JIHOČESKÁ UNIVERZITA V ČESKÝCH BUDĚJOVICÍCH

ZEMĚDĚLSKÁ FAKULTA

Katedra aplikované chemie

STUDIJNÍ PROGRAM: P1407 – Chemie

STUDIJNÍ OBOR: Zemědělská chemie

Magnetické biokompozitní materiály pro odstranění významných xenobiotik z vodních systémů

Ing. Eva Baldíková

Školitel: Prof. Ing. Ivo Šafařík, DrSc.

2017

Prohlašuji, že jsem předloženou disertační práci vypracovala samostatně za použití citované literatury.

V Českých Budějovicích, dne 14. 6. 2017

Balcárková

Prohlášení spoluautorů

Safarik I, Pospiskova K, Maderova Z, **Baldikova E**, Horska K, Safarikova M. Microwave-synthesized magnetic chitosan microparticles for the immobilization of yeast cells. *Yeast* 32, **2015**, 239-242.

Podíl: 10 %

Safarik I, Maderova Z, Horska K, **Baldikova E**, Pospiskova K, Safarikova M. Spent rooibos (*Aspalathus linearis*) tea biomass as an adsorbent for organic dyes removal. *Bioremed. J*. 19, **2015**, 183-187.

Podíl: 15 %

Baldikova E, Safarikova M, Safarik I. Organic dyes removal using magnetically modified rye straw. *J. Magn. Magn. Mater.* 380, **2015**, 181-185.

Podíl: 80 %

Safarik I, Maderova Z, Pospiskova K, **Baldikova E**, Horska K, Safarikova M. Magnetically responsive yeast cells: methods of preparation and application. *Yeast* 32, **2015**, 227-237.

Podíl: 10 %

Baldikova E, Politi D, Maderova Z, Pospiskova K, Sidiras D, Safarikova M, Safarik I. Utilization of magnetically responsive cereal by-product for organic dyes removal. *J. Sci. Food Agric*. 96, **2016**, 2204-2214.

Podíl: 65 %

Baldikova E, Pospiskova K, Maderova Z, Safarikova M, Safarik I. Příprava magnetických kompozitních materiálů - experimenty pro studenty středních škol. *Chem. listy* 110, **2016**, 64-68.

Podíl: 70 %

Safarik I, Nydlova L, Pospiskova K, **Baldikova E**, Maderova Z, Safarikova M. Rapid determination of iron oxide content in magnetically modified particulate materials. *Particuology* 26, **2016**, 114-117.

Podíl: 15 %

Safarik I, Pospiskova K, **Baldikova E**, Maderova Z, Safarikova M. Magnetic modification of cells. In: *Applications of NanoBioMaterials*, Volume II: Engineering of NanoBioMaterials (Grumezescu, A., ed.), Elsevier: US, **2016**, pp 145 – 181.

Podíl: 15 %

Safarik I, Pospiskova K, **Baldikova E**, Safarikova M. Magnetically responsive biological materials and their applications. *Adv. Mater. Lett.* 7, **2016**, 254-261.

Podíl: 15 %

Safarik I, Ashoura N, Maderova Z, Pospiskova K, **Baldikova E**, Safarikova M. Magnetically modified *Posidonia oceanica* biomass as an adsorbent for organic dyes removal. *Mediterr. Mar. Sci.* 17, **2016**, 351-358.

Podíl: 10 %

Maderova Z, **Baldikova E**, Pospiskova K, Safarik I, Safarikova M. Removal of dyes by adsorption on magnetically modified activated sludge. *Int. J. Environ. Sci. Technol.*13, **2016,** 1653-1664.

Podíl: 30 %

Safarik I, **Baldikova E,** Pospiskova K, Safarikova M. Magnetic modification of diamagnetic agglomerate forming powder materials. *Particuology* 29, **2016**, 169-171.

Podíl: 30 %

Angelova R, **Baldikova E**, Pospiskova K, Maderova Z, Safarikova M, Safarik I. Magnetically modified *Sargassum horneri* biomass as an adsorbent for organic dye removal. *J. Clean. Product.* 137, **2016**, 189-194.

Podíl: 25 %

Safarik I, Maderova Z, Pospiskova K, Schmidt HP, **Baldikova E**, Filip J, Krizek M, Malina O, Safarikova M. Magnetically modified biochar for organic xenobiotics removal. *Water Sci. Technol.* 74, **2016**, 1706-1715.

Podíl: 10 %

Baldikova E, Pospiskova K, Ladakis D, Kookos IK, Koutinas AA, Safarikova M, Safarik I. Magnetically modified bacterial cellulose: a promising carrier for immobilization of affinity ligands, enzymes, and cells. *Mater. Sci. Eng. C* 71, **2017**, 214-221.

Podíl: 50 %

Angelova R, **Baldikova E**, Pospiskova K, Safarikova M, Safarik I. Magnetically modified sheaths of *Leptothrix* sp. as an adsorbent for Amido black 10B removal. *J. Magn. Magn. Mater.* 427, **2017**, 314-319.

Podíl: 20 %

Safarik I, Pospiskova K, **Baldikova E,** Safarikova M. Magnetically responsive microbial cells for metal ions removal and detection. In: *Metal-Microbe Interactions and Bioremediation: Principles and Applications for Toxic Metals*, (Das S, Dash HR, Eds.), CRC Press, **2016**, 769-778.

Podíl: 10 %

Safarik I, Angelova R, **Baldikova E**, Pospiskova K, Safarikova M. *Leptothrix* sp. sheats modified with iron oxide particles: magnetically responsive, high aspect ratio functional material. *Mater. Sci. Eng. C* 71, **2017**, 1342-1346.

Podíl: 10 %

Svým podpisem stvrzujeme, že autorský podíl Ing. Evy Baldíkové je u jednotlivých publikací uveden správně.

V České Budějovicích dne 5. 6. 2017 Prof. Ing. Ivo Šafařík, DrSc .....

V Olomouci dne 31. 5. 2017 Mgr. Kristýna Pospíšková, Ph.D .....

V České Budějovicích dne 5. 6. 2017 Ing. Mirka Šafaříková, Ph.D.....

V Praze dne 22. 5. 2017 Mgr. Ralitsa Angelova, Ph.D.....

Poděkování

Na tomto místě bych ráda poděkovala svému školiteli, prof. Ivu Šafaříkovi, DrSc. za odborné vedení, cenné rady a připomínky.

Dále děkuji svým spoluautorům za vynikající spolupráci při sepisování publikací a celému Oddělení nanobiotechnologií Biologického centra AV ČR za přátelskou atmosféru.

Velký dík patří také prof. Pavlu Kalačovi, CSc. a doc. Evě Dadákové, Ph.D. za jejich ochotu kdykoliv pomoci.

V neposlední řadě děkuji své rodině, příteli a blízkým přátelům za podporu a trpělivost.

Abstrakt

Teoretická část předložené dizertační práce poskytuje ucelený pohled na problematiku přípravy a následného využití magnetických derivátů biologických materiálů pro separace xenobiotik z vod. Pozornost je zaměřena zejména na magnetickou modifikaci odpadních materiálů či vedlejších produktů zemědělského a potravinářského průmyslu, které reprezentují široce dostupné materiály za minimální cenu, a také na mikrobiální buňky. Kromě popisu přípravy magnetických částic a jednotlivých dostupných technik magnetické modifikace je zde uvedena stručná charakteristika vybraných polutantů a rozsáhlý tabulkový přehled využití biomateriálů s adekvátní magnetickou odezvou pro biosorpce organických barviv, těžkých kovů, farmaceutických preparátů a přípravků osobní péče společně s všudypřítomnými průmyslovými endokrinními disruptory a v neposlední řadě také ropných derivátů.

Experimentální část se zabývá přípravou a optimalizací nových typů magnetických materiálů. Důraz je kladen na využití jednoduchých, rychlých a zároveň cenově přijatelných magnetizačních technik (např. postmagnetizace magnetickými oxidy železa připravenými pomocí mikrovlnného záření či jednokroková modifikace magnetickými kapalinami). Vybrané rostlinné materiály (ječná a žitná sláma) byly chemicky modifikovány za účelem významného (až pětinásobného) navýšení maximálních adsorpčních kapacit pro testovaná barviva. Veškeré připravené biomateriály vykazovaly dobrou magnetickou odezvu a zároveň relativně vysokou adsorpční kapacitu pro vybraná xenobiotika v testovaných podmínkách. Byly studovány faktory významně ovlivňující adsorpci, jako je pH, počáteční koncentrace, inkubační doba či teplota. Adsorpční rovnovážná data byla vyhodnocena pomocí Langmuirova, Freundlichova či Sipsova modelu. Experimentální data z časové závislosti byla analyzována pomocí vybraných kinetických modelů, konkrétně modelu pseudo-prvního a pseudo-druhého řádu a intračásticového difúzního modelu. Termodynamické parametry (Gibbsova volná energie, entalpie a entropie) popisující povahu adsorpce byly taktéž zahrnuty do studie.

Klíčová slova: adsorpce; rostlinná biomasa; magnetické částice; magnetická modifikace; magnetická separace; magnetický biokompozit; mikrobiální biomasa; odstranění xenobiotik

Abstract

The theoretical part of this doctoral thesis provides a comprehensive overview on the topic of preparation and subsequent utilization of magnetic derivatives of biological materials for xenobiotic separation from water. Main attention is paid to magnetic modification of waste materials and by-products originating from agricultural and food industry, which represent widely available and low-cost materials, and also to magnetic modification of microbial cells. In addition to the description of magnetic particle preparation and individual developed techniques of magnetic modification, a brief characterization of selected pollutants and a detailed table overview on utilization of magnetically responsive biomaterials for biosorption of organic dyes, heavy metals, pharmaceutical and personal care products together with ubiquitous industrial endocrine disruptors and also of crude oil derivatives is presented.

Experimental part of this thesis is focused on the preparation and optimization of new types of magnetic materials. Emphasis is placed on the employment of simple, fast and simultaneously low-cost magnetic modification techniques (e.g., postmagnetization using microwave-synthesized magnetic iron oxides or one-step modification by magnetic fluids). Selected plant materials (barley and rye straw) were chemically modified to significantly (up to five-times) increase the maximum adsorption capacities for tested dyes. All prepared biomaterials exhibited a great magnetic response and simultaneously relatively high adsorption capacity for selected xenobiotics under experimental conditions used. Factors substantially affecting adsorption process, such as pH, initial concentration, incubation time or temperature were also studied. Adsorption equilibrium data were assessed using Langmuir, Freundlich or Sips isotherm models. Experimental data from time dependence study were analyzed by chosen kinetic models, namely the pseudo-first-order and pseudo-second-order ones and by intraparticle diffusion model. Thermodynamic parameters (Gibbs free energy, enthalpy and entropy) describing the nature of adsorption were also included in study.

Key words: adsorption; plant biomass; magnetic particles; magnetic modification; magnetic separation; magnetic biocomposite; microbial biomass; xenobiotic removal

Obsah

1. ÚVOD…… 11
2. CÍLE PRÁCE…… 12
3. LITERÁRNÍ PŘEHLED…….. 13
3.1 Charakteristika magnetických (bio)kompozitních materiálů……..... 13
3.2 Příprava magnetických (bio)kompozitů……. 14
3.2.1 Magnetické částice…….. 14
3.2.2 Způsoby magnetické modifikace…… 16
3.2.3 Magnetická separace, magnetické separátory……. 20
3.3 Odstraňování xenobiotik pomocí biosorpce……... 23
3.3.1 Rostlinná biomasa……... 24
3.3.2 Mikrobiální biomasa……... 26
3.4. Stručná charakteristika vybraných xenobiotik a jejich odstranění pomocí magnetických biokompozitů……. 27
3.4.1 Organická barviva…….. 27
3.4.2 Těžké kovy…… 31
3.4.3 Farmaceutické preparáty a přípravky osobní péče / endokrinní disruptory……. 36
3.4.4 Ropné deriváty…… 39
4. MATERIÁL A METODY…… 41
4.1 Materiál……... 41
4.2 Metody……..... 42
5. DOSAŽENÉ VÝSLEDKY…….. 46
5.1 Magnetická modifikace diamagnetických materiálů…….. 46
5.1.1 Magnetické biomateriály a jejich využití…… 46
5.1.2 Příprava magnetických biokompozitních materiálů pro studenty SŠ…… 48
5.1.3 Magnetická modifikace buněk…… 50
5.1.4 Magneticky modifikované kvasinkové buňky…… 52
5.1.5 Magnetická modifikace materiálů tvořících aglomeráty……. 54
5.1.6 Kvantifikace navázaných magnetických částic na povrchu modifikovaného materiálu……. 56
5.2 Adsorpce organických barviv…… 58

5.2.1 Chitosan/kvasinkový kompozit……... 58
5.2.2 Čaj Rooibos……. 60
5.2.3 Žitná sláma…….. 62
5.2.4 Ječná sláma……. 64
5.2.5 Mořská tráva *Posidonia oceanica*……... 66
5.2.6 Makrořasa *Sargassum horneri*…… 68
5.2.7 Aktivovaný kal…… 70
5.2.8 Biouhel…… 72
5.2.9 *Leptothrix* sp. ……. 74
5.2.10 Bakteriální celulóza……... 77
5.3 Adsorpce těžkých kovů…….. 79
5.3.1 Mikrobiální buňky……... 79
5.4 Adsorpce endokrinních disruptorů……. 81
5.4.1 Adsorpce bisfenolu A na biouhel…… 81
5.5 Adsorpce ropných derivátů……. 83
5.5.1 Odstranění ropných derivátů pomocí ječné slámy…….. 83
6. DISKUSE…….. 88
7. ZÁVĚR……. 91
8. LITERÁRNÍ ZDROJE……. 92
9. PŘÍLOHY……. 106
9.1 Seznam obrázků…….. 106
9.2 Seznam grafů…….. 106
9.3 Seznam tabulek……... 106
9.4 Seznam zkratek……... 107
9.5 Má publikační aktivita…… 108
9.5.1 Články v impaktovaných vědeckých časopisech…… 108
9.5.2 Články v neimpaktovaných vědeckých časopisech…… 109
9.5.3 Knižní kapitoly…… 110

1. ÚVOD

Znečištění vodních toků představuje v celosvětovém měřítku obrovský problém, a to nejen pro lidské zdraví, ale také pro životní prostředí i organismy v něm žijící. Některé nežádoucí látky (či jejich metabolity) produkované lidskou činností mají často toxické, karcinogenní či mutagenní účinky, jiné zase negativně ovlivňují reprodukční schopnosti, a tím i celé životní cykly organismů. V životním prostředí obvykle vykazují vysokou perzistenci, neboť bývají velmi obtížně biodegradovatelné.

Bylo popsáno mnoho metod, založených na fyzikálně - chemických principech, které lze pro odstraňování xenobiotik z vodních toků s úspěchem využít. Mezi tyto techniky lze zařadit například iontovou výměnu, membránové technologie, koagulaci, flokulaci, oxidaci, ozonaci, aerobní či anaerobní biodegradaci, fotodegradaci nebo chemickou degradaci. Avšak za jednu z nejefektivnějších a ekonomicky nejméně náročných technik je považována biosorpce.

Jako sorbenty mohou sloužit nejen živé i mrtvé buňky, ale také ostatní biologické materiály či jejich komponenty, které obsahují některé funkční skupiny, jako např. hydroxy-, karboxy-, amino-, amido-, thiol- a mnoho dalších. Pro nativní materiály, zejména rostlinného původu, jsou charakteristické nižší hodnoty maximálních adsorpčních kapacit, které však mohou být významně navýšeny pomocí vhodné fyzikální či chemické metody. Nejčastěji je využíváno účinku kyselin či hydroxidů, avšak některé publikace popisují také extrakci či karbonizaci.

Výhoda magnetické modifikace spočívá v získání materiálu, který lze rychle a selektivně odstranit z prostředí, a to pomocí vnějšího magnetického pole (NdFeB magnetu, komerčně dostupných magnetických separátorů či elektromagnetu). V některých případech se i samotné magnetické částice mohou účastnit adsorpce.

2. CÍLE PRÁCE

1) Vypracování literární rešerše k dané problematice
2) Příprava nových typů magnetických materiálů z diamagnetických prekurzorů, zejména rostlinného a mikrobiálního původu
3) Chemická či fyzikální modifikace magnetických materiálů za účelem zvýšení maximálních adsorpčních kapacit
4) Studium adsorpce vybraných xenobiotik v různých experimentálních podmínkách

3. LITERÁRNÍ PŘEHLED

3.1 Charakteristika magnetických (bio)kompozitních materiálů

Magnetické (bio)kompozitní materiály reprezentují velice významnou skupinu materiálů využitelných v nejrůznějších odvětvích přírodních i technických věd. Jedná se o materiály, které jsou složeny ze dvou nebo více složek s různými fyzikálními a chemickými vlastnostmi (Safarik et al., 2013), kde jednu z komponent tvoří ferimagnetické, feromagnetické či superparamagnetické nano- a mikročástice, zatímco další složky mají diamagnetický (nemagnetický) charakter. V případě biokompozitního materiálu mohou být diamagnetické části zastoupeny biopolymery (např. alginát, chitosan, κ-karagenan) a rostlinnou či mikrobiální biomasou, zatímco kompozity nebiologického původu jsou tvořeny syntetickými polymery (např. PVA, polystyren) či anorganickými materiály (např. oxid křemičitý nebo jíly).

Nespornou výhodnou magnetických (bio)kompozitů jsou jejich magnetické vlastnosti, díky kterým mohou být snadno a rychle odstraněny z libovolného prostředí pomocí vhodného magnetického separátoru. Magnetické struktury tak byly izolovány nejen z vodné suspenze či kultivačních médií, ale také přímo ze surových materiálů, jako je krev a ostatní tělní tekutiny, kostní dřeň či potraviny (Mosiniewicz-Szablewska et al., 2010). Díky této jedinečné schopnosti jsou také někdy nazývány „inteligentními (smart)“ materiály.

Magnetické biokompozity nacházejí uplatnění v různých sférách přírodních věd, především v biotechnologiích, biochemii, medicíně a environmentální technologii, neboť mohou sloužit jako levné a snadno připravitelné adsorbenty nejrůznějších xenobiotik (barviv, těžkých kovů, metabolitů léčiv) či biologicky aktivních látek, ale také jako nosiče pro imobilizované enzymy, kontrastní látky pro magnetickou rezonanci či jako celobuněčné biokatalyzátory (Safarik et al., 2013; Safarik et al., 2011b).

3.2 Příprava magnetických biokompozitů

Naprostá většina biologických materiálů má diamagnetické vlastnosti, neboť nevykazují vlastní magnetický moment (výjimky tvoří pouze redukovaný hemoglobin, erytrocyty, ferritin a magnetotaktické bakterie).

Realizace magnetické modifikace by nebyla úspěšná bez použití magnetických částic, separace pak bez vhodného magnetického separátoru.

3.2.1 Magnetické částice

Magnetická modifikace může být provedena nejen pomocí magnetických částic (o velikosti > 1μm), nýbrž také pomocí magnetických koloidů a kapalin (10-200 nm), magnetolipozómů nebo molekulových magnetických značek (Safarik and Safarikova, 1999, 2000). Nejčastěji používanými magnetickými materiály jsou práškové oxidy železa magnetit (Fe_3O_4) a maghemit (γ-Fe_2O_3) nebo jejich směsi, méně často pak oxid chromičitý, práškové železo, nikl a ferity (MeO. Fe_2O, kde Me = Ni, Co, Mg, Zn, Mn..) (Safarikova and Safarik, 1995).

Právě magnetické částice dodávají modifikovanému materiálu velice ceněnou vlastnost, umožňující selektivní separaci ze vzorku za využití vnějšího magnetického pole. Samotná jejich aplikovatelnost je však mnohem širší. Mohou sloužit také k citlivé detekci cílových biologicky aktivních sloučenin, směřování a následnému udržení magnetických částic v cílové oblasti pomocí magnetického pole, tvorbě tepla ve střídavém magnetickém poli (využívané při experimentální léčbě rakoviny) či k tvorbě negativního T2 kontrastu při zobrazení magnetickou rezonancí (Dutz et al., 2009; Safarik et al., 2011b; Safarik and Safarikova, 2009).

Magnetické částice různých velikostí i tvarů mohou být připraveny několika technikami, např. klasickou koprecipitační reakcí, hydrotermálními a vysokoteplotními reakcemi, sol-gel metodou, elektrosprejovou a průtokovou injekční metodou, mikrovlnnou syntézou či mechanochemickou syntézou (Laurent et al., 2008).

Klasická spolusrážecí reakce spočívá ve srážení železnatých a železitých solí v přesně definovaném poměru v alkalickém prostředí. Po úpravě pH na hodnotu 8 – 14 vzniká magnetit (viz rovnice 1). Ten je však nestabilní a v přítomnosti kyslíku podléhá oxidaci na maghemit (viz rovnice 2).

$$Fe^{2+} + 2\ Fe^{3+} + 8\ OH^- \rightarrow Fe_3O_4 + 4\ H_2O \qquad (1)$$

$$Fe_3O_4 + 2\ H^+ \rightarrow \gamma\text{-}Fe_2O_3 + Fe^{2+} + H_2O \quad (2)$$

Hlavní výhodou této metody je možnost přípravy velkého množství částic, na druhou stranu lze obtížněji ovlivňovat jejich velikost. Velikost a tvar částic je určována hodnotou pH, iontovou silou, teplotou, druhem použité soli a poměrem obsahu železnatých a železitých iontů. Přídavek chelatačních organických iontů (např. kyselina citrónová, glukonová nebo olejová) či polymerů (dextran, škrob, polyvinylalkohol) může zabránit agregacím vznikajících částic, a tím napomoci ke kontrole jejich velikosti (Laurent et al., 2008). První příprava superparamagnetických částic v podobě vodné magnetické kapaliny byla poprvé popsána v roce 1981 (Massart, 1981). Dle Massartova postupu lze magnetickou kapalinu stabilizovat pomocí kyseliny chloristé nebo hydroxidu tetraamonného. Magnetické částice lze dispergovat také v nepolárních kapalinách (olej, organická rozpouštědla) za účelem přípravy magnetických emulzí či kapsulí.

Hydrotermální syntéza probíhá ve vodných médiích v reaktorech anebo autoklávech za vysokého tlaku (> 2000 psi) a teploty 200 ^oC. Tento proces zahrnuje dva způsoby vzniku magnetických oxidů železa, a sice hydrolýzu a oxidaci. Na výsledný charakter částic má vliv typ rozpouštědla, teplota a čas (Laurent et al., 2008).

Sol-gel reakce je charakteristická přípravou nanočástic mokrou cestou a je založena na hydroxylaci a kondenzaci molekulových prekurzorů v roztoku za vzniku „sol“ částic o rozměrech nanometrů. Další kondenzací a anorganickou polymerací vzniká trojrozměrná sít oxidů kovu v gelu. Zahřívání na vysoké teploty vede k tvorbě konečného krystalického stavu (Laurent et al., 2008).

Pro přípravu oxidů železa lze také využít mikrovlnnou syntézu. Prekurzory částic mohou být tvořeny buďto směsí železnaté a železité soli (Hong et al., 2008) nebo pouze železnatou solí (Zheng et al., 2010). Po vysrážení hydroxidů železa v alkalickém prostředí je suspenze podrobena mikrovlnnému záření, které oproti klasickému záhřevu významně urychluje syntézu částic a částečnou konverzi železnatých iontů na železité ionty.

Další zajímavou technikou je mechanochemická syntéza částic, probíhající za dodání mechanické energie oběma prekurzorům železa a hydroxidu sodnému. Přídavek NaCl zabraňuje nežádoucím agregacím částic (Safarik et al., 2014).

3.2.2 Způsoby magnetické modifikace

Proces magnetické modifikace nejčastěji spočívá v navázání magnetických nano- či mikročástic oxidů železa na povrch diamagnetického materiálu či do jeho pórů (Safarik et al., 2012c), s úspěchem lze ale využít také kovalentní imobilizaci na magnetické nosiče, uzavření materiálu (společně s magnetickými částicemi) do polymeru, zesítění v přítomnosti magnetických částic pomocí bifunkčního činidla, srážení paramagnetických částic na povrchu materiálu či modifikaci erbitými ionty, které vykazují mimořádně vysoký atomový dipólový moment (Safarik et al., 2012c; Safarik and Safarikova, 2007, 2009).

Výběr způsobu modifikace vždy závisí jednak na charakteru modifikovaného materiálu, neboť jiné procedury byly popsány pro živou a jiné pro neživou biomasu, jednak na účelu použití výsledného biokompozitního materiálu. Úspěšná modifikace již byla provedena u široké škály materiálů zahrnující anorganické materiály (např. jíl), rostlinné deriváty (sláma, piliny, čajové lístky, kávová sedlina), mikrobiální buňky, polymery (syntetické i přírodní), dřevěné uhlí, aktivované uhlí a spousty dalších.

- **Navázání magnetických nano- či mikročástic na povrch**

K navázání magnetických nano- či mikročástic oxidů železa na povrch diamagnetického práškového materiálu lze v praxi použít několik jednoduchých metod. Nejstarší z nich je založena na smíchání modifikovaného materiálu s (převážně kyselou) magnetickou kapalinou a následném sušení. Postup lze využít buď přímý (Safarik et al., 2012a) nebo s využitím metanolu (Safarik and Safarikova, 2010).

Magnetické materiály lze připravit pomocí mikrovlnného záření generovaného běžnou kuchyňskou mikrovlnnou troubou. I v tomto případě lze využít dva postupy. První z nich je založen na jednokrokové *in situ* syntéze magnetického kompozitu a spočívá v mikrovlnném ozařování suspenze složené z modifikovaného diamagnetického materiálu a hydroxidů železa, které vznikly alkalizací síranu železnatého (Safarik et al., 2013). Tento přístup však není vhodný pro modifikaci materiálů, jež jsou citlivé na některé podmínky reakce, zejména na vysoké pH a teplotu nad 100 ^{o}C, a proto byla vyvinuta dvoukroková metoda, kde jsou mikrovlnnou syntézou nejdříve připraveny samotné magnetické částice, které jsou pak následně smíchány s modifikovaným materiálem (Pospiskova et al., 2013;

Safarik and Safarikova, 2014). Důležitým krokem je nejen důkladné promíchání směsi, ale také její sušení, které je nezbytné pro fixaci magnetických částic.

Na Obr. 1 je zdokumentována magnetická modifikace *Leptothrix* sp. využívající obou zmíněných magnetizačních postupů, konkrétně magnetizaci pomocí magnetické kapaliny stabilizované kyselinou chloristou (postup s využitím metanolu) a mikrovlnně-syntetizovanými magnetickými nano- a mikročásticemi Fe_3O_4 (MS magnetitem; postup nepřímý). Z téhož obrázku je patrné, že modifikace magnetickou kapalinou vedla k rovnoměrnému rozprostření magnetických nanočástic na povrchu buněk *Leptothrix* sp., zatímco MS magnetit vytvořil větší, nerovnoměrně rozložené agregáty. V obou případech vykazoval magnetický derivát rychlou magnetickou odezvu.

Obrázek 1: SEM bakterie *Leptothrix* sp. modifikované pomocí kyselé magnetické kapaliny (vlevo) a magnetických oxidů železa syntetizovanými mikrovlnným zářením (vpravo).

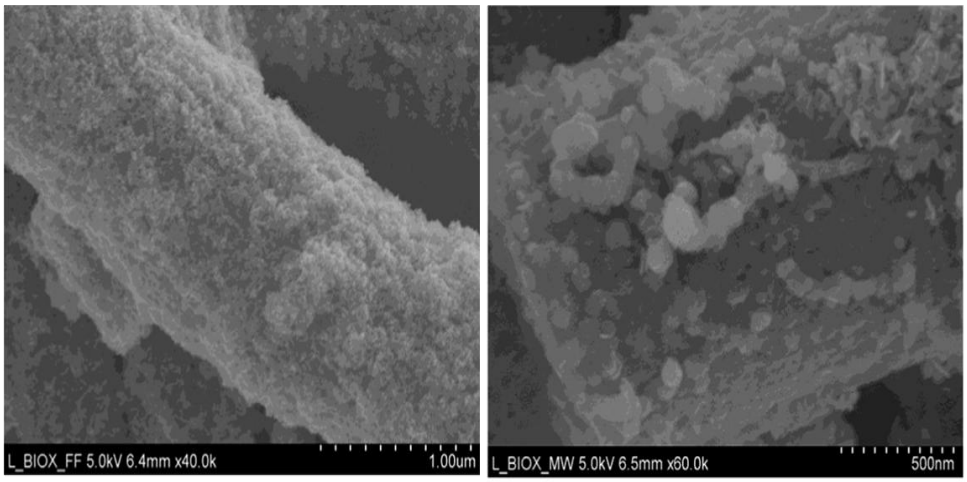

Zdroj: (Angelova et al., 2017)

Další zajímavou, i když ne příliš častou metodou přípravy různých typů látek a materiálů je mechanochemická syntéza. Typickým znakem je, že reakce probíhají za účasti mechanické energie dodané reaktantům např. v kulovém mlýnu nebo při tření materiálů tloučkem v třecí misce (Safarik et al., 2014).

- **Kovalentní imobilizace na magnetické nosiče**

Tato metoda je široce využívána zejména při imobilizaci nejrůznějších biopolymerů (Safarik and Safarikova, 2007), avšak jsou známy i případy, kdy byla použita pro mikrobiální buňky. Např. Safarik et al. (2015b) popisuje kovalentní imobilizaci kvasinek (*Saccharomyces cerevisiae)* na částice magnetického chitosanu (viz Obr. 2) za vzniku biokompozitního materiálu využitelného nejen jako potenciální adsorbent různých organických barviv, ale také jaké účinný celobuněčný biokatalyzátor pro degradaci peroxidu vodíku či tvorbu invertního cukru.

Obrázek 2: Kvasinkové buňky kovalentně vázané na částice magnetického chitosanu.

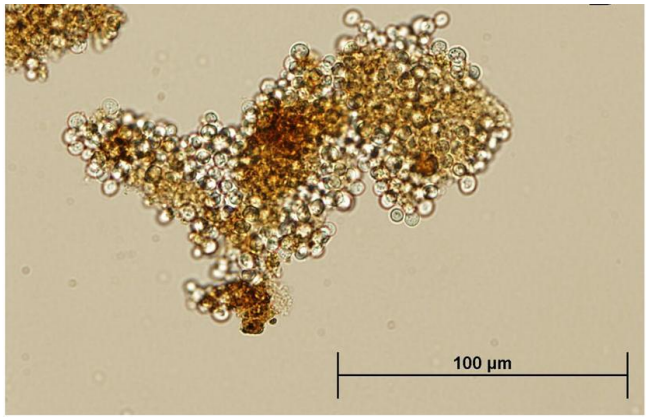

Zdroj: (Safarik et al., 2015b)

Kovalentní vazba je možná díky reaktivním skupinám na nosiči nebo prostřednictvím reaktivní vazby, která spojuje buňky a nosiče (Brodelius and Vandamme, 1987). K zavedení specifické skupiny na povrch nosiče mohou být také použita různá vazná činidla, jako např. aminosilan, karbodiimid, glutaraldehyd (Krumphanzl and Řeháček, 1988).

Jako nosiče lze zvolit magnetické deriváty polysacharidů, syntetických polymerů či anorganických materiálů (detailní rozdělení uvádí Tabulka 1), které ideálně vykazují tyto vlastnosti (Brena and Batista-Viera, 2006): velký povrch a vysokou permeabilitu; hydrofilní charakter a nerozpustnost ve vodě; chemickou, tepelnou a mechanickou stálost; schopnost regenerace; resistenci vůči mikroorganismům; toxikologickou bezpečnost; a co nejnižší cenu.

Tabulka 1: Nosiče používané pro kovalentní imobilizace.

Biopolymery		**Syntetické polymery**	**Syntetické materiály**	**Minerály**
polysacharidy	agar a agaróza	polyakrylát	neporézní sklo	bentonit
	celulóza	polyakrylamid	řízené porézní sklo	pemza
	chitin a chitosan	polyamid	oxidy kovů (Fe, Al, Zr)	
	dextran	polymetakrylát	keramika	
	karagenan	polystyren		
	škrob	polyuretan		
	xantanová guma	polyvinylalkohol		
proteiny	albumin	polyvinylchlorid		
	kolagen			
uhlíkové materiály	aktivované uhlí			

Zdroj: upraveno dle (Chibata et al., 1987; Kuncová and Trögl, 2001)

- **Enkapsulace/entrapment**

Principem této metody je uzavření materiálu (často buněk) společně s magnetickými částicemi do nosiče přírodního či syntetického charakteru. Jedná se o velmi oblíbenou techniku imobilizace mikrobiálních, rostlinných i živočišných buněk, nicméně uzavřít lze i rostlinný materiál, jak je popisováno např. Chengem et al. (2012), využívajícího chitosan jako vazný reagent pro enkapsulaci pilin a Fe_3O_4 částic.

Nosiče mohou být dále rozděleny dle mechanismu tvorby gelu (viz Tabulka 2) (Brodelius and Vandamme, 1987; Krumphanzl and Řeháček, 1988; Safarik and Safarikova, 2007).

Tabulka 2: Rozdělení nosičů dle mechanismu tvorby gelu (MČ = magnetické částice).

Mechanismus tvorby gelu	**Princip**	**Polymer**
Precipitace (srážení)	Smísení vodní suspenze materiálu + MČ s polymerem rozpuštěným ve vhodném organickém rozpouštědle a následné srážení směsi v jiném rozpouštědle, ve vodě či na vzduchu.	Celulóza, Triacetát celulózy
Termální gelace	Vmíchání materiálu + MČ do teplého roztoku přírodního polymeru-gelu rozpustného za tepla ve vodě a následné ztuhnutí směsi.	Kolagen, Želatina, Agar/agaróza
Ionotropní gelace	Vmíchání materiálu + MČ do teplého roztoku polymeru, srážení kapáním do studené vody obsahující soli (Ca, Ba, Sr, Fe, Al, K)	Alginát
Polymerace	Uzavření materiálu + MČ do sítě vznikajícího organického polymeru.	Polyakrylamid, Polymethakrylát
Polyadice		Polyuretan, Epoxidová pryskyřice
Zesítění	Kovalentí zesítění použitím bi- nebo multifunkčního činidla.	Proteiny

- **Zesítění (cross-linking)**

Jedná se o metodu založenou na zesítění obsahu materiálu, a to buď pomocí bi- či multifunkčního činidla (kovalentní zesítění) nebo flokulačními mechanismy vznikajícími přidáváním elektrolytů (iontové zesítění) (Chibata et al., 1987). Podstatou je reakce s amino-, hydroxy-, merkapto- a jinými funkčními skupinami materiálu. Většinou se používá v kombinaci s enkapsulací/entrapmentem.

3.2.3 Magnetická separace, magnetické separátory

Magnetické materiály mohou být ze vzorku odstraněny několika způsoby, dle typu použité magnetické separace. Magnetická separace je obecně rozdělována na pozitivní a negativní, a v případě magnetické separace buněk také na přímou a nepřímou (Obr. 3). Pomocí pozitivní separace jsou magneticky modifikovány a izolovány přímo žádané sloučeniny či buňky, zatímco v případě negativní separace

jsou cílové struktury získávány odstraňováním všech kontaminujících složek. V případě přímé separace je vhodný afinitní ligand spojen s magnetickou částicí nebo magneticky modifikovaným biopolymerem a poté je tento komplex přidán přímo do vzorku obsahující cílovou strukturu, kam se naváže. V nepřímé separaci reaguje cílová sloučenina nejprve s primárními afinitními ligandy, ke kterým mají afinitu přidávané sekundární ligandy a teprve posléze se navážou magnetické částice (Safarik and Safarikova, 1999; Safarikova and Safarik, 2001).

Obrázek 3: Schéma metod magnetické separace mikrobiálních buněk.

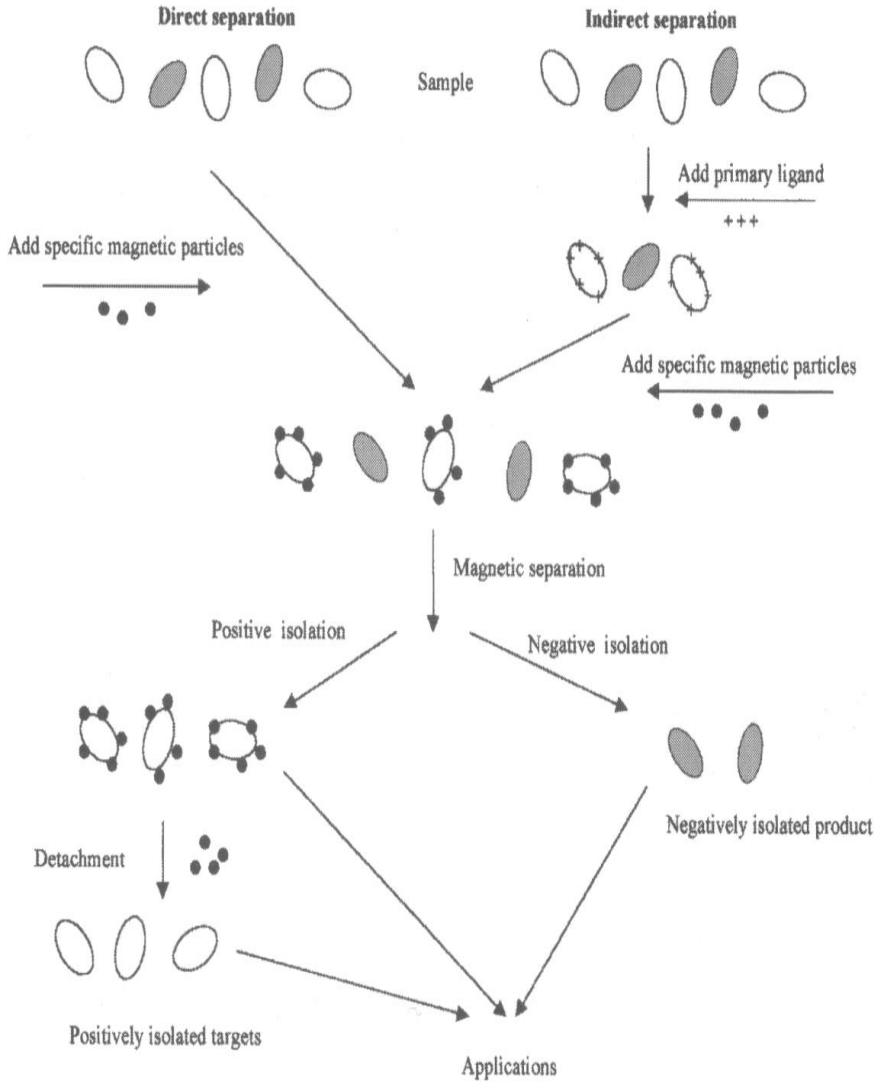

Zdroj: Safarikova and Safarik (2001)

Většina magnetických separátorů je tvořena velmi silnými permanentními magnety na bázi kovů vzácných zemin nebo elektromagnety (Safarik et al., 2012c; Safarik and Safarikova, 2000; Safarikova and Safarik, 1995). Jejich vhodnost pro zvolenou aplikaci závisí nejen na velikosti částic, které mají být separovány, ale také na celkovém objemu, ze kterého mají být odstraněny. Magnetické separátory lze obecně rozdělit na dvě skupiny, a sice na vsádkové a průtočné.

Vsádkové separátory reprezentují velmi oblíbené jednoduché typy separátorů, určené pro nejrůznější objemy: pro separaci mikročástic lze využít separátory typu Eppendorf (< 2 mL), zkumavkové (< 50 mL) či ploché magnety (< 1000 mL), pro manipulaci s nanočásticemi kvadrupólové a hexapólové separátory. Průtočné separátory jsou charakteriské průtokem kapaliny magnetických struktur separačním systémem. Tento typ separátorů bývá také označován jako vysokogradientový (HGMS – high gradient magnetic separator) a stejně jako vsádkové separátory jsou dostupné od řady komerčních společností. Ukázka různých typů komerčních vsádkových magnetických separátorů včetně magnetické separace je zdokumentována na Obr. 4.

Obrázek 4: Ukázka magnetické separace pomocí různých typů komerčně dostupných vsádkových magnetických separátorů.

3.3 Odstraňování xenobiotik pomocí biosorpce

Ač bylo popsáno mnoho metod, založených na fyzikálně - chemických principech, které lze pro odstraňování xenobiotik z vodních toků s úspěchem využít (např. iontová výměna, membránové technologie, koagulace, flokulace, oxidace, ozonace, aerobní či anaerobní biodegradace, fotodegradace nebo chemická degradace), za jednu z nejefektivnějších a ekonomicky nejméně náročných technik je stále považována (bio)sorpce.

Biosorpce je poměrně nová technologie nacházející své uplatnění v bioremediačních procesech, zejména ve vodních systémech. Dle Aksu (2005) ji lze definovat jako pasivní, metabolicky nezávislé odstraňování cílových nežádoucích látek pomocí biologických materiálů, k čemuž jsou využívány různé typy mechanismů, jako je chemická či fyzikální adsorpce, elektrostatické interakce, komplexace, chelatace, iontová výměna či precipitace.

Biosorpční proces probíhá vždy na rozhraní dvou fází: pevné (adsorbent) a kapalné, jež obsahuje polutant (adsorbát). Díky afinitě adsorbentu a adsorbátu dochází k vazbě (pomocí různých mechanismů), přičemž tento proces pokračuje až do dosažení adsorpční rovnováhy (Safarik et al., 2011b).

Jedná se tedy o fyzikálně chemický děj, charakteristický pro živé i mrtvé buňky, ostatní biologické materiály a jejich komponenty (Safarik et al., 2011b), jehož nespornými výhodami jsou vysoká selektivita a účinnost a zároveň nízká cena (hlavně při využití odpadních materiálů).

Nezbytnou podmínkou biosorpce je přítomnost některých funkčních skupin (např. hydroxy-, karboxy-, amino-, ester-, amido-, thiol-, acetamido-, fenol-, imidazol- a mnoho dalších), které jsou schopné interagovat s individuálními xenobiotiky (Wang and Chen, 2009). Na druhou stranu ani přítomnost těchto skupin vždy nezaručuje použití v biosorpčních procesech, neboť se mohou objevit různé sférické, konformační či jiné bariéry (Safarik et al., 2011b). Účinnost adsorpce je ovlivňována nejen povahou polutantu (velikost, náboj), ale také vnějšími faktory, jako pH, teplota, iontová síla či inkubační doba (Aksu, 2005; Tonk et al., 2011).

V posledních letech se zájem vědců obrací na levné, snadno připravitelné a zároveň účinné adsorbenty, které často představují odpadní materiály či vedlejší produkty zemědělského či potravinářského průmyslu. K biosorpci lze kromě rostlinné a mikrobiální biomasy úspěšně využít také živočišnou biomasu, kal a ostatní biologické odpady.

3.3.1 Rostlinná biomasa

Každý rok roste počet publikací zaměřených na využití rostlinné biomasy, reprezentující skupinu levných a snadno dostupných materiálů, které mohou být získávány i ve větším množství. Podstatnou část těchto funkčních materiálů tvoří nejen vedlejší produkty zemědělství, ale také potravinářské odpady. Odhaduje se, že více než 1/3 celosvětové produkce potravin přijde nazmar. Jen v EU bylo v roce 2012 vyprodukováno 88 milionů tun odpadu; 72 % připadalo na domácnosti a zpracování potravin, zbylých 28 % pak pocházelo z primární produkce, gastronomie, zásobování, maloobchodů a velkoobchodů (Stenmarck et al., 2016). I z tohoto hlediska je nutné odpadní materiály dále zpracovávat a hledat jejich nová využití.

Rostlinné deriváty získávají různá uplatnění, mohou sloužit nejen jako adsorbenty organických barviv (Zuorro et al., 2014), těžkých kovů (Fan et al., 2016) a radionuklidů (Wang et al., 2014), ale také jako adsorbenty pro imobilizaci enzymů (Safarik et al., 2013), absorbenty elektromagnetických vln (Chen et al., 2012) či katalyzátory (Latha et al., 2015).

V nativní i magnetické verzi již byla testována řada rostlinných materiálů, od běžnější slámy či pilin až po kůry citrusových plodů (Ong et al., 2012) či slupek od okurek (Akkaya and Guzel, 2014).

Obecně platí, že většina nativních rostlinných materiálů disponuje nižší adsorpční kapacitou. Tu je však možné pomocí vhodné metody modifikace významně navýšit. Např. jeden gram nativní pšeničné slámy navázal 57 (Zhang et al., 2011a) - 61 mg (Wu et al., 2009) metylenové modři, zatímco po ošetření chloridem 3-chloro-2-hydroxypropyltrimetylamonným, NaOH a kyselinou chlorooctovou dosáhla maximální adsorpční kapacita hodnoty 152 mg/g (Zhang et al., 2012). Karboxymetylací byla maximální adsorpční kapacita navýšena na 253 mg/g (Zhang et al., 2011a) a modifikace slámy kyselinou citrónovou, NaOH a $Pb(NO)_3$ vedla k hodnotě 397 mg/g (Han et al., 2010). Stejně tak maximální adsorpční kapacitu rýžové slámy pro dvojmocné olovo lze navýšit z 24 mg/g (Singha and Das, 2012) na 104 mg/g po esterifikaci kyselinou thioglykolovou v přítomnosti anhydridu kyseliny octové, kyseliny octové a katalyzátoru - kyseliny sírové (Gong et al., 2011).

V posledních letech se do popředí dostává příprava, modifikace a využití biocharu (biouhlu), a to jak v nemagnetické, tak magnetické verzi. Biouhel může být

připraven prakticky z libovolného rostlinného materiálu, a to prostřednictvím termochemických procesů (pyrolýzy, gasifikace či hydrotermální karbonizace), vedoucích k různému výtěžku biohlu (viz Tabulka 3). Na fyzikální a chemické vlastnosti biouhlu má ale vliv nejen použitá metoda a její parametry (teplota, tlak, atd.), nýbrž také charakter biomasy (velikost a tvar částic, fyzikální vlastnosti, složení, obsah popelu) (Parmar et al., 2014). Pro zvětšení povrchu biocharu (spojeným často s navýšením maximálních adsorpčních kapacit) lze také využít některou z chemických či fyzikálních modifikací. Tu je možné provést buď před termochemickým procesem, nebo po něm. Kromě klasických modifikací kyselinami a zásadami bylo v literatuře popsáno také využití např. manganistanu draselného (Wang et al., 2015), metanolu (Jing et al., 2014), peroxidu vodíku (Yakout et al., 2015), amoniaku či oxidu uhličitého (Zhang et al., 2013b), nejrůznějších chloridů (Creamer et al., 2016) apod. Z fyzikálních technik našla uplatnění aktivace mikrovlnami (Shen et al., 2015) či elektromodifikace (Jung et al., 2015).

Tabulka 3: Porovnání výtěžnosti biouhlu při použití různých termochemických procesů.

Proces	**Teplota (^{o}C)**	**Výtěžky (%)**			**Reference**
		Biouhel	**Bioolej**	**bioplyn**	
Pomalá pyrolýza	400	45	30	25	(Hernandez-Mena et al., 2014)
Rychlá pyrolýza	500	21	54	25	(Choi et al., 2015)
Mikrovlnná pyrolýza	170	27	42	31	(Gronnow et al., 2013)
Hydrotermální karbonizace	235	58	34	8	(Hoekman et al., 2013)
Gasifikace	800	10	5	85	(Nartey and Zhao, 2014)

3.3.2 Mikrobiální biomasa

Mikrobiální buňky mohou být využity nejen jako účinné adsorbenty široké škály xenobiotik, ale také (díky přítomnosti nejrůznějších enzymů) jako celobuněčné biokatalyzátory, a to jak ve volné, tak imobilizované formě. Imobilizované buňky jsou však upřednostňovány, neboť poskytují několik výhod, a sice jednodušší manipulaci s mikroorganismy, snazší oddělení produktů a substrátu, možnost opakovaného použití, zlevnění výroby (odstranění kroků jako extrakce, izolace či purifikace intracelulárních enzymů) a zvýšení odolnosti biomateriálu (Chibata et al., 1987; Kuncová and Trögl, 2001).

Ačkoliv bylo popsáno mnoho imobilizačních technik, mikrobiální buňky bývají nejčastěji imobilizovány (uzavírány) do biopolymerních nosičů (jako je alginát, κ-karagenan či chitosan), a to především díky biokompatibilitě a netoxicitě matrice vůči buňkám.

Obecně platí, že využití adsorbentů složených z živých mikroorganismů se oproti adsorbentům z mikroorganismů mrtvých (tepelně modifikovaných, vysušených, chemicky ošetřených) jeví méně výhodné, neboť je velice náročné tuto biomasu udržet životaschopnou (dodávaní živin, zachování mírných podmínek, zabránění styku s toxickými látkami). Navíc mrtvé buňky mají stejné ne-li vyšší adsorpční kapacity a je daleko snazší je regenerovat (Aksu, 2005).

Příprava magneticky modifikovaných buněk a jejich nejrůznější aplikace byly podrobně popsány v přehledných článcích či kapitolách knih (Safarik et al., 2015a; Safarik et al., 2016c).

3.4 Stručná charakteristika vybraných xenobiotik a jejich odstranění pomocí magnetických biokompozitů

Tato kapitola je rozdělena do čtyř částí dle typu adsorbovaného xenobiotika a poskytuje tak ucelený pohled na problematiku využití magneticky modifikovaných materiálů rostlinného či mikrobiálního původu pro sorpci organických barviv, těžkých kovů, farmaceutických preparátů a přípravků osobní péče (PPCP) zahrnující také endokrinní disruptory, a v neposlední řadě ropných látek.

3.4.1 Organická barviva

Organická barviva představují velice pestrou skupinu xenobiotik zahrnující více než 100 000 komerčně dostupných sloučenin (Aksu, 2005). Odhaduje se, že ročně je spotřebováno $7x10^5$ tun barviv (Rafatullah et al., 2010), přičemž za více než 60 % je odpovědný textilní průmysl (Celekli and Bozkurt, 2013). Uvádí se, že 10 – 15 % z produkovaných barviv vstupuje do vodních toků (Liu et al., 2016b).

Jedná se o sloučeniny, které jsou charakteristické svou vysokou perzistencí v životním prostředí a které často mají toxické, karcinogenní či mutagenní vlastnosti (Gong et al., 2006). Je prokázáno, že již nízká koncentrace barviva (10-50 mg/L) může negativně ovlivnit estetickou hodnotu vody a omezit propustnost pro sluneční záření, což má neblahý vliv na fotosyntetickou aktivitu, a tím i na život vodních organismů (Safarikova et al., 2005).

Organická barviva mohou být klasifikována na základě původu (přírodní a syntetická), rozpustnosti (rozpustná ve vodě či tucích), chemické struktury (diazo, trifenylmetanové, akridinové, chinoniminové, indigo) či Colour Indexu (C. I.; kyselá, přímá, disperzní, sirná, bazická, reaktivní).

Odstraňování barviv pomocí sorpce na magnetické biokompozitní materiály je shrnuto v Tabulce 4.

Tabulka 4: Magnetické biokompozitní materiály pro odstranění organických barviv (EDTA = etylendiamintetraoctová kyselina; GA = glutaraldehyd; PMDA = pyromelitický dianhydrid).

Rostlinná biomasa				
Rostlinný materiál	**Způsob magnetické modifikace**	**Adsorbát**	**q_m (mg/g) nebo jiné**	**Reference**
Arašídové slupky	Ošetření MK stabilizovanou kyselinou chloristou	Akridinová oranž; Bismarckova hněď Y; Krystalová violeť; Safranin O	71,4-95,7	(Safarik and Safarikova, 2010)
Arašídové slupky	Mikrovlnné ozařování suspenze materiálu s $Fe(OH)_2$ připravenými alkalizací $FeSO_4$	Bismarckova hněď Y; Safranin O	70,2; 72,2	(Safarik et al., 2013)
Arašídové slupky	Koprecipitace Fe_3O_4 připraveného z $FeSO_4$ a $FeCl_3$	Metylenová modř	9,0	(Taha and El-Maghraby, 2016)
Biochar z kukuřičného stébla	Karbonizace (400 ^oC/120 min), poté *in situ* koprecipitace	Krystalová violeť	349,4	(Sun et al., 2015)
Cukrová třtina	*In situ* koprecipitace Fe_3O_4 vzniklého z $FeCl_3$ a $FeSO_4$ na povrchu PMDA třtiny	Metylenová modř; Magenta	315,5; 304,9	(Yu et al., 2012)
Ječná sláma	Modifikace MS magnetitem	Bismarkova hněď Y; Safranin O; Krystalová violeť; Metylenová modř	86,5 -124,3	(Baldikova et al., 2016)
Kávová sedlina	Ošetření MK stabilizovanou kyselinou chloristou	7 barviv	1,24 – 73,4	(Safarik et al., 2012b)
Kávová sedlina	Mikrovlnné ozařování suspenze materiálu s $Fe(OH)_2$ připravenými alkalizací $FeSO_4$	Bismarckova hněď Y; Safranin O	49,3; 146,6	(Safarik et al., 2013)
Kukuřičný klas (vřeteno)	Navázání Fe_3O_4 na klas modifikovaný hydroxidem amonným	Metylenová modř	neurčeno	(Tan et al., 2012)

Kukuřičné klas (vřeteno)	*In situ* koprecipitace magnetických oxidů železa; modifikace etandiaminem	Kongo červeň	198,2	(Liu et al., 2016a)
Kukuřičná sláma	Impregnace Fe_3O_4; zesítění GA a ošetření kyselinou glutamovou	Metylenová modř	194,5	(Zhao et al., 2014)
Mláto	Ošetření MK stabilizovanou kyselinou chloristou	Anilinová modř; Bismarckova hněď Y; Krystalová violeť; Nilská modř	Nejvyšší q_m pro Bismarckovu hněď Y (72,4)	(Safarik et al., 2011a)
Odpad při zpracování kávy	Ošetření MK stabilizovanou hydroxidem tetrametylamonným	Metylenová modř	556,0	(Zuorro et al., 2013)
Pšeničná sláma	Navázání magnetitu na povrch	Metylenová modř	627,0	(Pirbazari et al., 2016)
Smrkové piliny	Koprecipitace $CuFe_2O_4$ na povrchu pilin	Cyaninová modř	178,6	(Hashemian and Salimi, 2012)
Smrkové piliny	Mikrovlnné ozařování suspenze materiálu s $Fe(OH)_2$ připravenými alkalizací $FeSO_4$	Bismarckova hněď Y; Safranin O	50,1; 72,4	(Safarik et al., 2013)
Upotřebené čajové lístky	Povrchová modifikace magnetitem	7 barviv	Kationtová barviva vyšší q_m	(Madrakian et al., 2012)
Upotřebené čajové lístky	Mikrovlnné ozařování suspenze materiálu s $Fe(OH)_2$ připravené alkalizací $FeSO_4$	Bismarckova hněď Y; Safranin O	120,7;148,5	(Safarik et al., 2013)
Mikrobiální buňky				
Mikroorganismus	**Způsob magnetické modifikace**	**Adsorbát**	**q_m v mg/g**	**Reference**
Chlorella vulgaris	Promytí 0,1M kyselinou octovou, poté přidání kyselé MK	6 barviv	24,3- 257,9	(Safarikova et al., 2008)
Kluyveromyces marxianus	Promytí 0,1M kyselinou octovou, poté přidání kyselé MK	7 barviv	29,9 – 138,2	(Safarik et al., 2007)

Saccharomyces cerevisiae	Inkubace buněk s $FeCl_2$, ultrazvuková oxidace pomocí H_2O_2, přídavek $FeCl_2$ a alkalizace	Metylenová modř	141,8	(Du et al., 2017)
Saccharomyces cerevisiae	Suspendace ve fyz. roztoku, poté v acetát. pufru (pH 4,6), přidání kyselé MK	5 barviv	19,6 – 430,2	(Safarik et al., 2002)
Saccharomyces cerevisiae	Zesítění (buňky + GA + Fe_3O_4)	Metylová violeť	60,8	(Tian et al., 2010)
Saccharomyces cerevisiae	Imobilizace *S. cerevisiae* na částice magnetického chitosanu	Safranin O, krystalová violeť	99; 63	(Safarik et al., 2015b)
Saccharomyces cerevisiae subsp. *uvarum*	PMDA modifikace, poté *in situ* koprecipitace Fe_3O_4 vzniklého z $FeCl_3$ a $FeSO_4$, promyv EDTA	Metylenová modř	609,0	(Yu et al., 2013b)
Saccharomyces cerevisiae subsp. *uvarum*	Suspendace ve fyz. roztoku, poté v acetát. pufru (pH 4,6), přidání kyselé MK	5 barviv	11,6 – 228,0	(Safarikova et al., 2005)

3.4.2 Těžké kovy

Znečištění těžkými kovy představuje závažný problém celého světa. Do lidského podvědomí se dostávají v 50. letech 20. století společně s výskytem onemocnění zvaných Itai-Itai (způsobené kadmiem) a Minamata (původcem rtuť), která se objevila v Japonsku (Wang et al., 2013b).

Těžké kovy vstupují do životního prostředí jak přirozenou cestou (vulkanická činnost, eroze minerálů), tak antropogenní činností (těžba a zpracování rud, galvanizace apod.) (Srivastava et al., 2015), a jsou charakteristické nejen vysokou perzistencí v životním prostředí a toxickými účinky, ale také svou akumulací v potravním řetězci. Byly popsány tři typy těžkých kovů, které nemohou být degradovány na neškodné produkty, a sice toxické kovy (Hg, Cr, Pb, Zn, Cu, Ni, Cd, As, Co, Sn), drahé kovy (Pd, Pt, Ag, Au, Ru) a radionuklidy (U, Th, Ra, Am) (Safarik et al., 2011b; Wang and Chen, 2009):

Využití rostlinných odpadních materiálů a vedlejších produktů pro sorpci těžkých kovů, leč v nemagnetické verzi, bylo podrobně sepsáno v přehledných článcích (Abdolali et al., 2014; Sud et al., 2008). Vybrané magnetické biomateriály, které byly úspěšně využity pro testování sorpce těžkých kovů a radionuklidů jsou shrnuty v Tabulce 5.

Tabulka 5: Magnetické biokompozitní materiály pro odstranění těžkých kovů (EDTAD = dianhydrid kyseliny etylendiamintetraoctové, GA = glutaraldehyd, PMDA = pyromelitický dianhydrid, TRIS = tris(hydroxymetyl)aminometan).

Rostlinná biomasa				
Rostlinný materiál	**Magnetické modifikace; další modifikace**	**Adsorbát**	**q_m v mg/g a jiné**	**Reference**
Arašídové slupky	Ošetření MK stabilizovanou kyselinou chloristou	Pb (II)	34,3	(Rozumova et al., 2012)
Biouhel z kokosových skořápek	Impregnace $FeCl_3$, mikrovlnná pyrolýza při 800W/20 min	Pb (II); Cd (II)	4,1; 3,8	(Yap et al., 2017)
Biouhel z rýžové slámy	*In situ* koprecipitace Fe_3O_4, pyrolýza 400 ^oC/40 min	Cd (II)	49,3	(Tan et al., 2017)
Biouhel z rýžových plev	NaOH modifikace; *in situ* koprecipitace Fe_3O_4; karbonizace 800 ^oC/2h	Cr (VI)	157,7	(Fan et al., 2016)
Biouhel z kůry borovice	*In situ* koprecipitace $CoFe_2O_4$ vzniklých z $Co(NO_3)_2$ a $Fe(NO_3)_3$; termálně ošetřeno při 950 ^oC/2h	Pb (II); Cd (II)	25,2; 15,0	(Reddy and Lee, 2014)
Biouhel z kůry dubu	Pyrolýza 450 ^oC; *in situ* koprecipitace částic vzniklých z $Fe_2(SO_4)_3$ a $FeSO_4$	Pb (II); Cd (II)	55,9; 8,3 při 45 ^oC	(Mohan et al., 2014)
Biouhel z topolu amerického	*In situ* koprecipitace γ-Fe_2O_3 vzniklého z $FeCl_3$; pyrolýza 600 ^oC	As (V)	3,1	(Zhang et al., 2013a)
Cukrová třtina	PMDA modifikace, poté *in situ* koprecipitace Fe_3O_4 částic vzniklých z $FeSO_4$ a $FeCl_3$	Pb (II); Cd (II)	Komparativní studie, $Pb^{2+} > Cd^{2+}$	(Yu et al., 2013a)
Cukrová třtina	Karbonizace (300 ^oC/30 min), *in situ* koprecipitace Fe_3O_4 částic z $FeCl_2$ a $FeCl_3$	Uran	17,2	(Yamamura et al., 2011)
Cukrová třtina	Karbonizace (300 ^oC), *in situ* koprecipitace Fe_3O_4 částic z $FeCl_2$ a $FeCl_3$, přídavek HCl	Uran	71,4	(Rahnama et al., 2014)
Kukuřičné stéblo	*In situ* koprecipitace magnetitu vzniklého z $FeSO_4$ a $FeCl_3$; amino-funkcionalizace	Cr (VI)	227 při 45 ^oC	(Song et al., 2015)

Kukuřičná sláma	*In situ* koprecipitace Fe_3O_4 vzniklého z $FeSO_4$ a $FeCl_3$, amino-funkcionalizace	Cr (VI)	345 při 45 ^oC	(Wang et al., 2016)
Piliny	Impregnace Fe_3O_4 částic na povrch pilin	Cd (II)	22,5	(Shah et al., 2016)
Piliny	Modifikace využívající Fe_3O_4 chitosan (z prekurzorů $FeCl_3$ a $FeCl_2$) jako vazný reagent	Sr (II)	12,6	(Cheng et al., 2012)
Pomerančové slupky	*In situ* koprecipitace Fe_3O_4 částic vzniklých z $FeSO_4$ a $FeCl_3$	Cd (II)	76,9	(Gupta and Nayak, 2012)
Použité čajové lístky	*In situ* koprecipitace Fe_3O_4 částic vzniklých z $FeCl_3$	As (III); As (V)	188,7; 153,8	(Lunge et al., 2014)
Použité čajové lístky	Modifikace kyselou MK s využitím metanolu	Pb (II)	44,5	(Rozumova et al., 2014)
Použité čajové lístky	Impregnace Fe_3O_4 částic vzniklých z $FeSO_4$ a $FeCl_3$	Ni (II)	38,3 při pH 4	(Panneerselvam et al., 2011)
Pšeničné otruby	Modifikace MS magnetitem vzniklého z $FeSO_4$	Uran	29	(Wang et al., 2014)
Pšeničná sláma	*In situ* koprecipitace Fe_3O_4 vzniklých z $FeSO_4$ a $FeCl_3$	As (III); As (V)	Čím více magnetitu tím vyšší q_m	(Tian et al., 2011)
Pšeničná sláma	*In situ* koprecipitace Fe_3O_4	Pb (II)	50,7	(Haghighat and Ameri, 2016)
Rýžová sláma	*In situ* koprecipitace Fe_3O_4 částic vzniklých z $FeCl_3$ a $FeCl_2$	Cu (II); Pb (II)	16,3; 19,5	(Khandanlou et al., 2015)
Rašelina	Smíchání $Fe(OH)_3$ z prekurozu $FeCl_3$ s homogenizovanou rašelinou	As (V)	15,0	(Ansone et al., 2013)

Slupky z pomela	Koprecipitace Fe_3O_4	Cu (II)	Nejvyšší q_m, když váhový poměr 1:3 (MČ:pomelo)	(Pengsaket et al., 2016)
Slupky z litchi	Postmagnetizace s Fe_3O_4	Pb (II)	78,7	(Jiang et al., 2015)
Topolové piliny	*In situ* koprecipitace Fe_3O_4 vzniklých z $FeCl_3$ a $FeCl_2$; modifikace 3-merkaptopropyl-trimethoxysilanem	Pb (II); Cu (II); Cd (II)	12,5; 5,5; 4	(Gan et al., 2016a)
Mikrobiální buňky				
Mikroorganismus	**Způsob magnetické modifikace**	**Adsorbát**	**q_m v mg/g**	**Reference**
Amphibacillus KSUCr3	Imobilizace buněk do silika-sodného alginátu s Fe_3O_4	Cr (VI)	Opt. pH 7 a 45^oC	(Ibrahim et al., 2013)
Enterobacter	Imobilizace buněk (ošetřených TRIS pufrem) s magnetitem	Ni (II)	Opt. 37 ^oC, 30 min inkubace	(Wong and Fung, 1997)
Kluyveromyces marxianus	Promytí 0,1M kyselinou octovou, poté přidání kyselé MK	Sr (II)	140,8	(Ji et al., 2010)
Penicillium sp.	Inkubace spor s Fe_3O_4 připravenými koprecipitací $FeCl_3$ a $FeCl_2$	Sr (II); U (VI); Th (IV)	100,9; 223,9; 280,8	(Ding et al., 2015)
Rhodotorula glutinis	Promytí acetátovým pufrem (pH 4,6) a přidání kyselé MK	Uran	187-226 V závislosti na rostoucí teplotě	(Bai et al., 2012)
Rhizopus cohnii	Uzavření *R. cohnni* a magnetitu do alginátu sodného a polyvinylalkoholu	Cr (VI)	5,8 při 28 ^oC	(Li et al., 2008)
Saccharomyces cerevisiae	Aktivace buněk (1-ethyl-3-(3-dimetylaminopropyl)karbodiimidem a *N*-hydroxysukcinimidem), poté inkubace s Fe_3O_4 modifikovanými dietylaminem	As (V)	28,7	(Rajesh Kumar et al., 2016)
Saccharomyces cerevisiae	Modifikace pomocí Fe^0 připraveného borohydridovou redukcí	Ni (II)	54.2	(Guler and Ersan, 2016)

Saccharomyces cerevisiae	*In situ* koprecipitace Fe_3O_4 na aktivní uhlí, poté imobilizace buněk	Hg (II)	MSPE	(Mahmoud et al., 2015)
Saccharomyces cerevisiae	Zesítění (buňky + GA + Fe_3O_4), poté ošetření EDTAD	Ca (II); Cd (II); Pb (II)	26,5; 41,0; 89,2	(Xu et al., 2011)
Saccharomyces cerevisiae	Zesítění (buňky + GA + Fe_3O_4), poté ošetření EDTAD	Pb (II); Cd (II)	88,2; 40,7	(Zhang et al., 2011b)
Saccharomyces cerevisiae	Zesítění (buňky + GA + Fe_3O_4), poté ošetření EDTAD	Pb (II); Cd (II)	99,3;48,7	(Zhang et al., 2011c)
Saccharomyces cerevisiae	Imobilizace s Fe_3O_4 obalených chitosanem	Cu (II)	144,9	(Peng et al., 2010)
Saccharomyces cerevisiae	Imobilizace s magnetitem	Cu (II); Cd (II); Ag (I)	14,3; 10,1; 8,6	(Patzak et al., 1997)
Saccharomyces cerevisiae subsp. u*varum*	Suspendace ve fyz. roztoku, poté v glycin-HCl pufru (pH 2,2) a přidání kyselé MK	Cu (II)	76,2	(Uzun et al., 2011)
Saccharomyces cerevisiae subsp. *uvarum*	Suspendace ve fyz. roztoku, poté v glycin-HCl pufru (pH 2,2) a přidání kyselé MK	Cu (II); Hg (II); Ni (II); Zn (II); Cd (II)	29,9; 76,2; 14,1; 11,8;12,3	(Yavuz et al., 2006)
Yarowia lipolytica NCIM3589 a NCIM 3590	Suspendace v acetátovém pufru (pH 4,5), přidání Fe^0/Fe_3O_4 připraveného koprecipitací $(NH_4)_2Fe(SO_4)_2$ a $NH_4Fe(SO_4)_2$ v extraktu z granátového jablka	Cr (VI)	186,3; 137,3	(Rao et al., 2013)

3.4.3 Farmaceutické preparáty a přípravky osobní péče / endokrinní disruptory

Farmaceutické preparáty a přípravky osobní péče, z anglického Pharmaceutical and personal care products (PPCPs), zahrnují tisíce různých chemických sloučenin, které jsou součástí humánních a veterinárních léčiv, hormonálních přípravků, desinfekčních a pracích prostředků, opalovacích krémů (UV filtry), vůní, repelentů, různých doplňků stravy apod. Přítomnost těchto látek je v čističkách odpadních vod detekována již od 80. let 20. století a je často spojována s výskytem fyziologických abnormalit u ryb.

Endokrinní disruptory (EDCs) představují extrémně různorodou skupinou sloučenin, napodobující funkce přírodních hormonů v endokrinním systému. Jsou všudypřítomné, neboť tvoří nedílnou součást nejen hormonálních léčiv, ale také pesticidů, průmyslových a potravinářských aditiv, kosmetických a čistících přípravků, hraček, obalů potravin, nábytku apod.

Do vodních systémů se PPCP/EDCs dostávají buďto v nativní formě či jako metabolity, přičemž nejčastějším vstupem je odpadní voda domácností, nemocnic či průmyslových zón. Obavy však nezpůsobují jen vysoké objemy produkovaných sloučenin, ale také jejich perzistence v životním prostředí v kombinaci s významnou biologickou aktivitou (např. vysoká toxicita, vliv na klíčové biologické funkce jako je reprodukce). Příkladem může být 17α-ethinylestradiol, syntetický steroidní hormon obsažený v antikoncepčních pilulkách, který je jen v EU produkován v množství několika set kilogramů ročně a který vykazuje estrogenní aktivitu u ryb už při koncentraci nižší než 1-4 ng/L (Fent et al., 2006).

Jedním z významných zástupců EDCs je bisfenol A (BFA), také nazývaný jako dian. Uvádí se, že 95 % veškeré spotřeby BFA připadá na výrobu polykarbonátových plastů (71 %) a epoxidových pryskyřic (29 %), zbylých 5 % pak slouží jako vazné a plnící materiály, aditiva v brzdových kapalinách, retardátorech hoření apod. Roční celosvětová produkce BFA činila v roce 2005 3,8 milionů tun (Rancière et al., 2015), zatímco v roce 2010 již 5 milionů tun (Huang et al., 2012). Není tedy divu, že přítomnost BFA byla detekována ve všech typech vod, a to v koncentracích pohybujících se od 3,5-59,8 ng/L v pitné vodě, 12 μg/L v tekoucích vodách a až 17,2 mg/L v průsakové vodě ze skládek (Zhou et al., 2012).

O všudypřítomnosti bisfenolu A svědčí také jeho detekovatelné množství v moči u 90 % testovaných jedinců (Vandenberg et al., 2010).

Ačkoliv bylo připraveno mnoho magnetických materiálů pro sorpci zástupců PPCP/EDCs, pouze malá část (viz Tabulka 6) byla tvořena rostlinnou biomasou.

Tabulka 6: Magnetické biokompozitní materiály pro odstranění PPCP/EDCs (ATB = antibiotika, N/A = neděláno).

Materiál	**Magnetická modifikace**	**Další modifikace materiálu**	**Adsorbát**	**q_m (mg/g) nebo jiné**	**Reference**
Aktivní uhlí získané z palmy	Koprecipitace částic vzniklých z $FeSO_4$	Silanizace (pomocí triethoxyphenylsilanu)	Ibuprofen; karbamazepin	120; 150	(Wong et al., 2016)
Aktivní uhlí získané z palmy	Koprecipitace částic vzniklých z $FeSO_4$	Silanizace (pomocí triethoxyphenylsilanu)	Bisfenol A	150	(Wong et al., 2016)
Aktivní uhlí připravené z rýžových plev	*In situ* koprecipitace Fe_3O_4	Aktivace pomocí $ZnCl_2$	Tetracyklinová ATB	MSPE	(Lou et al., 2016)
Aktivní uhlí připravené z rýžové slámy (resp. z hydrocharu)	Hydrotermální koprecipitace	N/A	Triclosan	303	(Liu et al., 2014)
Biouhel z borovicových pilin	Koprecipitace Fe_3O_4 vzniklých oxidační hydrolýzou z $FeCl_2$	N/A	Sulfomethoxazol	13.8	(Reguyal et al., 2017)
Biouhel z cukrové třtiny	*In situ* koprecipitace částic vzniklých z $FeSO_4 . 7H_2O$ a $FeCl_3 . 6H_2O$	N/A	Tetracyklinová ATB	48.4	(Rattanachueskul et al., 2017)
Biouhel z reziduí Kozince blanitého	*In situ* koprecipitace Fe_3O_4 připravených z $FeCl_3$ a $FeSO_4$	N/A	Ciprofloxacin	68.9	(Kong et al., 2017)

3.4.4 Ropné deriváty

Každý rok vstupuje do světových oceánů okolo 210 miliónů galonů ropy pocházející z její těžby či převozu a dalších 180 milionů galonů kontaminující vodu průsaky (Coleman et al., 2002).

Dle Colemana et al. (2002) zabíjí tento druh znečištění ryby, savce, ptáky, a jejich potomstvo, ničí rostliny a redukuje množství potravy pro přeživší organismy, čímž narušuje strukturu a funkci mořského společenstva a ekosystému. Banerjee et al. (2006) považuje za nejtoxičtější složky ropy ve vodě rozpustné aromáty a uvádí, že dospělý mořský organismus nepřežije jejich expozici v rozsahu 1-100 ppm, zatímco u larev byla letální dávka stanovena na 0,1 ppm.

Biosorpce ropných derivátů byla již úspěšně testována u mnoha nemagnetických rostlinných materiálů, např. pšeničné slámy (Sidiras and Konstantinou, 2012), ječné slámy (Husseien et al., 2009), rýžové slámy (Sun et al., 2002) a rýžových pluch (Kudaybergenov et al., 2012), cibulových slupek (Sayed and Zayed, 2006), vláken banánovníku (Sathasivam and Haris, 2010) a cukrové třtiny (Behnood et al., 2013), neboť se ukázalo, že mohou být stejně účinné jako často využívaný polypropylen či polyuretan. Ve verzi magnetické však snaha o využití rostlinných materiálů byla zaznamenána až poměrně nedávno (viz Tabulka 7).

Tabulka 7: Magnetické biokompozitní materiály pro odstranění ropných látek.

Materiál	**Magnetická modifikace**	**Adsorbát**	**q_m v g/g nebo jiné**	**Reference**
Mnohostěnné uhlíkaté nanotrubičky	Koprecipitace Fe_3O_4 na povrchu trubiček	Nafta	6,6	(Wang et al., 2013a)
Vysoce porézní uhlíkaté nanotrubičky (houbičky)	Chemická depozice částic z plynné fáze za využití ferrocenu a dichlorbenzenu	Nafta	56,0	(Gui et al., 2013)
Slupky pomela	Solvotermální metoda	Nafta	28,0	(Zou et al., 2016)
Topolové piliny	Hydrotermální syntéza (koprecipitace $CoFe_2O_4$ na povrchu pilin), poté silanizace	Lubrikační gel	11,5	(Gan et al., 2016b)
Celulózové houbičky	*In situ* koprecipitace Fe_3O_4 částic vzniklých z $FeCl_3$. 6 H_2O a $FeCl_2$. 4 H_2O, poté silanizace	Parafínový olej, petroleum ether, cyklohexan, toluen	Neurčeno, účinnost separace > 90%	(Peng et al., 2016)

4. MATERIÁL A METODY

4.1 Materiál

Chemikálie:

Chemikálie použité pro přípravu magnetických částic a pro sorpci organických barev byly p. a. čistoty, zatímco pro sorpci bisfenolu A byly využity chemikálie v HPLC kvalitě.

Zásobní roztoky barev o koncentraci 1 mg/mL (vyjma sorpčních experimentů s chemicky modifikovanou slámou, kde byla použita koncentrace 10 mg/mL) byly připraveny v destilované vodě a uchovávány při 4 ^{o}C. Bisfenol A (1 mg/mL) byl rozpuštěn v metanolu HPLC kvality, a všechna další ředění na požadovanou koncentraci byla provedena pomocí destilované vody.

Materiály:

Rostlinné materiály (ječná, žitná a pšeničná sláma, čaj Rooibos), makrořasa *Sargassum horneri* a mořská tráva *Posidonia oceanica* byly důkladně promyty vodou k odstranění nečistot a částeček prachu, a sušeny při pokojové teplotě (24 ^{o}C). Po vysušení byl testovaný materiál rozemlet v běžném kávovém mlýnku a přesítován standardizovanými síty k získání částic konkrétní velikosti.

Saccharomyces cerevisiae (pekařské droždí) byly zakoupeny v místním supermarketu, buňky *Leptothrix* sp. byly odebrány v bezejmenném potoce ve Stromovce v Českých Budějovicích během února 2016, aktivovaný kal pocházel z čističky odpadních vod ve Zlivi, a bakteriální celulóza byla věnována Zemědělskou univerzitou v Athénách (Řecko).

4.2 Metody

Příprava mikročástic chitosanu pomocí mikrovlnné syntézy (MS):

Chitosan byl rozpuštěn v kyselině octové, poté byla přidána destilovaná voda a roztok síranu železnatého. Promíchaná směs byla následně alkalizována přídavkem hydroxidu sodného (na pH 10-12) a po menších dávkách podrobována mikrovlnnému záření. Magnetické částice MS chitosanu byly opakovaně promývány vodou. Podrobný postup je uveden v publikaci (Safarik et al., 2015b).

Imobilizace buněk *S. cerevisiae* na částice MS chitosanu:

Částice MS chitosanu byly nejprve aktivovány a zesítěny pomocí glutaraldehydu, a po důkladném promyvu byly navázány kvasinkové buňky.

Příprava MS magnetitu:

Roztok síranu železnatého byl pozvolna alkalizován pomocí hydroxidu sodného na pH 12. Po přidání vody byla suspenze vysrážených hydroxidů železa ozařována mikrovlnami. Vzniklé magnetické částice byly několikrát promyty vodou (Safarik and Safarikova, 2014).

Magnetická modifikace pomocí MS magnetitu:

Jeden gram modifikovaného materiálu byl důkladně smíchán se 2 mL suspenze MS magnetitu, tvořené jedním dílem kompletně sedlých magnetických částic (18 h, v 50 mL kalibrovaných válcích) a čtyřmi díly destilované vody. Výsledná směs byla sušena při 60 ^{o}C do konstantní hmotnosti, standardně 24 h.

Pro získání materiálu s vyšší magnetickou odezvou je možné přidat větší objem suspenze MS magnetitu.

U materiálů tvořících po magnetizaci s vodnou suspenzí MS magnetitu tvrdé klastry lze použít alternativní způsob magnetické modifikace (Safarik et al., 2016a), spočívající ve smíchání materiálu s MS magnetitem v organickém rozpouštědle (nejlépe metanolu, popř. acetonu, izopropylalkoholu či propanolu).

Magnetická modifikace magnetickou kapalinou (MK):

K modifikovanému materiálu suspendovanému ve vodě nebo metanolu byla přidána kyselá MK. Po společné inkubaci byl materiál důkladně promyt vodou k odstranění přebytečných magnetických částic a ponechán ve vodné suspenzi (Safarik and Safarikova, 2010).

Mechanochemická syntéza magnetických biokompozitů:

Směs anorganických solí ($FeCl_3$. 6 H_2O a $FeCl_2$. 4 H_2O) a chloridu sodného byla důkladně homogenizována ve třecí misce. Posléze byl přidán modifikovaný materiál a směs byla opět důkladně třena. Následovala alkalizace směsi přídavkem hydroxidu sodného a další tření. Výsledný materiál byl několikrát promyt vodou a uchován buď ve vodné suspenzi, či ve vysušeném stavu (Safarik et al., 2014).

Chemická modifikace ječné a žitné slámy:

K částicím slámy byla nejdříve přidána kyselina citronová. Po společné inkubaci následovalo sušení při teplotě 50 ^{o}C, zvýšení teploty na 120 ^{o}C k realizaci termochemické reakce a důkladný promyv materiálu. Po dosažení neutrálního pH byla sláma smíchána s hydroxidem sodným, důkladně promyta a znovu sušena při 50 ^{o}C (Baldikova et al., 2016).

Adsorpční experimenty (BFA, barviva):

Veškeré adsorpční experimenty byly prováděny v 15 mL plastových uzavíratelných zkumavkách s 30 mg testovaného materiálu a celkovým objemem analytu 10 mL. Vzorky byly promíchávány na vertikálním rotátoru při 24 rpm po přesně stanovenou dobu, dle typu experimentu. Po ukončení inkubace byl vzorek separován pomocí magnetického separátoru a supernatant byl analyzován pomocí spektrofotometru (organická barviva) či HPLC (BFA). K určení množství navázaného analytu na jednotku sorbentu v rovnováze (q_e; mg/g) nebo čase t (q_t; mg/g) byly použity následující rovnice:

$$q_e = \frac{V\,(C_0 - C_e)}{m} \qquad (1)$$

$$q_t = \frac{V\,(C_o - C_t)}{m} \quad (2)$$

kde V je celkový objem (L), C_0 počáteční koncentrace analytu (mg/L), m množství sorbentu (g) a C_e a C_t koncentrace volného barviva v rovnováze a čase t (mg/L). C_e a C_t byly vypočteny z kalibrační rovnice.

Časová závislost k určení času potřebného k dosažení adsorpční rovnováhy byla testována standardně v časech 0 - 300 min. Experimentální data ze závislosti na čase byla dále použita ke stanovení kinetických parametrů, s využitím kinetických modelů pseudo-prvního (rovnice 3) a pseudo-druhého řádu (rovnice 4), popřípadě také intračásticového difúzního modelu (rovnice 5):

$$\ln(q_e - q_t) = \ln q_e - k_1 t \quad (3)$$

kde k_1 je rychlostní konstanta pseudo-prvního kinetického modelu (1/min), jež byla získána z lineární rovnice po vynesení ln (q_e-q_t) proti času t (min).

$$\frac{t}{q_t} = \frac{1}{k_2 {q_e}^2} + \frac{1}{q_e} t \quad (4)$$

kde k_2 je rychlostní konstanta pseudo-druhého kinetického modelu (g/mg min). Hodnoty k_2 a q_e byly vypočteny z lineární rovnice po vynesení t/qt proti t.

$$q_t = k_{id} t^{1/2} + C \quad (5)$$

kde ki_d je rychlostní konstanta intračásticového difúzního modelu (mg/g $\text{min}^{1/2}$) a C je konstanta přímo úměrná s tloušťkou vrstvy (mg/g).

Rovnovážné izotermy byly provedeny ve třech různých teplotách (ca 9, 24 a 40 ^{o}C). Experimentální data byla analyzována pomocí nelineární regresní analýzy (v programu Microsoft Excel a funkce Řešitel) a dvou nejčastěji používaných adsorpčních rovnovážných modelů, a sice Langmuirova a Freundlichova modelu.

Langmuirův model (rovnice 6) předpokládá jednovrstevnou adsorpci analytu a žádné interakce mezi molekulami, zatímco Freundlichův model (rovnice 7) vychází z vícevrstevné adsorpce na heterogenním povrchu adsorbentu.

$$q_e = \frac{q_m K_L C_e}{1+K_L C_e} \quad (6)$$

$$q_e = K_f C_e^{1/n} \quad (7)$$

kde K_L je Langmuirova konstanta (L/mg), K_F Freundlichova konstanta [(mg/g) (L/mg)1/n] spojená s množstvím navázaného analytu a n konstanta vyjadřující úroveň heterogenity.

Termodynamické parametry, volná Gibbsova energie ($\Delta G°$; J/mol), entalpie ($\Delta H°$, J/mol) a entropie ($\Delta S°$; J/mol K) byly vypočteny z rovnic (8) a (9). Termodynamická rovnovážná konstanta K_d byla zjištěna z úseku na ose y po vynesení ln (q_e/C_e) proti q_e (Khan and Singh, 1987).

$$\Delta G^o = -R\,T \ln(K_d) \quad (8)$$

$$\ln(K_d) = \frac{\Delta S^o}{R} - \frac{\Delta H^o}{RT} \quad (9)$$

kde R je univerzální plynová konstanta (8,314 J/ mol K) a T je teplota (K). $\Delta H°$ a $\Delta S°$ byly vypočteny po vynesení ln(K_d) proti 1/T.

5. DOSAŽENÉ VÝSLEDKY

5.1 Magnetická modifikace diamagnetických materiálů

5.1.1 Magnetické biomateriály a jejich využití

Magnetické částice a kompozitní materiály nacházejí uplatnění v nejrůznějších oblastech biologických věd, medicíně i environmentálních technologiích. Díky odezvě k vnějšímu magnetickému poli lze magneticky značené materiály nejen selektivně separovat z prostředí pomocí permanentních magnetů a magnetických separátorů, ale také dopravit do cílového orgánu, kde pomocí vysokofrekvenčního magnetického pole generují teplo, které efektivně zabíjí nádorové buňky.

Tento stručný přehledný článek shrnuje techniky magnetické modifikace vyvinuté Oddělením nanobiotechnologie Biologického centra AV ČR v Českých Budějovicích, konkrétně modifikaci magnetickými kapalinami, mikrovlnnou a mechanochemickou syntézu. Úspěšná magnetická modifikace byla provedena na diamagnetických materiálech nejrůznějšího charakteru; biopolymerech, rostlinných derivátech, mikrobiálních a řasových buňkách, mořských makrořasách i anorganických materiálech, o čemž svědčí doložené mikroskopické snímky pořízené optickou, skenovací a transmisní elektronovou mikroskopií, na kterých jsou patrné navázané magnetické částice či jejich agregáty na povrchu modifikovaného materiálu.

Magnetické biomateriály byly (v závislosti na typu diamagnetického materiálu) využity pro široké spektrum aplikací, od nosičů imobilizovaných mikrobiálních buněk či enzymů, přes afinitní sorbenty, sorbenty xenotibiok a katalyzátory, až po biosenzory.

Příloha 1:

Magnetically responsive biological materials and their applications

Safarik I, Pospiskova K, Baldikova E, Safarikova M

Adv. Mater. Lett. 7, **2016**, 254-261

www.vbripress.com/aml, DOI: 10.5185/amlett.2016.6176 Published online by the VBRI Press in 2016

Magnetically responsive biological materials and their applications

Ivo Safarik[1,2,3*], Kristyna Pospiskova[2], Eva Baldikova[1,4], Mirka Safarikova[1,3]

[1]*Department of Nanobiotechnology, Institute of Nanobiology and Structural Biology of GCRC, Ceske Budejovice, Czech Republic*
[2]*Regional Centre of Advanced Technologies and Materials, Palacky University, Olomouc, Czech Republic*
[3]*Department of Nanobiotechnology, Biology Centre – ISB, CAS, Ceske Budejovice, Czech Republic*
[4]*Department of Applied Chemistry, Faculty of Agriculture, University of South Bohemia, Ceske Budejovice, Czech Republic*

[*]Corresponding author. Tel: (+420) 387775608; E-mail: ivosaf@yahoo.com

Received: 15 September 2015, Revised: 20 December 2015 and Accepted: 22 January 2016

ABSTRACT

Diamagnetic biological materials of various origins (e.g., prokaryotic and eukaryotic microbial cells, lignocellulosic materials, food wastes, soluble and insoluble biopolymers etc.) can be magnetically modified in order to obtain smart biomaterials exhibiting an appropriate response to external magnetic field. Magnetic modification of originally nonmagnetic biological materials is usually based on the attachment of magnetic iron oxides nano- and microparticles on the surface or within the pores of the treated material, or by their entrapment in the gel structure. Magnetic modification can be performed using different procedures, e.g., by magnetic fluid treatment, mechanochemical synthesis and by direct or indirect microwave assisted synthesis. This short review will summarize magnetic modification procedures developed by the authors and applications of advanced magnetically modified biomaterials as adsorbents of both organic and inorganic xenobiotics and radionuclides, affinity adsorbents for isolation of target biomolecules, carriers for various affinity ligands, biologically active compounds and cells or whole-cell biocatalysts. The potential of magnetically responsive biomaterials will increase in the near future.

Keywords: Biological materials; magnetic modification; adsorbents; carriers; whole-cell biocatalysts.

Introduction

Magnetically responsive nano- and microparticles have been efficiently used in many areas of biosciences, biotechnology, medicine and environmental technology. Such materials can be described as smart materials, exhibiting several types of responses to external magnetic field. That's why magnetically responsive materials can be utilized for various applications. Such materials can be selectively separated from difficult-to-handle environments by means of a magnetic separator. Alternatively, they can be targeted and localized in a specific place using an appropriate magnetic system. Magnetic particles subjected to high frequency alternating magnetic field generate heat, which can be used for hyperthermia therapy of cancer diseases. Magnetic iron oxide nanoparticles increase a negative T_2 contrast during magnetic resonance imaging. Magnetorheological fluids increase their apparent viscosity when subjected to a magnetic field [**1**]. Recently, it was observed that both naked magnetic nanoparticles and magnetoferritin exhibit peroxidase-like activity [**2, 3**].

Magnetic nano- and microparticles can be successfully used for magnetic modification of diamagnetic biological materials (e.g. prokaryotic and eukaryotic cells or plant-derived materials), biopolymers, organic polymers and inorganic materials, and for magnetic labeling of biologically active compounds and affinity ligands (e.g., antibodies, enzymes, aptamers etc.).

The group of naturally magnetic materials is usually represented by magnetic iron oxides magnetite and maghemite, various types of ferrites or metallic iron, cobalt and nickel. On the contrary, majority of particulate materials exhibit diamagnetic (non-magnetic) behavior. In addition to inorganic particulate materials (e.g., different types of clays, sand, silica, aluminium oxide, titanium dioxide) and organic particulate materials (e.g., polystyrene-based ion exchangers), diverse biological materials are of great interest. Various types of non-magnetic particulate materials can be efficiently used as adsorbents, catalysts, chromatography materials, carriers or whole-cell catalysts. In many cases the application potential of these materials could be improved by their modification leading to the formation of magnetically responsive materials. Such a modification can substantially simplify separation of magnetic materials from complex systems, such as suspensions, culture media etc [**1**].

Magnetic modification procedures

Many procedures for the conversion of non-magnetic biological materials into their magnetic derivatives have been already described [**4**]. Magnetic modification is usually caused by the presence of magnetic labels within

the treated biomaterials pores, on the biomaterials surface or within the biopolymer gels. In general, magnetic properties of the modifiers (labels) are caused by the presence of nano- or microparticles of magnetic iron oxides, namely magnetite (Fe_3O_4) or maghemite (γ-Fe_2O_3) or their mixtures; in some cases also ferrite particles [**5**], chromium dioxide particles [**6**], nickel [**7**] or metallic cobalt [**8**] have been employed for specific magnetization purposes. Alternatively, magnetic labels are formed by paramagnetic cations [**9**] or by (magneto) ferritin [**10**].

The simplest and most often used approach for magnetic modification of non-magnetic materials is based on the alkali precipitation of ferrous and ferric salts in the presence of the treated material, followed by heating of the aqueous suspension. Magnetic iron oxides (magnetite, maghemite or their mixtures) are usually formed [**4**]. However, specific biomaterials may require more appropriate treatment. Selected, efficiently used magnetic modification procedures are described below.

Magnetic fluid modification

Diverse types of ionically and sterically stabilized magnetic fluids nanoparticles (magnetic fluids, ferrofluids, FF) can be used for magnetic modification. In the simplest way, perchloric acid stabilized magnetic fluid was mixed with methanol suspension of the powder material to be modified (e.g., sawdust). During mixing magnetic iron oxide nanoparticles from magnetic fluid firmly precipitated on the particles surface [**1, 11**] (**Fig. 1**).

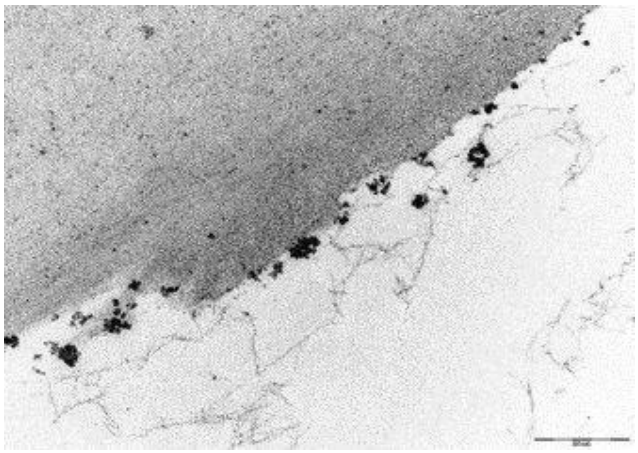

Fig. 1. TEM of ferrofluid modified sawdust particle; the bar corresponds to 200 nm. Reproduced, with permission, from [**1**].

Living baker's or brewer's yeast cells were washed with and suspended in acetate buffer, pH 4.6 or in glycine–HCl buffer, pH 2.2 for magnetic modification with perchloric acid stabilized ferrofluid; alternatively, tetramethyl-ammonium hydroxide stabilized magnetic fluid was utilized for baker's yeast cells modification in 0.1 M glycin–NaOH buffer, pH 10.6. After a short time period, magnetic nanoparticles precipitated on the cell surface (**Fig. 2**). The different physiological state of yeast cells can lead to various magnetic modification; using dormant yeast cells only surface modified cells were obtained, while magnetic modification of actively growing cells led to the accumulation of magnetic modifier in the periplasmic space [**12**].

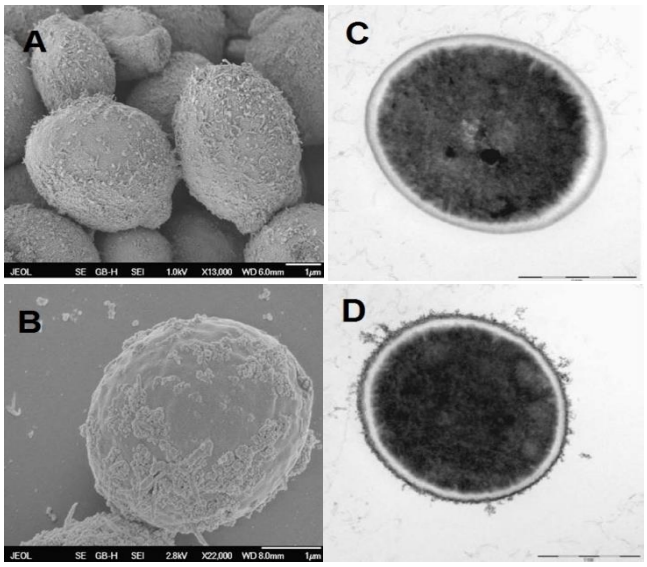

Fig. 2. (A, B) SEM images of ferrofluid-modified *Saccharomyces cerevisiae* cells, showing attached magnetic nanoparticles and their aggregates on the cell surface; bars =1 μm. (C) TEM image of a native *Saccharomyces cerevisiae* cell; bar =1 μm. (D) TEM image of a ferrofluid modified cell with attached magnetic iron oxide nanoparticles on the cell wall; bar =1 μm. Reproduced with permission from [**13**].

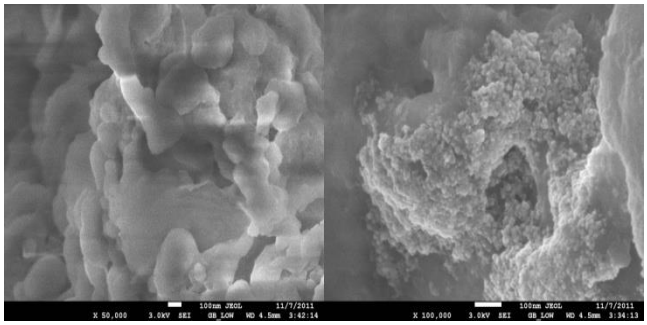

Fig. 3. SEM of native tea leaves (left) and tea leaves modified by direct ferrofluid treatment (right). Reproduced, with permission, from [**14**].

New and efficient postmagnetization procedure is based on the use of water based magnetic fluid stabilized with perchloric acid, which was directly thoroughly mixed with material to be modified (in a typical procedure, 1 g of nonmagnetic powder and 1 mL of FF is used) and dried completely. This technique is extremely simple and various biological, inorganic and polymer materials have been successfully transferred into their magnetic derivatives [**14**]. Tea leaves modified by this procedure are presented on **Fig. 3**.

Microwave assisted magnetic modification

Microwave assisted synthesis of magnetic iron oxides particles from ferrous sulfate has been described recently [**15**]. In general, microwave irradiation can accelerate many chemical reactions in organic and inorganic syntheses. In comparison with conventional heating methods, reactions under microwave irradiation have usually higher reaction

rates and the product can be obtained in a shorter period of time.

Extremely simple, one-pot, direct magnetic modification procedure employing just iron(II) salt (e.g., very cheap iron(II) sulfate) at high pH in the presence of the treated material has been developed recently. The suspension was treated in the regular kitchen microwave oven (700-750 W, 2450 MHz) for appropriate time. Submicrometer magnetic iron oxides nano- and microparticles formed during the microwave treatment deposited on the surface of the treated materials in the form of individual particles and their aggregates [**16**].

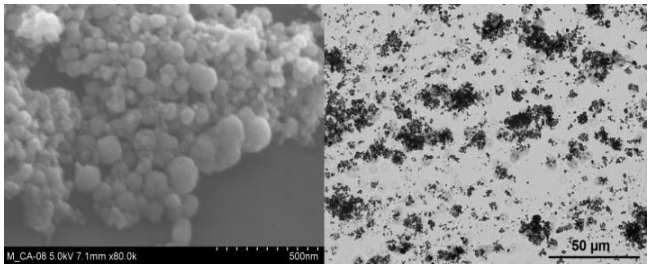

Fig. 4. SEM (left) and optical microscopy (right) images of magnetic iron oxides particles prepared by microwave-assisted synthesis. Reproduced, with permission, from [**18**].

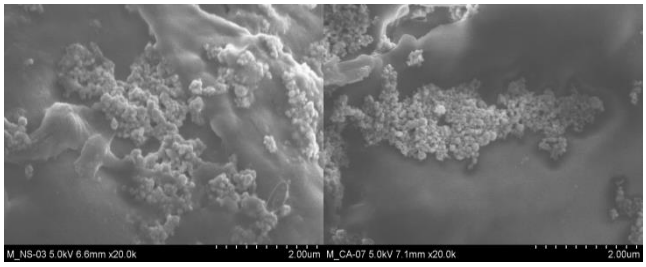

Fig. 5. SEM image of native (left) and chemically treated (right) barley straw magnetically modified with microwave synthesized magnetic iron oxides nano- and microparticles. Reproduced, with permission, from [**18**].

Direct microwave assisted magnetization procedure can be especially used for modification of heat and high pH stable materials. However, in order to enable magnetic modification of also more sensitive materials, an indirect microwave assisted modification has been developed [**17**]. At first, magnetic iron oxides nano- and microparticles (the nanoparticles diameter ranged between ca 25 and 100 nm; during the synthesis, the nanoparticles formed micrometer-sized stable aggregates with the maximum aggregate size ca 20 µm, see **Fig. 4**) have been synthesized from ferrous sulfate at high pH in a microwave oven. After particles washing, materials to be magnetically modified were thoroughly mixed with iron oxides particles suspension and dried completely at slightly increased temperature (e.g., 60º C). Magnetic modification led to the stable deposition of iron oxide nanoparticle aggregates on the surface of the modified material (**Fig. 5**).

Modified indirect magnetization procedure employing microwave synthesized magnetic particles can also be used for magnetic treatment of thermally sensitive materials, e.g., powdered enzymes. Enzyme powders were suspended in liquid media not allowing their solubilization (e.g., saturated ammonium sulfate and highly concentrated polyethylene glycol solutions, ethanol, methanol) and subsequently cross-linked with glutaraldehyde. Magnetic modification using magnetic iron oxides nano- and microparticles prepared by microwave-assisted synthesis was successfully performed at low temperature in a freezer (-20 °C). It can take several days or even weeks to dry magnetic enzyme powder completely [**19**]. Low temperature drying procedure has also been employed for magnetic modification of enzymes immobilized on non-magnetic carriers and for other sensitive biomaterials such as starch grains [**20**].

Mechanochemical magnetic modification

Recently, mechanochemical procedures have been used to synthesize magnetic iron oxides and ferrites nanoparticles [**21**]. Mechanochemistry represents one of several ways of chemical activation. In solid-state mechanochemistry, nonthermal chemical reactions occur because of the deformation and fracture of solids, which are technically induced by milling or grinding of the materials. During this process the mechanical energy induces chemical reactions and phase transformations [**22**].

In the standard mechanochemical synthesis of magnetic composite materials, hydrated ferrous and ferric chlorides were grounded in a mortar at room temperature for 10 min; to avoid agglomeration, the excess of sodium chloride was added to the precursors before grinding. Then, appropriate amount of target nonmagnetic powdered material was added and after thorough mixing the process continued for another 10 min. As the last step, powdered alkaline hydroxide was added and after mixing the grinding continued for 10 min. After finishing the mechanochemical process, the magnetically modified material was thoroughly washed with water. Variety of inorganic and biological materials, including e.g., potato and maize starch grains (**Fig. 6**), pollen grains, powdered lignocellulosic materials and many others has been successfully modified using this procedure [**23**].

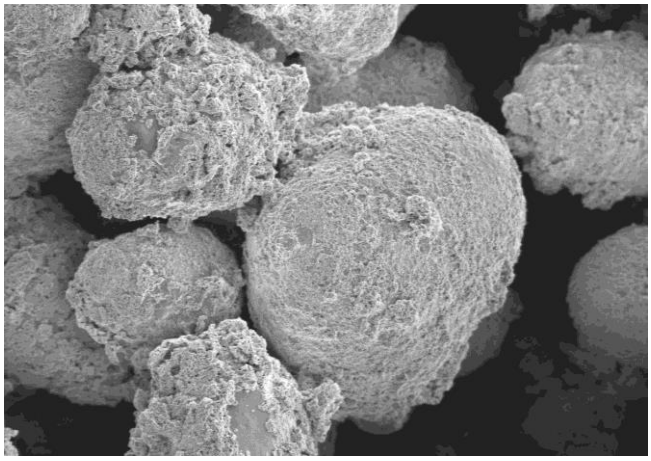

Fig. 6. SEM image of native potato starch magnetically modified using mechanochemical procedure. Reproduced, with permission, from [23].

Magnetically modified biomaterials and their applications

Different types of biological materials have been converted into their magnetic derivatives and subsequently used as adsorbents, carriers, biocatalysts etc. Especially the following materials are of our interest:

1) Individual biopolymers of various origin, such as polysaccharides (e.g., cellulose, chitin, chitosan, alginate, agar, agarose, plant gums), proteins (e.g., casein, keratin, gelatin, ovalbumin, hen egg white) or polyhydroxyalcanoates (e.g., polyhydroxybutyrate)
2) Complex biopolymers, especially lignocellulosic materials of plant origin (e.g., sawdust, straw, spent barley grain, spent coffee grounds)
3) Microbial and microalgae cells, such as baker's yeast (*Saccharomyces cerevisiae*), fodder yeast (*Kluyveromyces marxianus*) or unicellular alga *Chlorella vulgaris*
4) Marine seagrass and marine macroalgae, such as *Posidonia oceanica* (forming so called Neptune balls) or various species of *Sargassum*
5) Inorganic biomaterials, such as egg shells, sheaths of *Leptothrix ochracea* or various diatoms.

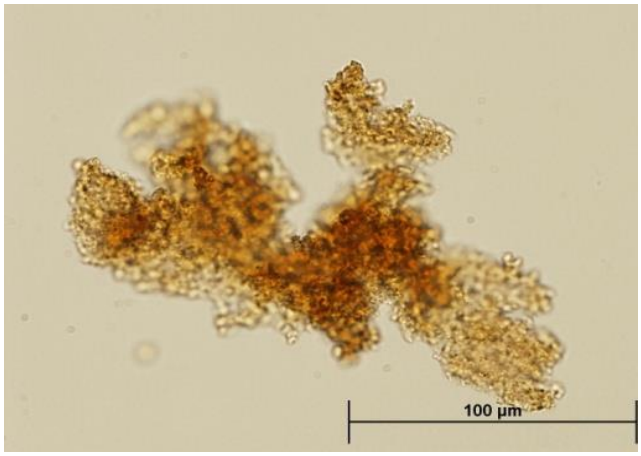

Fig. 7. Optical microscopy image of microwave-synthesized magnetic chitosan microparticles [24]. Reproduced, with permission, from [25].

Applications of magnetically modified biological materials are shortly described in the following section.

1. Chitin and chitosan belong to intensively studied and used polysaccharides. Huge amount of magnetic chitin and chitosan derivatives have been prepared. Recently, an extremely simple, one-pot procedure for magnetic chitosan particles preparation has been developed. In this procedure, chitosan was dissolved in diluted acetic acid solution and then solution of ferrous sulfate was added. Subsequently, solution of sodium hydroxide was added under intensive stirring and the formed brown precipitate was treated in a microwave oven [**24**]. After glutaraldehyde activation, target proteins [**24**] or microbial cells [**25**] can be immobilized. The character of the prepared magnetic chitosan particles is shown in **Fig. 7**.

Magnetic chitin and chitosan derivatives exhibit affinity for specific biologically active compounds, such as hen egg white lysozyme [**26, 27**], lysozyme from the gut of the soft tick *Ornithodoros moubata* [**28**] or plant chitinase from the latex of *Euphorbia characias* [**29**]. Potato (*Solanum tuberosum*) tuber lectin was isolated from tuber extract [**30**] or from potato starch industry waste water; the adsorbed lectin was eluted with glycine/HCl buffer, pH 2.2 and the specific activity of separated lectin increased 27 times during the isolation process [**31**]. Chitin and chitosan binding proteins can be substantially purified in one step using magnetic affinity adsorption [**32**].

Magnetic chitosan can be easily activated by glutaraldehyde and employed as a carrier for enzymes [**24, 33**] and microbial cells [**25**] immobilization. Organic affinity ligands (e.g., reactive textile dyes) have also been successfully immobilized; Ostazin turquoise (a reactive Cu phthalocyanine dye) immobilized on magnetic chitosan or silanized magnetite selectively bound planar organic dyes [**34, 35**] and was used for their magnetic solid phase extraction from water and urine samples [**35-37**].

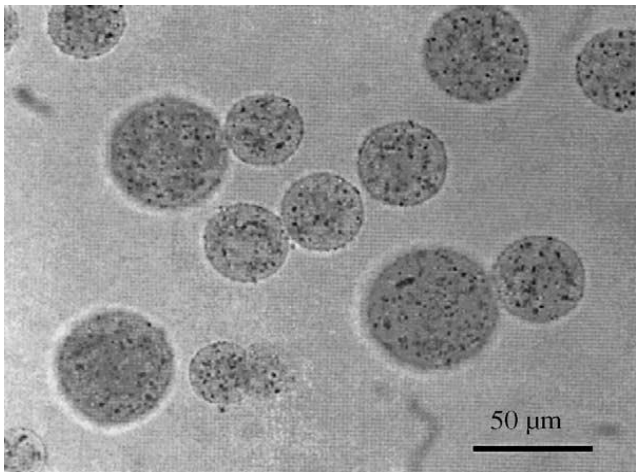

Fig. 8. Optical microscopy image of magnetic alginate microparticles. Reproduced, with permission, from [**40**].

Magnetic cellulose particles in the form of ion exchanger have also been successfully utilized for magnetic ion exchange separation of hen egg white lysozyme directly from native egg white [**38**].

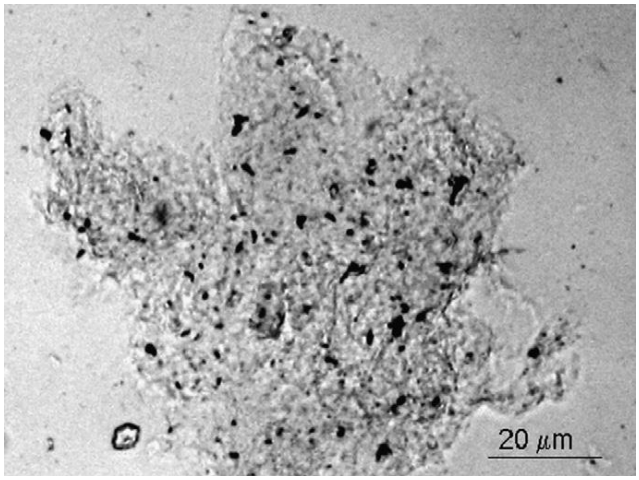

Fig. 9. Optical microscopy image of magnetic ovalbumin microparticles. Reproduced, with permission, from [42].

Magnetic alginate beads have been used for the entrapment of microbial cells [**39**] and as a pseudo affinity adsorbent; spherical magnetic alginate microparticles (25-60 µm in diameter, **Fig. 8**) were prepared using the

microemulsion system, with water-saturated 1-pentanol as the organic phase. The limited solubility of 1-pentanol in water enabled simple removal of the organic solvent from the prepared beads with water solution. The washed alginate microparticles were utilized as magnetic affinity adsorbents for specific purification of alpha-amylases; enzyme activity was eluted by 1.0 M maltose [**40**].

Magnetic porous corn starch was employed as an affinity adsorbent for the efficient and simple scale-up procedure for one-step purification of cyclodextrin glucanotransferase from *Bacillus circulans* culture media; the enzyme purification factor was 19-25 in different batches [**41**].

Simple and low-cost preparation of new magnetic adsorbents from ovalbumin and egg white, based on methanol precipitation and subsequent glutaraldehyde cross-linking has been developed. These adsorbents (**Fig. 9**) were used for preconcentration of two plant lectins from potato (*Solanum tuberosum*) tubers and from wheat (*Triticum* spp.) germs extracts. The adsorbed lectins were eluted with diluted hydrochloric acid. The specific activities of both lectins increased approximately 30–40 times during the preconcentration process [**42**].

Table 1. Comparison of maximum adsorption capacities Q_{max} (mg/g) of magnetically modified plant-based materials for tested dyes.

Dyes	Maximum adsorption capacities of magnetically responsive plant materials (mg/g)					
	Spruce sawdust [45]	Peanut husk [47]	Spent coffee grounds [49]	Spent grain [48]	Spent rooibos [51]	Rye straw [50]
Acridine orange	24.1	71.4	49.3		79.8	42.9
Aniline blue				44.7		
Bismarck brown Y	52.1	95.3	97.8	72.4	119	
Brilliant green					62.4	
Crystal violet	52.4	80.9	36.7	40.2	98.4	
Malachite green			62.9			
Methyl green					117	95.2
Methylene blue					96.5	
Nile blue					142	
Safranin O	25.0	86.1	34.3		128	

A procedure for the determination of proteolytic activity with dyed magnetic gelatine as an insoluble chromolytic substrate has been described; the magnetic nature of the substrate enabled magnetic separation of unhydrolysed substrate from the hydrolysed dyed peptide fragments [**43**]. New magnetic adsorbents for batch isolation and removal of various proteolytic enzymes were prepared by glutaraldehyde cross-linking of bovine, porcine and human erythrocytes in the presence of fine magnetic particles; serine proteinases and proteinases present in various commercial enzyme preparations were efficiently adsorbed on these adsorbents [**44**].

2. Magnetically modified materials of plant origin have been tested as efficient adsorbents of organic and inorganic pollutants. Several magnetic modification procedures have been used, namely ferrofluid treatment for sawdust [**11, 45, 46**], peanut husk [**47**], spent grain [**48**], spent coffee grounds [**49**] or spent tea leaves [**14**], and microwave assisted modification procedure for straw [**18, 50**] or spent rooibos (*Aspalathus linearis*) tea biomass [**51**]. These materials exhibited efficient adsorption of various water soluble dyes (see **Table 1**).

Table 2. Comparison of maximum adsorption capacities Q_{max} (mg/g) of magnetically modified yeast and microalgae cells for tested dyes.

Dyes	Maximum adsorption capacities of magnetically modified yeast and microalgae cells (mg/g)				
	S. cere-visiae [55]	*S. cerevisiae* (*uvarum*) [56]	*K. marxianus [57]*	*S. cerevi-siae* on chitosan [25]	*Ch. vulgaris* [63]
Acridine orange	82.8		62.2		
Amido black 10B		11.6	29.9		
Aniline blue	430	228			258
Bismarck brown Y			75.7		202
Congo red		93.1	49.7		157
Crystal violet	85.9	41.7	42.9	68	42.9
Malachite green	19.6				
Safranin O	90.3	46.6	138.2	111	116
Saturn blue LBRR			33.0		24.2

Wheat grain derived material, namely wheat bran magnetically modified with microwave synthesized iron oxides particles, has been successfully employed for adsorption of uranium [**52**].

Plant derived materials can also be used as low cost, biocompatible carriers for enzyme immobilization. Ferrofluid-modified spent grain was utilized as a low-cost, biocompatible and magnetically responsive carrier for the immobilization of *Candida rugosa* lipase. Several immobilization procedures were tested using both native and poly (ethyleneimine)-modified magnetic spent grain. This material can be a promising low-cost magnetic carrier for enzyme immobilization, applicable e.g. in food and feed technology and biotechnology [**53**].

3. Magnetically modified microbial and microalgae cells have found important applications both as adsorbents of important organic and inorganic pollutants [**54**] and whole-cell biocatalysts. Very simple treatment of baker's, brewer's and fodder yeast cells with ionic magnetic fluids led to the formation of magnetic adsorbents of organic water soluble dyes [**55-58**] (see **Table 2**), heavy metal ions [**59,60**] and strontium ions [**61**]. Magnetically modified *S. cerevisiae* cell walls [**62**] and unicellular alga *Chlorella vulgaris* [**63**] can also be used for the same purpose.

Magnetically modified microbial cells can be utilized as whole cell biocatalysts. Several magnetization procedures have been employed, namely application of acid ferrofluid and acetic acid buffer [**13**] (**Fig. 2**), entrapment of cells in magnetically modified millimeter or micron sized alginate particles [**39**] (**Fig. 10**), covalent binding to magnetic chitosan particles [**25**] (**Fig. 11**) or binding of microwave synthesized magnetic iron oxide nano- and microparticles on the cell surface [**64**] (**Fig. 12**).

Magnetic iron oxides particles, especially those prepared by microwave assisted synthesis, can be efficiently used for magnetic flocculation of microalgae cells, e.g., *Chlorella vulgaris* [**65-68**].

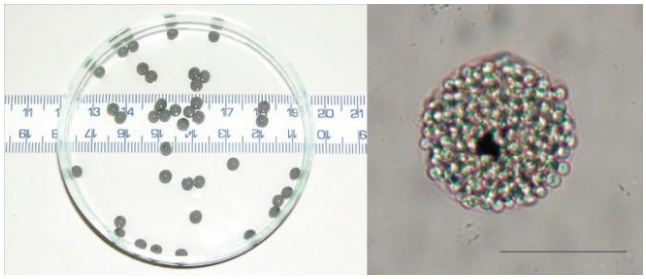

Fig. 10. Magnetically responsive alginate beads containing entrapped *Saccharomyces cerevisiae* cells and magnetite microparticles. Millimeter-sized beads (left) and microbeads (right; the scale bar corresponds to 50 μm). Reproduced, with permission, from [**39**].

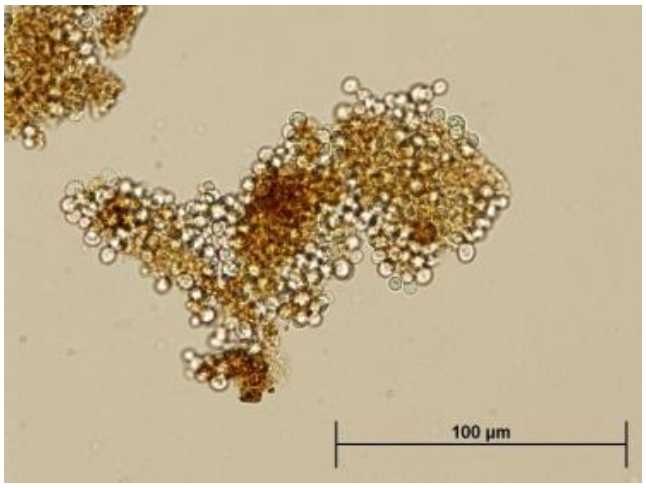

Fig. 11. Optical microscopy image of microwave-synthesized magnetic chitosan microparticles with immobilized *Saccharomyces cerevisiae* cells. Reproduced, with permission, from [**25**].

In order to decompose hydrogen peroxide (a potential chemical sanitizer for use in the food industry), magnetically responsive alginate beads containing entrapped *Saccharomyces cerevisiae* cells and magnetite microparticles (**Fig. 10**) were utilized. Larger beads (2-3 mm in diameter) were prepared by dropping the mixture into calcium chloride solution, while microbeads (the diameter of majority of particles ranged between 50 and 100 μm) were prepared using the water in oil emulsification process. In general, microbeads enabled more efficient hydrogen peroxide decomposition. The biocatalyst was stable; the same catalytic activity was observed after one month storage at 4 °C, and the microbeads could be used at least five times [**39**]. The same catalyst has also been employed for the hydrolysis of sucrose into glucose and fructose (invert sugar) [**69**].

4. Marine seagrass and marine macroalgae represent interesting and valuable biomaterials, often available in huge quantities. Recently, we have prepared magnetic derivatives of *Posidonia oceanica* (forming so called Neptune balls) and *Sargassum horneri*; both materials exhibited high capacity for dyes adsorption (manuscripts in preparation).

5. Biogenic iron oxides formed mainly by *Leptothrix ochracea*, collected from local water streams and subsequently magnetically modified using water-based magnetic fluid have been characterized in detail and used as an inexpensive magnetically responsive adsorbent for the removal of selected organic dyes from aqueous solutions. The observed maximum adsorption capacities ranged between 34.3 and 97.8 mg of dye per 1 g of absorbent [**70**].

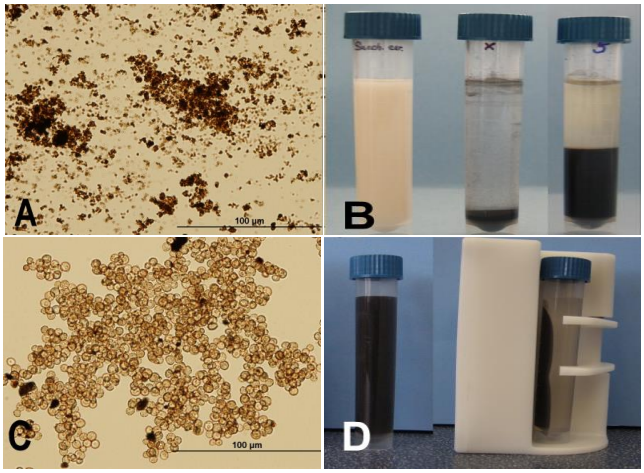

Fig. 12. Optical microscopy of magnetic iron oxide microparticles prepared by microwave-assisted synthesis (A); process of magnetic modification of yeast cells (left tube – *Saccharomyces cerevisiae* cells suspension; middle tube – sedimented iron oxides microparticles for magnetic modification; and right tube – sedimented magnetically modified yeast cells) (B); optical microscopy of *S. cerevisiae* cells modified by iron oxides microparticles (C); magnetic separation of magnetically modified yeast cells (D). Reproduced, with permission, from [**64**].

Conclusion

Different types of progressive materials, among them magnetically responsive nano- and micro(bio)materials, have enormous potential to significantly influence different areas of biosciences, medicine, biotechnology, environmental technology etc., where dozens of extremely important applications, both *in vitro* and *in vivo*, have already been described. It was shown that prepared magnetic (bio)materials can serve not only as adsorbents of diverse inorganic or organic xenobiotics, such as heavy metal ions, radionuclides, water-soluble dyes, endocrine disruptors or drug metabolites highly endangering environment and organisms living in, but also as carriers for immobilization of cells, enzymes and biologically active compounds or as biosensors. Moreover, their application potential is much wider. Due to the presence of magnetic particles, these materials can be successfully employed as contrast agents in MRI or for drug targeting; additional information about their possible utilization can be found in review papers of the authors [**71-86**]. Further progress can be expected particularly in biotechnology and environmental technology, where preparation of cost-effective and biocompatible magnetic particles or (bio) composites is increasingly required. Extremely inexpensive magnetic nanocomposites and microparticles for large scale applications (e.g. separation of biologically active compounds from agricultural wastes and culture media, removal of xenobiotics from wastewater or immobilization

of affinity ligands or biocatalysts) are necessary. Safety and biocompatibility studies of magnetically responsive materials, in particular long-term toxicity studies, have to be carried out. The collaboration of scientists from different fields is necessary. Potential of magnetic nano- and micromaterials will expand in the future.

Acknowledgements

This research was supported by the Grant Agency of the Czech Republic (Projects No. 13-13709S and 14-11516S), by the projects LD14066, LD14075 and LO1305 (Ministry of Education, Youth and Sports of the Czech Republic) and by the COST Actions TD1107 "Biochar as option for sustainable resource management" and MP1206 "Electrospun nano-fibres for bio inspired composite materials and innovative industrial applications".

Reference

1. Safarik, I.; Pospiskova, K.; Horska, K.; Safarikova, M. *Soft Matter*. **2012,** *8*, 5407. **DOI:** 10.1039/C2SM06861C
2. Wei, H.; Wang, E. *Anal. Chem.* **2008,** *80*, 2250. **DOI:** 10.1021/ac702203f
3. Melnikova, L.; Pospiskova, K.; Mitroova, Z.; Kopcansky, P.; Safarik, I. *Microchim. Acta* **2014,** *181*, 295. **DOI:** 10.1007/s00604-013-1105-5
4. Safarik, I.; Horska, K.; Pospiskova, K.; Safarikova, M. *Int. Rev. Chem. Eng.* **2012,** *4*, 346. **ISSN:** 2035-1755
5. Park, J. H.; Im, K. H.; Lee, S. H.; Kim, D. H.; Lee, D. Y.; Lee, Y. K.; Kim, K. M.; Kim, K. N. *J. Magn. Magn. Mater.* **2005,** *293*, 328. **DOI:** 10.1016/j.jmmm.2005.02.027
6. Hughes, S.; Dobson, J.; El Haj, A. J. *J. Biomech.* **2007,** *40*, S96. **DOI:** 10.1016/j.jbiomech.2007.03.002
7. Choi, D.; Fung, A.; Moon, H.; Ho, D.; Chen, Y.; Kan, E.; Rheem, Y.; Yoo, B.; Myung, N. *Biomed. Microdevices* **2007,** *9*, 143. **DOI:** 10.1007/s10544-006-9008-4
8. Bromberg, L.; Chang, E. P.; Alvarez-Lorenzo, C.; Magarinos, B.; Concheiro, A.; Hatton, T. A. *Langmuir* **2010,** *26*, 8829. **DOI:** 10.1021/la904589p
9. Zborowski, M.; Malchesky, P. S.; Jan, T. F.; Hall, G. S. *J. Gen. Microbiol.* **1992,** *138*, 63. **DOI:** 10.1099/00221287-138-1-63
10. Zborowski, M.; Fuh, C. B.; Green, R.; Baldwin, N. J.; Reddy, S.; Douglas, T.; Mann, S.; Chalmers, J. J. *Cytometry* **1996,** *24*, 251. **DOI:** 10.1002/(SICI)1097-0320(19960701)24:3<251::AID-CYTO8>3.0.CO;2-K
11. Safarik, I.; Lunackova, P.; Mosiniewicz-Szablewska, E.; Weyda, F.; Safarikova, M. *Holzforschung* **2007,** *61*, 247. **DOI:** 10.1515/HF.2007.060
12. Azevedo, R. B.; Silva, L. P.; Lemos, A. P. C.; Bao, S. N.; Lacava, Z. G. M.; Safarik, I.; Safarikova, M.; Morais, P. C. *IEEE Trans. Magn.* **2003,** *39*, 2660. **DOI:** 10.1109/TMAG.2003.815547
13. Safarikova, M.; Maderova, Z.; Safarik, I. *Food Res. Int.* **2009,** *42*, 521. **DOI:** 10.1016/j.foodres.2009.01.001
14. Safarik, I.; Horska, K.; Pospiskova, K.; Safarikova, M. *Powder Technol.* **2012,** *229*, 285. **DOI:** 10.1016/j.powtec.2012.06.006
15. Zheng, B. Z.; Zhang, M. H.; Xiao, D.; Jin, Y.; Choi, M. M. F. *Inorg. Mater.* **2010,** *46*, 1106. **DOI:** 10.1134/S0020168510100146
16. Safarik, I.; Horska, K.; Pospiskova, K.; Maderova, Z.; Safarikova, M. *IEEE Trans. Magn.* **2013,** *49*, 213. **DOI:** 10.1109/TMAG.2012.2221686
17. Safarik, I.; Safarikova, M. *Int. J. Mater. Res.* **2014,** *105*, 104. **DOI:** 10.3139/146.111009
18. Baldikova, E.; Politi, D.; Maderova, Z.; Pospiskova, K.; Sidiras, D.; Safarikova, M.; Safarik, I. *J. Sci. Food Agric.* **2015**, in press. **DOI:** 10.3139/146.111009
19. Pospiskova, K.; Safarik, I. *J. Magn. Magn. Mater.* **2015,** *380*, 197. **DOI:** 10.1016/j.jmmm.2014.10.037
20. Pospiskova, K.; Safarik, I. *Mater. Lett.* **2015,** *142*, 184. **DOI:** 10.1016/j.matlet.2014.11.163
21. Lin, C. R.; Chu, Y. M.; Wang, S. C. *Mater. Lett.* **2006,** *60*, 447. **DOI:** 10.1016/j.matlet.2005.09.009
22. Beyer, M. K.; Clausen-Schaumann, H. *Chem. Rev.* **2005,** *105*, 2921. **DOI:** 10.1021/cr030697h
23. Safarik, I.; Horska, K.; Pospiskova, K.; Filip, J.; Safarikova, M. *Mater. Lett.* **2014,** *126*, 202. **DOI:** 10.1016/j.matlet.2014.04.045
24. Pospiskova, K.; Safarik, I. *Carbohydr. Polym.* **2013**, *96*, 545. **DOI:** 10.1016/j.carbpol.2013.04.014
25. Safarik, I.; Pospiskova, K.; Maderova, Z.; Baldikova, E.; Horska, K.; Safarikova, M. *Yeast* **2015**, *32*, 239. **DOI:** 10.1002/yea.3017
26. Safarik, I.; Safarikova, M. *J. Biochem. Biophys. Meth.* **1993,** *27*, 327. **DOI:** 10.1016/0165-022X(93)90013-E
27. Safarik, I. *Biotechnol. Tech.* **1991,** *5*, 111. **DOI:** 10.1007/BF00159981
28. Kopacek, P.; Vogt, R.; Jindrak, L.; Weise, C.; Safarik, I. *Insect Biochem. Molec. Biol.* **1999**, *29*, 989. **DOI:** 10.1016/S0965-1748(99)00075-2
29. Spanò, D.; Pospiskova, K.; Safarik, I.; Pisano, M. B.; Pintus, F.; Floris, G.; Medda, R. *Protein Expr. Purif.* **2015**, *116*, 152. **DOI:** 10.1016/j.pep.2015.08.026
30. Safarikova, M.; Safarik, I. *Biotechnol. Lett.* **2000**, *22*, 941. **DOI:** 10.1023/A: 1005698616574
31. Safarik, I.; Horska, K.; Martinez, L. M.; Safarikova, M. *AIP Conf. Proc.* **2010**, *1311*, 146. **DOI:** 10.1063/1.3530004
32. Safarik, I.; Safarikova, M. *BioMagn. Res. Technol.* **2004**, *2*, 7. **DOI:** 10.1186/1477-044X-2-7
33. Pospiskova, K.; Safarik, I.; Sebela, M.; Kuncova, G. *Microchim. Acta* **2013**, *180*, 311. **DOI:** 10.1007/s00604-012-0932-0
34. Safarik, I. *Water Res.* **1995**, *29*, 101. **DOI:** 10.1016/0043-1354(94)E0110-R
35. Safarik, I.; Safarikova, M. *Water Res.* **2002,** *36*, 196. **DOI:** 10.1016/S0043-1354(01)00243-3
36. Safarikova, M.; Safarik, I. *J. Magn. Magn. Mater.* **1999,** *194*, 108. **DOI:** 10.1016/S0304-8853(98)00566-6
37. Safarikova, M.; Safarik, I. *Eur. Cells Mater.* **2002,** *3* (Suppl. 2), 192. **ISSN:** 1473 -2262
38. Safarik, I.; Sabatkova, Z.; Tokar, O.; Safarikova, M. *Food Technol. Biotechnol.* **2007,** *45*, 355. **ISSN:** 1330-9862
39. Safarik, I.; Sabatkova, Z.; Safarikova, M. *J. Agric. Food Chem.* **2008,** *56*, 7925. **DOI:** 10.1021/jf801354a
40. Safarikova, M.; Roy, I.; Gupta, M. N.; Safarik, I. *J. Biotechnol.* **2003,** *105*, 255. **DOI:** 10.1016/j.jbiotec.2003.07.002
41. Safarikova, M.; Horska, K.; Maderova, Z.; Tonkova, A.; Ivanova-Pashkoulova, V.; Safarik, I. *Biocatal. Biotransformation* **2012,** *30*, 96. **DOI:** 10.3109/10242422.2012.646665
42. Sabatkova, Z.; Safarikova, M.; Safarik, I. *Biochem. Eng. J.* **2008,** *40*, 542. **DOI:** 10.1016/j.bej.2008.02.003
43. Safarikova, M.; Safarik, I. *Biotechnol. Tech.* **1999,** *13*, 621. **DOI:** 10.1023/A:1008930813267
44. Safarik, I.; Safarikova, M. *J. Magn. Magn. Mater.* **2001,** *225*, 169. **DOI:** 10.1016/S0304-8853(00)01247-6
45. Safarik, I.; Safarikova, M.; Weyda, F.; Mosiniewicz-Szablewska, E.; Slawska-Waniewska, A. *J. Magn. Magn. Mater.* **2005,** *293*, 371. **DOI:** 10.1016/j.jmmm.2005.02.033
46. Mosiniewicz-Szablewska, E.; Safarikova, M.; Safarik, I. *J. Phys. D - Appl. Phys.* **2007,** *40*, 6490. **DOI:** 10.1088/0022-3727/40/21/003
47. Safarik, I.; Safarikova, M. *Physics Procedia* **2010,** *9*, 274. **DOI:** 10.1016/j.phpro.2010.11.061
48. Safarik, I.; Horska, K.; Safarikova, M. *J. Cereal Sci.* **2011,** *53*, 78. **DOI:** 10.1016/j.jcs.2010.09.010
49. Safarik, I.; Horska, K.; Svobodova, B.; Safarikova, M. *Eur. Food Res. Technol.* **2012,** *234*, 345.

DOI: 10.1007/s00217-011-1641-3
50. Baldikova, E.; Safarikova, M.; Safarik, I. *J. Magn. Magn. Mater.* **2015,** *380*, 181. **DOI:** 10.1016/j.jmmm.2014.09.003
51. Safarik, I.; Maderova, Z.; Horska, K.; Baldikova, E.; Pospiskova, K.; Safarikova, M. *Bioremed. J.* **2015,** *19*, 183. **DOI:** 10.1080/10889868.2014.979279
52. Wang, H.; Ji, Y.; Tian, Q.; Horska, K.; Shao, X.; Maderova, Z.; Miao, X.; Safarikova, M.; Safarik, I. *Sep. Sci. Technol.* **2014,** *49*, 2534. **DOI:** 10.1080/01496395.2014.926931
53. Pospiskova, K.; Safarik, I. *J. Sci. Food Agric.* **2013,** *93*, 1598. **DOI:** 10.1002/jsfa.593
54. Safarik, I.; Safarikova, M. *China Particuol.* **2007,** *5*, 19. **DOI:** 10.1016/j.cpart.2006.12.003
55. Safarik, I.; Ptackova, L.; Safarikova, M. *Eur. Cells Mater.* **2002**, *3* (Suppl. 2), 52. **ISSN:** 1473 -2262
56. Safarikova, M.; Ptackova, L.; Kibrikova, I.; Safarik, I. *Chemosphere* **2005**, *59*, 831. **DOI:** 10.1016/j.chemosphere.2004.10.062
57. Safarik, I.; Rego, L. F. T.; Borovska, M.; Mosiniewicz-Szablewska, E.; Weyda, F.; Safarikova, M. *Enzyme Microb. Technol.* **2007**, *40*, 1551. **DOI:** 10.1016/j.enzmictec.2006.10.034
58. Mosiniewicz-Szablewska, E.; Safarikova, M.; Safarik, I. *J. Nanosci. Nanotechnol.* **2010,** *10*, 2531. **DOI:** 10.1166/jnn.2010.1394
59. Yavuz, H.; Denizli, A.; Gungunes, H.; Safarikova, M.; Safarik, I. *Sep. Purif. Technol.* **2006,** *52*, 253. **DOI:** 10.1016/j.seppur.2006.05.001
60. Uzun, L.; Saglam, N.; Safarikova, M.; Safarik, I.; Denizli, A. *Sep. Sci. Technol.* **2011,** *46*, 1045. **DOI:** 10.1080/01496395.2010.541400
61. Ji, Y. Q.; Hu, Y. T.; Tian, Q.; Shao, X. Z.; Li, J. Y.; Safarikova, M.; Safarik, I. *Sep. Sci. Technol.* **2010,** *45*, 1499. **DOI:** 10.1080/01496391003705664
62. Patzak, M.; Dostalek, P.; Fogarty, R. V.; Safarik, I.; Tobin, J. M. *Biotechnol. Tech.* **1997,** *11*, 483. **DOI:** 10.1023/A:1018453814472
63. Safarikova, M.; Pona, B. M. R.; Mosiniewicz-Szablewska, E.; Weyda, F.; Safarik, I. *Fresenius Environ. Bull.* **2008,** *17*, 486. **ISSN:** 10184619
64. Pospiskova, K.; Prochazkova, G.; Safarik, I. *Lett. Appl. Microbiol.* **2013,** *56*, 456. **DOI:** 10.1111/lam.12069
65. Prochazkova, G.; Safarik, I.; Branyik, T. *Procedia Eng.* **2012,** *42*, 1778. **DOI:** 10.1016/j.proeng.2012.07.572
66. Prochazkova, G.; Safarik, I.; Branyik, T. *Bioresour. Technol.* **2013,** *130*, 472. **DOI:** 10.1016/j.biortech.2012.12.060
67. Prochazkova, G.; Podolova, N.; Safarik, I.; Zachleder, V.; Branyik, T. *Colloid Surf. B - Biointerfaces* **2013,** *112*, 213. **DOI:** 10.1016/j.colsurfb.2013.07.053
68. Safarik, I.; Prochazkova, G.; Pospiskova, K.; Branyik, T. *Crit. Rev. Biotechnol.* **2015**, in press. **DOI:** 10.3109/07388551.2015.1064085
69. Safarik, I.; Sabatkova, Z.; Safarikova, M. *J. Magn. Magn. Mater.* **2009,** *321*, 1478. **DOI:** 10.1016/j.jmmm.2009.02.056
70. Safarik, I.; Filip, J.; Horska, K.; Nowakova, M.; Tucek, J.; Safarikova, M.; Hashimoto, H.; Takada, J.; Zboril, R. *Int. J. Environ. Sci. Technol.* **2015,** *12*, 673. **DOI:** 10.1007/s13762-013-0455-1
71. Safarik, I.; Safarikova, M. *Chem. Listy.* **1994,** *88*, 464. **ISSN:** 1213-7103
72. Safarik, I.; Safarikova, M.; Forsythe, S. J. *J. Appl. Bacteriol.* **1995,** *78*, 575. **ISSN**: 0021-8847
73. Safarik, I.; Safarikova, M. In *Scientific and Clinical Applications of Magnetic Carriers.* Hafeli, U.; Schutt, W.; Teller, J.; Zborowski, M., Eds. Plenum Press: New York and London, **1997**, pp. 323. **ISBN:** 978-0-306-45687-9
74. Safarik, I.; Safarikova, M. *J. Chromatogr. B* **1999**, *722*, 33. **DOI:** 10.1016/S0378-4347(98)00338-7
75. Safarikova, M.; Safarik, I. *Magn. Electr. Sep.* **2001**, *10*, 223. **DOI:** 10.1155/2001/57434
76. Safarik, I.; Safarikova, M. *Mon. Chem.* **2002**, *133*, 737. **DOI:** 10.1007/s007060200047
77. Safarik, I.; Safarikova, M. In *Bioactive Egg Compounds.* Huopalahti, R.; López-Fandiño, R.; Anton, M.; Schade, R., Eds. **2007**, pp. 275. **ISBN:** 978-3-540-37883-9
78. Safarik, I.; Safarikova, M. *Solid State Phenomena* **2009**, *151*, 88. **DOI:** 10.4028/www.scientific.net/SSP.151.88
79. Safarik, I.; Safarikova, M. *Chem. Papers* **2009**, *63*, 497. **DOI:** 10.2478/s11696-009-0054-2
80. Mosiniewicz-Szablewska, E.; Safarikova, M.; Safarik, I. In *Applied Physics in the 21st Century (Horizons in World Physics, Volume 266).* Valencia, R. P., Ed. Nova Publishers: **2010**, pp. 301. **ISBN:** 978-1-60876-074-9
81. Safarik, I.; Safarikova, M. *Hacettepe J. Biol. Chem.* **2010,** *38*, 1. **ISSN:** 1303 5002
82. Safarik, I.; Horska, K.; Safarikova, M. In *Microbial Biosorption of Metals.* Kotrba, P.; Mackova, M.; Macek, T., Eds. Springer **2011**; pp. 301. **ISBN:** 978-94-007-0442-8
83. Safarik, I.; Safarikova, M. In *Magnetic Nanoparticles: From Fabrication to Biomedical and Clinical Applications.* Thanh, N. T. K., Ed. CRC Press/Taylor and Francis: **2012**, pp. 215. **ISBN:** 9781439869321
84. Safarik, I.; Horska, K.; Pospiskova, K.; Safarikova, M. *Anal. Bioanal. Chem.* **2012,** *404*, 1257. **DOI:** 10.1007/s00216-012-6056-x
85. Safarik, I.; Maderova, Z.; Pospiskova, K.; Horska, K.; Safarikova, M. In *Cell Surface Engineering: Fabrication of Functional Nanoshells.* Fakhrullin, R. F.; Choi, I.; Lvov, Y. M., Eds. RSC: **2014**, pp. 185. **ISBN:** 978-1-84973-902-3
86. Safarik, I.; Maderova, Z.; Pospiskova, K.; Baldikova, E.; Horska, K.; Safarikova, M. *Yeast* **2015,** *32*, 227. **DOI:** 10.1002/yea.3043

.

5.1.2 Příprava magnetických kompozitních materiálů pro studenty SŠ

Cílem této publikace je seznámení studentů středních škol s problematikou perspektivních a rychle se rozvíjejících odvětví biotechnologie, nanotechnologie a materiálové vědy. Prostřednictvím jednoduchých a na vybavení nenáročných experimentů si studenti mohou vyzkoušet dvě zajímavé techniky magnetické modifikace původně diamagnetických materiálů a jejich následné využití jako adsorbentů organických barviv (zde zvolena krystalová violeť, nicméně lze použít jakékoliv jiné dostupné). Pozornost je zaměřena především na magnetizaci odpadních a vedlejších produktů zemědělského (sláma, piliny) a potravinářského (kávová sedlina, použitý čaj) průmyslu, které by pro školní laboratoř mohly být snadno získatelné a zároveň poukazovaly na možnost jejich dalšího zužitkování. Úspěšnost magnetické modifikace mohou studenti ověřit jednak reakcí na permanentní NdFeB magnet, jednak Perlsovo barvením, které selektivně reaguje se syntetizovanými Fe(III) ionty na povrchu modifikovaného materiálu.

Příloha 2:

Příprava magnetických kompozitních materiálů - experimenty pro studenty středních škol

Baldíková E, Pospíšková K, Maděrová Z, Šafaříková M, Šafařík I

Chem. listy 110, **2016**, 64-68

VÝUKA CHEMIE

PŘÍPRAVA MAGNETICKÝCH KOMPOZITNÍCH MATERIÁLŮ: EXPERIMENTY PRO STUDENTY STŘEDNÍCH ŠKOL

EVA BALDÍKOVÁ[a], KRISTÝNA POSPÍŠKOVÁ[b], ZDEŇKA MADĚROVÁ[a], MIRKA ŠAFAŘÍKOVÁ[a] a IVO ŠAFAŘÍK[a,b]

[a] *Oddělení nanobiotechnologie, Ústav nanobiologie a strukturní biologie CVGZ, AV ČR, Na Sádkách 7, 370 05 České Budějovice,* [b] *Regionální centrum pokročilých technologií a materiálů, Univerzita Palackého, Šlechtitelů 27, 783 71 Olomouc*
baldie@email.cz

Došlo 23.3.15, přepracováno 26.6.15, přijato 8.7.15.

Klíčová slova: magnetická modifikace, magnetické kompozitní materiály, magnetická separace, mikrovlnná syntéza, mechanochemická syntéza

Úvod

Materiálový výzkum je zaměřen na vývoj nových materiálů se zlepšenými nebo zcela novými vlastnostmi. Jednou z významných skupin jsou také tzv. kompozitní materiály, jež jsou charakteristické tím, že přídavek (příměs) malého množství jednoho materiálu zásadním způsobem ovlivní vlastnosti dominantního materiálu (např. tvrdost, odolnost proti tahu nebo ohybu, elektrickou vodivost apod.)[1].

Magnetické kompozity představují velice atraktivní skupinu materiálů využitelných v nejrůznějších oblastech přírodních a technických věd, mimo jiné v biotechnologiích, biochemii, mikrobiologii, medicíně, analytické chemii či environmentálních technologiích. Jedná se o materiály složené ze dvou či více složek s různými fyzikálními a chemickými vlastnostmi[2], kde jednu z komponent tvoří nano- nebo mikročástice tvořené z feromagnetických či ferimagnetických materiálů, zatímco další složky magnetických kompozitů, zastoupené např. biopolymery, syntetickými polymery, rostlinnou a mikrobiální biomasou či anorganickými látkami, mají diamagnetické (nemagnetické) vlastnosti[3–6].

Obecně lze říci, že z hlediska potenciálního využití v biotechnologiích a environmentálních technologiích mají velký význam magnetické kompozity připravené z levných a snadno dostupných materiálů, především rostlinného a mikrobiálního původu, které mnohdy představují odpadní produkty v zemědělském či potravinářském průmyslu. Úspěšná magnetická modifikace již byla provedena např. u pšeničné slámy[7], použitých čajových lístků[8], použitých mletých pražených kávových zrn[9], pilin[10], mletých arašídových slupek[11], pomerančových slupek[12], rostlinného pylu[13] a mnoha dalších.

Magnetické kompozitní materiály jsou ceněny hlavně pro své magnetické vlastnosti, díky kterým mohou být snadno, rychle a selektivně odděleny z prostředí prostřednictvím vnějšího magnetického pole (vytvořeného vhodným magnetickým separátorem)[14]. Izolace je tak možná nejen z roztoků, ale také ze suspenzních systémů jako je krev, lymfa a ostatní tělní tekutiny, kostní dřeň, kultivační média, tekuté potraviny, environmentální vzorky a jiné[15]. Rovněž jsou zaznamenány případy úspěšné magnetické separace z extrémně viskózních roztoků, např. vaječného bílku[16].

Naprostá většina materiálů vyskytujících se v živé přírodě (vyjma erytrocytů, hemoglobinu a magnetotaktických bakterií) vykazuje diamagnetické vlastnosti a jejich magnetická susceptibilita (fyzikální veličina popisující chování materiálu ve vnějším magnetickém poli) je menší než nula. Konverzi z nemagnetického prekurzoru do magnetické formy lze však provést mnoha způsoby. Ty nejjednodušší z nich jsou zpravidla založeny na navázání magnetických nano- či mikročástic oxidů železa, zejména magnetitu (Fe_3O_4), maghemitu (γ-Fe_2O_3) nebo jejich směsí na povrch či do porézní struktury modifikovaného materiálu. Jednou z „klasických“ technik přípravy magnetických kompozitních materiálů je modifikace magnetickou kapalinou stabilizovanou kyselinou chloristou[11,17]. Tato procedura je sama o sobě velmi jednoduchá, nicméně složitost přípravy magnetické kapaliny, či její vysoká pořizovací cena vedly k hledání nových a lacinějších technik. Různé způsoby magnetické modifikace aktivního uhlí byly shrnuty v přehledném článku[18].

V posledních desetiletích se v různých oblastech chemie využívá mikrovlnné záření, a to nejen pro urychlení chemických reakcí a procesů[19,20], ale také pro přípravu nových sloučenin a materiálů[21,22]. Kromě nákladných systémů umožňujících práci s mikrovlnným zářením za definovaných podmínek je možné pro vybrané syntézy (např. příprava magnetických oxidů železa) použít i standardní kuchyňskou mikrovlnnou troubu[23]. Takto připravené magnetické částice lze využít pro extrémně jednoduchou přípravu magnetických kompozitů, která spočívá ve smíchání suspenze magnetických částic se zvoleným práškovým diamagnetickým materiálem a následným vysušením; tento proces vede ke stabilní fixaci částic na povrchu magnetizovaného materiálu[23].

Zajímavou, i když ne příliš častou metodou přípravy různých typů látek a materiálů je mechanochemická syntéza. Typickým znakem je, že reakce probíhají za účasti

mechanické energie dodané reaktantům např. v kulovém mlýnu nebo při tření materiálů tloučkem v třecí misce[24,25].

Uvedené procesy magnetické modifikace diamagnetických materiálů, společně s dalšími modifikačními metodami, jsou vhodné pro úpravu snadno dostupných a levných materiálů vykazujících zajímavé vlastnosti, které jsou využitelné jako adsorbenty nebo nosiče v environmentálních technologiích a biotechnologiích (např. potenciální adsorbenty pro nejrůznější anorganická i organická xenobiotika; afinitní materiály; nosiče enzymů, lektinů a dalších biologicky aktivních látek; nebo biokatalyzátory). Využití magnetických nano- a mikročástic a magnetických kompozitů může být však mnohem širší, dle jejich typu a velikosti, např. i v medicíně jako kontrastní látky při zobrazení magnetickou rezonancí, nosiče při cíleném transportu látek v těle nebo při léčbě rakoviny (hypertermie)[3,26].

Cílem této stručné práce je ukázat učitelům a studentům středních škol potenciál magnetických (bio)kompozitů a současně také jejich snadnou přípravu, kterou lze provést v běžně vybavené chemické laboratoři, zejména v chemických zájmových kroužcích.

Experimentální část

Pomůcky

K přípravě magnetických kompozitních materiálů je nutné mít k dispozici předvážky, váženky, lžičku, kádinky, skleněné tyčinky, kapátko, odměrný válec, pH papírky, standardní kuchyňskou mikrovlnnou troubu (cca 700 W, 2450 MHz), pipetu (nejlépe o objemu 5 ml), horkovzdušnou sušárnu, třecí misku a tlouček, ochranné brýle a rukavice, střičku, (kávový) mlýnek, čajové sítko (s oky cca 0,5–1 mm × 0,5–1 mm), permanentní NdFeB magnet (např. válec o průměru cca 20–25 mm a výšce 10 mm, dostupný od firem prodávajících magnetické materiály). Pro adsorpční test jsou zapotřebí analytické váhy a uzavíratelné plastové či skleněné zkumavky.

Chemikálie

K mikrovlnné syntéze[23,27] magnetických oxidů železa je zapotřebí $FeSO_4 . 7 H_2O$, zatímco mechanochemická syntéza vychází z prekurzorů $FeCl_2 . 4 H_2O$, $FeCl_3 . 6 H_2O$ a NaCl, jenž slouží jako prostředí zabraňující agregaci modifikovaných materiálů[28]. Obě modifikace vyžadují alkalizaci pomocí NaOH, popř. KOH. Pro adsorpční experimenty je vhodné např. organické barvivo krystalová violeť.

Nemagnetické materiály pro experimenty

Pro magnetizační experimenty lze zvolit nejrůznější běžně dostupné nemagnetické materiály, např. použitý čaj, kávovou sedlinu, piliny, pšeničnou slámu, arašídové slupky či mláto. V případě čaje, kávy a mláta je však nutné důkladné promývání horkou vodou, dokud nedojde k odstranění hnědého zbarvení a prachového podílu. Materiály o větší velikosti částic je nutné rozemlít (např. kávovým mlýnkem) a prosít přes síto o velikosti ok cca 0,5–1 mm × 0,5–1 mm.

Modifikace diamagnetických materiálů magnetickými částicemi oxidů železa připravenými mikrovlnnou syntézou[23]

Pro přípravu magnetických částic je rozpuštěn 1 g $FeSO_4 . 7 H_2O$ ve 100 ml vody (v 600 až 800 ml kádince). Za stálého míchání skleněnou tyčinkou je pomalu přikapáván 1 mol l^{-1} hydroxid sodný, dokud nedojde ke zvýšení pH na hodnotu 12 (sledováno indikátorovým pH papírkem) a vytvoření tmavé sraženiny hydroxidů železa. K této suspenzi je přidáno dalších 100 ml vody, neboť během následného varu dojde k odparu tohoto objemu (suspenze nesmí vyschnout). Kádinka je vložena do běžné kuchyňské mikrovlnné trouby (700 W, 2450 MHz), kde je suspenze podrobena působení mikrovlnného záření po dobu 10 min při maximálním výkonu. Vzniklé magnetické částice jsou promývány vodou pomocí magnetického separátoru, dokud hodnota pH nedosáhne neutrální hodnoty (opakovaný proces separace částic ke stěně kádinky pomocí magnetu, odlití vody a rozmíchání částic ve vodě v nepřítomnosti magnetu). Promytá suspenze magnetických částic je ponechána sedimentovat v odměrném válci po dobu 24 h; poté je poměr upraven na jeden díl kompletně sedimentovaných částic a čtyři díly vody.

Dalším krokem při přípravě magnetického kompozitu je smíchání 1 g práškového diamagnetického materiálu se 2 ml předem řádně rozmíchané suspenze magnetických částic. Směs materiálu a částic musí být důkladně promíchána skleněnou tyčinkou nebo špachtlí a následně sušena při 60 °C po dobu nejméně 24 h. Pokud není k dispozici vhodná sušárna, je možno materiál vysušit pomocí infralampy. Důkladné vysušení je nezbytné pro získání stabilního magnetického kompozitního materiálu.

Mechanochemická magnetická modifikace diamagnetických materiálů[28]

Směs anorganických solí v poměru 1,35 g $FeCl_3 . 6 H_2O$, 0,50 g $FeCl_2 . 4 H_2O$ a 4 g NaCl je v třecí misce důkladně a velkou silou třena pomocí tloučku po dobu 10 min. V průběhu tření dojde ke vzniku mazlavého materiálu, proto je během tohoto procesu vhodné seškrabávat materiál ze stěn. Posléze je přidán 1 g zvoleného nemagnetického materiálu pro modifikaci a pokračuje se v dalším desetiminutovém důkladném tření. Celá směs je alkalizována (při práci s hydroxidem je nutné chránit oči ochrannými brýlemi) přisypáním 1,22 g práškového (připraveného předem v jiné třecí misce) hydroxidu sodného (či draselného) a pokračuje se v tření po dobu 10 min, během kterého dojde ke změně zbarvení materiálu na hnědé až černé. Výsledný materiál je několikrát promyt vodou, aby byl zbaven všech rozpustných složek a volných

oxidů železa; při promývání je připravený magnetický materiál zachycován pomocí silného magnetu. Magnetický kompozit lze uchovávat buď ve vodné suspenzi, nebo ve vysušeném stavu.

Optická mikroskopie magnetických biokompozitů

Přítomnost oxidů železa obsahujících Fe^{3+} ionty je možno na modifikovaném materiálu prokázat Perlsovou reakcí[29]; materiál je na několik minut ponořen do čerstvě připraveného činidla (směs stejných objemů 4% roztoků hexakyanoželeznatanu draselného, známého jako „žlutá krevní sůl“, a kyseliny chlorovodíkové) a po následném oplachu vodou je připraven mikroskopický preparát.

Alternativní postup barvení pozorovaného materiálu (přímo v mikroskopickém preparátu) spočívá v opatrném nakápnutí čerstvého činidla ke hraně krycího sklíčka; dochází k pomalé difuzi činidla do prostoru mezi sklíčky.

Jednoduchý adsorpční experiment

Do uzavíratelných plastových zkumavek je naváženo 40 mg magnetického materiálu (např. magnetická pšeničná sláma), ke kterému je přidáno 6,6 ml vody a 0,4 ml roztoku krystalové violeti (1 mg ml^{-1}; při práci s organickými barvivy je nutné používat ochranné rukavice). Poměry lze měnit dle uvážení a účinnosti adsorpce jednotlivých sorbentů. Na rotátoru je suspenze pomalu promíchávána po dobu 10, 30 a 60 min. Pokud není k dispozici rotátor, lze pro demonstrativní účely zkumavky občas protřepat v ruce. Poté je zkumavka přiložena k magnetu, aby došlo k separaci magnetického sorbentu, a tím bylo umožněno vizuální srovnání poklesu intenzity zbarvení roztoku oproti původnímu srovnávacímu roztoku barviva neobsahujícího sorbent.

Výsledky a diskuse

V tomto článku jsou prezentovány dva jednoduché postupy pro magnetickou modifikaci vhodných diamagnetických materiálů. V prvním případě jsou pro modifikaci použity nano- a mikročástice magnetitu (primárně vznikají nanočástice o rozměrech cca 40–60 nm, které tvoří agregáty o rozměrech cca 0,1–20 μm; viz obr. 1). V průběhu syntézy dochází k následujícím chemickým reakcím[27]:

$$Fe^{2+} + 2\ OH^- \rightarrow Fe(OH)_2$$

$$3\ Fe(OH)_2 + ½\ O_2 \xrightarrow{\text{mikrovlny}} Fe_3O_4 + 3\ H_2O$$

Během mikrovlnného záření dochází k částečné oxidaci Fe^{2+} na Fe^{3+} a následné syntéze magnetitu.

Mechanochemická modifikace mláta je v jednotlivých krocích znázorněna na obr. 2. V průběhu syntézy dochází v prvé fázi k tvorbě magnetitu[28]:

$$2\ Fe^{3+} + Fe^{2+} + 8\ OH^- \rightarrow Fe_3O_4 + 4\ H_2O$$

Vzhledem k reakčním podmínkám (přítomnost atmosférického kyslíku, produkce tepla v průběhu tření) dochá-

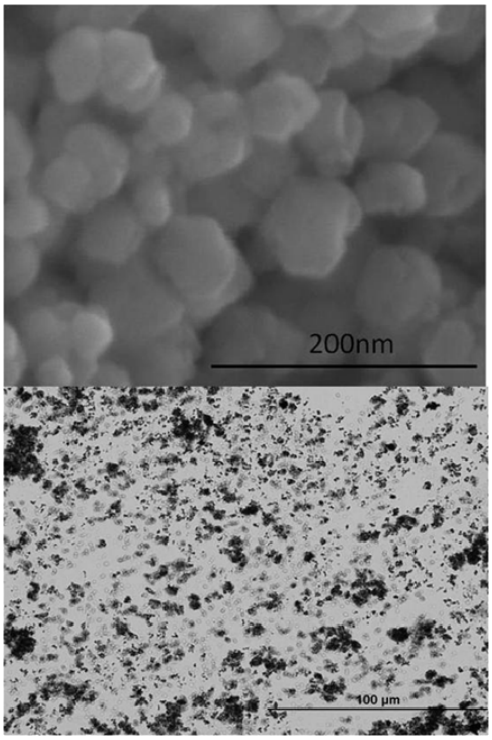

Obr. 1. **SEM (skenovací elektronová mikroskopie) magnetických nanočástic oxidů železa připravených mikrovlnnou syntézou (nahoře) a optická mikroskopie vzniklých agregátů částic (dole)**

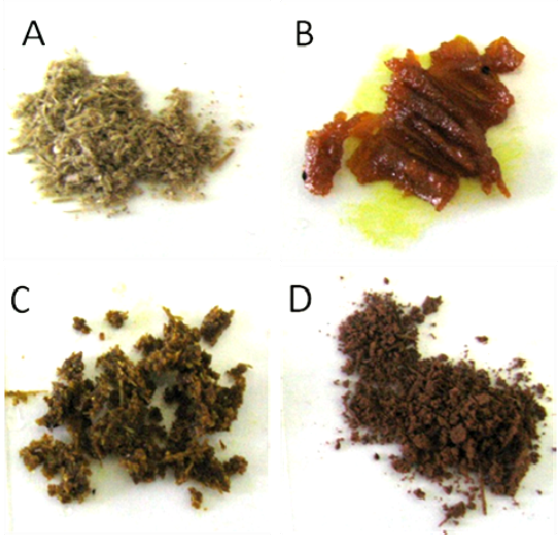

Obr. 2. **Změna zbarvení modifikovaného materiálu během jednotlivých kroků mechanochemické modifikace (A – původní promyté mláto, B – rozetřené soli železa po důkladném tření, C – rozetřené soli železa s mlátem, D – výsledné vysušené magneticky modifikované mláto).** Barevná fotografie je k dispozici v online verzi článku

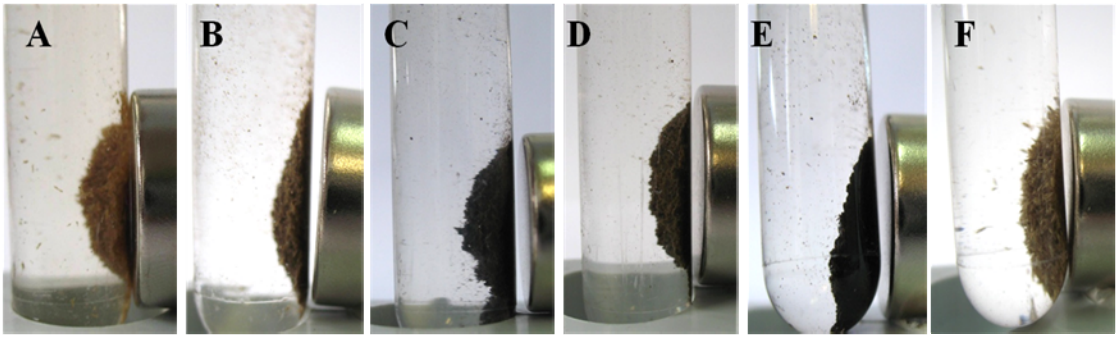

Obr. 3. **Magnetická separace magnetických biokompozitů modifikovaných částicemi oxidů železa připravenými mikrovlnnou syntézou (A – sláma, B – mláto, C – čaj, D – arašídové slupky, E – káva, F – piliny).** Barevná fotografie je k dispozici v online verzi článku

zí následně k přeměně magnetitu na maghemit (γ-Fe_2O_3):

$$4\ Fe_3O_4 + O_2 \rightarrow 6\ \gamma\text{-}Fe_2O_3$$

Úspěšnost magnetické modifikace původně nemagnetických materiálů lze ověřit jejich reakcí na přítomnost permanentního magnetu (viz obr. 3).

Vzhled původních a magneticky modifikovaných materiálů lze pozorovat optickým mikroskopem. Povrch magneticky modifikovaných materiálů (např. pilin) je pokryt magnetickými částicemi oxidů železa a jejich shluky, v mikroskopu viditelné jako tmavé plochy (viz obr. 4). Perlsovo barvení[29] umožňuje detegovat oxidy železa obsahující Fe^{3+} ionty na základě jejich reakce s hexakyanoželeznatanem draselným v kyselém prostředí. V průběhu reakce s kyselinou chlorovodíkovou dochází k uvolnění železitých iontů z přítomných částic oxidů železa, které okamžitě s druhým činidlem vytváří modrý nerozpustný komplex hexakyanoželeznatanu železitého (Berlínskou modř). V mikroskopickém preparátu jsou tedy magnetické kompozity zbarvené modře (obr. 4). V případě nakápnutí čerstvého činidla ke hraně krycího sklíčka mikroskopického preparátu je možné pozorovat postupné zabarvování magneticky modifikovaného materiálu do modra.

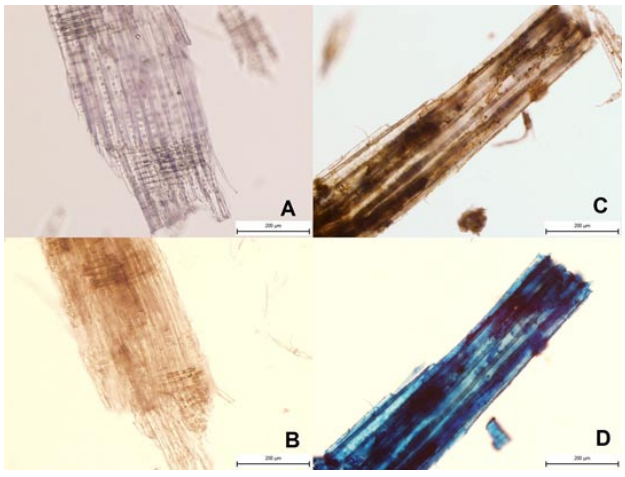

Obr. 4. **Optická mikroskopie nemagnetických pilin (A), nemagnetických pilin po barvení Perlsovou metodou (B), magneticky modifikovaných pilin pomocí částic oxidů železa připravených mikrovlnnou syntézou (C) a magnetických pilin po barvení Perlsovou metodou (D).** Barevná fotografie je k dispozici v online verzi článku

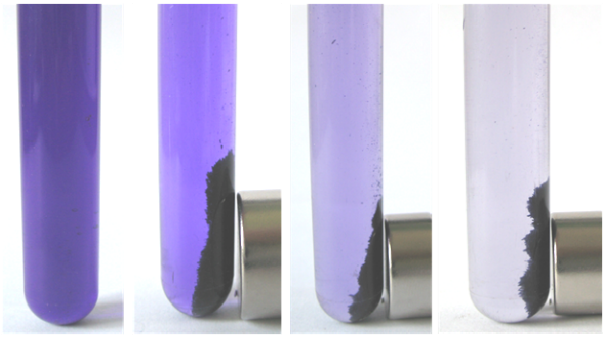

Obr. 5. **Adsorpce krystalové violeti na magneticky modifikovanou pšeničnou slámu v čase 0, 10, 30 a 60 min.** Barevná fotografie je k dispozici v online verzi článku

Magnetické adsorbenty, připravené modifikací lacinějších (často odpadních) biologických materiálů, mohou být využity pro odstranění významných kontaminantů životního prostředí, např. iontů těžkých kovů, radionuklidů nebo různých organických látek[4]. Významnou kontaminaci vodních zdrojů způsobují i organická barviva; možnost jejich odstranění je demonstrována jednoduchým experimentem (obr. 5).

Závěr

Tento příspěvek, zaměřený na vybrané metody magnetické modifikace původně nemagnetických materiálů,

umožňuje studentům a pedagogům nahlédnutí do zajímavé, velmi perspektivní a rychle se rozvíjející oblasti (nano) biotechnologií. Prostřednictvím netradičních, přitom jednoduchých a časově nenáročných experimentů mohou učitelé chemie motivovat své žáky k aktivnímu zájmu o tento obor. Studenti se mohou seznámit s jednou z metod přípravy magnetických částic, které následně využijí pro magnetickou modifikaci snadno dostupných levných materiálů. S připravenými kompozitními materiály lze snadno manipulovat v suspenzích pomocí magnetu. Jednoduchá ukázka jejich aplikace představuje také jednu z možností zužitkování nevšedních či odpadních materiálů z průmyslu nebo zemědělství.

Práce byla podpořena Grantovou agenturou České republiky (projekt 13-13709S). Autoři děkují vyučujícím chemie (Mgr. Marek Navrátil – Gymnázium Olomouc-Hejčín a PaedDr. Antonín Pospíšek – ZŠ Nedvědova, Olomouc, v důchodu) za cennou pomoc.

LITERATURA

1. Thomas V., Namdeo M., Mohan Y. M., Bajpai S. K., Bajpai M.: J. Macromol. Sci. Part A: Pure Appl. Chem. *45*, 107 (2008).
2. Safarik I., Horska K., Pospiskova K., Maderova Z., Safarikova M.: IEEE Trans Magn. *49*, 213 (2013).
3. Safarik I., Safarikova M.: Chem. Pap. *63*, 497 (2009).
4. Safarik I., Horska K., Safarikova M., v knize: *Microbial Biosorption of Metals* (Kotrba P., Mackova M., Macek T., eds.), str. 301. Springer, Dodrecht 2011.
5. Babayan V., Kazantseva N. E., Moučka R., Vilčáková J., Saha P:. Chem. Listy *108*, 4 (2014).
6. Sopčák T., Bureš R., Strečková M., Faberová M.: Chem. Listy *105*, 427 (2011).
7. Tian Y., Wu M., Lin X., Huang P., Huang Y.: J. Hazard. Mater. *193*, 10 (2011).
8. Yeo S. Y., Choi S., Dien V., Sow-Peh Y. K., Qi G., Hatton T. A., Doyle P. S., Thio B. J. R.: Plos One *8*, Article No. e66648 (2013).
9. Safarik I., Horska K., Svobodova B., Safarikova M.: Eur. Food Res.Technol. *234*, 345 (2012).
10. Cheng Z., Gao Z., Ma W., Sun Q., Wang B., Wang X.: Chem. Eng. J. *209*, 451 (2012).
11. Safarik I., Safarikova M.: Phys. Procedia *9*, 274 (2010).
12. Gupta V. K., Nayak A.: Chem. Eng. J. *180*, 81 (2012).
13. Thio B. J. R., Clark K. K., Keller A. A.: J. Hazard. Mater. *194*, 53 (2011).
14. Safarik I., Safarikova M.: J. Chromatogr. B *722*, 33 (1999).
15. Mosiniewicz-Szablewska E., Safarikova M., Safarik I., v knize: *Applied Physics in the 21st Century* (Valencia R. P., ed.), str. 301. Nova Science Publishers, Hauppauge, NY 2010.
16. Safarik I., Sabatkova Z., Tokar O., Safarikova M.: Food Technol. Biotechnol. *45*, 355 (2007).
17. Safarik I., Horska K., Safarikova M.: J. Cereal Sci. *53*, 78 (2011).
18. Safarik I., Horska K., Pospiskova K., Safarikova M.: Int. Rev. Chem. Eng. *4*, 346 (2012).
19. Halko R., Hutto M.: Chem. Listy *101*, 649 (2007).
20. Šauliová J.: Chem. Listy *96*, 761 (2002).
21. Larhed M., Olofsson K. (ed.): *Microwave Methods in Organic Synthesis*. Springer, Berlin 2006.
22. Horikoshi S., Serpone N. (ed.): *Microwaves in Nanoparticle Synthesis: Fundamentals and Applications*. Wiley, Weinheim 2013.
23. Safarik I., Safarikova M.: Int. J. Mater. Res. *105*, 104 (2014).
24. Balaz P., Achimovicova M., Balaz M., Billik P., Cherkezova-Zheleva Z., Manuel Criado J., Delogu F., Dutkova E., Gaffet E., Jose Gotor F., Kumar R., Mitov I., Rojac T., Senna M., Streletskii A., Wieczorek-Ciurowa K.: Chem. Soc. Rev. *42*, 7571 (2013).
25. Balaz P., Balaz M., Bujnakova Z.: Chem. Eng. Technol. *37*, 747 (2014).
26. Dutz S., Clement J. H., Eberbeck D., Gelbrich T. Hergt R., Mueller R., Wotschadlo J., Zeisberger M.: J. Magn. Magn. Mater. *321*, 1501 (2009).
27. Zheng B. Z., Zhang M. H., Xiao D., Jin Y., Choi M. M. F.: Inorg. Mater. *46*, 1106 (2010).
28. Safarik I., Horska K., Pospiskova K., Filip J., Safarikova M.: Mater. Lett. *126*, 202 (2014).
29. Safarik I., Horska K., Svobodova B., Safarikova M.: Eur. Food Res. Technol. *234*, 345 (2012).

E. Baldíková[a], K. Pospíšková[b], Z. Maděrová[a], M. Šafaříková[a], and I. Šafařík[a,b] *([a] Department of Nanobiotechnology, Institute of Nanobiology and Structural Biology of GCRC, Academy of Sciences of the Czech Republic, Ceske Budejovice, [b] Palacky University, Olomouc):*

Preparation of Magnetic Composite Materials: Experiments for Secondary School Students

Selected methods of magnetic modification of the originally non-magnetic materials are presented to show the importance of new materials and technologies for secondary school students and teachers. Through innovative, simple, smart and rapid experiments, chemistry teachers can motivate their students to foster an active interest in this field. The magnetic composite materials prepared can easily be manipulated in the suspensions with a magnet and used for, e.g., the removal of organic dyes.

5.1.3 Magnetická modifikace buněk

Prokaryotické a eukaryotické organismy mohou interagovat s nano- i mikročásticemi tvořenými nejrůznějšími prvky a sloučeninami, např. zlatem, stříbrem, paladiem, oxidy železa, uhličitanem vápenatým, fosforečnanem lantanitým, silikou apod. Přítomnost těchto částic byla pozorována jak na povrchu buněčné stěny, tak v protoplasmě či intracelulárních organelách, aniž by došlo ke snížení životaschopnosti buněk. Po vhodné modifikaci vykazují mikrooganismy nejrůznější přídavné vlastnosti.

Magnetické částice lokalizované na/v mikroorganismech umožňují nejen selektivní separaci či cílený transport, ale také vytvářejí negativní kontrast při zobrazení magnetickou rezonancí. Magneticky značené buňky tak nacházejí široké uplatnění v různých oblastech věd, a proto je problematika magnetické modifikace buněk obzvláště důležitá.

Tato knižní kapitola shrnuje publikované metody přípravy magnetických derivátů mikrobiálních buněk, a to od těch běžnějších (přímé navázání magnetických oxidů železa na povrch buněčné stěny, zabudování do magnetických nosičů či zesítění) až po ty méně časté (modifikace pomocí kvantových teček, magnetolipozómů či magnetoferritinu). Rozsáhlá část je věnována také specifickým interakcím s imunomagnetickými částicemi či magnetickými částicemi s naimobilizovanou biologicky aktivní látkou. Každá technika magnetické modifikace je vždy doprovázena nejen konkrétními příklady magnetizace vybraných buněk (bakterií, cyanobakterií, kvasinek, mikrořas, kmenových buněk, lymfocytů, nádorotvorných buněk apod), ale také obsahuje informaci o jejich následné aplikaci.

Příloha 3:

Magnetic modification of cells

Safarik I, Pospiskova K, Baldikova E, Maderova Z, Safarikova M

In: *Applications of NanoBioMaterials*, Volume II:

Engineering of NanoBioMaterials (Grumezescu, A., ed.), Elsevier: US, **2016**, pp 145 – 181

CHAPTER

Magnetic modification of cells

5

Ivo Safarik[1,2], Kristyna Pospiskova[2], Eva Baldikova[1], Zdenka Maderova[1] and Mirka Safarikova[1]

[1]Department of Nanobiotechnology, Institute of Nanobiology and Structural Biology of GCRC, Ceske Budejovice, Czech Republic [2]Regional Centre of Advanced Technologies and Materials, Palacky University, Olomouc, Czech Republic

5.1 INTRODUCTION

Different types of prokaryotic and eukaryotic cells exhibiting a wide variety of morphologies and sizes can interact with a wide range of nano- and microparticles made of diverse materials, such as gold, silver, palladium, iron oxides, calcium phosphate, calcium carbonate, carbon nanotubes, lanthanide phosphate, silica, titania, etc. (Fakhrullin and Lvov, 2012; Park et al., 2014). The modified cells can maintain their viability; the presence of foreign material on their surfaces, in protoplasm or in intracellular organelles can provide additional functionalities. Cells modified using various procedures can be employed as new therapeutic agents, efficient systems for high-resolution imaging, whole-cell biosensors, whole-cell biocatalysts, applied in toxicity microscreening devices and also as efficient adsorbents of different types of organic and inorganic xenobiotics; in addition, magnetically modified cells can be rapidly and selectively separated from complex mixtures (Fakhrullin and Lvov, 2012; Safarik et al., 2012; Safarik and Safarikova, 2007; Safarik et al., 2014; Safarik et al., 2015a, Brian et al., 2015).

Modification of cells with magnetic nano- and microparticles is exceptionally important and magnetically modified cells have been used in many applications. This review chapter focuses on the detailed description of various procedures and materials used to prepare magnetically responsive prokaryotic and eukaryotic cells from their diamagnetic precursors. Naturally occurring magnetically responsive cells, such as magnetotactic bacteria synthesizing intracellular biogenic magnetic nanoparticles (based either on magnetite [Fe_3O_4] or greigite [Fe_3S_4]) (Schüler, 2007) and magnetotactic algae (De Araujo et al., 1986), as well as genetically engineered magnetotactic cells will not be covered here.

Engineering of Nanobiomaterials. DOI: http://dx.doi.org/10.1016/B978-0-323-41532-3.00005-1

5.2 MAGNETIC MODIFICATION OF CELLS

The magnetization of originally diamagnetic prokaryotic and eukaryotic cells is usually performed by the attachment of magnetic nano- or microparticles on the cell surface; during endocytosis and related processes magnetic particles can be internalized into protoplasm. Alternatively, magnetic molecular labels or paramagnetic ions can be employed for cell-magnetic modification, as well as cell immobilization to magnetic carriers or entrapment to magnetically responsive polymers and gels (Safarik et al., 2014).

The modified cells can be arbitrarily divided into two large groups, namely cells with cell walls (prokaryotes and some eukaryotes) and cells covered by cell membrane (mammalian cells). The structure, biochemical composition, and physical properties of the cell surface play an important role in the process of magnetic (nano)material deposition and their spatial arrangement.

Several expressions can be found in the literature to describe the preparation of magnetically modified cells. The term "decorated cells" generally describes the cells covered with a high amount of nanoparticles (NPs), in some cases also in several layers; the particles usually do not cross the cell membrane or cell wall. On the contrary, target cells can be magnetically labeled just by a single (or only a few) magnetically responsive particle(s) attached to the cell wall or membrane. However, the term "magnetic modification" also represents the situation when magnetic NPs cross the cell membrane/wall and enter the cytoplasm or a periplasmic space. The terms "magnetically modified cells" or "magnetically responsive cells" will be applied throughout this chapter. The common characteristics of all magnetically modified cells are their specific interactions with an external magnetic field (Safarik et al., 2014).

Magnetic nano- and microparticles used as cells magnetic labels exhibit several types of responses to an external magnetic field, namely the possibility of their selective separation, targeting and localization, heat generation (which is caused by magnetic particles subjected to a high-frequency alternating magnetic field), increase of a negative T_2 contrast during magnetic resonance imaging (MRI) or great increase of apparent viscosity of magnetorheological fluids when subjected to a magnetic field. In addition, magnetic iron oxide(s) NPs can exhibit peroxidase-like activity (Safarik et al., 2014; Xie et al., 2012).

An absolute majority of prokaryotic and eukaryotic cells is diamagnetic. When an ability to respond to an external magnetic field should be added, several basic procedures can be utilized for the modification of the cell surface, such as the non-specific attachment of magnetic NPs (e.g., by the magnetic fluid treatment) (Safarikova et al., 2005), by binding of maghemite or magnetite particles on the cell surface (Dauer and Dunlop, 1991; Pospiskova et al., 2013), using layer-by-layer polyelectrolyte nanocoating (Fakhrullin and Lvov, 2012), by covalent immobilization of magnetic particles on the cell surface or vice versa (Ivanova et al., 2011), by specific interactions with immunomagnetic nano- and

microparticles (Safarik and Safarikova, 1999) or magnetoliposomes (Ito et al., 2004), etc. In general, magnetic properties of the modifiers (labels) are caused by the presence of nano- or microparticles of magnetic iron oxides, namely magnetite (Fe_3O_4) or maghemite (γ-Fe_2O_3) or their mixtures; in some cases also ferrite particles (Fortin et al., 2008; Liu et al., 2009a), chromium dioxide particles (Hughes et al., 2007), nickel (Choi et al., 2007) or metallic cobalt (Bromberg et al., 2010) have been employed for specific purposes. Alternatively, magnetic labels are formed by paramagnetic cations (Zborowski et al., 1992) or by (magneto)ferritin (Zborowski et al., 1995; Zborowski et al., 1996). The attached magnetic labels usually do not have a negative effect on the viability and phenotype alternation of modified cells. It should be taken into account that in specific cases the surface-bound magnetic particles can be internalized by the treated cells and will appear in protoplasm. Magnetic iron oxide particles prepared by different routes (e.g., combustion synthesis versus co-precipitation ones) can exhibit various effects on the treated cells (Bojin and Paunescu, 2015); also magnetic particles' surface modification (coating, stabilization) can dramatically influence the magnetic particles' biocompatibility (Bromberg et al., 2010). Interestingly, it has been demonstrated recently that the addition of magnetic iron oxide NPs in composite nanofibrous films (scaffolds) used to bind mammalian cells could induce a significantly higher proliferation rate and faster differentiation of specific cells, such as osteoblasts (Li et al., 2014).

As already mentioned, there are two general procedures to prepare magnetically modified cells. The first method is based on the modification of the cell surface (either cell wall or cellular membrane) with magnetic labels (modifiers) in order to obtain hybrid systems suitable for simple magnetic separation and enrichment, and for specific applications (e.g., construction of biosensors or application as xenobiotics adsorbents). In the second method the main aim is to deliver magnetic labels inside the cells in order to enable their MRI or histology detection, creation of potential agents for targeted drug and gene delivery, or to study intracellular processes. In fact, in some cases simple deposition of magnetic labels on the cell surface is followed by the labels' uptake into the cytoplasm via endocytosis and related processes. Cell membranes enable uptake of surface-bound particles, as well as particles present in the vicinity of the modified cell. The basic process is endocytosis via enclosure by the cell's membrane; this is divided into two steps, membrane invagination and particle wrapping. Pinocytosis (fluid endocytosis) is a mode of endocytosis in which small particles are transferred into the cell, forming an invagination, and then suspended within small vesicles which subsequently fuse with lysozomes. Phagocytosis is a specific form of endocytosis involving the vesicular internalization of solids such as bacteria. Receptor-mediated endocytosis, also called clathrin-dependent endocytosis, is a process by which cells absorb molecules by the inward budding of plasma membrane vesicles containing proteins with receptor sites specific to the molecules or particles being absorbed (Doherty and McMahon, 2009; Li et al., 2012; Kettler et al., 2014).

The individual magnetic modification procedures of both prokaryotic and eukaryotic cells, leading to surface or intracellularly modified derivatives, will be described in more detail below.

5.2.1 INTERACTION OF TARGET CELLS WITH NAKED AND SURFACE-STABILIZED MAGNETIC NANO- AND MICROPARTICLES

Diverse types of magnetic iron oxide microparticles, as well as ionically and sterically stabilized magnetic NPs (magnetic fluids), have been used for magnetic cell modification. In the simplest way, perchloric acid-stabilized magnetic fluid was mixed with baker's or brewer's yeast cells washed with and suspended in acetate buffer, pH 4.6 or in glycine−HCl buffer, pH 2.2; alternatively, tetramethylammonium-hydroxide-stabilized magnetic fluid was utilized for baker's yeast cell modification in 0.1 M glycin−NaOH buffer, pH l0.6. After a short time period magnetic particles precipitated on the cell surface (Figure 5.1). The different physiological state of the yeast cells can lead to various magnetic modifications; using dormant yeast cells only surface-modified cells were obtained, while magnetic modification of actively growing cells led to the accumulation of magnetic modifier in the periplasmic space (Azevedo et al., 2003). After washing, the magnetically modified cells were applied as whole-cell biocatalysts for hydrogen peroxide degradation or sucrose hydrolysis. Alternatively, the modified cells were heated in a boiling water bath to kill the cells, resulting in the formation of a stable adsorbent for the removal of selected organic and inorganic xenobiotics (Safarikova et al., 2009; Safarikova et al., 2005; Yavuz et al., 2006; Uzun et al., 2011; Safarik et al., 2002).

An alternative procedure was used when working with dried *Kluyveromyces fragilis* (fodder yeast) and *Chlorella vulgaris* cells. The cells were thoroughly washed several times with 0.1 M acetic acid to remove a substantial portion of soluble macromolecules which otherwise caused spontaneous precipitation of magnetic fluid. After washing and suspending the cells in acetic acid solution the addition of perchloric acid-stabilized magnetic fluid resulted in the formation of magnetically modified yeast and algae cells (see Figure 5.2) (Safarik et al., 2007; Safarikova et al., 2008). The same magnetic fluid was successfully employed for magnetic modification of selected diatoms or chrysomonads (*Diadesmis gallica*, *Mallomonas kalinae*); in this case magnetic modification can be performed in methanol (Kratosova et al., 2013).

Another procedure was based on the attachment of submicron, acicular maghemite particles on the yeast cells; the binding occurred irrespective of the solution pH and surface charge and was essentially irreversible (Dauer and Dunlop, 1991). Also magnetite microparticles were utilized to capture bacterial cells; cell adsorption was best in the pH range 3−6 (in the absence of calcium and magnesium ions), but the pH range was extended up to pH 10 in the presence of these two cations (MacRae and Evans, 1983).

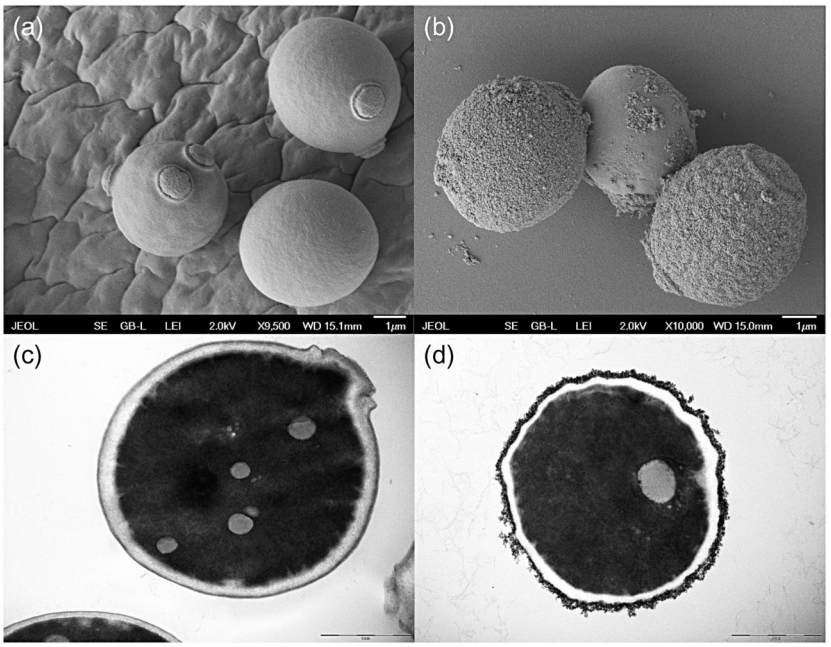

FIGURE 5.1

(a) Scanning electron microscope (SEM) image of native *Saccharomyces cerevisiae* cells. (b) SEM image of ferrofluid-modified *S. cerevisiae* cells, showing attached magnetic nanoparticles and their aggregates on the cell surface. (c) Transmission electron microscope (TEM) image of a native *S. cerevisiae* cell. (d) TEM image of a ferrofluid-modified *S. cerevisiae* cell with attached magnetic iron oxide nanoparticles on the cell wall. Bars correspond to 1 μm. Magnetic modification of dormant cells was performed using perchloric acid-stabilized magnetic fluid as described previously (Safarikova et al. (2009)).

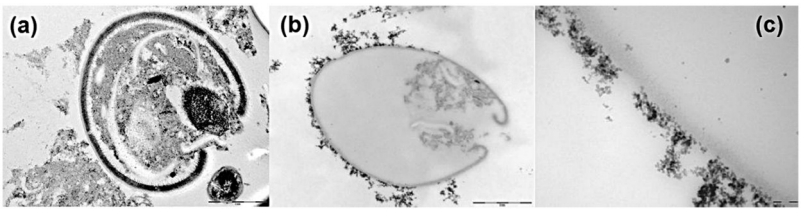

FIGURE 5.2

Transmission electron microscopy of dried *Chlorella vulgaris* cell ((a), bar line is 1 μm) and magnetic fluid modified *Chlorella* cell ((b, c), bar lines are 2 μm and 200 nm, respectively).

Reproduced, with permission, from Safarikova et al. (2008).

Algae in water were separated by using a superconducting high-gradient magnet after magnetization of algae by means of attaching the colloidal particles of hydrous iron(III) oxide. It was found that the percentage of recovery of algae depends on the added amount of iron oxide particles. The percentage of recovery was also found to reach almost 100% when the very small amount of particles was added to the algae suspension. These results demonstrated the feasibility of the magnetic separation of algae with no addition of polymer modifier (Takeda et al., 2000). Alternatively, magnetite particles in combination with aluminum sulfate (a flocculant) were employed for the magnetization and separation of *Anabaena* and *Aphanizomenon* cells (Bitton et al., 1975), while magnetite particles combined with ferric chloride were used for magnetization and subsequent separation of *Scenedesmus obliquus* cells (Yadidia et al., 1977).

An extremely simple procedure for the magnetic modification of yeast and algae cells, based on the use of microwave-synthesized magnetic iron oxide nano- and microparticles, has been developed recently. Two very cheap starting chemicals are needed (ferrous sulfate heptahydrate and sodium or potassium hydroxide); after their mixing and formation of mixed iron hydroxide precipitate the suspension underwent microwave treatment (a regular kitchen microwave oven can be used successfully) and microparticles of magnetic iron oxides formed (Pospiskova et al., 2013; Zheng et al., 2010). Mixing of magnetic particles with algae cell (*Chlorella vulgaris*) and yeast cell (*Saccharomyces cerevisiae*) suspensions caused cell flocculation and magnetically responsive cell aggregates (usually ca. 100−300 μm in diameter) were formed (see Figure 5.3) (Pospiskova et al., 2013; Prochazkova et al., 2013).

Diatoms have been magnetically labeled with human serum albumin (HSA)-coated iron oxide NPs, prepared from oleic acid/oleylamine-coated NPs; subsequently the NPs were surface-exchanged with dopamine and added to an aqueous solution of HSA, where the protein molecules were adsorbed onto the particle surface to grant them good aqueous stability. Diatoms were mixed with the modified particles in phosphate-buffered saline at room temperature for 2 h. Multiple amine groups on the surface of the magnetic NPs ensured their partial positive charge, making them appropriate to interact with negatively charged cell surfaces (Todd et al., 2014).

Alternatively, *Chlorella* sp. cells were magnetized after simple mixing with magnetic iron oxide NPs modified with chitosan. It was also shown that magnetic NPs can enter the cells; the internalization of NPs may proceed through a passive uptake or adhesive interaction (Toh et al., 2014a, 2014b).

Biopolymer-stabilized magnetic NPs can be utilized for intracellular magnetic modification of target cells in order to enable their localization via MRI. MRI is currently the most commonly used, noninvasive and repetitive imaging of biological structures in living organisms providing many advantages, such as excellent spatial resolution and independence on radioactive isotopes. Due to the fact that stem-cell-based therapies are currently under intensive clinical investigation, it is necessary to monitor the time course, migration, and distribution of stem cells following their transplantation into patients in order to provide critical

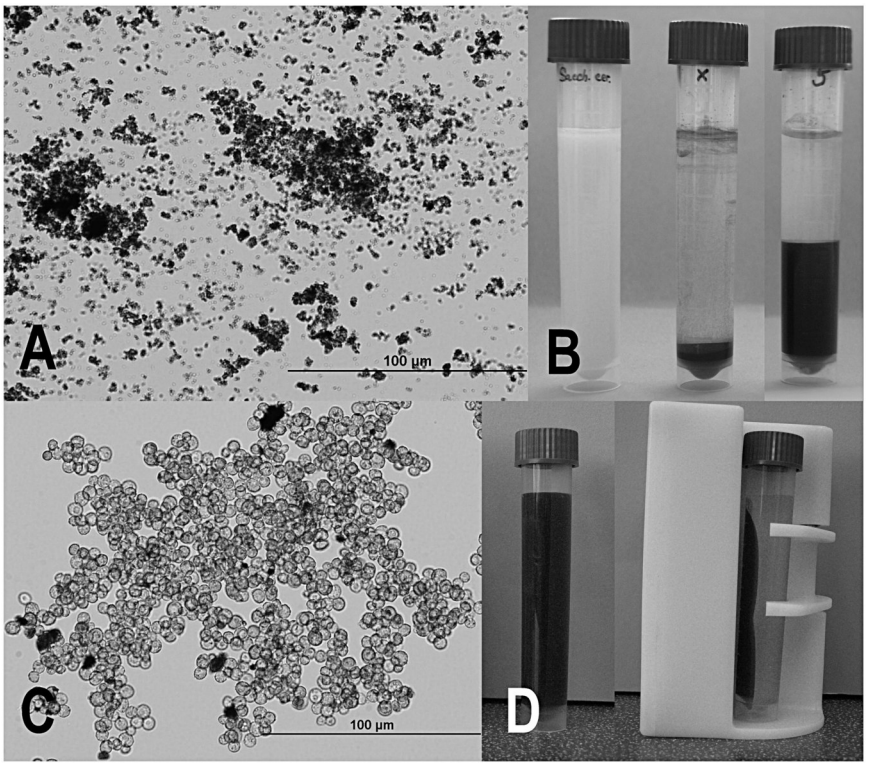

FIGURE 5.3

Optical microscopy of magnetic iron oxides microparticles prepared by microwave assisted synthesis (a); process of magnetic modification of yeast cells (left tube—*S. cerevisiae* cells suspension; center tube—sedimented iron oxides microparticles for magnetic modification; right tube—sedimented magnetically modified yeast cells) (b); optical microscopy of *S. cerevisiae* cells modified by iron oxide microparticles (c); magnetic separation of magnetically modified yeast cells (d).

Reproduced, with permission, from Pospiskova et al. (2013).

information for optimizing treatment regimens; preloading the cells with superparamagnetic iron oxide nanoparticles (SPIONs) enables their tracking using MRI. In recent decades, numerous studies focusing on the use of different contrast agents (CAs) for cell labeling and MRI tracking have been published. SPIONs have become the most preferred CA, especially because of their high relaxivities, biocompatibility, biodegradability, and possible control of magnetic properties through the size of cores and type of coating surface (Liu and Frank, 2009; Gutova et al., 2013; Jendelova et al., 2004).

Magnetic CAs need to be optimized or modified to have an appropriate surface layer that not only binds to cellular membranes, but also induces

internalization of the particles into the cytoplasm (Bulte et al., 2004). Different iron oxide NPs coated by dextran were used, especially CAs for MRI based on dextran-coated iron oxide NPs which can be taken up by cells during cultivation by endocytosis. Dendrimer-encapsulated superparamagnetic iron oxides, as well as NPs coated with lipids or proteins, have also been utilized for magnetic labeling and *in vivo* tracking of mammalian cells (Jendelova et al., 2003; Sykova and Jendelova, 2005; Bulte et al., 2004).

Labeling of the target mammalian cells can be performed in several ways. As can be seen from Table 5.1, the most often used technique is incubation of cells with the magnetic NP-based CAs *in vitro*. Internalization of CAs into cells is caused by either endocytosis or passive uptake by cell. Cells such as macrophages can be labeled *in vivo* by introducing the CA into the bloodstream, with the uptake of the CA occurring by phagocytosis (Cunningham et al., 2005). Nevertheless, another method, specifically electroporation (Wang and Cuschieri, 2013), has been reported recently; in comparison with "classical" incubation fast labeling can be achieved. Magnetic labeling of cancer cells has been successfully used during magnetic fluid hyperthermia (Ito et al., 2006; Latorre and Rinaldi, 2009). Typical examples of labeled cells containing intracellularly localized magnetic iron oxides are shown in Figure 5.4.

Under appropriate conditions red blood cells (RBCs) can be separated magnetically (Owen, 1978). Alternatively, the RBCs were modified with aminated and carboxylated core-shell magnetic NPs; it was shown that only aminated NPs could modify the RBCs and their adsorption interaction was caused by electrostatic attraction between the positively charged amino groups on the particles and the abundant sialic acid groups on the outer surface of RBCs (Mai et al., 2013). Also, SPIONs were used for RBC modification; for loading, the RBC's membrane was opened by swelling under hypo-osmotic conditions and subsequently resealed. SPIONs could be loaded into RBCs in a concentration sufficient to obtain strong contrast enhancement in MRI (Brahler et al., 2006).

5.2.2 MAGNETOFECTION

Magnetic cell labeling has also been employed during the magnetofection process. Magnetofection is a simple and highly efficient transfection method that uses magnetic fields to concentrate magnetic particles containing nucleic acid into the target cells. Magnetofection is based on three steps: formulating a magnetic vector, its addition to the medium covering cultured cells, and applying a magnetic field in order to direct the vector towards the target cells. The simplest approach to forming magnetic derivatives of nucleic acids employs magnetic nanocomposites covered with charged biocompatible polymers which enable formation of ionic complexes with nucleic acids. Magnetofection can be performed with viral and synthetic nucleic acid vectors, and can be used to overexpress nucleic acids or to silence endogenous gene expression. It can improve the efficacy of nucleic acid delivery by concentrating and/or retaining an applied vector dose both in primary cells in culture as well as in explanted tissue specimens and in living

Table 5.1 Magnetic Intracellular Labeling of Different Cell Types

Targeted Cells	Magnetic Particles	Magnetization Process	Other Notes	Loading Assessment	References
Human mesenchymal stem cells	Dex(U)SPIONs:	Incubation C + MP in presence of TA	Without TA endosomal incorporation very low	Prussian blue staining	Frank et al., 2002
Mouse T-cells	Feridex	PLL		MRI	
Rat oligodendrocyte progenitor (CG-4)	MION-46L	PLUS/Lipofectamine	Cellular viability and proliferation unaffected		
Human cervical carcinoma					
Human promonocytic cell line THP-1	CarboxyDexSPIONs:	Incubation C + MP for 5 days	Threshold detection using 3D FIESTA	ICP-MS susceptometry technique	Heyn et al., 2005
	SHU 555A			RMM method	
Bone marrow stromal cells	dexSPIONs:	Incubation C + MP for 72 h	Cells remain viable, MP inside the cells,	Prussian Blue staining	Jendelova et al., 2004
pEGFP-C1-transfected mouse embryonic stem cells	Endorem		*In vivo* MR tracking	TEM Histological staining MRI	
Rat C6 glioma cells	SPIONs coated with aminosilane, dextran, PVA or starch	Incubation C + MP at 37 °C and 5% CO_2 with and without PLL overnight	Dextran, PVA and starch internalized even when complexed with PLL (low uptake capacity)	Prussian Blue staining Optical microscope MRI	Mamani et al., 2012
Rat C6 glioma cells	PEI-SPIONs	Incubation C + MP for 12 h at 37 °C in 5% CO_2	*In vivo* monitoring, MP $<$ 100 nm, viability $>$93.5%	MRI	Liao et al., 2013
Rat C6 glioma cells	dexSPIONs conjugated with human EGF	Incubation of dexSPIONs-EGF by shaking for 1 h at 20 °C	*In vitro* and *in vivo* imaging No toxic influence on cell viability and proliferation	TEM Reflected laser scanning Immunogold labeling MRI	Shevtsov et al., 2014
Human lymphocytes 9L rat gliosarcoma cells	PS-Dex(U)SPIONs: Feridex	Incubation C + MP + protamine sulfate at 37 °C and 5% CO_2 overnight	Cell division and viability unaltered, $>$95% labeled, *ex vivo* experiment (rat brain), MP size 80–150 nm	Prussian Blue staining UV-VIS spectrophotometer MRI	Rad et al., 2007

(*Continued*)

Table 5.1 Magnetic Intracellular Labeling of Different Cell Types *Continued*

Targeted Cells	Magnetic Particles	Magnetization Process	Other Notes	Loading Assessment	References
Human lymphocytes	Dex(U)SPIONs Endorem Feridex	Incubation C + MP for 30 s, 2, 4, and 6 h	Labeling efficiency optimal at 4 h Fe incubation, T2 signal in cell incubated > 2 h	MRI	Sipe et al., 1999
LacZ-transfected mouse neural stem cell line C17.2	Dex(U)SPIONs	Magnetoelectroporation	Various condition 75–400 V, 0.3–30 ms *In vivo* MR tracking (mouse)	Prussian blue staining Antidextran staining	Walczak et al., 2005
Bone marrow rat and human mesenchymal stem cells	Feridex			Histochemistry MRI	
Rat bone marrow mesenchymal stem cells	3-Aminopropyl triethoxysilane-modified Fe_2O_3 nanoparticles	Incubation C + MP for 24 h at 37 °C and 5% CO_2	99% of the particles in cell cytoplasm, cells viable MP size 10–15 nm, *in vivo* MR tracking	Prussian blue staining MRI	Hua et al., 2015
Rat bone marrow mesenchymal stem cells	SPIOs	Incubation C + MP for 24 h	No significant difference in cell viability during 7 days at 0–100 μg/mL SPIO, *in vivo* experiment (rat)	Prussian blue staining High-power field microscopy	Zhao et al., 2014
Pancreatic cancer cells	BSA-SPIONs	Incubation C + BSA-SPIONs-mAb conjugates at 37 °C, 5% CO_2 for 24 h	BSA-SPIONs 18 nm, biocompatibility, high relaxivity, specific cellular binding	Fluorescent and MRI X-ray diffraction	Wang et al., 2014b
Endothelial progenitor cells	Cationic thiolated chitosan-TGA-SPIONs	Incubation C + MP for 24 h	MP size <15 nm; High biocompatibility Viability >90% after 24 h	ICP TEM Prussian blue staining MRI	Shahnaz et al., 2013
Endothelial progenitor cells	Tetramethylammonium hydroxide stabilized SPIONs	Incubation (early and outgrown) C + MP for 24 h at 37 °C	MP in cytoplasm Cell viability unaltered, *in vivo* brain targeting of magnetized cells	TEM Prussian blue staining SQUID magnetometry MRI	Carenza et al., 2014

Human mesenchymal stem cells	SPIONs Fe_3O_4 and Fe_3O_4@SiO_2	Incubation C + MP for 24 h	Determination of MP fate *in vivo*; coating with SiO_2 shell, higher stability and higher efficiency also during cell proliferation	TEM MRI	Tian et al., 2014
Human mesenchymal stem cells	PEG-coated SPIOs	Incubation C + MP in high magnetic field	SPIOs core size 14.9 nm, MP in cytoplasm, cell magnetically attracted *in vivo*	Confocal microscopy TEM MRI	Landazuri et al., 2013
Human carcinoma cells (A375M, DLD1, MCF7, SW480, U2OS)	PS-dexSPIOs	Incubation C + MP in presence of transfection agent protamine sulfate (PS) for 16–18 h	Labeling efficiency 95%, cell viability not affected	Prussian blue staining	Wang and Cuschieri, 2013
	dexSPIOs	Electroporation with and without PS	Labeling efficiency without PS 72%, with PS 88%, electroporation with PS significantly improved cell viability, without decrease, fast labeling (30 min) in comparison with TA	Quantichrom iron assay	
Dog bone marrow stem cells	Fe_3O_4-DMSA-PLL-SPIOs	Incubation of C + MP for 24 h	*In vivo* imaging (dog), MP size 12.2 nm, no effect on cell viability	Prussian blue staining TEM MRI	Lu et al., 2013
Human dental pulp stem cells	PLL-SPIOs Endorem	Incubation of C + MP for 24 h at 37 °C	Intracytoplasmatic deposits of MP by endocytosis, without PLL metabolic activity altered, *in vivo* tracking (mouse)	Prussian blue staining Atomic absorption spectroscopy	Struys et al., 2013
Human cardiosphere-derived stem cells	Ferumoxytol nanoparticles Feraheme	Incubation in presence of heparin sulfate and PS for 12 h	Intracellular uptake, nontoxic	Fluorescence and MRI imaging Prussian blue staining TEM	Vandergriff et al., 2014

TA, transfection agents; (U)SPIO(n)s, (ultrasmall) superparamagnetic iron oxide (nano)particle; C, cells; MP, magnetic particles; MION, monocrystalline iron oxide nanocolloid; ICP-MS, inductively coupled plasma mass spectrometry; RMM, the Reilly-Mc-Connel-Meisenheimer method; BSA, bovine serum albumin; Dex, dextran; PLL, poly-L-lysine; PS, protamine sulfate; PEG, polyethylene glycol; PEI, polyethyleneimine; DMSA, meso-2,3-dimercaptosuccinic acid; MRI, magnetic resonance imaging; TEM, transmission electron microscopy; TGA, thioglycolic acid; EGF, epidermal growth factor; AES, atomic emission spectroscopy; PVA, polyvinyl alcohol; SQUID, superconducting quantum interference device.

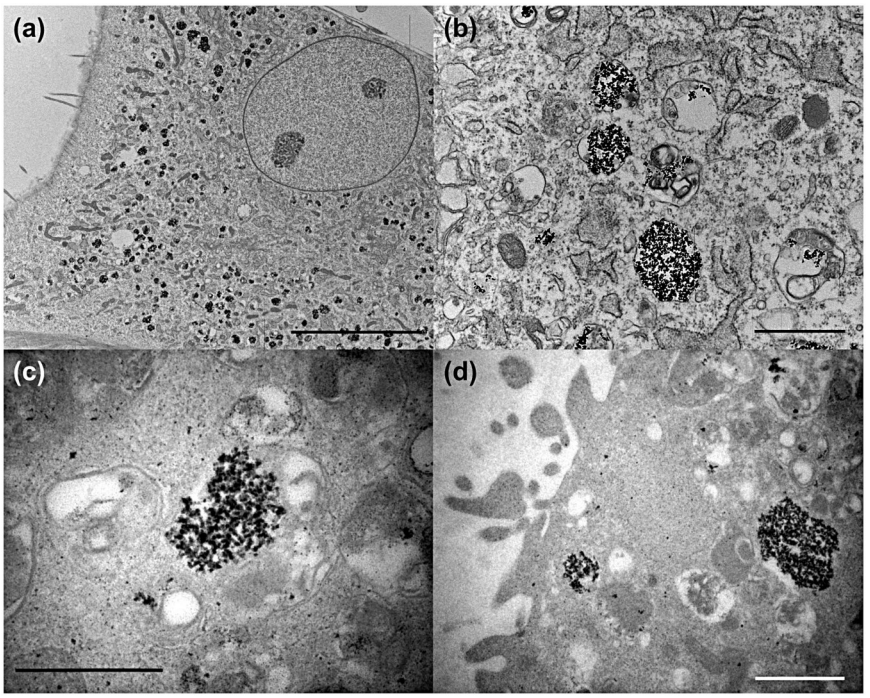

FIGURE 5.4

(a,b) Transmission electron microscope (TEM) micrographs of rat mesenchymal stem cells labeled with D-mannose-coated γ-Fe_2O_3 nanoparticles. Scale bars (a) 10 μm, (b) 1 μm. Reproduced, with permission, from Horak et al. (2009). (c) TEM micrograph of rat bone marrow stromal cells labeled with D-mannose-modified γ-Fe_2O_3 nanoparticles; scale bar 500 nm. Reproduced, with permission, from Horak et al. (2007). (d) TEM micrographs of rat bone marrow stromal cells labeled with poly(L-lysine)-modified γ-Fe_2O_3 nanoparticles; scale bar 2 μm. Reproduced, with permission, from Babic et al. (2008).

animals. Transfected cells can be separated from nontransfected ones using an appropriate magnetic separation technique (Mykhaylyk et al., 2007; Plank et al., 2011; Arora et al., 2013). Optimized magnetofection procedures employ oscillating magnet arrays to enhance the overall transfection efficiency of magnetofection and decrease transfection duration maintaining the high cell viability. In this system, magnetic NP−DNA complexes are added into the cell culture, and the presence of the oscillating magnet arrays, positioned beneath the cell culture plate, introduces a lateral motion to the particle−DNA complexes, which results in more efficient, mechanical stimulation of endocytosis and an increase in transfection efficiency in most cell types when compared to static magnetofection (Kamau et al., 2006; McBain et al., 2008).

5.2.3 LAYER-BY-LAYER POLYELECTROLYTE-ASSISTED BINDING OF MAGNETIC PARTICLES

An interesting procedure for coating yeast cells by magnetite NPs via electrostatic interactions has been described recently. At first poly(allylamine hydrochloride) (PAH) was coated onto the hydrated yeast cells whose surfaces were negatively charged in water, then the cells were coated with poly(sodium polystyrene sulfonate) (PSS). After repeating the procedure to build PAH/PSS/PAH coatings on the cells, magnetite NPs were deposited on the cells before the deposition of two additional polyelectrolyte layers. The final products had the layer structures of PAH/PSS/PAH/magnetic NPs/PAH/PSS, which preserve the viability of the yeast cells. Magnetic NPs formed a multilayered coating on the outer side of the yeast cell walls. Using yeast cells expressing GFP it was shown that magnetic modification had little effect on the fluorescence emission (Fakhrullin et al., 2010a). In another procedure PAH-stabilized positively charged magnetic NPs (average diameter around 15 nm) were used for the magnetization of living *Chlorella pyrenoidosa* cells. The single-step magnetization procedure is very simple and consisted of the dropwise introduction of the aqueous suspension of algae cells into a NP suspension followed by intensive shaking for 10 min. TEM images demonstrated the uniform layer of magnetic NPs on the cell walls with thickness around 90 ± 20 nm (Fakhrullin et al., 2010b) (see Figure 5.5). Great reviews on this topic have been written recently (Fakhrullin and Lvov, 2012; Fakhrullin et al., 2012).

5.2.4 COVALENT IMMOBILIZATION OF CELLS ON MAGNETIC PARTICULATE CARRIERS

Covalent binding is an extensively used technique for the immobilization of biopolymers, but this technique is not used so often for the immobilization of living cells. Covalent binding of microbial cells on a magnetic carrier is usually possible via reactive groups on the surface or through the aid of a reactive binding which links the cells to the carrier. Various coupling agents (e.g., aminosilane, carbodiimide, glutaraldehyde) may be employed to introduce a specific group on the carrier surface, which subsequently can interact with reactive groups on the cell surface. In typical examples of cell covalent immobilization, magnetic chitosan particles, activated by glutaraldehyde have been utilized for *Saccharomyces cerevisiae* immobilization (Ivanova et al., 2011; Safarik et al., 2015b). Alternatively, magnetic cellulose microparticles, after their activation with periodic acid, were employed for yeast cell immobilization (Ivanova et al., 2011). Magnetic polyacrolein microspheres carrying reactive aldehyde groups on their surface were used for covalent binding of fresh human RBCs (Margel et al., 1981). The photosynthetic microorganism *Synechocystis* sp. PCC 6803 was immobilized on amine-functionalized magnetic beads (Dynabeads M-270 Amine) by 1-ethyl-3-(3-dimethylaminopropyl)carbodiimide (EDC)−N-hydroxysulfosuccinimide (NHS) coupling chemistry; the carboxylic groups present on the *Synechocystis* cell

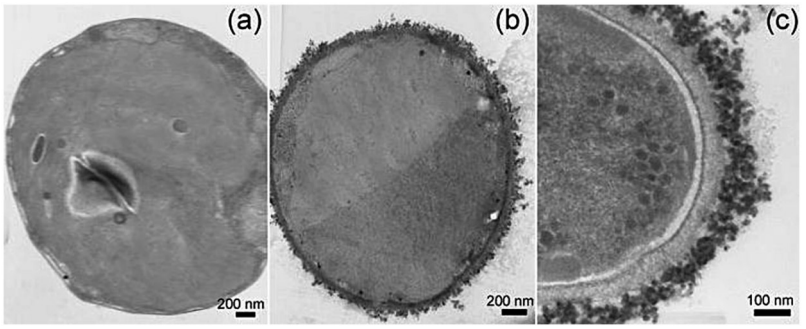

FIGURE 5.5

TEM images of the thin sections of (a) bare and (b) and (c) PAH-stabilized magnetic nanoparticle-coated *Chlorella pyrenoidosa* cells.

Reproduced, with permission, from Fakhrullin et al. (2010b).

wall were activated with EDC and then subjected to NHS to produce amine-reactive NHS esters enabling interaction with amine-functionalized magnetic beads to produce covalent amide bonds (Venu et al., 2013).

In addition to magnetic biopolymer and synthetic polymer particles, different types of magnetic iron oxides have been used for covalent cell immobilization or modification (Robatjazi et al., 2010; Robatjazi et al., 2013; Safarikova et al., 2007). Carboxylate- and amino-modified magnetic NPs were utilized for covalent modification of *Flavobacterium* ATCC 27,551. Under optimal conditions, the magnetic cells displayed specific activity ratios of 93−89% compared with untreated cells, after the covalent coupling with carboxylate and amino-modified magnetic NPs, respectively (Robatjazi et al., 2010). Silanized magnetite (20−40 nm, activated by (3)-aminopropyltriethoxysilane followed by glutaraldehyde treatment) was covalently bound to cells of the alkalotolerant producer of cyclodextrin glucanotransferase (CGTase) *Bacillus circulans* ATCC 21783 in order to increase the produced enzyme activity. The highest CGTase production was achieved after 96 h of semicontinuous process using this type of immobilized cells when the specific enzyme activity was 8.4-fold higher compared to that of free cells. Magnetic NPs linked on the cell walls by the covalent bond between the activated magnetite and the cells were very stable (Safarikova et al., 2007). An iron-based ammonia synthesis catalyst covered by a stable film of amino groups containing epoxy resin was used for *Saccharomyces cerevisiae* cell immobilization after glutaraldehyde activation (Ivanova et al., 1996).

5.2.5 BINDING OF CELLS ON MAGNETIC NANOFIBERS

Nanofibers and nanotextile prepared from biocompatible polymers have been successfully used as materials for scaffold manufacture. It has been

demonstrated recently that the addition of magnetic NPs in composite nanofibrous films could induce a significantly higher proliferation rate and faster differentiation of osteoblast cells. Therefore, scaffolds containing magnetic NPs may provide great potential in bone-regenerative medicine. That is why magnetically responsive nanofibers and nanotextile have been utilized to immobilize various cells (Wang et al., 2014a; Li et al., 2014). Magnetic nanofibers of different types have been tested as cell immobilization matrices/scaffold, such as those prepared from poly-L-lactide (Wang et al., 2014a; Li et al., 2014; Shan et al., 2013), poly(caprolactone) (Singh et al., 2014), chitosan/polyvinyl alcohol (Wei et al., 2011), or poly(lactic-co-glycolide) (Hu et al., 2013).

5.2.6 CROSSLINKING OF CELLS OR CELL WALLS IN THE PRESENCE OF MAGNETIC PARTICLES

Microbial cell walls contain free amino and/or carboxyl groups, which can easily be crosslinked by bi- or multifunctional reagents such as glutaraldehyde or toluene diisocyanate. The cells are usually crosslinked in the presence of an inert protein like gelatine, albumin, raw hen egg white, and collagen. Microbial cells can also be immobilized by ionic crosslinking through a flocculation mechanism by addition of polyelectrolytes. If magnetic particles are used throughout the crosslinking process, magnetic cells or cell wall derivatives can be prepared (Patzak et al., 1997).

5.2.7 SPECIFIC INTERACTIONS WITH IMMUNOMAGNETIC NANO- AND MICROPARTICLES

Immunomagnetic modification of cells is based on the use of magnetic nano- and microparticles with bound specific antibodies (Abs) against appropriate cell surface epitopes. After particle addition to the cell suspension they are selectively attached to target cells. After incubation, target cells with attached magnetic particles (and also excess particles) are isolated with the help of an appropriate magnetic separator. Both monoclonal and polyclonal mammalian Abs have been predominantly used in the course of immunomagnetic modification. In the direct method the appropriate Abs are coupled to the magnetic particles, which are then directly added to the cells-containing sample. Ideally, the antibody should be oriented with its F_c (fragment crystallizable) region towards the magnetic particle so that the F_{ab} (fragment antigen-binding) region is pointing outwards from the particle (Safarik and Safarikova, 1999; Safarik and Safarikova, 2007; Safarik et al., 2014).

Alternatively, the indirect method can be employed. In the first step, the cell suspension is incubated with primary Abs which bind to the target cells. Prior sensitization of the target cells will ensure a proper orientation of the Abs and an optimal number of interaction possibilities between magnetic particles

and cells. Not only purified primary Abs have to be used; crude antibody preparations or serum can be used too. After incubation, the unbound Abs are usually removed by washing. Thereafter, the magnetic particles with immobilized secondary Abs are added, permitting the beads to bind rapidly and firmly to the primary Abs on the target cells. Target cells−primary antibody complexes can also be captured by protein A or protein G immobilized on magnetic carriers. Alternatively, primary Abs can be biotinylated or labeled with fluorescein and magnetic particles with immobilized streptavidin or antifluorescein Abs are used for capturing the target cells (Safarik and Safarikova, 1999; Safarik and Safarikova, 2007).

In addition to mammalian-derived Abs, chicken egg yolk Abs (IgYs) can be used; they represent a promising alternative to animal Abs because eggs are obtained non-invasively, and the phylogenetic distance between chickens and mammals results in differences in antibody specificities (Schade et al., 2005). A few reports describing the use of IgYs immobilized on magnetic particles for microbial pathogens labeling and detection have been published (Mine, 1997).

The binding of magnetic particles to the cell surface mediated by a specific antigen−antibody reaction is preferably used in immunomagnetic separation of target prokaryotic and eukaryotic cells (e.g., microbial pathogens, stem and cancer cells, etc.). Both magnetic NPs and microparticles can be employed as antibody carriers. After target cell labeling the modified cells are usually magnetically separated from the sample. Target diamagnetic cells can be separated using two basic strategies, namely positive selection or depletion. The optimal separation strategy depends on the frequency of target cells in the cell sample, their phenotype compared with the other cells in the sample, the availability of reagents and a full consideration of how the target cells are to be used. Positive selection means that the desired target cells are magnetically labeled and isolated directly as the positive cell fraction (Figure 5.6). It is the most direct and specific way to isolate the target cells from a heterogeneous cell suspension. Positive selection is particularly well suited for the isolation of rare cells. Both fractions, labeled and unlabeled, can be recovered and used. Depletion means that the unwanted cells are magnetically labeled and eliminated from the cell mixture, and the nonmagnetic, untouched fraction contains the cells of interest. Potential effects on the functional status of cells are minimized (Safarik and Safarikova, 1999; Safarik and Safarikova, 2012).

The positively selected cells, in many cases, may not show any interference from the larger magnetic particles and may also be analyzed or used with the particles attached to them. In some cases, however, it is necessary to remove larger immunomagnetic particles from the cells after their isolation. The detachment process can be performed in several ways, namely (Safarik and Safarikova, 1999, 2012):

- Incubating captured cells overnight in cell culture medium and subsequent mechanical treatment (e.g., firm pipetting flushing the suspension 5−10 times through a narrow-tipped pipette).

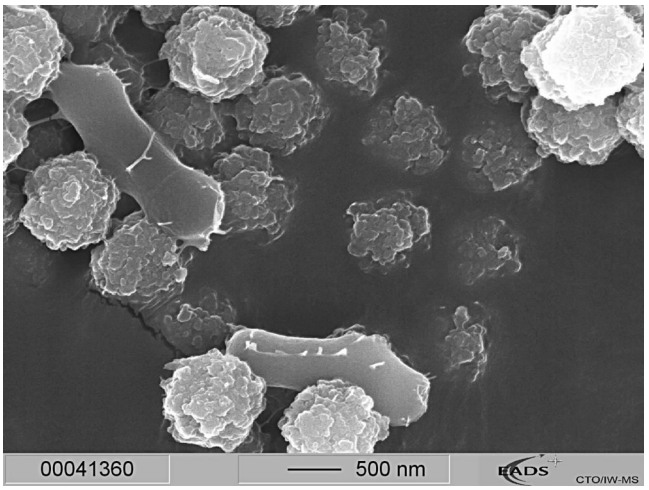

FIGURE 5.6

Electron microscopy of *Legionella pneumophila* bound to immunomagnetic beads (Dynabeads My One Streptavidin (Invitrogen) with bound biotinylated polyclonal anti-*Legionella* antibody).

Reproduced, with permission, from Reidt et al. (2011).

- Proteolytic enzymes can be used to release isolated cells from magnetic particles by selective cleavage of the protein epitope or Ab involved in the immunomagnetic binding.
- Application of an Ab that reacts with the F_{ab} fragments of primary monoclonal Abs on magnetic beads and thus enables direct dissociation of the antigen−Ab binding, thereby producing cells without Abs remaining on the surface and with unchanged antigen expression.
- Synthetic peptides that bind specifically to the antigen-binding site of primary Abs compete with the target cell−magnetic particle complexes and enable to obtain target cells with unchanged antigen expression.
- Carbohydrate units on the F_c part of the Abs allow reversible attachment of the Abs to the magnetic particles with immobilized $-B(OH)_3$ groups. After selective isolation of the target cells, sorbitol is added, which replaces the Ab on the magnetic bead.
- A complex primary Ab−DNA linker can be immobilized on magnetic particles, and after cell binding, the DNA linker can be split enzymatically using DNase.
- In specific cases, decrease of pH can cause immunomagnetic particle release.

5.2.8 INTERACTION WITH MAGNETIC PARTICLES BEARING IMMOBILIZED BIOLOGICALLY ACTIVE COMPOUNDS

Magnetic selective labeling of target cells can employ different types of biological interactions. In addition to antigen−antibody interaction described in Section 5.2.7, the following affinity ligands have been immobilized to magnetic particles and employed for cell labeling, namely:

- Specific lectins or other sugar-binding proteins
- Sugars and glycoproteins
- Avidin or streptavidin
- Annexin V
- Metal-binding proteins (transferrin (Tf), lactoferrin (Lf), ceruloplasmin)
- Cell-penetrating peptides
- Aptamers
- Integrin-binding ligands
- Vankomycin
- Folic acid.

Different types of lectins, such as those produced from *Triticum vulgaris* and *Agaricus bisporus*, or concanavalin A, immobilized on magnetic microspheres, were used to magnetically label specific bacterial pathogens, such as *Escherichia coli*. Recovered cell populations were free from environmental impurities and a high percentage of the culturable cells was extracted. Specific cell recovery was found to be variable, but the use of lectins may offer some promise as an alternative cell discriminator (Payne et al., 1993; Porter and Pickup, 1998; Porter et al., 1998). The *Ulex europaeus* lectin bound to submicron magnetic particles was used to label and separate human pluripotent stem cells (Wang et al., 2011).

Sugars or glycoproteins bound to magnetic particles can interact with specific cells; in a typical example, *Escherichia coli* strain ORN178 containing the mannose-binding protein FimH in its fimbriae was magnetically labeled using magnetic particles bearing mannose; subsequently the labeled cells were magnetically separated (Behra et al., 2013; El-Boubbou et al., 2007; El-Boubbou et al., 2010). D-Mannose-modified iron oxide NPs were used to modify rat bone marrow stromal cells; optical and transmission electron microscopy confirmed the presence of modified NPs inside the cells (Horak et al., 2007). Magnetic glyconanoparticles, based on immobilized mannose, galactose, fucose, sialic acid, and N-acetylglucose, were employed to detect and differentiate cancer cells bearing specific lectins on their surface (El-Boubbou et al., 2010). Oligosaccharide-coated magnetic particles were used for the selection of human carbohydrate-binding cell phenotypes (Rye and Bovin, 1997). Lactose functionalized anionic magnetoliposomes exhibiting affinity to asialoglycoprotein receptor (ASGP-r) were utilized as a magnetic resonance (MR) CA to target hepatocytes *in vivo* (Ketkar-Atre et al., 2014). Pigeon ovalbumin (a glyco- and phosphoprotein containing high levels of terminal galactose units recognizing a specific galactophilic lectin on the outer

cell membrane of *Pseudomonas aeruginosa*) was immobilized on magnetic NPs to label *P. aeruginosa* specifically. This procedure enables rapid detection, separation, and characterization of *P. aeruginosa* from clinical samples without their culturing (Liu et al., 2009b).

In another procedure cell membrane proteins were first biotinylated and then bound to streptavidin magnetic particles. HeLa and TE671 cells were used as model cells; their viability was not changed and this magnetic labeling method was not toxic to cells. Partial internalization of magnetic particles was observed; uptake of these particles did not affect cell viability (Ho et al., 2009).

Magnetic (nano)particles with immobilized annexin V have been employed for simple and efficient separation of apoptotic cells from normal culture. Annexin V is a Ca^{2+}-dependent phospholipid-binding protein with high affinity for negatively charged phosphatidylserine (PS). This phospholipid is redistributed from the inner to the outer plasma membrane leaflet in apoptotic or dead cells; once on the cell surface, PS can be bound to annexin V and any of its magnetic conjugates (Dirican et al., 2008; Makker et al., 2008; Lobascio et al., 2007).

Various cancer cells are characterized by the overexpression of endogenous transferrin receptor (TfR). TfR thus represents a suitable target for magnetic cancer cell labeling using magnetic (nano)particles with immobilized Tf (Hogemann-Savellano et al., 2003). In order to delineate the location of the tumor cells both before and during operation, bifunctional magnetic polymeric micelles for MR and fluorescence imaging in liver tumors have been prepared; after transferrin and near-infrared fluorescence molecule Cy5.5 conjugation onto the surface of the magnetic polymeric micelles an efficient accumulation in HepG2 cells was observed (Qi et al., 2014). Transferrin-conjugated magnetic silica/poly(D,L-lactic-co-glycolic acid) NPs were formulated in order to overcome the blood−brain barrier. These NPs were loaded with doxorubicin and paclitaxel, and their antiproliferative effect was evaluated in U-87 cells. The delivery and the subsequent cellular uptake of drug-loaded NPs could be enhanced by the presence of a magnetic field and the usage of Tf as targeting ligand, respectively (Cui et al., 2013).

Lf belongs to the transferrin family, and shares 60−80% sequence identity with Tf. Lf has low plasma concentration under physiological conditions, which makes Lf a promising ligand to target tumor; Lf receptors express highly on the cell surface of glioblastomas. Thus, Lf conjugated magnetic NPs could become promising CAs for brain tumors (Xie et al., 2011). Lf- or ceruloplasmin-coated magnetic NPs attached to the cell membrane of human dermal fibroblasts while the underivatized magnetic particles were internalized by the fibroblasts probably due to endocytosis, which resulted in disruption of the cell membrane and disorganized cell cytoskeleton (Gupta and Curtis, 2004).

Cell-penetrating peptides (CPP), including the HIV−Tat, the third helix of the homeodomain of Antennapedia, transportant, a peptide derived from anti-DNA monoclonal antibody, VP22 herpes virus protein, and other synthetic peptides provide a new way of delivering cargo molecules and (nano)particles through cellular membrane. Magnetically responsive (nano)particles with immobilized CPP have

been used to deliver the particles (together with the possible cargo) into cells. Magnetic particle internalization allows *in vivo* tracking of labeled cells in intact micro- and macroenvironments over time, MRI tracking of labeled cells, magnetic isolation of cells, and using the labeled cells as nanosensors (Tung and Weissleder, 2002; Torchilin, 2008). Derivatized particles were internalized into the target cells with substantially higher efficiency than non-modified particles (Josephson et al., 1999).

Magnetic nano- and microparticles with bound aptamers have similar application potential as immunomagnetic particles. These particles have been used for labeling and subsequent magnetic separation of both microbial (Suh and Jaykus, 2013; Dwivedi et al., 2013) and mammalian cells (Chen et al., 2008; Ding et al., 2010; Hua et al., 2013).

Integrin-expressing tumor cells have been successfully magnetically labeled using magnetic NPs with bound cyclic arginine−glycine−aspartic acid; the NPs could image $\alpha_v\beta_3$ integrins expressed in BT-20 tumor cells (Montet et al., 2006).

In order to magnetically separate the target bacteria, vancomycin (an antibiotic) was bound to the surface of FePt NPs to capture Gram-positive bacteria via molecular recognition between vancomycin and the terminal peptide, D-Ala-D-Ala, on the surface of Gram-positive bacteria (Gu et al., 2003).

Folic acid immobilized on magnetic NPs could be used to facilitate uptake to specific cancer cells overexpressing folate receptor for cancer therapy and diagnosis (Saltan et al., 2011).

5.2.9 MODIFICATION BY MAGNETIC QUANTUM DOTS

Quantum dots (QDs) are nanocrystals made of semiconductor material that are small enough to display quantum mechanical properties; in bioapplications they are particularly significant for optical applications due to their high extinction coefficient. Composite materials composed of magnetic particles and QDs can be successfully used also in magnetic cell labeling (Kale et al., 2011; Medintz et al., 2008; Medintz et al., 2005; Wang et al., 2004). Nanocomposite NPs consisting of polymer-coated γ-Fe_2O_3 superparamagnetic cores and CdSe/ZnS QDs shell with an average diameter of 30 nm were modified with carboxylic groups to increase their miscibility in aqueous solution. To demonstrate their utility anticyclin E Abs were immobilized on their surface and then bound to MCF7 breast cancer cells containing cyclin E, a protein which is specifically expressed on the surface of breast cancer cells. The separated breast cancer cells were easily observed by fluorescence imaging microscopy due to the strong luminescence of the luminescent/magnetic nanocomposite particles (Wang et al., 2004). Other possible applications of magnetic QDs can be found elsewhere (Mahajan et al., 2013).

5.2.10 MODIFICATION BY MAGNETOLIPOSOMES

Magnetoliposomes consist of vesicles composed of a phospholipid membrane encapsulating magnetic NPs. These systems have several important applications,

such as in MRI CAs, drug and gene carriers, and cancer treatment devices (Cintra et al., 2009). Different types of magnetoliposomes and other magnetic lipidic vesicles have been used as cells labels (Margolis et al., 1983).

Mesenchymal stem cells (MSCs), which can differentiate into multiple mesodermal tissues, have been magnetically labeled using cationic magnetoliposomes (leading to the concentration of 20 pg of magnetite per cell), in order to enrich them magnetically from bone marrow. The magnetoliposomes exhibited no toxicity against MSCs in proliferation and differentiation to osteoblasts and adipocytes. During subsequent culture, a substantially higher density of cells was obtained, compared to culture prepared without magnetoliposome treatment (Ito et al., 2004).

Alternatively, another methodology for enriching and proliferating MSCs from bone marrow aspirates has been developed using antibody-conjugated magnetoliposomes (AMLs). The AMLs were liposomes conjugated to anti-CD105 antibody (immunoliposomes) and containing magnetite NPs (diameter 10 nm). AMLs successfully labeled MSCs which could be separated by magnetic force. The MSCs proliferated and formed colonies (Ito et al., 2005). Other immunomagnetic systems based on magnetoliposomes bearing specific Abs have been used for magnetic labeling of target cells followed by their positive selection from a cell mixture. Anti-CD34 poly(ethylene glycol)-grafted immunomagnetoliposomes were prepared and used for CD34+ cells separation (Domingo et al., 1999, 2001). In an *in vivo* application example, tumor-specific magnetoliposomes were conjugated with an antibody fragment to give specificity to target glioma cells. After injection of magnetoliposomes to mice and exposure to the alternating magnetic field, the temperature of tumor tissue increased to 43 °C and the growth of the tumor was found to be arrested over 2 weeks. Magnetoliposomes could target the glioma cells *in vitro* and *in vivo*, and could be efficiently applicable to the hyperthermia of tumors (Le et al., 2001). Lactose functionalized anionic magnetoliposomes were used as an MR CA to target hepatocytes *in vivo*; lactose moieties were used for targeting the ASGP-r, which is highly expressed in hepatocytes (Ketkar-Atre et al., 2014).

5.2.11 BINDING OF FERRITIN AND MAGNETOFERRITIN ON THE CELL SURFACE

Ferritin is a globular protein complex consisting of 24 protein subunits and is the primary intracellular iron-storage protein in both prokaryotes and eukaryotes, keeping iron in a soluble and nontoxic form. Ferritin can be *in vitro* converted into magnetoferritin-containing magnetic iron oxides within the protein cavity (Mitroova et al., 2012).

Human lymphocytes were incubated with cationized horse spleen ferritin (N,N-dimethyl-1,3-propanediamine derivative of the native horse spleen ferritin) exhibiting a net positive charge at pH 7.5. Under these conditions, the cationized ferritin readily formed ionic bonds with the anionic sites on the cell membrane; the labeled cells were used during the experiments with analytical magnetapheresis (Zborowski et al., 1995).

A secondary antibody-staining method was employed to couple selectively magnetoferritin or native ferritin to human lymphocytes. The (magneto)ferritin surface was modified by biotin conjugation in preparation for avidin–biotin binding to the antibody complex. The biotinylated (magneto)ferritin was bound to specific biotinylated Abs via an avidin bridge. Detailed study of the labeled cells' movement in a ferrograph was performed; it was shown that the magnetic moment of magnetoferritin was sufficient for immunomagnetic isolation of lymphocytes from mononuclear cell preparations in the modified ferrograph (Zborowski et al., 1996).

Recombinant magnetoferritin formed from human heavy-chain ferritin protein subunits can be used to target and visualize tumor tissues overexpressing TfR1. The iron oxide core catalyzes the oxidation of peroxidase substrates in the presence of hydrogen peroxide to produce a color reaction that is used to visualize tumor tissues (Fan et al., 2012). Magnetoferritin derived from the genetically engineered human H-chain ferritin containing both a fluorescent dye and a cell-specific targeting peptide, RGD-4C, which binds $\alpha_v\beta_3$ integrins upregulated on tumor vasculature, was prepared and subsequently used to bind C32 melanoma cells *in vitro*. The results have shown that genetically modified magnetic ferritin can serve as a multifunctional nanoscale container for simultaneous iron oxide loading and cell-specific targeting (Uchida et al., 2006). The same magnetoferritin was used as a CA to label macrophages which play important roles in the immunological defense system; the composite material exhibited the R_2 relaxivity comparable to known iron oxide MRI CAs (Uchida et al., 2008).

5.2.12 BINDING OF PARAMAGNETIC CATIONS ON THE CELL SURFACE

Lanthanides, especially erbium in the form of erbium chloride ($ErCl_3$), have been used for magnetic labeling of a variety of cells. Erbium ions have a high affinity for the external cell surface and preserve their exceptionally high atomic magnetic dipole moment (9.3 Bohr magnetons) in various chemical structures. The mechanism of Er binding to the cell surface is mostly ionic, with many different Er-binding sites, such as carboxyl groups in glycoproteins, differing in affinity and binding capacity. The other well-recognized lanthanide-binding sites are the Ca receptor sites on the cell wall. Both Gram-positive and -negative bacteria can be magnetically modified (Zborowski et al., 1991, 1992, 1993; Tada et al., 1991–1992). Yeast cells labeled with erbium ions were efficiently separated using an analytical magnetapheresis device (Fuh et al., 2000) or used for measuring the volumetric magnetic susceptibility (Russell et al., 1987).

5.2.13 BIOLOGICALLY DRIVEN PRECIPITATION OF PARAMAGNETIC COMPOUNDS ON THE CELL SURFACE

Specific microorganisms such as *Desulfovibrio* (Gram-negative sulfate-reducing bacteria) can precipitate heavy metals on their surfaces as a consequence of their metabolism and growth. This, therefore, gives them the ability to accumulate such metals in large quantities from external surroundings. Microorganisms growing on glycerol-3-phosphate enzymatically produce phosphate anions in the vicinity of the cells. Heavy metal phosphates are usually insoluble and that is why they precipitate on the cell surface. Other strains of microorganisms reduce sulfate ions into sulfide under anaerobic conditions. As a consequence of this phenomenon, insoluble paramagnetic salts precipitate on the cells if paramagnetic cations (e.g., iron ions) are present in the medium. Microbial cells modified in this way can be magnetically separated using a high-gradient magnetic separation technique (Bahaj et al., 1991).

5.2.14 ENTRAPMENT OF CELLS INTO BIOCOMPATIBLE MAGNETIC POLYMERS AND GELS

Microbial cells can be entrapped in natural or biocompatible synthetic carriers (gels). The carriers can be grouped according to the mechanism leading to the gel formation. Gels can be formed by polymerization (e.g., polyacrylamide, polymethacrylate), crosslinking (e.g., proteins), polycondensation (polyurethane, epoxy resins), thermal gelation (e.g., gelatin, agar, agarose), ionotropic gelation (e.g., alginate, chitosan) and precipitation (cellulose, cellulose triacetate). The gel is formed in the presence of the cells and appropriate magnetic materials. There are various methods available to obtain particles (beads) containing entrapped cells and magnetic particles (Brodelius and Vandamme, 1987; Safarik et al., 2014).

The gel formation procedure can be very mild, enabling magnetic modification of living cells and subsequently employing their biological activities. One of the major drawbacks of the entrapment technique is the possible diffusional limitation as well as the steric hindrance, especially when the macromolecular compounds have to be treated with immobilized cells (Safarik et al., 2014). In a typical example, magnetically responsive alginate beads containing entrapped *S. cerevisiae* cells and magnetite microparticles were prepared. Larger beads (2−3 mm in diameter) were prepared by dropping the mixture into a calcium chloride solution, while microbeads (the diameter of the majority of particles was in the range 50−100 μm) were prepared using the water-in-oil emulsification process (Figure 5.7). The presence of magnetic material had no negative effect on activity of cells. The yeast cells immobilized in magnetic alginate beads were used as whole-cell biocatalysts for hydrogen peroxide degradation (Safarik et al., 2008), sucrose hydrolysis (Safarik et al., 2009), and for ethanol production (Birnbaum and Larsson, 1982; Ivanova et al., 2011; Larsson and Mosbach, 1979; Liu et al., 2009a).

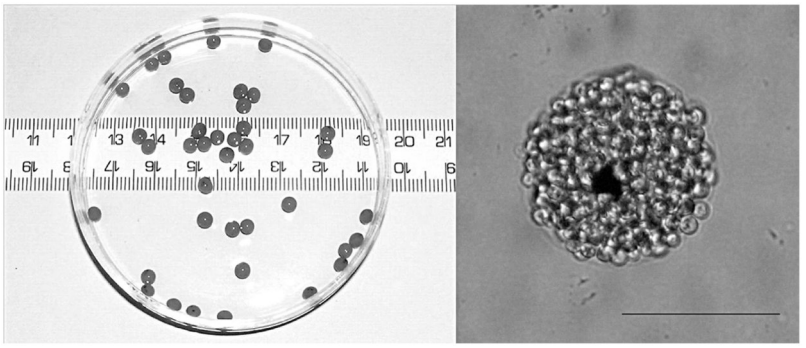

FIGURE 5.7

Magnetically responsive alginate beads containing entrapped *Saccharomyces cerevisiae* cells and magnetite microparticles. Millimeter-sized beads (left) and microbeads (right). The scale bar corresponds to 50 μm.

Reproduced, with permission, from Safarik et al. (2008).

Bacterial alkaliphilic cells, *Amphibacillus* sp. KSUCr3, were immobilized in silica-coated magnetic alginate gel beads and applied for detoxification of hexavalent chromate. In comparison with the cells immobilized into nonmagnetic matrix, the magnetic beads with cells showed approximately 16% higher reduction activity. Coating of magnetic alginate beads with a dense silica layer (using sol–gel procedure; silica layer was deposited by addition of ammonia and tetraethylorthosilicate to dispersed beads) improved physical and mechanical properties and thermal stability of immobilized cells (Ibrahim et al., 2013).

Microbial cells, *Spinghomonas* sp., were immobilized into magnetic gellan gum gel beads and applied for degradation of carbazole. Magnetic gel beads were prepared by mixing of gellan gel with cells and magnetite NPs (average diameter 20 nm) suspensions and extruding the mixtures through a syringe into calcium chloride solution. Magnetically immobilized cells showed higher carbazole biodegradation activity compared with cells immobilized in nonmagnetic matrix or free cells. Another interesting investigation from recycling experiments demonstrates a gradual increase of the degradation activity of magnetically immobilized cells during the eight repeated reaction cycles (Wang et al., 2007).

Crude egg white containing magnetic particles was used for entrapment and co-crosslinking of archaebacterial acidothermophilic cells of *Caldariella acidophila* with the help of glutaraldehyde. This material had good mechanical properties suitable for both batch and continuous-flow reactors. Determination of enzyme ß-galactosidase activity, evaluated as a marker of the integrity of enzyme machinery in immobilized cells, showed a 30-fold increase in egg-white entrapped cells in comparison with free cells, probably due to increase in cellular membrane permeability caused by the entrapment process (De Rosa et al., 1981).

Bacterial cells of *Pseudomonas dalafieldii* R-8 were immobilized in magnetic polyvinyl alcohol (PVA) beads and utilized for biodesulfurization. The suspension of cells in phosphate buffer was mixed with aqueous solution of PVA and oleic acid stabilized magnetic fluid and subsequently dropped into liquid nitrogen for quick freezing. Formed beads with immobilized cells underwent thawing by slow increase of the temperature under vacuum. In these PVA-cryogel beads, immobilized cells do not grow in the center, but propagate well at the edges. This biocatalyst could be used repeatedly over 12 times (Guobin et al., 2005). Microalgal cells (*Chlorella vulgaris*) were entrapped within a nontoxic polyvinylpyrrolidone (PVP) polymer matrix containing superparamagnetic magnetite NPs using a continuous-flow vortex fluidic device; high entrapment efficiency (up to 95%) was obtained. Entrapped cells can be separated from the PVP matrix using mild sonication (Eroglu et al., 2013).

Escherichia coli cells were encapsulated in a magnetic inorganic sol−gel matrix. Magnetic particles of this ferrihydrite gel, iron oxyhydroxide NPs (diameter ca. 5 nm), was prepared by alkalinization of an iron (III) chloride solution with subsequent removal of chloride anions to reduce ionic strength. Addition of phosphate buffer solution with or without glycerol formatted brown and opaque gel. The long-term viability of bacterial cells encapsulated in ferrihydrite gels was quite high, probably due to the neutral gel surface and its weaker interactions with cells and beneficial effect of iron species for bacteria metabolism (Amoura et al., 2009).

5.3 CONCLUSIONS

Modification of prokaryotic and eukaryotic cells with diverse magnetic labels creates opportunities for numerous bioapplications. In this review chapter we have focused our attention on the presentation of available procedures used to prepare magnetically responsive cells from originally diamagnetic precursors. Different approaches for magnetic modification have been developed; some of them (e.g., immunomagnetic techniques) have become widely used tools in cell biology, medicine, and microbiology. The unique properties of magnetically responsive cells enable their selective magnetic separation, MRI imaging, cancer treatment, etc. Cell labeling methods using magnetic particles have been widely developed, usually showing no adverse effect on cell proliferation and functionalities while conferring magnetic properties to various cell types. Further progress will be based on the application of novel functionalized magnetic NPs for cell modification; magnetically modified cells will become an important part of selective biosensors, cell tissue constructs, and magnetically responsive whole-cell biocatalysts or adsorbents.

The list of available magnetically modified cells will increase in the near future which will lead to a broader application of these interesting magnetically responsive biomaterials.

ACKNOWLEDGMENTS

This research was supported by the Grant Agency of the Czech Republic (Project No. 13-13709S) and by the Ministry of Education of the Czech Republic (Project LD 14075—Action COST MP1206 and LO1305).

REFERENCES

Amoura, M., Brayner, R., Perullini, M., Sicard, C., Roux, C., Livage, J., et al., 2009. Bacteria encapsulation in a magnetic sol-gel matrix. J. Mater. Chem. 19, 1241−1244.

Arora, S., Gupta, G., Singh, S., Singh, N., 2013. Advances in magnetofection—magnetically guided nucleic acid delivery: a review. J. Pharm. Technol. Res. Manage. 1, 19−29.

Azevedo, R.B., Silva, L.P., Lemos, A.P.C., Bao, S.N., Lacava, Z.G.M., Safarik, I., et al., 2003. Morphological study of *Saccharomyces cerevisiae* cells treated with magnetic fluid. IEEE Trans. Magn. 39, 2660−2662.

Babic, M., Horak, D., Trchova, M., Jendelova, P., Glogarova, K., Lesny, P., et al., 2008. Poly(L-lysine)-modified iron oxide nanoparticles for stem cell labeling. Bioconjug. Chem. 19, 740−750.

Bahaj, A.S., Ellwood, D.C., Watson, J.H.P., 1991. Extraction of heavy metals using micro-organisms and high gradient magnetic separation. IEEE Trans. Magn. 27, 5371−5374.

Behra, M., Azzouz, N., Schmidt, S., Volodkin, D.V., Mosca, S., Chanana, M., et al., 2013. Magnetic porous sugar-functionalized PEG microgels for efficient isolation and removal of bacteria from solution. Biomacromolecules 14, 1927−1935.

Birnbaum, S., Larsson, P.O., 1982. Application of magnetic immobilized microorganisms. Ethanol production by *Saccharomyces cerevisiae*. Appl. Biochem. Biotechnol. 7, 55−57.

Bitton, G., Fox, J.L., Strickland, H.G., 1975. Removal of algae from Florida lakes by magnetic filtration. Appl. Microbiol. 30, 905−908.

Bojin, F.M., Paunescu, V., 2015. Pros and cons on magnetic nanoparticles use in biomedicine and biotechnologies applications. In: Mihai Lungu, M., Neculae, A., Bunoiu, M., Biris, C. (Eds.), Nanoparticles' Promises and Risks. Heidelberg Springer, pp. 103−135.

Brahler, M., Georgieva, R., Buske, N., Muller, A., Muller, S., Pinkernelle, J., et al., 2006. Magnetite-loaded carrier erythrocytes as contrast agents for magnetic resonance imaging. Nano Lett. 6, 2505−2509.

Brian, D.P., Shashi, K.M., Laura, H.L., 2015. Fundamentals and application of magnetic particles in cell isolation and enrichment: a review. Rep. Prog. Phys. 78, 016601.

Brodelius, P., Vandamme, E.J., 1987. Immobilized cell systems. In: Rehm, H.-J., Reed, G. (Eds.), Biotechnology (Enzyme Technology), Vol. 7a. Verlag Chemie, Weinheim, pp. 405−464.

Bromberg, L., Chang, E.P., Alvarez-Lorenzo, C., Magarinos, B., Concheiro, A., Hatton, T.A., 2010. Binding of functionalized paramagnetic nanoparticles to bacterial lipopolysaccharides and DNA. Langmuir 26, 8829−8835.

Bulte, J.W.M., Arbab, A.S., Douglas, T., Frank, J.A., 2004. Preparation of magnetically labeled cells for cell tracking by magnetic resonance imaging. Methods Enzymol. 386, 275−299.

Carenza, E., Barcelo, V., Morancho, A., Levander, L., Boada, C., Laromaine, A., et al., 2014. *In vitro* angiogenic performance and *in vivo* brain targeting of magnetized endothelial progenitor cells for neurorepair therapies. Nanomedicine 10, 225–234.

Chen, H.W., Medley, C.D., Sefah, K., Shangguan, D., Tang, Z.W., Meng, L., et al., 2008. Molecular recognition of small-cell lung cancer cells using aptamers. Chemmedchem 3, 991–1001.

Choi, D., Fung, A., Moon, H., Ho, D., Chen, Y., Kan, E., et al., 2007. Transport of living cells with magnetically assembled nanowires. Biomed. Microdevices 9, 143–148.

Cintra, E.R., Ferreira, F.S., Santos, J.L., Campello, J.C., Socolovsky, L.M., Lima, E.M., et al., 2009. Nanoparticle agglomerates in magnetoliposomes. Nanotechnology 20, Article No. 045103.

Cui, Y.N., Xu, Q.X., Chow, P.K.H., Wang, D.P., Wang, C.H., 2013. Transferrin-conjugated magnetic silica PLGA nanoparticles loaded with doxorubicin and paclitaxel for brain glioma treatment. Biomaterials 34, 8511–8520.

Cunningham, C.H., Arai, T., Yang, P.C., Mcconnell, M.V., Pauly, J.M., Conolly, S.M., 2005. Positive contrast magnetic resonance imaging of cells labeled with magnetic nanoparticles. Magn. Reson. Med. 53, 999–1005.

Dauer, R.R., Dunlop, E.H., 1991. High-gradient magnetic separation of yeast. Biotechnol. Bioeng. 37, 1021–1028.

de Araujo, F.F.T., Pires, M.A., Frankel, R.B., Bicudo, C.E.M., 1986. Magnetite and magnetotaxis in algae. Biophys. J. 50, 375–378.

de Rosa, M., Gambacorta, A., Lama, L., Nicolaus, B., Buonocore, V., 1981. Immobilization of thermophilic microbial cells in crude egg white. Biotechnol. Lett. 3, 183–186.

Ding, C.F., Ge, Y., Zhang, S.S., 2010. Electrochemical and electrochemiluminescence determination of cancer cells based on aptamers and magnetic beads. Chem. Eur. J. 16, 10707–10714.

Dirican, E.K., Ozgun, O.D., Akarsu, S., Akin, K.O., Ercan, O., Ugurlu, M., et al., 2008. Clinical outcome of magnetic activated cell sorting of non-apoptotic spermatozoa before density gradient centrifugation for assisted reproduction. J. Assist. Reprod. Genet. 25, 375–381.

Doherty, G.J., Mcmahon, H.T., 2009. Mechanisms of endocytosis. Annu. Rev. Biochem. 78, 857–902.

Domingo, J.C., Mercadal, M., Petriz, J., De Madariaga, M.A., 2001. Preparation of PEG-grafted immunomagnetoliposomes entrapping citrate stabilized magnetite particles and their application in CD34 + cell sorting. J. Microencapsul. 18, 41–54.

Domingo, J.C., Mercadal, M., Petriz, J., Garcia, J., De Madariaga, M.A., 1999. Preparation of PEG-grafted immunomagnetoliposomes and their application in cell sorting. Cell. Mol. Biol. Lett. 4, 583–597.

Dwivedi, H.P., Smiley, R.D., Jaykus, L.A., 2013. Selection of DNA aptamers for capture and detection of *Salmonella typhimurium* using a whole-cell SELEX approach in conjunction with cell sorting. Appl. Microbiol. Biotechnol. 97, 3677–3686.

El-Boubbou, K., Gruden, C., Huang, X., 2007. Magnetic glyco-nanoparticles: a unique tool for rapid pathogen detection, decontamination, and strain differentiation. J. Am. Chem. Soc. 129, 13392–13393.

El-Boubbou, K., Zhu, D.C., Vasileiou, C., Borhan, B., Prosperi, D., Li, W., et al., 2010. Magnetic glyco-nanoparticles: a tool to detect, differentiate, and unlock the glycocodes of cancer via magnetic resonance imaging. J. Am. Chem. Soc. 132, 4490–4499.

Eroglu, E., D'alonzo, N.J., Smith, S.M., Raston, C.L., 2013. Vortex fluidic entrapment of functional microalgal cells in a magnetic polymer matrix. Nanoscale 5, 2627−2631.

Fakhrullin, R.F., Lvov, Y.M., 2012. "Face-lifting" and "make-up" for microorganisms: layer-by-layer polyelectrolyte nanocoating. ACS Nano 6, 4557−4564.

Fakhrullin, R.F., Garcia-Alonso, J., Paunov, V.N., 2010a. A direct technique for preparation of magnetically functionalised living yeast cells. Soft Matter 6, 391−397.

Fakhrullin, R.F., Shlykova, L.V., Zamaleeva, A.I., Nurgaliev, D.K., Osin, Y.N., Garcia-Alonso, J., et al., 2010b. Interfacing living unicellular algae cells with biocompatible polyelectrolyte-stabilised magnetic nanoparticles. Macromol. Biosci. 10, 1257−1264.

Fakhrullin, R.F., Zamaleeva, A.I., Minullina, R.T., Konnova, S.A., Paunov, V.N., 2012. Cyborg cells: functionalisation of living cells with polymers and nanomaterials. Chem. Soc. Rev. 41, 4189−4206.

Fan, K.L., Cao, C.Q., Pan, Y.X., Lu, D., Yang, D.L., Feng, J., et al., 2012. Magnetoferritin nanoparticles for targeting and visualizing tumour tissues. Nat. Nanotechnol. 7, 459−464.

Fortin, J.P., Gazeau, F., Wilhelm, C., 2008. Intracellular heating of living cells through Neel relaxation of magnetic nanoparticles. Eur. Biophys. J. Biophys. Lett. 37, 223−228.

Frank, J.A., Zywicke, H., Jordan, E.K., Mitchell, J., Lewis, B.K., Miller, B., et al., 2002. Magnetic intracellular labeling of mammalian cells by combining (FDA-approved) superparamagnetic iron oxide MR contrast agents and commonly used transfection agents. Acad. Radiol. 9, S484−S487.

Fuh, C.B., Lin, L.Y., Lai, M.H., 2000. Analytical magnetapheresis of magnetically susceptible particles. J. Chromatogr. A 874, 131−142.

Gu, H., Ho, P.L., Tsang, K.W.T., Wang, L., Xu, B., 2003. Using biofunctional magnetic nanoparticles to capture vancomycin-resistant enterococci and other gram-positive bacteria at ultralow concentration. J. Am. Chem. Soc. 125, 15702−15703.

Guobin, S., Jianmin, X., Chen, G., Huizhou, L., Jiayong, C., 2005. Biodesulfurization using *Pseudomonas delafieldii* in magnetic polyvinyl alcohol beads. Lett. Appl. Microbiol. 40, 30−36.

Gupta, A.K., Curtis, A.S.G., 2004. Lactoferrin and ceruloplasmin derivatized superparamagnetic iron oxide nanoparticles for targeting cell surface receptors. Biomaterials 25, 3029−3040.

Gutova, M., Frank, J.A., D'apuzzo, M., Khankaldyyan, V., Gilchrist, M.M., Annala, A.J., et al., 2013. Magnetic resonance imaging tracking of Ferumoxytol-labeled human neural stem cells: studies leading to clinical use. Stem Cells Transl. Med. 2, 766−775.

Heyn, C., Bowen, C.V., Rutt, B.K., Foster, P.J., 2005. Detection threshold of single SPIO-labeled cells with FIESTA. Magn. Reson. Med. 53, 312−320.

Ho, V.H.B., Mueller, K.H., Darton, N.J., Darling, D.C., Farzaneh, F., Slater, N.K.H., 2009. Simple magnetic cell patterning using streptavidin paramagnetic particles. Exp. Biol. Med. 234, 332−341.

Hogemann-Savellano, D., Bos, E., Blondet, C., Sato, F., Abe, T., Josephson, L., et al., 2003. The transferrin receptor: a potential molecular imaging marker for human cancer. Neoplasia 5, 495−506.

Horak, D., Babic, M., Jendelova, P., Herynek, V., Trchova, M., Pientka, Z., et al., 2007. D-Mannose-modified iron oxide nanoparticles for stem cell labeling. Bioconjug. Chem. 18, 635−644.

Horak, D., Babic, M., Jendelova, P., Herynek, V., Trchova, M., Likavcanova, K., et al., 2009. Effect of different magnetic nanoparticle coatings on the efficiency of stem cell labeling. J. Magn. Magn. Mater. 321, 1539–1547.

Hu, H., Jiang, W., Lan, F., Zeng, X.B., Ma, S.H., Wu, Y., et al., 2013. Synergic effect of magnetic nanoparticles on the electrospun aligned superparamagnetic nanofibers as a potential tissue engineering scaffold. RSC Adv. 3, 879–886.

Hua, P., Wang, Y.Y., Liu, L.B., Liu, J.L., Liu, J.Y., Yang, Y.Q., et al., 2015. *In vivo* magnetic resonance imaging tracking of transplanted superparamagnetic iron oxide-labeled bone marrow mesenchymal stem cells in rats with myocardial infarction. Mol. Med. Rep. 11, 113–120.

Hua, X., Zhou, Z., Yuan, L., Liu, S., 2013. Selective collection and detection of MCF-7 breast cancer cells using aptamer-functionalized magnetic beads and quantum dots based nano-bio-probes. Anal. Chim. Acta 788, 135–140.

Hughes, S., Dobson, J., El Haj, A.J., 2007. Magnetic targeting of mechanosensors in bone cells for tissue engineering applications. J. Biomech. 40, S96–S104.

Ibrahim, A.S.S., Al-Salamah, A.A., El-Toni, A.M., El-Tayeb, M.A., Elbadawi, Y.B., Antranikian, G., 2013. Detoxification of hexavalent chromate by *Amphibacillus* sp KSUCr3 cells immobilised in silica-coated magnetic alginate beads. Biotechnol. Bioprocess Eng. 18, 1238–1249.

Ito, A., Hibino, E., Honda, H., Hata, K., Kagami, H., Ueda, M., et al., 2004. A new methodology of mesenchymal stem cell expansion using magnetic nanoparticles. Biochem. Eng. J. 20, 119–125.

Ito, A., Hibino, E., Shimizu, K., Kobayashi, T., Yamada, Y., Hibi, H., et al., 2005. Magnetic force-based mesenchymal stem cell expansion using antibody-conjugated magnetoliposomes. J. Biomed. Mater. Res. Part B Appl. Biomater. 75B, 320–327.

Ito, A., Honda, H., Kobayashi, T., 2006. Cancer immunotherapy based on intracellular hyperthermia using magnetite nanoparticles: a novel concept of "heat-controlled necrosis" with heat shock protein expression. Cancer Immunol. Immunother. 55, 320–328.

Ivanova, V., Hristov, J., Dobreva, E., Al-Hassan, Z., Penchev, I., 1996. Performance of a magnetically stabilized bed reactor with immobilized yeast cells. Appl. Biochem. Biotechnol. 59, 187–198.

Ivanova, V., Petrova, P., Hristov, J., 2011. Application in the ethanol fermentation of immobilized yeast cells in matrix of alginate/magnetic nanoparticles, on chitosan-magnetite microparticles and cellulose-coated magnetic nanoparticles. Int. Rev. Chem. Eng. 3, 289–299.

Jendelova, P., Herynek, V., Decroos, J., Glogarova, K., Andersson, B., Hajek, M., et al., 2003. Imaging the fate of implanted bone marrow stromal cells labeled with superparamagnetic nanoparticles. Magn. Reson. Med. 50, 767–776.

Jendelova, P., Herynek, V., Urdzikova, L., Glogarova, K., Kroupova, J., Andersson, B., et al., 2004. Magnetic resonance tracking of transplanted bone marrow and embryonic stem cells labeled by iron oxide nanoparticles in rat brain and spinal cord. J. Neurosci. Res. 76, 232–243.

Josephson, L., Tung, C.H., Moore, A., Weissleder, R., 1999. High-efficiency intracellular magnetic labeling with novel superparamagnetic-Tat peptide conjugates. Bioconjug. Chem. 10, 186–191.

Kale, A., Kale, S., Yadav, P., Gholap, H., Pasricha, R., Jog, J.P., et al., 2011. Magnetite/CdTe magnetic-fluorescent composite nanosystem for magnetic separation and bio-imaging. Nanotechnology 22, Article No. 225101.

Kamau, S.W., Hassa, P.O., Steitz, B., Petri-Fink, A., Hofmann, H., Hofmann-Amtenbrink, M., et al., 2006. Enhancement of the efficiency of non-viral gene delivery by application of pulsed magnetic field. Nucleic Acids Res. 34, e40.

Ketkar-Atre, A., Struys, T., Dresselaers, T., Hodenius, M., Mannaerts, I., Ni, Y., et al., 2014. *In vivo* hepatocyte MR imaging using lactose functionalized magnetoliposomes. Biomaterials 35, 1015−1024.

Kettler, K., Veltman, K., Van De Meent, D., Van Wezel, A., Hendriks, A.J., 2014. Cellular uptake of nanoparticles as determined by particle properties, experimental conditions, and cell type. Environ. Toxicol. Chem. 33, 481−492.

Kratosova, G., Schrofel, A., Safarik, I., Horska, K., Urban, M., Rosenbergova, K., et al., 2013. Bionanocomposite, the way of its production and application. Czech Patent, 304046.

Landazuri, N., Tong, S., Suo, J., Joseph, G., Weiss, D., Sutcliffe, D.J., et al., 2013. Magnetic targeting of human mesenchymal stem cells with internalized superparamagnetic iron oxide nanoparticles. Small 9, 4017−4026.

Larsson, P.O., Mosbach, K., 1979. Alcohol production by magnetic immobilized yeast. Biotechnol. Lett. 1, 501−506.

Latorre, M., Rinaldi, C., 2009. Applications of magnetic nanoparticles in medicine: magnetic fluid hyperthermia. Puerto Rico Health Sci. J. 28, 227−238.

Le, B., Shinkai, M., Kitade, T., Honda, H., Yoshida, J., Wakabayashi, T., et al., 2001. Preparation of tumor-specific magnetoliposomes and their application for hyperthermia. J. Chem. Eng. Jpn. 34, 66−72.

Li, L., Yang, G., Li, J., Ding, S., Zhou, S., 2014. Cell behaviors on magnetic electrospun poly-D,L-lactide nanofibers. Mater. Sci. Eng. C. 34, 252−261.

Li, Y., Yue, T.T., Yang, K., Zhang, X.R., 2012. Molecular modeling of the relationship between nanoparticle shape anisotropy and endocytosis kinetics. Biomaterials 33, 4965−4973.

Liao, J., Xia, R., Liu, T., Feng, H., Ai, H., Song, B., et al., 2013. *In vivo* dynamic monitoring of the biological behavior of labeled C6 glioma by MRI. Mol. Med. Rep. 7, 1397−1402.

Liu, C.Z., Wang, F., Ou-Yang, F., 2009a. Ethanol fermentation in a magnetically fluidized bed reactor with immobilized *Saccharomyces cerevisiae* in magnetic particles. Bioresour. Technol. 100, 878−882.

Liu, J.C., Chen, W.J., Li, C.W., Mong, K.K.T., Tsai, P.J., Tsai, T.L., et al., 2009b. Identification of *Pseudomonas aeruginosa* using functional magnetic nanoparticle-based affinity capture combined with MALDI MS analysis. Analyst 134, 2087−2094.

Liu, W., Frank, J.A., 2009. Detection and quantification of magnetically labeled cells by cellular MRI. Eur. J. Radiol. 70, 258−264.

Lobascio, A.M., Klinger, F.G., De Felici, M., 2007. Isolation of apoptotic mouse fetal oocytes by AnnexinV assay. Int. J. Dev. Biol. 51, 157−160.

Lu, S.S., Liu, S., Zu, Q.Q., Xu, X.Q., Yu, J., Wang, J.W., et al., 2013. *In vivo* MR imaging of intraarterially delivered magnetically labeled mesenchymal stem cells in a canine stroke model. PLoS One 8, e54963.

Macrae, I.C., Evans, S.K., 1983. Factors influencing the adsorption of bacteria to magnetite in water and wastewater. Water Res. 17, 271−277.

Mahajan, K.D., Fan, Q., Dorcéna, J., Ruan, G., Winter, J.O., 2013. Magnetic quantum dots in biotechnology − synthesis and applications. Biotechnol. J. 8, 1424−1434.

Mai, T.D., D'orlye, F., Menager, C., Varenne, A., Siaugue, J.-M., 2013. Red blood cells decorated with functionalized core-shell magnetic nanoparticles: elucidation of the adsorption mechanism. Chem. Commun. 49, 5393−5395.

Makker, K., Agarwal, A., Sharma, R.K., 2008. Magnetic activated cell sorting (MACS): utility in assisted reproduction. Indian J. Exp. Biol. 46, 491−497.

Mamani, J.B., Pavon, L.F., Miyaki, L.A.M., Sibov, T.T., Rossan, F., Silveira, P.H., et al., 2012. Intracellular labeling and quantification process by magnetic resonance imaging using iron oxide magnetic nanoparticles in rat C6 glioma cell line. Einstein (São Paulo) 10, 216−221.

Margel, S., Beitler, U., Ofarim, M., 1981. A novel synthesis of polyacrolein microspheres and their application for cell labeling and cell separation. Immunol. Commun. 10, 567−575.

Margolis, L.B., Namiot, V.A., Kljukin, L.M., 1983. Magnetoliposomes: another principle of cell sorting. Biochim. Biophys. Acta 735, 193−195.

Mcbain, S.C., Griesenbach, U., Xenariou, S., Keramane, A., Batich, C.D., Alton, E., et al., 2008. Magnetic nanoparticles as gene delivery agents: enhanced transfection in the presence of oscillating magnet arrays. Nanotechnology 19, Article No. 405102.

Medintz, I.L., Uyeda, H.T., Goldman, E.R., Mattoussi, H., 2005. Quantum dot bioconjugates for imaging, labelling and sensing. Nat. Mater. 4, 435−446.

Medintz, I.L., Mattoussi, H., Clapp, A.R., 2008. Potential clinical applications of quantum dots. Int. J. Nanomed. 3, 151−167.

Mine, Y., 1997. Separation of *Salmonella enteritidis* from experimentally contaminated liquid eggs using a hen IgY immobilized immunomagnetic separation system. J. Agric. Food Chem. 45, 3723−3727.

Mitroova, Z., Melnikova, L., Kovac, J., Timko, M., Kopcansky, P., 2012. Synthesis and characterization of magnetoferritin. Acta Phys. Pol. A 121, 1318−1320.

Montet, X., Montet-Abou, K., Reynolds, F., Weissleder, R., Josephson, L., 2006. Nanoparticle imaging of integrins on tumor cells. Neoplasia 8, 214−222.

Mykhaylyk, O., Antequera, Y.S., Vlaskou, D., Plank, C., 2007. Generation of magnetic nonviral gene transfer agents and magnetofection *in vitro*. Nat. Protoc. 2, 2391−2411.

Owen, C.S., 1978. High gradient magnetic separation of erythrocytes. Biophys. J. 22, 171−178.

Park, J.H., Lee, J., Kim, B.J., Yang, S.H., 2014. Bioinspired encapsulation of living cells within inorganic nanoshells. In: Fakhrullin, R.F., Choi, I., Lvov, Y.M. (Eds.), Cell Surface Engineering: Fabrication of Functional Nanoshells. RSC, Cambridge, pp. 48−79.

Patzak, M., Dostalek, P., Fogarty, R.V., Safarik, I., Tobin, J.M., 1997. Development of magnetic biosorbents for metal uptake. Biotechnol. Tech. 11, 483−487.

Payne, M.J., Campbell, S., Kroll, R.G., 1993. Lectin-magnetic separation can enhance methods for the detection of *Staphylococcus aureus*, *Salmonella enteritidis* and *Listeria monocytogenes*. Food Microbiol. 10, 75−83.

Plank, C., Zelphati, O., Mykhaylyk, O., 2011. Magnetically enhanced nucleic acid delivery. Ten years of magnetofection-progress and prospects. Adv. Drug Deliv. Rev. 63, 1300−1331.

Porter, J., Pickup, R.W., 1998. Separation of natural populations of coliform bacteria from freshwater and sewage by magnetic-bead cell sorting. J. Microbiol. Methods 33, 221−226.

Porter, J., Robinson, J., Pickup, R., Edwards, C., 1998. An evaluation of lectin-mediated magnetic bead cell sorting for the targeted separation of enteric bacteria. J. Appl. Microbiol. 84, 722–732.

Pospiskova, K., Prochazkova, G., Safarik, I., 2013. One-step magnetic modification of yeast cells by microwave-synthesized iron oxide microparticles. Lett. Appl. Microbiol. 56, 456–461.

Prochazkova, G., Safarik, I., Branyik, T., 2013. Harvesting microalgae with microwave synthesized magnetic microparticles. Bioresour. Tech. 130, 472–477.

Qi, H., Li, Z., Du, K., Mu, K., Zhou, Q., Liang, S., et al., 2014. Transferrin-targeted magnetic/fluorescence micelles as a specific bi-functional nanoprobe for imaging liver tumor. Nanoscale Res. Lett. 9, Article No. 595.

Rad, A.M., Arbab, A.S., Iskander, A.S.M., Jiang, Q., Soltanian-Zadeh, H., 2007. Quantification of superparamagenetic iron oxide (SPIO)-labeled cells using MRI. J. Magn. Reson. Imaging 26, 366–374.

Reidt, U., Geisberger, B., Heller, C., Friedberger, A., 2011. Automated immunomagnetic processing and separation of *Legionella pneumophila* with manual detection by sandwich ELISA and PCR amplification of the ompS gene. J. Lab. Autom. 16, 157–164.

Robatjazi, S.M., Shojaosadati, S.A., Khalilzadeh, R., Farahani, E.V., 2010. Optimization of the covalent coupling and ionic adsorption of magnetic nanoparticles on *Flavobacterium* ATCC 27551 using the Taguchi method. Biocatal. Biotransform. 28, 304–312.

Robatjazi, S.M., Shojaosadati, S.A., Khalilzadeh, R., Farahani, E.V., Zeinoddini, M., 2013. Continuous biodegradation of parathion by immobilized *Sphingomonas* sp. in magnetically fixed-bed bioreactors and evaluation of the enzyme stability of immobilized bacteria. Biotechnol. Lett. 35, 67–73.

Russell, A.P., Evans, C.H., Westcott, V.C., 1987. Measurement of the susceptibility of paramagnetically labeled cells with paramagnetic solutions. Anal. Biochem. 164, 181–189.

Rye, P.D., Bovin, N.V., 1997. Selection of carbohydrate-binding cell phenotypes using oligosaccharide-coated magnetic particles. Glycobiology 7, 179–182.

Safarik, I., Safarikova, M., 1999. Use of magnetic techniques for the isolation of cells. J. Chromatogr. B 722, 33–53.

Safarik, I., Safarikova, M., 2007. Magnetically modified microbial cells: a new type of magnetic adsorbents. China Particuol. 5, 19–25.

Safarik, I., Safarikova, M., 2012. Magnetic nanoparticles for *in vitro* biological and medical applications: an overview. In: Thanh, N.T.K. (Ed.), Magnetic Nanoparticles: From Fabrication to Biomedical and Clinical Applications. CRC Press/Taylor and Francis, Boca Raton, pp. 215–242.

Safarik, I., Ptackova, L., Safarikova, M., 2002. Adsorption of dyes on magnetically labeled baker's yeast cells. Eur. Cells Mater. 3 (Suppl. 2), 52–55.

Safarik, I., Rego, L.F.T., Borovska, M., Mosiniewicz-Szablewska, E., Weyda, F., Safarikova, M., 2007. New magnetically responsive yeast-based biosorbent for the efficient removal of water-soluble dyes. Enzyme Microb. Technol. 40, 1551–1556.

Safarik, I., Sabatkova, Z., Safarikova, M., 2008. Hydrogen peroxide removal with magnetically responsive *Saccharomyces cerevisiae* cells. J. Agric. Food Chem. 56, 7925–7928.

Safarik, I., Sabatkova, Z., Safarikova, M., 2009. Invert sugar formation with *Saccharomyces cerevisiae* cells encapsulated in magnetically responsive alginate microparticles. J. Magn. Magn. Mater. 321, 1478–1481.

Safarik, I., Pospiskova, K., Horska, K., Safarikova, M., 2012. Potential of magnetically responsive (nano)biocomposites. Soft Matter 8, 5407–5413.

Safarik, I., Maderova, Z., Pospiskova, K., Horska, K., Safarikova, M., 2014. Magnetic decoration and labeling of prokaryotic and eukaryotic cells. In: Fakhrullin, R.F., Choi, I., Lvov, Y.M. (Eds.), Cell Surface Engineering: Fabrication of Functional Nanoshells. RSC, Cambridge, pp. 185–215.

Safarik, I., Maderova, Z., Pospiskova, K., Baldikova, E., Horska, K., Safarikova, M., 2015a. Magnetically responsive yeast cells: methods of preparation and applications. Yeast 32, 227–237.

Safarik, I., Pospiskova, K., Maderova, Z., Baldikova, E., Horska, K., Safarikova, M., 2015b. Microwave-synthesized magnetic chitosan microparticles for the immobilization of yeast cells. Yeast 32, 239–243.

Safarikova, M., Ptackova, L., Kibrikova, I., Safarik, I., 2005. Biosorption of water-soluble dyes on magnetically modified *Saccharomyces cerevisiae* subsp. *uvarum* cells. Chemosphere 59, 831–835.

Safarikova, M., Atanasova, N., Ivanova, V., Weyda, F., Tonkova, A., 2007. Cyclodextrin glucanotransferase synthesis by semicontinuous cultivation of magnetic biocatalysts from cells of *Bacillus circulans* ATCC 21783. Process Biochem. 42, 1454–1459.

Safarikova, M., Pona, B.M.R., Mosiniewicz-Szablewska, E., Weyda, F., Safarik, I., 2008. Dye adsorption on magnetically modified *Chlorella vulgaris* cells. Fresenius Environ. Bull. 17, 486–492.

Safarikova, M., Maderova, Z., Safarik, I., 2009. Ferrofluid modified *Saccharomyces cerevisiae* cells for biocatalysis. Food Res. Int. 42, 521–524.

Saltan, N., Kutlu, H.M., Hur, D., Iscan, A., Say, R., 2011. Interaction of cancer cells with magnetic nanoparticles modified by methacrylamido-folic acid. Int. J. Nanomed. 6, 477–484.

Schade, K., Calzado, E.G., Sarmiento, R., Chacana, P.A., Porankiewicz-Asplund, J., Terzolo, H.R., 2005. Chicken egg yolk antibodies (IgY-technology): a review of progress in production and use in research and human and veterinary medicine. Atla Altern. Lab. Anim. 33, 129–154.

Schüler, D. (Ed.), 2007. Magnetoreception and Magnetosomes in Bacteria. Springer, Berlin, Heidelberg.

Shahnaz, G., Kremser, C., Reinisch, A., Vetter, A., Laffleur, F., Rahmat, D., et al., 2013. Efficient MRI labeling of endothelial progenitor cells: design of thiolated surface stabilized superparamagnetic iron oxide nanoparticles. Eur. J. Pharm. Biopharm. 85, 346–355.

Shan, D.Y., Shi, Y.Z., Duan, S., Wei, Y., Cai, Q., Yang, X.P., 2013. Electrospun magnetic poly(L-lactide) (PLLA) nanofibers by incorporating PLLA-stabilized Fe_3O_4 nanoparticles. Mater. Sci. Eng. C Mater. Biol. Appl. 33, 3498–3505.

Shevtsov, M.A., Nikolaev, B.P., Yakovleva, L.Y., Marchenko, Y.Y., Dobrodumov, A.V., Mikhrina, A.L., et al., 2014. Superparamagnetic iron oxide nanoparticles conjugated with epidermal growth factor (SPION-EGF) for targeting brain tumors. Int. J. Nanomed. 9, 273–287.

Singh, R.K., Patel, K.D., Lee, J.H., Lee, E.J., Kim, J.H., Kim, T.H., et al., 2014. Potential of magnetic nanofiber scaffolds with mechanical and biological properties applicable for bone regeneration. PLoS One 9, e91584.

Sipe, J.C., Filippi, M., Martino, G., Furlan, R., Rocca, M.A., Rovaris, M., et al., 1999. Method for intracellular magnetic labeling of human mononuclear cells using approved iron contrast agents. Magn. Reson. Imaging 17, 1521–1523.

Struys, T., Ketkar-Atre, A., Gervois, P., Leten, C., Hilkens, P., Martens, W., et al., 2013. Magnetic resonance imaging of human dental pulp stem cells *in vitro* and *in vivo*. Cell Transplant. 22, 1813–1829.

Suh, S.H., Jaykus, L.A., 2013. Nucleic acid aptamers for capture and detection of *Listeria* spp. J. Biotechnol. 167, 454–461.

Sykova, E., Jendelova, P., 2005. Magnetic resonance tracking of implanted adult and embryonic stem cells in injured brain and spinal cord. Ann. N. Y. Acad. Sci. 1049, 146–160.

Tada, Y., Dohi, T., Horiuchi, T., Malchesky, P.S., Zborowski, M., 1991. Study on analytical magnetic separation system of bacterial species. J. Life Support Technol. 4, 17–27.

Takeda, S., Furuyoshi, T., Tari, I., Nakahira, A., Kakehi, Y., Kusaka, T., et al., 2000. Separation of algae with magnetic iron(III) oxide particles using superconducting high gradient magnetic field. Nippon Kagaku Kaishi 9 (9), 661–663.

Tian, F., Chen, G., Yi, P., Zhang, J., Li, A., Zhang, J., et al., 2014. Fates of Fe_3O_4 and $Fe_3O_4@SiO_2$ nanoparticles in human mesenchymal stem cells assessed by synchrotron radiation-based techniques. Biomaterials 35, 6412–6421.

Todd, T., Zhen, Z.P., Tang, W., Chen, H.M., Wang, G., Chuang, Y.J., et al., 2014. Iron oxide nanoparticle encapsulated diatoms for magnetic delivery of small molecules to tumors. Nanoscale 6, 2073–2076.

Toh, P.Y., Ng, B.W., Ahmad, A.L., Chieh, D.C.J., Lim, J., 2014a. Magnetophoretic separation of *Chlorella* sp.: role of cationic polymer binder. Process Saf. Environ. Prot. 92, 515–521.

Toh, P.Y., Ng, B.W., Chong, C.H., Ahmad, A.L., Yang, J.W., Derek, C.J.C., et al., 2014b. Magnetophoretic separation of microalgae: the role of nanoparticles and polymer binder in harvesting biofuel. RSC Adv. 4, 4114–4121.

Torchilin, V.P., 2008. Tat peptide-mediated intracellular delivery of pharmaceutical nanocarriers. Adv. Drug Deliv. Rev. 60, 548–558.

Tung, C.-H., Weissleder, R., 2002. Cell-penetrating peptide conjugations and magnetic cell labels. In: Langel, U. (Ed.), Cell-Penetrating Peptides: Processes and Applications. CRC Press, Boca Raton, pp. 327–346.

Uchida, M., Flenniken, M.L., Allen, M., Willits, D.A., Crowley, B.E., Brumfield, S., et al., 2006. Targeting of cancer cells with ferrimagnetic ferritin cage nanoparticles. J. Am. Chem. Soc. 128, 16626–16633.

Uchida, M., Terashima, M., Cunningham, C.H., Suzuki, Y., Willits, D.A., Willis, A.F., et al., 2008. A human ferritin iron oxide nano-composite magnetic resonance contrast agent. Magn. Reson. Med. 60, 1073–1081.

Uzun, L., Saglam, N., Safarikova, M., Safarik, I., Denizli, A., 2011. Copper biosorption on magnetically modified yeast cells under magnetic field. Sep. Sci. Technol. 46, 1045–1051.

Vandergriff, A.C., Hensley, T.M., Henry, E.T., Shen, D., Anthony, S., Zhang, J., et al., 2014. Magnetic targeting of cardiosphere-derived stem cells with ferumoxytol nanoparticles for treating rats with myocardial infarction. Biomaterials 35, 8528–8539.

Venu, R., Lim, B., Hu, X.H., Jeong, I., Ramulu, T.S., Kim, C.G., 2013. On-chip manipulation and trapping of microorganisms using a patterned magnetic pathway. Microfluid. Nanofluid. 14, 277–285.

Walczak, P., Kedziorek, D.A., Gilad, A.A., Lin, S., Bulte, J.W.M., 2005. Instant MR labeling of stem cells using magnetoelectroporation. Magn. Reson. Med. 54, 769–774.

Wang, D.S., He, J.B., Rosenzweig, N., Rosenzweig, Z., 2004. Superparamagnetic Fe_2O_3 beads-CdSe/ZnS quantum dots core-shell nanocomposite particles for cell separation. Nano Lett. 4, 409–413.

Wang, H.T., Chan, Y.H., Feng, S.W., Lo, Y.J., Teng, N.C., Huang, H.M., 2014a. Development and biocompatibility tests of electrospun poly-L-lactide nanofibrous membranes incorporating oleic acid-coated Fe_3O_4. J. Polym. Eng. 34, 241–245.

Wang, X., Gai, Z.H., Yu, B., Feng, J.H., Xu, C.Y., Yuan, Y., et al., 2007. Degradation of carbazole by microbial cells immobilized in magnetic gellan gum gel beads. Appl. Environ. Microbiol. 73, 6421–6428.

Wang, X., Xing, X., Zhang, B., Liu, F., Cheng, Y., Shi, D., 2014b. Surface engineered antifouling optomagnetic SPIONs for bimodal targeted imaging of pancreatic cancer cells. Int. J. Nanomed. 9, 1601–1615.

Wang, Y.-C., Nakagawa, M., Garitaonandia, I., Slavin, I., Altun, G., Lacharite, R.M., et al., 2011. Specific lectin biomarkers for isolation of human pluripotent stem cells identified through array-based glycomic analysis. Cell Res. 21, 1551–1563.

Wang, Z., Cuschieri, A., 2013. Tumour cell labelling by magnetic nanoparticles with determination of intracellular iron content and spatial distribution of the intracellular iron. Int. J. Mol. Sci. 14, 9111–9125.

Wei, Y., Zhang, X.H., Song, Y., Han, B., Hu, X.Y., Wang, X.Z., et al., 2011. Magnetic biodegradable Fe_3O_4/CS/PVA nanofibrous membranes for bone regeneration. Biomed. Mater. 6, Article No. 055008.

Xie, H., Zhu, Y.H., Jiang, W.L., Zhou, Q., Yang, H., Gu, N., et al., 2011. Lactoferrin-conjugated superparamagnetic iron oxide nanoparticles as a specific MRI contrast agent for detection of brain glioma *in vivo*. Biomaterials 32, 495–502.

Xie, J.X., Zhang, X.D., Wang, H., Zheng, H.Z., Huang, Y.M., 2012. Analytical and environmental applications of nanoparticles as enzyme mimetics. Trends Anal. Chem. 39, 114–129.

Yadidia, R., Abeliovich, A., Belfort, G., 1977. Algae removal by high gradient magnetic filtration. Environ. Sci. Technol. 11, 913–916.

Yavuz, H., Denizli, A., Gungunes, H., Safarikova, M., Safarik, I., 2006. Biosorption of mercury on magnetically modified yeast cells. Sep. Purif. Technol. 52, 253–260.

Zborowski, M., Malchesky, P.S., Savon, S.R., Green, R., Hall, G.S., Nose, Y., 1991. Modification of ferrography method for analysis of lymphocytes and bacteria. Wear 142, 135–149.

Zborowski, M., Malchesky, P.S., Jan, T.F., Hall, G.S., 1992. Quantitative separation of bacteria in saline solution using lanthanide Er(III) and a magnetic field. J. Gen. Microbiol. 138, 63–68.

Zborowski, M., Tada, Y., Malchesky, P.S., Hall, G.S., 1993. Dark-field microscopy analysis of the magnetic deposition of bacteria on a glass surface. Colloids Surf. A Physicochem. Eng. Aspects 77, 209–218.

Zborowski, M., Fuh, C.B., Green, R., Sun, L., Chalmers, J.J., 1995. Analytical magnetapheresis of ferritin-labeled lymphocytes. Anal. Chem. 67, 3702–3712.

Zborowski, M., Fuh, C.B., Green, R., Baldwin, N.J., Reddy, S., Douglas, T., et al., 1996. Immunomagnetic isolation of magnetoferritin-labeled cells in a modified ferrograph. Cytometry 24, 251–259.

Zhao, S., Wang, Y., Gao, C., Zhang, J., Bao, H., Wang, Z., et al., 2014. Superparamagnetic iron oxide magnetic nanomaterial-labeled bone marrow mesenchymal stem cells for rat liver repair after hepatectomy. J. Surg. Res. 191, 290–301.

Zheng, B.Z., Zhang, M.H., Xiao, D., Jin, Y., Choi, M.M.F., 2010. Fast microwave synthesis of Fe_3O_4 and Fe_3O_4/Ag magnetic nanoparticles using Fe^{2+} as precursor. Inorg. Mater. 46, 1106–1111.

5.1.4 Magneticky modifikované kvasinkové buňky

Kvasinky rodu *Saccharomyces* reprezentují velice významnou skupinu mikroorganismů, jež jsou používány nejen k přípravě pokrmů a nápojů, pro produkci bioetanolu a léčiv, ale navíc mohou sloužit jako efektivní nástroje pro bioremediace. Na druhou stranu existují další rody kvasinek, např. *Kluyveromyces*, *Rhodotorula* a *Yarrowia*, které také mohou vykazovat zajímavé vlastnosti a být využity k nejrůznějším bioaplikacím.

První kapitola článku je věnována přípravě magnetických derivátů kvasinkových buněk. Jsou zde popisovány nejen základní techniky, jako je přímé navázání magnetických nanočástic na buněčné stěny materiálu, kovalentní imobilizace na magnetické nosiče, enkapsulace do magnetických polymerů či zesítění, ale také další méně časté a velmi specifické způsoby zahrnující například interakce s imunomagnetickými částicemi.

Druhá část článku je pak zaměřena na potenciální využití magneticky modifikovaných kvasinkových buněk, a to pro biokatalytické reakce používané v biotechnologiích (např. tvorba invertního cukru, produkce etanolu, degradace peroxidu vodíku), sorpce xenobiotik organického i anorganického původu, a v neposlední řadě také k detekci genotoxických látek prostřednictvím mikrofluidního biosenzoru.

Příloha 4:

Magnetically responsive yeast cells: methods of preparation and application

Safarik I, Maderova Z, Pospiskova K, Baldikova E, Horska K, Safarikova M

Yeast 32, **2015**, 227-237

Yeast
Yeast 2015; **32**: 227–237.
Published online 7 November 2014 in Wiley Online Library
(wileyonlinelibrary.com) **DOI:** 10.1002/yea.3043

Special Issue Article

Magnetically responsive yeast cells: methods of preparation and applications

Ivo Safarik[1,2]*, Zdenka Maderova[1], Kristyna Pospiskova[2], Eva Baldikova[1], Katerina Horska[1] and Mirka Safarikova[1]

[1]*Department of Nanobiotechnology, Institute of Nanobiology and Structural Biology of GCRC, Ceske Budejovice, Czech Republic*
[2]*Regional Centre of Advanced Technologies and Materials, Palacky University, Olomouc, Czech Republic*

**Correspondence to:*
I. Safarik, Department of Nanobiotechnology, Institute of Nanobiology and Structural Biology of GCRC, Na Sadkach 7, 370 05 Ceske Budejovice, Czech Republic.
E-mail: ivosaf@yahoo.com;
WWW: www.nh.cas.cz/people/safarik

Received: 15 March 2014
Accepted: 19 September 2014

Abstract

Magnetically modified yeast cells represent an interesting type of biocomposite material, applicable in various areas of bioanalysis, biotechnology and environmental technology. In this review, typical examples of magnetic modifications of yeast cells of the genera *Saccharomyces, Kluyveromyces, Rhodotorula and Yarrowia* are presented, as well as their possible applications as biocatalysts, active part of biosensors and biosorbents for the separation of organic xenobiotics, heavy metal ions and radionuclides.

Keywords: **yeast cells; *Saccharomyces*; *Kluyveromyces*; *Rhodotorula*; *Yarrowia*; magnetic modification**

Introduction

Yeasts are unicellular fungi that belong to different taxonomic groups. Among these, species of the *Saccharomyces sensu stricto* complex have been widely used by humans for preparing food and beverages. The yeast *Saccharomyces cerevisiae* and its relatives in the *Saccharomyces sensu stricto* complex are in fact the most useful and industrially exploited microorganisms. In addition to traditional production of food and beverages, this group of yeasts is currently used in the production of renewable fuels (bio-ethanol), food ingredients and pharmaceuticals. Another use of *S. cerevisiae* cells is in environmental applications, such as bioremediation of heavy metal ions and organic xenobiotics. *S. cerevisiae* cells can be obtained in large amounts because they are a by-product of large fermentation industries (e.g. the brewing, wine and bio-ethanol industries); the surplus yeast produced from these industries can be obtained at a low price. In addition, *S. cerevisiae* strains are described as 'generally recognized as safe' organisms by the US Food and Drug Administration (FDA) and are in the 'qualified presumption of safety' (QPS) list of the European Food Safety Authority, which means that these cells can be freely manipulated without public concern; this fact increases the feasibility of possible applications of yeast biomass in biotechnology and environmental technology processes (Sicard and Legras, 2011; Soares and Soares, 2012). In addition to *S. cerevisiae*, yeast cells belonging to other genera can also be used for important applications (Johnson, 2013a, 2013b).

Many prokaryotic and eukaryotic cells can interact with a wide range of nano- and microparticles. The modified cells usually maintain their viability, but the presence of foreign material on their surfaces, in protoplasm or in intracellular organelles, can provide additional functionalities (Fakhrullin and Lvov, 2012; Fakhrullin *et al*., 2014). Modification of cells with magnetic nano- and microparticles is exceptionally important and magnetically modified

cells have been used in many applications (Naumenko *et al*., 2014; Safarik *et al*., 2014a). Yeast cells magnetically modified using different procedures can be employed as whole-cell biosensors and whole-cell biocatalysts and be applied in toxicity microscreening devices and also as efficient adsorbents of different types of organic and inorganic xenobiotics (Safarik *et al*., 2014a; Safarik and Safarikova, 2007).

In this review, we focus on yeast species belonging to the genera *Saccharomyces*, *Kluyveromyces*, *Rhodotorula* and *Yarrowia* and on the interaction of these yeast cells with magnetic nano- and microparticles, in order to obtain magnetically responsive cells. Various procedures and materials used to prepare magnetic yeast cells are depicted and the most important examples of their applications are described.

Magnetic labelling of yeast cells

The magnetization of originally diamagnetic yeast cells can be usually performed by the attachment of magnetic nano- or microparticles on the cell surface; during growth of the cells, magnetic particles can be internalized into the periplasmic space. Alternatively, paramagnetic ions can be used for magnetic modification of the cells. The common characteristics of all magnetically modified cells are their specific interactions with an external magnetic field. In general, different types of responses of magnetic materials to an external magnetic field enable various applications, such as selective separation and localization of magnetically responsive cells using an external magnetic field, heat generation (which is caused by magnetic particles subjected to a high-frequency alternating magnetic field) or increase of a negative T2 contrast by magnetic iron oxide nanoparticles during magnetic resonance imaging (MRI) (Safarik *et al*., 2014a).

The individual magnetization procedures are described in more detail below.

Interaction of target cells with magnetic nano- and microparticles

Different types of magnetic microparticles, as well as ionically and sterically stabilized magnetic nanoparticles, have been used for the magnetic modification of target cells. Magnetic modification of yeast cells can be performed using an appropriate magnetic fluid. In the simplest way, perchloric acid-stabilized magnetic fluid was mixed with yeast cells washed with, and suspended in, acetate buffer, pH 4.6; alternatively, tetramethylammonium hydroxide-stabilized magnetic fluid was used for modification of yeast cells in 0.1 M glycine–NaOH buffer, pH 10.6; after a short time period, magnetic particles were precipitated on the cell surface (Figure 1). After washing, the magnetically modified cells were used as whole-cell biocatalysts for hydrogen peroxide degradation or sucrose hydrolysis. Alternatively, the modified cells were heated in a boiling water bath to kill the cells, resulting in the formation of a stable adsorbent for the removal of selected organic and inorganic xenobiotics (Azevedo *et al*., 2003; Bai *et al*., 2012; Safarik *et al*., 2002; Safarikova *et al*., 2005, 2009; Yavuz *et al*., 2006). Dried *Kluyveromyces marxianus* (fodder yeast) cells were thoroughly washed with 0.1 M acetic acid to remove soluble macromolecules, which caused spontaneous precipitation of magnetic fluid; after suspending the cells in the same solution, the addition of perchloric acid-stabilized magnetic fluid resulted in the formation of magnetically modified yeast cells (Mosiniewicz-Szablewska *et al*., 2010; Safarik *et al*., 2007).

Ferrofluid modification of dormant yeast cells or cells killed by high temperature led to the deposition of iron oxide nanoparticles, mainly on the cell surface; in contrast, ferrofluid modification of actively growing cells can lead to the accumulation of magnetic nanoparticles in the periplasmic space (Azevedo *et al*., 2003). Also, magnetic nanoparticles surface-functionalized with meso-2,3-dimercaptosuccinic acid (Morais *et al*., 2004) and poly(allylamine hydrochloride)-stabilized magnetic iron oxide nanoparticles (Garcia-Alonso *et al*., 2010) have been successfully used for baker's yeast magnetization.

Another procedure was based on the attachment of submicron, acicular maghemite particles on the yeast cells; the binding occurred irrespective of the solution pH and surface charge and was essentially irreversible (Dauer and Dunlop, 1991).

An extremely simple procedure for the magnetic modification of yeast cells has been developed recently, based on the use of microwave-synthesized magnetic iron oxides nano- and microparticles. Two very cheap starting chemicals were used, ferrous sulphate heptahydrate and sodium or potassium

DOI: 10.1002/yea

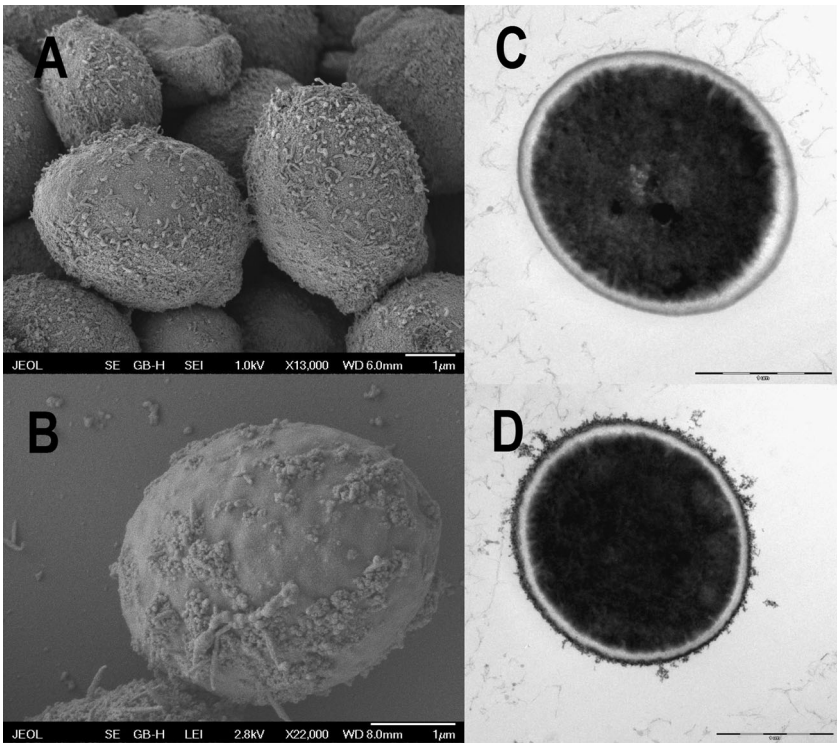

Figure 1. (A, B) SEM images of ferrofluid-modified *Saccharomyces cerevisiae* cells, showing attached magnetic nanoparticles and their aggregates on the cell surface; bars = 1 μm. (C) TEM image of a native *Saccharomyces cerevisiae* cell; bar = 1 μm. (D) TEM image of a ferrofluid modified cell with attached magnetic iron oxide nanoparticles on the cell wall; bar = 1 μm. Reproduced with permission from Safarikova *et al.* (2009)

hydroxide; after their mixing and formation of mixed iron hydroxides, the suspension underwent microwave treatment (a regular kitchen microwave oven can be used successfully) and microparticles of magnetic iron oxides formed (Pospiskova *et al.*, 2013; Zheng *et al.*, 2010). Mixing of magnetic particles with yeast cell (*S. cerevisiae*) suspensions caused cell flocculation and magnetically responsive cell aggregates, usually ca. 100–300 μm in diameter, were formed (Figure 2) (Pospiskova *et al.*, 2013). The magnetic iron oxide particles were also bound to the surface of *S. cerevisiae* cells at high pH values, where both reaction partners exhibited negative ζ-potential (Pospiskova *et al.*, 2013; Schwegmann *et al.*, 2010).

In an alternative procedure, the cells of *S. cerevisiae* and *S. bayanus* were made responsive to a magnetic field by the adsorption of superparamagnetic maghemite (γ-Fe_2O_3) nanoparticles coated with a thin layer of silica and grafted with (aminoethylamino)propylmethyldimethoxysilane (APMS). The terminal amino groups of the APMS molecules provided a positive charge on the nanoparticles' surfaces and promoted their electrostatic absorption onto the negatively charged surfaces of the yeast cells. The optimal mass ratio between the magnetic nanoparticles and the wine yeast cells was determined to be 1:10 (Berovic *et al.*, 2014).

It was shown that bottom-fermenting yeast cells adhere to magnetic, polystyrene-coated latex beads, which can be easily removed from the cell suspension by using a strong permanent magnet. At pH 4.5, electrostatic repulsion between yeast cells and magnetic latex beads was found to be minimal and yeast cell adhesion was predominantly based on hydrophobic interactions (Straver and Kijne, 1996).

An interesting procedure for coating *S. cerevisiae* yeast cells by magnetite nanoparticles via electrostatic interactions has been described recently. First, poly(allylamine hydrochloride) (PAH) was coated onto hydrated yeast cells whose surfaces were negatively charged in water, then the cells were coated with poly(sodium polystyrene sulphonate) (PSS).

DOI: 10.1002/yea

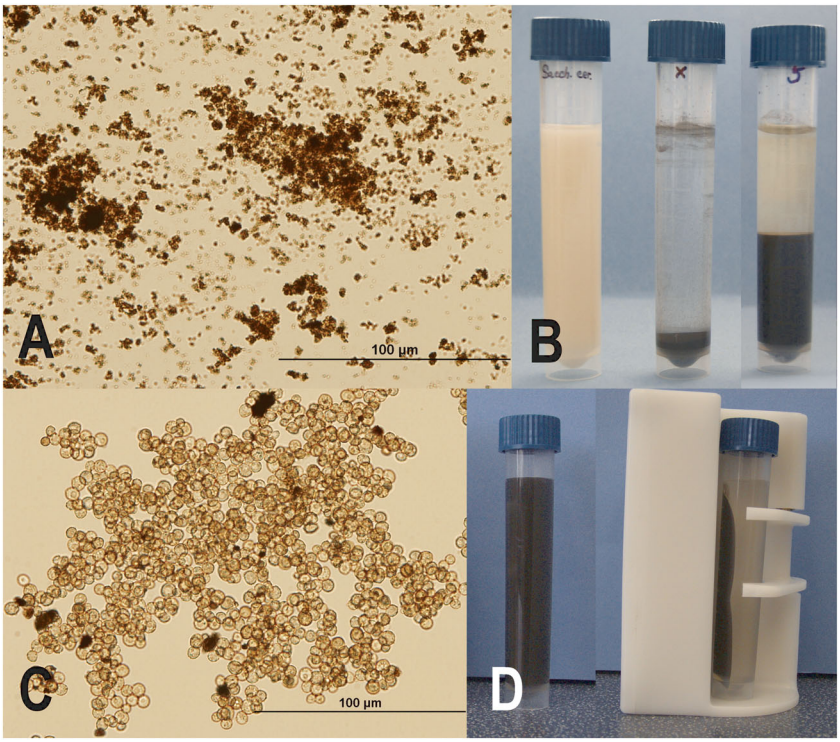

Figure 2. (A) Optical microscopy of magnetic iron oxides microparticles prepared by microwave assisted synthesis. (B) Process of magnetic modification of yeast cells: left tube, *S. cerevisiae* cell suspension; middle tube, sedimented iron oxide microparticles for magnetic modification; right tube, sedimented magnetically modified yeast cells. (C) Optical microscopy of *S. cerevisiae* cells modified by iron oxides microparticles. (D) Magnetic separation of magnetically modified yeast cells. Reproduced with permission from Pospiskova *et al.* (2013)

After repeating the procedure to build PAH–PSS–PAH coatings on the cells, magnetite nanoparticles were deposited on the cells before the deposition of two additional polyelectrolyte layers. The final product had the layer structure PAH–PSS–PAH–magnetic nanoparticles–PAH–PSS, which preserved the viability of the yeast cells. Magnetic nanoparticles formed a multilayered coating on the outer side of the yeast cell walls. Using yeast cells expressing GFP, it was shown that magnetic modification had little effect on fluorescence emission (Fakhrullin *et al.*, 2010).

Recently the modification of living yeast cells with multilayers of graphene oxide nanosheets via layer-by-layer self-assembly has been reported. Graphene oxide nanosheets with opposite charges were alternately coated together with magnetite nanoparticles onto the individual yeast cells while preserving their viability (Yang *et al.*, 2012).

Information about the depth of clusters penetration inside the biomembrane, the typical sizes of clusters and the dispersion of magnetic cluster sizes in magnetically modified *S. cerevisiae* cells has been obtained recently (Gorobets *et al.*, 2011, 2013a).

Covalent immobilization of cells on magnetic carriers

Covalent binding is an often-used technique for the immobilization of biopolymers, but is not used so often for the immobilization of living cells. Covalent binding of microbial cells on a magnetic carrier is usually possible via reactive groups on the surface, or through the aid of a reactive binding which links the cells to the carrier. Various coupling agents, e.g. aminosilane, carbodiimide or glutaraldehyde, may be employed to introduce a specific group onto the carrier surface, which can subsequently interact with reactive groups on the cell surface. In typical examples of covalent immobilization of cells, magnetic chitosan particles, activated by glutaraldehyde, have been used for

DOI: 10.1002/yea

S. cerevisiae immobilization (Ivanova *et al*., 2011; Safarik *et al*., 2014b). Alternatively, magnetic cellulose microparticles, after their activation with periodic acid, were used for immobilization of the same yeast cells (Ivanova *et al*., 2011).

Entrapment of cells into biocompatible polymers

Yeast cells can be entrapped in natural or biocompatible synthetic carriers (gels). The carriers can be grouped according to the mechanism leading to the gel formation. Gels can be formed by polymerization (e.g. polyacrylamide, polymethacrylate), crosslinking (e.g. proteins), polycondensation (polyurethane, epoxy resins), thermal gelation (e.g. gelatin, agar, agarose), ionotropic gelation (e.g. alginate, chitosan) and precipitation (cellulose, cellulose triacetate). The gel is formed in the presence of the cells and appropriate magnetic materials. There are various methods available to obtain particles (beads) containing entrapped cells and magnetic particles (Brodelius and Vandamme, 1987; Safarik *et al*., 2014a):

- *Block polymerization*, with subsequent mechanical disintegration into particles. This is a simple method but it results in irregular particles of a wide size distribution.
- *Moulding of particles (beads) in a template form*. This method results in a uniform preparation of immobilized cells but it is less suitable for the preparation of large quantities of immobilized cells.
- *Bead formation in a two-phase system*. Spherical beads can be prepared in large quantities by suspending an aqueous mixture of cells, magnetic particles and polymer in a hydrophobic phase under stirring and subsequently inducing gel formation.
- *Bead formation of ionotropic polymers* after dripping the mixture of cells, magnetic particles and polymer into a medium containing appropriate hardening ions.

Such a procedure can be very mild, enabling magnetic modification of living cells and subsequently employing their biological activities. One of the major drawbacks of the entrapment technique is a possible diffusional limitation, as well as steric hindrance (Safarik *et al*., 2014a). In a typical example, magnetically responsive alginate beads containing entrapped *S. cerevisiae* cells and magnetite microparticles were prepared. Larger beads (2–3 mm in diameter) were prepared by dropping the mixture into a calcium chloride solution, while microbeads (the diameter of the majority of particles was in the range 50–100 μm) were prepared using the water-in-oil emulsification process (Figure 3). The yeast cells immobilized in magnetic alginate beads were used as whole-cell biocatalysts for hydrogen peroxide degradation (Safarik *et al*., 2008), sucrose hydrolysis (Safarik *et al*., 2009) and for ethanol production (Birnbaum and Larsson, 1982; Ivanova *et al*., 2011; Larsson and Mosbach, 1979; Liu *et al*., 2009; Sakai *et al*., 1994).

Crosslinking of yeast cells or cell walls

Yeast cell walls contain free amino and/or carboxyl groups, which can easily be crosslinked by bi- or

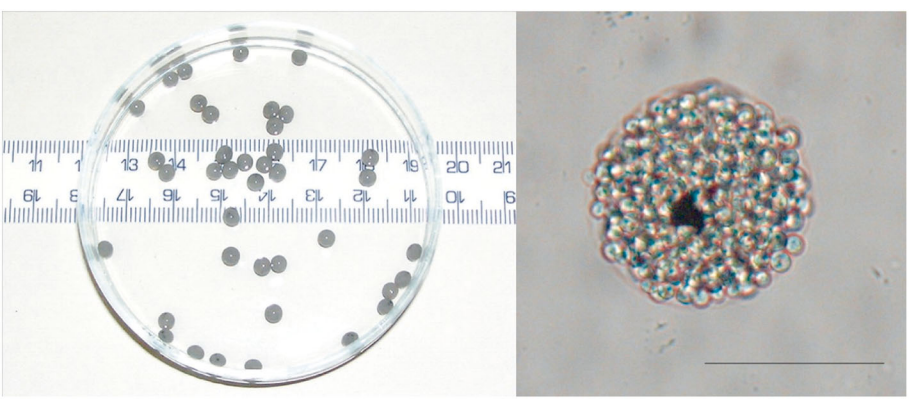

Figure 3. Magnetically responsive alginate beads containing entrapped *Saccharomyces cerevisiae* cells and magnetite microparticles: (left) millimeter-sized beads; (right) microbeads; scale bar =50 μm. Reproduced with permission from Safarik *et al.* (2008)

DOI: 10.1002/yea

multifunctional reagents, such as glutaraldehyde or toluene di-isocyanate. The cells can be also crosslinked in the presence of an inert protein such as gelatin, albumin, raw hen egg white or collagen. If magnetic particles are used throughout the crosslinking process, magnetic yeast cells can be prepared (Al-Hassan *et al.*, 1991; Ivanova *et al.*, 1996). Also, a recent patent describes the crosslinking of *S. cerevisiae* cells in the presence of magnetic iron oxide nanoparticles (Zhang *et al.*, 2012). A magnetic biosorbent has been prepared from epichlorhydrin-crosslinked *S. cerevisiae* cell walls in the presence of either native or silanized magnetite particles (Patzak *et al.*, 1997).

Specific interactions with immunomagnetic nano- and microparticles

Immunomagnetic detection and modification of cells implies the use of magnetic microbeads or magnetic nanoparticles–antibody systems, causing the particles to be selectively attached to target cells when added to a cell suspension. After incubation, target cells with attached magnetic particles (and also excess particles) are isolated with the help of an appropriate magnetic separator. Potential effects on the functional status of cells are minimized. This procedure is used especially for the detection of important microbial and protozoan pathogens and for the detection and removal of cancer cells (Safarik *et al.*, 2014a; Safarik and Safarikova, 1999, 2012).

Only a very limited number of papers have reported the application of immunomagnetic particles in yeast research. In one of the described procedures, sheep anti-mouse IgG-linked magnetic microspheres (Dynabeads M-280, Dynal) were coated with monoclonal antibody (mAb) 4E1 in order to magnetically separate *S. cerevisiae* transformants containing a *Candida albicans* gene of the mycelial surface antigen recognized by mAb 4E1 (Lamarre *et al.*, 2000).

Interaction with magnetic particles bearing immobilized biologically active compounds

Magnetic selective labelling of target cells can employ different types of biological interactions. In addition to the antigen–antibody interaction described above, interactions between biotin and avidin or streptavidin have recently been employed. In order to distinguish old and young brewer's yeast cells, the brewer's yeast was allowed to grow for an appropriate time. After centrifugation and washing, the cell suspension was biotinylated with a commercial biotinylating agent and the biotinylated cells were allowed to grow. After addition of Dynabeads–streptavidin, the old (parent biotinylated) cells were captured by the magnetic beads, while young cells appeared in the supernatant (Kurec, 2010; Kurec *et al.*, 2009).

Binding of paramagnetic cations on the cell surface

Lanthanides, especially erbium in the form of erbium chloride ($ErCl_3$), have been used for the magnetic labelling of a variety of cells. Erbium ions have a high affinity for the external cell surface and preserve their exceptionally high atomic magnetic dipole moment (9.3 Bohr magnetons) in various chemical structures. The mechanism of Er^{3+} binding to the cell surface is mostly ionic, with many different Er^{3+} binding sites, such as carboxyl groups in glycoproteins, differing in affinity and binding capacity. The other well-recognized lanthanide binding sites are the Ca^{2+} receptor sites on the cell wall (Safarik *et al.*, 2014a). Yeast cells labelled with erbium ions were efficiently separated by analytical magnetapheresis (Fuh *et al.*, 2000) or used for measuring volumetric magnetic susceptibility (Russell *et al.*, 1987).

Biosynthesis of magnetic particles within yeast cells

It has been shown recently that diamagnetic *S. cerevisiae* cells become magnetized (as observed by attraction towards a magnet) when grown with ferric citrate. The magnetization was further enhanced by genetic modification of iron homeostasis and introduction of ferritin. The acquired magnetizable properties enabled the cells to be attracted to a magnet and trapped by a magnetic column. Superconducting quantum interference device (SQUID) magnetometry confirmed and quantitatively characterized the acquired paramagnetism. Electron microscopy and energy-dispersive X-ray spectroscopy showed electron-dense, iron-containing aggregates within the magnetized cells. Magnetization-based screening of gene knock-outs identified *Tco89p*, a component of Target of rapamycin complex 1 (TORC1), as important for magnetization; loss

DOI: 10.1002/yea

of *TCO89* and treatment with rapamycin reduced magnetization in a *TCO89*-dependent manner. The *TCO89* expression level positively correlated with magnetization, enabling inducible magnetization (Nishida and Silver, 2012).

Applications of magnetically modified yeast cells

As mentioned in the previous section, different procedures are available to convert originally diamagnetic yeast cells into their magnetic derivatives. In this section, a selection of important applications of magnetically modified yeast cells are presented.

Magnetically modified yeast cells in biotechnology

Magnetic modification of living yeast cells can lead to the formation of magnetically responsive whole-cell biocatalysts. Both direct modification of cell walls with appropriate water-based magnetic fluids or magnetic microparticles, and entrapment of target yeast cells into biocompatible (bio) polymer gels in the presence of magnetic particles, can be performed in a simple way. The intracellular enzyme activities have not decreased substantially after the modification, as shown by hydrogen peroxide degradation and sucrose hydrolysis by intracellular enzymes catalase and invertase, respectively, present in magnetically modified *S. cerevisiae* cells (Pospiskova *et al*., 2013; Safarik *et al*., 2008, 2009; Safarikova *et al*., 2009). The same observation was made for the fermentation capacity and alcohol production, which were not influenced in the case of *S. cerevisiae* cells immobilized in calcium alginate gel together with varying concentrations of magnetic iron oxides or ferrites (Ivanova *et al*., 2011; Larsson and Mosbach, 1979). The production of ethanol by *K. marxianus* IMB3 immobilized in calcium alginate increased substantially when magnetite particles with immobilized β-galactosidase derived from the same strain were co-immobilized; the ethanol production increased further when Mn^{2+} ions were incorporated into fermentation media (Brady *et al*., 1997). Ethanol fermentation with magnetically modified *S. cerevisiae* cells was also performed in magnetically stabilized fluidized-bed reactors (Ivanova *et al*., 1996; Liu *et al*., 2009).

Also *S. cerevisiae* and *S. bayanus* cells modified with superparamagnetic maghemite nanoparticles, coated with a thin layer of silica and grafted with APMS, exhibited no negative influences of magnetization on the cell metabolism during the production of sparkling wine. The same results were confirmed in sensorial analyses of the sparkling wine produced. Separation of the magnetized waste yeast biomass in the bottle neck, using a relatively weak magnetic field gradient, could be successfully completed in approximately 15 min (Berovic *et al*., 2014).

In order to separate *S. cerevisiae* cells from aqueous suspensions, magnetically stabilized fluidized beds (MSFBs) can be employed. The magnetic particles consisted of a magnetic core of magnetite covered by a stable layer of activated carbon, used to adsorb the yeast cells from the suspension. The yeast cell concentration in the effluent was determined periodically by measuring the absorbance at 610 nm. It was shown that the continuous separation of yeast cells from aqueous suspensions by MSFB is possible. The removal efficiency was affected by different parameters, including the bed height, flow rate and initial concentration of cells. The removal efficiency reached 82%, and could be improved by varying the operational parameters (Al-Qodah and Al-Shannag, 2006).

Magnetic particles present within magnetic carriers are mainly used for magnetic manipulation. However, heat generation due to eddy currents and hysteresis induced by alternating magnetic field was utilized for the enhancement of ethanol formation, catalysed by yeasts immobilized together with iron powder or Ba-ferrite in alginate beads. Ethanol concentration increased by 12–14% with immobilized yeast; these effects were attributed to a 4 K rise in temperature inside the gel (Sakai *et al*., 1994).

A rapid and selective assay was developed to measure the cell surface hydrophobicity of brewer's yeast cells. During the so-called magnobead assay, bottom-fermenting yeast cells adhere to paramagnetic, polystyrene-coated latex beads, which can be easily removed from the cell suspension using a strong permanent magnet. At pH 4.5, electrostatic repulsion between yeast cells and latex beads was found to be minimal, and yeast cell adhesion was predominantly based on hydrophobic

DOI: 10.1002/yea

interactions. The percentage of cells adhering to the beads could be calculated and provided a measure for cell surface hydrophobicity (Straver and Kijne, 1996).

Magnetically modified yeast cells can be used as part of cost-effective microfluidic biosensor systems. One such screening method used viable, genetically modified green fluorescent protein (GFP) reporter yeast cells that were magnetically functionalized by biocompatible positively charged magnetic nanoparticles, with diameters of ca. 15 nm and held within a microfluidic device. The GFP reporter yeast cells were used to detect genotoxicity by monitoring the exposure of the cells to a well-known genotoxic chemical (methyl methane sulphonate); effective fluorescence emitted from the produced GFP was measured. The magnetically enhanced retention of the yeast cells, with their facile subsequent removal and reloading, allowed very convenient and rapid screening of genotoxic compounds (Fakhrullin *et al*., 2010; Garcia-Alonso *et al*., 2010).

Magnetically modified yeast cells as xenobiotic adsorbents

Yeast biomass represents an important and promising material for the biosorption of xenobiotics. In order to have a stabilized product enabling work for a long period of time, dead yeast cells are preferred. Fodder yeast cells of *K. marxianus* species are usually prepared in dried form, which enables their simple magnetic modification and the preparation of an inexpensive adsorbent (Safarik *et al*., 2007).

Magnetically modified *Saccharomyces* and *Kluyveromyces* cells were used for the adsorption of water soluble dyes from water solutions (Safarik *et al*., 2002, 2007; Safarikova *et al*., 2005; Tian *et al*., 2010; Wu *et al*., 2009; Yu *et al*., 2013). The maximum adsorption capacities vary greatly, depending on the structure of the dyes. Great differences can also be observed, even for dyes belonging to the same group (see Table 1). In most cases the adsorption process can be described by the Langmuir adsorption isotherm (Safarik *et al*., 2011). In order to increase the maximum adsorption capacity of magnetic brewer's yeast cells for cationic dyes, pyromellitic di-anhydride (PMDA)-modified yeast biomass in *N*,*N*-dimethylacetamide solution was prepared before the magnetization process (Yu *et al*., 2013).

Magnetically modified baker's, brewer's and fodder yeast cells were also tested as efficient adsorbents of heavy metal ions and radionuclides. Hg^{2+} and Cu^{2+} ions were separated by magnetic *S. cerevisiae* subsp. *uvarum* brewer's yeast. The adsorption equilibrium data were well fitted to the Langmuir isotherm; the yeast biomass could be easily regenerated by nitric acid with high effectiveness (Uzun *et al*., 2011; Yavuz *et al*., 2006). Strontium and ferrous ions could be successfully adsorbed on magnetic *K. marxianus* fodder yeast (Ji *et al*., 2010) and magnetic baker's yeast

Table 1. Comparison of maximum adsorption capacities, Q_{max} (mg/g), of magnetically modified yeast cells for tested dyes

Dyes	Colour index no.	*S. cerevisiae* (Safarik *et al*., 2002)	*S. cerevisiae* (Tian *et al*., 2010)	*S. cerevisiae* subsp. *uvarum* (Safarikova *et al*., 2005)	PMSA-modified brewer's yeast (Yu *et al*., 2013)	*Kluyveromyces marxianus* (Safarik *et al*., 2007)
Acridine orange	46005	82.8				62.2
Amido black 10B	20470			11.6		29.9
Aniline blue	42755	430.2		228.0		
Basic magenta	42510				520.9	
Bismarck brown	21000					75.7
Congo red	22120			93.1		49.7
Crystal violet	42555	85.9		41.7		42.9
Malachite green	42000	19.6				
Methyl violet	42535		60.84			
Methylene blue	52015				609.0	
Safranin O	50240	90.3		46.6		138.2
Saturn blue LBRR	34140					33.0

DOI: 10.1002/yea

(Gorobets *et al*., 2013b), respectively. Uranium ions were successfully isolated using ferrofluid-modified *Rhodotorula glutinis* cells (Bai *et al*., 2012), while hexavalent chromium ions were efficiently adsorbed on *Yarrowia lipolytica* cells modified with magnetite nanoparticles (Rao *et al*., 2013). *S. cerevisiae* cells immobilized on the surface of chitosan-coated magnetic nanoparticles were used for biosorption of Cu^{2+} (Peng *et al*., 2010) and Ce^{3+} (Ou *et al*., 2013) from aqueous solutions. Magnetically modified yeast cell walls were used for the adsorption of Cu^{2+}, Cd^{2+} and Ag^{+} ions (Patzak *et al*., 1997).

In some cases, yeast cells were modified to increase their adsorption capacities for heavy metal ions. Ethylenediamine-modified yeast biomass coated with magnetic chitosan microparticles was studied in a batch adsorption system for the removal of Pb^{2+} ions (Li *et al*., 2013). Ethylenediamine tetraacetic dianhydride-treated magnetic baker's yeast biomass was used to adsorb Ca^{2+}, Cd^{2+} and Pb^{2+} ions (Xu *et al*., 2011; Zhang *et al*., 2011).

Conclusion and outlook

In this review, we have focused our attention on the very interesting interdisciplinary topic of magnetically modified yeast cells. Different procedures for the magnetic modification of originally diamagnetic yeast cells have been developed. However, research on optimizing the magnetization of cells will continue, employing novel functionalized magnetic (nano)particles. Further progress can be especially expected in finding other interesting applications of magnetically modified cells in bioanalysis, biotechnology and environmental technology, e.g. as magnetically responsive whole cell biocatalysts or adsorbents.

Biocatalytic processes have become a very useful tool for the production of natural flavours and fragrances (Serra *et al*., 2005). Recently a few papers describing the use of (non-magnetic) immobilized yeast cells for bioflavour production have been published (Lalou *et al*., 2013; van der Sluis *et al*., 2001). Conversion of immobilized yeast cells into their magnetic derivatives would enable their simple removal from the reaction mixture and the application of magnetic field-assisted bioreactors (Hristov and Ivanova, 1999). Magnetic particles could also serve as carriers for the immobilization of target enzymes; after their co-entrapment to yeast cells containing gel particles or application into fermentation media, better bioflavour production could be achieved (Sun *et al*., 2013). In addition, magnetically modified yeast cells or yeast cell walls could serve as a cheap and biocompatible adsorbent for the elimination of off-odours in wines (Jimenez-Moreno and Ancin-Azpilicueta, 2009; Nieto-Rojo *et al*., 2014).

We believe that the number of applications of magnetically modified yeast cells will increase in the near future. There is still plenty of room for further work in this interesting area.

Acknowledgements

This review was prepared in the framework of COST Action FA0907 ***BIOFLAVOUR*** (www.bioflavour.insa-toulouse.fr), under the EU's Seventh Framework Programme for Research (FP7), and also by the Ministry of Education of the Czech Republic (Project No. LD13023, COST Action FA0907, Project No. LD13021–Action COST TD1003).

References

Al-Hassan Z, Ivanova V, Dobreva E, *et al.* 1991. Nonporous magnetic supports for cell immobilization. *J Ferment Bioeng* **71**: 114–117.

Al-Qodah Z, Al-Shannag M. 2006. Separation of yeast cells from aqueous solutions using magnetically stabilized fluidized beds. *Lett Appl Microbiol* **43**: 652–658.

Azevedo RB, Silva LP, Lemos APC, *et al*. 2003. Morphological study of *Saccharomyces cerevisiae* cells treated with magnetic fluid. *IEEE Trans Magn* **39**: 2660–2662.

Bai J, Wu X, Fan F, *et al*. 2012. Biosorption of uranium by magnetically modified *Rhodotorula glutinis*. *Enzyme Microb Technol* **51**: 382–387.

Berovic M, Berlot M, Kralj S, Makovec D. 2014. A new method for the rapid separation of magnetized yeast in sparkling wine. *Biochem Eng J* **88**: 77–84.

Birnbaum S, Larsson PO. 1982. Application of magnetic immobilized microorganisms. Ethanol production by *Saccharomyces cerevisiae*. *Appl Biochem Biotechnol* **7**: 55–57.

Brady D, Nigam P, Marchant R, *et al*. 1997. The effect of Mn^{2+} on ethanol production from lactose using *Kluyveromyces marxianus* IMB3 immobilized in magnetically responsive matrices. *Bioproc Eng* **17**: 31–34.

Brodelius P, Vandamme EJ. 1987. Immobilized cell systems. In Biotechnology (Enzyme Technology), vol **7a**, Rehm HJ, Reed G (eds). Verlag Chemie: Weinheim; 405–464.

Dauer RR, Dunlop EH. 1991. High-gradient magnetic separation of yeast. *Biotechnol Bioeng* **37**: 1021–1028.

Fakhrullin RF, Choi IS, Lvov Y (eds). 2014. Cell Surface Engineering: Fabrication of Functional Nanoshells. Royal Society of Chemistry: London; 252 pp.

Fakhrullin RF, Garcia-Alonso J, Paunov VN. 2010. A direct technique for preparation of magnetically functionalised living yeast cells. *Soft Matter* **6**: 391–397.

Fakhrullin RF, Lvov YM. 2012. 'Face-lifting' and 'make-up' for microorganisms: layer-by-layer polyelectrolyte nanocoating. *ACS Nano* **6**: 4557–4564.

Fuh CB, Lin LY, Lai MH. 2000. Analytical magnetapheresis of magnetically susceptible particles. *J Chromatogr A* **874**: 131–142.

Garcia-Alonso J, Fakhrullin RF, Paunov VN. 2010. Rapid and direct magnetization of GFP-reporter yeast for micro-screening systems. *Biosens Bioelectron* **25**: 1816–1819.

Gorobets SV, Gorobets OY, Demianenko IV. 2011. Self-organization of magnetic nanoparticles when giving magnetic properties to yeast *Saccharomyces cerevisiae*. *Res Bull NTUU 'KPI'* **3**: 27–33.

Gorobets SV, Gorobets OY, Demianenko IV, *et al*. 2013a. Self-organization of magnetite nanoparticles in providing *Saccharomyces cerevisiae* yeasts with magnetic properties. *J Magn Magn Mater* **337–338**: 53–57.

Gorobets SV, Karpenko YV, Kovalev OV, *et al*. 2013b. Application of magnetically labeled cells *S. cerevisiae* as biosorbents at treatment plants. *Res Bull NTUU 'KPI'* **3**: 42–47.

Hristov J, Ivanova V. 1999. Magnetic field assisted bioreactors. *Recent Res Devel Ferment Bioeng* **2**: 41–94.

Ivanova V, Hristov J, Dobreva E, *et al*. 1996. Performance of a magnetically stabilized bed reactor with immobilized yeast cells. *Appl Biochem Biotechnol* **59**: 187–198.

Ivanova V, Petrova P, Hristov J. 2011. Application in the ethanol fermentation of immobilized yeast cells in matrix of alginate/magnetic nanoparticles, on chitosan–magnetite microparticles and cellulose-coated magnetic nanoparticles. *Int Rev Chem Eng* **3**: 289–299.

Ji YQ, Hu YT, Tian Q, *et al*. 2010. Biosorption of strontium ions by magnetically modified yeast cells. *Sep Sci Technol* **45**: 1499–1504.

Jimenez-Moreno N, Ancin-Azpilicueta C. 2009. Sorption of volatile phenols by yeast cell walls. *Int J Wine Res* **1**: 11–18.

Johnson EA. 2013a. Biotechnology of non-*Saccharomyces* yeasts – the Ascomycetes. *Appl Microbiol Biotechnol* **97**: 503–517.

Johnson EA. 2013b. Biotechnology of non-*Saccharomyces* yeasts – the Basidiomycetes. *Appl Microbiol Biotechnol* **97**: 7563–7577.

Kurec M. 2010. Yeast biofilm – its formation and control during continuous alcohol-free beer production. PhD Thesis, Institute of Chemical Technology, Prague, Czech Republic.

Kurec M, Baszczynski M, Lehnert R, *et al*. 2009. Flow cytometry for age assessment of a yeast population and its application in beer fermentations. *J Inst Brew* **115**: 253–258.

Lalou S, Mantzouridou F, Paraskevopoulou A, *et al*. 2013. Bioflavour production from orange peel hydrolysate using immobilized *Saccharomyces cerevisiae*. *Appl Microbiol Biotechnol* **97**: 9397–9407.

Lamarre C, Deslauriers N, Bourbonnais Y. 2000. Expression cloning of the *Candida albicans CSA1* gene encoding a mycelial surface antigen by sorting of *Saccharomyces cerevisiae* transformants with monoclonal antibody-coated magnetic beads. *Mol Microbiol* **35**: 444–453.

Larsson PO, Mosbach K. 1979. Alcohol production by magnetic immobilized yeast. *Biotechnol Lett* **1**: 501–506.

Li T, Liu Y, Peng Q, *et al*. 2013. Removal of lead(II) from aqueous solution with ethylenediamine-modified yeast biomass coated with magnetic chitosan microparticles: kinetic and equilibrium modeling. *Chem Eng J* **214**: 189–197.

Liu CZ, Wang F, Ou-Yang F. 2009. Ethanol fermentation in a magnetically fluidized bed reactor with immobilized *Saccharomyces cerevisiae* in magnetic particles. *Bioresour Technol* **100**: 878–882.

Morais JPMG, Azevedo RB, Silva LP, *et al*. 2004. Magnetic resonance investigation of magnetic-labeled baker's yeast cells. *J Magn Magn Mater* **272–276**: 2400–2401.

Mosiniewicz-Szablewska E, Safarikova M, Safarik I. 2010. Magnetic studies of ferrofluid-modified microbial cells. *J Nanosci Nanotechnol* **10**: 2531–2536.

Naumenko EA, Dzamukova MR, Fakhrullin RF. 2014. Magnetically functionalized cells: fabrication, characterization, and biomedical applications. In Implantable Bioelectronics, Katz E (ed.) Wiley-VCH: Weinheim; 7–26.

Nieto-Rojo R, Ancin-Azpilicueta C, Garrido JJ. 2014. Sorption of 4-ethylguaiacol and 4-ethylphenol on yeast cell walls, using a synthetic wine. *Food Chem* **152**: 399–406.

Nishida K, Silver PA. 2012. Induction of biogenic magnetization and redox control by a component of the target of rapamycin complex 1 signaling pathway. *PLoS Biol* **10**: e1001269.

Ou H, Bian W, Weng X, *et al*. 2013. Adsorption of Ce(III) by magnetic chitosan/yeast composites from aqueous solution: kinetic and equilibrium studies. In Energy Engineering and Environmental Engineering, parts 1 and 2, Sun T (ed.). Trans Tech Publications: Hangzhou; 391–394.

Patzak M, Dostalek P, Fogarty RV, *et al*. 1997. Development of magnetic biosorbents for metal uptake. *Biotechnol Tech* **11**: 483–487.

Peng Q, Liu Y, Zeng G, *et al*. 2010. Biosorption of copper(II) by immobilizing *Saccharomyces cerevisiae* on the surface of chitosan-coated magnetic nanoparticles from aqueous solution. *J Hazard Mater* **177**: 676–682.

Pospiskova K, Prochazkova G, Safarik I. 2013. One-step magnetic modification of yeast cells by microwave-synthesized iron oxide microparticles. *Lett Appl Microbiol* **56**: 456–461.

Rao A, Bankar A, Kumar AR, *et al*. 2013. Removal of hexavalent chromium ions by *Yarrowia lipolytica* cells modified with phyto-inspired Fe^0/Fe_3O_4 nanoparticles. *J Contam Hydrol* **146**: 63–73.

Russell AP, Evans CH, Westcott VC. 1987. Measurement of the susceptibility of paramagnetically labeled cells with paramagnetic solutions. *Anal Biochem* **164**: 181–189.

Safarik I, Horska K, Safarikova M. 2011. Magnetically responsive biocomposites for inorganic and organic xenobiotics removal. In Microbial Biosorption of Metals, Kotrba P, Mackova M, Macek T (eds). Springer: Berlin; 301–320.

Safarik I, Maderova Z, Pospiskova K, *et al*. 2014a. Magnetic decoration and labelling of prokaryotic and eukaryotic cells. In Cell Surface Engineering: Fabrication of Functional Nanoshells, Fakhrullin RF, Choi I, Lvov YM (eds). Royal Society of Chemistry: London; 185–215.

Safarik I, Pospiskova K, Maderova Z, *et al*. 2014b. Microwave-synthesized chitosan microparticles for yeast cells immobilization. *Yeast*. doi: 10.1002/yea.3017.

Safarik I, Ptackova L, Safarikova M. 2002. Adsorption of dyes on magnetically labeled baker's yeast cells. *Eur Cell Mater* **3**(suppl 2): 52–55.

Safarik I, Rego LFT, Borovska M, *et al*. 2007. New magnetically responsive yeast-based biosorbent for the efficient removal of water-soluble dyes. *Enzyme Microb Technol* **40**: 1551–1556.

Safarik I, Sabatkova Z, Safarikova M. 2008. Hydrogen peroxide removal with magnetically responsive *Saccharomyces cerevisiae* cells. *J Agr Food Chem* **56**: 7925–7928.

Safarik I, Sabatkova Z, Safarikova M. 2009. Invert sugar formation with *Saccharomyces cerevisiae* cells encapsulated in magnetically responsive alginate microparticles. *J Magn Magn Mater* **321**: 1478–1481.

Safarik I, Safarikova M. 1999. Use of magnetic techniques for the isolation of cells. *J Chromatogr B* **722**: 33–53.

Safarik I, Safarikova M. 2007. Magnetically modified microbial cells: a new type of magnetic adsorbent. *China Particuol* **5**: 19–25.

Safarik I, Safarikova M. 2012. Magnetic nanoparticles for *in vitro* biological and medical applications: an overview. In Magnetic Nanoparticles: From Fabrication to Biomedical and Clinical Applications, Thanh NTK (ed.). CRC Press/Taylor and Francis: Boca Raton; 215–242.

Safarikova M, Maderova Z, Safarik I. 2009. Ferrofluid modified *Saccharomyces cerevisiae* cells for biocatalysis. *Food Res Int* **42**: 521–524.

Safarikova M, Ptackova L, Kibrikova I, Safarik I. 2005. Biosorption of water-soluble dyes on magnetically modified *Saccharomyces cerevisiae* subsp. *uvarum* cells. *Chemosphere* **59**: 831–835.

Sakai Y, Tamiya Y, Takahashi F. 1994. Enhancement of ethanol formation by immobilized yeast containing iron powder or Ba-ferrite due to eddy current or hysteresis. *J Ferment Bioeng* **77**: 169–172.

Schwegmann H, Feitz AJ, Frimmel FH. 2010. Influence of the zeta potential on the sorption and toxicity of iron oxide nanoparticles on *S. cerevisiae* and *E. coli*. *J Colloid Interface Sci* **347**: 43–48.

Serra S, Fuganti C, Brenna E. 2005. Biocatalytic preparation of natural flavours and fragrances. *Trends Biotechnol* **23**: 193–198.

Sicard D, Legras JL. 2011. Bread, beer and wine: yeast domestication in the *Saccharomyces sensu stricto* complex. *C R Biol* **334**: 229–236.

Soares EV, Soares HMVM. 2012. Bioremediation of industrial effluents containing heavy metals using brewing cells of *Saccharomyces cerevisiae* as a green technology: a review. *Environ Sci Pollut Res* **19**: 1066–1083.

Straver MH, Kijne JW. 1996. A rapid and selective assay for measuring cell surface hydrophobicity of brewer's yeast cells. *Yeast* **12**: 207–213.

Sun J, Lim Y, Liu SQ. 2013. Biosynthesis of flavor esters in coconut cream through coupling fermentation and lipase-catalysed biocatalysis. *Eur J Lipid Sci Technol* **115**: 1107–1114.

Tian Y, Ji CY, Zhao MJ, *et al*. 2010. Preparation and characterization of baker's yeast modified by nano-Fe_3O_4: application of biosorption of methyl violet in aqueous solution. *Chem Eng J* **165**: 474–481.

Uzun L, Saglam N, Safarikova M, *et al*. 2011. Copper biosorption on magnetically modified yeast cells under magnetic field. *Sep Sci Technol* **46**: 1045–1051.

van der Sluis C, Stoffelen CJP, Castelein SJ, *et al*. 2001. Immobilized salt-tolerant yeasts: application of a new polyethylene-oxide support in a continuous stirred-tank reactor for flavour production. *J Biotechnol* **88**: 129–139.

Wu Q, Shan Z, Shen M, *et al*. 2009. Biosorption of direct scarlet dye on magnetically modified *Saccharomyces cerevisiae* cells. *Chin J Biotech* **25**: 1477–1482.

Xu M, Zhang YS, Zhang ZM, *et al*. 2011. Study on the adsorption of Ca^{2+}, Cd^{2+} and Pb^{2+} by magnetic Fe_3O_4 yeast treated with EDTA dianhydride. *Chem Eng J* **168**: 737–745.

Yang SH, Lee T, Seo E, *et al*. 2012. Interfacing living yeast cells with graphene oxide nanosheaths. *Macromol Biosci* **12**: 61–66.

Yavuz H, Denizli A, Güngüneş H, *et al*. 2006. Biosorption of mercury on magnetically modified yeast cells. *Sep Purif Technol* **52**: 253–260.

Yu JX, Wang LY, Chi RA, *et al*. 2013. A simple method to prepare magnetic modified beer yeast and its application for cationic dye adsorption. *Environ Sci Pollut Res* **20**: 543–551.

Zhang Y, Liu W, Zhang L, *et al*. 2011. Application of bifunctional *Saccharomyces cerevisiae* to remove lead(II) and cadmium(II) in aqueous solution. *Appl Surf Sci* **257**: 9809–9816.

Zhang YS, Zhao MJ, Wang RG, *et al*. 2012. Method for preparing magnetic *Saccharomyces cerevisiae* and technique for processing printing and dying wastewater by using same. Chinese Patent No CN 102059100 B.

Zheng BZ, Zhang MH, Xiao D, *et al*. 2010. Fast microwave synthesis of Fe_3O_4 and Fe_3O_4/Ag magnetic nanoparticles using Fe^{2+} as precursor. *Inorg Mater* **46**: 1106–1111.

5.1.5 Magnetická modifikace materiálů tvořících aglomeráty

Příprava magnetických nano- a mikročástic či *in situ* syntéza magnetických biokompozitů, využívající prekurzor heptahydrát síranu železnatého, alkalizaci hydroxidem sodným a následné ošetření mikrovlnným ozařováním v běžné kuchyňské mikrovlnné troubě byla již důkladně popsána (Safarik et al., 2013; Safarik and Safarikova, 2014). Zatímco *in situ* příprava biokompozitů s magnetickou odezvou není vhodná pro materiály citlivé k vyšší teplotě či hodnotě pH, technika postmagnetizace založená na smísení vodné suspenze MS magnetických částic s modifikovaným materiálem vede u některých materiálů po vysušení (citrusové slupky, makrořasy *Sargassum* sp. a jíly) k tvorbě agregátů, které jsou jednak obtížně homogenizovatelné, jednak pro svůj malý povrch téměř nepoužitelné v sorpčních experimentech.

Tvorbě tvrdých klastrů lze zabránit několika způsoby popisovanými v této krátké publikaci. Jedním z možných postupů je převod vzniklého magnetitu z vodné suspenze do organického rozpouštědla (metanol, etanol, izopropylalkohol, aceton apod.), důkladné smíchání s modifikovaným materiálem a sušení. Alternativní postup spočívá v suspendaci materiálu v organickém rozpouštědle a přidání potřebného množství vodné suspenze magnetitu. Po krátké inkubaci je materiál odstředěn a vysušen.

Příloha 5:

Magnetic modification of diamagnetic agglomerate forming powder materials

Safarik I, Baldikova E, Pospiskova K, Safarikova M

Particuology 29, **2016**, 169-171

Particuology 29 (2016) 169–171

Contents lists available at ScienceDirect

Particuology

journal homepage: www.elsevier.com/locate/partic

Short communication

Magnetic modification of diamagnetic agglomerate forming powder materials

Ivo Safarik[a,b,c,*], Eva Baldikova[a,d], Kristyna Pospiskova[b], Mirka Safarikova[a,c]

[a] Department of Nanobiotechnology, Biology Centre, ISB, CAS, Na Sadkach 7, 370 05 Ceske Budejovice, Czech Republic
[b] Regional Centre of Advanced Technologies and Materials, Palacky University, Slechtitelu 27, 783 71 Olomouc, Czech Republic
[c] Global Change Research Institute, CAS, Na Sadkach 7, 370 05 Ceske Budejovice, Czech Republic
[d] Department of Applied Chemistry, Faculty of Agriculture, University of South Bohemia, Branisovska 1457, 370 05 Ceske Budejovice, Czech Republic

ARTICLE INFO

Article history:
Received 7 February 2016
Received in revised form 19 April 2016
Accepted 2 May 2016
Available online 17 June 2016

Keywords:
Magnetic modification
Magnetic separation
Powdered material
Magnetic iron oxide
Microwave assisted synthesis

ABSTRACT

A simple method for the magnetic modification of various types of powdered agglomerate forming diamagnetic materials was developed. Magnetic iron oxide particles were prepared from ferrous sulfate by microwave assisted synthesis. A suspension of the magnetic particles in water soluble organic solvent (methanol, ethanol, propanol, isopropyl alcohol, or acetone) was mixed with the material to be modified and then completely dried at elevated temperature. The magnetically modified materials were found to be stable in water suspension at least for 2 months.

Introduction

Vast numbers of diamagnetic powder materials with interesting properties exist; these materials can be used, for example, as catalysts, adsorbents, and carriers. In many cases their application potential could be improved by converting them into magnetically responsive forms. Different magnetic modification procedures are available (e.g., magnetic fluid treatment, microwave-assisted procedures, mechanochemical synthesis), which are usually based on the deposition of magnetic iron oxide nano- or microparticles onto the surface or within the pores of the treated materials (Safarik, Horska, Pospiskova, Filip, & Safarikova, 2014; Safarik, Horska, Pospiskova, & Safarikova, 2012; Safarik & Safarikova, 2014).

Recently, an extremely simple procedure based on the use of microwave-synthesized magnetic iron oxide nano- and microparticles has been developed and employed in the magnetic modification of several dozens of different diamagnetic powder and particulate materials (Safarik & Safarikova, 2014). Complete drying of the magnetically modified materials was found to be necessary to properly fix the magnetic iron oxide particles on the surface of the treated materials. However, some types of modified powder formed rough agglomerates after the drying process when the standard water suspension of magnetic iron oxide particles was used for the modification. These agglomerates exhibited magnetic properties, but their disintegration and conversion into fine magnetic powder was difficult.

To prevent the formation of magnetic agglomerates during the preparation of magnetically responsive materials, a modified magnetization procedure using selected organic solvents as the mobile phase of the magnetic suspension was developed in this work.

Experimental

Materials

Iron(II) sulfate heptahydrate ($FeSO_4 \cdot 7H_2O$), sodium hydroxide, methanol, ethanol, propanol, isopropyl alcohol, and acetone were supplied by Sigma-Aldrich, Prague, Czech Republic. Dried fodder yeast (*Kluyveromyces marxianus*) was obtained from Biocel, Paskov, Czech Republic. Dried powdered orange peel and pomelo peel were obtained locally, while brown macroalgae *Sargassum horneri* was collected from a beach in Qingdao, China. Bentonite clay was obtained from Tamda, Olomouc, Czech Republic.

* Corresponding author at: Department of Nanobiotechnology, Biology Centre, ISB, CAS, Na Sadkach 7, 370 05 Ceske Budejovice, Czech Republic. Tel.: +420 387775608.
E-mail address: ivosaf@yahoo.com (I. Safarik).

http://dx.doi.org/10.1016/j.partic.2016.05.002

Microwave assisted synthesis of magnetic iron oxide particles

$FeSO_4 \cdot 7H_2O$ (1 g) was dissolved in 100 mL of water in an 800-mL beaker, after which sodium hydroxide solution (1 mol/L) was added dropwise slowly under mixing until the pH of the mixture reached ca. 12. A precipitate of iron hydroxides formed during this process. Next, the suspension was diluted to 200 mL with water and placed in a standard kitchen microwave oven (700 W, 2450 MHz) for 10 min at maximum power. The formed magnetic iron oxide particles were repeatedly washed with water (Safarik & Safarikova, 2014).

To prepare suspensions of the magnetic particles for the modification of the agglomerate forming powder materials, the water phase was substituted with methanol or other tested water soluble organic solvents (ethanol, propanol, isopropyl alcohol, or acetone).

Magnetic modification of diamagnetic agglomerate forming powder materials

One gram of the material to be modified was thoroughly mixed (using a spatula or laboratory spoon) with 2 mL of the microwave-synthesized iron oxide microparticle suspension in methanol or other water soluble organic solvent (1 part of completely sedimented iron oxide particles to 4 parts of methanol or other solvent) in a short test-tube or small beaker. Other volumes of iron oxide particle suspension were used to prepare magnetically modified materials with different responses to an external magnetic field. Thorough mixing was important for homogeneous distribution of the magnetic particles within the material to be treated. The obtained mixture was completely dried in an oven at a temperature not exceeding 60 °C.

Additionally, a suspension of the material to be treated in methanol or other solvent was prepared and mixed with an appropriate amount of microwave-synthesized iron oxide microparticle suspension. After thorough mixing and subsequent sedimentation or centrifugation, the supernatant was removed and the well-mixed sediment was allowed to dry completely in an oven as described above.

Results and discussion

Recently, we developed a cheap and simple technique for modifying originally diamagnetic powdered materials into magnetic derivatives using microwave-synthesized magnetic iron oxide nano- and microparticles (Safarik & Safarikova, 2014). In most cases this technique gave excellent results, forming stable magnetically responsive powdered materials. However, some diamagnetic materials formed large agglomerates after modification with water suspensions of magnetic particles. Thus, herein we have developed a simple magnetization technique for agglomerate forming materials such as bentonite, dried orange and pomelo peel powders, dried *S. horneri* biomass, and dried fodder yeast cells (*K. marxianus*).

Modification of bentonite using the standard water-based magnetization procedure (Safarik & Safarikova, 2014) led to the formation of rough agglomerates after the drying process. In contrast, suspending the magnetic particles in ethanol instead of water resulted in the formation of fine powdered magnetic material after drying. The degree of magnetic modification could be tuned by changing the amount of magnetic modifier used (Fig. 1).

A similar situation was observed for the biological samples. Water and four organic solvents, i.e., methanol, isopropyl alcohol, propanol, and acetone were used to prepare magnetic particle suspensions subsequently used to magnetically modify the dried *K. marxianus* cells, pomelo peel, orange peel, and *S. horneri* biomass. In all cases, using the water-based suspension of magnetic particles

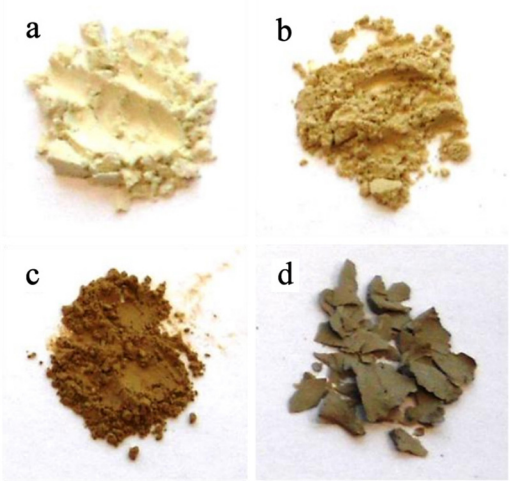

Fig. 1. Native bentonite clay powder (a), magnetic bentonite powder prepared by modification with an ethanol suspension of (b) lower and (c) higher amount of microwave-synthesized iron oxide magnetic particles, agglomerated magnetic bentonite prepared by modification with a water suspension of the magnetic particles (d).

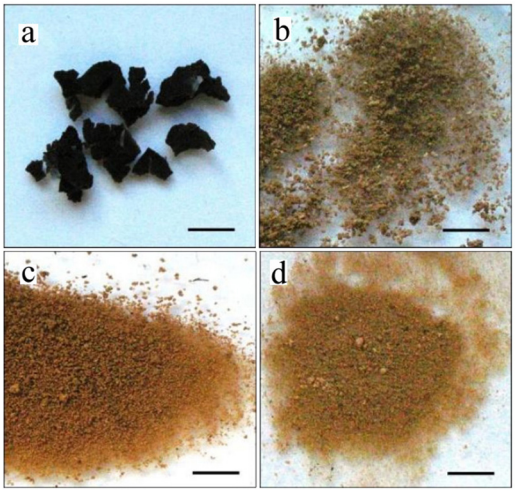

Fig. 2. Magnetically modified dried *Kluyveromyces marxianus* cells using microwave-synthesized magnetic iron oxide particles suspended in: (a) water, (b) methanol, (c) propanol, and (d) acetone. Bars correspond to 10 mm.

for the modification led to the formation of very durable clusters and agglomerates (Fig. 2(a)) that could not be converted into homogeneous suspensions when suspended in water. This situation substantially decreases the potential applicability of the magnetically responsive materials. Conversely, suspending the magnetic particles in an organic solvent resulted in the formation of fine magnetically responsive powders (Fig. 2(b)–(d)). As shown in Fig. 2, the colors of the dried materials differed slightly. However, no effects on the response of the powders to external magnetic field or the long-term stability of the suspensions were detected.

The diamagnetic materials were efficiently magnetically modified by the deposition of the microwave-synthesized iron oxide nano- and micro-particles onto their surface. The microwave synthesis produced nanoparticles with diameters ranging between ~25 and 100 nm that formed stable micrometer-sized aggregates. A scanning electron microscopy (SEM) image of the iron oxide nanoparticle aggregates on the surface of a magnetically modified material (pomelo peel powder) is shown in Fig. 3. The strong binding of the magnetic iron oxide particles to the diamagnetic materials was achieved by a subtle balance of van der Waals,

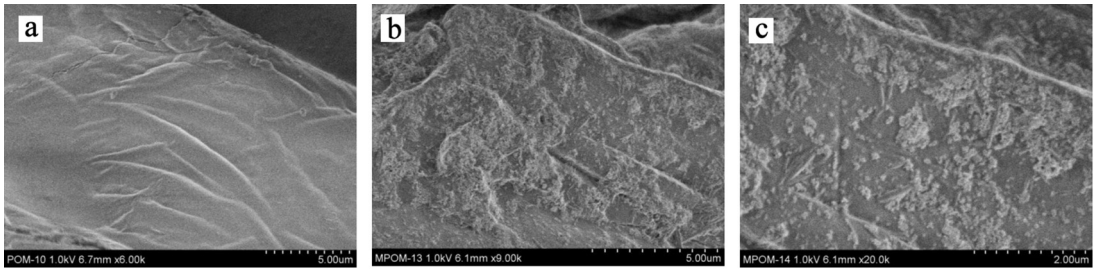

Fig. 3. SEM images of native pomelo peel powder (a) and of the same material modified with magnetic particles suspended in methanol (b and c).

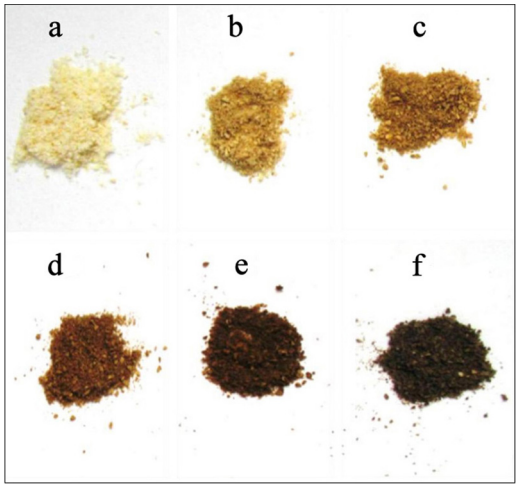

Fig. 4. Pomelo peel powder (1 g) modified with different volumes of magnetic particles in methanol suspension: (a) 0 mL (native powder), (b) 1 mL, (c) 2 mL, (d) 4 mL, (e) 6 mL, and (f) 10 mL.

electrostatic, and hydrophobic interactions between the magnetic particles and the modified materials (Saito, Koopal, Nagasaki, & Tanaka, 2008). The magnetically modified materials were found to be stable in water suspension for more than eight weeks, and could be very easily magnetically separated from the suspensions using permanent magnets or electromagnets.

Magnetically modified materials with different magnetic responses were easily prepared by changing the amount of magnetic iron oxide particles used in the modification procedure. Fig. 4 shows photos of pomelo peel powder and its magnetic derivatives prepared with different volumes of standard magnetic iron oxide suspension in methanol.

Various types of low cost, easily available materials (including food industry waste) have been tested and used as adsorbents for the removal of pollutants. The magnetic modification of such adsorbents to obtain magnetically responsive materials markedly simplifies their separation from the treated solutions or suspensions using an appropriate magnetic separator. The magnetically modified pomelo peel was evaluated as a biosorbent for the removal of acridine orange and methylene blue. The adsorption experiments were performed exactly as described in a previous work (Safarik, Horska, Svobodova, & Safarikova, 2012). The equilibrium adsorption isotherms for both dyes are shown in Fig. 5; the data followed the Langmuir isotherm equation. The calculated maximum adsorption capacity of the modified pomelo peel powder was 106.6 mg/g for acridine orange and 179.0 mg/g for methylene blue. These results indicate the promising potential of

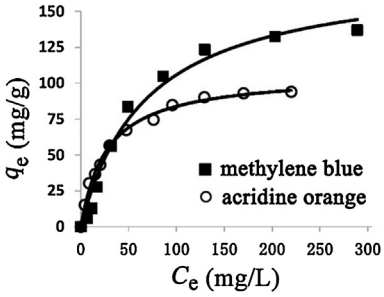

Fig. 5. Equilibrium adsorption isotherms of tested dyes on magnetically modified pomelo peel. C_e: equilibrium liquid-phase concentration of the unadsorbed (free) dye (mg/L); q_e: equilibrium solid-phase concentration of the adsorbed dye (mg/g).

the present magnetically modified low cost materials as pollutant adsorbents.

Conclusions

A new magnetization technique was developed for the magnetic modification of agglomerate forming materials using microwave-synthesized iron oxide nano- and microparticles suspended in water miscible organic solvents. Smart, simple, inexpensive, and scalable magnetic modification of various types of materials is possible using this technique.

Acknowledgments

This work was supported by the Grant Agency of the Czech Republic (Project No. 13-13709S) and by projects LO1305 and LD14066 of the Ministry of Education, Youth, and Sports of the Czech Republic. This research was also part of COST TD1203 activities.

References

Safarik, I., Horska, K., Pospiskova, K., Filip, J., & Safarikova, M. (2014). Mechanochemical synthesis of magnetically responsive materials from non-magnetic precursors. *Materials Letters*, *126*, 202–206.

Safarik, I., Horska, K., Pospiskova, K., & Safarikova, M. (2012). One-step preparation of magnetically responsive materials from non-magnetic powders. *Powder Technology*, *229*, 285–289.

Safarik, I., Horska, K., Svobodova, B., & Safarikova, M. (2012). Magnetically modified spent coffee grounds for dyes removal. *European Food Research and Technology*, *234*, 345–350.

Safarik, I., & Safarikova, M. (2014). One-step magnetic modification of non-magnetic solid materials. *International Journal of Materials Research*, *105*, 104–107.

Saito, T., Koopal, L. K., Nagasaki, S., & Tanaka, S. (2008). Adsorption of heterogeneously charged nanoparticles on a variably charged surface by the extended surface complexation approach: Charge regulation, chemical heterogeneity, and surface complexation. *Journal of Physical Chemistry B*, *112*, 1339–1349.

5.1.6 Kvantifikace navázaných magnetických částic na povrchu modifikovaného materiálu

V této krátké publikaci je představena inovativní metoda sloužící ke kvantifikaci navázaných magnetických nano- a mikročástic a jejich agregátů na povrchu modifikovaného materiálu, jež je založena na měření relativní magnetické permeability, která je přímo úměrná množství přítomných magnetických částic. K experimentům byly použity různé biologické materiály modifikované kyselou magnetickou kapalinou (stabilizovanou kyselinou chloristou) a MS magnetitem, s rozdílným stupněm magnetizace (tzv. různým množstvím přidaných částic).

Nově vyvinutá technika představuje velmi rychlé a reprodukovatelné měření množství navázaných magnetických částic na povrchu materiálu, které nevyžaduje předchozí modifikace. Lze pracovat jak s pevným materiálem, tak se suspenzí, a v obou případech je možné stanovit magnetické částice do 20 % hmotnosti testovaného materiálu.

Příloha 6:

Rapid determination of iron oxide content in magnetically modified particulate materials

Safarik I, Nydlova L, Pospiskova K, Baldikova E, Maderova Z, Safarikova M

Particuology 26, **2016**, 114-117

Particuology 26 (2016) 114–117

Contents lists available at ScienceDirect

Particuology

journal homepage: www.elsevier.com/locate/partic

Short communication

Rapid determination of iron oxide content in magnetically modified particulate materials

Ivo Safarik[a,b,c,*], Leona Nydlova[a], Kristyna Pospiskova[b], Eva Baldikova[a,d], Zdenka Maderova[a], Mirka Safarikova[a,c]

[a] Department of Nanobiotechnology, Institute of Nanobiology and Structural Biology of GCRC, Na Sadkach 7, 370 05 Ceske Budejovice, Czech Republic
[b] Regional Centre of Advanced Technologies and Materials, Palacky University, Slechtitelu 27, 783 71 Olomouc, Czech Republic
[c] Department of Nanobiotechnology, Biology Centre, CAS, Na Sadkach 7, 370 05 Ceske Budejovice, Czech Republic
[d] Department of Applied Chemistry, Faculty of Agriculture, University of South Bohemia, Branisovska 1457, 370 05 Ceske Budejovice, Czech Republic

ARTICLE INFO

Article history:
Received 6 October 2015
Received in revised form 9 November 2015
Accepted 18 November 2015
Available online 18 January 2016

Keywords:
Magnetic permeability meter
Magnetic iron oxides
Magnetically modified materials

ABSTRACT

Magnetically responsive composite materials have been used in interesting applications in various areas of bioscience, biotechnology, and environmental technology. In this work, a simple method to determine the amount of magnetic iron oxide nano- and microparticles attached to magnetically-modified particulate diamagnetic materials has been developed using a commercially available magnetic permeability meter. The procedure is fast and enables dry particulate magnetically modified materials to be analysed without any modification or pretreatment. We show that the magnetic permeability can be measured for materials containing up to 20% magnetic iron oxide. The magnetic permeability measurements are highly reproducible.

Introduction

Magnetically responsive nano- and microparticles have been used in many important applications in various areas of bioscience, medicine, biotechnology, and environmental technology. Such materials exhibit several types of responses to an external magnetic field, such as selective separation, targeting and localization, heat generation in high frequency alternating magnetic fields, increases in negative T2 contrast by magnetic iron oxides nanoparticles during magnetic resonance imaging, or great increases in apparent viscosity of magnetorheological fluids when subjected to a magnetic field (Safarik, Pospiskova, Horska, Maderova, & Safarikova, 2014). Currently, large amounts of diverse magnetic nano- and micromaterials can be obtained commercially, or can be produced in research laboratories using many different basic principles (Laurent et al., 2008; Kharissova, Dias, & Kharisov, 2015).

In the last two decades, a large number of magnetically responsive materials, prepared from a huge variety of diamagnetic ("nonmagnetic") particulate materials with interesting properties, have been described. Various modification techniques can be employed to convert nonmagnetic materials into magnetic derivatives (Safarik, Horska, Pospiskova, & Safarikova, 2012a). Recently, two extremely simple and widely applicable magnetic modification procedures have been developed based on the interaction of microwave synthesized magnetic iron oxide nano- and microparticles or perchloric acid stabilized magnetic fluid with modified diamagnetic materials. After thorough drying, stable magnetically responsive composite materials are formed. The magnetic iron oxide particles are mainly localized on the surface or within the pores of the treated materials, and their mutual interaction is quite strong and stable. The strong binding of magnetic iron oxide particles to nonmagnetic materials is thought to arise from a subtle balance of van der Waals, electrostatic, and hydrophobic interactions between the magnetic particles and the treated material (Saito, Koopal, Nagasaki, & Tanaka, 2008). The magnetic properties of the composites can be tuned simply by changing the amount of magnetic modifier used (Safarik & Safarikova, 2014; Safarik, Horska, Pospiskova, & Safarikova, 2012b). The prepared magnetic composites can be magnetically separated very easily using either NdFeB permanent magnets or commercially available magnetic separators (see Fig. 1).

Large amounts of magnetically responsive materials with different degrees of magnetic modification have been prepared in our lab in quantities ranging from grams to approximately one

* Corresponding author at: Prof. Ivo Safarik, Biology Centre, Czech Academy of Sciences, Department of Nanobiotechnology, Na Sadkach 7, 370 05 Ceske Budejovice, Czech Republic. Tel.: +420 387775608; fax: +420 385310133.
E-mail address: ivosaf@yahoo.com (I. Safarik).

http://dx.doi.org/10.1016/j.partic.2015.11.001

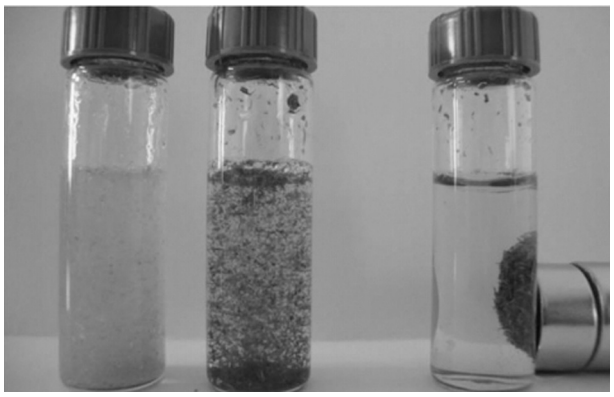

Fig. 1. Appearance of original straw particle suspension (left), suspension of straw after magnetic modification with microwave synthesized magnetic iron oxide particles (middle), and demonstration of magnetic separation of magnetically modified straw (right).

kilogram using both procedures. It became obvious that a rapid method enabling the measurement of the magnetic particle content of the modified materials was needed to confirm the proper magnetic modification of the final materials and to determine iron oxide content in mixtures prepared from materials with different levels of magnetic label coating. Thus, in this paper, a simple procedure to measure the amount of magnetic iron oxide on magnetically modified materials has been developed using a commercially available magnetic permeability meter. The method is rapid and allows dry powdered magnetically modified materials to be used for measurements without any modification.

Experimental

Materials

Bentonite clay was obtained from Tamda (Olomouc, Czech Republic), and montmorillonite, powdered magnetite, ferrous sulphate heptahydrate, and sodium hydroxide were obtained from Sigma-Aldrich (St. Louis, MO, USA). Oak sawdust and milled rye straw (about 0.1–2 mm in diameter) as well as potato starch were obtained locally. Water-based magnetic fluid stabilized with perchloric acid was prepared using a standard procedure (Massart, 1981). The ferrofluid was composed of magnetic iron oxide nanoparticles with diameters ranging between 10 and 20 nm (electron microscopy measurements). The relative magnetic fluid concentration (30.2 mg/mL) is given as the iron (II, III) oxide content determined by a colorimetric method (Kiwada, Sato, Yamada, & Kato, 1986).

Magnetic modification with microwave synthesized magnetic iron oxide particles

Nonmagnetic materials were magnetically modified using microwave-synthesized magnetic iron oxide particles (Safarik & Safarikova, 2014). In a typical procedure, 1 g $FeSO_4 \cdot 7H_2O$ was dissolved in 100 mL of water in a 600–800 mL beaker and sodium hydroxide solution (1 mol/L) was added slowly under mixing until the pH reached ca. 12; during this process a precipitate of iron hydroxides was formed. Then, the suspension was diluted to 200 mL with water and inserted into a standard kitchen microwave oven (700 W, 2450 MHz). The suspension was usually treated for 10 min at the maximum power of the oven. The beaker was then removed from the oven and the formed magnetic iron oxide nano- and microparticles were repeatedly washed with water until neutral pH was reached.

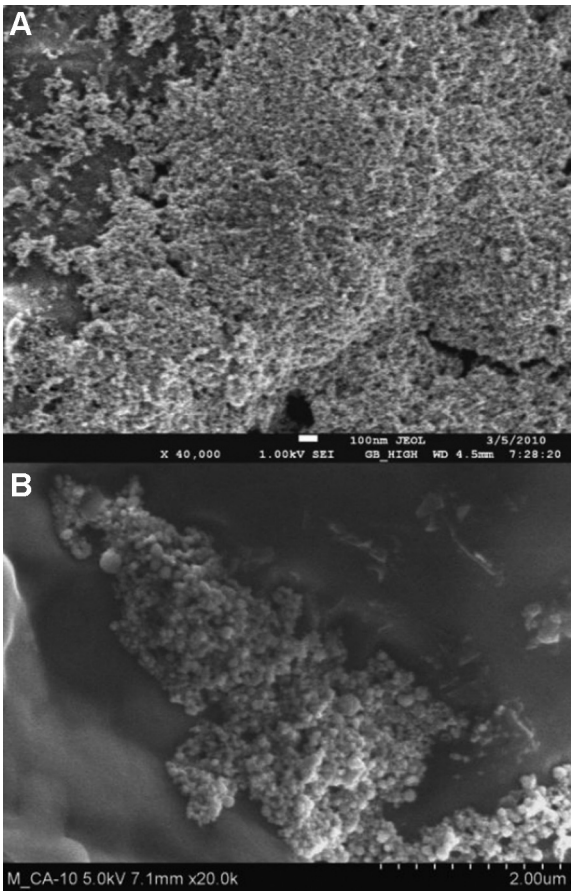

Fig. 2. Scanning electron microscope images of lignocellulosic materials modified with magnetic fluid (a) and with microwave-synthesized magnetic iron oxide nanoparticles (b).

To prepare magnetically responsive materials, 1 g of the target powdered material was thoroughly mixed in a short test-tube or a small beaker with an appropriate amount of microwave iron oxide nano- and microparticle suspension (one part completely sedimented iron oxide particles and four parts water; the exact iron oxide content was determined after drying to constant weight). Vigorous mixing with a spatula or laboratory spoon enabled homogeneous distribution of the magnetic nanoparticles and microparticles within the treated material. The mixture was allowed to dry completely at temperatures usually not exceeding 60 °C for 48 h. To change the magnetic response of the modified material, the amount of iron oxide particles (i.e., the volume of iron oxide suspension) was changed as required (Safarik & Safarikova, 2014). For specific materials (e.g., bentonite), the iron oxide particle suspension was prepared in ethanol.

Magnetic modification with magnetic fluid

In a typical procedure, 1 g of the powder to be modified was thoroughly mixed in a short test-tube or a small beaker with an appropriate amount (e.g., 1 mL) of water based ferrofluid stabilized with perchloric acid. Mixing with a spatula or laboratory spoon enabled homogeneous distribution of the magnetic fluid within the treated material. The mixture was allowed to dry completely at temperatures usually not exceeding 50–60 °C for 48 h (Safarik et al., 2012b). Use of a larger volume of magnetic fluid led to the formation of modified materials with higher magnetic responses.

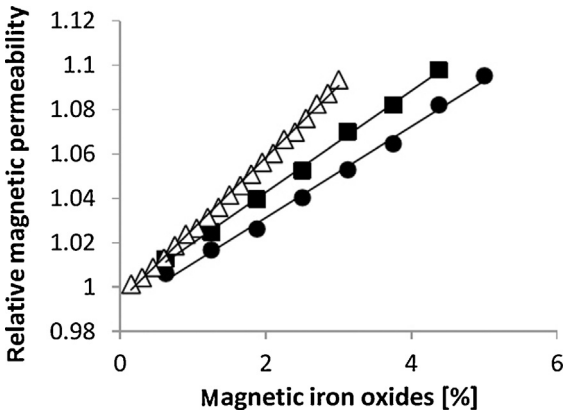

Fig. 3. Dependence of relative magnetic permeability on the concentration of commercial magnetite (●), microwave-synthesized magnetic iron oxides (■), and maghemite nanoparticles in water based magnetic fluid stabilized with perchloric acid (△). Powdered magnetic materials were diluted with potato starch.

Determination of iron oxide content in magnetically modified materials

The measurements were performed using an MPM-100 magnetic permeability meter (European Institute of Science, Lund, Sweden). The magnetically responsive powder material sample was added into the sample vial (ϕ8 mm × 40 mm) to a height of ca. 20 mm, and was then packed by mechanical tapping of the vial several times. The filled vial was then inserted into the device and the relative magnetic permeability of the sample was measured.

Results and discussion

Diamagnetic materials were successfully magnetically modified using two magnetic labels; microwave-synthesized magnetic iron oxide nano- and microparticles, and magnetic fluid. The content of magnetic iron oxide particles on the surface or within the pores of magnetically modified materials can usually be finely tuned by adjusting the amount of magnetic label used to modify each unit amount of diamagnetic material. A greater amount of magnetic label causes a stronger response of the magnetic composites to an external magnetic field. However, some of the important properties of the modified materials, such as their adsorption capacity, can be partially decreased as a result of the blockage of adsorption sites by the magnetic nano- or microparticles. Typical examples of lignocellulosic materials magnetically modified with large volumes of magnetic fluid and by the attachment of microwave-synthesized magnetic iron oxide nano- and microparticles are presented in Fig. 2. In the first case, individual nanoparticles of magnetic iron oxides (originating from magnetic fluid) and fine aggregates of nanoparticles can be clearly seen on the surface of the treated material (Fig. 2(a)). In the second case, nanoparticles with diameters ranging between ca. 25 and 100 nm were formed during the microwave synthesis. However, the nanoparticles formed micrometer-sized stable aggregates of up to approximately 20 μm in size during the synthesis. Thus, the magnetic modification led to the deposition of individual aggregates on the surface of the modified material (Fig. 2(b)).

The amount of magnetic label (usually magnetic iron oxide nano- and microparticles) fixed on a magnetically modified material is proportional to the relative magnetic permeability (μ_r) determined by the magnetic permeability meter (in this case MPM-100). This operational principle is based on the fact that the measured change in inductance of an internal coil is proportional to the amount of magnetic label on a magnetically modified sample present in the coil. Use of the magnetic permeability meter allows the relative magnetic permeability in any solution, suspension, or powder to be directly determined (Kriz, Gehrke, & Kriz, 1998; Abrahamsson, Kriz, Lu, & Kriz, 2004).

Dry powder material was able to be successfully used in the present magnetic permeability measurements. Fig. 3 shows the relative magnetic permeability values obtained for various concentrations of both commercial magnetite and microwave-synthesized magnetic iron oxide particles diluted with potato starch (a typical diamagnetic biological powder material made up of spherical granules of between 5 and 100 μm in size). For comparison, the relative magnetic permeability of water based magnetic fluid (diluted with water) is also presented. It can be seen that good linearity is obtained until an iron oxide concentration of ca. 5 wt%, with correlation coefficients higher than 0.9947.

Fig. 4 illustrates the dependence of the relative magnetic permeability on the amount of iron oxide particles deposited on the

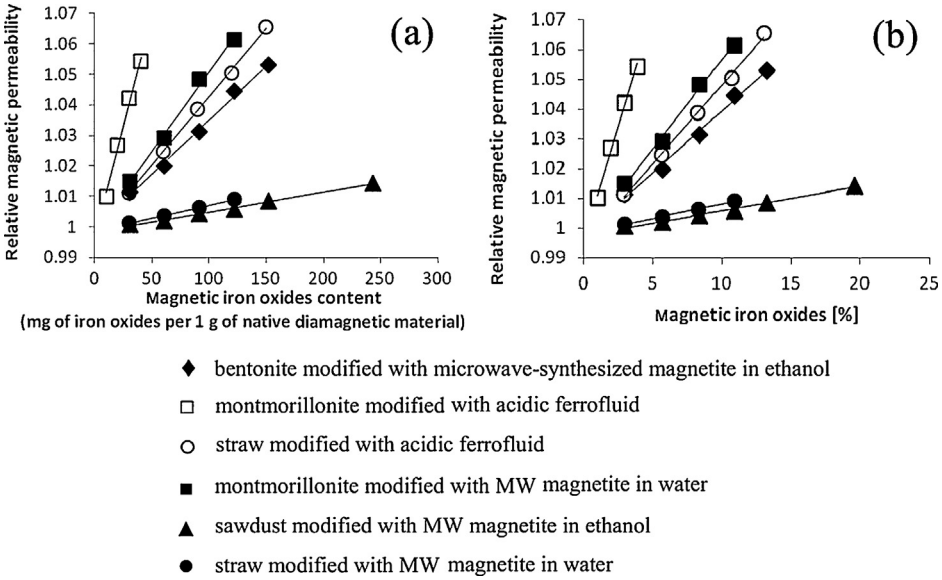

Fig. 4. Dependence of relative magnetic permeability on the amount of magnetic iron oxide (MIO) attached to the native material: (a) amount of MIO expressed in mg per 1 g of the native treated material; (b) amount of MIO in mass percent.

surface of the treated nonmagnetic materials. Magnetically responsive materials were highly reproducibly prepared using constant amounts of diamagnetic material and various amounts of magnetic label. Finely tuned magnetized materials were obtained. The resulting calibration curves were linear, with correlation coefficients higher than 0.9905. A quite high attachment of magnetic iron oxide (up to ca 250 mg of magnetic label per 1 g of native diamagnetic material, corresponding to 20% magnetic label concentration (mass/mass)) was measured for specific materials. Two ways of quantifying the iron oxide content are presented in Fig. 4. In the first case (Fig. 4(a)), the *x*-axis unit of the calibration graph has the form "mg of magnetic iron oxide per 1 g of the native (original unmodified) material". A simple calculation of the standard percent concentration (mass/mass) has been used for the second plot (Fig. 4(b)). It can be clearly seen that the slope of the calibration lines was strongly dependent both on the type of native diamagnetic material and the magnetic modification technique. This means that specific calibration curves have to be prepared for each target combination of treated diamagnetic material and magnetic label. Several factors have caused this situation, mainly the character of the materials to be modified, such as their appearance (e.g., fine or coarse powder), their diameter or aspect ratio, the simultaneous presence of both small and large particles, and their interparticle spacing.

The magnetic permeability measurements were highly reproducible; the relative standard deviations were found to be well below 1% for both between run repeatability and between day repeatability, as well as the repeatability within the three following days.

Conclusions

A very simple procedure for the determination of magnetic iron oxide concentration on magnetically modified powdered materials has been developed. A low cost, commercially available magnetic permeability meter was successfully used for the measurements.

Acknowledgements

This work was supported by the Grant Agency of the Czech Republic (Project No. 13-13709S) and by the projects LO1305 and LD14066 of the Ministry of Education, Youth and Sports of the Czech Republic. The research was also part of COST TD1203 activities.

References

Abrahamsson, D., Kriz, K. B., Lu, M., & Kriz, D. (2004). A preliminary study on DNA detection based on relative magnetic permeability measurements and histone HI conjugated superparamagnetic nanoparticles as magnetic tracers. *Biosensors and Bioelectronics*, *19*, 1549–1557.

Kharissova, O. V., Dias, H. R., & Kharisov, B. I. (2015). Magnetic adsorbents based on micro- and nano-structured materials. *RSC Advances*, *5*, 6695–6719.

Kiwada, H., Sato, J., Yamada, S., & Kato, Y. (1986). Feasibility of magnetic liposomes as a targeting device for drugs. *Chemical and Pharmaceutical Bulletin*, *34*, 4253–4258.

Kriz, K., Gehrke, J., & Kriz, D. (1998). Advancements toward magneto immunoassays. *Biosensors and Bioelectronics*, *13*, 817–823.

Laurent, S., Forge, D., Port, M., Roch, A., Robic, C., Elst, L. V., et al. (2008). Magnetic iron oxide nanoparticles: Synthesis, stabilization, vectorization, physicochemical characterizations, and biological applications. *Chemical Reviews*, *108*, 2064–2110.

Massart, R. (1981). Preparation of aqueous magnetic liquids in alkaline and acidic media. *IEEE Transactions on Magnetics*, *17*, 1247–1248.

Safarik, I., Horska, K., Pospiskova, K., & Safarikova, M. (2012a). Magnetically responsive activated carbons for bio- and environmental applications. *International Review of Chemical Engineering*, *4*, 346–352.

Safarik, I., Horska, K., Pospiskova, K., & Safarikova, M. (2012b). One-step preparation of magnetically responsive materials from non-magnetic powders. *Powder Technology*, *229*, 285–289.

Safarik, I., Pospiskova, K., Horska, K., Maderova, Z., & Safarikova, M. (2014). Magnetically responsive (nano) biocomposites. In A. Prokop, Y. Iwasaki, & A. Harada (Eds.), *Intracellular delivery* (Vol. 2) (pp. 17–34). New York, NY: Springer.

Safarik, I., & Safarikova, M. (2014). One-step magnetic modification of non-magnetic solid materials. *International Journal of Materials Research*, *105*(1), 104–107.

Saito, T., Koopal, L. K., Nagasaki, S., & Tanaka, S. (2008). Adsorption of heterogeneously charged nanoparticles on a variably charged surface by the extended surface complexation approach: Charge regulation, chemical heterogeneity, and surface complexation. *The Journal of Physical Chemistry B*, *112*(5), 1339–1349.

5.2 Adsorpce organických barviv

5.2.1 Chitosan/kvasinkový kompozit

Chitosan je přírodní polysacharid získávaný deacetylací chitinu. Pro svou netoxicitu a biodegradovatelnost se řadí mezi nejvíce využívané biomateriály sloužící jako nosiče pro imobilizované buňky i enzymy.

Magnetické chitosanové mikročástice (o velikosti 10 – 200 μm) byly vytvořeny jednoduchou *in situ* syntézou využívající heptahydrát síranu železnatého, hydroxid sodný a mikrovlnné ozařování v běžné mikrovlnné troubě. Vzniklý materiál byl zesítěn pomocí glutaraldehydu a posléze byly kovalentně navázány resuspendované kvasinkové buňky (pekařské droždí, *Saccharomyces cerevisiae*).

Výsledný biokompozitní materiál byl testován nejen pro sorpci modelových barviv, ale také jako celobuněčný biokatalyzátor (pro výrobu invertního cukru a degradaci peroxidu vodíku).

Pro sorpční experimenty byla vybrána krystalová violeť (zástupce trifenymetanových barviv) a safranin O (safraninová barviva). Ukázalo se, že samotné magnetické chitosanové mikročástice neadsorbují ani jedno z barviv, veškerá sorpce je tedy způsobena přítomností navázaných kvasinek. Získané hodnoty maximálních adsorpčních kapacit jsou proto srovnatelné s daty publikovanými v předchozí studii pracující s buňkami *S. cerevisiae* modifikovanými prostřednictvím kyselené magnetické kapaliny (Safarik et al., 2002).

Příloha 7:

Microwave-synthesized magnetic chitosan microparticles for the immobilization of yeast cells

Safarik I, Pospiskova K, Maderova Z, Baldikova E, Horska K, Safarikova M

Yeast 32, **2015**, 239-242

Yeast
Yeast 2015; **32**: 239–243.
Published online 13 May 2014 in Wiley Online Library
(wileyonlinelibrary.com) **DOI:** 10.1002/yea.3017

Special Issue Article

Microwave-synthesized magnetic chitosan microparticles for the immobilization of yeast cells

Ivo Safarik[1,2]*, Kristyna Pospiskova[2], Zdenka Maderova[1], Eva Baldikova[1], Katerina Horska[1] and Mirka Safarikova[1]

[1]*Department of Nanobiotechnology, Institute of Nanobiology and Structural Biology of GCRC, Ceske Budejovice, Czech Republic*
[2]*Regional Centre of Advanced Technologies and Materials, Palacky University, Olomouc, Czech Republic*

**Correspondence to:*
I. Safarik, Department of Nanobiotechnology, Institute of Nanobiology and Structural Biology of GCRC, Na Sadkach 7, 370 05 Ceske Budejovice, Czech Republic.
E-mail: ivosaf@yahoo.com;
WWW: www.nh.cas.cz/people/safarik

Abstract

An extremely simple procedure has been developed for the immobilization of *Saccharomyces cerevisiae* cells on magnetic chitosan microparticles. The magnetic carrier was prepared using an inexpensive, simple, rapid, one-pot process, based on the microwave irradiation of chitosan and ferrous sulphate at high pH. Immobilized yeast cells have been used for sucrose hydrolysis, hydrogen peroxide decomposition and the adsorption of selected dyes. Copyright © 2014 John Wiley & Sons, Ltd.

Keywords: **chitosan; magnetite; microwave irradiation; cells immobilization; yeast; *Saccharomyces cerevisiae***

Received: 1 January 2014
Accepted: 11 April 2014

Introduction

Immobilized microbial cells have been used extensively in various laboratory-scale, industrial, biotechnological and environmental technology applications. Many different carriers, especially natural polymers (e.g. algal polysaccharides – agar, agarose, alginate, carrageenan) and synthetic polymers (polyacrylamide, polystyrene, polyurethane) were successfully applied for the encapsulation of microbial cells (Cassidy *et al*., 1996). Among them, chitosan (a linear polysaccharide composed of randomly distributed β-(1,4)-linked D-glucosamine and *N*-acetyl-D-glucosamine) has been used several times (Aguilar-May and Sanchez-Saavedra, 2009; Li *et al*., 2007; Odaci *et al*., 2009). Chitosan is a cheap, biocompatible, hydrophilic, mechanically stable biopolymer containing reactive functional groups suitable and accessible for chemical modification. The immobilization of cells on chitosan carriers can usually be performed in a simple way.

Magnetic carriers enable simple magnetic separation of immobilized cells (Safarik and Safarikova, 2007, 2009). Magnetic chitosan derivatives have been already prepared and used for the immobilization of various enzymes (Ju *et al*., 2012; Peniche *et al*., 2005; Wu *et al*., 2009; Yang *et al*., 2010) or the isolation of target biologically active compounds, such as lectins (Safarik *et al*., 2010). In many cases, complicated procedures for magnetic chitosan particle preparations are used which are not applicable for large-scale synthesis.

In this paper we describe a simple procedure for the immobilization of *Saccharomyces cerevisiae* cells onto microwave-synthesized magnetic chitosan microparticles, which can be prepared in an extremely simple, one-pot procedure. The results show that immobilized yeast cells can be successfully used for sucrose hydrolysis, hydrogen peroxide decomposition and the adsorption of important xenobiotics, e.g. dyes.

Materials and methods

Materials

Chitosan [medium molecular weight (ca. 400 000), 75–85% deacetylated] was from Fluka, while

glutaraldehyde was obtained from Sigma. Iron(II) sulphate heptahydrate, sodium hydroxide, hydrogen peroxide, sucrose and common chemicals were from Lach-Ner, Czech Republic. *S. cerevisiae* cells (compressed baker's yeast) were obtained from a food shop. A domestic microwave oven (700 W, 2450 MHz, type 0205, Eta, Czech Republic) with a rotary plate was used for the preparation of the magnetic carrier.

Microwave-assisted preparation of magnetic chitosan microparticles

Microwave-synthesized magnetic chitosan microparticles were prepared as follows: Chitosan (1 g) was dissolved in 250 ml 5% v/v acetic acid solution under stirring with a mechanical overhead stirrer (300 rpm; RZR 2041, Heidolph, Germany). After dissolution of the chitosan, 250 ml water was added, followed by 100 ml 3.6% w/v solution of $FeSO_4 . 7H_2O$. Then 10% w/v NaOH was added dropwise under intense stirring (1000 rpm) until the pH of the suspension was at least 10 and a dark precipitate was formed; 250 ml fractions of the suspension were transferred into 1000 ml beakers and submitted to 10 min microwave treatment at the maximum power (700 W). The magnetically responsive chitosan microparticles formed were repeatedly washed with water (Pospiskova and Safarik, 2013).

Yeast cells immobilization

The microwave-synthesized magnetic chitosan microparticles were cross-linked and activated, using glutaraldehyde, before immobilization of yeast cells. 400 mg magnetic particles (wet weight) were mixed with 20 ml 5% v/v solution of glutaraldehyde in a capped Falcon tube and shaken at room temperature at 20 rpm for 3 h on an automatic rotator (Multi Bio RS-24, Biosan, Latvia). Then the particles were magnetically separated and washed with distilled water. Cross-linked and activated chitosan particles were mixed with a suspension of 3g *S. cerevisiae* cells in 30 ml distilled water (measured pH = 5.7) and shaken for 2 h at 18 rpm at room temperature. Finally, the magnetic particles with immobilized yeast cells were washed with distilled water until no free cells were detected in the supernatant (absorbance measurement at 600 nm). This immobilized biocatalyst was stored at 4 °C in 0.9% w/v NaCl.

Sucrose hydrolysis by immobilized yeast cells

Study of sucrose hydrolysis by immobilized yeast cells, their operational and storage stabilities and time dependence of substrate hydrolysis were performed as described recently (Pospiskova *et al.*, 2013).

Hydrogen peroxide degradation by immobilized yeast cells

Study of hydrogen peroxide degradation by immobilized yeast cells (effects of various amounts of magnetic biocatalyst) was performed as described recently (Safarik *et al.*, 2008). Briefly, different amounts of magnetic biocatalyst were incubated for 1 h in 50 ml reaction medium (0.15 M NaCl and 0.05 M $CaCl_2$) containing hydrogen peroxide at an initial concentration of 300 mM.

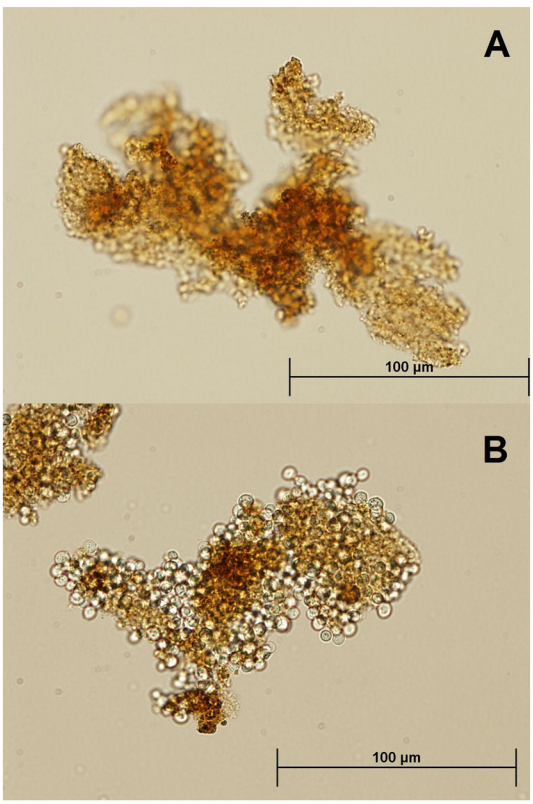

Figure 1. Optical microscopy images of microwave-synthesized magnetic chitosan microparticles (A) and magnetic chitosan microparticles with immobilized *S. cerevisiae* cells (B)

Adsorption of dyes by immobilized yeast cells

The adsorption of safranin O and crystal violet dyes was performed as described recently (Safarik *et al*., 2007). Briefly, 0.4 ml of the suspension of immobilized yeast cells (the volume of the settled adsorbent was 0.1 ml) was mixed with 4.8 ml water in a 15 ml test tube. Then 0.01–2.0 ml stock water solution (1 mg/ml) of a tested dye was added and the total volume of the suspension was made up to 10.0 ml with water. The suspension was mixed for 3 h at room temperature. Then the magnetic yeast cells were separated from the suspension using a magnetic separator and the clear supernatant was used for the spectrophotometric measurement. The concentration of free (unbound) dye in the supernatant (C_{eq}) was determined from the calibration curve. The amount of dye bound to the unit amount of the adsorbent (q_{eq}) was calculated using the following formula, taking into account that the dry weight of 1 ml sedimented immobilized yeast cells was 0.035 g:

$$q_{eq} = \left(10\, C_{init} - 10\, C_{eq}\right)/3.5\ (\mu g/\mu l \text{ or } mg/ml) \quad (1)$$

where C_{init} is the initial concentration of dye used in the experiment.

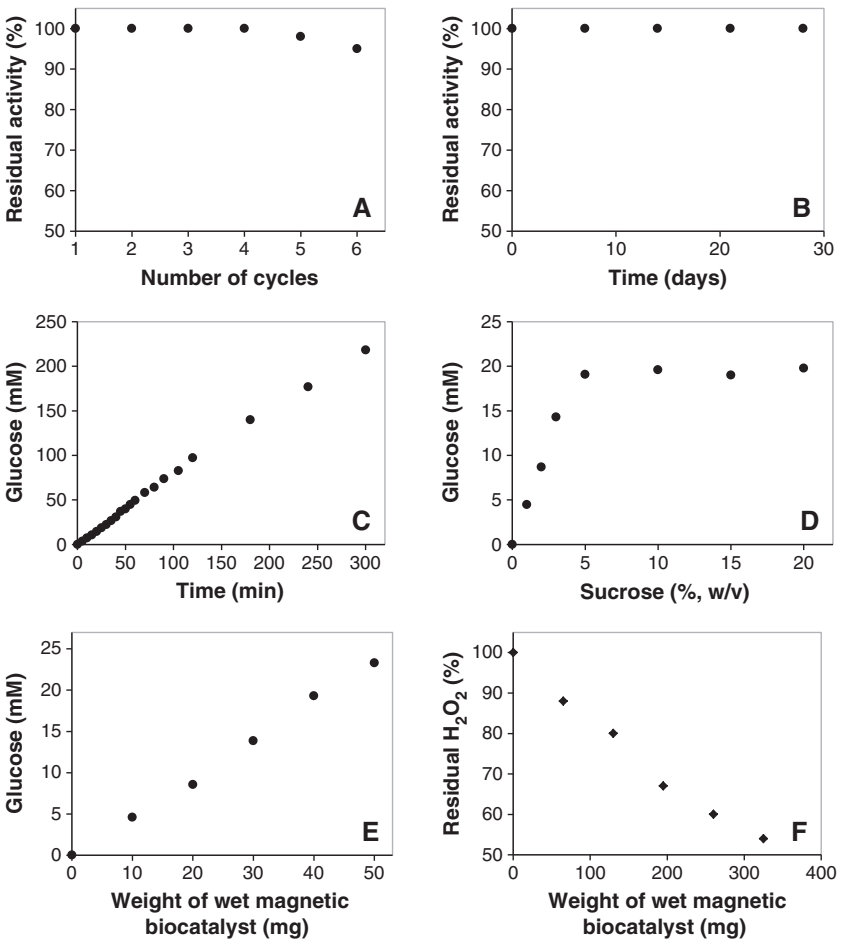

Figure 2. Operational stability of *S. cerevisiae* cells immobilized on magnetic chitosan microparticles, evaluated through invertase activity during repeated 20 min reaction cycles of sucrose hydrolysis (initial concentration 20% w/v) (A); time stability of magnetic biocatalyst (B); dependence of sucrose hydrolysis on the reaction time (C); dependence of sucrose hydrolysis after 20 min reaction on the initial concentration of sucrose (D); dependence of sucrose hydrolysis on the amount (wet weight) of magnetically responsive biocatalyst used for the reaction (E); dependence of hydrogen peroxide decomposition (initial concentration 300 mM) on the amount (wet weight) of magnetic biocatalyst (F)

DOI: 10.1002/yea

Results and discussion

An extremely simple, inexpensive, one-pot, microwave-assisted procedure has been used for the preparation of magnetically responsive chitosan microparticles with typical diameters of 10–200 μm (Figure 1A). The production of these particles is rapid, and they can be easily removed using an appropriate magnetic separator.

The magnetic chitosan microparticles activated with glutaraldehyde efficiently captured *S. cerevisiae* yeast cells by the simple mixing of cells and magnetic microparticles under defined conditions and a relatively short interaction time (2 h at room temperature). Washing out of the unbound cells was satisfactory. Optical microscopy images clearly showed the binding of yeast cells onto the surface of magnetic chitosan particles (Figure 1B). The yeast cells thus immobilized exhibited the same viability as native cells after vital staining with methylene blue (data not shown).

In the absence of glucose repression, the *S. cerevisiae* yeast chosen as the model microorganism for this study expressed invertase enzymatic activity (*β*-fructofuranosidase; EC 3.2.1.26) in the periplasmic space. Invertase catalyses the hydrolysis of the disaccharide sucrose into the monosaccharides glucose and fructose; this is why magnetically modified yeast cells were used as a whole-cell biocatalyst for sucrose hydrolysis. After six cycles of sucrose hydrolysis, the immobilized yeast retained 95% of the initial invertase activity (Figure 2A). The biocatalyst was very stable during 1 month of storage at 4 °C in saline (Figure 2B). Figure 2C shows sucrose hydrolysis in time (performed for 5 h), while Figure 2D illustrates the dependence of sucrose hydrolysis on the initial concentration of sucrose after 20 min reaction time. Figure 2E demonstrates the dependence of sucrose hydrolysis on the amount (wet weight) of magnetically responsive biocatalyst used for the reaction. Potential leaching of cells from the magnetic material was tested by turbidity measurement at 600 nm; the leaching was negligible during a 1 month period and had no significant impact on the enzyme activity of the biocatalyst (Figure 2B). No extracellular invertase activity was detected during the same period.

Immobilized yeast cells also enabled efficient degradation of hydrogen peroxide, due to the presence of intracellular catalase (hydrogen peroxide: hydrogen peroxide oxidoreductase; EC 1.11.1.6). Figure 2F shows the dependence of hydrogen peroxide decomposition on the amount of wet biocatalyst used.

Microbial cells can also be efficiently used as adsorbents for the removal of organic and inorganic xenobiotics. Yeast cells immobilized on magnetic chitosan microparticles adsorbed two important dyes belonging to different dye classes, viz. safranin O (safranin group) and crystal violet (triphenylmethane group). The adsorption was completely caused by the yeast cells, not by the chitosan carrier (Figure 3). The experimental data, analysed by means of both linear and non-linear regression, using SigmaPlot 2000 software (SPSS Inc., USA), fitted well to the Langmuir isotherm equation, usually expressed as:

$$q_{eq} = \frac{Q_{\max} b C_{eq}}{1 + b C_{eq}} \qquad (2)$$

where q_{eq} (expressed in mg/g) is the amount of the adsorbed dye/unit mass of immobilized yeast cells and C_{eq} (expressed in mg/l) is the unadsorbed dye concentration in solution at equilibrium. Q_{max} is the maximum amount of the dye/unit mass (mg/g) of immobilized yeast cells to form a complete monolayer on the surface, bound at high dye concentration, and b is a constant related to the affinity of the binding sites (expressed in l/mg).

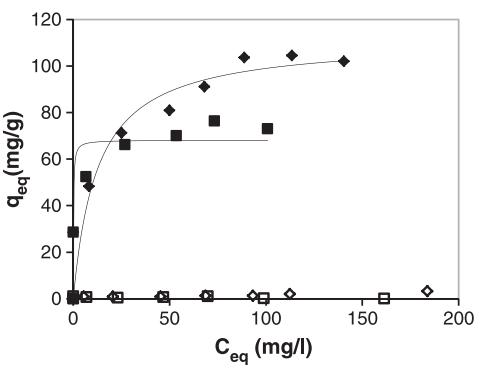

Figure 3. Equilibrium adsorption isotherms of safranin O (♦) and crystal violet (■) by *S. cerevisiae* cells immobilized on magnetic chitosan microparticles and by the native magnetic chitosan microparticles (◊, □), as measured at room temperature. Solid lines, fitted Langmuir isotherm functions; C_{eq}, equilibrium liquid-phase concentration of the unadsorbed (free) dye (mg/l); q_{eq}, equilibrium solid-phase concentration of the adsorbed dye (mg/g)

DOI: 10.1002/yea

This allowed the calculation of the maximum adsorption capacities of the magnetic biocomposite, which are very important parameters describing the adsorption process: the values 99 ± 5 and 69 ± 3 mg/g dry biosorbent for safranin and crystal violet, respectively, were calculated using the linear regression, while the values 111 ± 6 and 68 ± 3 mg/g dry biosorbent were calculated using non-linear regression. The values of r^2 (goodness of fit) were 0.986 for both dyes in linear regression. These maximum adsorption capacities are quite high and fully comparable with other described magnetic biosorbents used for the same purpose (Safarik and Safarikova, 2007).

Conclusions

This study demonstrated a fast, easy and inexpensive method for the preparation of magnetically responsive chitosan microparticles with immobilized yeast cells, and their use as a biocatalyst and/or biosorbent. Microwave-assisted synthesis of magnetic chitosan microparticles is very simple, and their interaction with *S. cerevisiae* cells leads to the formation of magnetically responsive biocomposites. These magnetic whole-cell biocatalysts retain their intracellular enzymatic activities and have very good stability; they can be used for sucrose hydrolysis by intracellular invertase and for hydrogen peroxide degradation by intracellular catalase. In addition, the prepared biocomposite can be used as an efficient adsorbent for the removal of xenobiotics.

Acknowledgements

This research was supported by the Grant Agency of the Czech Republic (Project No. 13-13709S), the Ministry of Education of the Czech Republic (Research Project Nos LD13023, CZ.1.05/2.1.00/03.0058 and CZ.1.07/2.4.00/31.0189) and the COST Action FA0907–***BIOFLAVOUR***.

References

Aguilar-May B, Sanchez-Saavedra MD. 2009. Growth and removal of nitrogen and phosphorus by free-living and chitosan-immobilized cells of the marine cyanobacterium *Synechococcus elongatus*. *J Appl Phycol* **21**: 353–360.

Cassidy MB, Lee H, Trevors JT. 1996. Environmental applications of immobilized microbial cells: a review. *J Ind Microbiol* **16**: 79–101.

Ju HY, Kuo CH, Too JR, *et al.* 2012. Optimal covalent immobilization of α-chymotrypsin on Fe_3O_4–chitosan nanoparticles. *J Mol Catal B Enzymatic* **78**: 9–15.

Li GY, Huang KL, Jiang YR, Ding P. 2007. Production of (*R*)-mandelic acid by immobilized cells of *Saccharomyces cerevisiae* on chitosan carrier. *Process Biochem* **42**: 1465–1469.

Odaci D, Timur S, Telefoncu A. 2009. A microbial biosensor based on bacterial cells immobilized on chitosan matrix. *Bioelectrochemistry* **75**: 77–82.

Peniche H, Osorio A, Acosta N, *et al.* 2005. Preparation and characterization of superparamagnetic chitosan microspheres: application as a support for the immobilization of tyrosinase. *J Appl Polym Sci* **98**: 651–657.

Pospiskova K, Prochazkova G, Safarik I. 2013. One-step magnetic modification of yeast cells by microwave-synthesized iron oxide microparticles. *Lett Appl Microbiol* **56**: 456–461.

Pospiskova K, Safarik I. 2013. Low-cost, easy-to-prepare magnetic chitosan microparticles for enzymes immobilization. *Carbohydr Polym* **96**: 545–548.

Safarik I, Horska K, Martinez LM, Safarikova M. 2010. Large scale magnetic separation of *Solanum tuberosum* tuber lectin from potato starch waste water. *AIP Conf Proc* **1311**: 146–151.

Safarik I, Rego LFT, Borovska M, *et al.* 2007. New magnetically responsive yeast-based biosorbent for the efficient removal of water-soluble dyes. *Enzyme Microb Technol* **40**: 1551–1556.

Safarik I, Sabatkova Z, Safarikova M. 2008. Hydrogen peroxide removal with magnetically responsive *Saccharomyces cerevisiae* cells. *J Agr Food Chem* **56**: 7925–7928.

Safarik I, Safarikova M. 2007. Magnetically modified microbial cells: a new type of magnetic adsorbents. *China Particuol* **5**: 19–25.

Safarik I, Safarikova M. 2009. Magnetic nano- and microparticles in biotechnology. *Chem Papers* **63**: 497–505.

Wu Y, Wang YJ, Luo GS, Dai YY. 2009. *In situ* preparation of magnetic Fe_3O_4–chitosan nanoparticles for lipase immobilization by cross-linking and oxidation in aqueous solution. *Bioresour Technol* **100**: 3459–3464.

Yang K, Xu NS, Su WW. 2010. Co-immobilized enzymes in magnetic chitosan beads for improved hydrolysis of macromolecular substrates under a time-varying magnetic field. *J Biotechnol* **148**: 119–127.

5.2.2 Čaj Rooibos

Čaj Rooibos představuje druhý nejvíce konzumovaný čaj na světě. Je charakteristický nepřítomností kofeinu a v porovnání s běžným černým čajem také nižším obsahem taninů. Ač již bylo napsáno mnoho publikací zaměřených na tento typ materiálu, zatím žádná z nich se nezaobírala jeho použitím jako adsorbentu organických barviv.

Čajový odpad byl magneticky modifikován smícháním s mikrovlnně syntetizovanými magnetickými nano- a mikročásticemi oxidů železa a následným sušením. Získaný materiál vykazoval výbornou odezvu vůči vnějšímu magnetickému poli, jak je v přiložené publikaci zdokumentováno na Obr. 1.

V rámci této práce bylo testováno 17 barviv s různou chemickou strukturou. Osm z nich vykázalo v rámci screeningových experimentů vynikající adsorpční účinnost (> 90 %), a proto byly podrobeny dalším testům, především analýze získaných adsorpčních rovnovážných dat pomocí Langmuirova a Freundlichova modelu.

Získané maximální adsorpční kapacity magnetického derivátu se pohybovaly v rozmezí 62-142 mg/g. Nativní čajový odpad vykazoval ve všech testovaných případech (vyjma safraninu O) vyšší hodnoty kapacit, a to v rozmezí ca 5 – 17 %. Nejvyšší hodnoty maximálních adsorpčních kapacit, ale také nejvýznamnější rozdíl mezi nativní a magnetickou verzí (67 %) byl pozorován u adsorpce Bismarckovo hnědi Y. Ačkoliv došlo po magnetizaci materiálu ke snížení účinnosti adsorpce, stále lze magnetický derivát preferovat, a to zejména díky jeho snadné separaci ze systému.

Příloha 8:

Spent Rooibos (*Aspalathus linearis*) tea biomass as an adsorbent for organic dyes removal

Safarik I, Maderova Z, Horska K, Baldikova E, Pospiskova K, Safarikova M

Bioremed. J. 19, **2015**, 183-187

Bioremediation Journal, 19(3):183–187, 2015

ISSN: 1088-9868 print / 1547-6529 online
DOI: 10.1080/10889868.2014.979279

Spent Rooibos (*Aspalathus linearis*) Tea Biomass as an Adsorbent for Organic Dye Removal

Ivo Safarik,[1,2]
Zdenka Maderova,[1]
Katerina Horska,[1]
Eva Baldikova,[1]
Kristyna Pospiskova,[2]
and Mirka Safarikova[1]
[1]Department of Nanobiotechnology, Institute of Nanobiology and Structural Biology of Global Change Research Centre, Ceske Budejovice, Czech Republic
[2]Regional Centre of Advanced Technologies and Materials, Palacky University, Olomouc, Czech Republic

ABSTRACT Spent rooibos (*Aspalathus linearis*) tea biomass can be used as an inexpensive biosorbent for xenobiotic removal. Seventeen dyes have been tested for their affinity to spent rooibos tea biomass. Eight dyes were used to study the adsorption process in detail. The dye adsorption has been described with the Langmuir isotherm. The calculated maximum adsorption capacities reached the value of over 200 mg of dye per gram of dried rooibos biomass for Bismarck brown Y. Spent rooibos tea biomass was also magnetically modified by contact with microwave-synthesized magnetic iron oxide nano- and microparticles. This new type of magnetically responsive biocomposite material can be easily separated by means of strong permanent magnets. Both native and magnetically modified spent rooibos biomass have shown excellent adsorption capacities for various types of organic dyes, so they are highly promising adsorbents in environmental technologies for selected xenobiotic removal.

KEYWORDS dye adsorption, postmagnetization, spent rooibos biomass

INTRODUCTION

The genus *Aspalathus* (Fabaceae, Tribe Crotalarieae) belongs to very important plants that are endemic to the Cape Floristic Region. Rooibos tea, produced from *A. linearis* (Burm. F.) Dahlg., is a well-known herbal tea, becoming the second most commonly consumed beverage tea ingredient in the world after ordinary tea (*Camellia sinensis*) (Joubert and de Beer 2011).

Rooibos is prized as a caffeine-free herbal tea, although traces of the alkaloid sparteine have been reported. When compared with black tea (*Camellia sinensis*), rooibos contains less tannins. Rooibos tea comprises two unique phenolic compounds, namely, aspalathin (a dihydrochalcone *C*-glucoside) and aspalalinin (a cyclic dihydrochalcone). Other major phenolic compounds present in rooibos tea include flavones (orientin, isoorientin, vitexin, isovitexin, luteolin, chrysoeriol), flavanones (dihydroorientin, dihydroisoorientin, hemiphlorin), and flavonols (quercetin, hyperoside, isoquercitrin, rutin). Phenolic acids, lignans, flavone diglycosides, (+)-catechin, a phenylpyruvic acid glycoside, the flavonol

Address correspondence to Ivo Safarik, Department of Nanobiotechnology, Institute of Nanobiology and Structural Biology of GCRC, Na Sadkach 7, 370 05 Ceske Budejovice, Czech Republic. E-mail: ivosaf@yahoo.com; www.nh.cas.cz/people/safarik

Color versions of one or more of the figures in the article can be found online at www.tandfonline.com/bbrm.

quercetin-3-*O*-robinobioside, and the coumarins, esculetin, and esculin have also been identified. The potential health benefits of rooibos tea have been linked to its phenolic content (Joubert and de Beer 2011).

Traditional or "conventional" rooibos is fermented to develop its characteristic red-brown leaf and infusion color and pleasant and slightly sweet flavor. In addition to "standard rooibos tea," an instant rooibos from the fermented plant material has been developed (Joubert and de Beer 2011). Rooibos extracts enriched in aspalathin, a potent antioxidant unique to rooibos, are also employed in cosmetic products (Joubert and de Beer 2011; Joubert and Schulz 2006).

Many research papers have described the rooibos composition, preparation, and health benefits. However, no attention has been paid to the utilization of spent rooibos biomass, originating after the tea preparation or during the rooibos extract production. In fact, spent (waste) plant materials have been often tested as potential biosorbents for the removal of wide variety of organic and inorganic xenobiotics (Fomina and Gadd 2014; Gadd 2009; Shukla et al. 2002; Srinivasan and Viraraghavan 2010; Sud, Mahajan, and Kaur 2008). During preliminary experiments, we have observed that spent rooibos biomass efficiently adsorbed a variety of organic dyes from water solutions. In this short paper, we describe the results of the adsorption experiments. In order to improve manipulation with spent rooibos biomass, a magnetically responsive rooibos derivative has been prepared using an extremely simple and low-cost procedure and tested as a magnetic biosorbent for dye removal.

MATERIALS AND METHODS

Materials

Rooibos tea was obtained in the local supermarket in Ceske Budejovice, Czech Republic. After preparation of the tea infusion, the spent material was soaked several times with boiling water until majority of brown-colored substances had been extracted. Then, the rooibos biomass was completely dried at ca. 60°C and milled to obtain fine particles (ca. 0.15–1.5 mm in diameter). The dyes used for the adsorption experiments are described in Table 1. Ferrous sulfate heptahydrate and sodium hydroxide were from Sigma-Aldrich, Prague, Czech Republic.

Magnetic Modification of Spent Rooibos Biomass

Spent rooibos biomass was magnetically modified using microwave-synthesized magnetic iron oxide particles (Safarik and Safarikova 2014). In a typical procedure, 1 g $FeSO_4 \cdot 7\ H_2O$ was dissolved in 100 mL of

TABLE 1 **Characteristics of the Water-Soluble Dyes Used and the Decrease in Free Dye Concentration after 4-h Incubation with Spent Rooibos Biomass**

Dye	CI Number	Type of dye	Manufacturer/Supplier	Decrease in free dye concentration (%)
Orange II, sodium salt	15510	Monoazo	Sigma, USA	6
Amido black 10B	20470	Disazo	Merck, Germany	0
Bismarck brown Y	21000	Disazo	Sigma, USA	96
Congo red	22120	Disazo	Sigma, USA	15
Saturn blue LBRR 200	34140	Polyazo	Synthesia, Czech Republic	0
Brilliant Green	42040	Triarylmethane	Lachema, Czech Republic	93
Crystal violet	42555	Triarylmethane	Lachema, Czech Republic	92
Methyl green	42585	Triarylmethane	Loba Feinchemie, Austria	95
Aniline blue, water-soluble	42755	Triarylmethane	Lachema, Czech Republic	70
Fluorescein natrium	45350	Fluorone	Geigy, Switzerland	2
Acridine orange	46005	Acridine	Loba Feinchemie, Austria	93
Azocarmine G	50085	Quinone-imine	Lachema, Czech Republic	22
Safranin O	50240	Safranin	Sigma, USA	95
Nigrosine, water-soluble	50420	Nigrosin	Lachema, Czech Republic	10
Nile blue A (sulfate)	51180	Oxazin	Chemische Fabrik GmbH, Germany	93
Methylene blue	52015	Quinone-imine	Sigma, USA	94
Indigocarmine	73015	Indigo	Lachema, Czech Republic	7

water in a 600–800-mL beaker, and a solution of sodium or potassium hydroxide (1 mol L^{-1}) was added slowly under mixing until the pH reached the value ca. 12; during this process, a precipitate of iron hydroxides was formed. Then, the suspension was diluted up to 200 mL with water and inserted into a standard kitchen microwave oven (700 W, 2450 MHz). The suspension was treated usually for 10 min at the maximum power. Then, the beaker was removed from the oven and the formed magnetic iron oxide nano- and microparticles were repeatedly washed with water until neutral pH of the magnetic suspension was reached.

To prepare magnetically responsive rooibos biomass, 1 g of rooibos powder was thoroughly mixed in a short test tube or a small beaker with 2 mL of microwave iron oxide nano- and microparticle suspension (1 part completely sedimented iron oxide particles and 4 parts water). Vigorous mixing with a spatula or laboratory spoon enabled homogeneous distribution of magnetic nano- and microparticles within the treated material. This mixture was allowed to dry completely at temperatures not exceeding 60°C for 48 h. In order to increase magnetic response of the rooibos composite, the amount of iron oxide particles can be increased (Safarik and Safarikova 2014).

Adsorption of Dyes on Spent Rooibos Biomass

To test the ability of the spent rooibos biomass to adsorb the tested dyes, 30 mg of spent rooibos biomass was mixed with 10 mL of tested dyes (100 μg mL^{-1}). After 4 h of incubation (rotation mixer; Dynal, Oslo, Norway) and subsequent centrifugation, the absorbances of supernatants (and control dye samples without adsorbent) were measured using Cintra 20 spectrophotometer (GBC Scientific Equipment, Braeside, Australia) and the percentage of the adsorbed dye calculated.

The following procedure was used to study the adsorption properties (Safarik et al. 2012). Thirty milligram of native or magnetically modified spent rooibos biomass were mixed with 4.0 mL of water in a test tube. Then, a 1–6-mL portion of stock water solution (1 mg mL^{-1}) of a tested dye was added and the total volume of the solution was made up to 10.0 mL with water. The suspension was mixed for 4 h at room temperature. Then, the native rooibos biomass was centrifuged out while magnetic rooibos derivative was separated from the suspension using a magnetic separator (MPC-1 or MPC-6; Dynal) and the clear supernatant was used for the spectrophotometric measurement. The concentration of free (unbound) dye in the supernatant (C_{eq}) was determined from the calibration curve. The amount of dye bound to the unit mass of the adsorbent (q_{eq}) was calculated using the following formula:

$$q_{eq} = (C_{tot} - C_{eq})/3 \ (mg\,g^{-1}) \quad (1)$$

where C_{tot} is the total (initial) concentration (μg mL^{-1}) of dye used in the experiment. The value q_{eq} was expressed in mg of adsorbed dye per 1 g of adsorbent.

Other Procedures

Equilibrium adsorption data were fit to Langmuir adsorption isotherms using SigmaPlot software (Systat Software GmbH, Erkrath, Germany).

RESULTS AND DISCUSSION

Many types of biomaterials have been tested as potential adsorbents for the removal of organic xenobiotics. These works prompted our experiments with spent rooibos biomass. In order to simplify the adsorbent separation from the suspension, the spent rooibos biomass was also magnetically modified by contact with microwave-synthesized magnetic iron oxide nano- and microparticles (Safarik and Safarikova 2014). This modified material could be easily separated by rare earth permanent magnets or commercially available magnetic separators (see Figure 1).

FIGURE 1 Appearance of native spent rooibos biomass suspension (*left*), suspension of rooibos biomass after magnetic modification (*middle*), and demonstration of magnetic separation of magnetically modified rooibos biomass (*right*).

Dyes with the highest affinity for this material were identified among 17 types of water-soluble organic dyes belonging to different classes (see Table 1 for details). The decrease in free dye concentration after 4-h adsorption process under standard conditions (see Materials and Methods) was taken as a measure of the dye affinity for spent rooibos biomass. It can be clearly seen that various dyes exhibit very different affinities for rooibos biomass.

Eight water-soluble dyes belonging to different dye classes, selected according to their adsorption affinities during the preliminary experiments (see Table 1), were used to study the sorption on spent rooibos biomass. The tested dyes comprised crystal violet, brilliant green, and methyl green (triarylmethane group), Bismarck brown (azo dye group), acridine orange (acridine group), methylene blue (quinone-imine group), Nile blue (oxazin group), and safranin O (safranin group). The dyes used for adsorption experiments were dissolved in distilled water without buffering the solution. The adsorption of tested dyes reached equilibrium in approximately 2–3 h (see Figure 2); the incubation time of 4 h was used for adsorption experiments. The equilibrium adsorption isotherms for the tested dyes using both native rooibos biomass and magnetically modified rooibos biomass are shown in Figure 3.

In order to study the adsorption process, Langmuir and Freundlich isotherm equations are usually used for experimental data analysis. The Langmuir model is valid for monolayer adsorption onto a surface with a finite number of identical sites. The well-known expression for the Langmuir model is given by

$$q_{eq} = \frac{Q_{max}\, bC_{eq}}{1 + bC_{eq}} \qquad (2)$$

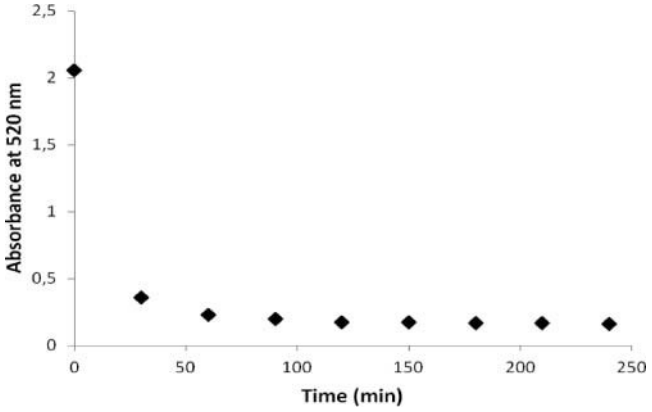

FIGURE 2 Time dependence of the adsorption of methylene blue on spent rooibos biomass.

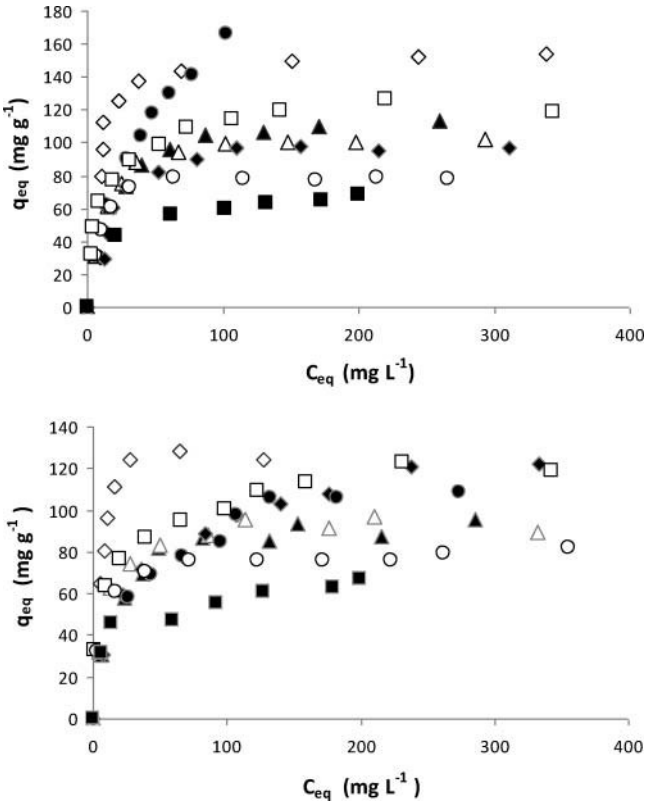

FIGURE 3 Equilibrium adsorption isotherms of tested dyes on native spent rooibos biomass (*top*) and on magnetically modified spent rooibos biomass (*bottom*). C_{eq}= equilibrium liquid-phase concentration of the unadsorbed (free) dye (mg L^{-1}); q_{eq}= equilibrium solid-phase concentration of the adsorbed dye (mg g^{-1}). (○) acridine orange; (●) Bismarck brown Y; (■) brilliant green; (▲) crystal violet; (Δ) methylene blue; (□) methyl green; (◊) Nile blue; (◆) safranin O.

where q_{eq} (expressed in mg g^{-1} or mg mL^{-1}) is the amount of the adsorbed dye per unit mass or sedimented volume of spent rooibos biomass and C_{eq} (expressed in mg L^{-1}) is the unadsorbed dye concentration in solution at equilibrium. Q_{max} is the maximum amount of the dye per unit mass (mg g^{-1}) or sedimented volume (mg mL^{-1}) of spent rooibos biomass to form a complete monolayer on the surface bound at high dye concentration and b is a constant related to the affinity of the binding sites (expressed in L mg^{-1}) (Safarik et al. 2012).

Nonlinear regression calculation using SigmaPlot software was used to fit the experimental data to Langmuir adsorption model and to obtain both constants (Q_{max}, b). The results are presented in Table 2. As it can be seen, the adsorption can be described by the Langmuir isotherm. Such a description allows a simple calculation of the maximum adsorption capacity, which is

TABLE 2 Isotherms Used for the Description of Dyes Adsorption on Both Native and Magnetically Modified Spent Rooibos Biomass and Calculated Adsorption (Q_{max}, b) Coefficients

	Langmuir isotherm $q_{eq} = \frac{Q_{max} b C_{eq}}{1 + b C_{eq}}$	
Dye	Nonmagnetic	Magnetic
Acridine orange	$Q_{max} = 83.6$ $b = 0.127$	$Q_{max} = 79.8$ $b = 0.199$
Bismarck brown Y	$Q_{max} = 202.7$ $b = 0.031$	$Q_{max} = 119.5$ $b = 0.036$
Brilliant green	$Q_{max} = 70.2$ $b = 0.072$	$Q_{max} = 62.4$ $b = 0.162$
Crystal violet	$Q_{max} = 120.5$ $b = 0.064$	$Q_{max} = 98.4$ $b = 0.072$
Methylene blue	$Q_{max} = 109.1$ $b = 0.087$	$Q_{max} = 96.5$ $b = 0.133$
Methyl green	$Q_{max} = 123.5$ $b = 0.109$	$Q_{max} = 116.6$ $b = 0.113$
Nile blue	$Q_{max} = 164.4$ $b = 0.087$	$Q_{max} = 141.8$ $b = 0.161$
Safranin O	$Q_{max} = 107.8$ $b = 0.055$	$Q_{max} = 128.4$ $b = 0.032$

Q_{max} is expressed in mg g^{-1}.

a very important parameter describing the adsorption process.

In the case of eight tested dyes, the highest calculated Q_{max} was found for Bismarck brown Y (202.7 mg g^{-1}), whereas the lowest Q_{max} value was obtained for brilliant green (70.2 mg g^{-1}). As it can be seen from Table 1, similar dyes belonging to the same group could exhibit completely different affinities for spent rooibos tea biomass. Congo red, amido black 10B, and Bismarck brown Y all belong to the azo dye group; however, the adsorption of Congo red and amido black 10B was very low in comparison with that of Bismarck brown Y.

The magnetic modification usually caused slight decrease of maximum adsorption capacity, most probably due to the partial blockage of adsorption sites by magnetic iron oxide particles. In specific cases, however, the presence of magnetic particles in the magnetic biocomposite can lead to the increase of adsorption capacity (see safranin in Table 2).

CONCLUSIONS

The results clearly demonstrate that spent rooibos tea biomass can be easily transformed into a magnetic form by microwave-synthesized magnetic iron oxide particles. Both native (nonmagnetic) and magnetically modified spent rooibos biomass have considerable potential for the removal of selected xenobiotics, such as dyes. It has to be taken into consideration, however, that the adsorption properties of this material are strongly dependent on the dye type.

FUNDING

This research was supported by the Grant Agency of the Czech Republic (Project No. 13-13709S).

REFERENCES

Fomina, M., and G. M. Gadd. 2014. Biosorption: Current perspectives on concept, definition and application. *Bioresour. Technol.* 160:3–14.

Gadd, G. M. 2009. Biosorption: Critical review of scientific rationale, environmental importance and significance for pollution treatment. *J. Chem. Technol. Biotechnol.* 84:13–28.

Joubert, E., and D. de Beer. 2011. Rooibos (*Aspalathus linearis*) beyond the farm gate: From herbal tea to potential phytopharmaceutical. *S. Afr. J. Bot.* 77:869–886.

Joubert, E., and H. Schulz. 2006. Production and quality aspects of rooibos tea and related products. A review. *J. Appl. Bot. Food Qual.* 80:138–144.

Safarik, I., K. Horska, B. Svobodova, and M. Safarikova. 2012. Magnetically modified spent coffee grounds for dyes removal. *Eur. Food Res. Technol.* 234:345–350.

Safarik, I., and M. Safarikova. 2014. One-step magnetic modification of non-magnetic solid materials. *Int. J. Mater. Res.*105:104–107.

Shukla, A., Y. H. Zhang, P. Dubey, J. L. Margrave, and S. S. Shukla. 2002. The role of sawdust in the removal of unwanted materials from water. *J. Hazard. Mater.* 95:137–152.

Srinivasan, A., and T. Viraraghavan. 2010. Decolorization of dye wastewaters by biosorbents: A review. *J. Environ. Manage.* 91:1915–1929.

Sud, D., G. Mahajan, and M. P. Kaur. 2008. Agricultural waste material as potential adsorbent for sequestering heavy metal ions from aqueous solutions—A review. *Bioresour. Technol.* 99:6017–6027.

5.2.3 Žitná sláma

V této krátké publikaci bylo testováno odstranění dvou organických barviv s různou chemickou strukturou, konkrétně akridinové oranže (skupina akridinových barviv) a metylové zeleně (trifenylmetanová barviva), pomocí typického zástupce vedlejších produktů zemědělského průmyslu, a sice žitné slámy.

Magnetická modifikace slámové materiálu byla provedena postmagnetizační technikou využívající MS magnetit. Chemická modifikace byla založena na ošetření materiálu kyselinou citronovou a hydroxidem sodným, po kterém následoval proces magnetizace.

Veškeré adsorpční experimenty byly provedeny v modelovém prostředí. Studiem závislosti účinnosti adsorpce na inkubační době byl stanoven čas nutný k dosažení adsorpční rovnováhy na dvě hodiny. Rovnovážná adsorpční data byla analyzována pomocí Langmuirova modelu, ze kterého byly vypočteny maximální adsorpční kapacity.

Maximální adsorpční kapacita nativní slámy byla pro obě testovaná barviva více než čtyřikrát nižší než u slámy chemicky modifikované. V porovnání s ostatními publikovanými materiály shrnutými v Tabulce 2 přiloženého článku lze konstatovat, že slámový materiál představuje nejen velice účinný, ale také velmi laciný biosorbent pro obě testovaná barviva.

V tomto článku byly slámové deriváty charakterizovány pouze prostřednictvím optické mikroskopie, proto nebyly nalezeny žádné rozdíly vedoucí k takto rozdílným hodnotám adsorpční účinnosti.

Příloha 9:

Organic dyes removal using magnetically modified rye straw

Baldikova E, Safarikova M, Safarik I

J. Magn. Magn. Mater. 380, **2015**, 181-185

Journal of Magnetism and Magnetic Materials 380 (2015) 181–185

Contents lists available at ScienceDirect

Journal of Magnetism and Magnetic Materials

journal homepage: www.elsevier.com/locate/jmmm

Organic dyes removal using magnetically modified rye straw

Eva Baldikova [a,*], Mirka Safarikova [a], Ivo Safarik [a,b,**]

[a] Department of Nanobiotechnology, Institute of Nanobiology and Structural Biology of GCRC, Na Sadkach 7, 370 05 Ceske Budejovice, Czech Republic
[b] Regional Centre of Advanced Technologies and Materials, Palacky University, Slechtitelu 11, 783 71 Olomouc, Czech Republic

ARTICLE INFO

Article history:
Received 24 June 2014
Received in revised form
28 August 2014
Accepted 2 September 2014
Available online 10 September 2014

Keywords:
Rye straw
Adsorbent
Dyes removal
Magnetic modification

ABSTRACT

Rye straw, a very low-cost material, was employed as a biosorbent for two organic water-soluble dyes belonging to different dye classes, namely acridine orange (acridine group) and methyl green (triarylmethane group). The adsorption properties were tested for native and citric acid–NaOH modified rye straw, both in nonmagnetic and magnetic versions. The adsorption equilibrium was reached in 2 h and the adsorption isotherms data were analyzed using the Langmuir model. The highest values of maximum adsorption capacities were 208.3 mg/g for acridine orange and 384.6 mg/g for methyl green.

1. Introduction

Enormous amounts of dyestuff are consumed annually by various sectors of industry, e. g. textile, paper, leather, plastics, rubber, cosmetics, pharmaceuticals and food industries [1]. These compounds or their metabolites cause concern for human health because of their toxicity, carcinogenity and mutagenity [2,3] and also due to high persistence in environment and non-biodegradable characteristics [4]. Moreover, the colored dye effluents can block the penetration of sunlight and oxygen which are both essential for various aquatic forms of life [5].

Many techniques have been employed to eliminate dyes from waste water. These methods involve e.g. ion exchange, coagulation and flocculation, oxidation and various forms of degradation (photo-, bio- and chemical-) [4,6]. Among them, adsorption is considered to be superior because of the high efficiency and subsequently economical value [7].

In recent years, many plant materials have been tested as low-cost adsorbents for various xenobiotics, such as organic dyes, heavy metals, radionuclides or endocrinne disruptors. For instance, wheat straw [8], barley straw [9], rice straw [10], rice husks [11], sawdust [1], tea waste [5], peanut husks [12], spent coffee grounds [13], coffee husks [14], spent grain [15], fruit peels [16] and sugarcane bagasse [17] have been succesfully used for organic dyes removal.

Rye straw represents a very interesting material that can be obtained in large amount and for low price. Nevertheless, there are only few publications focused on utilization of rye derivatives for xenobiotics removal. One of them describes adsorption of Cr (VI) [18] and the second one removal of azodyes [19].

Native plant materials usually show lower maximum adsorption capacities. Nevertheless, these values can be significantly increased using a suitable method such as treatment with various acids, hydroxides or combination of both; also less common carbonization or hydrolysis have been reported recently [9,11].

A successful combination of nonmagnetic powdered material with magnetic nano- or microparticles (often bound on the surface or within the pores of the modified material) results in a formation of magnetically responsive (bio)composites which exhibit response to external magnetic field. Magnetic materials facilitate and accelerate many manipulations, also in difficult-to-handle materials (including raw extracts, blood and other body fluid, environmental samples, cultivation media, suspensions, etc.) [20]. Originally diamagnetic materials can be easily and selectively separated using a permanent magnet, an appropriate magnetic separator or an electromagnet. Magnetic separations can also be performed in large scale due to the existence of industrial magnetic separators, currently employed e.g. in kaolin decolorization, steel industry, mineral beneficiation, etc. [20].

The aim of this paper is the comparison of adsorption properties of native and chemically modified rye straw, both in nonmagnetic and magnetic versions for organic dyes adsorption and a demonstration of the promising potential of this type of plant-based material.

* Corresponding author.
** Corresponding author at: Department of Nanobiotechnology, Institute of Nanobiology and Structural Biology of GCRC, Na Sadkach 7, 370 05 Ceske Budejovice, Czech Republic.
E-mail addresses: baldie@email.cz (E. Baldikova), ivosaf@yahoo.com (I. Safarik).

http://dx.doi.org/10.1016/j.jmmm.2014.09.003
0304-8853/

2. Materials and methods

2.1. Materials

Rye straw was supplied by the farm Tomsik in Horni Dubenky (Czech Republic). Ferrous sulfate heptahydrate and sodium hydroxide were from Sigma-Aldrich (Czech Republic), citric acid from Lachema (Czech Republic), acridine orange (CI (Colour Index) 46005) and methyl green (CI 42585) from Loba Feinchemie (Austria).

2.2. Preparation of rye derivative

Before all experiments, rye straw was cut into smaller pieces (ca. 5 cm), milled and sieved to obtain fine particles about 0.1–2 mm in diameter.

2.3. Magnetic modification

Magnetic modification was carried out according to the described procedure [21] using microwave-synthesized magnetic iron oxide nano- and microparticles. Briefly, 1 g $Fe(SO_4)\cdot 7H_2O$ was dissolved in 100 mL of water and solution of NaOH (mol/L) was added dropwise under stirring until the pH reached the value 12 and the precipitate of iron hydroxides was formed. Then the suspension was diluted up to 200 mL with water. The beaker was inserted into a standard kitchen microwave oven (700 W, 2450 MHz) and treated at maximum power for 10 min. Finally, the formed magnetic particles were repeatedly washed with water until the pH was neutral.

To prepare magnetic biosorbent derivate, 1 g of straw was thoroughly mixed with 2 mL of magnetic iron oxide nano- and microparticles suspension (1 part of completely sedimented magnetic particles and 4 part of water) and then this mixture was dried at 60 °C for 24 h.

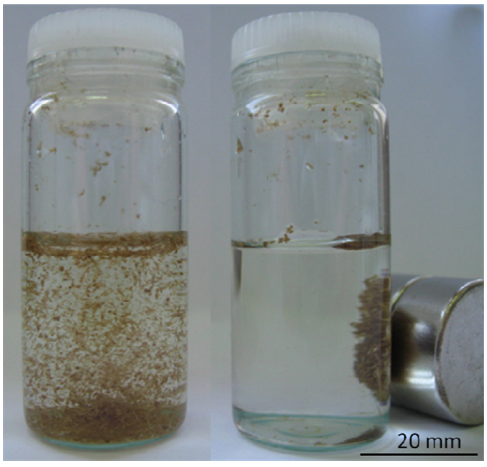

Fig. 1. Magnetic separation of magnetically modified rye straw using NdFeB permanent magnet (diametre: 20 mm; height: 10 mm; remanence: 1 T).

2.4. Citric acid–NaOH modification

The chemical modification of rye straw was performed as described previously [2]. Citric acid (0.5 mol/L) was added to rye straw in a ratio 12:1 (v/w). This mixture was stirred for 30 minutes and dried at 50 °C for 24 h. The termochemical reaction between rye straw and citric acid (CA) was carried out by increasing the temperature to 120 °C for 60 min. After cooling at room temperature, the CA-modified straw was thoroughly washed with distilled water to obtain neutral pH and filtered. Then a solution of NaOH (0.1 mol/L) was added to the filtrated residues in a ratio 12:1 (v/w) and the mixture was stirred for 90 min. Finally, the CA–NaOH modified straw derivative was extensively washed with distilled water to remove alkali residuals and dried at 50 °C for 24 h.

2.5. Adsorption of dyes on rye straw biomass

Testing of the adsorption properties slightly differed for untreated and chemically modified dye straw. In case of untreated derivative, 30 mg of biosorbent was mixed with 1 mL of distilled water and then 1–9 mL of dye (mg/mL) was added, while in the

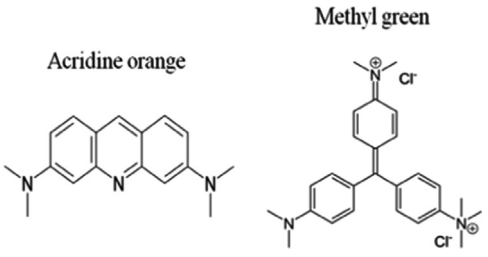

Fig. 3. Chemical structures of acridine orange and methyl green.

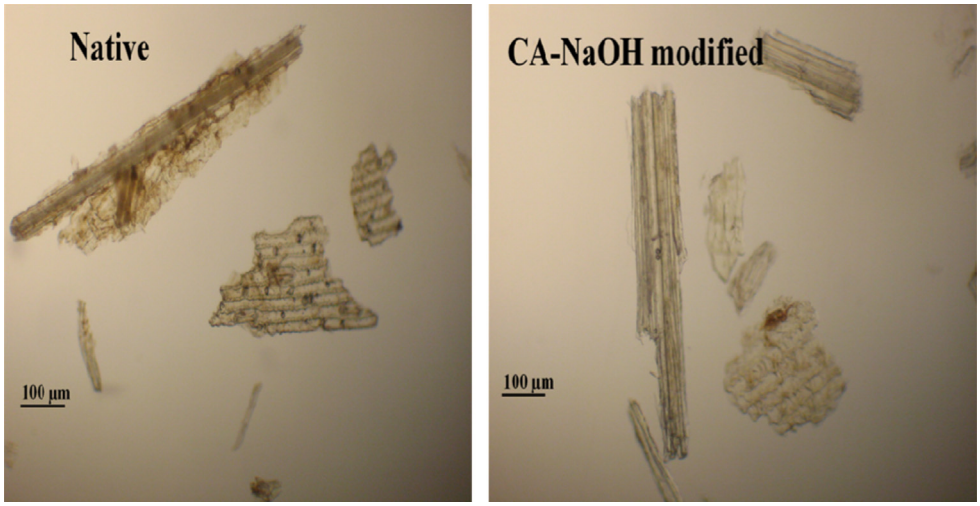

Fig. 2. Structures of native (left) and chemically modified (right) rye straw adsorbents.

Table 1
Other adsorbents for acridine orange and methyl blue removal. The maximum adsorption capacities (Q_{max}) were calculated using the Langmuir or Langmuir–Freundlich models.

Dye	Adsorbent	Q_{max} (mg/g)	Other notes	Reference
Acridine orange	Calcium alginate beads	41.8	Optimal pH 5–8	[22]
	Graphene alginic beads	61.3		
	Graphene oxide/calcium alginate beads	59.0		
	Graphene oxide/alginic beads	63.3		
	ZSM-5 nanozeolit	55.5	Optimal pH 9–11	[23]
	Fe-ZSM-5 nanozeolit	64.9	Q_{max} increases with increasing temperature	
	Spent coffee grounds/magnetic fluid	73.4	Used also for magnetic solid phase extraction	[13]
	Peanut husks/magnetic fluid	71.4	Equilibrium 60–90 min	[12]
	Magnetic particles (γ-Fe_2O_3)	59.0	Optimal pH 4–8	[24]
	Kluyveromyces fragilis/magnetic fluid	59.1	Equilibrium 60–90 min	[25]
	Spruce sawdust/magnetic fluid	24.1	Served also as an absorbent for lysozyme	[26]
	Native rye straw	42.9	Equilibrium in 2 h	This work
	Rye straw/microwave-synthesized magnetic iron oxides	36.9		
	Citric acid–NaOH rye straw	192.3		
	Citric acid–NaOH rye straw/ microwave-synthesized magnetic iron oxides	208.3		
Methyl green	Graphene sheets	203.5–312.8	Q_{max} increases with increasing temperature	[27]
	Graphene sheets decorated with $CoFe_2O_4$	147.1–149.8		
	Native rye straw	95.2	Equilibrium in 2 h	This work
	Rye straw/microwave-synthesized magnetic iron oxides	78.1		
	Citric acid-NaOH rye straw	384.6		
	Citric acid-NaOH rye straw/ microwave-synthesized magnetic iron oxides	357.1		

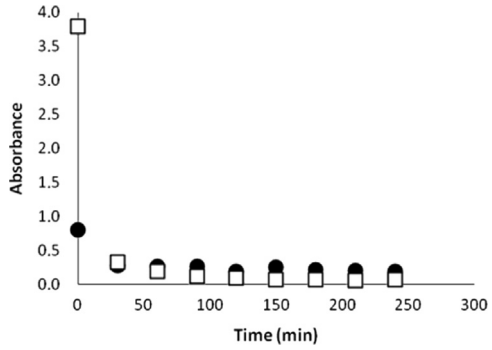

Fig. 4. Time necessary to reach the adsorption equilibrium for methyl green (• native and ▫ chemically modified).

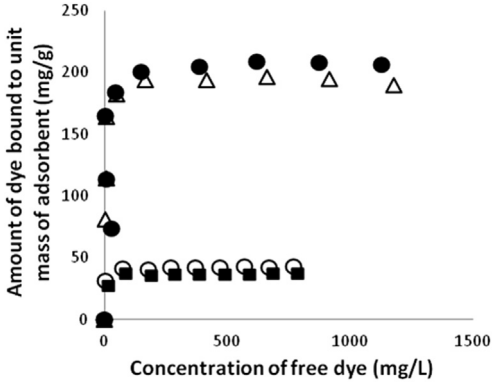

Fig. 5. The Langmuir isotherms for differently modified rye straw (○ native nonmagnetic, ■ native magnetic, Δ CA–NaOH modified, • magnetic CA–NaOH) and acridine orange.

second case, 30 mg of CA–NaOH straw was mixed with 4 mL of distilled water and 1–6 mL of dye (5 mg/mL) was added. The final volume was made up to 10 mL with distilled water. Both types of absorbents were incubated for 3 h at room temperature.

Subsequently the nonmagnetic derivatives were centrifuged out (8 min at 10000 g), while the magnetic materials were separated by means of magnetic separator (DynaMag™-15, Dynal,

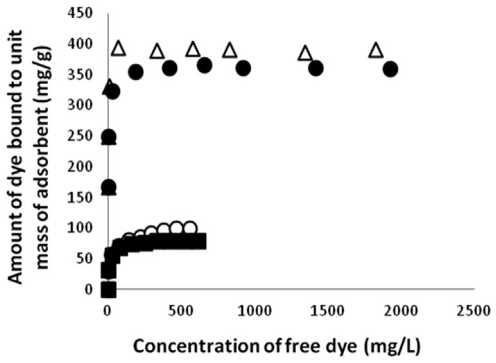

Fig. 6. The Langmuir isotherms for differently modified rye straw (○ native nonmagnetic, ■ native magnetic, Δ CA–NaOH modified, • magmetic CA–NaOH) and methyl green.

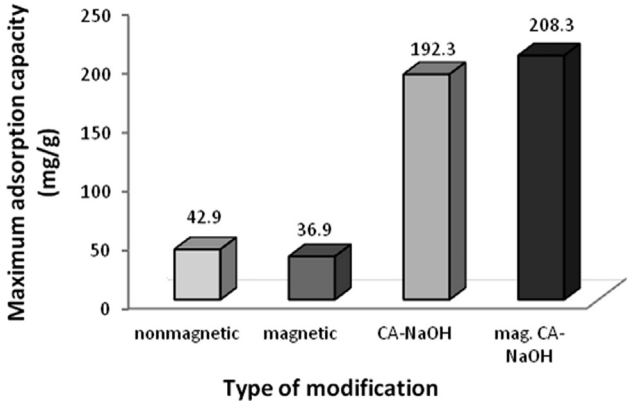

Fig. 7. Comparison of the maximum adsorption capacities for differently modified rye straw and acridine orange.

Norway) and the clear supernatant was used for spectrophotometric measurement (UV/VIS Spectrophotometer Cintra 20, GBC, Australia). The concentration of free (unbound) dye in the supernatant (C_{eq}) was determined from the calibration curve. The amount of dye bound to the unit mass of the adsorbent (Q_{eq})

Table 2
Some published methods for increasing of Q_{max} of straw.

Type of straw	Modification	Removal of	Other notes	References
Wheat	Graft copolymerization	Ammonium; phosphate	Potassium acrylate/polyvinylalcohol	[28]
	Succinoylation	Cr (VI)	Succinic anhydride, dimethylacetamide, catalyst 4-dimethylaminopryidine	[29]
	Esterification	Methyl orange; Acid green 25	30% NaOH, trimethylammonium chloride	[30]
	Mild acid hydrolysis	Methylene blue; Red Basic 22	100 °C, 18 M H_2SO_4; Q_{max} increased 3 times (RB22) and 9 times (MB)	[31]
	Surfactant modification	Acid blue 40; reactive black 5	Cetylpyridinium chloride	[32]
	Grafting method and amine-cross-linking	NO_3^-, PO_4^{3-}, $Cr_2O_7^{2-}$	Epichlorohydrin, triethylamine and ethylenediamine	[33]
		Acid Red 73; Reactive Red 24		[4]
	Solid-phase esterification	Copper ion; methylene blue	Citric acid–NaOH treatment with addition of $Pb(NO_3)_2$, Q_{max} increased ca 6 times	[34]
		Copper ion	Citric acid–NaOH treatment, 11 times higher Q_{max}	[8]
	Alkalization	Cu (II)	Treatment with 5% NaOH, 1% NaOH and 5% NaOH in combination with formaldehyde	[35]
		Cr (III)	2N NaOH, stirred for 10 min, left overnight	[36]
	Carbonization	Cr (VI)	No activation process	[37]
Rice	Alkalization with cross-linking	U (VI)	25% NaOH+epichlorohydrin	[38]
	Mercapto-grafting	Hg (II)	1.5% 3-Mercaptopropyltriethoxysilane	[39]
	Acetylation	Oil spill	Acetic anhydride, 100 and 120 °C, 1–4 h, 4 tertiary amine catalysts	[40]

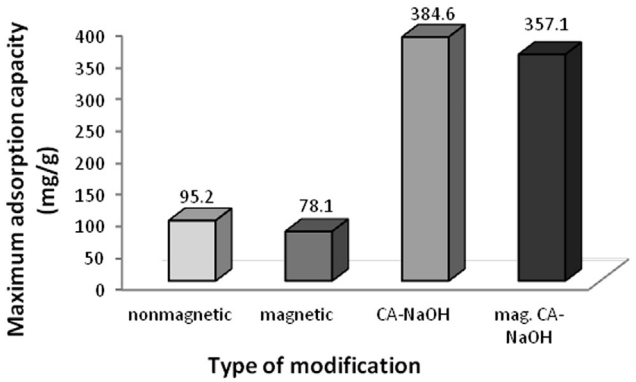

Fig. 8. Comparison of the maximum adsorption capacities for differently modified rye straw and methyl green.

was calculated using the following formula:

$$Q_{eq} = (0.01C_{tot} - 0.01C_{eq})/0.03 \quad (mg/g)$$

where C_{tot} is the total (initial) concentration (μg/mL) of dye used in the experiment.

3. Results and discussion

As can be seen on Fig. 1, magnetic modification of rye straw by microwave synthesized magnetic iron nano- and microparticles led to a formation of magnetically responsive material reacting to external magnetic field. During this procedure the whole amount of straw was magnetically modified. The presence of magnetic particles on the surface was detected using Perl's Prussian Blue Stain causing intense blue color of the Fe^{3+} containing material.

It was proven that the stability of magnetically modified straw is very high. This material can be stored in water suspension (at 4 °C) more than six months without releasing magnetic particles or other negative changes.

No substantial morphological differences in the structure of native and chemically modified rye straw were found as demonstrated in Fig. 2.

Rye straw derivatives were tested as potential adsorbents for two types of organic water-soluble dyes, namely acridine orange belonging to acridine group and methyl green representing triarylmethane group. Their chemical structures are illustrated in Fig. 3. Table 1 shows some published adsorption data of various adsorbent which have been recently used for acridine orange and methyl green removal.

The time necessary to reach the adsorption equilibrium was equal to approximately two hours for both native and chemically modified rye straw as shown in Fig. 4. Nevertheless, the incubation of all experiments was performed for three hours.

The adsorption properties of the prepared adsorbents were analyzed using the Langmuir isotherms (Figs. 5 and 6) and the maximum adsorption capacities (Q_{max}) were calculated by linear regression of these isotherms. The comparison of Q_{max} values is demonstrated in Fig. 7 (for acridine orange) and Fig. 8 (for methyl green). As can be seen from these figures, the presence of magnetic particles in native versions of straw slightly decreased the maximum adsorption capacities. After chemical modification, some significant differences in adsorption properties of tested dyes appeared. In the case of acridine orange, the magnetic Ca–NaOH rye straw derivatives reached higher maximum adsorption capacities than the nonmagnetic derivatives, while the trend for methyl green is opposite.

It is apparent that citric acid–NaOH modification considerably increased the maximum adsorption capacities, in all cases more than four times. Many published studies have been focused on improvement of adsorption properties of various types of straw recently. Some of these methods can be seen in Table 2.

4. Conclusion

The results clearly demonstrate that rye straw derivatives, especially the one obtained by after citric acid–NaOH modification, can be considered as a very promising low-cost material for various types of organic dyes removal. The manipulation with adsorbents can be significantly facilitated after their conversion into magnetically responsive materials using microwave-synthesized magnetic nano- or microparticles.

Acknowledgments

This research was supported by the Grant Agency of the Czech Republic (Project no. 13-13709S).

References

[1] S. Hashemian, M. Salimi, Nano composite a potential low cost adsorbent for removal of cyanine acid, Chem. Eng. J. 188 (2012) 57–63.
[2] R. Gong, Y. Jin, F. Chen, J. Chen, Z. Liu, Enhanced malachite green removal from aqueous solution by citric acid modified rice straw, J. Hazard. Mater. 137 (2006) 865–870.
[3] S. Chakraborty, S. Chowdhury, P. Das Saha, Artificial neural network (ANN) modeling of dynamic adsorption of crystal violet from aqueous solution using citric-acid-modified rice (*Oryza sativa*) straw as adsorbent, Clean Technol. Environ. Policy 15 (2013) 255–264.
[4] X. Xu, B.-Y. Gao, Q.-Y. Yue, Q.-Q. Zhong, Preparation and utilization of wheat straw bearing amine groups for the sorption of acid and reactive dyes from aqueous solutions, J. Hazard. Mater. 182 (2010) 1–9.
[5] T. Madrakian, A. Afkhami, M. Ahmadi, Adsorption and kinetic studies of seven different organic dyes onto magnetite nanoparticles loaded tea waste and removal of them from wastewater samples, Spectrochim. Acta Part A-Mol. Biomol. Spectrosc. 99 (2012) 102–109.
[6] W. Zhang, H. Yan, H. Li, Z. Jiang, L. Dong, X. Kan, H. Yang, A. Li, R. Cheng, Removal of dyes from aqueous solutions by straw based adsorbents: batch and column studies, Chem. Eng. J. 168 (2011) 1120–1127.
[7] W.S.W. Ngah, L.C. Teong, M.A.K.M. Hanafiah, Adsorption of dyes and heavy metal ions by chitosan composites: a review, Carbohydr. Polym. 83 (2011) 1446–1456.
[8] R. Gong, R. Guan, J. Zhao, X. Liu, S. Ni, Citric acid functionalizing wheat straw as sorbent for copper removal from aqueous solution, J. Health Sci. 54 (2008) 174–178.
[9] E. Pehlivan, T. Altun, S. Parlayici, Modified barley straw as a potential biosorbent for removal of copper ions from aqueous solution, Food Chem. 135 (2012) 2229–2234.
[10] S. Chowdhury, S. Chakraborty, P. Das, Adsorption of crystal violet from aqueous solution by citric acid modified rice straw: equilibrium, kinetics, and thermodynamics, Sep. Sci. Technol. 48 (2013) 1339–1348.
[11] B. Ramaraju, P.M.K. Reddy, C. Subrahmanyam, Low cost adsorbents from agricultural waste for removal of dyes, Environ. Prog. Sustain. Energy 33 (2014) 38–46.
[12] I. Safarik, M. Safarikova, Magnetic fluid modified peanut husks as an adsorbent for organic dyes removal, Phys. Proc. 9 (2010) 274–278.
[13] I. Safarik, K. Horska, B. Svobodova, M. Safarikova, Magnetically modified spent coffee grounds for dyes removal, Eur. Food Res. Technol. 234 (2012) 345–350.
[14] L.S. Oliveira, A.S. Franca, T.M. Alves, S.D.F. Rocha, Evaluation of untreated coffee husks as potential biosorbents for treatment of dye contaminated waters, J. Hazard. Mater. 155 (2008) 507–512.
[15] I. Safarik, K. Horska, M. Safarikova, Magnetically modified spent grain for dye removal, J. Cereal Sci. 53 (2011) 78–80.
[16] S.T. Ong, P.S. Keng, S.T. Ooi, Y.T. Hung, S.L. Lee, Utilization of fruits peel as a sorbent for removal of methylene blue, Asian J. Chem. 24 (2012) 398–402.
[17] C.B. Chandran, D. Singh, P. Nigam, Remediation of textile effluent using agricultural residues, Appl. Biochem. Biotechnol. 102 (2002) 207–212.
[18] H. Deveci, E. Pehlivan, The utilization of modified rye straws as biosorbents for Cr (VI) ions [online], in: Proceedings of the 2nd International Symposium on Sustainable Development, 2010. Available from: ⟨http://eprints.ibu.edu.ba/445⟩.
[19] W. Kaminski, E. Tomczak, S. Kuberski, Sorption equilibrium of selected azo dyes onto low-cost sorbents, Glob. J. Adv. Pure Appl. Sci. 1 (2013) 94–100.
[20] C.T. Yavuz, A. Prakash, J.T. Mayo, V.L. Colvin, Magnetic separations: from steel plants to biotechnology, Chem. Eng. Sci. 64 (2009) 2510–2521.
[21] I. Safarik, M. Safarikova, One-step magnetic modification of non-magnetic solid materials, Int. J. Mater. Res. 105 (2014) 104–107.
[22] L. Sun, B. Fugetsu, Graphene oxide captured for green use: influence on the structures of calcium alginate and macroporous alginic beads and their application to aqueous removal of acridine orange, Chem. Eng. J. 240 (2014) 565–573.
[23] S.K.H. Nejad-Darzi, A. Samadi-Maybodi, M. Ghobakhluo, Synthesis and characterization of modified ZSM-5 nanozeolite and their applications in adsorption of acridine orange dye from aqueous solution, J. Porous Mater. 20 (2013) 909–916.
[24] S. Qadri, A. Ganoe, Y. Haik, Removal and recovery of acridine orange from solutions by use of magnetic nanoparticles, J. Hazard. Mater. 169 (2009) 318–323.
[25] I. Safarik, L.F.T. Rego, M. Borovska, E. Mosiniewicz-Szablewska, F. Weyda, M. Safarikova, New magnetically responsive yeast-based biosorbent for the efficient removal of water-soluble dyes, Enzyme Microb. Technol. 40 (2007) 1551–1556.
[26] I. Safarik, M. Safarikova, F. Weyda, E. Mosiniewicz-Szablewska, A. Slawska-Waniewska, Ferrofluid-modified plant-based materials as adsorbents for batch separation of selected biologically active compounds and xenobiotics, J. Magn. Magn. Mater. 293 (2005) 371–376.
[27] A.A. Farghali, M. Bahgat, W.M.A. El Rouby, M.H. Khedr, Preparation, decoration and characterization of graphene sheets for methyl green adsorption, J. Alloys Compd. 555 (2013) 193–200.
[28] J. Liu, Y. Su, Q. Li, Q. Yue, B. Gao, Preparation of wheat straw based superabsorbent resins and their applications as adsorbents for ammonium and phosphate removal, Bioresour. Technol. 143 (2013) 32–39.
[29] X.-F. Sun, Z. Jing, H. Wang, Y. Li, Removal of low concentration Cr(VI) from aqueous solution by modified wheat straw, J. Appl. Polym. Sci. 129 (2013) 1555–1562.
[30] W. Zhang, H. Li, X. Kan, L. Dong, H. Yan, Z. Jiang, H. Yang, A. Li, R. Cheng, Adsorption of anionic dyes from aqueous solutions using chemically modified straw, Bioresour. Technol. 117 (2012) 40–47.
[31] F. Batzias, D. Sidiras, E. Schroeder, C. Weber, Simulation of dye adsorption on hydrolyzed wheat straw in batch and fixed-bed systems, Chem. Eng. J. 148 (2009) 459–472.
[32] B.C. Oei, S. Ibrahim, S. Wang, H.M. Ang, Surfactant modified barley straw for removal of acid and reactive dyes from aqueous solution, Bioresour. Technol. 100 (2009) 4292–4295.
[33] X. Xu, Y. Gao, B. Gao, Q. Yue, Q. Zhong, Adsorption studies of the removal of anions from aqueous solutions onto an adsorbent prepared from wheat straw, Sci. China Chem. 53 (2010) 1414–1419.
[34] R. Han, L. Zhang, C. Song, M. Zhang, H. Zhu, L. Zhang, Characterization of modified wheat straw, kinetic and equilibrium study about copper ion and methylene blue adsorption in batch mode, Carbohydr. Polym. 79 (2010) 1140–1149.
[35] M. Sciban, M. Klasnja, B. Skrbic, Adsorption of copper ions from water by modified agricultural by-products, Desalination 229 (2008) 170–180.
[36] A. Kumar, N.N. Rao, S.N. Kaul, Alkali-treated straw and insoluble straw xanthate as low cost adsorbents for heavy metal removal – preparation, characterization and application, Bioresour. Technol. 71 (2000) 133–142.
[37] R. Chand, T. Watari, K. Inoue, T. Torikai, M. Yada, Evaluation of wheat straw and barley straw carbon for Cr(VI) adsorption, Sep. Purif. Technol. 65 (2009) 331–336.
[38] X. Li, Y. Liu, M.Z. Hua, Y. Liu, Z. Zhang, X. Li, C. He, Adsorption of U(VI) from aqueous solution by cross-linked rice straw, J. Radioanal. Nucl. Chem. 298 (2013) 383–392.
[39] S.-T. Song, N. Saman, K. Johari, H. Mat, Removal of Hg(II) from aqueous solution by adsorption using raw and chemically modified rice straw as novel adsorbents, Ind. Eng. Chem. Res. 52 (2013) 13092–13101.
[40] X.F. Sun, R.C. Sun, J.X. Sun, Acetylation of rice straw with or without catalysts and its characterization as a natural sorbent in oil spill cleanup, J. Agric. Food Chem. 50 (2002) 6428–6433.

5.2.4 Ječná sláma

V této publikaci byla studována adsorpce čtyř organických barviv charakteristických různou chemickou strukturou. Vybrána byla krystalová violeť, jakožto zástupce trifenylmetanových barviv, Bismarckova hněď Y – azobarviva, safranin O – safraninová barviva, a metylenová modř – skupina chinoniminových barviv. Jako levný adsorbent byla testována ječná sláma, a to ve čtyřech verzích: nativní, nativní magnetické, nemagnetické chemicky modifikované a magnetické chemicky modifikované.

Chemická i magnetická modifikace byla provedena stejným způsobem, jaký je popsán v předchozím článku (viz příloha 9), tedy ošetřením kyselinou citronovou a hydroxidem sodným, a smícháním s MS magnetitem.

Do studie byla zahrnuta nejen časová závislost a analýza adsorpčních rovnovážných dat, ale byly také vypočteny parametry popisující kinetiku a termodynamiku adsorpce. Rovnovážný stav byl dosažen do dvou hodin, kinetika reakce vyhovovala kinetickému modelu pseudo-druhého řádu, adsorpční proces byl spontánní a endotermický.

Stejně jako v případě žitné slámy, i zde došlo po chemické modifikaci k mnohonásobnému navýšení maximálních adsorpčních kapacit. Zajímavým trendem v této publikaci je navíc to, že nativní magnetická verze vykazuje lehce vyšší maximální adsorpční kapacity než verze nativní nemagnetická.

Připravený biosorbent byl důkladně charakterizován pomocí skenovací elektronové mikroskopie (SEM), energiově disperzní spektroskopie (EDS) a infračervené spektrometrie s Fourierovou transformací (FTIR) provedené na Palackého univerzitě v Olomouci. Významné zvýšení adsorpční účinnosti po chemické modifikaci lze přikládat jednak zdrsnění povrchu materiálu, jednak přítomností většího počtu karboxylových skupin.

Příloha 10:

Utilization of magnetically responsive cereal by-product for organic dye removal

Baldikova E, Politi D, Maderova Z, Pospiskova K, Sidiras D, Safarikova M, Safarik I

J. Sci. Food Agric. 96, **2016**, 2204-2214

Research Article

Received: 9 April 2015 Revised: 25 June 2015 Accepted article published: 10 July 2015 Published online in Wiley Online Library: 10 August 2015

(wileyonlinelibrary.com) DOI 10.1002/jsfa.7337

Utilization of magnetically responsive cereal by-product for organic dye removal

Eva Baldikova,[a*] Dorothea Politi,[b] Zdenka Maderova,[a] Kristyna Pospiskova,[c] Dimitrios Sidiras,[b] Mirka Safarikova[a] and Ivo Safarik[a,c*]

Abstract

BACKGROUND: Barley straw, an agricultural by-product, can also serve as a low-cost and relatively efficient adsorbent of various harmful compounds. In this case, adsorption of four water-soluble dyes belonging to different dye classes (specifically Bismarck brown Y, representing the azo group; methylene blue, quinone-imine group; safranin O, safranin group; and crystal violet, triphenylmethane group) on native and citric acid–NaOH-modified barley straw, both in magnetic and non-magnetic versions, was studied.

RESULTS: The adsorption was characterized using three adsorption models, namely Langmuir, Freundlich and Sips. To compare the maximum adsorption capacities (q_{max}), the Langmuir model was employed. The q_{max} values reached 86.5–124.3 mg of dye per g of native non-magnetic straw and 410.8–520.3 mg of dye per g of magnetic chemically modified straw. Performed characterization studies suggested that the substantial increase in q_{max} values after chemical modification could be caused by rougher surface of adsorbent (observed by scanning electron microscopy) and by the presence of higher amounts of carboxyl groups (detected by Fourier transform infrared spectroscopy). The adsorption processes followed the pseudo-second-order kinetic model and thermodynamic studies indicated spontaneous and endothermic adsorption.

CONCLUSION: The chemical modification of barley straw led to a significant increase in maximum adsorption capacities for all tested dyes, while magnetic modification substantially facilitated the manipulation with adsorbent.

Supporting information may be found in the online version of this article.

Keywords: barley straw; magnetic modification; magnetic adsorbent; microwave-assisted synthesis; organic dyes

ABBREVIATIONS AND NOMENCLATURE

CA	citric acid
CA-NaOH-BS	citric acid–NaOH-modified barley straw
CA-NaOH-MBS	citric acid–NaOH-modified magnetic barley straw
NLRA	nonlinear regression analysis
SEE	standard error of estimate
C_e	equilibrium concentration of dye after adsorption (mg L^{-1})
C_o	initial concentration (mg L^{-1}) of dye used in experiment
C_t	concentration of dye in solution (mg L^{-1}) measured at time t
ΔG	standard free energy (J mol^{-1})
ΔH	enthalpy (J mol^{-1})
q_e	amount of dye bound to the unit mass of the adsorbent (mg g^{-1})
q_{max}	the maximum adsorption capacity (mg g^{-1})
q_t	amount of adsorbed dye per unit mass of adsorbent at time t (mg g^{-1})
k_1	rate constant (min^{-1}) for pseudo-first-order kinetic model
k_2	rate constant (g mg^{-1} min^{-1}) for pseudo-second-order kinetic model
K_d	thermodynamic equilibrium constant
K_F	Freundlich isotherm constant related to adsorption capacity ((mg g^{-1}) (L $mg^{-1})^{1/n}$)
K_L	Langmuir constant related to energy of adsorption (L mg^{-1})
m	mass of adsorbent (g)
n	Freundlich isotherm constant related to adsorption intensity
ΔS	entropy (J mol^{-1} K^{-1})

* *Correspondence to: Eva Baldikova or Ivo Safarik, Department of Nanobiotechnology, Institute of Nanobiology and Structural Biology of GCRC, Na Sadkach 7, 370 05 Ceske Budejovice, Czech Republic. E-mail: baldie@email.cz (Baldikova); ivosaf@yahoo.com (Safarik)*

a *Department of Nanobiotechnology, Institute of Nanobiology and Structural Biology of GCRC, 370 05 Ceske Budejovice, Czech Republic*

b *Laboratory of Simulation of Industrial Processes, Department of Industrial Management and Technology, University of Piraeus, 18534 Piraeus, Greece*

c *Regional Centre of Advanced Technologies and Materials, Palacky University, 783 71 Olomouc, Czech Republic*

V	total volume (L)
R	gas constant (8.314 J mol^{-1} K^{-1})
R_L	separation factor
T	absolute temperature (K)
t	time (min)

INTRODUCTION

Water pollution caused by organic dyes poses a huge global threat not only to the environment, but also to human and aquatic life. It was found that these compounds or their metabolites are often toxic, carcinogenic and mutagenic.[1,2] The danger for the environment especially lies in their high persistence in nature and non-biodegradable characteristic.[3] Moreover, even small concentrations of dyes (10–50 mg L^{-1}) can negatively change esthetical water value and its permeability to sunlight, which can significantly affect photosynthetic activity and thus the life of aquatic organisms.[4,5]

It is estimated that more than 7×10^5 tons of dyes are consumed annually[6,7] by various industrial sections, such as dyeing, printing, textile, leather, paper, coating, rubber, plastics, cosmetics, pharmaceuticals and food industries.[3] Among them, the textile industry consumes about 60% of total produced dyes[6] and around 10–15% of the used dyes enter the environment through effluent.[8]

The existence of a wide range of dyes (more than 100 000 compounds) has been described.[9] In general, many of these pollutants are very difficult to degrade because of their diversity in structure and stability to light, oxidizing agents, aerobic digestion and biodegradation.[3] Various techniques have been employed for removal of dyes from wastewaters. These methods include, for example, ion exchange, membrane technology, coagulation, flocculation, oxidation or ozonation, aerobic and anaerobic biodegradation, photodegradation or chemical degradation.[3,4,10] Nevertheless, biosorption is considered to be the cheapest and most effective method.[11]

In recent years, many studies have suggested that waste plant materials can be utilized as potential sources of cheap and easily available biosorbents for organic dyes, heavy metal ions, radionuclides or endocrine disruptors. Plant derivatives, such as wheat straw,[12] barley straw,[13] rice straw,[14] spent grain,[15] pumpkin husks,[6] peanut husks,[16] spent coffee grounds,[17] spent tea leaves,[5] sawdust,[18] sugarcane bagasse[19] and many others, have been successfully used for adsorption of water-soluble organic dyes from water systems.

In recent years, straw has been considered as an interesting biosorbent that can be obtained in large amounts and for very low prices. However, the application of native straw is not recommended because of lower adsorption capacity. Therefore, plant wastes are often modified or pretreated to improve their adsorption properties before being applied to xenobiotics removal. Many papers focusing on methods of increasing the maximum adsorption capacities of different types of straw have been published recently. These techniques include, most often, treatment using various acids and hydroxides, but hydrolysis[20] and carbonization,[21] for example, are also reported.

Adsorbents can also be magnetically modified to simplify manipulation. Thanks to magnetic iron oxides nano- or microparticles bound on the surface or within the pores of the modified materials, highly selective and very fast separation from water suspensions and difficult- to-handle media can be achieved by means of an external magnetic field (using an appropriate magnetic separator).[22]

This research is focused on the study of magnetically modified barley straw, its utilization for adsorption of organic water-soluble dyes belonging to different dye classes and on suitable methods to increase the maximum adsorption capacities using common chemicals. To our knowledge, this is the first study to investigate both magnetic and citric acid (CA)-NaOH-modified barley straw.

MATERIALS AND METHODS

Materials

Barley straw, supplied by a cooperative farm in Netrebice (Czech Republic), was cut into small pieces, milled and sieved to obtain fine particles (~0.15–2 mm in diameter). Ferrous sulfate heptahydrate, sodium hydroxide, Bismarck brown Y (CI: 21000), methylene blue (CI: 52015) and safranin O (CI: 50240) were purchased from Sigma-Aldrich (St Louis, MO, USA). Citric acid and crystal violet (CI: 42555) were obtained from Lachema (Brno, Czech Republic).

Magnetic modification of barley straw biomass

Barley straw biomass was magnetically modified using microwave-synthesized magnetic iron oxides:[23] 1 g $FeSO_4.7H_2O$ was dissolved in 100 mL water in a 600–800 mL beaker and a solution of sodium hydroxide (1 mol L^{-1}) was added slowly under stirring (Stuart SB 161-3 stirrer; Bibby Scientific Ltd, Stone, UK) until the pH reached a value of ~12. After forming a precipitate of iron hydroxides, the suspension was diluted up to 200 mL with water, inserted into a standard kitchen microwave oven (700 W, 2450 MHz) and treated for 10 min at maximum power. The formed magnetic iron oxides nano- and microparticles were then repeatedly washed with water to obtain a suspension with neutral pH.

The preparation of magnetically responsive barley straw biomass was carried out in the following steps: 1 g straw powder was thoroughly mixed with 2 mL microwave synthesized iron oxide nano- and microparticle suspension (1 part completely sedimented iron oxide particles and 4 parts water) and this mixture was dried at 60 °C for 24 h.[23]

Chemical modification of barley straw biomass

The chemical modification of barley straw biomass was performed as described previously.[24] Barley straw was mixed with 0.5 mol L^{-1} CA in a ratio of 1:12 (straw:citric acid, w/v) and stirred for 30 min at ambient temperature. The straw/acid slurries were dried at 50 °C for 24 h. The thermochemical reaction between acid and barley straw was then performed by increasing the temperature to 120 °C for 90 min. Barley straw (after cooling to room temperature) was thoroughly washed with distilled water to reach neutral pH and filtered. The filtered residue was suspended in NaOH solution (0.1 mol L^{-1}) and stirred for 60 min. The straw biomass was then extensively washed with water to remove alkaline residuals. The treated material was dried at 50 °C until constant weight.

Characterization of materials

The morphological study of both native and modified straw was performed using scanning electron microscopy (SEM) measurements; the samples were analyzed using a Hitachi SU6600 scanning electron microscope (Hitachi, Tokyo, Japan) with accelerating voltage 5 kV/3 kV. Energy dispersive X-ray spectroscopy (EDS) was acquired in SEM using Thermo Noran System 7 (Thermo Scientific, Waltham, MA, USA) with Si(Li) detector; accelerating

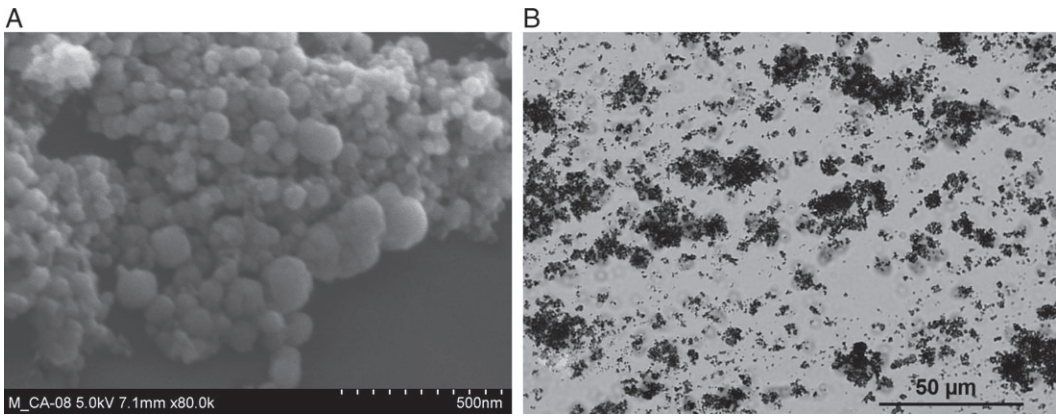

Figure 1. SEM (A) and optical microscopy (B) of magnetic particles prepared by microwave-assisted synthesis.

voltage was 15 kV and acquisition time was 300 s. Fourier transform infrared (FTIR) absorption spectra were measured using Thermo Scientific Nicolet iS5 FTIR spectrometer (Thermo Nicolet Corp., Madison, WI, USA) with iD Foundation accessory (ZnSe crystal, range 4000–650 cm^{-1}, 32 scans, resolution 4 cm^{-1}). The IR absorption spectra are presented in transmittance after advanced attenuated total reflectance (ATR) and automatic baseline corrections.

Adsorption of dyes on barley straw biomass

Testing of the adsorption properties was performed in a batch system without any pH adjustment. 10 mL dye solution (at a concentration of 100–900 mg L^{-1} for native and 250–2500 mg L^{-1} for chemically modified straw) was mixed with 30 mg biosorbent. These concentrations were chosen to reach the isotherm plateau according to previous experiments indicating different adsorption efficiencies of prepared materials. The suspension was incubated for 2 h at room temperature (rotation mixer; Dynal, Oslo, Norway).

The non-magnetic straw biomass was centrifuged out (8 min at 10 000 × *g*; Zentrifugen Universal 320; Hettich, Tuttlingen, Germany), while magnetic straw was separated from the suspension using a magnetic separator (DynaMag™-15, Dynal, Oslo, Norway). The clear supernatant was used for spectrophotometric measurement (Cintra 20; GBC Scientific Equipment, Braeside, Australia). The concentration of free (unbound) dye in the supernatant (C_e) was determined from the calibration curve. The amount of dye bound to the unit mass of the adsorbent q_e was calculated using the following formula:

$$q_e = \frac{V\ (C_0 - C_e)}{m} \quad (1)$$

The same procedure was used for thermodynamic studies, which were performed at 282.15, 295.15 and 313.15 K. For these experiments, safranin O was chosen as a model dye.

Adsorption kinetics were studied at 15, 30, 90, 120, 150 and 180 min for all dyes and all modifications at room temperature, using concentration of 350 mg L^{-1} for untreated and 1250 mg L^{-1} for chemically modified straw. The amount of adsorbed dye per unit mass of adsorbent q_t at time t was calculated from the following formula:

$$q_t = \frac{V\ (C_0 - C_t)}{m} \quad (2)$$

All adsorption experiments were carried out in triplicate.

RESULTS AND DISCUSSION

Magnetic modification of straw adsorbents

Both native and chemically modified straw were magnetically modified by microwave- synthesized iron oxides nano- and microparticles; nanoparticle diameter ranged between ~25 and 100 nm (Fig. 1A). During synthesis, the nanoparticles formed micrometer-sized stable aggregates (maximum aggregate size ~20 µm; see Fig. 1B). Magnetic modification led to the deposition of iron oxide nanoparticle aggregates on the surface of the straw particles (Fig. 2C, D). Energy-dispersive X-ray spectroscopy confirmed the presence of iron on the magnetized straw (Fig. 3). The presence of Fe^{3+} ions on the surface of magnetically modified straw was also verified by Perls' Prussian Blue stain, which caused intensive blue coloration of the whole material. Magnetic modification led to the formation of magnetically responsive material that could be easily separated using a permanent magnet or commercial magnetic separator (Fig. 4).

It was proved that the stability of magnetically modified straw is very high. This material could be stored in water suspension at 277.15 K longer than 7 months without any change in magnetic properties or release of magnetic particles. Therefore, it also could be used in long-term experiments.

Characterization of materials

IR spectra of both native and CA-NaOH straw displayed a number of absorption peaks, denoting the complex structure of the materials. As can be seen from Fig. 5, both tested materials exhibit several similar peaks; the first one was located at 3330 cm^{-1} and was attributed to O—H stretching indicating the presence of hydroxyl groups in the molecular structure of straw; the peak observed at 2920 cm^{-1} is characteristic of C—H stretching in methyl and methylene groups; the peak at 1510 cm^{-1} is associated with stretch vibration of aromatic rings; the peak in the region ~1160 cm^{-1} is related to C—O—C vibration in cellulose and hemicellulose; and the last one, at 1036 cm^{-1}, is characteristic of strong C—O bonds, confirming the presence of lignin. After chemical modification, increase in peaks at 1731, 1582 and 1391 cm^{-1} is apparent; the first one is attributed to C═O stretching of ester and carboxyl groups, another one is assigned to stretch vibration of C—O groups and the last one is related to C—H bond vibrations in methyl bonds. On the other hand, native straw showed some smaller peaks which were either not observed or were shifted in the spectrum of the chemically modified straw: specifically, the peak at 1641 cm^{-1} (stretching vibration of carbonyl groups conjugated to aromatic rings), 1423 cm^{-1} (stretching vibration of C—O

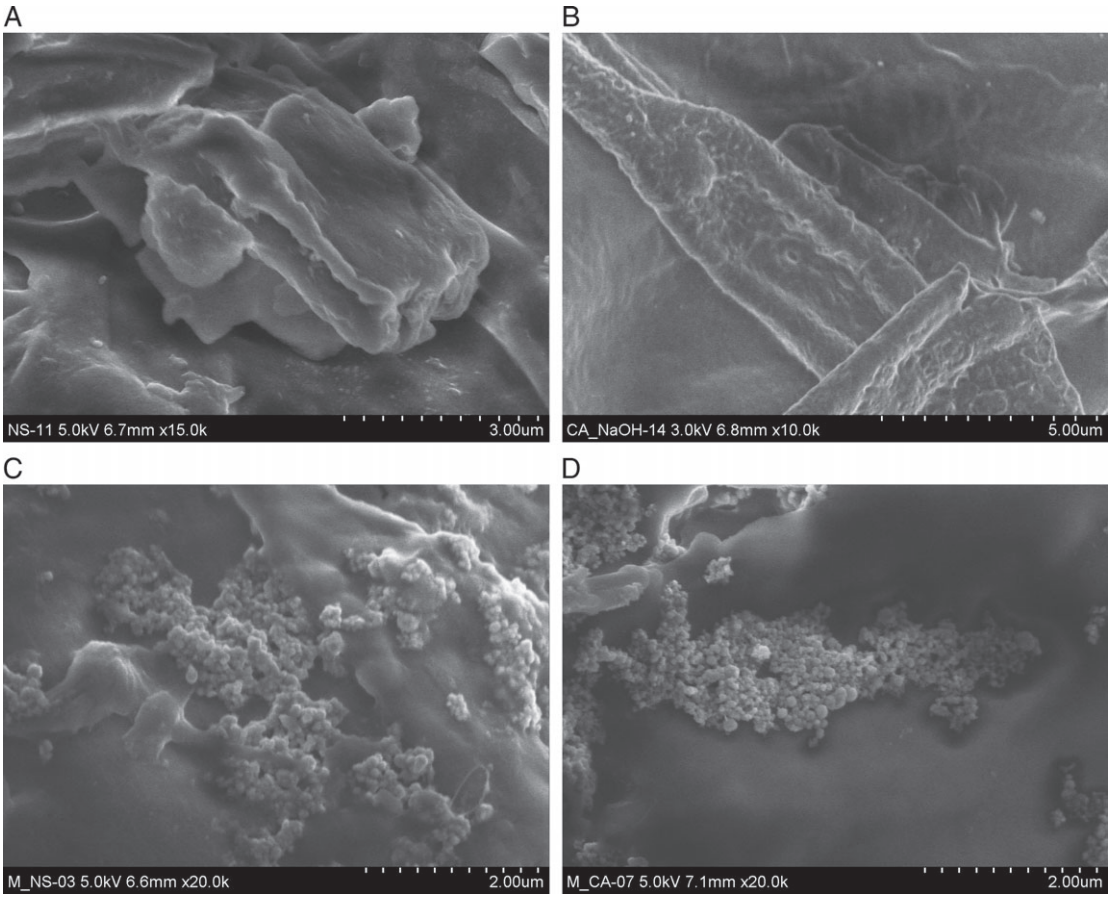

Figure 2. SEM images of (A) native, (B) CA-NaOH, (C) native magnetic and (D) magnetic CA-NaOH adsorbents.

from carboxyl group), 1369 cm^{-1} (C—H stretching vibration of cellulose/hemicellulose and other groups that are bound to methyl radicals, which are common in lignin) and at 1240 cm^{-1} (associated with C—O vibration in phenols and C—O—H deformation).[25–28]

The chemical treatment also led to a higher concentration of sodium in the sample, as documented by EDS (Fig. 3). The slightly rougher straw surface after chemical modification was confirmed by SEM (Fig. 2A, B).

The results indicating a rougher surface after CA-NaOH modification and the increase in carboxyl groups were also published by Han *et al.*[25] and Gong *et al.*[24]

Adsorption studies and isotherms

Native and chemically modified barley straw, both in non-magnetic and magnetic versions, were used as adsorbents to study the binding of four organic water-soluble dyes belonging to different dye classes. These dyes were selected according to the results of the preliminary screening experiment using a magnetically modified version of barley straw and 14 different dyes (data not shown). Therefore, Bismarck brown Y (azo dye group), crystal violet (triphenylmethane group), methylene blue (quinone-imine group) and safranin O (safranin group) were chosen for further experiments.

The equilibrium of the adsorption was reached in approximately 90–120 min. Both types of adsorbents were incubated for 2 h during the adsorption experiments.

The obtained adsorption experimental data (see Fig. 6; the standard deviations are presented as supporting information in Table S1) clearly indicated that the simple chemical pretreatment of the straw using two cheap chemicals, namely citric acid and sodium hydroxide, had a dramatic effect on the adsorption capacity. In order to study the adsorption processes, three isotherm models, including Freundlich, Langmuir and Sips equations,[26–28] were used to fit the experimental data. The first two models are widely used for investigating the adsorption of dyes on various lignocellulosic materials and activated carbons. The Freundlich isotherm model assumes that the surface of the adsorbent is heterogeneous and polymolecular layer adsorption takes place. This model can be described by the equation

$$q_e = K_F \left(C_e\right)^{\frac{1}{n}} \tag{3}$$

The linear form of the Freundlich isotherm model[29] can be defined by the following equation:

$$\log q_e = \log K_F + \frac{1}{n} \log C_e \tag{4}$$

The Langmuir isotherm model[30] is given as

$$q_e = \frac{K_L\, q_{max}\, C_e}{1 + K_L\, C_e} \tag{5}$$

Moreover, this equation in linearized form is

$$\frac{1}{q_e} = \left(\frac{1}{q_{max}}\right) + \left(\frac{1}{K_L q_{max}}\right)\left(\frac{1}{C_e}\right) \tag{6}$$

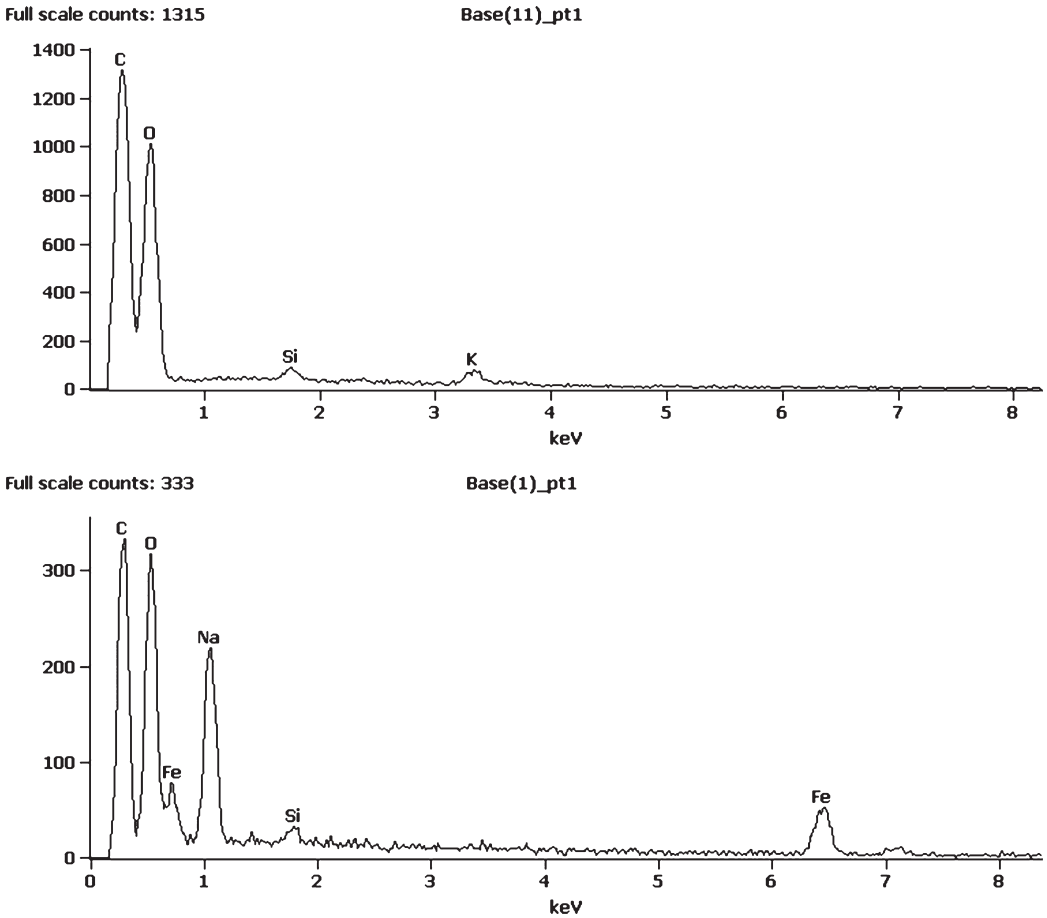

Figure 3. EDS of native (top) and magnetic CA-NaOH (bottom) straw derivatives.

Figure 4. Appearance of original barley straw suspension (left), suspension of straw after magnetic modification (middle) and demonstration of magnetic separation of magnetically modified straw (right).

In cases where the isotherm experimental data approximate the Langmuir equation, the parameters K_L and q_{max} can be estimated either by plotting $1/q_e$ versus $1/C_e$ or by nonlinear regression analysis (NLRA).

The Sips isotherm model[31] is a combination of the Langmuir and Freundlich isotherm type models and is expected to describe heterogeneous surface better. The Sips equation is presented by

$$q_e = \frac{q_{max}\left(K_L\, C_e\right)^{1/n}}{1 + \left(K_L\, C_e\right)^{1/n}} \tag{7}$$

The standard error of estimate (SEE) was calculated in each case as follows:

$$\mathrm{SEE} = \sqrt{\sum_{i=1}^{n'} \left(y_i - y_{i,\,\mathrm{theor}}\right)^2 / \left(n' - p'\right)} \tag{8}$$

where y_i is the experimental value of the dependent variable, $y_{i,\mathrm{theor}}$ is the theoretical or estimated value of the dependent variable, n' is the number of experimental measurements and p' is the number of parameters (the difference $n' - p'$ being the number of degrees of freedom).

The parameters of each adsorption isotherm model obtained by nonlinear regression (NLRA) are shown in Table 1. The Langmuir and Sips adsorption models were the most satisfactory ones for fitting methylene blue adsorption experimental data, as shown by the corresponding SEE values given in Table 1. The Freundlich isotherm model had the most satisfactory fitting for crystal violet. However, SEE values cannot serve as the only parameter to decide which adsorption model is better. It was shown that in some cases the Sips model has given constants lacking the correct physical meaning (specifically Bismarck brown Y – non-magnetic straw and citric acid–NaOH-modified barley straw (CA-NaOH-BS); safranin O – both magnetic versions of straw; and crystal violet – citric acid–NaOH-modified magnetic barley straw (CA-NaOH-MBS), CA-NaOH-BS and magnetic straw). However, the Langmuir adsorption model, enabling very simple calculation of maximum adsorption capacities with reasonable

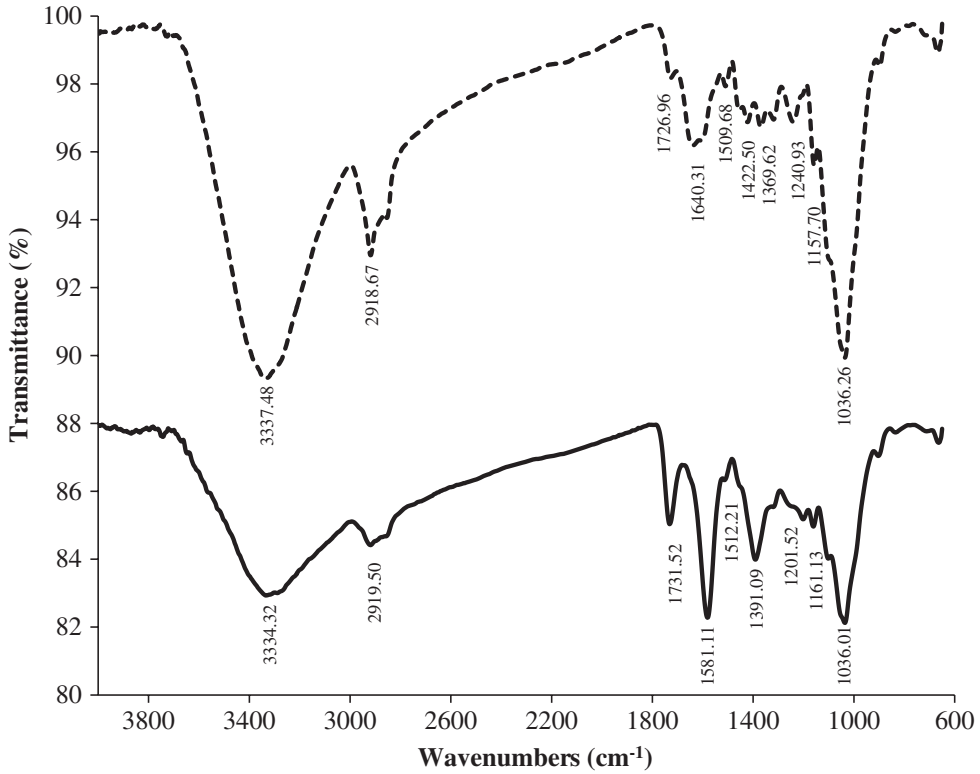

Figure 5. FTIR spectra of native (dashed line) and chemically modified (solid line) barley straw.

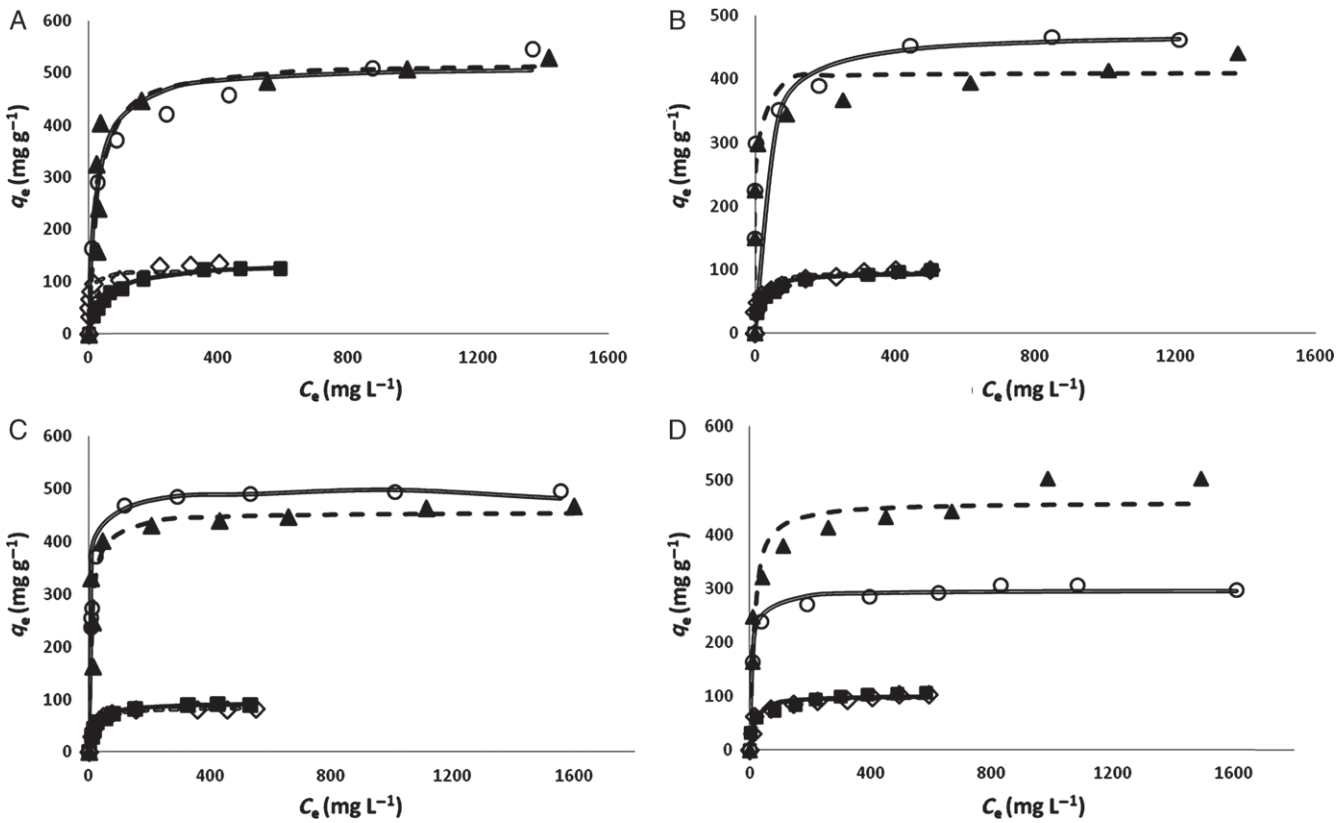

Figure 6. Langmuir isotherms: (A) Bismarck brown Y; (B) crystal violet; (C) methylene blue; (D) safranin O (◇ native, ■ magnetic, ○ non-magnetic CA-NaOH, ▲ magnetic CA-NaOH straw).

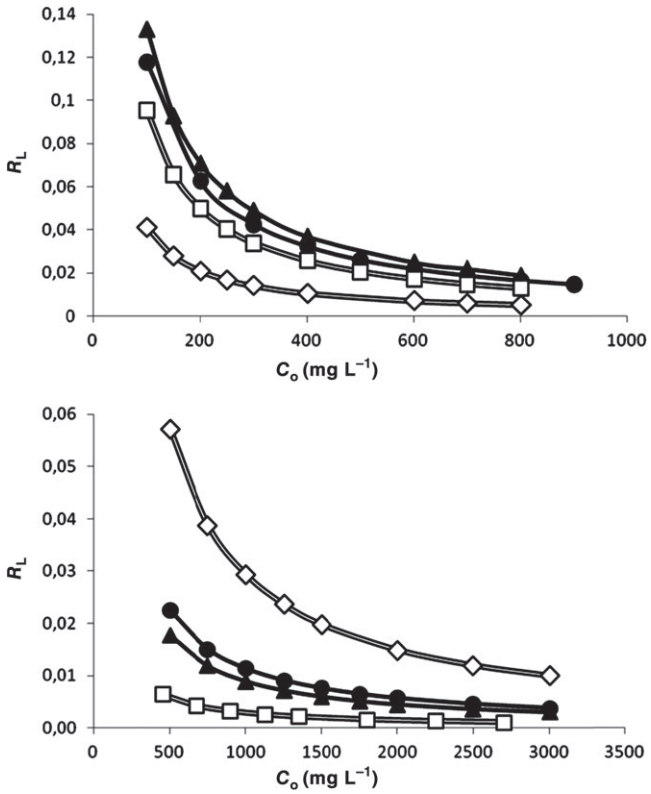

Figure 7. Calculated separation factor profiles for all tested dyes and native barley straw (top) and magnetic, chemically modified straw (bottom) as a function of dye initial concentration (mg L^{-1}) (◇ Bismarck brown Y, □ crystal violet, ▲ methylene blue, ● safranin O).

precision, was employed to compare the adsorption efficiencies of tested adsorbents.

Numerous studies[32,33] incorporate another important parameter, R_L, namely the separation factor. The value of R_L indicates the type of isotherm to be either unfavorable ($R_L > 1$), linear ($R_L = 1$), favorable ($0 < R_L < 1$) or irreversible ($R_L = 0$) and is expressed by the following equation:

$$R_L = \frac{1}{1 + K_L C_0} \quad (9)$$

The values of the separation factor R_L for all four tested dyes and two types of adsorbents (native and magnetic, chemically modified straw, respectively) were calculated and plotted against initial dye concentration. The data (Fig. 7) showed that the sorption process was favorable for dye removal at all concentrations investigated; additional data are presented as supporting information in Table S2.

As already mentioned, citric acid–NaOH modification substantially increased dye adsorption, as shown in Table 1 and Fig. 8. In most cases the additional magnetic modification not only enabled efficient magnetic separation of the adsorbents, but also maximum adsorption capacities increased. As a result of the modification procedure a four to five times increase in maximum adsorption capacity has been achieved.

Table 1. The Langmuir, Freundlich and Sips parameters of adsorption isotherms for all tested dyes obtained by nonlinear regression analysis (NLRA)

Adsorption model	Parameter	Bismarck brown Y				Crystal violet				Methylene blue				Safranin O			
		Native	Native mag.	CA-NaOH-BS	CA-NaOH-MBS	Native	Native mag.	CA-NaOH-BS	CA-NaOH-MBS	Native	Native mag.	CA-NaOH-BS	CA-NaOH-MBS	Native	Native mag.	CA-NaOH-BS	CA-NaOH-MBS
Langmuir	q_{max} (mg g^{-1})	124.3	137.6	524.3	520.3	95.8	96.1	473.2	410.8	86.5	94.1	498.1	455.8	99.7	102.0	296.6	460.7
	K_L (L mg^{-1})	0.233	0.018	0.039	0.033	0.095	0.063	0.039	0.345	0.065	0.051	0.133	0.111	0.075	0.068	0.140	0.087
	SEE	21.336	2.370	39.576	71.868	14.675	7.824	44.327	46.307	2.472	2.413	38.086	64.240	7.053	11.145	10.923	44.698
Sips	q_{max} (mg g^{-1})	260.2	139.2	691.2	526.0	95.8	148.4	1283.0	1273.7	83.3	97.2	502.1	504.6	112.7	344.1	320.3	601.6
	K_L (L mg^{-1})	0.003	0.015	0.013	0.040	0.095	0.0118	1.910^{-6}	4.310^{-6}	0.066	0.047	0.130	0.105	0.051	9.410^{-5}	0.146	0.029
	n	3.910	1.155	2.206	1.056	5.920	2.468	10.812	8.318	0.761	1.121	1.000	1.941	0.100	3.852	1.000	0.100
	SEE	16.315	2.412	19.824	78.710	8.128	1.888	34.104	23.063	1.101	2.298	40.606	64.900	6.968	2.807	6.551	30.292
Freundlich	K_F [(mg g^{-1}) (L mg^{-1})$^{1/n}$]	50.817	20.833	151.68	170.04	36.120	28.697	289.82	237.93	30.994	27.156	230.02	210.50	31.741	31.355	155.29	168.07
	n	6.118	3.419	5.567	6.185	5.920	4.883	14.653	11.357	5.990	4.903	8.648	8.647	5.264	5.069	10.270	6.429
	SEE	15.089	8.556	29.007	78.509	1.752	3.361	27.695	18.336	9.112	7.475	69.541	6.330	8.000	3.209	16.937	33.255

Adsorption kinetics

The adsorption kinetics of all tested dyes and all types of modifications are presented in Fig. 9; additional data are shown as supporting information in Table S3. The kinetic data were then fitted

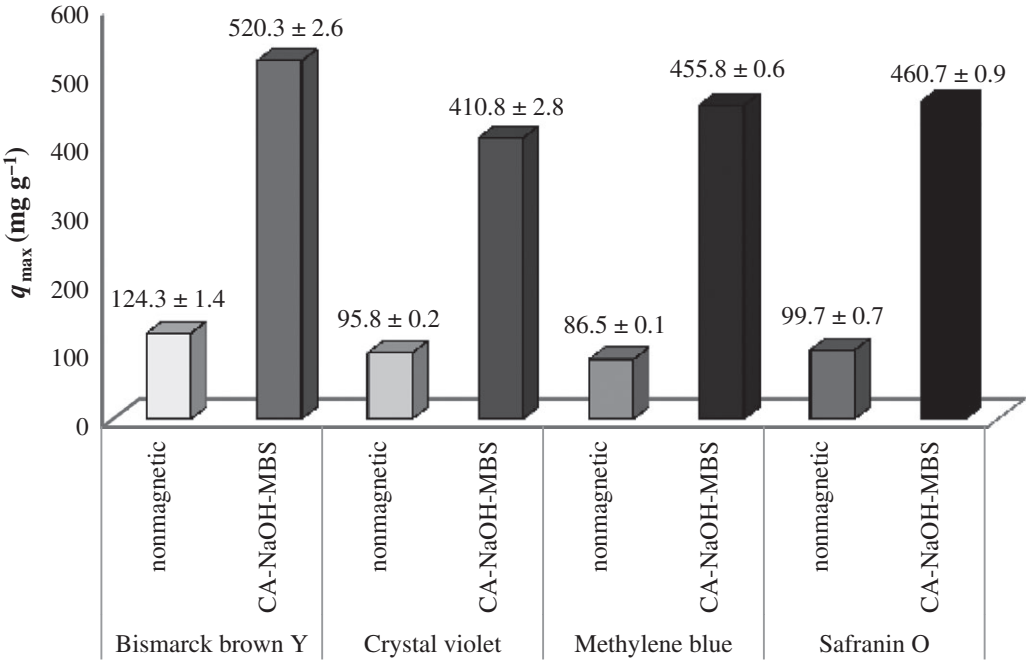

Figure 8. Comparison of maximum adsorption capacities q_{max} (mg g^{-1}; Langmuir equation used) obtained by nonlinear regression.

using the pseudo-first and pseudo-second-order kinetic models (see Table 2).

The linear form of pseudo-first kinetic order is given by Lagergren:[34]

$$\ln\left(q_e - q_t\right) = \ln\left(q_e\right) - k_1 t \tag{10}$$

where the rate constant k_1 can be obtained from the linear plot of $\ln(q_e - q_t)$ against time. If the plot is found to be linear with good correlation coefficients, it can be supposed that the Lagergren equation fitted well; thus the kinetic adsorption corresponds to the pseudo-first-order kinetic model. Nevertheless, in the case of tested dyes and all types of adsorbents, as can be seen from Table 2, the correlation coefficients were very low and the obtained q_e values absolutely disagreed with experimental q_{exp} values; that is why this model is inadequate.

The linear form of pseudo-second-order kinetics can be expressed by this formula:[35]

$$\frac{t}{q_t} = \frac{1}{k_2 q_e^2} + \frac{t}{q_e} \tag{11}$$

where the parameters q_e and k_2 can be determined from the slope and intercept of plot t/q_t versus t. As demonstrated in Table 2, the corresponding correlation coefficients reached values higher than 0.99 and simultaneously the calculated q_e values were very similar to experimental q_{exp} values, which indicated that these kinetic adsorption data conformed well the pseudo-second-order kinetic model.

Adsorption thermodynamics

The thermodynamic experiments were carried out at 282.15, 295.15 and 313.15 K for all types of modification. The thermodynamic equilibrium constant K_d was determined from intercept of the plots of $\ln(q_e/C_e)$ against q_e.[36] The other thermodynamic parameters, namely enthalpy (ΔH^o) and entropy (ΔS^o) were obtained from the Van't Hoff equation:

$$\ln\left(K_d\right) = \frac{\Delta S^o}{R} - \frac{\Delta H^o}{RT} \tag{12}$$

ΔH^o and ΔS^o were calculated from the slope and intercept of the linear plot of $\ln(K_d)$ versus $1/T$.

The standard free energy ΔG^o was calculated from the following formula:[37]

$$\Delta G^o = -RT \ln\left(K_d\right) \tag{13}$$

The obtained thermodynamic data are present in Table 3. The enthalpy changes are positive and this suggests the endothermic nature of adsorption process. The negative values of ΔG^o indicate that the adsorption of dyes is spontaneous and positive ΔS^o values correspond to an increase in degree of freedom of the adsorbed species. The identical nature of the adsorption process has been published for other plant-based adsorbents, such as orange peel[38] and tea waste.[39] The increase in ΔS^o value after chemical modification has also been described previously.[40]

CONCLUSIONS

Barley straw was chosen to study the biosorption of selected organic dyes. This material can be obtained at very low cost. Native barley straw exhibited sufficient dye adsorption, but simple chemical modification using citric acid and sodium hydroxide enabled us to prepare adsorbents with extremely high adsorption capacity. The characterization studies performed suggested that the enormous increase in q_{max} values could be caused by a rougher surface of adsorbents and due to higher number of carboxyl groups. Subsequent magnetic modification was used to prepare magnetically responsive adsorbent. The Langmuir adsorption model, enabling easy determination of q_{max} values with sufficient precision, was used to compare the adsorption efficiencies of tested materials. The adsorption processes could be described by the pseudo-second-order kinetic model and the thermodynamic studies indicated that the adsorption is spontaneous and endothermic.

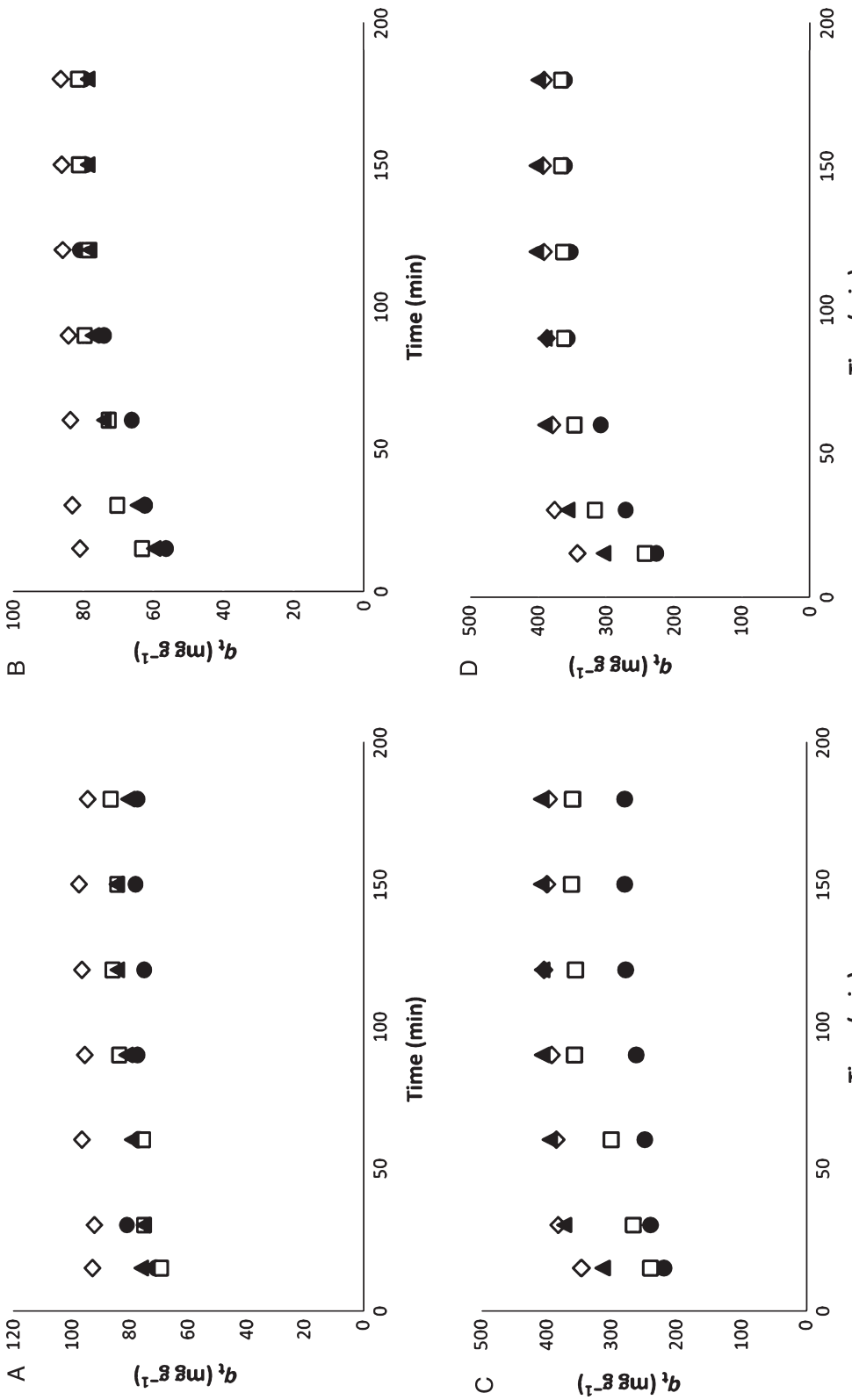

Figure 9. Adsorption kinetics of all tested dyes (◇ Bismarck brown Y, □ crystal violet, ▲ methylene blue, ● safranin O) adsorbed by native non-magnetic (A), native magnetic (B), CA-NaOH nonmagnetic (C) and CA-NaOH magnetic (D) barley straw; at room temperature, at natural pH, concentration of dye solution 350 mg L^{-1} (A, B) and 1250 mg L^{-1} (C, D).

Table 2. Pseudo-first and pseudo-second-order kinetic model parameters for all tested dyes (at room temperature).

Type of modification	Dye	q_{exp} (mg g^{-1})	Pseudo-first order			Pseudo-second order		
			k_1 (min^{-1})	q_e(mg g^{-1})	R^2	k_2 (g mg^{-1} min^{-1})	q_e (mg g^{-1})	R^2
Native	SAF	79	0.0139	9.1	0.3714	0.0594	77.5	0.9995
	CV	88	0.0198	35.8	0.8494	0.0028	87.7	0.9980
	BB	98	0.0156	11.5	0.4414	0.0601	96.1	0.9995
	MB	85	0.0212	20.9	0.5543	0.0092	83.3	0.9984
Native magnetic	SAF	83	0.0182	43.9	0.8380	0.0017	82.6	0.9949
	CV	83	0.0197	33.7	0.8900	0.0029	82.6	0.9985
	BB	88	0.0159	16.0	0.6729	0.0096	86.9	0.9998
	MB	80	0.0221	31.2	0.9001	0.0031	80.6	0.9990
CA-NaOH-BS	SAF	282	0.0268	145.7	0.9345	0.0007	285.7	0.9980
	CV	362	0.0297	225.1	0.9166	0.0004	370.4	0.9951
	BB	405	0.0195	86.4	0.6280	0.0017	400.0	0.9997
	MB	410	0.0291	124.9	0.8615	0.0009	416.7	0.9995
CA-NaOH-MBS	SAF	363	0.0316	257.3	0.9460	0.0004	370.4	0.9961
	CV	368	0.0300	167.4	0.9305	0.0006	370.4	0.9988
	BB	395	0.0243	87.9	0.8090	0.0017	400.0	0.9998
	MB	405	0.0264	135.5	0.8026	0.0008	416.7	0.9993

Table 3. Thermodynamic parameters for adsorption of safranin O on all types of adsorbent

Type of modification	ΔH^o (kJ mol^{-1})	ΔS^o (J mol^{-1} K^{-1})	ΔG^o (kJ mol^{-1})		
			282.15 K	295.15 K	313.15 K
Native	39.95	159.8	−5.26	−7.00	−10.20
Native magnetic	44.64	175.3	−4.75	−7.22	−10.19
CA-NaOH-BS	115.58	451.6	−11.38	−18.57	−25.43
CA-NaOH-MBS	110.02	436.6	−13.09	−19.02	−26.64

ACKNOWLEDGEMENTS

This research was supported by the Grant Agency of the Czech Republic (Project No. 13-13709S) and by the project LO1305 (Ministry of Education, Youth and Sports of the Czech Republic). This research has been co-financed by the ESF and Greek national funds through the NSRF (THALES, Project MIS 377356). The research was also part of COST TD1203 activities. The authors thank Ing. Petra Bazgerova for performing SEM and EDS analysis.

SUPPORTING INFORMATION

Supporting information may be found in the online version of this article.

REFERENCES

1 Gong R, Jin Y, Chen F, Chen J and Liu Z, Enhanced malachite green removal from aqueous solution by citric acid modified rice straw. *J Hazard Mater* **137**:865–870 (2006).
2 Chakraborty S, Chowdhury S and Das Saha P, Artificial neural network (ANN) modeling of dynamic adsorption of crystal violet from aqueous solution using citric-acid-modified rice (*Oryza sativa*) straw as adsorbent. *Clean Technol Environ Policy* **15**:255–264 (2013).
3 Xu X, Gao BY, Yue QY and Zhong QQ, Preparation and utilization of wheat straw bearing amine groups for the sorption of acid and reactive dyes from aqueous solutions. *J Hazard Mater* **182**:1–9 (2010).
4 Safarikova M, Ptackova L, Kibrikova I and Safarik I, Biosorption of water-soluble dyes on magnetically modified *Saccharomyces cerevisiae* subsp *uvarum* cells. *Chemosphere* **59**:831–835 (2005).
5 Madrakian T, Afkhami A and Ahmadi M, Adsorption and kinetic studies of seven different organic dyes onto magnetite nanoparticles loaded tea waste and removal of them from wastewater samples. *Spectrochim Acta A* **99**:102–109 (2012).
6 Celekli A and Bozkurt H, Predictive modeling of an azo metal complex dye sorption by pumpkin husk. *Environ Sci Pollut Res* **20**:7355–7366 (2013).
7 Rafatullah M, Sulaiman O, Hashim R and Ahmad A, Adsorption of methylene blue on low-cost adsorbents: a review. *J Hazard Mater* **177**:70–80 (2010).
8 Gupta VK, Application of low-cost adsorbents for dye removal: a review. *J Environ Manage* **90**:2313–2342 (2009).
9 Aksu Z, Application of biosorption for the removal of organic pollutants: a review. *Process Biochem* **40**:997–1026 (2005).
10 Zhang W, Li H, Kan X, Dong L, Yan H, Jiang Z *et al.*, Adsorption of anionic dyes from aqueous solutions using chemically modified straw. *Bioresour Technol* **117**:40–47 (2012).
11 Ngah WSW, Teong LC and Hanafiah MAKM, Adsorption of dyes and heavy metal ions by chitosan composites: a review. *Carbohydr Polym* **83**:1446–1456 (2011).
12 Tian Y, Wu M, Lin X, Huang P and Huang Y, Synthesis of magnetic wheat straw for arsenic adsorption. *J Hazard Mater* **193**:10–16 (2011).
13 Ibrahim S, Fatimah I, Ang HM and Wang S, Adsorption of anionic dyes in aqueous solution using chemically modified barley straw. *Water Sci Technol* **62**:1177–1182 (2010).
14 Chowdhury S, Chakraborty S, Das P, Adsorption of crystal violet from aqueous solution by citric acid modified rice straw: equilibrium, kinetics, and thermodynamics. *Sep Sci Technol* **48**:1339–1348 (2013).
15 Safarik I, Horska K and Safarikova M, Magnetically modified spent grain for dye removal. *J Cereal Sci* **53**:78–80 (2011).
16 Song J, Zou W, Bian Y, Su F and Han R, Adsorption characteristics of methylene blue by peanut husk in batch and column modes. *Desalination* **265**:119–125 (2011).

17 Kyzas GZ, A decolorization technique with spent 'Greek coffee' grounds as zero-cost adsorbents for industrial textile wastewaters. *Materials* **5**:2069–2087 (2012).
18 Safarik I, Lunackova P, Mosiniewicz-Szablewska E, Weyda F and Safarikova M, Adsorption of water-soluble organic dyes on ferrofluid-modified sawdust. *Holzforschung* **61**:247–253 (2007).
19 Yu JX, Chi RA, Zhang YF, Xu ZG, Xiao CQ and Guo J, A situ co-precipitation method to prepare magnetic PMDA modified sugarcane bagasse and its application for competitive adsorption of methylene blue and basic magenta. *Bioresour Technol* **110**:160–166 (2012).
20 Batzias F, Sidiras D, Schroeder E and Weber C, Simulation of dye adsorption on hydrolyzed wheat straw in batch and fixed-bed systems. *Chem Eng J* **148**:459–472 (2009).
21 Wang XS, Chen LF, Li FY, Chen KL, Wan WY and Tang YJ, Removal of Cr(VI) with wheat-residue derived black carbon: reaction mechanism and adsorption performance. *J Hazard Mater* **175**:816–822 (2010).
22 Safarik I, Pospiskova K, Horska K and Safarikova M, Potential of magnetically responsive (nano)biocomposites. *Soft Matter* **8**:5407–5413 (2012).
23 Safarik I and Safarikova M, One-step magnetic modification of non-magnetic solid materials. *Int J Mater Res* **105**:104–107 (2014).
24 Gong R, Guan R, Zhao J, Liu X and Ni S, Citric acid functionalizing wheat straw as sorbent for copper removal from aqueous solution. *J Health Sci* **54**:174–178 (2008).
25 Han R, Zhang L, Song C, Zhang M, Zhu H and Zhang L, Characterization of modified wheat straw, kinetic and equilibrium study about copper ion and methylene blue adsorption in batch mode. *Carbohydr Polym* **79**:1140–1149 (2010).
26 Sun XF, Sun RC and Sun JX, Acetylation of rice straw with or without catalysts and its characterization as a natural sorbent in oil spill cleanup. *J Agric Food Chem* **50**:6428–6433 (2002).
27 Nomanbhay SM, Hussain R and Palanisamy K, Microwave-assisted alkaline pretreatment and microwave assisted enzymatic saccharification of oil palm empty fruit bunch fiber for enhanced fermentable sugar yield. *J Sustain Bioenergy Syst* **3**:7–17 (2013).
28 Séné CFB, McCann MC, Wilson RH and Grinter R, Fourier-transform Raman and Fourier-transform infrared spectroscopy: an investigation of five higher plant cell walls and their components. *Plant Physiol* **106**:1623–1631 (1994).
29 Freundlich HMF, Über die Adsorption in Lösungen. *Z Phys Chem* **57**:385–471 (1906).
30 Langmuir I, The constitution and fundamental properties of solids and liquids. *J Am Chem Soc* **38**:2221–2295 (1916).
31 Sips R, Structure of a catalyst surface. *J Chem Phys* **16**:490–495 (1948).
32 Weber TW and Chakravorti RK, Pore and solid diffusion models for fixed bed adsorbers. *J Am Inst Chem Eng* **20**:228–238 (1974).
33 Reddy PMK, Krushnamurty K, Mahammadunnisa SK, Dayamani A and Subrahmanyam Ch, Preparation of activated carbons from bio-waste: effect of surface functional groups on methylene blue adsorption. *Int J Environ Sci Technol* **12**:1363–1372 (2015).
34 Lagergren SY, *Zur Theorie der sogenannten Adsorption gelöster Stoffe*, Vol. 24, No. 4. Kungliga Svenska Vetensakademiens, Handlingar, pp. 1–39 (1898).
35 Kumar KV, Linear and non-linear regression analysis for the sorption kinetics of methylene blue onto activated carbon. *J Hazard Mater* **137**:1538–1544 (2006).
36 Khan AA and Singh RP, Adsorption thermodynamics of carbofuran on Sn(IV) arsenosilicate in H^+, Na^+ and Ca^{2+} forms. *Colloids Surf* **24**:33–42 (1987).
37 Tan IAW, Ahmad AL and Hameed BH, Adsorption of basic dye on high-surface-area activated carbon prepared from coconut husk: equilibrium, kinetic and thermodynamic studies. *J Hazard Mater* **154**:337–346 (2008).
38 Gupta VK and Nayak A, Cadmium removal and recovery from aqueous solutions by novel adsorbents prepared from orange peel and Fe_2O_3 nanoparticles. *Chem Eng J* **180**:81–90 (2012).
39 Lunge S, Singh S and Sinha A, Magnetic iron oxide (Fe_3O_4) nanoparticles from tea waste for arsenic removal. *J Magn Mater* **56**:21–31 (2014).
40 Song ST, Saman N, Johari K and Mat H, Removal of Hg(II) from aqueous solution by adsorption using raw and chemically modified rice straw as novel adsorbents. *Ind Eng Chem Res* **52**:13092–13101 (2013).

5.2.5 Mořská tráva *Posidonia oceanica*

Sorpce organických barviv byla testována také na mořské trávě *Posidonia oceanica*, jež představuje odpadní materiál nacházející se v ohromném množství na plážích Středozemního moře.

Magnetická modifikace byla provedena třemi různými způsoby, a sice kyselou magnetickou kapalinou, mechanochemickou syntézou a mikrovlnně syntetizovanými magnetickými částicemi.

U jednotlivých magnetických modifikací byla studována adsorpce metylenové modře. Z dosažených výsledků je patrné, že nejvyšší adsorpční kapacity byly dosaženy pro modifikaci MS magnetitem, následované magnetickou kapalinou. Nejnižší účinnost adsorpce byla pozorována u mechanochemické syntézy.

Z tohoto důvodu byla pro další experimenty použita modifikace mikrovlnnou syntézou. Testováno bylo sedm barev s různou chemickou strukturou. Adsorpční rovnovážná data byla analyzována pomocí Langmuirova modelu, ze kterého byly vypočteny maximální adsorpční kapacity, pohybující se v rozmezí od 88,1 do 233,5 mg/g. Kinetiku adsorpce lze pro všechna barviva popsat kinetickým modelem pseudo-druhého řádu. Na základě vypočtených termodynamických parametrů je patrné, že adsorpční proces je spontánní a endotermní.

Přítomnost magnetických částic na povrchu materiálu byla detekována pomocí SEM vybavené energiově disperzním spektroskopem.

Příloha 11:

Magnetically modified *Posidonia oceanica* biomass as an adsorbent for organic dyes removal

Safarik I, Ashoura N, Maderova Z, Pospiskova K, Baldikova E, Safarikova M

Mediterr. Mar. Sci. 17, **2016**, 351-358

Research Article

Mediterranean Marine Science
Indexed in WoS (Web of Science, ISI Thomson) and SCOPUS
The journal is available on line at http://www.medit-mar-sc.net
DOI: http://dx.doi.org/10.12681/mms.1549

Magnetically modified *Posidonia oceanica* biomass as an adsorbent for organic dyes removal

I. SAFARIK[1,2,3], N. ASHOURA[4], Z. MADEROVA[3], K. POSPISKOVA[2], E. BALDIKOVA[3,5] and M. SAFARIKOVA[1,3]

[1] Department of Nanobiotechnology, Biology Centre, ISB, CAS, Na Sadkach 7, 370 05 Ceske Budejovice, Czech Republic
[2] Regional Centre of Advanced Technologies and Materials, Palacky University, Slechtitelu 27, 783 71 Olomouc, Czech Republic
[3] Global Change Research Institute, CAS, Na Sadkach 7, 370 05 Ceske Budejovice, Czech Republic
[4] Department of Chemistry, Florida Institute of Technology, 150 W. University Blvd., Melbourne, FL 32901, USA
[5] Department of Applied Chemistry, Faculty of Agriculture, University of South Bohemia, Branisovska 1457, 370 05 Ceske Budejovice, Czech Republic

Corresponding author: ivosaf@yahoo.com

Handling Editor: Argyro Zenetos

Received: 2 November 2015; Accepted: 9 February 2016; Published on line: 29 February 2016

Abstract

Magnetically modified *Posidonia oceanica* sea grass dead biomass was employed as an adsorbent of organic dyes. The adsorption of seven water-soluble organic dyes was characterized using Langmuir adsorption model. The highest calculated maximum adsorption capacity was found for Bismarck brown Y (233.5 mg g^{-1}), while the lowest capacity value was obtained for safranin O (88.1 mg g^{-1}). The adsorption processes followed the pseudo-second-order kinetic model and the thermodynamic studies indicated spontaneous and endothermic adsorption.

Keywords: *Posidonia oceanica*, Neptune balls, magnetic biomass, organic dyes, adsorbent.

Introduction

Posidonia oceanica (L.) Delile is a widely distributed, fast-growing sea grass playing important ecological roles in the Mediterranean ecosystem. The *P. oceanica* dead leaves in the form of so called "Neptune balls" (Fig. 1) are accumulated in a large scale on the beaches. This material is usually collected from the beaches as a waste because of their bad view and also distinctive odour. The collected dead leaves are usually burned to get beaches clean. However, this material contains ca 30% of cellulose and 29% of lignin with many functional groups, such as hydroxyl, sulphonyl, carbonyl and phenolic, that can be effectively used for adsorption purposes (Aydin *et al.*, 2012; Cengiz & Cavas, 2010; Chadlia *et al.,* 2009).

Waste *Posidonia* biomass has recently been tested as a sorbent for the removal of various organic dyes from water solutions. This adsorbent exhibited high maximum adsorption capacity (119.05 mg g^{-1}) towards methyl violet at 45 ºC. Pseudo-second-order kinetic model fitted well the experimental data. Negative values of Gibbs free energy implied that the process was spontaneous (Cengiz & Cavas, 2010). Some other dyes were also adsorbed well on the *Posidonia* biomass, as shown by relatively high maximum adsorption capacities; Astrazon red (68.97 mg g^{-1}, Cengiz *et al.*, 2012, Acid yellow 59 (76.9 mg g^{-1}; (Guezguez *et al.*, 2009)), Alpacide yellow (15.11 mg g^{-1}; (Ncibi *et al.,* 2009)) and Reactive red 228 (5.74 mg g^{-1}; (Ncibi *et al.*, 2007)) can serve as examples.

Magnetically modified adsorbents can be prepared by the attachment of magnetic iron oxides nano- or microparticles on the surface or within the pores of the treated materials. Magnetic materials can be easily separated from complex systems and difficult-to-handle media by means of magnetic separators (Safarikova & Safarik, 2001).

In order to improve manipulation with *Posidonia* biomass, magnetically responsive derivatives were prepared using three simple and low-cost procedures and tested as magnetic biosorbents for organic dyes removal. The best magnetic *Posidonia* adsorbent was characterized in detail.

Materials and Methods

Materials

Posidonia oceanica fibres balls, collected at the Poetto beach in Cagliari (Sardinia, Italy; the coordinates of the area are 39°11′43.50″ N – 9°09′33.52″ E) at the end of March 2013, were manually converted into fibres, washed thoroughly with water to remove sand and salt and then dried in an oven at 40 - 60 ºC for 48 h to a constant weight. After drying, the fibres were cut into small fragments and milled to obtain fine particles (length ca 0.1 – 0.6 mm, width ca 0.03 – 0.1 mm), see Fig. 2. Methylene blue (C.I. 52015), Bismarck brown Y (C.I. 21000) and safranin O (C.I. 50240) were purchased from Sigma, USA. Crystal

Fig. 1: "Neptune balls" (*Posidonia oceanica* dead biomass) on the Poetto beach, Cagliari, Sardinia, Italy.

violet (C.I. 42555) and brilliant green (C.I. 42040) were supplied by Lachema, Czech Republic. Acridine orange (C.I. 46005) was obtained from Loba Feinchemie, Austria, while Nile blue A sulphate (C.I. 51180) was from Chemische Fabrik GmbH, Germany. Common chemicals were from Sigma-Aldrich, Czech Republic. Water-based ionic magnetic fluid stabilized with perchloric acid (concentration 30.5 mg of maghemite per 1 mL) was prepared using a standard procedure (Massart, 1981).

Magnetic modification of Posidonia powdered biomass

a/ Microwave assisted modification procedure

Posidonia biomass was magnetically modified using microwave-synthesized magnetic iron oxides particles (Safarik & Safarikova, 2014). In a typical procedure, 1 g $FeSO_4 . 7 H_2O$ was dissolved in 100 mL of water in a 600 – 800 mL beaker and solution of sodium or potassium hydroxide (1 mol L^{-1}) was added slowly under mixing until the pH reached the value ca 12; during this process, a precipitate of iron hydroxides was formed. The suspension was then diluted up to 200 mL with water and inserted into a standard kitchen microwave oven (700 W, 2450 MHz). The suspension was usually treated for 10 min at the maximum power. Then the beaker was removed from the oven and the formed magnetic iron oxides nano- and microparticles were repeatedly washed with water until neutral pH of the magnetic suspension was reached.

Fig. 2: *Posidonia oceanica* fibres ball, separated fibres and fine biomass particles obtained by milling.

To prepare magnetically responsive *Posidonia* biomass, one gram of biomass was thoroughly mixed in a short test-tube or a small beaker with 2 mL of microwave iron oxides nano- and microparticles suspension (1 part of completely sedimented iron oxides particles and 4 parts of water). Vigorous mixing with a spatula or laboratory spoon enabled homogeneous distribution of magnetic nano- and microparticles within the treated material. This mixture was allowed to dry completely at temperatures not exceeding 60 °C for 48 hours. In order to increase magnetic response of the *Posidonia* composite, the amount of iron oxide particles can be increased (Safarik & Safarikova, 2014).

b/ Mechanochemical modification procedure

In the standard procedure, a mixture of 1.35 g of $FeCl_3 . 6H_2O$ (0.005 mol), 0.50 g of $FeCl_2 . 4 H_2O$ (0.0025 mol) and 4 g of sodium chloride (inert material used to avoid particles agglomeration) was ground in a mortar at room temperature for 10 min. One g of *Posidonia* biomass was then added and after thorough mixing, the process continued for another 10 min. As the last step, powdered potassium hydroxide (1.22 g) was added and after mixing, the grinding continued for 10 min. After KOH addition, the mixture became brown. During the grinding process, the material was scraped from the mortar wall occasionally. After finishing the mechanochemical process, the magnetically modified material was thoroughly washed with water (to remove soluble impurities and free iron oxides particles) and air dried (Safarik *et al.*, 2014).

c/ Modification with magnetic fluid

In a typical procedure, 1 g of *Posidonia* biomass was thoroughly mixed in a short test-tube or a small beaker with 1 mL of water based ferrofluid stabilized with perchloric acid. The mixing with a spatula or laboratory spoon enabled homogeneous distribution of magnetic fluid within the treated biomass. This mixture was allowed to dry completely at temperatures not exceeding 50 °C and then washed with water and/or methanol. The magnetically responsive biomass was air dried (Safarik *et al.*, 2012a).

Adsorption of dyes on magnetic Posidonia biomass

The following procedure was employed to study the adsorption properties (Safarik *et al.,* 2012b). 30 mg of magnetically modified *Posidonia* biomass were mixed with 4.0 mL of water in a test tube. Then 1-6 mL portion of stock water solution (1 mg mL^{-1}) of a tested dye was added and the total volume of the solution was made up to 10.0 mL with water. The suspension was mixed for 2

h at room temperature. Then the magnetic adsorbent was separated from the suspension by means of a magnetic separator (MPC-1 or MPC-6, Dynal, Norway) and the clear supernatant was used for the spectrophotometric measurement. The concentration of free (unbound) dye in the supernatant (C_{eq}) was determined from the calibration curve. The amount of dye bound to the unit mass of the adsorbent (q_{eq}) was calculated using the following formula:

$$q_{eq} = V\,(C_0 - C_{eq})\,/\,m \quad (1)$$

where V is the total volume (L), C_0 is the initial concentration (mg L^{-1}) of dye used in the experiment and m is the mass of adsorbent (g). The value q_{eq} was expressed in mg of adsorbed dye per 1 g of adsorbent. Equilibrium adsorption data were fitted to Langmuir adsorption isotherms using SigmaPlot software.

Adsorption kinetics

Adsorption kinetics was studied using Bismarck brown Y (initial dye concentration 150 mg L^{-1}, 25°C, pH not adjusted), in different time intervals (0-300 min). The amount of adsorbed dye per unit mass of adsorbent q_t (mg g^{-1}) in time t was calculated from this formula:

$$q_t = V\,(C_o - C_t)\,/\,m \quad (2)$$

where C_t is the concentration of dye in solution (mg L^{-1}) in time t (min). The obtained kinetic data were analyzed using the linear forms of pseudo-first (Lagergren, 1898) and pseudo-second (Kumar, 2006) order kinetic equations given as follows, respectively:

$$ln(q_{eq} - q_t) = ln(q_{eq}) - k_1 t \quad (3)$$

where the rate constant k_1 (min^{-1}) can be obtained from the linear plot of ln (q_{eq} - q_t) against time

$$t/q_t = 1/k_2 q_{eq}^{\,2} + t/q_{eq} \quad (4)$$

where the equilibrium adsorption capacity (q_{eq}) and the second-order rate constant k_2 (g mg^{-1} min^{-1}) can be determined from the slope and intercept of plot t/q_t versus t.

Thermodynamic studies

The studies of temperature effect of Bismarck brown Y adsorption on magnetically modified *Posidonia* biomass were carried out at 282.15, 298.15 and 313.15 K.

The thermodynamic equilibrium constant K_d was determined from intercept of the plot of ln (q_{eq}/C_{eq}) aqainst q_{eq} (Khan & Singh, 1987). The other thermodynamic parameters, namely Gibbs free energy change ΔG^o (J mol^{-1}), standard enthalpy change ΔH^o (J mol^{-1}) and standard entropy change ΔS^o (J mol^{-1} K^{-1}) of studied process were calculated by using these equations:

$$\Delta G^0 = -RT\,ln(K_d) \quad (5)$$

$$ln(K_d) = \Delta S^0/R - \Delta H^0/RT \quad (6)$$

where R is the universal gas constant (8.314 J mol^{-1} K^{-1}) and T is the absolute temperature (K). ΔH^o and ΔS^o were determined from the slope and intercept of the linear plot of ln (K_d) versus 1/T.

Results and Discussion

Magnetic modification of Posidonia biomass

Three procedures for magnetic modification of *Posidonia* biomass, namely modification with microwave synthesized magnetic iron oxides nano- and microparticles (Safarik & Safarikova, 2014), mechanochemical synthesis (Safarik *et al.,* 2014) and modification with water based magnetic fluid (Safarik *et al.*, 2012a) were tested in order to select an optimal magnetized adsorbent. Both the adsorbent maximum adsorption capacity and the simplicity and price of its preparation were taken into account. Preliminary adsorption experiments with methylene blue showed that magnetization with microwave synthesized magnetic iron oxides nano- and microparticles enabled to prepare magnetic adsorbent with the highest maximum adsorption capacity (calculated using Langmuir adsorption isotherm), see Table 1. This magnetization procedure is extremely simple, and very cheap chemicals (ferrous sulphate and sodium or potassium hydroxide) are used as precursors. During the microwave-assisted synthesis, magnetic iron oxide nanoparticles (ca 25 to 100 nm) formed micrometer-sized stable aggregates (maximum aggregate size ca 20 μm; Baldikova *et al.,* in press). Magnetic modification led to the deposition of iron oxide nanoparticle aggregates on the surface of the *Posidonia* biomass providing sufficient surface area for efficient dye adsorption (see Fig. 3). Energy-dispersive X-ray spectroscopy confirmed the presence of iron on the magnetized biomass (Fig. 4). The presence of Fe^{3+} ions on the surface of magnetically modified *Posidonia* biomass was confirmed by Perls´ Prussian Blue Stain that caused intensive blue coloration of the whole material (Fig. 5). The stability of magnetically modified biomass was very high (stable at least two months in water suspension). The formed magnetically responsive *Posidonia*

Table 1. Maximum adsorption capacity (q_{max}) of magnetic *Posidonia* adsorbents for methylene blue.

Magnetic modification of *Posidonia* adsorbents	q_{max} **(mg g^{-1})**
Microwave synthesized magnetic iron oxides nano- and microparticles	143.7
Mechanochemical synthesis	102.5
Modification with magnetic fluid	133.3

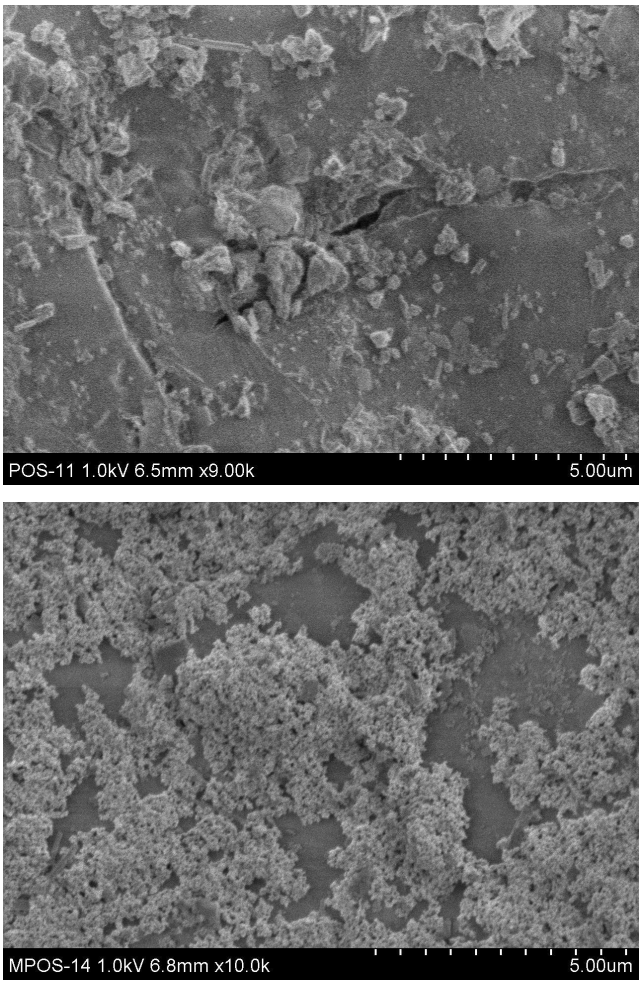

Fig. 3: SEM images of native (top) and magnetically modified (bottom) *Posidonia* biomass.

adsorbent can be easily separated using permanent magnet or commercial magnetic separator (Fig. 6).

Adsorption studies and isotherms

Posidonia biomass modified with microwave synthesized magnetic iron oxides nano- and microparticles was used as an adsorbent to study binding of 7 organic water-soluble dyes belonging to different dye classes. These dyes were selected according to the results of the preliminary screening experiment using 18 different dyes.

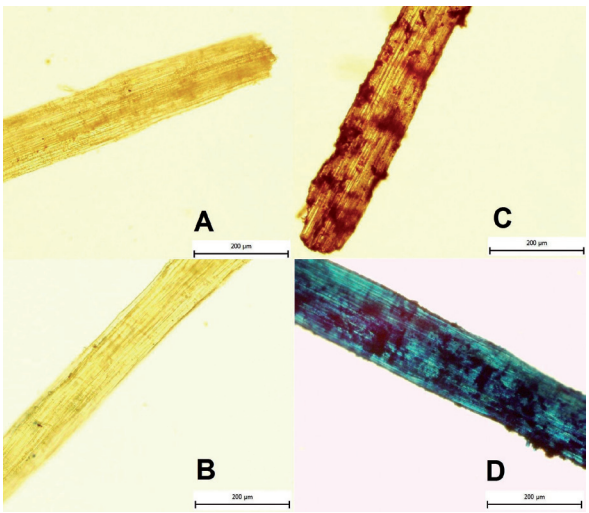

Fig. 5: Optical microscopy of native (A) and magnetically modified (C) *Posidonia* biomass. After Perls' stain, almost no coloration is visible on native biomass (B), while deep blue coloration is observed on magnetically modified biomass (D). Bar is 200 µm.

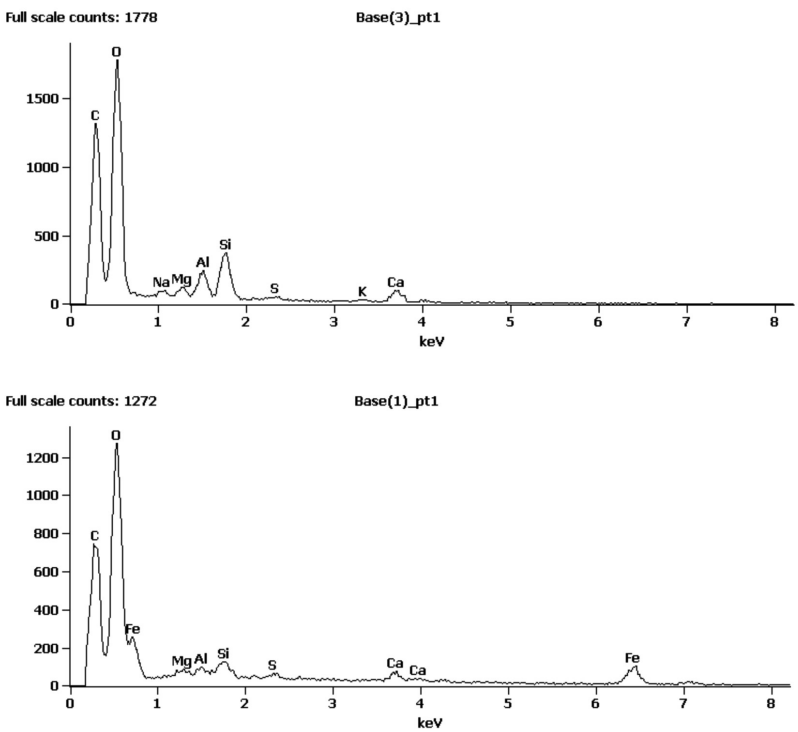

Fig. 4: EDS of native (top) and magnetically modified (bottom) *Posidonia* biomass.

Fig. 6: Appearance of original *Posidonia* biomass suspension (left), suspension of biomass after magnetic modification (middle) and demonstration of magnetic separation of magnetically modified biomass (right).

Therefore, Bismarck brown Y (azodyes group), crystal violet and brilliant green (triphenylmethane group), methylene blue (quinone-imine group), acridine orange (acridine group), Nile blue (oxazin group) and safranin O (safranin group) were chosen for further experiments. The chemical structures are shown in Table 2.

The contact time is one of the most important adsorption parameters required for determination of time necessary to reach the equilibrium. As can be seen from the Fig. 7, the adsorption process was very fast; more than 96% of Bismarck brown Y was adsorbed within 5 min. However, to reach the equilibrium approximately 1 h is needed. Two hours incubation was used for the adsorption experiments. The equilibrium adsorption isotherms

Table 2. Dye structures and maximum adsorption capacities (q_{max}) and dissociation constants (b) describing the dyes adsorption on magnetically modified *Posidonia* biomass, calculated from the Langmuir equation; q_{max} is expressed in mg g^{-1}.

Dye	Dye structure	Adsorption coefficients
Acridine orange	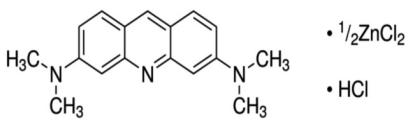	q_{max} = 119.8 b = 0.424
Bismarck brown Y	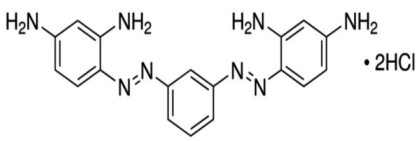	q_{max} = 233.5 b = 0.084
Brilliant green	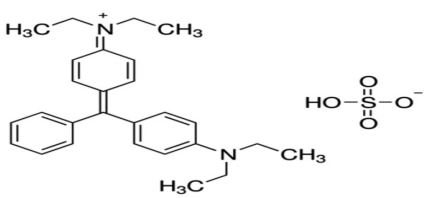	q_{max} = 151.8 b = 0.588
Crystal violet	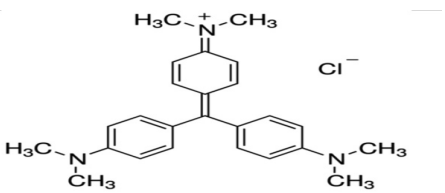	q_{max} = 99.9 b = 0.299
Methylene blue	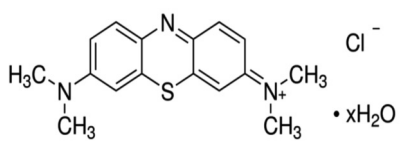	q_{max} = 143.7 b = 0.060
Nile blue A sulphate	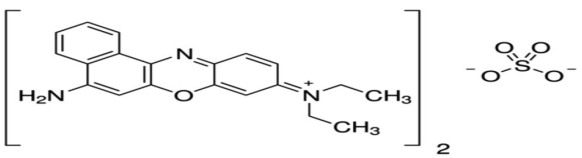	q_{max} = 193.7 b = 0.041
Safranin O	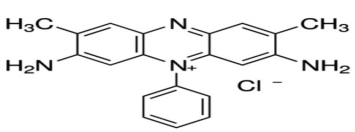	q_{max} = 88.1 b = 0.307

for the tested dyes using magnetically modified *Posidonia* biomass are shown in Fig. 8.

In order to study the adsorption process, Langmuir and Freundlich isotherm equations are usually used for experimental data analysis. The Langmuir model is valid for monolayer adsorption onto a surface with a finite number of identical sites. The well-known expression for the Langmuir model is given by

$$q_{eq} = \frac{q_{\max} b C_{eq}}{1 + b C_{eq}} \quad (7)$$

where q_{eq} (expressed in mg g^{-1} or mg mL^{-1}) is the amount of the adsorbed dye per unit mass or sedimented volume of magnetic *Posidonia* biomass and C_{eq} (expressed in mg L^{-1}) is the unadsorbed dye concentration in solution at equilibrium. The parameter q_{max} is the maximum amount of the dye per unit mass (mg g^{-1}) or sedimented volume (mg mL^{-1}) of magnetic *Posidonia* biomass to form a complete monolayer on the surface bound at high dye concentration and b is a constant related to the affinity of the binding sites (expressed in L mg^{-1}) (Safarik *et al.*, 2012b).

Non-linear regression calculation using SigmaPlot software was used to fit the experimental data to Langmuir adsorption model and to obtain both constants (q_{max}, b). The results are presented in Table 2. The value of the maximum adsorption capacity is a very important parameter describing the adsorption process.

In the case of seven tested dyes, the highest calculated q_{max} was found for Bismarck brown Y (233.5 mg g^{-1}), while the lowest q_{max} value was obtained for safranin O (88.1 mg g^{-1}).

Adsorption kinetics

As already shown in the Fig. 7, the adsorption process was very fast with more than 96% of Bismarck brown Y adsorbed within 5 min. The obtained data were subsequently analyzed to investigate kinetics of adsorption process using pseudo-first and pseudo-second order kinetic models. It is apparent from results summarized in Table 3 that the pseudo-first order kinetic model did not fit well; the correlation coefficient was low and the calculated q_{eq} absolutely disagreed with the experimental $q_{eq\,exp}$ value, while in case of pseudo-second order kinetic model (see Table 3 and Fig. 9) the correlation coefficient reached the value close to 1.0 and the theoretical q_{eq} value calculated from this equation approached the experimental $q_{eq\,exp}$.

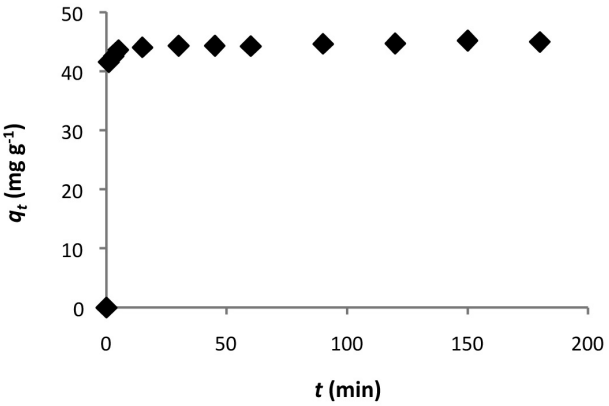

Fig. 7: Dependence of Bismarck brown Y adsorption on time (dye initial concentration 150 mg L^{-1}, 25°C, pH not adjusted).

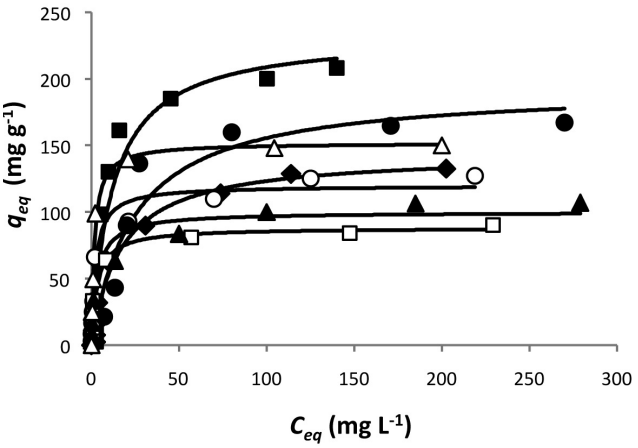

Fig. 8: Equilibrium adsorption isotherms of tested dyes on magnetically modified *Posidonia* biomass. C_{eq} - equilibrium liquid-phase concentration of the unadsorbed (free) dye (mg L^{-1}); q_{eq} - equilibrium solid-phase concentration of the adsorbed dye (mg g^{-1}). (○) - acridine orange; (■) - Bismarck brown Y; (Δ) - brilliant green; (▲) - crystal violet; (♦) - methylene blue; (●) - Nile blue; (□) - safranin O.

Thermodynamic studies

Thermodynamic studies were performed at three different temperatures, namely 282.15, 298.15 and 313.15 K. All obtained thermodynamic parameters are presented in Table 4. Negative values of Gibbs free energy change (ΔG^o) indicate the spontaneous process, positive ΔH^o the endothermic nature of adsorption and positive ΔS^o suggests an increase of the randomness at the solid/solution

Table 3. The pseudo-first and pseudo-second order kinetic model parameters for Bismarck brown Y (25°C, pH not adjusted).

C_o (mg L^{-1})	$q_{eq\,exp}$ (mg g^{-1})	Pseudo-first order			Pseudo-second order		
		k_1 (min^{-1})	q_{eq} (mg g^{-1})	R^2	k_2 (g mg^{-1} min^{-1})	q_{eq} (mg g^{-1})	R^2
150	45.2	0.0137	2.0	0.7593	0.0632	45.0	0.9999

Table 4. The thermodynamic parameters for Bismarck brown Y adsorption on magnetically modified *Posidonia oceanica*.

ΔH^o (kJ mol^{-1})	ΔS^o (kJ mol^{-1} K^{-1})	ΔG^o (kJ mol^{-1})		
		282.15	**298.15**	**313.15**
14.977	0.073	-5.514	-7.235	-7.731

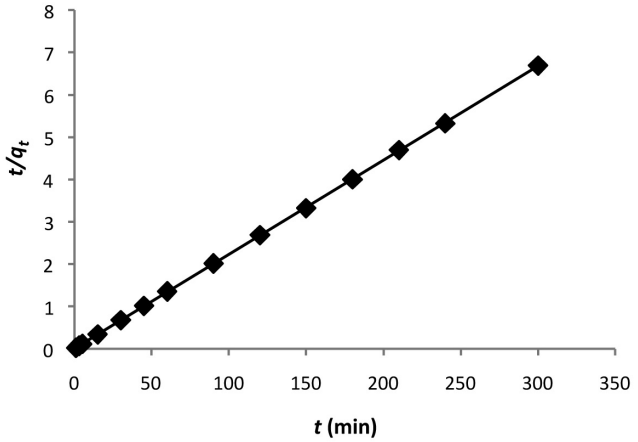

Fig. 9: The pseudo-second order kinetic model plot (Bismarck brown Y, initial concentration 150 mg L^{-1}, pH not adjusted, 25°C).

interface during sorption process. Similar results have been published recently (Cengiz & Cavas, 2010).

Conclusions

Posidonia oceanica dead biomass, known also as Neptune balls, was chosen to study the biosorption of selected organic water-soluble dyes. This material can be obtained at very low cost; in fact in many localities it is a waste. To simplify the manipulation with the adsorbent, *Posidonia* biomass was magnetically modified using three different techniques. Although all tested magnetization procedures led to the preparation of magnetically responsive adsorbents, the method using microwave synthesized magnetic iron oxides nano- and microparticles enabled to prepare material with the highest dye removal efficiency.

Langmuir adsorption model, enabling very simple calculation of maximum adsorption capacities, could be applied with reasonable accuracy for fitting all the experimental adsorption data. The obtained values of maximum adsorption capacity ranged between 88.1 mg g^{-1} for safranin O and 233.5 mg g^{-1} for Bismarck brown Y, respectively.

The adsorption processes could be described by the pseudo-second-order kinetic model and the thermodynamic studies indicated that the adsorption is spontaneous and endothermic. Due to the low price, high adsorption efficiency and simplicity of magnetic modification process, the magnetic *Posidonia* biomass represents a perspective low-cost adsorbent for organic pollutants removal.

Acknowledgements

This research was supported by the Grant Agency of the Czech Republic (Project No. 13-13709S) and by the projects LO1305 and LD14066 of the Ministry of Education, Youth and Sports of the Czech Republic. The research was also part of COST TD1203 activities.

References

Aydin, M., Cavas, L., Merdivan, M., 2012. An alternative evaluation method for accumulated dead leaves of *Posidonia oceanica* (L.) Delile on the beaches: removal of uranium from aqueous solutions. *Journal of Radioanalytical and Nuclear Chemistry*, 293, 489-496.

Baldikova, E., Politi, D., Maderova, Z., Pospiskova, K., Sidiras, D., Safarikova, M., Safarik, I., 2016. Utilization of magnetically responsive cereal by-product for organic dye removal. *Journal of the Science of Food and Agriculture*, in press (DOI: 10.1002/jsfa.7337).

Cengiz, S., Cavas, L., 2010. A promising evaluation method for dead leaves of *Posidonia oceanica* (L.) in the adsorption of methyl violet. *Marine Biotechnology*, 12, 728-736.

Cengiz, S., Tanrikulu, F., Aksu, S., 2012. An alternative source of adsorbent for the removal of dyes from textile waters: *Posidonia oceanica* (L.). *Chemical Engineering Journal*, 189, 32-40.

Guezguez, I., Dridi-Dhaouadi, S., Mhenni, E., 2009. Sorption of Yellow 59 on *Posidonia oceanica*, a non-conventional biosorbent: Comparison with activated carbons. *Industrial Crops and Products,* 29, 197-204.

Chadlia, A., Mohamed, K., Najah, L., Farouk, M. M., 2009. Preparation and characterization of new succinic anhydride grafted *Posidonia* for the removal of organic and inorganic pollutants. *Journal of Hazardous Materials*, 172, 1579-1590.

Khan, A. A., Singh, R. P., 1987. Adsorption thermodynamics of carbofuran on Sn(IV) arsenosilicate in H^+, Na^+ and Ca^{2+} forms. *Colloids and Surfaces*, 24, 33-42.

Kumar, K. V., 2006. Linear and non-linear regression analysis for the sorption kinetics of methylene blue onto activated carbon. *Journal of Hazardous Materials,* 137, 1538-1544.

Lagergren, S. Y., 1898. Zur Theorie der sogenannten Adsorption gelöster Stoffe. *Kungliga Svenska Vetenskapsakademiens Handlingar*, 24 (4), 1-39.

Massart, R., 1981. Preparation of aqueous magnetic liquids in alkaline and acidic media. *IEEE Transactions on Magnetics,* 17, 1247-1248.

Ncibi, M. C., Mahjoub, B., Ben Hamissa, A. M., Ben Mansour, R., Seffen, M., 2009. Biosorption of textile metal-complexed dye from aqueous medium using *Posidonia oceanica* (L.) leaf sheaths: Mathematical modelling. *Desalination*, 243, 109-121.

Ncibi, M. C., Mahjoub, B., Seffen, M., 2007. Adsorptive removal of textile reactive dye using *Posidonia oceanica* (L.) fibrous biomass. *International Journal of Environmental Science and Technology*, 4, 433-440.

Safarik, I., Horska, K., Pospiskova, K., Filip, J., Safarikova, M., 2014. Mechanochemical synthesis of magnetically responsive materials from non-magnetic precursors. *Materials Letters,* 126, 202-206.

Safarik, I., Horska, K., Pospiskova, K., Safarikova, M., 2012a. One-step preparation of magnetically responsive materials from non-magnetic powders. *Powder Technology*, 229, 285-289.

Safarik, I., Horska, K., Svobodova, B., Safarikova, M., 2012b. Magnetically modified spent coffee grounds for dyes removal. *European Food Research and Technology*, 234, 345-350.

Safarik, I., Safarikova, M., 2014. One-step magnetic modification of non-magnetic solid materials. *International Journal of Materials Research*, 105, 104-107.

Safarikova, M., Safarik, I., 2001. The application of magnetic techniques in biosciences. *Magnetic and Electrical Separation*, 10, 223-252.

5.2.6 Makrořasa *Sargassum horneri*

Stejně tak jako mořská tráva *Posidonia oceanica* se makrořasa *Sargassum horneri* může vyskytovat ve velkém množství na plážích (zejména v jižním Pacifiku). Přestavuje tak odpadní materiál, který by mohl být dále zužitkován.

Biomasa makrořasy byla magnetizována pomocí MS magnetitu suspendovaným v metanolu. Charakterizace připraveného biosorbentu byla provedena pomocí SEM, EDS a FTIR.

V této práci byla testována sorpce pěti organických barviv: akridinové oranže, krystalové violeti, malachitové zeleně, metylenové modře a safraninu O. Studována byla závislost na čase i teplotě. Rovnovážná adsorpční data byla analyzována pomocí Langmuirova a Freundlichova modelu. Hodnota maximálních adsorpčních kapacit byla ve všech studovaných případech vyšší než 110 mg/g. Kinetický proces lze popsat kinetickým modelem pseudo-druhého řádu. Na rozdíl od *Posidinie* je adsorpční proces exotermní.

Příloha 12:

Magnetically modified *Sargassum horneri* biomass as an adsorbent for organic dyes removal

Angelova R, Baldikova E, Pospiskova K, Maderova Z, Safarikova M, Safarik I

J. Clean. Product. 137, **2016**, 189-194

Journal of Cleaner Production 137 (2016) 189–194

Contents lists available at ScienceDirect

Journal of Cleaner Production

journal homepage: www.elsevier.com/locate/jclepro

Short communication

Magnetically modified *Sargassum horneri* biomass as an adsorbent for organic dye removal

Ralitsa Angelova [a, b, c], Eva Baldikova [d, e], Kristyna Pospiskova [f], Zdenka Maderova [d], Mirka Safarikova [a, d], Ivo Safarik [a, d, f, *]

[a] Department of Nanobiotechnology, Biology Centre, ISB, CAS, Na Sadkach 7, 370 05 Ceske Budejovice, Czech Republic
[b] Department of General and Industrial Microbiology, Faculty of Biology, Sofia University "St. Kliment Ohridski", 8 Dragan Tsankov Blvd, 1164 Sofia, Bulgaria
[c] Laboratory Microwave Magnetics, Institute of Electronics, Bulgarian Academy of Sciences, 72 Tzarigradsko Chaussee Blvd, 1784 Sofia, Bulgaria
[d] Global Change Research Institute, CAS, Na Sadkach 7, 370 05 Ceske Budejovice, Czech Republic
[e] Department of Applied Chemistry, Faculty of Agriculture, University of South Bohemia, Branisovska 1457, 370 05 Ceske Budejovice, Czech Republic
[f] Regional Centre of Advanced Technologies and Materials, Palacky University, Slechtitelu 27, 783 71 Olomouc, Czech Republic

ARTICLE INFO

Article history:
Received 1 April 2016
Received in revised form
7 July 2016
Accepted 12 July 2016
Available online 15 July 2016

Keywords:
Sargassum horneri
Brown seaweed
Magnetic adsorbent
Microwave synthesis
Magnetic iron oxide

ABSTRACT

Adsorption of five water-soluble dyes of different chemical structures from aqueous solutions was investigated using magnetically responsive brown algae *Sargassum horneri*. The simple magnetic modification of *Sargassum* biomass employing microwave-synthesized iron oxide nano- and microparticles enabled rapid and selective separation by means of external magnetic field. The biosorption was studied in a batch system under different conditions. Time necessary to reach equilibrium was less than 2 h for all tested dyes. The adsorption equilibrium data were analyzed by Langmuir and Freundlich isotherm models. The highest maximum adsorption capacity was observed for acridine orange (193.8 mg/g), the lowest one for malachite green (110.4 mg/g). The sorption kinetics could be described by pseudo-second-order model, and the thermodynamic studies indicated exothermic nature of biosorption process in the temperature range studied. It can be concluded that *Sargassum horneri* biomass, exhibiting a satisfactory efficacy in dye removal, can be used as an effective, low-cost adsorbent.

1. Introduction

Dyes are important color compounds widely used in many sections of industry, such as food, textile, plastic, paper, pharmaceutical and cosmetic ones. It is estimated that more than 7×10^5 tons of diverse dyes are produced annually (Celekli and Bozkurt, 2013), and 10–15% of them enter the water system (Ausavasuhki et al., 2016; Liu et al., 2016). Even very low dye concentration is highly visible and can significantly affect aquatic life as well as food web (Banat et al., 1996; Robinson et al., 2001). Many of these pollutants or their metabolites have also toxic, carcinogenic and mutagenic effects. Furthermore, they are very difficult to degrade because of the diversity in structure and high persistence in nature caused by stability to light, oxidizing agents, aerobic digestion and biodegradation (Aravindhan et al., 2007; Sun and Yang, 2003; Xu et al., 2010).

Development of efficient and inexpensive treatment techniques applicable for dye removal from the wastewater before discharging to natural water streams is necessary. Conventional methods, such as precipitation, filtration, oxidation, ozonation, irradiation, ion exchange or photodegradation have already been employed, however, utilization of these techniques is usually connected with high economical cost, operational problems, formation of hazardous by-products or intensive energy requirement (Gupta and Suhas, 2009; Zhou et al., 2014).

Application of biosorption for the removal of toxic pollutants from wastewaters is one of the progressive developments in environmental technology. This process can exhibit high efficiency, while producing low amount of waste (Park et al., 2010). Many biosorbents, including bacteria, fungi, algae, industrial wastes, agricultural wastes and other polysaccharide materials, have already been used for dye removal (Crini, 2006; Lee et al., 2016; Çelekli et al., 2013). Marine macroalgae, popularly known as

* Corresponding author. Department of Nanobiotechnology, Biology Centre, ISB, CAS, Na Sadkach 7, 370 05 Ceske Budejovice, Czech Republic.
E-mail address: ivosaf@yahoo.com (I. Safarik).

http://dx.doi.org/10.1016/j.jclepro.2016.07.068
0959-6526/

Table 1
Chemical structures and other related information about tested dyes.

Dye	Colour index (CI) number	Molecular weight	Chemical structure	Dye class	Manufacturer/supplier
Acridine orange	46005	301.82	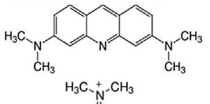	Acridine	Loba Feinchemie, Austria
Crystal violet	42555	407.98	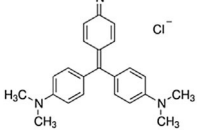	Triphenylmethane	Lachema, Czech Republic
Malachite green	42000	364.91	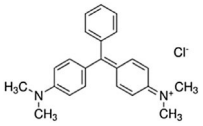	Triphenylmethane	Lachner, Czech Republic
Methylene blue	52015	319.85	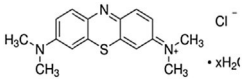	Quinone-imine	Sigma, USA
Safranin O	50240	350.84	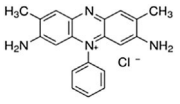	Safranin	Sigma, USA

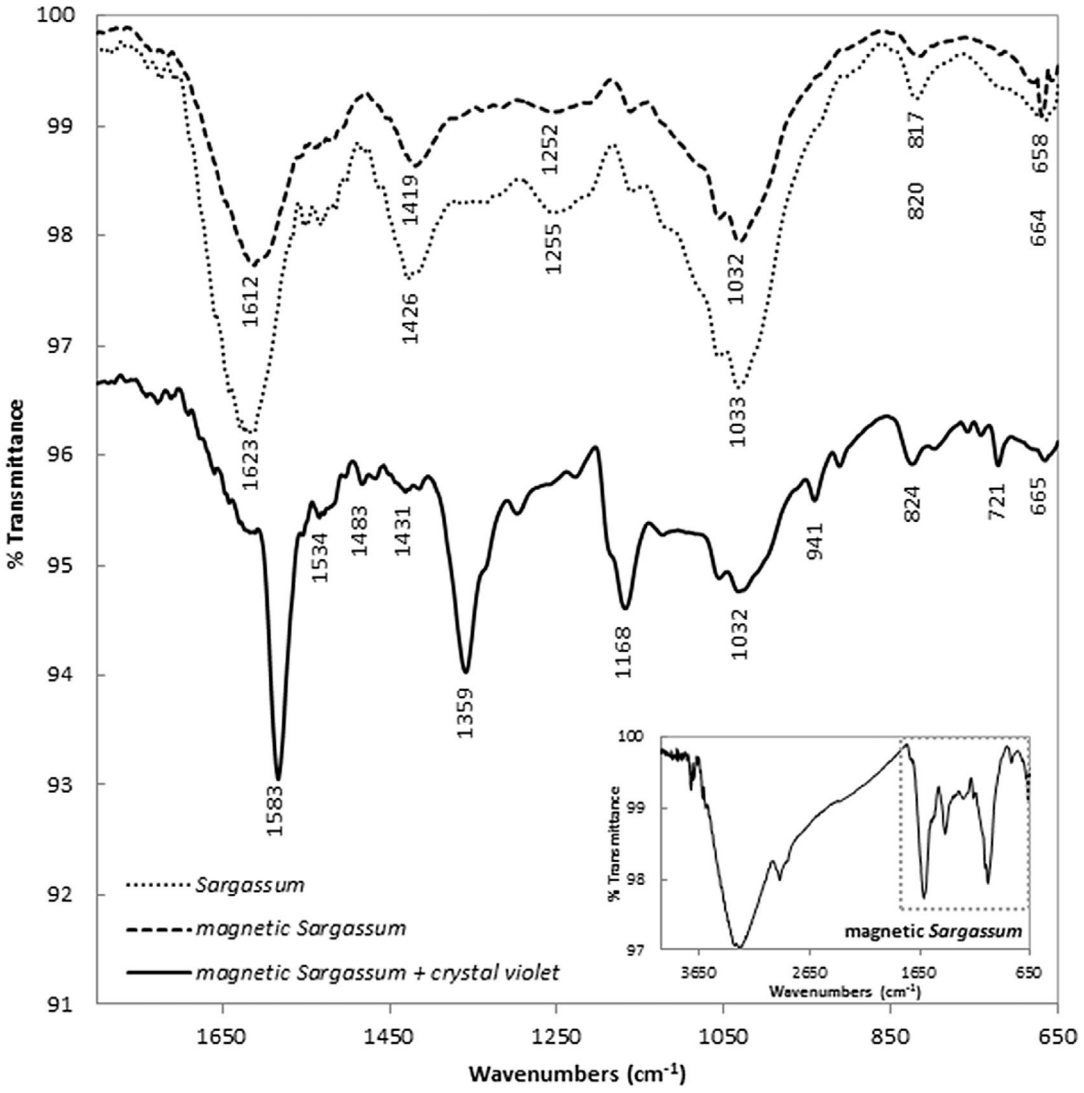

Fig. 1. Fourier transform infrared spectrum of native (… … …), magnetically modified (- - - - - -) and crystal violet bound to magnetically modified (_____) *Sargassum horneri* biomass.

seaweeds, represent very interesting adsorbent materials typical of zero-cost and easy availability in many parts of the world (Pozdniakova et al., 2016; Rathod et al., 2014; Vijayaraghavan et al., 2009). Especially *Sargassum horneri* can be locally very abundant (mainly in the eastern Pacific); its continued expansion throughout the temperate and tropical oceans combined with its high growth rates and long floating thalli may pose a major threat to the sustainability of native marine ecosystems. Large amounts of *Sargassum* biomass can be found occasionally on beaches (Marks et al., 2015).

In the present study, the removal of several dyes (acridine orange, crystal violet, malachite green, methylene blue and safranin O) from aqueous solution was studied using magnetically modified *Sargassum horneri* biomass as a natural, renewable and low-cost biosorbent. Magnetic modification of the biomass enabled simple and rapid magnetic separation after the adsorption process. Several experimental factors affecting the adsorption were studied in detail. The equilibrium biosorption data were fitted to Langmuir and Freundlich adsorption isotherm equations. Thermodynamic parameters were also determined to study the nature of the adsorption process.

2. Materials and methods

2.1. Chemicals

NaOH was obtained from Penta (Czech Republic), $FeSO_4 \cdot 7H_2O$ and methanol were supplied by Lachner (Czech Republic); all chemicals were of GR grade. Related information about tested dyes is summarized in Table 1.

2.2. Biosorbent material

Macroalgae biomass (*Sargassum horneri*) was collected by one of the authors (I. S.) at the Golden Sandy Beach, Qingdao, China (35°57′17.08″N, 120°14′26.67″E), at the end of October 2014. The biomass was washed with water, dried (at temperature below 60 °C), ground in a coffee mill and sieved through test sieves (Retsch GmbH, Germany) to obtain particles with size below 0.7 mm.

The magnetic modification of native *Sargassum* biomass was performed using microwave-synthesized iron oxide nano- and microparticles which were prepared as described recently (Safarik and Safarikova, 2014; Zheng et al., 2010). After washing with water, the formed iron oxide particles were transferred to methanol. The magnetic modification of diamagnetic algae biomass was carried out by thorough mixing one gram of *Sargassum* biomass with 2 mL of iron oxide suspension in methanol (1 part of completely sedimented iron oxide particles and 4 parts of methanol); the modified material was dried completely at 60 °C for 24 h (Safarik et al., 2016b).

Native and magnetically modified *Sargassum* biomass was characterized using Fourier transform infrared spectroscopy (FTIR; the spectra were recorded in a Thermo Scientific Nicolet iS5 FT-IR Spectrometer with iD Foundation accessory (ZnSe crystal, range 4000–650 cm^{-1}, 32 scans, resolution of 4 cm^{-1})), scanning electron microscopy (SEM; Hitachi SU6600 with accelerating voltage 5 kV) and optical microscopy (detection of iron on magnetically modified *Sargassum* biomass using Perls' staining procedure (Safarik et al., 2012)).

2.3. Dye adsorption experiments

The structures of dyes (acridine orange, crystal violet, malachite green, methylene blue, safranin O) tested in this work are shown in Table 1. All concentrations were prepared by diluting 1 g/L stock dye solution with distilled water; the pH values of the dye solutions were 3.1 for malachite green, 3.2 for acridine orange, 4.6 for crystal violet, 5.8 for methylene blue and 6.5 for safranin O. The sorption experiments were carried out in batch systems without any pH adjustment, similarly as described previously (Baldikova et al., 2016; Safarik et al., 2016a); for details, see the Electronic Supplement.

3. Results and discussion

Sargassum biomass, as well as other related materials of biological origin, contains various functional groups which can act as binding sites to capture various molecules via electrostatic attraction, ion exchange and complexation (Daneshvar et al., 2012). The functional groups of *Sargassum* sp. biomass were detected by using FTIR spectra in the range of 650–4000 cm^{-1} (Fig. 1). The broad and strong absorption vibration around 3000 – 3500 cm^{-1} shows the presence of O-H and N-H groups on algae biomass. The weak band occurring around 2924 cm^{-1} can be assigned to stretching vibration of alkyl CH groups. The strong absorption peak at around 1612 cm^{-1} and a weak absorption band at 1419 cm^{-1} represent carboxyl groups. The absorption bands at around 1252 and 1032 cm^{-1} are due to S=O stretching vibrations (Kannan, 2014). The adsorption of crystal violet (one of the dyes used for the experiments) on magnetic *Sargassum* sp. biomass caused changes in FTIR spectrum, mainly within 1800–800 cm^{-1} region. The peak at

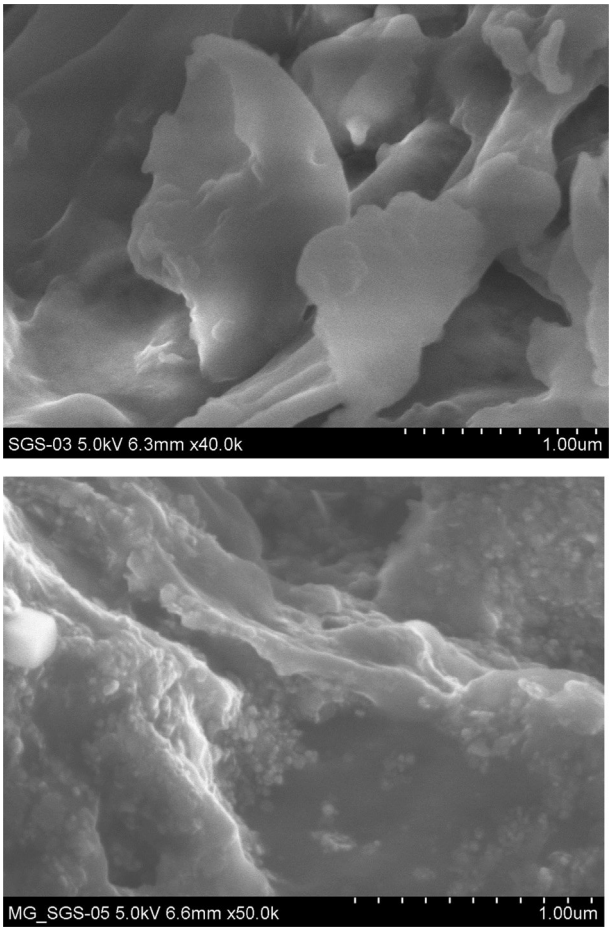

Fig. 2. SEM images of native (top) and magnetically modified (bottom) *Sargassum horneri* biomass.

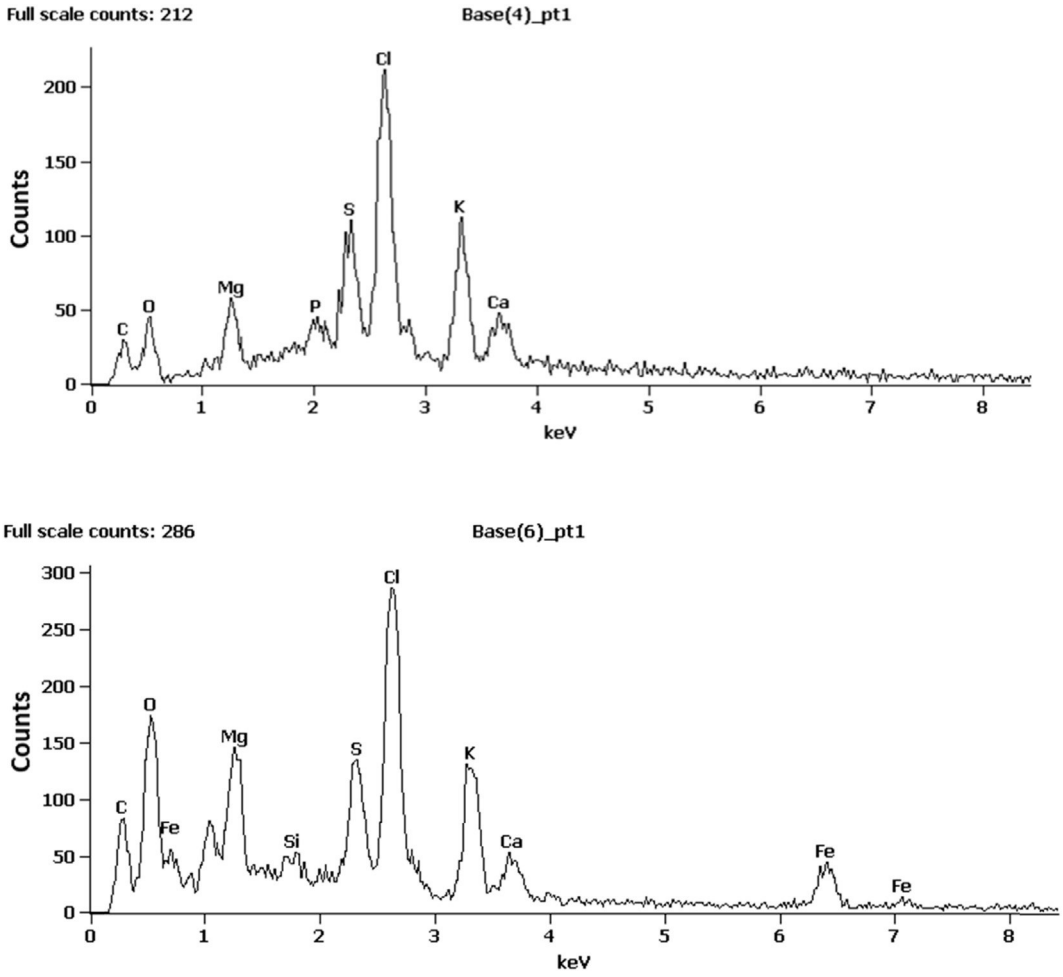

Fig. 3. EDS of native (top) and magnetically modified (bottom) *Sargassum horneri* biomass.

1583 cm^{-1} corresponds to the C=C stretching of the benzene ring while the peak for the C–N stretch of aromatic tertiary amine can be observed at 1359 cm^{-1}. Spectrum shows also a peak at 1168 cm^{-1} corresponding to the C–N stretching vibrations (Cheriaa et al., 2012).

An extremely simple procedure was used to prepare magnetically modified *Sargassum* biomass; this modification led to the deposition of magnetic iron oxide nano- and microparticles on the surface of individual macroalgae particles. Optical microscopy enabled to observe magnetic particles both in native preparations (brown deposits) and especially after Perls' staining indicating the presence of Fe(III) ions in magnetic particles as intensively blue deposits (see Supplement Fig. S1). The magnetic particles deposition was confirmed using SEM; it can be clearly seen that magnetic iron oxide nanoparticles form aggregates firmly adhering to the biomass surface (Fig. 2).

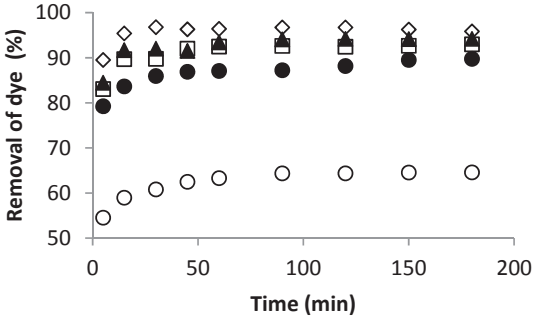

Fig. 4. Effect of contact time on dye adsorption at 298.15 K; adsorbent 30 mg; initial dye concentration 250 mg/L. □ – acridine orange, ● – crystal violet, ○ – malachite green, ◊ – methylene blue, ▲ – safranin O.

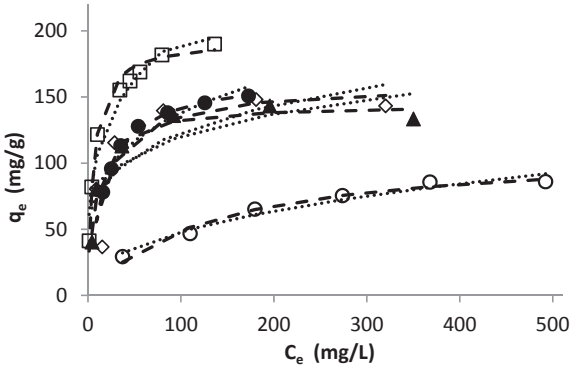

Fig. 5. Equilibrium adsorption isotherms of tested dyes on magnetically modified *Sargassum* biomass. C_e – equilibrium liquid-phase concentration of the unadsorbed (free) dye (mg/L); q_e – equilibrium solid-phase concentration of the adsorbed dye (mg/g). □ – acridine orange, ● – crystal violet, ○ – malachite green, ◊ – methylene blue, ▲ – safranin O. Langmuir isotherm (- - - - - -), Freundlich isotherm (…. …. …. …. ….).

Table 2
The Langmuir and Freundlich isotherm parameters for tested dyes.

		Acridine orange	Crystal violet	Malachite green	Methylene blue	Safranin O
Langmuir	q_{max} (mg/g)	193.8	167.0	110.4	158.9	144.4
	b (L/mg)	0.167	0.056	0.008	0.061	0.112
	SEE	7.73	1.83	3.72	25.24	7.18
Freundlich	K_f [(mg/g) (L/mg)$^{1/n}$]	57.64	45.00	7.39	44.70	49.90
	n	3.767	4.106	2.460	4.536	5.240
	SEE	3.20	7.84	4.93	29.01	20.00

Table 3
Kinetic parameters of dye uptake on magnetic *Sargassum* biomass.

Model	Parameters	Acridine orange	Crystal violet	Malachite green	Methylene blue	Safranin O
	$q_{e,exp}$ (mg/g)	75.8	74.8	48.6	80.2	70.1
Pseudo-first-order	$k_1 \times 10^2$ (1/min)	0.87	0.76	0.94	0.94	0.70
	q_e (mg/g)	4.5	8.1	5.8	1.6	5.0
	R^2	0.65	0.88	0.80	0.27	0.67
Pseudo-second-order	$k_2 \times 10^2$ (g/mg min)	0.19	0.85	1.28	10.3	1.82
	q_e (mg/g)	75.8	75.2	49.0	80.6	70.4
	R^2	1.00	0.99	1.00	1.00	0.99

Energy-dispersive X-ray spectroscopy (EDS) confirmed the presence of iron on the magnetized biomass (Fig. 3). The stability of magnetically modified biomass was very high (stable at least for two months in water suspension). The magnetically responsive *Sargassum* adsorbent formed can be easily separated using permanent magnet or commercial magnetic separator.

Adsorption process requires sufficient time to reach the equilibrium. As can be seen from Fig. 4, the adsorption equilibrium was achieved for each dye (chemical structures of tested dyes and other related information are presented in Table 1) at another time, in the range between 30 min for methylene blue and 90 min for malachite green. Two hours incubation time was used for the adsorption experiments.

The equilibrium adsorption isotherms for the tested dyes using magnetically modified *Sargassum* biomass are shown in Fig. 5. In order to study the adsorption process, Langmuir and Freundlich isotherm equations were used for experimental data analysis. The nonlinear fits of isotherm models to the experimental data are displayed in Fig. 5. The corresponding models constants and the standard error of estimate (SEE) are summarized in Table 2. The Langmuir parameter q_{max} provides information about maximum monolayer sorption capacity on the biomass; the highest q_{max} was obtained for acridine orange (193.8 mg/g).

The values of standard error of estimate were applied as the fitting criteria for comparing the isotherm models. The Langmuir model fitted sufficiently well with the experimental data for all dyes.

The adsorption is a multi step process involving the following four steps: (i) bulk diffusion, (ii) film diffusion, (iii) pore diffusion or intra-particle diffusion and (iv) adsorption of dye on the adsorbent surface (Khaled et al., 2009). The adsorption efficiency and a possible rate controlling step are obtained from adsorption kinetics. The kinetic data were analyzed by pseudo-first-order and pseudo-second-order models (see Supplement Fig. S2). Table 3 represents the calculated parameters using kinetic models.

The fitting of experimental data to both kinetic models was evaluated on the basis of obtained correlation coefficients (R^2) and calculated q_e values. It is apparent from results summarized in Table 3 that adsorption of all tested dyes on magnetically responsive *Sargassum* biomass followed well the pseudo-second-order kinetic model.

The thermodynamic parameters including the Gibbs free energy change (ΔG°), enthalpy (ΔH°) and entropy (ΔS°) assist to describe the thermodynamic behavior of the sorption. One model dye (crystal violet) was selected for prediction of its adsorption behavior on *Sargassum* biomass in the range of temperature 282.15–313.15 K.

ΔG° was calculated to be −10.12, −10.9 and −10.19 kJ/mol at 282.15, 298.15 and 313.15 K, respectively. The negative values of Gibbs free energy change show the spontaneous nature of the sorption. The negative value of ΔH° (−9.56 kJ/mol), calculated from the slope of the plot of ln K_d vs 1/T, indicates the exothermic nature of

Table 4
Comparison of various macro- and microalgae and seagrass as adsorbents for organic dyes removal.

Adsorbent	Adsorbent modification	Adsorbed dye	Maximum adsorption capacity (q_{max}; mg/g)	Reference
Sargassum muticum	Removal of lipids by acetone	Methylene blue	860	Rubín et al., 2010
Sargassum muticum	HCl treatment	Methylene blue	279	Rubin et al., 2005
Chaetophora elegans	–	Methylene blue	333	El Jamal and Ncibi, 2012
Carolina	No pretreatment	Methylene blue	55	Hammud et al., 2011
	Crosslinking with formaldehyde		64	
Posidonia oceanica	–	Methylene blue	5.5	Ncibi et al., 2007
Spirogyra majuscula	–	Reactive red 120	722	Celekli et al., 2009
Chara contraria	–	Reactive red 120	113	Çelekli et al., 2012
Chara contraria	–	Lanaset red G	163	Çelekli et al., 2011
Chlorella vulgaris	Magnetic modification	Safranin O	115	Safarikova et al., 2008
		Crystal violet	43	Safarikova et al., 2008
Sargassum horneri	Magnetic modification	Acridine orange	194	This paper
		Crystal violet	167	This paper
		Malachite green	110	This paper
		Methylene blue	159	This paper
		Safranin O	144	This paper

biosorption process in the temperature range studied. The small negative value of the standard enthalpy change suggests that the adsorption is physical in nature involving weak forces of attraction (El-Bindary et al., 2015). Similar results of thermodynamic parameters of the biosorption of methylene blue onto algal biomass have been achieved recently (Kumar et al., 2015). Furthermore, the positive value of ΔS° (1.94 J/mol K) implies the increased randomness at the solid–solution interface during the sorption process.

4. Conclusion

The applicability of magnetically modified *Sargassum* biomass as a biosorbent for dye removal was demonstrated. The presence of microwave-synthesized magnetic iron oxide particles on *Sargassum* surface enabled rapid separation of biosorbent by means of appropriate magnetic separator. Five dyes were chosen for adsorption experiments. The adsorption equilibrium time was lower than 90 min for all the dyes. In all cases, the calculated maximum adsorption capacities were relatively high (>110 mg/g), also in comparison with the literature values for other macro- and microalgae (Table 4). Kinetic data fitted well the pseudo-second-order kinetic model, and thermodynamic studies indicated the spontaneous and exothermic process. *Sargassum* biomass has a potential to become a promising low-cost biosorbent.

Acknowledgements

The authors thank to Prof. Pengcheng Li (Institute of Oceanology, Chinese Academy of Sciences, Qingdao, China) for the determination of collected macroalgae. This research was supported by the Grant Agency of the Czech Republic (Project No. 13-13709S) and by the projects LO1305 and LD14066 of the Ministry of Education, Youth and Sports of the Czech Republic. The research was also part of COST TD1203 activities.

Appendix A. Supplementary data

Supplementary data related to this article can be found at http://dx.doi.org/10.1016/j.jclepro.2016.07.068.

References

Aravindhan, R., Rao, J.R., Nair, B.U., 2007. Removal of basic yellow dye from aqueous solution by sorption on green alga *Caulerpa scalpelliformis*. J. Hazard. Mater. 142 (1–2), 68–76.

Ausavasuhki, A., Kampoosaen, C., Kengnok, O., 2016. Adsorption characteristic of Congo red on carbonized leonardite. J. Clean. Prod. http://dx.doi.org/10.1016/j.clepro.2015.10.034 in press.

Baldikova, E., Politi, D., Maderova, Z., Pospiskova, K., Sidiras, D., Safarikova, M., Safarik, I., 2016. Utilization of magnetically responsive cereal by-product for organic dye removal. J. Sci. Food Agric. 96, 2204–2214.

Banat, I.M., Nigam, P., Singh, D., Marchant, R., 1996. Microbial decolorization of textile-dyecontaining effluents: a review. Bioresour. Technol. 58 (3), 217–227.

Celekli, A., Bozkurt, H., 2013. Predictive modeling of an azo metal complex dye sorption by pumpkin husk. Environ. Sci. Pollut. Res. 20 (10), 7355–7366.

Çelekli, A., Bozkurt, H., Geyik, F., 2013. Use of artificial neural networks and genetic algorithms for prediction of sorption of an azo-metal complex dye onto lentil straw. Bioresour. Technol. 129, 396–401.

Celekli, A., Yavuzatmaca, M., Bozkurt, H., 2009. Kinetic and equilibrium studies on the adsorption of reactive red 120 from aqueous solution on *Spirogyra majuscula*. Chem. Eng. J. 152 (1), 139–145.

Çelekli, A., Tanrıverdi, B., Bozkurt, H., 2011. Predictive modeling of removal of Lanaset Red G on *Chara contraria*; kinetic, equilibrium, and thermodynamic studies. Chem. Eng. J. 169 (1), 166–172.

Çelekli, A., İlgün, G., Bozkurt, H., 2012. Sorption equilibrium, kinetic, thermodynamic, and desorption studies of Reactive Red 120 on *Chara contraria*. Chem. Eng. J. 191, 228–235.

Cheriaa, J., Khaireddine, M., Rouabhia, M., Bakhrouf, A., 2012. Removal of triphenylmethane dyes by bacterial consortium. Sci. World J. 2012, Article ID 512454.

Crini, G., 2006. Non-conventional low-cost adsorbents for dye removal: a review. Bioresour. Technol. 97 (9), 1061–1085.

Daneshvar, E., Kousha, M., Jokar, M., Koutahzadeh, N., Guibal, E., 2012. Acidic dye biosorption onto marine brown macroalgae: isotherms, kinetic and thermodynamic studies. Chem. Eng. J. 204–206, 225–234.

El-Bindary, A.A., El-Sonbati, A.Z., Al-Sarawy, A.A., Mohamed, K.S., Farid, M.A., 2015. Removal of hazardous azopyrazole dye from an aqueous solution using rice straw as a waste adsorbent: kinetic, equilibrium and thermodynamic studies. Spectrochim. Acta A 136, 1842–1849. Part C.

El Jamal, M.M., Ncibi, M.C., 2012. Biosorption of methylene blue by *Chaetophora elegans* algae: kinetics, equilibrium and thermodynamic studies. Acta Chim. Slov. 59, 24–31.

Gupta, V.K., Suhas, I.A., 2009. Application of low-cost adsorbents for dye removal – a review. J. Environ. Manage. 90 (8), 2313–2342.

Hammud, H.H., Fayoumi, L., Holail, H., Mostafa, E.S.M., 2011. Biosorption studies of methylene blue by Mediterranean algae *Carolina* and its chemically modified forms. Linear and nonlinear models' prediction based on statistical error calculation. Int. J. Chem. 3 (4), 147.

Kannan, S., 2014. FT-IR and EDS analysis of the seaweeds *Sargassum wightii* (brown algae) and *Gracilaria corticata* (red algae). Int. J. Curr. Microbiol. App. Sci. 3 (4), 341–351.

Khaled, A., Nemr, A.E., El-Sikaily, A., Abdelwahab, O., 2009. Removal of Direct N Blue-106 from artificial textile dye effluent using activated carbon from orange peel: adsorption isotherm and kinetic studies. J. Hazard. Mater. 165 (1–3), 100–110.

Kumar, P.S., Pavithra, J., Suriya, S., Ramesh, M., Kumar, K.A., 2015. *Sargassum wightii*, a marine alga is the source for the production of algal oil, bio-oil, and application in the dye wastewater treatment. Desalin. Water Treat. 55, 1342–1358.

Lee, L.Y., Gan, S., Tan, M.S.Y., Lim, S.S., Lee, X.J., Lam, Y.F., 2016. Effective removal of Acid Blue 113 dye using overripe *Cucumis sativus* peel as an eco-friendly biosorbent from agricultural residue. J. Clean. Prod. 113, 194–203.

Liu, X.X., Gong, W.P., Luo, J., Zou, C.T., Yang, Y., Yang, S.J., 2016. Selective adsorption of cationic dyes from aqueous solution by polyoxometalate-based metal-organic framework composite. Appl. Surf. Sci. 362, 517–524.

Marks, L.M., Salinas-Ruiz, P., Reed, D.C., Holbrook, S.J., Culver, C.S., Engle, J.M., Kushner, D.J., Caselle, J.E., Freiwald, J., Williams, J.P., Smith, J.R., Aguilar-Rosas, L.E., Kaplanis, N.J., 2015. Range expansion of a non-native, invasive macroalga *Sargassum horneri* (Turner) C. Agardh, 1820 in the eastern Pacific. BioInvasions Rec. 4 (4), 243–248.

Ncibi, M.C., Mahjoub, B., Seffen, M., 2007. Kinetic and equilibrium studies of methylene blue biosorption by *Posidonia oceanica* (L.) fibres. J. Hazard. Mater. B139, 280–285.

Park, D., Yun, Y.-S., Park, J.M., 2010. The past, present, and future trends of biosorption. Biotechnol. Bioprocess Eng. 15 (1), 86–102.

Pozdniakova, T.A., Mazur, L.P., Boaventura, R.A.R., Vilar, V.J.P., 2016. Brown macroalgae as natural cation exchangers for the treatment of zinc containing wastewaters generated in the galvanizing process. J. Clean. Prod. 119, 38–49.

Rathod, M., Mody, K., Basha, S., 2014. Efficient removal of phosphate from aqueous solutions by red seaweed, *Kappaphycus alverezii*. J. Clean. Prod. 84, 484–493.

Robinson, T., McMullan, G., Marchant, R., Nigam, P., 2001. Remediation of dyes in textile effluent: a critical review on current treatment technologies with a proposed alternative. Bioresour. Technol. 77 (3), 247–255.

Rubin, E., Rodriguez, P., Herrero, R., Cremades, J., Barbara, I., de Vicente, S., Manuel, E., 2005. Removal of methylene blue from aqueous solutions using as biosorbent *Sargassum muticum*: an invasive macroalga in Europe. J. Chem. Technol. Biotechnol. 80 (3), 291–298.

Rubín, E., Rodríguez, P., Herrero, R., Sastre de Vicente, M.E., 2010. Adsorption of methylene blue on chemically modified algal biomass: equilibrium, dynamic, and surface data. J. Chem. Eng. Data 55 (12), 5707–5714.

Safarik, I., Ashoura, N., Maderova, Z., Pospiskova, K., Baldikova, E., Safarikova, M., 2016a. Magnetically modified *Posidonia oceanica* biomass as an adsorbent for organic dyes removal. Mediterr. Mar. Sci. 17 (2), 351–358.

Safarik, I., Baldikova, E., Pospiskova, K., Safarikova, M., 2016b. Magnetic modification of diamagnetic agglomerate forming powder materials. Particuology in press.

Safarik, I., Horska, K., Svobodova, B., Safarikova, M., 2012. Magnetically modified spent coffee grounds for dyes removal. Eur. Food Res. Technol. 234 (2), 345–350.

Safarik, I., Safarikova, M., 2014. One-step magnetic modification of non-magnetic solid materials. Int. J. Mater. Res. 105 (1), 104–107.

Safarikova, M., Pona, B.M.R., Mosiniewicz-Szablewska, E., Weyda, F., Safarik, I., 2008. Dye adsorption on magnetically modified *Chlorella vulgaris* cells. Fresenius Environ. Bull. 17, 486–492.

Sun, Q., Yang, L., 2003. The adsorption of basic dyes from aqueous solution on modified peat–resin particle. Water Res. 37 (7), 1535–1544.

Vijayaraghavan, K., Teo, T.T., Balasubramanian, R., Joshi, U.M., 2009. Application of *Sargassum* biomass to remove heavy metal ions from synthetic multi-metal solutions and urban storm water runoff. J. Hazard. Mater. 164, 1019–1023.

Xu, X., Gao, B.-Y., Yue, Q.-Y., Zhong, Q.-Q., 2010. Preparation and utilization of wheat straw bearing amine groups for the sorption of acid and reactive dyes from aqueous solutions. J. Hazard. Mater. 182 (1–3), 1–9.

Zheng, B.Z., Zhang, M.H., Xiao, D., Jin, Y., Choi, M.M.F., 2010. Fast microwave synthesis of Fe_3O_4 and Fe_3O_4/Ag magnetic nanoparticles using Fe^{2+} as precursor. Inorg. Mater. 46 (10), 1106–1111.

Zhou, K., Zhang, Q., Wang, B., Liu, J., Panyue, W., Gui, Z., Hu, Y., 2014. The integrated utilization of typical clays in removal of organic dyes and polymer nanocomposites. J. Clean. Prod. 81, 281–289.

5.2.7 Aktivovaný kal

Tento článek je zaměřen na odstraňování organických barviv pomocí aktivovaného kalu získaného z čističky odpadních vod ve Zlivi. Kal byl použit jednak v nativní verzi, jednak po tepelném ošetření (120 ^{o}C/15 min).

Magnetická modifikace byla provedena inkubací kalu s MS magnetitem, a to v poměru 1:0,1 (1 mL kalu:0,1 mL sedlého magnetitu), který vedl k vytvoření materiálu s dostatečnou magnetickou odezvou.

Materiál byl stejně jako v některých předchozích publikacích charakterizován pomocí optické a skenovací elektronové mikroskopie, EDS a FTIR. MS magnetit byl ale navíc analyzován rentgenovou krystalografií (XRD), která prokázala typické znaky nano- a mikročástic magnetitu.

V rámci screeningových experimentů bylo testováno 12 barviv, avšak pro detailní popis adsorpce byly vybrány pouze čtyři, které vykazovaly nejvyšší adsorpční účinnost. Studována byla závislost nejen na čase či teplotě, ale také na pH. Rovnovážná adsorpční data byla modelována pomocí Langmuirova, Freundlichova a Sipsova modelu. Maximální adsorpční kapacita získaná z Langmuirova modelu (pro tepelně ošetřený magnetický kal) dosahovala hodnot od 246,9 do 768,2 mg/g. Neošetřený kal vykazoval hodnoty mnohem nižší (anilinová modř: 768,2 versus 493,0 mg/g).

Kinetiku adsorpce lze s 99,9% spolehlivostí popsat pomocí kinetického modelu pseudo-druhého řádu. Termodynamické studie prokázaly spontánní a endotermní adsorpční proces.

Příloha 13:

Removal of dyes by adsorption on magnetically modified activated sludge

Maderova Z, Baldikova E, Pospiskova K, Safarik I, Safarikova M

Int. J. Environ. Sci. Technol. 13, **2016**, 1653-1664

Int. J. Environ. Sci. Technol. (2016) 13:1653–1664
DOI 10.1007/s13762-016-1001-8

ORIGINAL PAPER

Removal of dyes by adsorption on magnetically modified activated sludge

Z. Maderova[1] · E. Baldikova[1,2] · K. Pospiskova[3] · I. Safarik[1,3,4] · M. Safarikova[1,4]

Received: 18 January 2016 / Revised: 29 February 2016 / Accepted: 12 April 2016 / Published online: 25 April 2016

Abstract The ability of magnetically modified activated sludge affected by thermal treatment to remove water-soluble organic dyes was examined. Twelve different dyes were tested. Based on the results of the initial sorption study, four dyes (namely aniline blue, Nile blue, Bismarck brown Y and safranin O) were chosen for further experiments due to their promising binding onto magnetic activated sludge. Significant factors influencing adsorption efficiency such as dependence of contact time, initial pH or temperature were studied in detail. The adsorption process was very fast; more than 88 % of dye content (55 mg/L) was adsorbed within 15 min under experimental conditions used. The equilibrium adsorption data were analyzed by Freundlich, Langmuir and Sips adsorption isotherm models, and the fitting of each isotherm model to experimental data was assessed on the basis of error functions. The maximum adsorption capacities of magnetic activated sludge were 768.2, 246.9, 515.1 and 326.8 mg/g for aniline blue, Bismarck brown Y, Nile blue and safranin O, respectively. The kinetic studies indicated that adsorption of all selected dyes could be well described by the pseudo-second-order kinetic model, and the thermodynamic data suggested the spontaneous and endothermic process.

Keywords Biosorption · Dyes · Magnetic adsorbent · Magnetic modification · Microwave-assisted synthesis

Abbreviations

ARE	The average relative error
AS	Activated sludge
MIOP	Magnetic iron oxides particles
SEE	The standard error of estimate
A_0	The initial absorbance of dye used in the experiment
A_f	The final absorbance of dye used in the experiment
a_L	The Langmuir constant related to the energy of adsorption (L/mg)
C_0	The initial concentration of used dye (mg/L)
C_e	The concentration of free (unbound) dye in the supernatant (mg/L)
C_t	The concentration at time t (mg/L)
$\Delta G°$	The standard free energy change of sorption (kJ/mol)
$\Delta H°$	The standard enthalpy change (kJ/mol)
k_1	The rate constant of pseudo-first-order kinetic model (1/min)
k_2	The rate constant of pseudo-second-order kinetic model (g/mg min)
K_F	The Freundlich isotherm constant related to adsorption capacity [(mg/g) $(L/mg)^{1/n}$]
K_L	The thermodynamic equilibrium constant
n	The Freundlich isotherm constant connected with adsorption intensity
n'	The number of the experimental measurements
p'	The number of parameters

✉ E. Baldikova
baldie@email.cz

[1] Global Change Research Institute, CAS, Na Sadkach 7, 370 05 Ceske Budejovice, Czech Republic

[2] Department of Applied Chemistry, Faculty of Agriculture, University of South Bohemia, Branisovska 1457, 370 05 Ceske Budejovice, Czech Republic

[3] Regional Centre of Advanced Technologies and Materials, Palacky University, Slechtitelu 27, 783 71 Olomouc, Czech Republic

[4] Department of Nanobiotechnology, Biology Centre, ISB, CAS, Na Sadkach 7, 370 05 Ceske Budejovice, Czech Republic

q_e	The amount of dye bound to the unit mass of the adsorbent (mg/g)
q_m	The maximum adsorption capacity (mg/g)
q_t	The amount of dye bound to the unit mass of the adsorbent at time t (mg/g)
R	The universal gas constant (8.314 J/mol K)
$\Delta S°$	The standard entropy chase (J/mol K)
t	Time (min)
T	Temperature (K)
V	Volume of solution (L)
w	Dry mass of magnetic AS (g)
y_i	The experimental value of the dependent variable
$y_{i,theor}$	The estimated value of the dependent variable

Introduction

Organic dyes are important water pollutants; currently, more than 100,000 dyes are available commercially. It is estimated that over 7×10^5 tons of dyestuffs is produced annually (Celekli and Bozkurt 2013; Ramaraju et al. 2014). Two percent of produced dyes are discharged directly in aqueous effluent, and 10–15 % are subsequently lost during the textile coloration process (Liu et al. 2016). These data indicate a scale of threat to water systems. The presence of very small amounts of dyes in water (<1 ppm for some dyes) is highly visible and undesirable (Banat et al. 1996). Many of these dyes are also toxic and even carcinogenic, and this poses a serious hazard to aquatic living organisms (Kyzas et al. 2013). Wide range of dyes which are diversified in their structure and physicochemical properties exists, such as acidic, basic, reactive, disperse, azo, diazo, anthroquinone-based and metal complex dyes (Buthelezi et al. 2012).

Numerous techniques focusing on dye removal have been published (Banat et al. 1996; Salleh et al. 2011; Srinivasan and Viraraghavan 2010). Among them, adsorption provides prime results and can be used to remove different types of dyes. In the specific type of adsorption, named biosorption, dead bacteria (Nacèra and Aicha 2006), yeast (Yu et al. 2013), fungi (Aydogan and Arslan 2015) and microalgae (Hernandez-Zamora et al. 2015) have been employed as biosorbents for the removal of target dyes.

Activated sludge (AS) is formed by particles produced in wastewater treatment process containing many living organisms (such as bacteria, fungi, yeasts, algae and protozoa). The cell walls of the microorganisms contain various functional groups that can interact with different organic and inorganic matter. This material is easily available and has a great potential for applications. Recently, a lot of studies have been reported on the removal of heavy metal ions and organic compounds from water systems by differently treated activated sludge (Chu and Chen 2002; Gobi et al. 2011; Gulnaz et al. 2004; Hammaini et al. 2007; Hyland et al. 2012; Ju et al. 2008).

Magnetic modification of originally diamagnetic materials using various ferro- and ferrimagnetic nano- and microparticles [see an excellent review describing various procedures for their preparation (Laurent et al. 2008)] provides new unique characteristics of such materials. Magnetic modification facilitates the separation process in the presence of external magnetic field. This is widely applied to separations in complex and difficult-to-handle media (blood, waste waters etc.). Very simple and easy to scale-up method for magnetization of cells was developed by our group. Inspired by previous studies of magnetic modification of pure yeast and algae cell cultures (Pospiskova et al. 2013; Prochazkova et al. 2013), we employed this method for activated sludge as an example of mixed cultures. Subsequently, magnetic AS was tested as a low-cost adsorbent for removal of organic compounds, specifically organic dyes. The dyes adsorption on magnetic biomass was quantified by means of three adsorption models, namely Langmuir, Freundlich and Sips ones. The kinetic model and thermodynamic parameters were also determined.

Materials and methods

Materials

The AS samples were taken from the Sewage Treatment Plant, Zliv, Czech Republic, which handles 668 m^3/day of wastewater and uses primary (mechanical) and secondary (biological–denitrification and nitrification) treatments, in May 2015. A fraction of particles obtained by passing through a sieve of mesh size 100 μm was utilized. Twelve water-soluble dyes (see Table 1) were tested during the study. Iron (II) sulfate heptahydrate and HCl were supplied by LachNer (Neratovice, Czech Republic), while NaOH was obtained from Penta (Prague, Czech Republic). All chemicals were of guaranteed reagent (G.R.) grade.

Preparation of magnetic iron oxide particles (MIOP)

As described earlier (Safarik and Safarikova 2014; Zheng et al. 2010), magnetic iron oxides nano- and microparticles were prepared from ferrous sulfate at high pH using microwave irradiation. For small-scale experiments, 1 g $FeSO_4 \cdot 7\ H_2O$ was dissolved in 100 mL of water in an

Table 1 Specification of tested dyes

Dye	Synonym	CI number	Declared purity (%)	Type of dye	Manufacturer/supplier	Sorption [%]
Acridine orange	Basic orange 14	46,005	75	Acridine	Loba Feinchemie, Austria	51.8
Amido black 10B	Acid black 1	20,470	50	Disazo	Merck, Germany	2.0
Aniline blue	Acid blue 22	42,755	55	Triarylmethane	Lachema, Czech Republic	81.8
Azocarmine G	Acid red 101	50,085	60	Quinone-imine	Lachema, Czech Republic	17.7
Bismarck brown Y	Basic brown 1	21,000	56	Disazo	Sigma, USA	81.7
Congo red	Direct red 28	22,120	50	Disazo	Sigma, USA	12.3
Crystal violet	Basic violet 3	42,555	75	Triarylmethane	Lachema, Czech Republic	56.8
Indigo carmine	Acid blue 74	73,015	85	Indigo	Lachema, Czech Republic	8.1
Methylene blue	Basic blue 9	52,015	75	Quinone-imine	Sigma, USA	53.4
Nigrosine, water soluble	Acid black 2	50,420	not declared	Nigrosin	Lachema, Czech Republic	15.0
Nile blue A (sulfate)	Basic blue 12	51,180	75	Oxazin	Chemische Fabrik GmbH, Germany	82.0
Safranin O	Basic red 2	50,240	96	Safranin	Sigma, USA	45.5

The higher the sorption [%], the better the adsorption properties

800 mL beaker and solution of sodium or potassium hydroxide (1 mol/L) was dropped slowly under mixing until the pH reached the value ca 12; during this process, a precipitate of iron hydroxides was formed. Then the suspension was diluted up to 200 mL with water and inserted into a standard kitchen microwave oven (700 W, 2450 MHz). The suspension was treated for 10 min at the maximum power. Then, the beaker was removed from the oven and the formed magnetic iron oxides microparticles were repeatedly washed with water. The synthesized MIOP were suspended in water until further use.

Preparation of magnetic adsorbent

In order to prepare a safe adsorbent based on AS, the sludge was heated in the autoclave for 15 min at 120 °C (75 mL settled volume of activated sludge in 1L Erlenmeyer flask). The magnetization of sterilized AS with microwave-synthesized MIOP was performed by simple mixing of both suspended materials similarly as described previously (Pospiskova et al. 2013) using the ratio 1 mL of settled volume of activated sludge (corresponding to 16.9 mg, dry weight) to 0.1 mL of settled volume of MIOP (corresponding to 7.6 mg, dry weight) in 10 mL of water. The settled volumes of both materials were measured in calibrated containers after 18 h of sedimentation. The mixture of MIOP and AS was mixed by rotator at 25 rpm for 30 min at room temperature. The resultant magnetic activated sludge was washed and suspended in water until further use.

The magnetic untreated (living) activated sludge was prepared by the same method in order to compare the adsorption capacity of heat-treated and untreated magnetic adsorbents.

Batch adsorption experiments

The sorption of dyes onto magnetic AS was studied in batch systems. Twelve different dyes (Table 1) were chosen to test magnetic AS as an adsorbent. In total, 100 μL settled volume of AS (1.69 mg dry weight) was mixed with 9 mL of water and 1 mL of selected dye (1 mg/mL). After 1 h of incubation on orbital rotator (25 rpm) and subsequent magnetic separation by magnetic separator, the samples (supernatants and control dye samples without adsorbent) were analyzed by UV–Vis spectrophotometer. The percentage of sorption was determined by the formula

$$(\%) = 100\frac{A_0 - A_f}{A_0} \quad (1)$$

For isotherms studies, the experiments were carried out using 100 μL settled volume of AS and 10 mL of dye solutions with the initial concentrations of 10–500 mg/L. The tubes were agitated on orbital rotator (25 rpm) under constant temperature (295.15 K) for 90 min. The magnetic AS was separated from the suspension by magnetic separator, and samples were analyzed by UV–Vis spectrophotometer.

The studies of temperature effect on the sorption of dyes onto magnetic heat-treated AS were performed as

isotherms studies at different temperature (282.15, 295.15 and 313.15 K).

The concentration of free dye in the supernatant (C_e) was determined from the calibration curve. The amount of dye bound to the unit mass of the adsorbent at equilibrium (q_e) was calculated using the following formula:

$$q_e = \frac{(C_0 - C_e)V}{w} \quad (2)$$

The amount of dye bound to the unit mass of the adsorbent at time t (q_t) was calculated using the following formula

$$q_t = \frac{(C_0 - C_t)V}{w} \quad (3)$$

All experiments were repeated three times. Average values obtained during the experiments are presented.

Adsorption kinetics

The adsorption kinetics study was determined by evaluation of dye quantity adsorbed onto magnetic AS at different time intervals (0–140 min). The initial concentration of dye solution was 55 mg/L. Amount of adsorbent, volume of dye solution and sample analysis were kept in the same way as isotherm studies.

The data were analyzed using the Lagergren equation, pseudo-first-order model (Chairat et al. 2008) and pseudo-second-order model (Ho 2006).

The linear form of Lagergren pseudo-first-order model is represented by following equation

$$\ln(q_e - q_t) = \ln q_e - k_1 t \quad (4)$$

where k_1 and q_e were calculated from the slope and intercept of the plots of $\ln(q_e - q_t)$ versus t.

The linear form of pseudo-second-order kinetic model is presented by following equation

$$\frac{t}{q_t} = \frac{1}{k_2 q_e^2} + \frac{1}{q_e} t \quad (5)$$

where the values of k_2 and q_e were calculated from the slope and intercept of the plots of t/q_t versus t.

Degree of fit of the model is evaluated on the basis of the correlation coefficient R^2 value.

Adsorption isotherms

The equilibrium data were fitted using two (Freundlich and Langmuir isotherms) and three (Sips isotherm) parameter equations. The adsorption isotherms were processed using nonlinear regression analysis (solver add-in function of the Microsoft Excel). Langmuir isotherm model (Langmuir 1918) assumes monolayer adsorption on the surface of adsorbent and no interaction between adsorbed molecules. The mathematic expression of Langmuir isotherm model is

$$q_e = \frac{q_m a_L C_e}{1 + a_L C_e} \quad (6)$$

Freundlich isotherm model (Freundlich 1906) is used to describe the non-ideal and reversible adsorption. It is applied to the adsorption on heterogeneous surface. The mathematic expression of Freundlich isotherm model is defined as

$$q_e = K_f C_e^{1/n} \quad (7)$$

Sips isotherm model (Sips 1948) is a combination of the Langmuir and Freundlich isotherm models and is expected to describe better adsorption on heterogeneous surfaces. The Sips equation is presented by:

$$q_e = \frac{q_m (a_L C_e)^{1/n}}{1 + (a_L C_e)^{1/n}} \quad (8)$$

The assessment of applicability of isotherm models for experimental data processing is discussed by error functions. In this study, the standard error of estimate and average relative error were used to confirm the best fitting. If data from the model are similar to the experimental data, error is a small number.

The standard error of estimate (SEE) was calculated in each case as follows:

$$\mathrm{SEE} = \sqrt{\frac{\sum_{i=1}^{n'} (y_i - y_{i,\mathrm{theor}})^2}{(n' - p')}} \quad (9)$$

Average relative error (ARE) is expressed by:

$$\mathrm{ARE}\,(\%) = \frac{100}{n'} \sum_{i=1}^{n'} \left| \frac{(y_i - y_{i,\mathrm{theor}})}{y_i} \right| \quad (10)$$

Thermodynamic parameters

The data measured from the study of temperature effect were analyzed, and thermodynamic parameters were calculated by the following equations (Gobi et al. 2011)

$$\Delta G^\circ = -RT \ln K_L \quad (11)$$

$$\Delta G^\circ = \Delta H^\circ - T\Delta S^\circ \quad (12)$$

Equation (13) is obtained by combining Eqs. (11) and (12).

$$\ln K_L = \frac{\Delta S^\circ}{R} - \frac{\Delta H^\circ}{RT} \quad (13)$$

where K_L was computed according to Liu (2009) and ΔH° and ΔS° values were calculated from the slope and intercept of the plot of $\ln K_L$ versus $1/T$ using Eq. (13).

Materials characterization

The morphological study was performed using scanning electron microscopy (SEM) measurements. The samples were analyzed by SEM 120 Hitachi SU6600 (Hitachi, Tokyo, Japan) with accelerating voltage 5 kV, equipped with energy-dispersive spectroscopy (EDS)—Thermo Noran System 7 (Thermo Scientific, Waltham, MA, USA) with Si (Li) detector (accelerating voltage of 15 kV and acquisition time 300 s). X-ray powder diffraction (XRD) pattern of synthesized magnetite was recorded on PANalytical ẊPert PRO (Almelo, the Netherlands) instrument in Bragg–Brentano geometry with Fe-filtered Co$K\alpha$ radiation (40 kV, 30 mA). The acquired pattern was evaluated using the ẊPert HighScore Plus software (PANalytical, Almelo, the Netherlands), PDF-4+ and ICSD databases. Fourier transform infrared (FTIR) absorption spectra were measured using Thermo Scientific Nicolet iS5 FTIR spectrometer (Thermo Nicolet Corp., Madison, WI, USA) with iD Foundation accessory (ZnSe crystal, range 4000–650 cm^{-1}, 32 scans, resolution 4 cm^{-1}). The IR absorption spectra are presented in transmittance after advanced attenuated total reflectance (ATR) and automatic baseline corrections.

Results and discussion

Magnetic modification of activated sludge

The combination of microwave-synthesized magnetic iron oxide nano- and microparticles and AS led to the formation of "smart" magnetically responsive material. One of the great advantages of this material is its easy manipulation using a permanent magnet or commercially available magnetic separator. The magnetic AS prepared as described was completely magnetically separated in a short time (<20 s).

Microwave-assisted synthesis resulted in the formation of iron oxides nanoparticles with diameters ranging between ca 25 and 100 nm (Fig. 1a). During synthesis, the nanoparticles formed micrometer-sized stable aggregates (maximum aggregate size ca 20 μm) (Baldikova et al. 2016). XRD pattern of the synthesized magnetic particles shows features typical of magnetite nano- to microparticles (Fig. 1b); further analysis using Mössbauer spectroscopy confirmed the presence of non-stoichiometric magnetite (Ochmann 2015).

The appropriate ratio between AS and MIOP was selected on the basis of separation velocity of the formed magnetic composite in the external magnetic field (created by the NdFeB magnet, diameter 20 mm, height 10 mm, remanence 1 T) in preliminary experiments (data not shown). Magnetic modification led to the interaction of iron oxide nanoparticle aggregates with the microorganisms and released material present in activated sludge; flocs with diameters between tens and several hundred micrometers were formed (Fig. 1c). SEM has confirmed efficient interaction of microbial cells and magnetic nanoparticles; surface of microbial cells is covered by the magnetic nanoparticles (Fig. 1d). Energy-dispersive X-ray spectroscopy verified the presence of iron in the magnetically responsive activated sludge (Fig. 2a).

The formation of magnetic adsorbent by direct mixing of MIOP and AS is an extremely rapid, inexpensive and simple method, which can be easily scaled up. On the contrary, Hu and Hu (2014) used dried sewage sludge for magnetic modification by coprecipitation method; however, this method is time and energy consuming. Lakshmanan and Rajarao (2014) described the application of magnetic nanoparticles as suitable flocculants for reduction in sludge water content and enhancement of sludge settling in the presence of external magnetic field, thereby reducing the sludge handling time and simplifying future processing.

Activated sludge contains, in addition to microbial cells, also extracellular polymeric substances (EPSs), which are microorganism-produced macromolecules, mainly consisting of polysaccharides, proteins and nucleic acids (Zhang et al. 2006); they represent a large pool of functional groups, which are involved in adsorption of various dyes and other compounds of interest.

FTIR spectral analysis (Fig. 2b) shows typical peaks indicating the presence of important groups. Peaks between 3100 and 2900 cm^{-1} (main at 3077 and 2924) represent the asymmetric and symmetric stretchings of $–CH_2$ from proteins, polysaccharides and lipids. Peaks with their maxima at 1622 and 1547 cm^{-1} are typical of primary and secondary amino group in proteins (peptide bond). The peaks at 1114 and 1033 cm^{-1} are characteristic of all sugar derivatives (O–C–O stretching vibrations in polysaccharide groups) (Andreassen 2008).

The bacteria present in the activated sludge have isoelectric points between pH 2 and 4, and thus, their surface will be negatively charged at higher pH (Sanin 2002). Some pretreatment processes can modify the adsorption capacity of the microbial biomass, such as autoclaving as high-temperature treatment causes cell rupture with a consecutive increase in surface area (Solis et al. 2012).

Screening of dyes

The adsorption properties of magnetically modified heat-treated AS were studied using water-soluble organic dyes (Table 1). The dyes used for preliminary adsorption experiments were selected to cover wide range of dye types. Dyes were dissolved in distilled water without

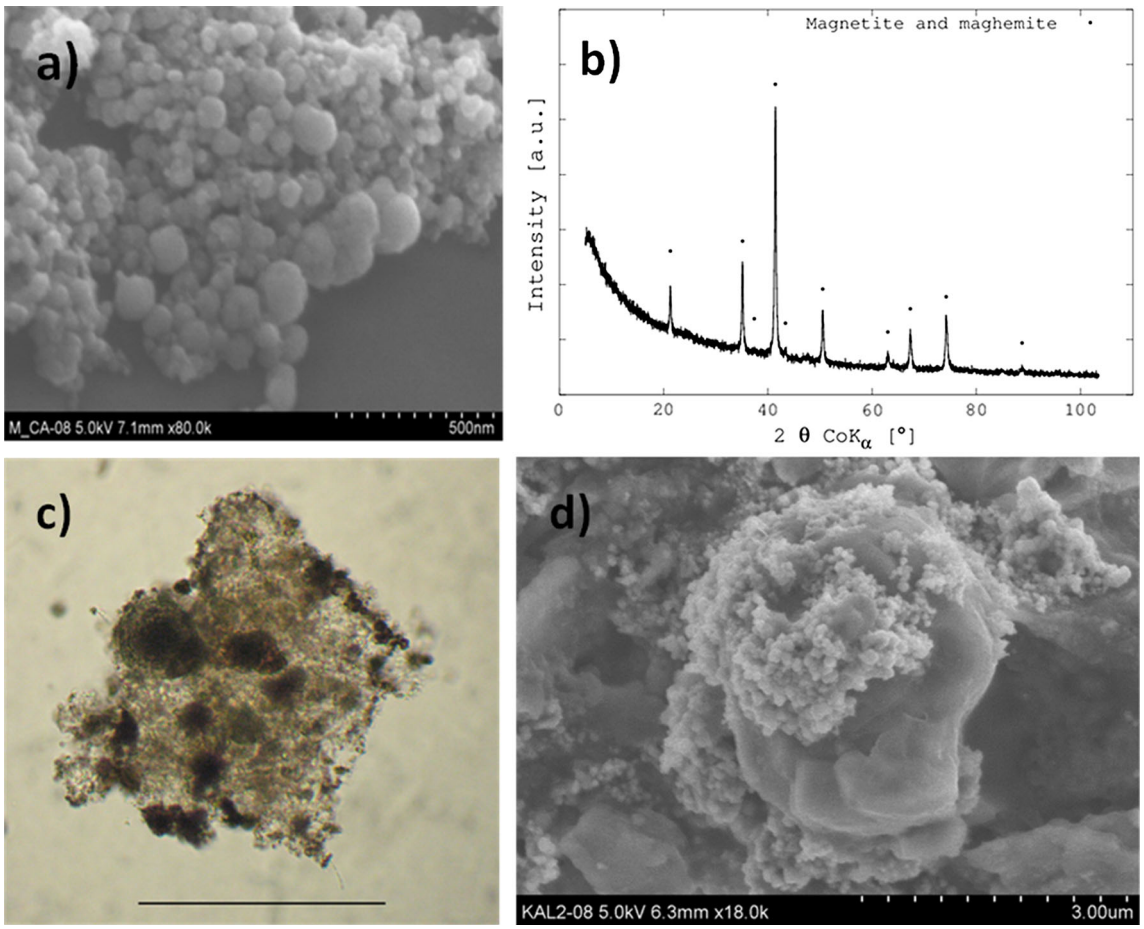

Fig. 1 **a** SEM of magnetic nanoparticles prepared by microwave-assisted synthesis (80,000× magnification). Reproduced, with permission, from (Baldikova et al. 2016); **b** XRD pattern of magnetic nano- and microparticles prepared by microwave-assisted synthesis (*black dots* mark the position of magnetite and maghemite diffractions); **c** optical microscopy of the typical magnetic activated sludge floc (the *bar* corresponds to 100 μm); **d** SEM of magnetically modified activated sludge (18,000× magnification)

buffering the solution. Several dyes exhibiting high biosorption, belonging to the different dye classes, namely aniline blue, Nile blue, Bismarck brown Y and safranin O (see Fig. 3a) were selected for detailed adsorption study. The dyes exhibiting good adsorption properties can be in most cases characterized as basic dyes, which suggest strong involvement of ion exchange interactions between dyes and cell surfaces.

Effect of pH

The effect of pH on adsorption of tested dyes onto magnetic heat-treated activated sludge was investigated. As can be seen from Fig. 3b, each dye exhibits different behavior at various pH. The adsorption efficiency of safranin O remained nearly constant up to pH 7, but at pH 8 there is a significant decrease. The lowest percentage removal of Nile blue was found at pH 3, and at higher pH values, the adsorption efficiencies significantly increased and kept almost the same values up to pH 8. The behavior of Bismarck brown Y seemed to be very similar to Nile blue; nevertheless, at pH higher than 6, there is apparent a slight fall. Aniline blue exhibited definitely another behavior; the most suitable pH values took place at pH 4 and 5, while at pH 3 and at pH values higher than 5 the adsorption efficiencies decreased substantially.

Adsorption kinetics

The contact time is one of the important factors to achieve equilibrium required for description of the adsorption process. The adsorption equilibrium studies for removal of selected dyes (aniline blue, Bismarck brown Y, safranin O, Nile blue, 55 mg/L) on magnetic AS and kinetic studies were performed in batch system at room temperature (295.15 K) under mixing. The effect of contact time on the adsorption of tested dyes is shown in Fig. 3c; it is evident that the dyes adsorption was a fast process, and 93 % of the

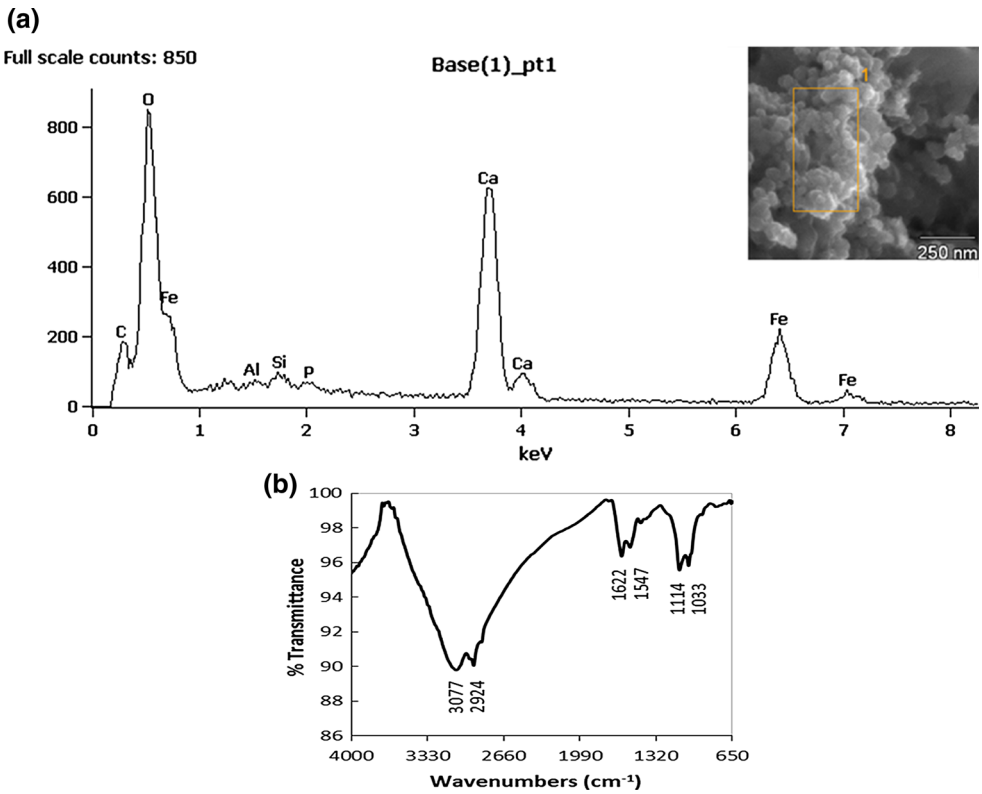

Fig. 2 **a** EDS of magnetically modified activated sludge; **b** FTIR spectrum of magnetically modified activated sludge

sorption took place in the first 15 min except Bismarck brown Y sorption where only 88 % of dye was adsorbed in the first 15 min. Nevertheless, the process needs approximately 60 min to reach the equilibrium.

The results obtained during examination of contact time dependence were subsequently analyzed to investigate kinetics of adsorption process. Pseudo-first- and pseudo-second-order kinetic equations were used. The pseudo-first-order kinetic model is the earliest known one describing the adsorption rate based on the adsorption capacity (Ho 2006). It is apparent from the predicted values of q_e and correlation coefficient R^2 shown in Table 2 that the kinetic data of the dyes sorption on magnetic heat-treated AS were not well fitted to the pseudo-first-order model. On the other side, the values of correlation coefficient R^2 for pseudo-second-order model (see Table 2) were close to 1.0 for all cases and the theoretical values of q_e calculated from this model approached the experimental data. This indicates that the sorption mechanism of selected dyes on magnetically modified heat-treated AS follows the pseudo-second-order model.

Adsorption isotherms study

The adsorption isotherm is a significant parameter to understand the behavior of the adsorption process. In this study, the distribution of dyes between liquid phase and solid phase (magnetic AS) was described using two and three parameters isotherm models, namely Langmuir, Freundlich and Sips ones. The first two models are widely used for investigating the adsorption of dyes on various materials. Figure 4 demonstrates the plots of the experimental data and predicted isotherm models for sorption of selected dyes onto magnetic heat-treated activated sludge. Determined isotherm parameters computed for all examined dyes are listed in Table 3. The average relative error (ARE) and standard error of estimate (SEE) based on the actual deviation between the experimental points and predicted values are also shown.

Langmuir isotherm model is the two parameters model. This empirical model assumed monolayer adsorption, and all sites possess equal affinity for the sorbate (Vijayaraghavan et al. 2006). High value of a_L indicates high affinity. In the case of aniline blue (Table 3), SEE and ARE for Langmuir isotherm model exhibited lower values than for Freundlich and Sips isotherm models. Consequently, Langmuir isotherm model was considered to be a better fit compared to the other two.

Freundlich isotherm model (two parameters model) assumes that the surface of adsorbent is heterogeneous, and surface sites have a spectrum of different binding energies. The constant K_F relates to the effectiveness of magnetic AS to adsorb dyes. Higher values of K_F indicate larger capacities of adsorption. The constant n is a function of the strength of

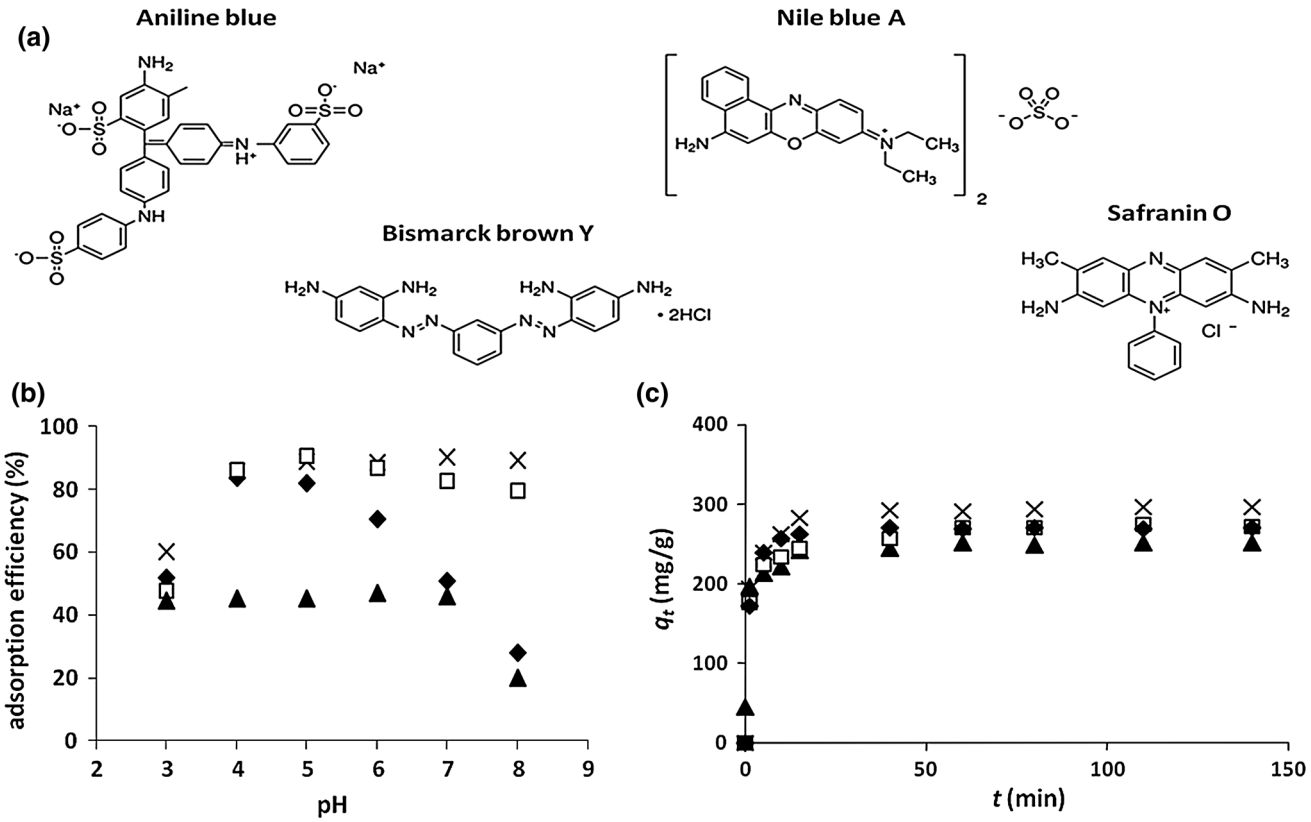

Fig. 3 **a** Chemical structures of dyes used for the experiments; **b** the effect of pH on dye adsorption on heat-treated magnetic AS (agitation time 90 min, 10 mL of 100 mg/L dye solution, 1.69 mg of magnetic AS, 295.15 K); **c** time dependence of dye adsorption on heat-treated magnetic AS at 295.15 K. [aniline blue (*filled diamond*), Bismarck brown Y (*open square*), safranin O (*filled triangle*) and Nile blue (*cross mark*)]

Table 2 Values of rate constants, capacities and regression coefficients from pseudo-first- and pseudo-second-order kinetic models

Dye	q_e (mg/g)	Pseudo-first-order model			Pseudo-second-order model		
		q_e (mg/g)	k_1 (1/min)	R^2	q_e (mg/g)	k_2 (g/mg min)	R^2
Aniline blue	274	24.3	0.0200	0.6293	270	0.0069	1.0000
Bismarck brown Y	275	54.0	0.0332	0.7920	278	0.0025	0.9998
Safranin O	254	29.6	0.0236	0.7683	256	0.0004	0.9999
Nile blue	299	45.5	0.0286	0.8689	303	0.0030	0.9999

adsorbent and indicates the favorability of adsorption. It is generally stated that the values n in the range of 2–10 represent good, 1–2 moderately difficult and <1 poor adsorption characteristics (Hadi et al. 2010). Error values (Table 3) and Fig. 4 representing adsorption fitting curves for dyes onto magnetic AS suggest that the Freundlich isotherm is more accurate to describe the Nile blue—magnetic AS interaction in comparison with other three dyes.

Sips isotherm model (three parameters model) combines the features of Freundlich and Langmuir models. As shown (Table 3), the Sips isotherm generated a satisfactory fit to the experimental data as indicated by the error functions. However, the Langmuir isotherm showed a better fit to the adsorption data for aniline blue and the Freundlich isotherm in the sorption of Nile blue. Nevertheless, for aniline blue Sips model closely approached the Langmuir model with their exponents (α_L) being close to unity.

Table 4 represents some other adsorbents, and their adsorption capacity employed for adsorption of selected dyes from water; it can be observed that heat-treated magnetically responsive AS is an efficient adsorbent for dyes removal.

The effect of activated sludge heat treatment on dyes adsorption

The three isotherm models (Langmuir, Freundlich and Sips) were applied to describe the adsorption process of aniline blue on living and heat-treated magnetic AS.

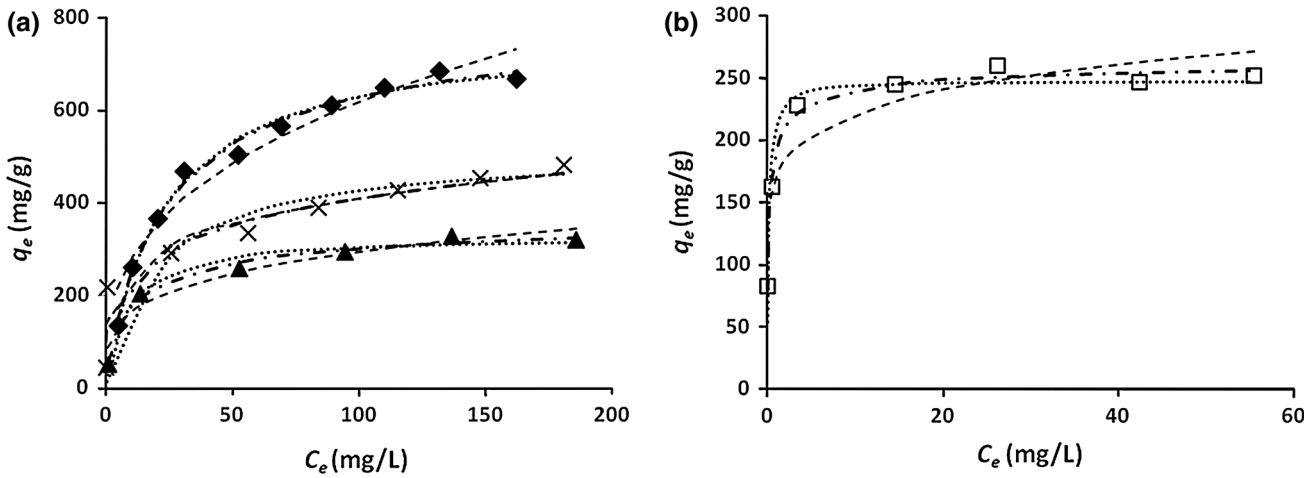

Fig. 4 Comparison of isotherms models of aniline blue (*filled diamond*), Nile blue (*cross mark*), safranin O (*filled triangle*) (**a**) and Bismarck brown Y (*open square*) (**b**) onto heat-treated magnetic AS; *dotted line* Langmuir model; *straight line* Freundlich model; *dashed line* Sips model

Table 3 Parameters of Langmuir, Freundlich and Sips adsorption isotherm models

Type of adsorbent	Dye	Langmuir		Sips		Freundlich	
Heat-treated magnetic AS	Safranin O	q_m (mg/g)	326.8	q_m (mg/g)	385.9	K_F [(mg/g)(L/mg)$^{1/n}$]	92.2
		a_L (L/mg)	0.12	a_L (L/mg)	0.08	n	3.97
		SEE	20.23	n	1.60	SEE	25.39
		ARE (%)	11.00	SEE	13.20	ARE (%)	15.64
				ARE (%)	4.15		
Heat-treated magnetic AS	Nile blue	q_m (mg/g)	515.1	q_m (mg/g)	492.2	K_F [(mg/g)(L/mg)$^{1/n}$]	155.8
		a_L (L/mg)	0.05	a_L (L/mg)	0.004	n	4.77
		SEE	75.35	n	9.55	SEE	36.22
		ARE (%)	21.86	SEE	38.72	ARE (%)	19.03
				ARE (%)	19.03		
Heat-treated magnetic AS	Bismarck brown Y	q_m (mg/g)	246.9	q_m (mg/g)	265.9	K_F [(mg/g)(L/mg)$^{1/n}$]	167.3
		a_L (L/mg)	5.72	a_L (L/mg)	4.69	n	8.31
		SEE	19.03	n	1.74	SEE	25.45
		ARE (%)	7.83	SEE	7.87	ARE (%)	11.93
				ARE (%)	2.69		
Heat-treated magnetic AS	Aniline blue	q_m (mg/g)	768.2	q_m (mg/g)	806.9	K_F [(mg/g)(L/mg)$^{1/n}$]	123.9
		a_L(L/mg)	0.05	a_L (L/mg)	0.04	n	2.87
		SEE	20.11	n	1.10	SEE	43.92
		ARE (%)	2.87	SEE	20.59	ARE (%)	10.36
				ARE (%)	3.33		
Live magnetic AS	Aniline blue	q_m (mg/g)	493.0	q_m (mg/g)	570.4	K_F [(mg/g)(L/mg)$^{1/n}$]	65.6
		a_L (L/mg)	0.03	a_L (L/mg)	0.02	n	2.76
		SEE	14.37	n	1.26	SEE	19.307
		ARE (%)	3.30	SEE	12.93	ARE (%)	5.90
				ARE (%)	3.09		

Computed isotherm parameters and errors (ARE and SEE) are shown in Table 3. In both cases, the Sips model closely approached the Langmuir model. Sips isotherm fitted better the experimental data for the living magnetic AS and Langmuir isotherm for heat-treated magnetic AS as indicated by the error functions. The maximum amount of pure dye adsorbed at equilibrium by heat-treated magnetic AS was 806.9 mg/g adsorbent, while it was only 570.4 mg/

Table 4 Comparison of maximum adsorption capacities (q_m) of different adsorbents for selected dyes according to Langmuir isotherm model

Dye	Adsorbent	q_m (mg/g)	References
Safranin O	Biopolymer poly(γ-glutamic acid)	502.8	(Inbaraj et al. 2006)
	Heat-treated magnetic activated sludge	326.8	This study
	Magnetically modified yeast cells	138.2	(Safarik et al. 2007)
	Sugarcane bagasse	58.8	(Farahani et al. 2015)
Nile blue	Heat-treated magnetic activated sludge	515.1	This study
	Magnetic spent tea leaves	87.1	(Safarik et al. 2012)
	Magnetically modified spent grain	64.1	(Safarik et al. 2011)
	Cocoa shell activated carbon	55.8	(Mylsamy 2013)
Bismarck brown Y	Biopolymer poly(γ-glutamic acid)	667.1	(Inbaraj et al. 2008)
	Heat-treated magnetic activated sludge	246.9	This study
	Magnetically modified spent grain	72.4	(Safarik et al. 2011)
	Flower like iron oxide nanostructure	64.1	(Khosravi and Azizian 2014)
Aniline blue	Heat-treated magnetic activated sludge	768.2	This study
	Magnetic *Saccharomyces cerevisiae*	228.0	(Safarikova et al. 2005)
	Iodo polyurethane foam	188.9	(Moawed et al. 2015)
	Magnetically modified spent grain	44.7	(Safarik et al. 2011)

g adsorbent by live magnetic AS according to Sips isotherm model. The higher sorption ability of dead microorganisms in comparison with live microorganisms was observed in the literature (Du et al. 2012; Srinivasan and Viraraghavan 2010); it was proposed that the increased biosorption of dyes by the heat-treated biomass could be caused by increased permeability of the cell walls after heating, such that the dye could enter into the cells and be adsorbed to the intracellular adsorption sites.

Thermodynamic parameters

Thermodynamic parameters (associated with the dye adsorption process) were determined from adsorption data at different temperatures (282.15; 295.15 and 313.15 K, respectively). The sorption increased with increasing temperature indicating that sorption process was endothermic in nature. Similar observations were reported, suggesting that this situation may be caused by increasing the mobility of the dye molecules and an increase in the porosity and in the total pore volume of the adsorbent with the increase in temperature (Salleh et al. 2011; Senthilkumaar et al. 2006).

The thermodynamic data are summarized in Table 5. The plot ln K_L versus 1/T straight lines ($R^2 > 0.98$) for all the four systems and R^2 values indicate that the values of enthalpy and entropy calculated for adsorbent are convenient. The negative values of Gibbs free energy change indicated the spontaneous reactions. The endothermic nature of selected dyes sorption on magnetic heat-treated AS was confirmed by the positive values of $\Delta H°$. The positive values of $\Delta S°$ suggested an increase in randomness at the solid/liquid interface.

Potential fate of the used adsorbent

One of the important characteristics of a biosorbent is its processing after finishing the sorption process. Biosorbents can be regenerated by selected organic solvents (e.g., methanol, ethanol), surfactants (e.g., Tween), as well as acidic and alkaline solutions; alternatively they are disposed in an environmentally acceptable manner. Thorough economical calculation is necessary to suggest the potential optimal setup of the pollutant adsorption process using low-cost biosorbents formed from biological waste materials.

Conclusions

The activated sludge was easily modified by microwave-synthesized magnetic iron oxides nano- and microparticles and used as an adsorbent for removal of dyes from aqueous solution. The prepared adsorbent can be selectively removed from many difficult-to-handle samples using an appropriate magnetic separator. It was demonstrated that magnetic activated sludge (especially heat treated) could be effective sorbent for dyes removal. This material contains a large number of functional groups, which are involved in efficient adsorption of various dyes. It was observed that Sips isotherm model described well the adsorption of safranin O and Bismarck brown Y, while Langmuir isotherm model was better for aniline blue adsorption and Freundlich isotherm model for Nile blue adsorption on magnetic heat-treated activated sludge, respectively.

Table 5 Thermodynamic parameters of the adsorption of selected dyes on magnetic heat-treated AS

Dye	R^2	ΔH° (kJ/mol)	ΔS° (J/mol/K)	ΔG° (kJ/mol)		
				282.15 K	295.15 K	313.15 K
Aniline blue	0.985	25.219	192.63	−29.030	−31.822	−35.013
Bismarck brown Y	0.996	42.773	263.29	−31.429	−35.097	−39.601
Safranin O	0.987	12.871	127.89	−23.260	−24.788	−27.220
Nile blue	0.989	28.441	197.44	−27.169	−30.016	−33.300

The kinetic study revealed that the process followed pseudo-second-order kinetics. The thermodynamic parameters obtained in all cases confirmed spontaneous and endothermic process.

Acknowledgments This research was supported by the Grant Agency of the Czech Republic (Project No. 13-13709S) and by the Ministry of Education, Youth and Sports of the Czech Republic (Project LO1305). Authors also thank to Ing. Petra Bazgerova for technical assistance.

References

Andreassen HM (2008) New topics in water resources research and management. Nova Publishers, New York

Aydogan MN, Arslan NP (2015) Removal of textile dye reactive black 5 by the cold-adapted, alkali- and halotolerant fungus *Aspergillus flavipes* MA-25 under non-sterile conditions. Desalin Water Treat 56:2258–2266. doi:10.1080/19443994.2014.960463

Baldikova E, Politi D, Maderova Z, Pospiskova K, Sidiras D, Safarikova M, Safarik I (2016) Utilization of magnetically responsive cereal by-product for organic dye removal. J Sci Food Agric 96:2204–2214. doi:10.1002/jsfa.7337

Banat IM, Nigam P, Singh D, Marchant R (1996) Microbial decolorization of textile-dyecontaining effluents: a review. Bioresour Technol 58:217–227. doi:10.1016/S0960-8524(96)00113-7

Buthelezi SP, Olaniran AO, Pillay B (2012) Textile dye removal from wastewater effluents using bioflocculants produced by indigenous bacterial isolates. Molecules 17:14260–14274. doi:10.3390/molecules171214260

Celekli A, Bozkurt H (2013) Predictive modeling of an azo metal complex dye sorption by pumpkin husk. Environ Sci Pollut Res 20:7355–7366. doi:10.1007/s11356-013-1751-5

Chairat M, Rattanaphani S, Bremner JB, Rattanaphani V (2008) Adsorption kinetic study of lac dyeing on cotton. Dyes Pigm 76:435–439. doi:10.1016/j.dyepig.2006.09.008

Chu HC, Chen KM (2002) Reuse of activated sludge biomass: I. Removal of basic dyes from wastewater by biomass. Process Biochem 37:595–600. doi:10.1016/s0032-9592(01)00234-5

Du LN, Wang B, Li G, Wang S, Crowley DE, Zhao YH (2012) Biosorption of the metal-complex dye Acid Black 172 by live and heat-treated biomass of *Pseudomonas* sp. strain DY1: kinetics and sorption mechanisms. J Hazard Mater 205–206:47–54. doi:10.1016/j.jhazmat.2011.12.001

Farahani M, Kashisaz M, Abdullah SRS (2015) Adsorption of safranin O from aqueous phase using sugarcane bagasse. Int J Ecol Sci Environ Eng 2:17–29

Freundlich HMF (1906) Over the adsorption in solution. J Phys Chem 57:385–470

Gobi K, Mashitah MD, Vadivelu VM (2011) Adsorptive removal of methylene blue using novel adsorbent from palm oil mill effluent waste activated sludge: equilibrium, thermodynamics and kinetic studies. Chem Eng J 171:1246–1252. doi:10.1016/j.cej.2011.05.036

Gulnaz O, Kaya A, Matyar F, Arikan B (2004) Sorption of basic dyes from aqueous solution by activated sludge. J Hazard Mater 108:183–188. doi:10.1016/j.jhazmat.2004.02.012

Hadi M, Samarghandi MR, McKay G (2010) Equilibrium two-parameter isotherms of acid dyes sorption by activated carbons: study of residual errors. Chem Eng J 160:408–416. doi:10.1016/j.cej.2010.03.016

Hammaini A, González F, Ballester A, Blázquez ML, Muñoz JA (2007) Biosorption of heavy metals by activated sludge and their desorption characteristics. J Environ Manage 84:419–426. doi:10.1016/j.jenvman.2006.06.015

Hernandez-Zamora M, Cristiani-Urbina E, Martinez-Jeronimo F, Perales-Vela H, Ponce-Noyola T, Montes-Horcasitas MD, Canizares-Villanueva RO (2015) Bioremoval of the azo dye Congo red by the microalga *Chlorella vulgaris*. Environ Sci Pollut Res 22:10811–10823. doi:10.1007/s11356-015-4277-1

Ho YS (2006) Review of second-order models for adsorption systems. J Hazard Mater 136:681–689. doi:10.1016/j.jhazmat.2005.12.043

Hu SH, Hu SC (2014) Kinetics of ionic dyes adsorption with magnetic-modified sewage sludge. Environ Prog Sustain Energy 33:905–912. doi:10.1002/ep.11872

Hyland KC, Dickenson ERV, Drewes JE, Higgins CP (2012) Sorption of ionized and neutral emerging trace organic compounds onto activated sludge from different wastewater treatment configurations. Water Res 46:1958–1968. doi:10.1016/j.watres.2012.01.012

Inbaraj BS, Chien JT, Ho GH, Yang J, Chen BH (2006) Equilibrium and kinetic studies on sorption of basic dyes by a natural biopolymer poly(γ-glutamic acid). Biochem Eng J 31:204–215. doi:10.1016/j.bej.2006.08.001

Inbaraj BS, Chiu CP, Ho GH, Yang J, Chen BH (2008) Effects of temperature and pH on adsorption of basic brown 1 by the bacterial biopolymer poly(γ-glutamic acid). Bioresour Technol 99:1026–1035. doi:10.1016/j.biortech.2007.03.008

Ju DJ, Byun IG, Park JJ, Lee CH, Ahn GH, Park TJ (2008) Biosorption of a reactive dye (Rhodamine-B) from an aqueous solution using dried biomass of activated sludge. Bioresour Technol 99:7971–7975. doi:10.1016/j.biortech.2008.03.061

Khosravi M, Azizian S (2014) Synthesis of different nanostructured flower-like iron oxides and study of their performance as adsorbent. Adv Powder Technol 25:1578–1584. doi:10.1016/j.apt.2014.05.010

Kyzas GZ, Fu J, Matis KA (2013) The change from past to future for adsorbent materials in treatment of dyeing wastewaters. Materials 6:5131–5158. doi:10.3390/ma6115131

Lakshmanan R, Rajarao GK (2014) Effective water content reduction in sewage wastewater sludge using magnetic nanoparticles. Bioresour Technol 153:333–339. doi:10.1016/j.biortech.2013.12.003

Langmuir I (1918) The adsorption of gases on plane surfaces of glass, mica and platinum. J Am Chem Soc 40:1361–1403

Laurent S, Forge D, Port M, Roch A, Robic C, Vander Elst L, Muller RN (2008) Magnetic iron oxide nanoparticles: synthesis, stabilization, vectorization, physicochemical characterizations, and biological applications. Chem Rev 108:2064–2110. doi:10.1021/cr068445e

Liu Y (2009) Is the free energy change of adsorption correctly calculated? J Chem Eng Data 54:1981–1985. doi:10.1021/je800661q

Liu XX, Gong WP, Luo J, Zou CT, Yang Y, Yang SJ (2016) Selective adsorption of cationic dyes from aqueous solution by polyoxometalate-based metal-organic framework composite. Appl Surf Sci 362:517–524. doi:10.1016/j.apsusc.2015.11.151

Moawed EA, Abulkibash AB, El-Shahat MF (2015) Synthesis and characterization of iodo polyurethane foam and its application in removing of aniline blue and crystal violet from laundry wastewater. J Taibah Univ Sci 9:80–88. doi:10.1016/j.jtusci.2014.07.003

Mylsamy S (2013) Adsorption of basic blue 12 from cocoa (*Theobroma Cacao*) shell activated carbon—equilibrium isotherm analyses. Int J Sci Res 2:70–72. doi:10.15373/22778179

Nacèra Y, Aicha B (2006) Equilibrium and kinetic modelling of methylene blue biosorption by pretreated dead *streptomyces rimosus*: effect of temperature. Chem Eng J 119:121–125. doi:10.1016/j.cej.2006.01.018

Ochmann M (2015) Microwave synthesis of magnetic iron oxides nanoparticles. Dissertation, Palacky University

Pospiskova K, Prochazkova G, Safarik I (2013) One-step magnetic modification of yeast cells by microwave-synthesized iron oxide microparticles. Lett Appl Microbiol 56:456–461. doi:10.1111/lam.12069

Prochazkova G, Safarik I, Branyik T (2013) Harvesting microalgae with microwave synthesized magnetic microparticles. Bioresour Technol 130:472–477. doi:10.1016/j.biortech.2012.12.060

Ramaraju B, Reddy PMK, Subrahmanyam C (2014) Low cost adsorbents from agricultural waste for removal of dyes. Environ Prog Sustain Energy 33:38–46. doi:10.1002/ep.11742

Safarik I, Safarikova M (2014) One-step magnetic modification of non-magnetic solid materials. Int J Mat Res 105:104–107. doi:10.3139/146.111009

Safarik I, Rego LFT, Borovska M, Mosiniewicz-Szablewska E, Weyda F, Safarikova M (2007) New magnetically responsive yeast-based biosorbent for the efficient removal of water-soluble dyes. Enzyme Microb Technol 40:1551–1556. doi:10.1016/j.enzmictec.2006.10.034

Safarik I, Horska K, Safarikova M (2011) Magnetically modified spent grain for dye removal. J Cereal Sci 53:78–80. doi:10.1016/j.jcs.2010.09.010

Safarik I, Horska K, Pospiskova K, Safarikova M (2012) One-step preparation of magnetically responsive materials from non-magnetic powders. Powder Technol 229:285–289. doi:10.1016/j.powtec.2012.06.006

Safarikova M, Ptackova L, Kibrikova I, Safarik I (2005) Biosorption of water-soluble dyes on magnetically modified *Saccharomyces cerevisiae* subsp. *uvarum* cells. Chemosphere 59:831–835. doi:10.1016/j.chemosphere.2004.10.062

Salleh MAM, Mahmoud DK, Karim WAWA, Idris A (2011) Cationic and anionic dye adsorption by agricultural solid wastes: a comprehensive review. Desalination 280:1–13. doi:10.1016/j.desal.2011.07.019

Sanin DF (2002) Effect of solution physical chemistry on the rheological properties of activated sludge. Water SA 28:207–211

Senthilkumaar S, Kalaamani P, Subburaam CV (2006) Liquid phase adsorption of crystal violet onto activated carbons derived from male flowers of coconut tree. J Hazard Mater 136:800–808. doi:10.1016/j.jhazmat.2006.01.045

Sips R (1948) Structure of a catalyst surface. J Chem Phys 16:490–495

Solis M, Solis A, Perez HI, Manjarrez PN, Flores M (2012) Microbial decolouration of azo dyes: a review. Process Biochem 47:1723–1748. doi:10.1016/j.procbio.2012.08.014

Srinivasan A, Viraraghavan T (2010) Decolorization of dye wastewaters by biosorbents: a review. J Environ Manage 91:1915–1929. doi:10.116/j.jenvman.2010.05.003

Vijayaraghavan K, Padmesh TVN, Palanivelu K, Velan M (2006) Biosorption of nickel(II) ions onto *Sargassum wightii*: application of two-parameter and three-parameter isotherm models. J Hazard Mater 133:304–308. doi:10.1016/j.jhazmat.2005.10.016

Yu JX, Wang LY, Chi RA, Zhang YF, Xu ZG, Guo J (2013) A simple method to prepare magnetic modified beer yeast and its application for cationic dye adsorption. Environ Sci Pollut Res 20:543–551. doi:10.1007/s11356-012-0903-3

Zhang D, Wang J, Pan X (2006) Cadmium sorption by EPSs produced by anaerobic sludge under sulfate-reducing conditions. J Hazard Mater 138:589–593. doi:10.1016/j.jhazmat.2006.05.092

Zheng B, Zhang M, Xiao D, Jin Y, Choi MF (2010) Fast microwave synthesis of Fe_3O_4 and Fe_3O_4/Ag magnetic nanoparticles using Fe^{2+} as precursor. Inorg Mater 46:1106–1111. doi:10.1134/S0020168510100146

5.2.8 Biouhel

Biouhel připravený ze směsi dřev pomalou pyrolýzou byl magneticky modifikován pomocí MS magnetitu v klasickém poměru.

Charakterizace materiálu zahrnovala studium morfologie materiálu pomocí skenovací a transmisní elektronové mikroskopie a studium magnetických vlastností, které bylo provedeno pomocí XRD a supravodivého kvantového interferenčního zařízení (SQUID). Také byla určena velikost specifického povrchu a porozita.

Magnetický biouhel byl testován pro sorpci pěti organických barviv. Zjišťována byla závislost na čase a teplotě. Rovnovážná adsorpční data byla vyhodnocena Langmuirovým modelem. Maximální adsorpční kapacita byla (až na akridinovou oranž) vyšší než 81 mg/g a roste se zvyšující se teplotou, což značí endotermní proces. Vhodným kinetickým modelem je na základě získaných koeficientů spolehlivosti kinetický model pseudo-druhého řádu.

Příloha 14:

Magnetically modified biochar for organic xenobiotics removal

Safarik I, Maderova Z, Pospikova K, Schmidt HP, Baldikova E, Filip J, Krizek M, Malina O, Safarikova M

Water Sci. Technol. 74, **2016**, 1706-1715

Magnetically modified biochar for organic xenobiotics removal

Ivo Šafařík, Zdenka Maděrová, Kristýna Pospíšková, Hans-Peter Schmidt, Eva Baldíková, Jan Filip, Michal Křížek, Ondřej Malina and Mirka Šafaříková

ABSTRACT

Large amounts of biochar are produced worldwide for potential agricultural applications. However, this material can also be used as an efficient biosorbent for xenobiotics removal. In this work, biochar was magnetically modified using microwave-synthesized magnetic iron oxide particles. This new type of a magnetically responsive biocomposite material can be easily separated by means of strong permanent magnets. Magnetic biochar has been used as an inexpensive magnetic adsorbent for the removal of water-soluble dyes. Five dyes (malachite green, methyl green, Bismarck brown Y, acridine orange and Nile blue A) were used to study the adsorption process. The dyes adsorption could be usually described with the Langmuir isotherm. The maximum adsorption capacities reached the value 137 mg of dye per g of dried magnetically modified biochar for Bismarck brown Y. The adsorption processes followed the pseudo-second-order kinetic model and the thermodynamic studies indicated spontaneous and endothermic adsorption. Extremely simple magnetic modification of biochar resulted in the formation of a new, promising adsorbent suggested for selected xenobiotics removal.

Key words | adsorption, biochar, magnetic iron oxide particles, magnetic modification, organic dyes

Ivo Šafařík (corresponding author)
Mirka Šafaříková
Department of Nanobiotechnology,
Biology Centre, ISB, ASCR,
Na Sádkách 7, České Budějovice 370 05,
Czech Republic
E-mail: *ivosaf@yahoo.com*

Ivo Šafařík
Kristýna Pospíšková
Jan Filip
Michal Křížek
Ondřej Malina
Regional Centre of Advanced Technologies and Materials,
Palacký University,
Šlechtitelů 27, Olomouc 783 71,
Czech Republic

Ivo Šafařík
Zdenka Maděrová
Eva Baldíková
Mirka Šafaříková
Global Change Research Institute, ASCR,
Na Sádkách 7, České Budějovice 370 05,
Czech Republic

Hans-Peter Schmidt
Ithaka Institute for Carbon Strategies,
Ancienne Eglise 9, Arbaz CH-1974,
Switzerland

ABBREVIATIONS

ADP	advanced data processing
b	constant related to the affinity of the binding sites (L/mg)
B_{C+}	positive coercivity
B_{C-}	negative coercivity
BET(3)	Brunauer Emmet Teller (model)
BJH	Barrett Joyner Halenda (model)
C_0	total (initial) concentration of dye used in the experiment (μg/mL)
C_{eq}	equilibrium liquid-phase concentration of the unadsorbed (free) dye in the supernatant (μg/mL; mg/L)
C_t	concentration of dye in solution (mg/L) in time t (min)
DFT	density functional theory
EDS	energy dispersive X-ray spectrometry
FC	field-cooled magnetization curve
ΔG^o	Gibbs free energy change (J/mol)
ΔH^o	standard enthalpy change (J/mol)
HK	Horvath and Kawazoe (model)
k_1	the first-order rate constant (1/min)
k_2	the second-order rate constant (g/mg min)
K_d	thermodynamic equilibrium constant
M_{max+} (5 T)	maximum magnetization at 5 T
M_{max-} (– 5 T)	maximum magnetization at –5 T
M_{R+}	positive remanent magnetization
M_{R-}	negative remanent magnetization
MD	molecular dynamics

doi: 10.2166/wst.2016.335

PSD	power spectral density calculations
q_{eq}	equilibrium solid-phase concentration of the adsorbed dye per unit mass or sedimented volume of magnetically modified biomass = eq. adsorption capacity (mg/g or mg/mL)
Q_{max}	maximum amount of the dye per unit mass of adsorbent to form a complete monolayer on the surface bound at high dye concentration = maximum adsorption capacity (mg/g)
q_t	amount of adsorbed dye per unit mass of adsorbent (mg/g) in time t (min)
R	universal gas constant (8.314 J/mol K)
ΔS^o	standard entropy change (J/mol K)
SEM	scanning electron microscopy
SQUID	superconducting quantum interference device
T	absolute temperature (K)
TEM	transmission electron microscopy
XRD	X-ray powder diffraction
ZFC	zero-field-cooled magnetization curve

INTRODUCTION

Biosorption of organic pollutants, heavy metal ions and radionuclides using a variety of low-cost biological materials represents an emerging possibility for the reduction of environmental pollution. Enormous amount of biological materials has already been tested (Volesky & Holan 1995; Srinivasan & Viraraghavan 2010). In most cases, the efficient biosorbents are based on plant materials, microbial biomass or different types of polysaccharides. Recently, biochar has become a useful adsorbent for many types of xenobiotics (Xie *et al.* 2015).

Biochar is a black carbon rich product formed during thermal decomposition of biomass (e.g. wood, manure, or leaves), under limited supply of oxygen and usually at temperatures between 350–900 °C. This material is primarily used as soil amendment in agriculture and soil remediation when it acts simultaneously as a carbon sink. After insertion to soils, biochar can provide multiple benefits, including improvement of soil fertility, increasing soil nutrient and water holding capacity, raising crop productivity, and reducing emissions of greenhouse gases from soils to mitigate global warming (Zhang *et al.* 2013; Nartey & Zhao 2014).

Recently, new biochar applications have been introduced, especially as adsorbents for removal of both inorganic and organic contaminants (Xie *et al.* 2015). Due to the typically low cost of biochar, this material could, in many cases, substitute more expensive activated charcoal.

Magnetically responsive biochar derivatives can substantially simplify the separation from difficult-to-handle environments. Several procedures for the preparation of magnetic biochar have been described. One of the approaches is based on the modification of native biomass with the solution of ferric chloride; after drying, the material was pyrolyzed to form biochar/maghemite composite (Zhang *et al.* 2013). Alternatively, mixture of ferrous and ferric salts was used under similar conditions to form biochar/magnetite composite (Chen *et al.* 2011).

Also, postmagnetization procedures have been used, based on the immersion of the biochar into the Fe^{2+} and Fe^{3+} solution followed by the addition of sodium hydroxide and heating (Wang *et al.* 2014; Han *et al.* 2015); unfortunately, these are procedures of several steps requiring time-consuming operations.

In this paper we present an extremely simple and generally applicable procedure for magnetic modification of already prepared biochar which requires just simple mixing of biochar with microwave synthesized magnetic iron oxide particles followed by a drying process. Virtually any type of biochar can be converted into its magnetic derivative using this extremely simple procedure. Prepared magnetic biochar was characterized in detail and used as an efficient adsorbent of several water soluble dyes.

EXPERIMENTAL

Materials

Malachite green (CI 42000, MW 364.91 g/mol) was obtained from Roth, Germany while Bismarck brown Y (C.I. 21000, MW 419.31 g/mol) was from Sigma, USA. Acridine orange (C.I. 46005, MW 265.36 g/mol) and methyl green (C.I. 42585, MW 364.85 g/mol) were purchased from Loba Feinchemie, Austria while Nile blue A sulphate (C.I. 51180, MW 732.85 g/mol) was from Chemische Fabrik GmbH, Germany. All other used common chemicals were from Sigma-Aldrich, Czech Republic.

Biochar preparation and characterization

The biochar used for magnetization and adsorption experiments was produced from the fine fraction (<10 mm) of sieved mixed wood. The feedstock consisted of even

portions of coniferous and hard wood. It was treated by the continuous slow pyrolysis production system Pyreg 500 at Swiss Biochar GmbH in Belmont sur Lausanne. Pyrolysis time was 22 min with continuous heating from ambient temperature to a highest treatment temperature of 700 °C. To minimize syngas condensates formation inside the biochar structure and on its surface, the biochar was subjected for 5 min to an active outgassing under ambient air after its evacuation from the pyrolysis reactor. The basic characterization of the biochar was undertaken in accordance to the analytical methods of the European Biochar Foundation (EBC) guidelines (EBC 2012).

Preparation of magnetic biochar

Biochar was magnetically modified using microwave-synthesized magnetic iron oxide particles (Safarik & Safarikova 2014). In a typical procedure, 1 g of $FeSO_4 \cdot 7 H_2O$ was dissolved in 100 mL of water in a 600–800 mL beaker and a solution of sodium or potassium hydroxide (1 mol/L) was added slowly under mixing until the pH reached the value of ca 12; during this process, a precipitate of iron hydroxides was formed. Subsequently, the suspension was diluted up to 200 mL with water and inserted into a standard kitchen microwave oven (700 W, 2,450 MHz). The suspension was treated usually for 10 min at the maximum power. Then, the beaker was removed from the oven and the formed magnetic iron oxide nano- and microparticles were repeatedly washed with water until neutral pH of the magnetic suspension was reached.

To prepare magnetically responsive biochar, one gram of biochar was thoroughly mixed in a short test-tube or a small beaker with 2 mL of microwave iron oxide nano- and microparticles suspension (one part of completely sedimented iron oxide particles and four parts of water). Vigorous mixing with a spatula or laboratory spoon enabled homogeneous distribution of magnetic nano- and microparticles within the treated material. This mixture was allowed to dry completely at temperatures not exceeding 60 °C for 48 h. In order to increase magnetic response of the biochar composite, the amount of iron oxide particles can be increased (Safarik & Safarikova 2014).

Characterization of native and magnetic biochar

X-ray powder diffraction (XRD) patterns of both native and magnetically modified biochar were recorded on PANalytical X´Pert PRO (The Netherlands) instrument in Bragg-Brentano geometry with Fe-filtered CoK_α radiation (40 kV, 30 mA). The samples were inserted into conventional back-loading cavity sample holder and scanned in the 2θ range of 5–100 ° in steps of 0.017 °. The commercial standards SRM640 (Si) and SRM660 (LaB_6) from NIST were used for evaluation of the line positions and instrumental line broadening, respectively. The acquired pattern was evaluated using the X´Pert HighScore Plus software (PANalytical), PDF-4+ and ICSD databases.

The morphological study was performed using scanning electron microscopy (SEM) and transmission electron microscopy (TEM) measurements. To each sample in a small Eppendorf tube, purified water was added and the content was ultra-sonicated for 5 min. Suspensions of samples were dropped on either conductive carbon tape (for SEM) or copper grid with holey carbon film (for TEM) and air-dried. The samples were analyzed by SEM Hitachi SU6600 with accelerating voltage 15 kV, equipped with energy dispersive spectroscopy (EDS) – Thermo Noran System 7 with Si(Li) Detector (accelerating voltage of 15 kV and acquisition time 300 s). TEM analysis was done on JEOL JEM 2010F at 160 kV of accelerating voltage.

A superconducting quantum interference device (SQUID, MPMS XL-7, Quantum Design) was used for the magnetic measurements. The hysteresis loops were collected at temperatures of 5 and 300 K and in external magnetic fields ranging from −5 to +5 T.

Specific surface area and porosity of the samples were evaluated using the nitrogen adsorption-desorption measurement method at temperature of 77.13 K (molecular cross-sectional area 0.162 nm^2 of the N_2 molecule was assumed). Isotherms were acquired by the statistic volumetric technique and obtained by Sorptomatic 1990 analyzer (ThermoFinnigan). General preparation of the sample surface was realized by degassing at room temperature for at least 20 h before the measurement, to reach pressure below 0.13 Pa. Specific surface areas were calculated using the multipoint Brunauer Emmet Teller model (BET(3)). The best fits of the BET lines were obtained using adsorption data in the region of relative pressures from 0.005 to 0.4 (p/p_0). Pore size distributions were calculated from the desorption branch of the nitrogen isotherms using Barrett Joyner Halenda model assuming the presence of mesoporosity (exhibited by intra-particle voids). Low-pressure part of the adsorption branches of the nitrogen isotherms were used for calculating the microporosity using the Horvath and Kawazoe model. For pore size analysis by density functional theory and molecular dynamics (Evans *et al.* 1986; Ravikovitch *et al.* 1998) software AsiQwin 2.0 (Quantachrome) was used for calculations. Macroscopic and

semi-empirical analyses were performed with the Advanced Data Processing 4.0 software package (CE Instruments).

Adsorption of dyes on magnetically modified biochar

30 mg of magnetically modified biochar were mixed with 5.0 mL of water in a test tube. Then 0.1–5 mL portion of stock water solution (1 mg/mL) of a tested dye was added and the total volume of the solution was made up to 10.0 mL with water. The suspension was mixed at 27 rpm (vertical rotator, Dynal, Oslo, Norway) at room temperature (297.15 K) for 3 h. Then the magnetic adsorbent was separated from the suspension using a magnetic separator (MPC-1 or MPC-6, Dynal, Norway) and the clear supernatant was used for the spectrophotometric measurement. The concentration of free (unbound) dye in the supernatant (C_{eq}) was determined from the calibration curve. The amount of dye bound to the unit mass of the adsorbent (q_{eq}) was calculated using the following formula:

$$q_{eq} = \frac{(C_0 - C_{eq})}{3}\left(\frac{\text{mg}}{g}\right) \quad (1)$$

where C_0 is the total (initial) concentration (μg/mL) of dye used in the experiment. The value q_{eq} was expressed in mg of adsorbed dye per 1 g of adsorbent. Equilibrium adsorption data were fitted to Langmuir adsorption isotherms using SigmaPlot software.

Adsorption kinetics

Adsorption kinetics was studied under similar conditions using Bismarck brown Y, Nile blue A and malachite green (initial dye concentration 150 mg/L, 297.15 K, pH not adjusted), in different time intervals (0–180 min). The amount of adsorbed dye per unit mass of adsorbent q_t (mg/g) in time t was calculated from this formula:

$$q_t = \frac{V(C_o - C_t)}{m} \quad (2)$$

where C_t is the concentration of dye in solution (mg/L) in time t (min). The obtained kinetic data were analyzed using the linear forms of pseudo-first-order (Lagergren 1898) and pseudo-second-order (Kumar 2006) kinetic equations given as follows, respectively:

$$\ln(q_{eq} - q_t) = \ln(q_{eq}) - k_1 t \quad (3)$$

where the rate constant k_1 (1/min) can be obtained from the linear plot of ln (q_{eq}–q_t) against time

$$\frac{t}{q_t} = \frac{1}{k_2 q_{eq}^2} + \frac{t}{q_{eq}} \quad (4)$$

and the equilibrium adsorption capacity (q_{eq}) and the second-order rate constant k_2 (g/mg min) can be determined from the slope and intercept of plot t/q_t versus t.

Thermodynamic studies

Adsorption of Bismarck brown Y, Nile blue A and malachite green on magnetically modified biochar was carried out under similar conditions as above at 282.15, 297.15 and 313.15 K.

The thermodynamic equilibrium constant K_d was determined from intercept of the plot of ln (q_{eq}/C_{eq}) against q_{eq} and extrapolating q_e to zero (Khan & Singh 1987). The other thermodynamic parameters, namely Gibbs free energy change ΔG^o (J/mol), standard enthalpy change ΔH^o (J/mol) and standard entropy change ΔS^o (J/mol K) of studied process were calculated by using these equations (Gobi *et al.* 2011):

$$\Delta G^o = -RT\ln(K_d) \quad (5)$$

$$\ln(K_d) = \frac{\Delta S^o}{R} - \frac{\Delta H^o}{RT} \quad (6)$$

where R is the universal gas constant (8.314 J/mol K) and T is the absolute temperature (K). ΔH^o and ΔS^o were determined from the slope and intercept of the linear plot of ln (K_d) versus $1/T$.

RESULTS AND DISCUSSION

Native and magnetic biochar characterization

The biochar used for the preparation of magnetic derivative was partially characterized at the Ithaka Institute; it had an organic carbon content of 80% with a molar H/C_{org} ratio of 0.18 and molar O/C_{org} ratio of 0.04 indicating a comparably high aromaticity of the biochar carbon. The soluble electrolytes electrical conductivity was 0.1 S/m. The iron content of the biochar before its magnetisation was 1,840 mg/kg (dry mass). All threshold for the premium certificate of the European Biochar Foundation (EBC 2012) were respected.

An extremely simple magnetization procedure employing very cheap microwave assisted production of magnetic iron oxide particles from ferrous sulfate was used to prepare magnetic biochar. The synthesized magnetic iron oxide particles (nanoparticles with diameters between 20–60 nm, forming aggregates 0.1–20 μm in diameter; analysis using Mössbauer spectroscopy identified this material as a non-stoichiometric magnetite (Maderova *et al.* 2016)) are localized on the surface of biochar after its magnetic modification (see SEM and TEM images, Figure 1). The presence of iron oxide particles on the surface of the modified biochar was confirmed using energy-dispersive X-ray spectroscopy (see Figure 2). In case of this magnetic modification procedure, it can be expected that the strong binding of magnetic iron oxide particles to the surface of native biochar has been achieved by a subtle balance of van der Waals, electrostatic and hydrophobic interactions between the magnetic particles and the treated material surface (Saito *et al.* 2008). The stability of magnetically modified biochar is very high (stable at least two months in water suspension without leakage of magnetic particles). The formed magnetically responsive biochar can be easily separated using permanent magnet or commercial magnetic separator.

The XRD characterization confirmed that both unmodified and magnetically modified biochar samples are mostly of amorphous character, with just SiO_2 and $CaCO_3$ as the only crystalline components (Figure 3); the observed slight variations in relative contents of both phases are given by the heterogeneity of biochar material and do not reflect the influence of magnetic modification process. The magnetically modified biochar sample contains in addition also features typical for poorly crystalline magnetite (nano- to microparticles).

The surface area and porosity of both native and magnetically modified biochar were analyzed under the same conditions with identical settings of the number of adsorption and desorption points (Supplement Table S1, Supplement Figure S1, available with the online version of this paper). Surface area of non-magnetic biochar was 348 m^2/g and of magnetically modified biochar was 269 m^2/g. Both samples exhibit an identical type of isotherm, combination of types I and IV (Sing *et al.* 1985; Rouquerol *et al.* 1999; Lowell *et al.* 2004) according to the IUPAC classification, with hysteresis

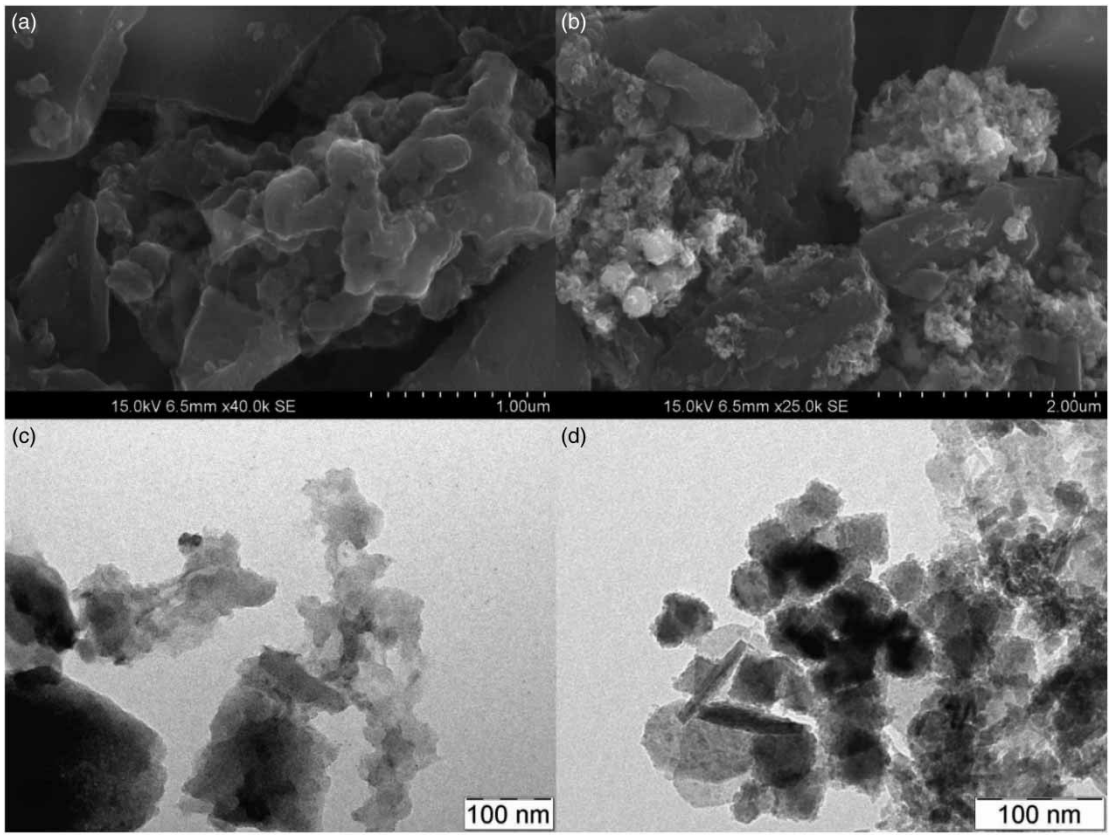

Figure 1 | SEM of non-magnetic (a) and magnetically modified (b) biochar. TEM of non-magnetic (c) and magnetically modified (d) biochar.

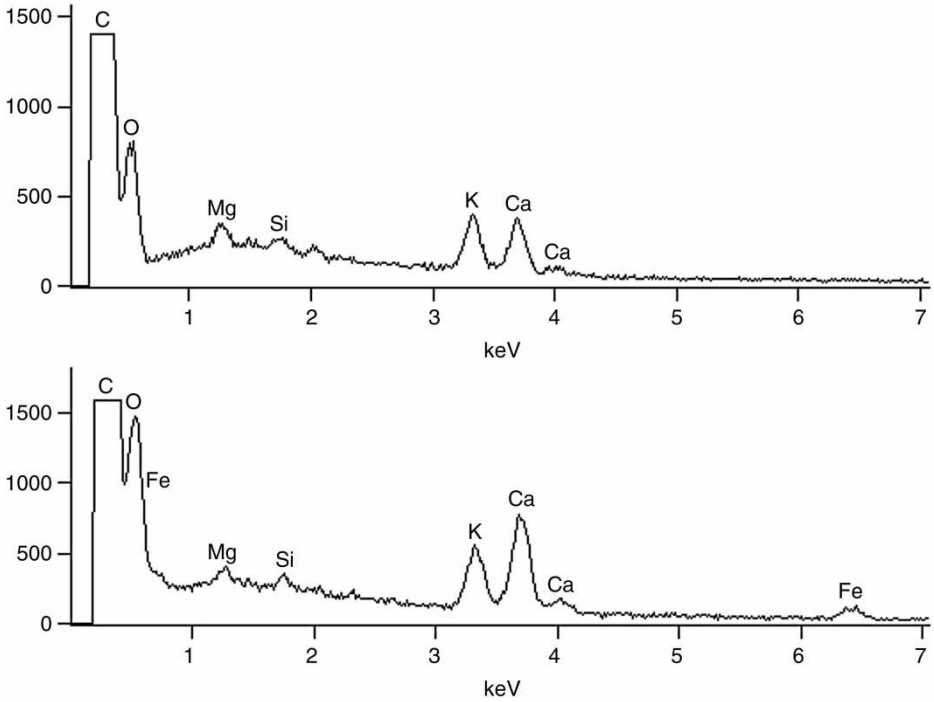

Figure 2 | Energy-dispersive X-ray spectroscopy: EDS spectrum of non-magnetic (top) and magnetically modified (bottom) biochar.

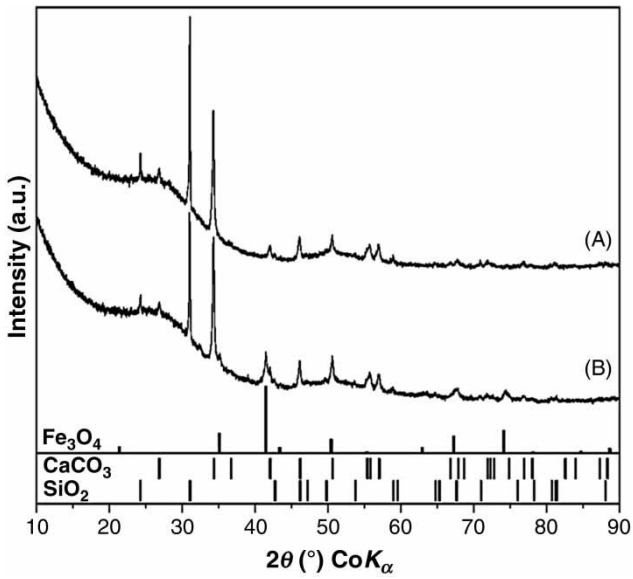

Figure 3 | XRD patterns of non-modified (A) and magnetically modified (B) biochar samples. Vertical bars mark the positions of diffractions of identified crystalline phases (SiO_2: PDF card No. 03-065-0466; $CaCO_3$: PDF card No. 01-086-2334), theoretical XRD pattern of magnetite is also shown (PDF card No. 01-075-0033).

loop type to be H3. This type of isotherms indicates the presence of both micro- and mesoporosity in material. Illustrated behavior of the adsorption–desorption hysteresis loop is typical for slit pores in carbon porous materials. This shape of isotherms and type of hysteresis loops is well described (Thommes 2010) and is exhibited by complicated pore-network structures of micro-mesoporous materials with ink-bottle type pores. This concept can easily be adopted for description of the intra-aggregate voids and spaces between the nanoparticles, as well as for voids in biochar particles itself. Power spectral density calculations demonstrate mostly microporous-like material, with small presence of mesoporosity.

In order to get a deeper insight into the magnetic properties of magnetically modified biochar sample, magnetization measurements were performed (see Supplement Figures S2 and S3, available with the online version of this paper). As already discussed above, the magnetic biochar was prepared by modification with magnetic iron oxide particles (nanoparticles with diameters of 20–60 nm forming aggregates with typical sizes of 0.1–20 μm in diameter). The sample's magnetic response is in a full accordance with SEM/TEM observations – i.e. the magnetic system is not superparamagnetic at room temperature with respect to the characteristic measuring time of the SQUID magnetometer (~10 s); the temperature of irreversibility marking the separation between the zero-field-cooled (ZFC) and field-cooled (FC) magnetization curve is above the room temperature. In addition, the average blocking temperature was found to be at ~172 K; the maximum is very broad implying broad

particles size distribution. It is hypothesized that the presence of diamagnetic matrix in biochar significantly slows down the relaxation mechanism. The increase in the ZFC magnetization curve at low temperature is probably due to the presence of some paramagnetic substance (most probably of organic nature) present in biochar. The coercivity values fall into the range expected for nonhydrated iron oxides (γ-Fe_2O_3, Fe_3O_4 or their non-stoichiometric analogues). The decrease in the saturation magnetization is due to the presence of paramagnetic and diamagnetic contributions from some organic and inorganic substances present in biochar (see XRD results). The detailed parameters of the hysteresis loops are presented in Table 1.

Adsorption of organic dyes on magnetic biochar

Magnetic biochar was applied as an adsorbent to study the binding of five water-soluble dyes belonging to different dye classes. The tested dyes comprehended methyl green and malachite green (triphenylmethane group), Bismarck brown Y (azodyes group), acridine orange (acridine group) and Nile blue A (oxazine group). Commercially available dyes were used during the experiments; they were dissolved in distilled water without buffering the solution. The pH values of the dyes stock solutions (1 mg/mL) ranged between 3.0 and 4.5 (malachite green – 3.0; acridine orange – 3.2; Bismarck brown Y – 3.2; Nile blue – 4.0; methyl green – 4.5).

The contact time is an important adsorption parameter required for determination of time necessary to reach the equilibrium. As can be seen from the Figure 4, removal of Bismarck brown Y and Nile blue A is very fast in comparison with removal of malachite green. The adsorption equilibrium was reached within 45 min for the first two dyes, while it took 150 min for malachite green. 3 h incubation was used for the adsorption experiments.

The equilibrium adsorption isotherms for the unbuffered aqueous solutions of the tested dyes are shown in Figure 5.

Table 1 | Parameters of the hysteresis loops of the magnetic biochar sample, measured at a temperature of 5 K and 300 K, where M_{max+} (5 T) is a maximum magnetization at 5 T, M_{max-} (−5 T) is a maximum magnetization at –5 T, B_{C+} is a positive coercivity, B_{C-} is negative coercivity, M_{R+} is a positive remanent magnetization and M_{R-} is a negative remanent magnetization

T (K)	M_{max+} (5 T) (Am²/kg)	M_{max-} (5 T) (Am²/kg)	B_{C+}(mT)	B_{C-} (mT)	M_{R+} (Am²/kg)	M_{R-} (Am²/kg)
5	1.90	−1.90	27.0	−26.8	0.41	−0.41
300	1.27	−1.27	3.9	−3.9	0.11	−0.11

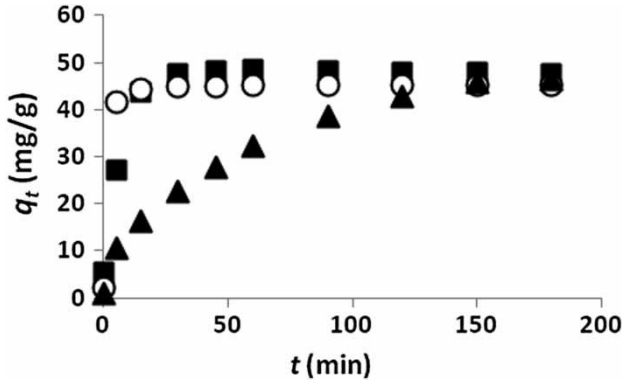

Figure 4 | Effect of time on uptake of dyes on magnetic biochar (standard conditions used, initial dye concentration was 150 mg/L). ○–Bismarck brown Y, ▲–malachite green, ■–Nile blue A.

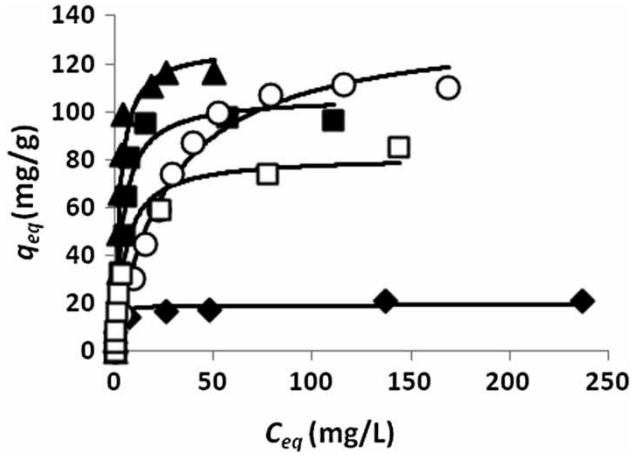

Figure 5 | Equilibrium adsorption isotherms of tested dyes on magnetically modified biochar. C_{eq}–equilibrium liquid-phase concentration of the unadsorbed (free) dye (mg/L); q_{eq}–equilibrium solid-phase concentration of the adsorbed dye (mg/g). ▲–malachite green, ○–Bismarck brown Y, ■–Nile blue A, □–methyl green, ◆–acridine orange.

These isotherms represent distribution of dyes between the aqueous and solid phases as the dye concentration increases. Langmuir and Freundlich isotherm equations are usually used for experimental data analysis in order to study the adsorption of target species from water solutions.

The Langmuir model is valid for monolayer adsorption onto a surface with a finite number of identical sites. A well known expression for the Langmuir model is given by

$$q_{eq} = \frac{Q_{\max} b C_{eq}}{1 + b C_{eq}} \tag{7}$$

where q_{eq} (expressed in mg/g or mg/mL) is the amount of the adsorbed dye per unit mass or sedimented volume of

magnetically modified biomass and C_{eq} (expressed in mg/L) is the unadsorbed dye concentration in solution at equilibrium. Q_{max} (mg/g) is the maximum amount of the dye per unit mass of adsorbent to form a complete monolayer on the surface bound at high dye concentration and b is a constant related to the affinity of the binding sites (expressed in L/mg).

Non-linear regression calculation is currently the preferred way to calculate the constants (Q_{max}, b). The results are presented in Table 2. The highest Q_{max} was found for Bismarck brown Y (137.0 mg/g), while the lowest Q_{max} value was obtained for acridine orange (19.3 mg/g). The values of standard error of estimate indicate that Langmuir isotherm can be used for the description of adsorption of all the tested dyes.

The maximum adsorption capacity values Q_{max} obtained for magnetically modified biochar are in most cases at least comparable with literature data for other biomaterials (both in non-magnetic and magnetic forms) (Srinivasan & Viraraghavan 2010). Adsorption of Nile blue A (this dye exhibited relatively good adsorption on magnetic biochar) on various sorbents has been compared (see Table 3). Evidently, the low-cost magnetic biochar exhibits good adsorption properties for this dye and should be considered as a promising adsorbent for specific groups of organic dyes.

Adsorption kinetics

The adsorption process of Bismarck brown, Nile blue A and malachite green is documented in Figure 4. The obtained data were subsequently analyzed to investigate kinetics of adsorption process using pseudo-first- and pseudo-second-order kinetic models (see also Supplement Figure S4). It is apparent from results summarized in Supplement Table S2 that the pseudo-first-order kinetic model did not fit well; the correlation coefficient was low and the calculated q_{eq} absolutely disagreed with the experimental $q_{eq\ exp}$ value, while in the case of pseudo-second-order kinetic model the correlation coefficient reached the value close to 1.0 and the theoretical q_{eq} value calculated from this equation approached the experimental $q_{eq\ exp}$. (Supplement Figure S4 and Supplement Table S2 are available with the online version of this paper.)

Table 2 | Maximum adsorption capacities (Q_{max}) and constants related to the affinity of binding sites (b) describing the dyes adsorption on magnetically modified biochar, calculated from the Langmuir equation. Q_{max} is expressed in mg/g or μmol/g, while b is expressed in L/mg

Dye	Adsorption coefficients
Acridine orange	$Q_{max} = 19.25$ mg/g (73 μmol/g) $b = 1.358$
Bismarck brown Y	$Q_{max} = 137.0$ mg/g (327 μmol/g) $b = 0.038$
Malachite green	$Q_{max} = 127.3$ mg/g (349 μmol/g) $b = 0.417$
Methyl green	$Q_{max} = 81.2$ mg/g (223 μmol/g) $b = 0.198$
Nile blue A	$Q_{max} = 106.2$ mg/g (145 μmol/g) $b = 0.265$

Table 3 | Comparison of maximum adsorption capacities (mg/g) of Nile blue A onto low-cost biosorbents and studied magnetic biochar

Adsorbent	Q_{max} (mg/g)	Reference
Acrylamide-maleic acid hydrogels	1.6–3.9	Saraydin *et al.* (1996)
Biogenic iron oxides, magnetically modified	50.1	Safarik *et al.* (2015)
Dimethyl terephthalate distillation residue	21.2	Guclu (2010)
Spent grain, magnetically modified	64.1	Safarik *et al.* (2011)
Spent tea leaves, magnetically modified	87.1	Safarik *et al.* (2012)
Sulfonated phenol–formaldehyde resin	107	Iyim *et al.* (2008)
Magnetic biochar	106.2	This paper

Thermodynamic studies

The effect of temperature on the uptake of the above mentioned three dyes onto biochar can indicate the sorption nature, i.e. whether it is an exothermic or endothermic process. Thermodynamic studies were performed at three different temperatures, namely 282.15, 297.15 and 313.15 K. The higher uptake of dyes was achieved at higher temperature (Supplement Figure S5). This observation indicates that adsorption of the tested dyes (Bismarck brown Y, Nile blue A and malachite green) onto biochar may be endothermic. All obtained thermodynamic parameters are presented in Supplement Table S3 and Supplement Figure S6. Negative values of Gibbs free energy change (ΔG^o) indicate the spontaneous process, positive ΔH^o the endothermic nature of adsorption and positive ΔS^o suggests an increase of the randomness at the solid/solution

interface during sorption process. (Supplement Figures S5 and S6 and Supplement Table S3 are available with the online version of this paper.)

CONCLUSION

Magnetically responsive derivative of biochar has been prepared. This material was used as an adsorbent for the removal of selected dyes. Maximum adsorption capacities of magnetic biochar reached values up to 137 mg of adsorbed dye per one gram of adsorbent which is fully comparable with other described non-magnetic and magnetic biosorbents used for the same purpose. Extremely simple, cheap and scalable magnetic modification of biochar enabling its simple magnetic separation makes the described biosorbent superior with respect to other non-magnetic materials. It should be taken into consideration, however, that the adsorption properties of this material are strongly dependent on the dye type and conditions during the adsorption process.

ACKNOWLEDGEMENTS

This research was supported by the Grant Agency of the Czech Republic (Project No. 13-13709S), by the projects LO1305 and LD14066 (Ministry of Education, Youth and Sports of the Czech Republic) and by the COST Action TD1107 'Biochar as option for sustainable resource management'. The authors also thank the internal IGA grant of Palacky University in Olomouc, Czech Republic (IGA_PrF_2015_021) and Assoc. Prof. Jiří Pechoušek, Assoc. Prof. Jiří Tuček and Jana Stráská, MSc for technical assistance.

REFERENCES

Chen, B. L., Chen, Z. M. & Lv, S. F. 2011 A novel magnetic biochar efficiently sorbs organic pollutants and phosphate. *Bioresource Technology* **102** (2), 716–723.

EBC 2012 *European Biochar Certificate – Guidelines for A Sustainable Production of Biochar.* European Biochar Foundation (EBC), Arbaz, Switzerland.

Evans, R., Marconi, U. M. B. & Tarazona, P. 1986 Capillary condensation and adsorption in cylindrical and slit-like pores. *Journal of the Chemical Society, Faraday Transactions 2* **82**, 1763–1787.

Gobi, K., Mashitah, M. D. & Vadivelu, V. M. 2011 Adsorptive removal of methylene blue using novel adsorbent from palm oil mill effluent waste activated sludge: equilibrium, thermodynamics and kinetic studies. *Chemical Engineering Journal* **171** (3), 1246–1252.

Guclu, G. 2010 Removal of basic dyes from aqueous solutions by dimethyl terephthalate distillation residue. *Desalination* **259** (1–3), 53–58.

Han, Z., Sani, B., Akkanen, J., Abel, S., Nybom, I., Karapanagioti, H. K. & Werner, D. 2015 A critical evaluation of magnetic activated carbon's potential for the remediation of sediment impacted by polycyclic aromatic hydrocarbons. *Journal of Hazardous Materials* **286**, 41–47.

Iyim, T. B., Acar, I. & Ozgumus, S. 2008 Removal of basic dyes from aqueous solutions with sulfonated phenol-formaldehyde resin. *Journal of Applied Polymer Science* **109** (5), 2774–2780.

Khan, A. A. & Singh, R. P. 1987 Adsorption thermodynamics of carbofuran on Sn(IV) arsenosilicate in H^+, Na^+ and Ca^{2+} forms. *Colloids and Surfaces* **24** (1), 33–42.

Kumar, K. V. 2006 Linear and non-linear regression analysis for the sorption kinetics of methylene blue onto activated carbon. *Journal of Hazardous Materials* **137** (3), 1538–1544.

Lagergren, S. Y. 1898 Zur Theorie der sogenannten Adsorption gelöster Stoffe. *Kungliga Svenska Vetenskapsakademiens Handlingar* **24** (4), 1–39.

Lowell, S., Shields, J. E., Thomas, M. A. & Thommes, M. 2004 *Characterization of Porous Solids and Powders: Surface Area, Pore Size and Density.* Springer, Heidelberg, Germany.

Maderova, Z., Baldikova, E., Pospiskova, K., Safarik, I. & Safarikova, M. 2016 Removal of dyes by adsorption on magnetically modified activated sludge. *International Journal of Environmental Science and Technology* **13**, 1653–1664.

Nartey, O. D. & Zhao, B. W. 2014 Biochar preparation, characterization, and adsorptive capacity and its effect on bioavailability of contaminants: an overview. *Advances in Materials Science and Engineering* Article ID 715398.

Ravikovitch, P. I., Haller, G. L. & Neimark, A. V. 1998 Density functional theory model for calculating pore size distributions: pore structure of nanoporous catalysts. *Advances in Colloid and Interface Science* **76–77**, 203–226.

Rouquerol, F., Rouquerol, J. & Sing, K. eds. 1999 *Adsorption by Powders and Porous Solids. Principles, Methodology and Applications.* Academic Press, London, UK.

Safarik, I. & Safarikova, M. 2014 One-step magnetic modification of non-magnetic solid materials. *International Journal of Materials Research* **105** (1), 104–107.

Safarik, I., Horska, K. & Safarikova, M. 2011 Magnetically modified spent grain for dye removal. *Journal of Cereal Science* **53** (1), 78–80.

Safarik, I., Horska, K., Pospiskova, K. & Safarikova, M. 2012 One-step preparation of magnetically responsive materials from non-magnetic powders. *Powder Technology* **229**, 285–289.

Safarik, I., Filip, J., Horska, K., Nowakova, M., Tucek, J., Safarikova, M., Hashimoto, H., Takada, J. & Zboril, R. 2015 Magnetically-modified natural biogenic iron oxides for organic xenobiotics removal. *International Journal of Environmental Science and Technology* **12** (2), 673–682.

Saito, T., Koopal, L. K., Nagasaki, S. & Tanaka, S. 2008 Adsorption of heterogeneously charged nanoparticles on a variably charged surface by the extended surface complexation approach: charge regulation, chemical heterogeneity, and surface complexation. *Journal of Physical Chemistry B* **112** (5), 1339–1349.

Saraydin, D., Karadag, E. & Guven, O. 1996 Adsorption of some basic dyes by acrylamide-maleic acid hydrogels. *Separation Science and Technology* **31** (3), 423–434.

Sing, K. S. W., Everett, D. H., Haul, R. A. W., Moscou, L., Pierotti, R. A., Rouquerol, J. & Siemieniewska, T. 1985 Reporting physisorption data for gas solid systems with special reference to the determination of surface-area and porosity (Recommendations 1984). *Pure and Applied Chemistry* **57** (4), 603–619.

Srinivasan, A. & Viraraghavan, T. 2010 Decolorization of dye wastewaters by biosorbents: a review. *Journal of Environmental Management* **91** (10), 1915–1929.

Thommes, M. 2010 Physical adsorption characterization of nanoporous materials. *Chemie Ingenieur Technik* **82** (7), 1059–1073.

Volesky, B. & Holan, Z. R. 1995 Biosorption of heavy metals. *Biotechnology Progress* **11** (3), 235–250.

Wang, S. Y., Tang, Y. K., Li, K., Mo, Y. Y., Li, H. F. & Gu, Z. Q. 2014 Combined performance of biochar sorption and magnetic separation processes for treatment of chromium-contained electroplating wastewater. *Bioresource Technology* **174**, 67–73.

Xie, T., Reddy, K. R., Wang, C. W., Yargicoglu, E. & Spokas, K. 2015 Characteristics and applications of biochar for environmental remediation: a review. *Critical Reviews in Environmental Science and Technology* **45** (9), 939–969.

Zhang, M., Gao, B., Varnoosfaderani, S., Hebard, A., Yao, Y. & Inyang, M. 2013 Preparation and characterization of a novel magnetic biochar for arsenic removal. *Bioresource Technology* **130**, 457–462.

First received 17 February 2016; accepted in revised form 28 June 2016. Available online 22 July 2016

5.2.9 ***Leptothrix* sp.**

V následujících dvou přiložených publikacích je studována schopnost adsorpce organických barviv pomocí bakterií *Leptothrix* sp., které byly na konci února 2016 odebrány v bezejmenném potoce ve Stromovce v Českých Budějovicích.

Magnetická modifikace *Leptothrix* sp. byla v obou případech realizována jak prostřednictvím kyselé MK, tak MS magnetitem. V první publikaci je však testována sorpce amidové černě 10B, zatímco publikace druhá je zaměřena na odstranění krystalové violeti. Oba články obsahují základní charakterizace připravených materiálů, optickou mikroskopii a SEM.

Nejvhodnější hodnotou pH pro odstranění amidové černě 10B z vodního systému bylo pH 2, při kterém byly dosaženy velmi vysoké maximální adsorpční kapacity: 339,2 mg/g pro MK a 286,1 mg/g pro MS magnetitem modifikované bakterie. Jako nejvhodnější adsorpční model byl ustanoven Freundlichův model a kinetika reakce s 99,999% spolehlivostí souhlasila s kinetickým modelem pseudo-druhého řádu. Na základě vypočtených termodynamických parametrů bylo prokázáno, že adsorpční proces je spontánní a endotermní.

Zjištěné ideální pH pro sorpci krystalové violeti bylo pH 10. Zde byl však pozorován opačný trend než v předešlé publikaci, a sice maximální adsorpční kapacita pro modifikaci MS magnetitem (243,1 mg/g) byla vyšší než pro modifikaci kyselou MK (166,6 mg/g). Rovnovážná adsorpční data korelovala lépe s Langmuirovým modelem. Kinetiku lze popsat stejně jako u sorpce amidové černě 10B kinetickým modelem pseudo-druhého řádu.

Příloha 15:

Magnetically modified sheaths of *Leptothrix* sp. as an adsorbent for Amido black 10B removal

Angelova R, Baldikova E, Pospiskova K, Safarikova M, Safarik I

J. Magn. Magn. Mater. 427, **2017**, 314-319

Journal of Magnetism and Magnetic Materials 427 (2017) 314–319

Contents lists available at ScienceDirect

Journal of Magnetism and Magnetic Materials

journal homepage: www.elsevier.com/locate/jmmm

Magnetically modified sheaths of *Leptothrix* sp. as an adsorbent for Amido black 10B removal

Ralitsa Angelova[a,b,c], Eva Baldikova[d,e], Kristyna Pospiskova[f], Mirka Safarikova[a,d], Ivo Safarik[a,d,f,*]

[a] Department of Nanobiotechnology, Biology Centre, ISB, CAS, Na Sadkach 7, 370 05 Ceske Budejovice, Czech Republic
[b] Department of General and Industrial Microbiology, Faculty of Biology, Sofia University "St. Kliment Ohridski", 8 Dragan Tsankov Blvd, 1164 Sofia, Bulgaria
[c] Laboratory Microwave Magnetics, Institute of Electronics, Bulgarian Academy of Sciences, 72 Tzarigradsko Chaussee Blvd, 1784 Sofia, Bulgaria
[d] Global Change Research Institute, CAS, Na Sadkach 7, 370 05 Ceske Budejovice, Czech Republic
[e] Department of Applied Chemistry, Faculty of Agriculture, University of South Bohemia, Branisovska 1457, 370 05 Ceske Budejovice, Czech Republic
[f] Regional Centre of Advanced Technologies and Materials, Palacky University, Slechtitelu 27, 783 71 Olomouc, Czech Republic

ARTICLE INFO

Keywords:
Leptothrix sp.
Sheaths
Magnetic fluid
Magnetic iron oxide
Magnetic adsorbent
Amido black 10B

ABSTRACT

The goal of this study was to assess the biosorption of Amido black 10B dye from aqueous solutions on magnetically modified sheaths of *Leptothrix* sp. in a batch system. The magnetic modification of the sheaths was performed using both microwave synthesized iron oxide nano- and microparticles and perchloric acid stabilized ferrofluid. The native and both magnetically modified sheaths were characterized by SEM. Various parameters significantly affecting the adsorption process, such as pH, contact time, temperature and initial concentration, were studied in detail using the adsorbent magnetized by both methods.

The highest adsorption efficiency was achieved at pH 2. The maximum adsorption capacities of both types of magnetized material at room temperature were found to be 339.2 and 286.1 mg of dye per 1 g of ferrofluid modified and microwave synthesized particles modified adsorbent, respectively. Thermodynamic study of dye adsorption revealed a spontaneous and endothermic process in the temperature range between 279.15 and 313.15 K. The data were fitted to various equilibrium and kinetic models. Experimental data matched well with the pseudo-second-order kinetics and Freundlich isotherm model.

The *Leptothrix* sheaths have excellent efficacy for dye adsorption. This material can be used as an effective, low-cost adsorbent.

1. Introduction

Various chemical industries including textile, plastic, paint, paper, leather and rubber ones generate large volumes of toxic dye wastes. Many dyes are difficult to decolorize due to their complex structure and synthetic origin [1]. Even a very low dye concentration is highly visible and can significantly affect aquatic life as well as food web.

Application of biosorption to remove toxic pollutants from wastewaters is one of the progressive environmental technologies. Adsorption is a very simple method compared to other procedures, and has often been used in the treatment of wastewater containing colored impurities and heavy metal ions [2]. Dye removal by adsorption is often based on the use of natural adsorbents so that the process becomes economically feasible. In addition, natural biosorbents are renewable, available in large amounts and less expensive compared to other materials that are used as adsorbents, such as activated carbon [3], zeolite [4], carbon nanotubes [5], noble metals like Pb and Ag loaded on activated carbon [6] or ZnO nanoparticles on activated carbon [7]. The use of microorganisms as biosorbents for removal of synthetic dyes from textile wastewater is promising due to their good performance and low cost [8]. However, no studies have been reported on the removal of Amido black 10B dye using *Leptothrix* sheaths as adsorbent. The synthetic dye chosen (Amido black 10B, also known as Naphthol blue black or Acid black 1) is usually used for staining of proteins in biochemical research, nevertheless, it can be applied to all kind of both natural (cotton, wool, silk) or synthetic (acrylic, polyester, and rayon) fibers or can also be employed in paints, inks, plastics and leather industries [9]. This dye can cause damages of the human respiratory system and skin and eye irritations. Hence, it is considered worthwhile to develop a low-cost adsorbent for the effective removal of

* Corresponding author at: Department of Nanobiotechnology, Biology Centre, ISB, CAS, Na Sadkach 7, 370 05 Ceske Budejovice, Czech Republic.
E-mail address: ivosaf@yahoo.com (I. Safarik).

http://dx.doi.org/10.1016/j.jmmm.2016.10.094
Received 23 June 2016; Received in revised form 16 October 2016; Accepted 18 October 2016
Available online 19 October 2016
0304-8853/

Amido Black 10B dye from its aqueous solutions [4].

The sheathed bacteria from the genus *Leptothrix* belong to the group of neutrophilic iron bacteria. They can be found in different aquatic habitats as lakes, streams, springs, swamps, iron seeps, and springs rich in iron and manganese, as well as in wastewater treatment systems [10]. Their metal-oxidizing ability is important in biogeochemical cycles of these metals.

Leptothrix sp. is able to accumulate Fe and Mn ions into their sheaths. This ability is employed for removal of iron and manganese from groundwater to clean water for drinking purposes. This technology is used in many water-treatment plants all over the world. Filamentous-looking sheaths of *Leptothrix* sp. as well as the ferric oxides formed are of great interest for different nanotechnology and bioengineering applications as pigments, adsorbents, carriers and others [11–15].

The purpose of this work was to investigate the adsorption potential of magnetically responsive *Leptothrix* sp. sheaths (MLS) prepared by modification with both microwave synthesized iron oxide nano- and microparticles, and perchloric acid stabilized magnetic fluid. Adsorption of a model dye, namely Amido black 10B was performed in a batch system where MLS with adsorbed dye were easily removed using an appropriate magnetic separator.

2. Materials and methods

2.1. Materials

Natural ocherous sediment containing *Leptothrix* sp. sheaths was collected using glass vessels from an unnamed stream in Ceske Budejovice, Czech Republic (48°58′22.57′′N, 14°27′39.93′′E) (Fig. 1) at the end of February 2016. Sample was concentrated during collection by letting the biomaterial settle down and decanting overlying water. Subsequently, the sediment was promptly transported to the laboratory, where it was repeatedly washed with water. Ferrous sulfate heptahydrate, sodium hydroxide and other common chemicals were obtained from Lach-Ner, Czech Republic. Magnetic fluid stabilized with perchloric acid was prepared using a standard procedure [16]; the relative magnetic fluid concentration (39.5 mg/mL) is given as the maghemite content determined by a colorimetric method [17].

2.2. Modification of Leptothrix sheaths with microwave synthesized magnetic iron oxide nano- and microparticles

The magnetic iron oxide nano- and microparticles were synthesized using a microwave (MW) assisted procedure described previously [18]. 400 mL of completely sedimented (earth gravity, 24 h) *Leptothrix* sheaths (either native or sterilized at 121 °C for 20 min, pH around 7.0) was mixed with 120 mL of iron oxide suspension in water (1 part of completely sedimented (earth gravity, 24 h) microwave synthesized iron oxide nano- and microparticles and 4 parts of water, pH 7.0). The mixture was incubated on a sample mixer (Dynal Biotech Inc., NY, USA; 27 rpm) for 3 h at room temperature, and then, magnetically modified sheaths were repeatedly washed with water (using a magnetic separator) until nonmagnetic material was washed out. Next, magnetized *Leptothrix* sheaths were used to prepare a suspension (1 part of completely sedimented (earth gravity, 24 h) sheaths and 4 parts of distilled water) used in the adsorption experiments. The prepared magnetically responsive sheaths were stored in water at 4 °C.

Fig. 1. The sampling place of ocherous *Leptothrix* sp. sheaths.

2.3. Modification of Leptothrix sheaths with magnetic fluid

400 mL of completely sedimented *Leptothrix* sheaths (the same as above) was mixed with 20 mL of perchloric acid stabilized magnetic fluid (FF). After mixing on a sample mixer (27 rpm) for 3 h at room temperature, the modified sheaths were washed with water. Next, the same suspension as above was prepared for adsorption experiments. The prepared magnetically responsive material was stored in water at 4 °C.

2.4. Characterization of magnetically modified Leptothrix sheaths

The morphology and structure of both native and magnetically modified *Leptothrix* sheaths were studied by optical microscopy and scanning electron microscopy (SEM). The samples were analyzed using a Hitachi SU6600 scanning electron microscope (Hitachi, Japan) with accelerating voltage 1, 3 or 5 kV. Energy dispersive X-ray spectra (EDS) were acquired in SEM using Thermo Noran System 7 (Thermo Scientific, MA, USA) with Si(Li) detector (accelerating voltage of 10 kV, acquisition time 300 s).

2.5. Dye

Amido black 10B is a synthetic amino acid staining diazo dye (CI 20470, molecular formula: $C_{22}H_{14}N_6Na_2O_9S_2$, molar mass: 616.5 g/mol). It was obtained from Merck, Germany (purity: 50%) and was used without further purification. Amido black 10B is a dark red to black powder soluble in water and used as a stain for protein materials. The chemical structure of Amido Black 10B dye is given in Fig. 2. The wavelength corresponding to maximum absorbance for the dye was found to be 618 nm.

2.6. Adsorption of dye on magnetically modified Leptothrix sheaths

One mL of settled magnetic *Leptothrix* suspensions (corresponding to 19 mg of dried magnetically modified material) in a series of test tubes was mixed with 1–8 mL portion of stock water solution of tested dye (1 mg/mL; pH 2) and the total volume of the solutions was filled up to 10.0 mL with water (pH 2). The suspensions were incubated on a rotary mixer (Dynal, Norway, 27 rpm) for 2.5 h at room temperature. Various parameters were varied keeping the other parameters constant, to study the influence of pH (2–10), initial dye concentration (0–800 mg/L), contact time (0–240 min), and temperature (6–40 °C). After adsorption, the magnetic adsorbents were separated from the suspensions using a magnetic separator (MPC-1 or MPC-6, Dynal, Norway) and the clear supernatants were used for the spectrophotometric measurements. The concentration of free (unbound) dye in the supernatants (C_e; mg/L) was determined from the calibration curve.

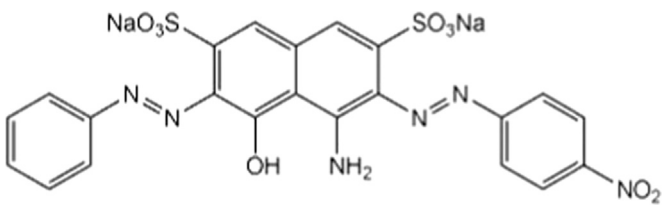

Fig. 2. Structure of Amido black 10B dye.

The amount of dye bound to the unit mass of the adsorbent (q_e; mg/g) was calculated using the following formula:

$$q_e = (C_{tot} - C_e)/1.9 \quad (1)$$

where C_{tot} is the total (initial) concentration of dye (mg/L) used in the experiment. Equilibrium adsorption data were analyzed by the Langmuir and Freundlich adsorption isotherm models using non-linear regression analysis (solver add – in function of the Microsoft Excel), and kinetic data were fitted to the pseudo-first-order and pseudo-second-order kinetic models as described previously [19]. Thermodynamic parameters, namely the standard free energy change ($\Delta G°$; J/mol), enthalpy ($\Delta H°$; J/mol), entropy ($\Delta S°$; J/mol K) and thermodynamic equilibrium constant (K_L) were calculated according to Maderova et al. [20].

3. Results and discussion

3.1. Characterization of the adsorbent

Native *Leptothrix* sheaths were collected from a natural water source. Long sheaths (with the lengths often exceeding 50 μm) are clearly visible using both optical and scanning electron microscopy (Fig. 3). The sheaths were magnetically modified by both simple and quick procedures employing mixing of native *Leptothrix* sheaths with either microwave synthesized magnetic iron oxide particles or water-based magnetic fluid.

The first modification is based on a preparation of nonstoichiometric magnetite particles from an iron(II) salt precursor at high pH. The use of a single salt during the microwave synthesis makes this approach substantially simpler in comparison with analogous techniques where both iron(II) and iron(III) salts have been used simultaneously [18,21].

Water-based magnetic fluid stabilized with perchloric acid was utilized as a second magnetic modifier. Magnetic fluid was composed of maghemite nanoparticles with diameters ranging between 10 and 20 nm (electron microscopy measurements), with a mean particle diameter ca. 12.5–14 nm [22,23].

Thorough mixing of target non-magnetic *Leptothrix* sheaths with

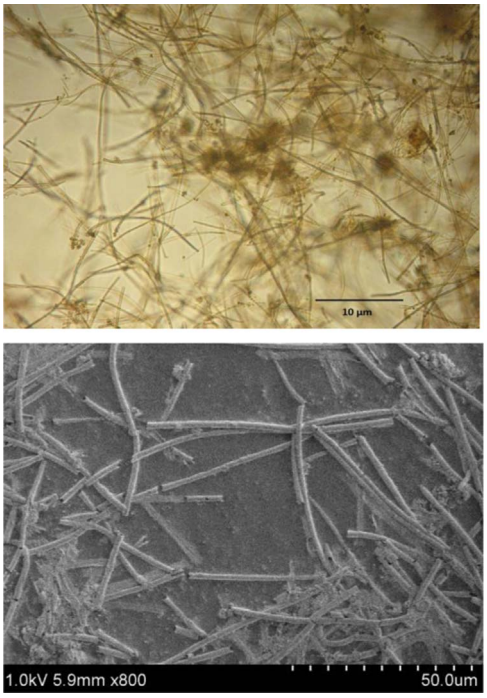

Fig. 3. Images of native *Leptothrix* sp. sheaths: optical microscopy (top); scanning electron microscopy (bottom).

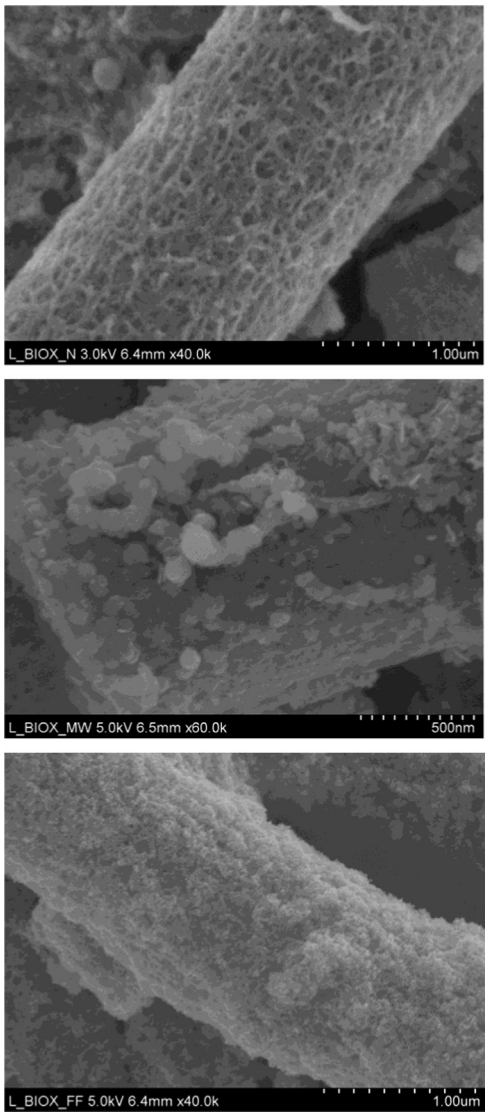

Fig. 4. SEM images of native *Leptothrix* sheaths (top); sheaths modified by microwave synthesized magnetite particles (middle); and sheaths modified by magnetic fluid (bottom).

Fig. 5. Appearance of native *Leptothrix* sheaths suspension (left), suspension of sheaths after magnetic modification (middle) and demonstration of magnetic separation of magnetically modified sheaths (right). Almost the same appearance was observed after magnetic modification with microwave synthesized magnetite particles and with magnetic fluid.

both magnetic modifiers led to the deposition of magnetic iron oxide particles onto the surface of the *Leptothrix* sheaths. The presence of iron oxide particles and their aggregates on the surface of the treated sheaths was confirmed by SEM (Fig. 4). The magnetically modified

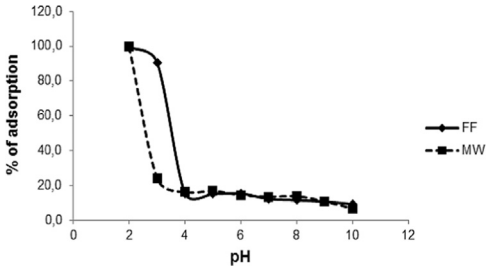

Fig. 6. Dependence of dye removal efficiency on solution pH using MW-MLS and FF-MLS.

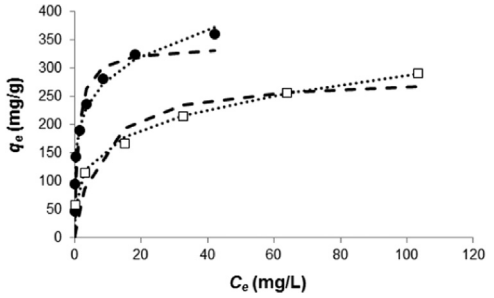

Fig. 7. Langmuir (- - -) and Freundlich (.....) equilibrium adsorption isotherms of Amido black 10B on *Leptothrix* sheaths modified with microwave synthesized magnetite (□) and magnetic fluid (•).

Table 1
Langmuir and Freundlich parameters for Amido black 10B obtained by non-linear regression analysis.

Isotherm model	Parameters	279.15 K		297.15 K		313.15 K	
		FF	MW	FF	MW	FF	MW
Langmuir	q_m (mg/g)	320.8	299.2	339.2	286.1	368.4	382.1
	α_L (L/mg)	0.59	0.83	0.94	0.14	0.95	0.97
	SEE	28.61	44.50	50.27	37.28	75.59	41.73
Freundlich	K_F [(mg/g) (L/mg)$^{1/n}$]	131.8	135.5	178.1	88.9	204.4	190.0
	n	3.44	3.03	5.06	3.94	5.04	2.86
	SEE	23.84	35.31	44.35	7.79	53.42	34.88

materials could be easily separated by rare earth permanent magnets or commercially available magnetic separators (Fig. 5).

3.2. Effect of solution pH on the adsorption process

pH is an important parameter significantly affecting the adsorption processes. To study the effect of initial pH on the adsorption of Amido black 10 B on magnetic *Leptothrix* sheaths, batch adsorption experiments were performed at pH values between 2 and 10 using 100 mg/L dye solution at 27 rpm stirrer speed and 24 °C (297.15 K) for 150 min. Fig. 6 shows the dye removal efficiency (%) profile of MLS over a pH range studied. The percent removal of the dye decreased significantly with the increase in initial pH of the solution as Amido black 10B is anionic in nature [4]. Better adsorption took place at low pH. Hence, all further experiments were conducted at the initial pH of 2.

Table 3
Thermodynamic parameters for both type magnetized *Leptothrix* sheaths.

Adsorbent	ΔH° (kJ/mol)	ΔS° (kJ/mol/K)	ΔG° (kJ/mol)		
			279.15 K	297.15 K	313.15 K
FF	27.161	0.193	−27.285	−28.618	−34.100
MW	8.230	0.128	−28.786	−26.555	−33.685

3.3. Adsorption isotherms, kinetics and thermodynamics

The dye adsorption on both types of the magnetically modified *Leptothrix* sheaths was tested with a water soluble organic dye Amido black 10B at 279.15 K, 297.15 K and 313.15 K. All experiments were carried out at pH 2 where maximum adsorption was achieved. Dye adsorption on both tested magnetic biosorbents was analyzed by two commonly used adsorption isotherm models, namely the Langmuir and Freundlich ones. The fitting of experimental data to each isotherm model was assessed on the basis of standard error of estimate (SEE). 95% of dye content (100 mg/L) was adsorbed within 5 min in both cases of magnetically modified *Leptothrix*. Although the adsorption equilibrium was reached within 15 min, incubation time was set to 150 min. The equilibrium adsorption isotherm models for both tested materials are shown in Fig. 7. The adsorption of Amido black 10B could be well described by the Freundlich model; the values of calculated coefficients are shown in Table 1. The observed maximum adsorption capacity of both types of magnetized materials (MW and FF) with Amido black 10B at room temperature were 286.1 and 339.2 mg of dye per 1 g of adsorbent at pH 2, respectively.

The fitting of experimental kinetic data to the pseudo-first-order and pseudo-second-order kinetic models was evaluated on the basis of obtained correlation coefficients and calculated q_e values; kinetic parameters are summarized in Table 2. The adsorption process followed the pseudo-second-order kinetic model.

Thermodynamic parameters were calculated as described recently [20]. As can be seen from the Table 3, the Amido black 10B adsorption on both FF-MLS and MW-MLS adsorbents is a spontaneous (negative value of Gibbs energy) and endothermic (positive value of enthalpy) process. Positive value of entropy indicates an increase in degree of freedom of adsorbed species.

The described procedure for the removal of Amido black 10B employs inexpensive biomaterial produced also during biological water treatment (removal of iron and manganese); the biomass of iron bacteria formed during the process has to be periodically removed. Currently the potential application of this “biological waste” is studied in several countries [13]. The adsorption capacity of magnetic derivative of *Leptothrix* sp. sheaths was quite high, as can be seen from Table 4 where other adsorbents for Amido black 10B are summarized, together with their maximum adsorption capacities.

Table 2
Values of the rate constants, capacities and regression coefficients from pseudo-first-order and pseudo-second-order kinetic models.

Adsorbent	C_{tot} (mg/L)	q_e (mg/g)	Pseudo-first-order model			Pseudo-second-order model		
			q_e (mg/g)	k_1 (1/min)	R^2	q_e (mg/g)	k_2 (g/mg min)	R^2
FF	100	48	1.4	0.0125	0.9431	47.4	0.0742	0.9999
	500	232	73.1	0.0040	0.8523	232.6	0.0023	0.9998
MW	100	58	2.2	0.0170	0.8735	57.8	0.0491	0.9999
	500	276	48.8	0.0156	0.9337	277.8	0.0014	0.9997

Table 4
Examples of adsorbents for Amido black 10B removal.

Adsorbent	q_m (mg/g)	Conditions	Other comments	References
Porous chitosan aerogels doped with graphene oxide	573.5	At 20 °C	P-2-O model followed	[24]
Leptothrix sheaths modified with magnetic fluid	339.2	pH 2 and 24 °C	Endothermic process, Freundlich and P-2-O models followed	Present study
Cross-linked chitosan/bentonite composite	323.6	pH 2 and 20 °C	Endothermic process, Langmuir and P-2-O models followed	[25]
Leptothrix sheaths modified with microwave-synthesized magnetic iron oxides	286.1	pH 2 and 24 °C	Endothermic process, Freundlich and P-2-O models followed	Present study
Mesoporous carbon	270.0	pH 7 and 20 °C	Freundlich model followed	[26]
Polyaniline/iron oxide composite	147.1	At 30 °C	Endothermic process, Freundlich and P-2-O models followed	[27]
Hen feather	88.9	pH 3 and 30 °C	Freundlich model followed	[9]
Kluyveromyces marxianus cells modified with magnetic fluid	29.9	RT	Langmuir model followed	[28]
Fly ash	18.9	At 20 °C	Endothermic process, Freundlich and P-2-O models followed	[29]
Saccharomyces cerevisiae subsp. *uvarum* cells modified with magnetic fluid	11.6	RT	Langmuir model followed	[30]
Palm flower activated carbon	3.8	At 27 °C	Endothermic process, Freundlich and P-2-O models followed	[31]

Notes: RT=room temperature, P-2-O=pseudo-second-order kinetic model.

4. Conclusion

Microwave synthesized iron oxide nano- and microparticles, and water-based magnetic fluid were used for rapid magnetic modification of non-magnetic native *Leptothrix* sheaths. The magnetically responsive materials were used as magnetic adsorbents for the removal of Amido black 10B in a batch system. Maximum adsorption of dye appeared at pH 2. The adsorption kinetics followed the pseudo-second-order kinetic model. It is clearly evident that magnetic *Leptothrix* sheaths have high adsorption capacity towards Amido black 10B dye. The results obtained show that the magnetic *Leptothrix* derivatives are efficient and biocompatible magnetically responsive materials which can substantially improve and simplify biotechnology and environmental technology processes.

Acknowledgements

This research was supported by the Czech Science Foundation (Grant No. 14-11516S), Ministry of Education, Youth and Sports of the CR (projects LD14075, LO1305 and LM2015073) and the Bulgarian National Science Fund of Ministry of Education and Science (project T02-17/2014).

References

[1] M. Ghaedi, E. Nazari, R. Sahraie, M.K. Purkait, Kinetic and isotherm study of Bromothymol Blue and Methylene blue removal using Au-NP loaded on activated carbon, Desalin. Water Treat. 52 (2013) 5504–5512.
[2] P. Monash, G. Pugazhenthi, Removal of crystal violet dye from aqueous solution using calcined and uncalcined mixed clay adsorbents, Separat. Sci. Technol. 45 (2009) 94–104.
[3] M. Ghaedi, H.A. Larki, S.N. Kokhdan, F. Marahel, R. Sahraei, A. Daneshfar, M.K. Purkait, Synthesis and characterization of zinc sulfide nanoparticles loaded on activated carbon for the removal of methylene blue, Environ. Prog. Sustain Energy 32 (2013) 535–542.
[4] A. Garg, M. Mainrai, V.K. Bulasara, S. Barman, Experimental investigation on adsorption of Amido black 10B dye onto zeolite synthesized from fly ash, Chem. Eng. Commun. 202 (2015) 123–130.
[5] M. Sheibani, M. Ghaedi, F. Marahel, A. Ansari, Congo red removal using oxidized multiwalled carbon nanotubes: kinetic and isotherm study, Desalin. Water Treat. 53 (2015) 844–852.
[6] M. Ghaedi, M. Ghayedi, S.N. Kokhdan, R. Sahraei, A. Daneshfar, Palladium, silver, and zinc oxide nanoparticles loaded on activated carbon as adsorbent for removal of bromophenol red from aqueous solution, J. Ind. Eng. Chem. 19 (2013) 1209–1217.
[7] M. Ghaedi, A. Ansari, M.H. Habibi, A.R. Asghari, Removal of malachite green from aqueous solution by zinc oxide nanoparticle loaded on activated carbon: kinetics and isotherm study, J. Ind. Eng. Chem. 20 (2014) 17–28.
[8] D. Charumathi, N. Das, Packed bed column studies for the removal of synthetic dyes from textile wastewater using immobilised dead *C. tropicalis*, Desalination 285 (2012) 22–30.
[9] A. Mittal, V. Thakur, V. Gajbe, Adsorptive removal of toxic azo dye Amido Black 10B by hen feather, Environ. Sci. Pollut. Res. 20 (2013) 260–269.
[10] D.H. Bergey, J.G. Holt, Sheathed bacteria, in: J.G. Holt (Ed.)Bergey's manual of systematic bacteriology, The Williams & Wilkins Co., Baltimore, 1994, pp. 477–482.
[11] A.K. Gupta, M. Gupta, Synthesis and surface engineering of iron oxide nanoparticles for biomedical applications, Biomaterials 26 (2005) 3995–4021.
[12] M. Sawayama, T. Suzuki, H. Hashimoto, T. Kasai, M. Furutani, N. Miyata, H. Kunoh, J. Takada, Isolation of a *Leptothrix* strain, OUMS1, from ocherous deposits in groundwater, Curr. Microbiol. 63 (2011) 173–180.
[13] T. Kunoh, H. Kunoh, J. Takada, Perspectives on the biogenesis of iron oxide complexes produced by *Leptothrix*, an iron-oxidizing bacterium and promising industrial applications for their functions, J. Microb. Biochem. Technol. 7 (2015) 419–426.
[14] T. Kunoh, H. Hashimoto, T. Suzuki, N. Hayashi, K. Tamura, M. Takano, H. Kunoh, J. Takada, Direct adherence of Fe(III) particles onto sheaths of *Leptothrix* sp. strain OUMS1 in culture, Minerals 6 (2016) (Article No. 4).
[15] S. Veleva, R. Angelova, L. Stoyanov, V. Groudeva, D. Kovacheva, M. Mladenov, R. Raicheff, Biogenic iron oxide-based nanocomposites electrodes for hybrid battery-supercapacitor systems, Nanosci. Nanotechnol. 14 (2014) 50–52.
[16] R. Massart, Preparation of aqueous magnetic liquids in alkaline and acidic media, IEEE Trans. Magn. 17 (1981) 1247–1248.
[17] H. Kiwada, J. Sato, S. Yamada, Y. Kato, Feasibility of magnetic liposomes as a targeting device for drugs, Chem. Pharm. Bull. 34 (1986) 4253–4258.
[18] I. Safarik, M. Safarikova, One-step magnetic modification of non-magnetic solid materials, Int. J. Mater. Res. 105 (2014) 104–107.
[19] E. Baldikova, D. Politi, Z. Maderova, K. Pospiskova, D. Sidiras, M. Safarikova, I. Safarik, Utilization of magnetically responsive cereal by-product for organic dye removal, J. Sci. Food Agric. 96 (2016) 2204–2214.
[20] Z. Maderova, E. Baldikova, K. Pospiskova, I. Safarik, M. Safarikova, Removal of dyes by adsorption on magnetically modified activated sludge, Int. J. Environ. Sci. Technol. 13 (2016) 1653–1664.
[21] B.Z. Zheng, M.H. Zhang, D. Xiao, Y. Jin, M.M.F. Choi, Fast microwave synthesis of Fe_3O_4 and Fe_3O_4/Ag magnetic nanoparticles using Fe^{2+} as precursor, Inorg. Mater. 46 (2010) 1106–1111.
[22] E. Mosiniewicz-Szablewska, M. Safarikova, I. Safarik, Magnetic studies of ferrofluid-modified spruce sawdust, J. Phys. D: Appl. Phys. 40 (2007) 6490–6496.
[23] E. Mosiniewicz-Szablewska, M. Safarikova, I. Safarik, Magnetic studies of ferrofluid-modified microbial cells, J. Nanosci. Nanotechnol. 10 (2010) 2531–2536.
[24] Y. Wang, G. Xia, C. Wu, J. Sun, R. Song, W. Huang, Porous chitosan doped with graphene oxide as highly effective adsorbent for methyl orange and amido black 10B, Carbohydr. Polym. 115 (2015) 686–693.
[25] Q. Liu, B. Yang, L. Zhang, R. Huang, Adsorption of an anionic azo dye by cross-linked chitosan/bentonite composite, Int. J. Biol. Macromol. 72 (2015) 1129–1135.
[26] J. Galán, A. Rodríguez, J.M. Gómez, S.J. Allen, G.M. Walker, Reactive dye adsorption onto a novel mesoporous carbon, Chem. Eng. J. 219 (2013) 62–68.

[27] R. Ahmad, R. Kumar, Conducting polyaniline/iron oxide composite: a novel adsorbent for the removal of amido black 10B, J. Chem. Eng. Data 55 (2010) 3489–3493.
[28] I. Safarik, L.F.T. Rego, M. Borovska, E. Mosiniewicz-Szablewska, F. Weyda, M. Safarikova, New magnetically responsive yeast-based biosorbent for the efficient removal of water-soluble dyes, Enzym. Microb. Technol. 40 (2007) 1551–1556.
[29] D. Sun, X. Zhang, Y. Wu, X. Liu, Adsorption of anionic dyes from aqueous solution on fly ash, J. Hazard. Mater. 181 (2010) 335–342.
[30] M. Safarikova, L. Ptackova, I. Kibrikova, I. Safarik, Biosorption of water-soluble dyes on magnetically modified *Saccharomyces cerevisiae* subsp. *uvarum* cells, Chemosphere 59 (2005) 831–835.
[31] S. Nethaji, A. Sivasamy, Adsorptive removal of an acid dye by lignocellulosic waste biomass activated carbon: equilibrium and kinetic studies, Chemosphere 82 (2011) 1367–1372.

Příloha 16:

Leptothrix sp. sheats modified with iron oxide particles: magnetically responsive, high aspect ratio functional material

Safarik I, Angelova R, Baldikova E, Pospiskova K, Safarikova M

Mater. Sci. Eng. C 71, **2017**, 1342-1346

Materials Science and Engineering C 71 (2017) 1342–1346

Contents lists available at ScienceDirect

Materials Science and Engineering C

journal homepage: www.elsevier.com/locate/msec

Short communication

Leptothrix sp. sheaths modified with iron oxide particles: Magnetically responsive, high aspect ratio functional material

Ivo Safarik [a,b,c,*], Ralitsa Angelova [a,d,e], Eva Baldikova [b,f], Kristyna Pospiskova [c], Mirka Safarikova [a,b]

[a] Department of Nanobiotechnology, Biology Centre, ISB, CAS, Na Sadkach 7, 370 05 Ceske Budejovice, Czech Republic
[b] Global Change Research Institute, CAS, Na Sadkach 7, 370 05 Ceske Budejovice, Czech Republic
[c] Regional Centre of Advanced Technologies and Materials, Palacky University, Slechtitelu 27, 783 71 Olomouc, Czech Republic
[d] Department of General and Industrial Microbiology, Faculty of Biology, Sofia University "St. Kliment Ohridski", 8 Dragan Tsankov Blvd., 1164 Sofia, Bulgaria
[e] Laboratory Microwave Magnetics, Institute of Electronics, Bulgarian Academy of Sciences, 72 Tzarigradsko Chaussee Blvd., 1784 Sofia, Bulgaria
[f] Department of Applied Chemistry, Faculty of Agriculture, University of South Bohemia, Branisovska 1457, 370 05 Ceske Budejovice, Czech Republic

ARTICLE INFO

Article history:
Received 11 August 2016
Received in revised form 27 September 2016
Accepted 23 October 2016
Available online 26 October 2016

Keywords:
Leptothrix
Magnetic modification
Iron oxide
High aspect ratio material

ABSTRACT

Smart materials of biological origin are attracting a lot of attention nowadays, especially as catalysts, carriers or adsorbents. Among them, magnetically modified biomaterials are especially important due to their response to external magnetic field. This report demonstrates that naturally occurring micrometer sized, high aspect ratio material (native and autoclaved *Leptothrix* sp. sheaths) efficiently bind synthetically prepared magnetite and maghemite nanoparticles and their aggregates. Magnetic modification of *Leptothrix* sheaths enables to prepare a promising material for advanced biotechnology and environmental technology applications. The prepared magnetically responsive sheaths were tested as inexpensive adsorbent for crystal violet removal from aqueous solutions. The observed maximum adsorption capacity was 243.1 mg of dye per 1 g of adsorbent.

1. Introduction

Various microorganisms are involved in the process of biomineralization which leads to the formation of specific inorganic solid deposits with specific functions. A group of Fe-/Mn-oxidizing bacteria, such as *Gallionella*, *Sphaerotilus*, *Leptothrix*, and *Clonothrix*, are often found in ocherous ferromanganese deposits that form in neutral waters of lakes, ponds, swamps, drainage ditches, and springs [1]. Their metal-oxidizing ability is important in biogeochemical cycling of these metals.

Leptothrix sp. is able to accumulate Fe and Mn ions into their sheaths; this ability is employed for removal of iron and manganese from groundwater to clean water for drinking purposes. This technology is used in many water-treatment plants all over the world. As a consequence, huge amounts of Fe-/Mn-rich precipitates are formed. Recently, an intensive research in Japan has shown that this waste material can have very interesting application potential [2].

Leptothrix sp. forms filamentous-looking microtubular, cell-encasing sheaths containing large amounts of oxidized Fe or Mn nanoparticles. The metal encrustation of *Leptothrix* sheaths results from the interaction of the sheath skeleton active groups originating from polysaccharides, proteins, and lipids, and aqueous-phase cations. There is a strong correlation between the presence of acidic polysaccharides with carboxyl functional groups binding metal ions and the distribution of iron oxyhydroxides in *Leptothrix* sheaths. Actively dividing *Leptothrix* cells also excrete exopolymers from their surface, providing a platform for the formation of Fe-enriched sheaths [3,4].

It was observed recently that not only metal ions, but also Fe(III) based particles formed in uninoculated culture medium for *Leptothrix* cultivation bind spontaneously onto the sheaths of both living and dead *Leptothrix* culture. These results show that a direct adherence of Fe(III) particles onto sheaths has to be considered as an alternative way of sheath encrustation in addition to regular interactions between bacterial polymers and metal ions [3].

Based on the above mentioned findings it can be expected that *Leptothrix* sheaths could also interact with synthetically prepared iron oxide nano- and microparticles. If magnetic particles bind on *Leptothrix* sheaths, the whole *Leptothrix* – iron oxide particles complex will exhibit response to external magnetic field. Experiments with magnetic fluid and microwave-synthesized magnetic iron oxide particles have confirmed our expectations. Magnetically responsive *Leptothrix* sheaths

Abbreviations: α_L, Langmuir constant (L/mg); ATR, attenuated total reflectance; C_{eq}, concentration of free (unbound) dye in the supernatant (μg/mL); C_{tot}, total (initial) concentration of dye (μg/mL); EDS, energy dispersive X-ray spectra; FF, ferrofluid; FTIR, Fourier transform infrared spectroscopy; K_F, Freundlich isotherm constant [(mg/g)(L/mg)$^{1/n}$]; P-1-O, pseudo-first order; P-2-O, pseudo-second order; q_{eq}, amount of dye bound to the unit mass of the adsorbent (mg/g); q_m, maximum adsorption capacity calculated by Langmuir equation (mg/g); RT, room temperature; SEM, scanning electron microscopy; SEE, standard error of estimate.

* Corresponding author at: Department of Nanobiotechnology, Biology Centre, ISB, CAS, Na Sadkach 7, 370 05 Ceske Budejovice, Czech Republic.
E-mail address: ivosaf@yahoo.com (I. Safarik).

http://dx.doi.org/10.1016/j.msec.2016.10.056
0928-4931/

can be successfully used also as an inexpensive adsorbent for selected pollutant removal. Application potential of this material has been demonstrated via crystal violet adsorption study.

2. Materials and methods

2.1. Materials

The natural ocherous sediment containing *Leptothrix* sp. sheaths was collected using glass vessels from an unnamed stream in Ceske Budejovice, Czech Republic (48°58′22.57″N, 14°27′39.93″E) during the end of February 2016. Sample was concentrated during collection by letting the biomaterial settle down and decanting overlying water. Subsequently, the sediment was promptly transported to the laboratory, where it was repeatedly washed with water. Ferrous sulfate heptahydrate, sodium hydroxide and other common chemicals were obtained from Lach-Ner, Czech Republic. Magnetic fluid stabilized with perchloric acid was prepared using a standard procedure [5]. The relative magnetic fluid concentration (39.5 mg/mL) is given as the maghemite content determined by a colorimetric method [6].

2.2. Preparation of iron oxide microparticles using microwave-assisted synthesis

One gram of $FeSO_4 \cdot 7\ H_2O$ was dissolved in 100 mL of water in 800-mL glass beaker. A solution of sodium hydroxide (1 mol/L) was slowly added with continuous stirring until the pH reached the value ca 12. During this process, a precipitate of iron hydroxides was formed. After adjusting the volume to 200 mL with water, the beaker containing the precipitate was placed into a regular kitchen microwave oven (700 W, 2450 MHz) and treated by microwaves at the maximum power for 10 min. The formed suspension of magnetically responsive iron oxide nano- and microparticles was thoroughly washed with water [7].

2.3. Modification of Leptothrix sheaths with magnetic iron oxide nano- and microparticles

400 mL of completely sedimented *Leptothrix* sheaths (earth gravity, 24 h; either native or sterilized at 121 °C for 20 min., pH around 7.0) was mixed with 120 mL of iron oxide suspension in water (1 part of completely sedimented microwave synthesized iron oxide nano- and microparticles and 4 parts of water, pH 7.0). The mixture was mixed

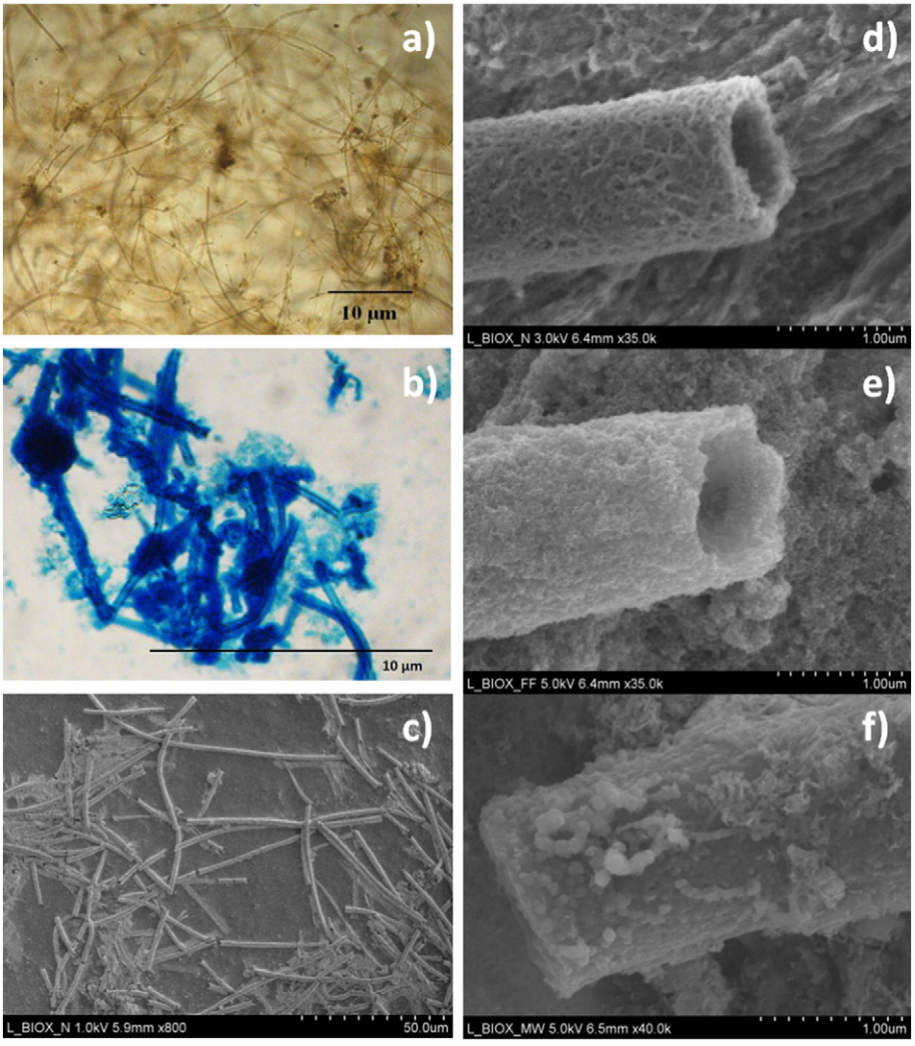

Fig. 1. Optical microscopy of native *Lepthothrix* sp. sheaths (a) and native sheaths after Perls' Prussian Blue Staining (b); scanning electron microscopy of native *Lepthothrix* sp. sheaths (c and d); sheaths modified with magnetic fluid (e) and sheaths modified with microwave synthesized magnetite particles (f).

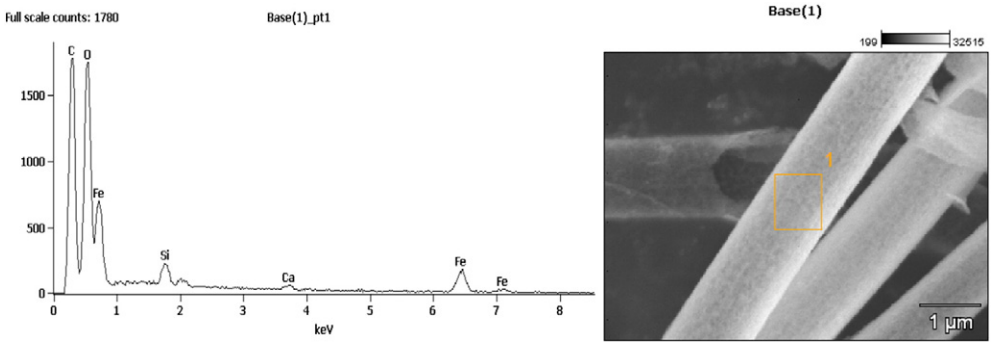

Fig. 2. Energy-dispersive X-ray spectroscopy of native *Leptothrix* sheaths.

on a sample mixer (Dynal Biotech Inc., NY, USA; 27 rpm) for 3 h at room temperature, and then, magnetically modified sheaths were repeatedly washed with water (using a magnetic separator) until nonmagnetic material was washed out. Next, magnetized *Leptothrix* sheaths were used to prepare a suspension (1 part of completely sedimented (earth gravity, 24 h) sheaths and 4 parts of distilled water) for the adsorption experiments. The prepared magnetically responsive sheaths were stored in water at 4 °C.

2.4. Modification of Leptothrix sheaths with magnetic fluid

400 mL of completely sedimented *Leptothrix* sheaths (the same as above) was mixed with 20 mL of perchloric acid stabilized magnetic fluid. After mixing on a sample mixer (27 rpm) for 3 h at room temperature, the modified sheaths were washed with water. Next, the same suspension as above was prepared for adsorption experiments. The prepared magnetically responsive material was stored in water at 4 °C.

2.5. Characterization of magnetically modified Leptothrix sheaths

The morphology and structure of both native and magnetically modified *Leptothrix* sheaths was studied by optical microscopy and scanning electron microscopy (SEM). The samples were analyzed using a Hitachi SU6600 scanning electron microscope (Hitachi, Tokyo, Japan) with accelerating voltage 1, 3 or 5 kV. Energy dispersive X-ray spectra (EDS) were acquired in SEM using Thermo Noran System 7 (Thermo Scientific, Waltham, MA, USA) with Si(Li) detector (accelerating voltage of 10 kV, acquisition time 300 s).

Characteristic functional groups of samples were identified by Fourier transform infrared (FTIR) spectroscopy. Absorption spectra were measured using Thermo Scientific Nicolet iS5 FTIR spectrometer (Thermo Nicolet Corp., Madison, WI, USA) with iD Foundation accessory (ZnSe crystal, range 4000–650 cm^{-1}, 32 scans, resolution 4 cm^{-1}, N_2 atmosphere). The IR absorption spectra are presented in transmittance after advanced attenuated total reflectance (ATR) and automatic baseline corrections.

2.6. Adsorption of dyes on magnetically modified Leptothrix sheaths

One mL of settled magnetic *Leptothrix* suspensions (corresponding to 19 mg of dried magnetically modified material) in a series of test tubes was mixed with 1–8 mL portion of stock water solution of tested dye (1 mg/mL; pH 10) and the total volume of the solutions was filled up to 10.0 mL with water (pH 10). The suspensions were mixed on a rotary mixer (Dynal, Norway, 27 rpm) for 2.5 h at room temperature. Then the magnetic adsorbents were separated from the suspensions using a magnetic separator (MPC-1 or MPC-6, Dynal, Norway) and the clear supernatants were used for the spectrophotometric measurements. The concentration of free (unbound) dye in the supernatants (C_{eq}) was determined from the calibration curve. The amount of dye bound to the unit mass of the adsorbent (q_{eq}) was calculated using the following formula:

$$q_{eq} = (C_{tot} - C_{eq})/1.9 (\mathrm{mg/g}) \quad (1)$$

where C_{tot} is the total (initial) concentration of dye (μg/mL) used in the

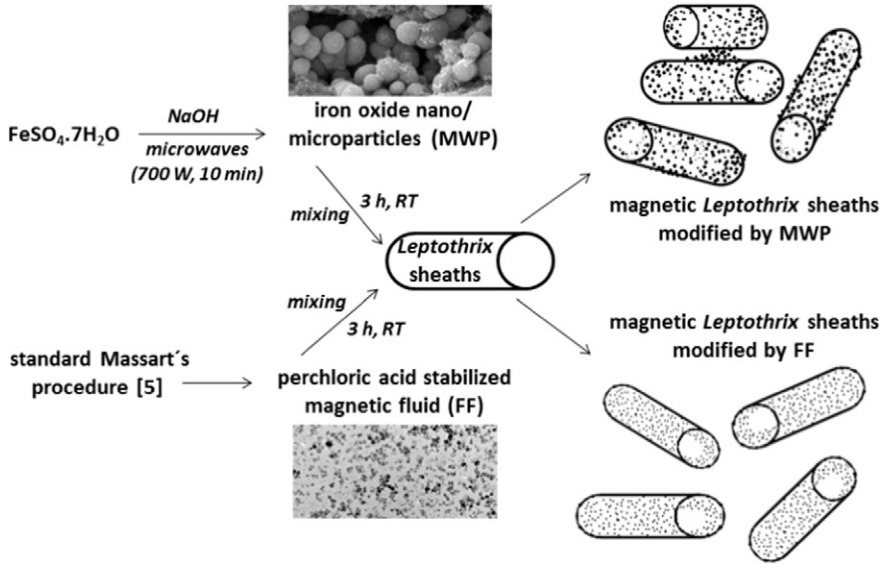

Fig. 3. Reaction scheme showing the process of magnetic modification of native *Lepthothrix* sp. sheaths.

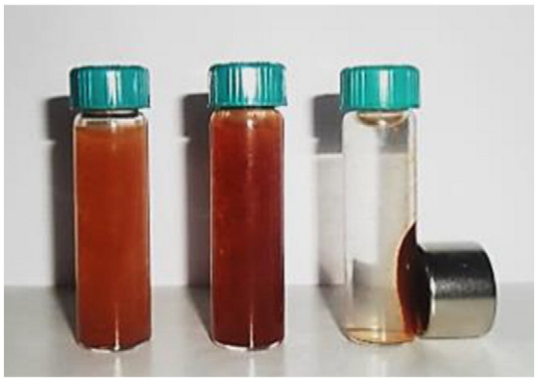

Fig. 4. A demonstration of magnetic separation of magnetically modified sheaths. Appearance of native *Leptothrix* sheaths suspension (left), suspension of sheaths after magnetic modification with magnetic fluid (middle) and demonstration of magnetic separation of magnetically modified sheaths (right).

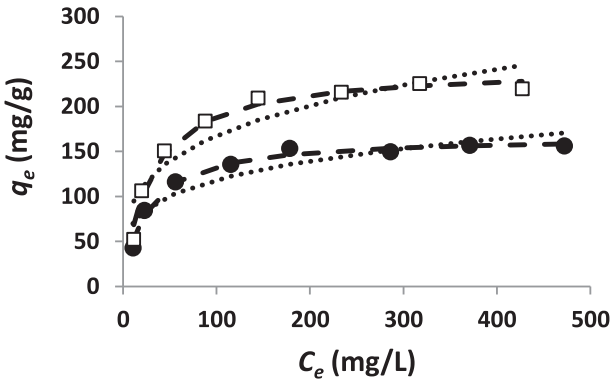

Fig. 6. Lagmuir (- - -) and Freundlich (.....) equilibrium adsorption isotherms of crystal violet on *Leptothrix* sheaths modified with microwave synthesized magnetite (□) and magnetic fluid (●).

experiment. The value q_{eq} was expressed in mg of adsorbed dye per 1 g of adsorbent. The equilibrium adsorption data were fitted to Langmuir and Freundlich isotherms models using nonlinear analysis (solver add-in function of the Microsoft excel), and kinetic data were analyzed with pseudo-first and pseudo-second order kinetic models, as described [8,9]. All adsorption experiments were performed in triplicate at pH 10 and room temperature.

3. Results and discussion

Native *Leptothrix* sheaths were collected from natural water sources. Using both optical and scanning electron microscopy, long sheaths (with the lengths often exceeding 50 μm) are clearly visible (Fig. 1a, c). At higher magnification a typical structure of the microtubules can be seen (Fig. 1d); the typical diameter of the sheaths is 1–1.5 μm.

Energy-dispersive X-ray spectroscopy, as well as the Perls' Prussian blue staining verified the presence of iron in the native *Leptothrix* sheaths (Figs. 1b and 2).

Sheaths interaction with synthetic iron oxide nano- and microparticles was studied using two types of materials (see the reaction scheme in Fig. 3). The first material was synthesized from ferrous sulfate at high pH by the action of microwave irradiation. The use of a single iron(II) salt as a precursor during the microwave synthesis makes this procedure substantially simpler, in comparison with analogous procedures where both iron(II) and iron(III) salts have been used simultaneously [7,10]. Microwave-assisted synthesis resulted in the formation of iron oxide nanoparticles with diameters ranging between ca 25 and 100 nm; during synthesis, the nanoparticles form micrometer-sized stable aggregates (maximum aggregate size ca 20 μm). XRD pattern of the synthesized magnetic particles shows features typical of magnetite nano- to microparticles; further analysis using Mössbauer spectroscopy confirmed the presence of non-stoichiometric magnetite [11]. Water based magnetic fluid stabilized with perchloric acid [5], composed of maghemite nanoparticles with diameters ranging between 5 and 20 nm and a mean particle diameter ca 13 nm [12,13] was used as the second iron oxide material.

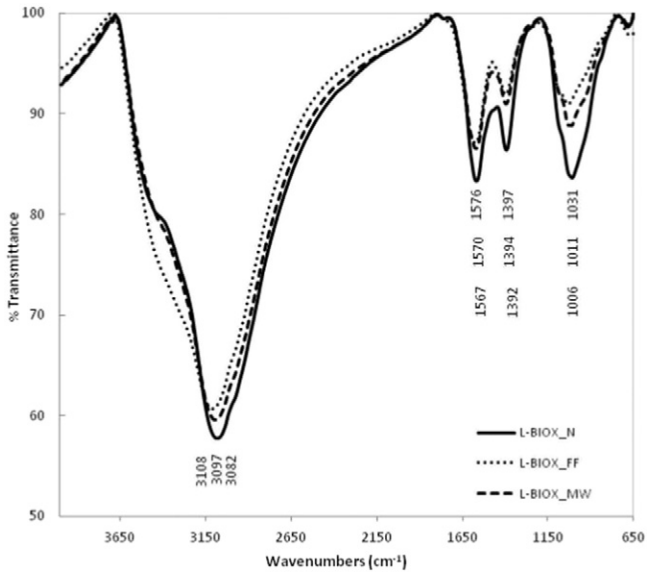

Fig. 5. Fourier transform infrared spectra of native (____) and magnetically modified (....., magnetic fluid; - - - - - - -, microwave synthesized magnetite) *Leptothrix* sheaths.

Thorough mixing of water suspension of both native and autoclaved *Leptothrix* sheaths with both studied materials led to the deposition of iron oxide nanoparticles and their aggregates onto sheath surface, as confirmed by scanning electron microscopy (SEM) (Fig. 1e, f); maghemite nanoparticles covered the *Leptothrix* sheath surface homogeneously, while magnetite particles occurred in irregularly located clusters. In all cases, the binding of synthetic iron oxide particles was firm and stable for at least two months. No difference in the particles binding to the native and autoclaved sheaths was observed. Energy-dispersive X-ray spectra of magnetically modified sheaths were similar to spectra of native sheaths (Fig. 2).

Due to the fact that both magnetite and maghemite particles exhibit ferrimagnetic behavior, modified *Leptothrix* sheaths can be easily separated by rare earth permanent magnets or commercially available magnetic separators (Fig. 4).

The functional groups of both native and magnetically modified *Leptothrix* sp. biomass were detected by using FTIR spectra in the range of 650–4000 cm^{-1}. All three samples showed similar pattern with only some small shifts of band positions, which can be caused by a slight effect of deposited iron oxide particles on the native *Leptothrix* sheaths (Fig. 5). The broad and strong absorption vibration around 3100 cm^{-1} can be attributed to the —OH stretching vibrations of the polysaccharide chains. The deprotonated carboxyl group shows two strong bands near 1400 and 1570 cm^{-1} for the symmetric and the

Table 1
Langmuir and Freundlich parameters for crystal violet adsorption obtained by non-linear analysis.

Isotherm model	Parameters	MF	MW
Langmuir	q_m (mg/g)	166.6	243.1
	α_L (L/mg)	0.040	0.035
	SEE	4.80	8.73
Freundlich	K_F [(mg/g) (L/mg)$^{1/n}$]	40.33	50.05
	N	4.27	3.81
	SEE	16.40	25.29

Table 2
Values of rate constants, capacities and regression coefficients from pseudo-first and pseudo-second-order kinetic models.

Adsorbent	C_{tot} (mg/L)	$q_{eq\ exp.}$ (mg/g)	Pseudo-first-order model			Pseudo-second-order model		
			q_{eq} (mg/g)	k_1 (1/min)	R^2	q_{eq} (mg/g)	k_2 (g/mg min)	R^2
FF	100	49.0	6.0	0.0315	0.6461	48.1	0.0307	0.9998
MW	100	58.5	2.5	0.0323	0.6302	57.8	0.3325	0.9999

asymmetric stretching vibration, respectively. Magnetic iron oxides have a distinct spectrum within the so-called Fe–O range (ca 350–1000 cm^{-1}); the band around 1010 cm^{-1} can be assigned to the presence of γ-FeOOH in the sample [14–16].

The adsorption properties of the magnetically modified *Leptothrix* sheaths were tested with a water soluble organic dye crystal violet, belonging to triarylmethane group. The dye adsorption on both types of magnetically modified biosorbent at room temperature and pH 10 was examined. It was shown in preliminary experiments that the adsorption process was very fast; the adsorption equilibrium was reached within 15–30 min. The equilibrium adsorption isotherms (incubation time 2.5 h) for both adsorbents are shown in Fig. 6; the experimental data analysis was performed using Langmuir and Freundlich isotherm equations. The adsorption of crystal violet could be well described by the Langmuir model; the values of calculated coefficients are shown in Table 1. The values of maximum adsorption capacities for crystal violet at pH 10 were 243.1 mg of dye per 1 g of dry adsorbent for sheaths modified with microwave synthesized magnetite particles, and 166.6 mg of dye per 1 g of dry adsorbent for sheaths modified with magnetic fluid, respectively.

The fitting of experimental kinetic data to pseudo-first (P-1-O) and pseudo-second order (P-2-O) kinetic models was evaluated on the basis of obtained correlation coefficients and calculated q_{eq} values. As summarized in Table 2, the correlation coefficients for both tested materials obtained from P-2-O model are much higher (>0.999) than those from P-1-O kinetic model (0.630–0.646). Simultaneously, the q_{eq} values calculated from the P-2-O kinetic model ($q_{eq\ calc}$) approached more closely the experimental q_{eq} values ($q_{eq\ exp}$). Based on these results, it can be assumed that the adsorption process followed the pseudo-second-order kinetic model.

To conclude, *Leptothrix* sheaths spontaneously bound synthetic iron oxide nano- and microparticles and formed magnetically responsive material, which can be used for environmental technology and potential biotechnology applications. In addition to magnetic adsorbents described in present paper, this material could be used as a carrier for immobilization of biologically active compounds or as high aspect ratio micro-containers.

Acknowledgements

This research was supported by the Czech Science Foundation (Grant No. 14-11516S), Ministry of Education, Youth and Sports of the Czech Republic (projects LO1305 and LD14075) and the Bulgarian National Science Fund of Ministry of Education and Science (project T02-17/2014). The authors acknowledge the assistance provided by the Research Infrastructure NanoEnviCz, supported by the Ministry of Education, Youth and Sports of the Czech Republic under Project No. LM2015073.

References

[1] W.C. Ghiorse, Biology of iron- and manganese-depositing bacteria, Annu. Rev. Microbiol. 38 (1984) 515–550.
[2] T. Kunoh, H. Kunoh, J. Takada, Perspectives on the biogenesis of iron oxide complexes produced by *Leptothrix*, an iron-oxidizing bacterium and promising industrial applications for their functions, J. Microb. Biochem. Technol. 7 (2015) 419–426.
[3] T. Kunoh, H. Hashimoto, T. Suzuki, N. Hayashi, K. Tamura, M. Takano, H. Kunoh, J. Takada, Direct adherence of Fe(III) particles onto sheaths of *Leptothrix* sp. strain OUMS1 in culture, Minerals 6 (1) (2016) (Article No. 4).
[4] C.S. Chan, S.C. Fakra, D.C. Edwards, D. Emerson, J.F. Banfield, Iron oxyhydroxide mineralization on microbial extracellular polysaccharides, Geochim. Cosmochim. Acta 73 (13) (2009) 3807–3818.
[5] R. Massart, Preparation of aqueous magnetic liquids in alkaline and acidic media, IEEE Trans. Magn. 17 (2) (1981) 1247–1248.
[6] H. Kiwada, J. Sato, S. Yamada, Y. Kato, Feasibility of magnetic liposomes as a targeting device for drugs, Chem. Pharm. Bull. 34 (10) (1986) 4253–4258.
[7] I. Safarik, M. Safarikova, One-step magnetic modification of non-magnetic solid materials, Int. J. Mater. Res. 105 (1) (2014) 104–107.
[8] E. Baldikova, D. Politi, Z. Maderova, K. Pospiskova, D. Sidiras, M. Safarikova, I. Safarik, Utilization of magnetically responsive cereal by-product for organic dye removal, J. Sci. Food Agric. 96 (6) (2016) 2204–2214.
[9] I. Safarik, N. Ashoura, Z. Maderova, K. Pospiskova, E. Baldikova, M. Safarikova, Magnetically modified *Posidonia oceanica* biomass as an adsorbent for organic dyes removal, Mediterr. Mar. Sci. 17 (2) (2016) 351–358.
[10] B.Z. Zheng, M.H. Zhang, D. Xiao, Y. Jin, M.M.F. Choi, Fast microwave synthesis of Fe_3O_4 and Fe_3O_4/Ag magnetic nanoparticles using Fe^{2+} as precursor, Inorg. Mater. 46 (10) (2010) 1106–1111.
[11] Z. Maderova, E. Baldikova, K. Pospiskova, I. Safarik, M. Safarikova, Removal of dyes by adsorption on magnetically modified activated sludge, Int. J. Environ. Sci. Technol. 13 (2016) 1653–1664.
[12] E. Mosiniewicz-Szablewska, M. Safarikova, I. Safarik, Magnetic studies of ferrofluid-modified spruce sawdust, J. Phys. D. Appl. Phys. 40 (21) (2007) 6490–6496.
[13] E. Mosiniewicz-Szablewska, M. Safarikova, I. Safarik, Magnetic studies of ferrofluid-modified microbial cells, J. Nanosci. Nanotechnol. 10 (4) (2010) 2531–2536.
[14] M. Shopska, Z.P. Cherkezova-Zheleva, D.G. Paneva, M. Iliev, G.B. Kadinov, I.G. Mitov, V.I. Groudeva, Biogenic iron compounds: XRD, Mossbauer and FTIR study, Cent. Eur. J. Chem. 11 (2) (2013) 215–227.
[15] M.G. Shopska, Z.P. Cherkezova-Zheleva, D.G. Paneva, V. Petkova, G.B. Kadinov, I.G. Mitov, Treatment of biogenic iron-containing materials, Croat. Chem. Acta 87 (2) (2014) 161–170.
[16] H.M. Khanlou, B.C. Ang, S. Talebian, M.M. Barzani, M. Silakhori, H. Fauzi, A systematic study of maghemite/PMMA nano-fibrous composite via an electrospinning process: synthesis and characterization, Measurement 70 (2015) 179–187.

5.2.10 Bakteriální celulóza

Na bakteriální celulózu, produkovanou bakterií *Komagataeibacter sucrofermentas,* bylo imobilizováno reaktivní barvivo ostazinová tyrkys, vyznačující se vysokou afinitou vůči planárním molekulám. Magnetická modifikace byla provedena inkubací s kyselou MK. Byla porovnávána schopnost odstraňovat planární molekulu krystalové violeti, a to jednak pomocí magnetické nativní, jednak pomocí magnetické bakteriální celulózy s imobilizovaným afinitním ligandem. Dle očekávání byla vypočtená hodnota maximální adsorpční kapacity bakteriální celulózy po imobilizaci (388,4 mg/g) výrazně vyšší než u té nemodifikované (179,4 mg/g). Adsorpční proces lze popsat Freundlichovým modelem, je spontánní a exotermní.

Magneticky modifikovaná bakteriální celulóza byla také testována jako nosič pro imobilizované buňky *S. cerevisiae* či modelový enzym trypsin. Kvasinkové buňky byly aktivovány, zesítěny glutaraldehydem a poté opakovaně využity jako celobuněčný biokatalyzátor pro hydrolýzu sacharózy. Nejvhodnější způsob imobilizace trypsinu spočíval v aktivaci a kovalentním navázáním na nosič. Vzniklý enzymo-bakteriální komplex lze použít 10x po sobě bez ztráty původní enzymové aktivity.

Příloha 17:

Magnetically modified bacterial celulose: a promising carrier for immobilization of affinity ligands, enzymes, and cells

Baldikova E, Pospiskova K, Ladakis D, Kookos IK, Koutinas AA, Safarikova M, Safarik I

Mater. Sci. Eng. C 71, **2017**, 29-33

Materials Science and Engineering C 71 (2017) 214–221

Contents lists available at ScienceDirect

Materials Science and Engineering C

journal homepage: www.elsevier.com/locate/msec

Magnetically modified bacterial cellulose: A promising carrier for immobilization of affinity ligands, enzymes, and cells

Eva Baldikova [a], Kristyna Pospiskova [b], Dimitrios Ladakis [c], Ioannis K. Kookos [c], Apostolis A. Koutinas [d], Mirka Safarikova [a,e], Ivo Safarik [a,b,e,*]

[a] Global Change Research Institute, CAS, Na Sadkach 7, 370 05 Ceske Budejovice, Czech Republic
[b] Regional Centre of Advanced Technologies and Materials, Palacky University, Slechtitelu 27, 783 71 Olomouc, Czech Republic
[c] Department of Chemical Engineering, University of Patras, 26504 Patras, Rio, Greece
[d] Department of Food Science and Human Nutrition, Agricultural University of Athens, Iera Odos 75, Athens 11855, Greece
[e] Department of Nanobiotechnology, Biology Centre, ISB, CAS, Na Sadkach 7, 370 05 Ceske Budejovice, Czech Republic

ARTICLE INFO

Article history:
Received 23 May 2016
Received in revised form 9 September 2016
Accepted 7 October 2016
Available online 8 October 2016

Keywords:
Bacterial cellulose
Komagataeibacter sucrofermentans
Copper phthalocyanine
Crystal violet
Yeast cells
Trypsin

ABSTRACT

Bacterial cellulose (BC) produced by *Komagataeibacter sucrofermentans* was magnetically modified using perchloric acid stabilized magnetic fluid. Magnetic bacterial cellulose (MBC) was used as a carrier for the immobilization of affinity ligands, enzymes and cells. MBC with immobilized reactive copper phthalocyanine dye was an efficient adsorbent for crystal violet removal; the maximum adsorption capacity was 388 mg/g. Kinetic and thermodynamic parameters were also determined. Model biocatalysts, namely bovine pancreas trypsin and *Saccharomyces cerevisiae* cells were immobilized on MBC using several strategies including adsorption with subsequent cross-linking with glutaraldehyde and covalent binding on previously activated MBC using sodium periodate or 1,4-butanediol diglycidyl ether. Immobilized yeast cells retained approximately 90% of their initial activity after 6 repeated cycles of sucrose solution hydrolysis. Trypsin covalently bound after MBC periodate activation was very stable during operational stability testing; it could be repeatedly used for ten cycles of low molecular weight substrate hydrolysis without loss of its initial activity.

1. Introduction

Cellulose is the most abundant macromolecule in nature and conventionally found in plants as a structural component forming the lignocellulosic structure together with lignin and hemicellulose. Bacterial cellulose (BC), produced by bacterial strains of the genera *Acetobacter*, demonstrates high purity, high water holding capacity, high hydrophilicity, high crystallinity, high porosity and comparable mechanical behavior to other complex and synthetically produced polymers and fibers [1]. BC is nowadays considered a functional biomaterial with numerous applications in various fields including skin tissue repair [2], potential scaffold for tissue-engineering [3], wound healing applications [4], immobilization, paper manufacturing, cosmetics, dye decolorization [5] and as a thickening and stabilizing agent in the food industry [6]. One of the main disadvantages of industrial BC production is the high cost of manufacture mainly due to the commercial raw materials used in the formulation of fermentation media and the low productivity achieved during fermentation. To alleviate the former drawback, waste and by-product streams from various industrial sectors (e.g. the food industry, the biodiesel industry using oilseeds) could be used as low cost sources of nutrients [7]. For instance, the utilization of hydrolysates from confectionary industry waste streams or by-products from a sunflower-based biodiesel process (i.e. crude glycerol, sunflower meal hydrolysate) led to the production of around 13 g/L of BC [7].

Recently, diverse types of biological materials have been magnetically modified and used for various applications [8,9]. Also BC has already been converted into its magnetic derivatives using different approaches, e.g. by *in situ* thermal decomposition of iron(III) acetylacetonate under microwave irradiation [10] or by homogenizing the BC pellicle in the solution of ferrous and ferric salts, followed by the addition of sodium hydroxide [11]. Alternatively, magnetic bacterial cellulose (MBC) can be produced during the BC biosynthesis process in a culture medium containing dispersed magnetite nanoparticles [12].

The present work describes a new, extremely simple procedure to prepare magnetically responsive bacterial cellulose employing a simple entrapment of magnetic nanoparticles during the contact of BC with water-based magnetic fluid. MBC was used as an efficient carrier for the immobilization of affinity ligands, enzymes and cells.

Abbreviations: BC, bacterial cellulose; FF, ferrofluid; MBC, magnetic bacterial cellulose; PM-MBC, phthalocyanine-modified magnetic bacterial cellulose.

* Corresponding author.
E-mail address: safarik@nh.cas.cz (I. Safarik).

http://dx.doi.org/10.1016/j.msec.2016.10.009
0928-4931/

2. Materials and methods

2.1. Materials

Reactive copper phthalocyanine dye (Ostazin turquoise V-G; C.I. Reactive Blue 21) was supplied by Spolek pro chemickou a hutni vyrobu, Usti nad Labem, Czech Republic. Crystal violet (C.I. 42555), N_{α}-benzoyl-DL-arginine 4-nitroanilide hydrochloride (BAPNA), sodium (meta)periodate, 1,4-butanediol diglycidyl ether and glutaraldehyde were obtained from Sigma-Aldrich (St. Louis, MO, USA). Crystalline trypsin from bovine pancreas and anhydrous Na_2CO_3 were from Lachema (Brno, Czech Republic). Reagent for the measurement of glucose concentration was obtained from Biosystems (Barcelona, Spain). *Saccharomyces cerevisiae* cells (compressed baker's yeast) were purchased in a local market. Other common chemicals were from Lachner (Neratovice, Czech Republic). Crude glycerol used in this study was kindly provided by the biodiesel producer P. N. Pettas S. A. industry (Patras, Greece). The crude glycerol (92.4% w/w) of slightly higher purity was obtained via decanting of the original crude glycerol using separation funnels [13].

2.2. Bacterial production of bacterial cellulose

Bacterial cellulose was produced by the bacterial strain *Komagataeibacter sucrofermentans* DSM 15973. Bacterial stock cultures were maintained at −85 °C in cryovials with a respective ratio of commercial glycerol to preculture of 1:1. Liquid media for the preparation of inoculum and fermentation media consisted of (g/L): 20 carbon source; 5 peptone; 5 yeast extract; 2.7 Na_2HPO_4; 1.15 citric acid. In the case of the inocula, the carbon source used was glucose, while in the case of fermentation medium, crude glycerol was employed. The pH of the medium was adjusted to 6 with 5 M NaOH.

Fermentations were carried out at 30 °C in a 32 L PVC container with working volume of 2 L. The container was sterilized under Ultra Violet light for 20 min. The volume of the inocula was 10% (v/v). The container was statically incubated for 8 days. After the completion of fermentation, BC was removed from the culture broth and treated with 2 M NaOH to remove bacterial cells and subsequently washed repeatedly until a neutral pH was achieved.

2.3. Characterization of materials

The morphology and structure of bacterial cellulose samples was studied by optical microscopy (OM) and scanning electron microscopy (SEM). Samples were analyzed using a Hitachi SU6600 scanning electron microscope (Hitachi, Tokyo, Japan) with accelerating voltage 1 or 3 kV. Energy dispersive X-ray spectra (EDS) were acquired in SEM using Thermo Noran System 7 (Thermo Scientific, Waltham, MA, USA) with Si(Li) detector; accelerating voltage was 5 or 15 kV and acquisition time was 300 s.

Fourier transform infrared (FTIR) absorption spectra were measured using Thermo Scientific Nicolet iS5 FTIR spectrometer (Thermo Nicolet Corp., Madison, WI, USA) with iD Foundation accessory (ZnSe crystal, range 4000–650 cm^{-1}, 32 scans, resolution 4 cm^{-1}). The IR absorption spectra are presented in transmittance after advanced attenuated total reflectance (ATR) and automatic baseline corrections.

2.4. Magnetic modification of bacterial cellulose

BC was magnetically modified using perchloric acid stabilized magnetic fluid (ferrofluid, FF) prepared according to the described procedure [14]. 25 mL of distilled water and 5 mL of FF (c = 30.24 mg/mL) were added to 10 g of BC particles (prepared using a mixer), followed by incubation on rotator mixer (Dynal, Oslo, Norway) for 24 h. Prepared magnetically responsive BC was thoroughly washed with water to remove excess magnetic fluid, sieved with a sieve with 0.7 × 0.7 mm opening, and stored at 4 °C. In the same way, cut pieces of BC pellicle were also magnetically modified.

2.5. Phthalocyanine modification of magnetic bacterial cellulose

MBC was allowed to sediment in a graduated cylinder for 18 h. Immobilization of reactive copper phthalocyanine dye was described previously by Safarik [15]. Briefly, 2 g of Ostazine turquoise and 6 g of NaCl were mixed with 100 mL of MBC suspension (1:1; sediment:water) and warmed to 70 °C. After 15 min, 5 g of anhydrous Na_2CO_3 was added and the suspension was stirred at 70 °C for next 3 h. Then the mixture was left overnight at ambient temperature without mixing. The phthalocyanine modified magnetic bacterial cellulose (PM-MBC) was thoroughly washed with water and methanol to dispose unbound dye and stored at 4 °C. The dry weight of 1 mL of settled MBC and PM-MBC was equal to 3 mg.

2.6. Adsorption of crystal violet

The adsorption of crystal violet by PM-MBC was tested in a batch system without any pH adjustment. Kinetic parameters were evaluated using 0.5 mL of settled PM-MBC mixed with 10 mL of 100 mg/L solution of crystal violet and incubated on rotator mixer (Dynal, Oslo, Norway) for 5–180 min at room temperature (22.0 °C). Thermodynamic parameters were determined at 11.0, 22.0 and 40.0 °C, using 0.3 mL of settled PM-MBC and dye concentrations ranging between 25 and 450 mg/L. Incubation time was set according to kinetic results to 2 h. To compare adsorption efficiency of MBC after phthalocyanine dye immobilization, the adsorption isotherm for MBC at room temperature was also prepared.

The absorbance of supernatant was measured after magnetic separation (separator DynaMag™-15, Dynal, Oslo, Norway) by spectrophotometer (Cintra 20, GBC Scientific Equipment, Braeside, Australia). The concentration of unbound dye in equilibrium (C_e, mg/L) or at time t (C_t, mg/L) was determined from calibration curve, while the amount of dye adsorbed on unit mass of adsorbent in equilibrium (q_e, mg/g) or at time t (q_t, mg/g) was calculated from these formulae:

$$q_e = \frac{V\,(C_0 - C_e)}{m} \tag{1}$$

$$q_t = \frac{V\,(C_0 - C_t)}{m} \tag{2}$$

where C_0 is the initial concentration of dye (mg/L) and m is the mass of adsorbent (g).

2.7. Adsorption kinetics

The data were analyzed using pseudo-first and pseudo-second-order kinetic models. The linear form of pseudo-first-order (P-1-O) kinetic model is given by the equation [16]:

$$\ln(q_e - q_t) = \ln(q_e) - k_1\,t \tag{3}$$

where the rate constant k_1 (1/min) can be obtained from the linear plot of ln ($q_e - q_t$) against time.

The linear form of pseudo-second-order (P-2-O) model can be expressed as described by Ho and McKay [17]:

$$\frac{t}{q_t} = \frac{1}{k_2\,q_e{}^2} + \frac{t}{q_e} \tag{4}$$

where the equilibrium adsorption capacity (q_e), and the second-order rate constant k_2 (g/mg min) can be determined from the slope and intercept of plot t/q_t versus t [18,19].

2.8. Adsorption thermodynamics

The thermodynamic parameter ΔG° (the standard free energy change of sorption (J/mol)) was calculated from following formula:

$$\Delta G^\circ = -RT \ln K_D \tag{5}$$

where ln K_D is the thermodynamic distribution constant computed from the plot of ln(q_e/C_e) against q_e, where q_e was extrapolated to zero [18].

ΔH° (the standard enthalpy change (J/mol)) and ΔS° (the standard entropy change (J/mol K)) were calculated from Van't Hoff equation:

$$\ln K_D = \frac{\Delta S^\circ}{R} - \frac{\Delta H^\circ}{RT} \tag{6}$$

where R is the universal gas constant (8.314 J/mol K) and T is temperature (K). ΔH° and ΔS° values were determined from the slope and intercept of the plot of ln K_D versus 1/T.

2.9. Adsorption isotherms models

Adsorption equilibrium data were evaluated using two adsorption isotherm models, namely the Langmuir and Freundlich ones. The adsorption isotherms were processed using non-linear regression analysis (solver add- in function of the Microsoft Excel). All experiments were carried out in triplicate.

The Langmuir model assumes the monolayer adsorption and no interaction between adsorbed molecules, and can be expressed as follows:

$$q_e = \frac{q_m\, a_L\, C_e}{1 + a_L\, C_e} \tag{7}$$

where α_L is the Langmuir constant related to the energy of adsorption (L/mg) and q_m is the amount of dyes adsorbed (mg/g).

Freundlich isotherm model, assuming that the surface of adsorbent is heterogeneous and polymolecular layer adsorption takes place, can be defined by the following equation:

$$q_e = K_F\, (C_e)^{\frac{1}{n}} \tag{8}$$

where K_F is the Freundlich constant related to adsorption capacity [(mg/g) (L/mg)$^{1/n}$] and n is the Freundlich isotherm constant associated with adsorption intensity.

The fitting of data to both isotherm models were evaluated by the standard error of estimate (SEE):

$$SEE = \sqrt{\frac{\sum_{i=1}^{n\prime} (y_i - y_{i,theor})^2}{(n\prime - p\prime)}} \tag{9}$$

where y_i is the experimental value of the dependent variable, $y_{i,theor}$ is the theoretical or estimated value of the dependent variable, n' is the number of the experimental measurements and p' is the number of parameters [18,19].

2.10. Immobilization of trypsin on MBC

Small particles of MBC were modified using two types of activating agents, namely by incubating 100 mg of this material (wet weight) either in 1% (w/v) solution of sodium (meta)periodate ($NaIO_4$) in 0.1 M sodium acetate buffer pH 4 or in 3% (v/v) solution of 1,4-butanediol diglycidyl ether (BDDE) in 0.25 M sodium hydroxide on automatic rotator for 20 h at room temperature in the dark. Then, MBC samples were thoroughly washed with distilled water (magnetically separated by NdFeB permanent magnet) and trypsin was covalently bound. Activated MBC was mixed with 2 mL of trypsin solution (2 mg/mL in 0.05 M phosphate buffer solution, pH 7) and incubated for 20 h at 4 °C. After binding step, material was properly washed with phosphate buffer to remove unbound enzyme. Immobilized sample was stored in buffer at 4 °C.

2.11. Immobilization of yeast cells on MBC

Saccharomyces cerevisiae cells were immobilized into MBC via physical adsorption with subsequent cross-linking of cells with glutaraldehyde (GA). 100 mg of MBC (wet weight) was mixed with 2 mL of yeast cell suspension (50 mg/mL in distilled water) and incubated for 20 h at 4 °C. After binding step, material was properly washed with distilled water to remove unbound cells. The adsorbed cells were cross-linked with 2% (v/v) GA solution (on automatic rotator for 3 h at room temperature) and then properly washed with water. Alternatively, yeast cells were covalently immobilized on MBC activated with $NaIO_4$ or BDDE as described above. In both cases, 100 mg of activated MBC (wet weight) was mixed with 2 mL of yeast cell suspension (50 mg/mL in distilled water) and incubated for 20 h at 4 °C. After binding step, material was properly washed with distilled water to remove unbound cells. MBC samples containing immobilized cells were stored in 0.9% (w/v) sodium chloride solution at 4 °C.

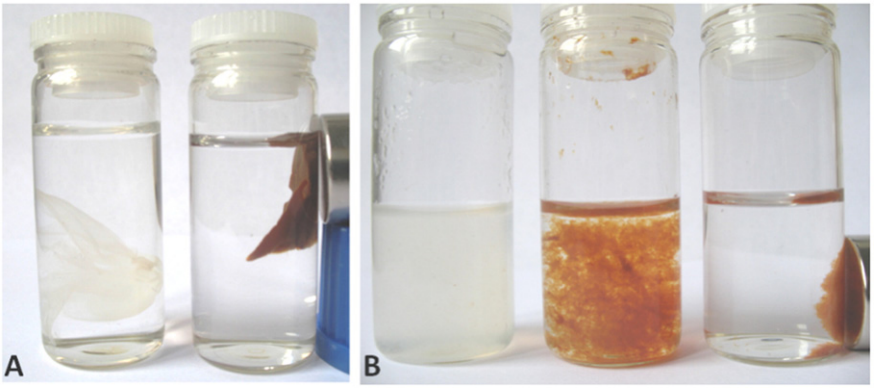

Fig. 1. Appearance and magnetic separation of MBC. A) BC pellicle (left tube nonmagnetic BC, right tube MBC); B) BC particles (left tube nonmagnetic BC, middle tube MBC before and right tube after magnetic separation).

2.12. Immobilized trypsin activity assay (BAPNA hydrolysis)

Activity of trypsin immobilized on MBC was determined by spectrophotometric measurement (405 nm) of yellow-colored product resulting from cleaved artificial substrate BAPNA (1.25 mM in reaction; stock solution in dimethyl sulfoxide) in 0.05 M Tris-HCl buffer, pH 8.5 with 0.02 M $CaCl_2$ at 37 °C [20].

2.13. Immobilized Saccharomyces cerevisiae activity assay (sucrose hydrolysis)

Enzyme activity of immobilized yeast cells was assessed by measurement of the activity of intracellular invertase that catalyzes the hydrolysis of sucrose. Approx. 30 mg of wet weight sample was mixed with 5 mL of 20% (w/v) aqueous sucrose solution and shaken for 20 min at room temperature on automatic rotator; then the reaction was stopped by removing the biocatalyst using magnetic separation. An aliquot (5 μL) was taken from the supernatant and concentration of the reaction product glucose was determined using commercial reagent solution; pink-colored complex was measured spectrophotometrically at 500 nm [21].

2.14. Operational stability of immobilized trypsin and Saccharomyces cerevisiae cells

Operation stability of immobilized enzyme and cells was tested during repeated reaction cycles (trypsin 10 cycles, cells 6 cycles; after each cycle, biocatalysts were washed with appropriate buffer/water). Activities of biocatalysts were measured as described and their activities after each reaction cycle were determined as residual activities in % (initial activity in the first cycle is 100%).

3. Results and discussion

3.1. Magnetically modified bacterial cellulose

Magnetic modification of bacterial cellulose by means of an extremely simple procedure using perchloric acid stabilized magnetic fluid resulted in a formation of material responsive to external magnetic field as documented in Fig. 1. Both the native BC pellicle and BC particles (see optical microscopy in Fig. 2A) have been successfully modified. Magnetic modification led to the deposition of iron oxide nanoparticle aggregates on the surface of the BC fibrils (see Fig. 2B, C). Energy-dispersive X-ray spectroscopy confirmed the presence of iron in the magnetically modified BC (Fig. 3). The presence of Fe^{3+} ions within the MBC was confirmed by Perls´ Prussian Blue Stain [22] that caused intensive blue coloration of the whole material. The stability of magnetically modified BC was very high (stable at least two months in water suspension). The formed MBC can serve as magnetic carrier for the immobilization of target compounds and cells.

Basic characteristic absorption peaks were identified according the measured IR absorption spectra of BC and MBC (Fig. 4). Both types of samples, native and magnetically modified, showed very similar pattern. The band at 3343 cm^{-1} was attributed to the characteristic O—H stretch. The absorption peaks at 2896 and 1428 cm^{-1} were related to the C—H stretching of —CH_2 and —CH_2 symmetric bending respectively. The peaks at 1110, 1059 and 1034 cm^{-1} in BC spectra indicated C_2O_2, C_3O_3 and C_6O_6 stretching, respectively [23]. After comparison of our spectrum with FTIR spectra of BC published in the relevant literature, it can be concluded that the purity of our preparation is high.

3.2. Adsorption of crystal violet on phthalocyanine modified MBC

MBC was used as a carrier for the immobilization of a reactive textile dye Ostazin turquoise V-G. This phthalocyanine dye exhibits affinity for several groups of planar organic compounds, such as polyaromatic hydrocarbons [24] or triphenylmethane dyes [25,26]. In this work, we evaluated adsorption of crystal violet (a typical triphenylmethane dye with a carcinogenic potential) on phthalocyanine modified MBC. It also has to be taken into account that native BC itself can adsorb relatively high amounts of various organic dyes [27].

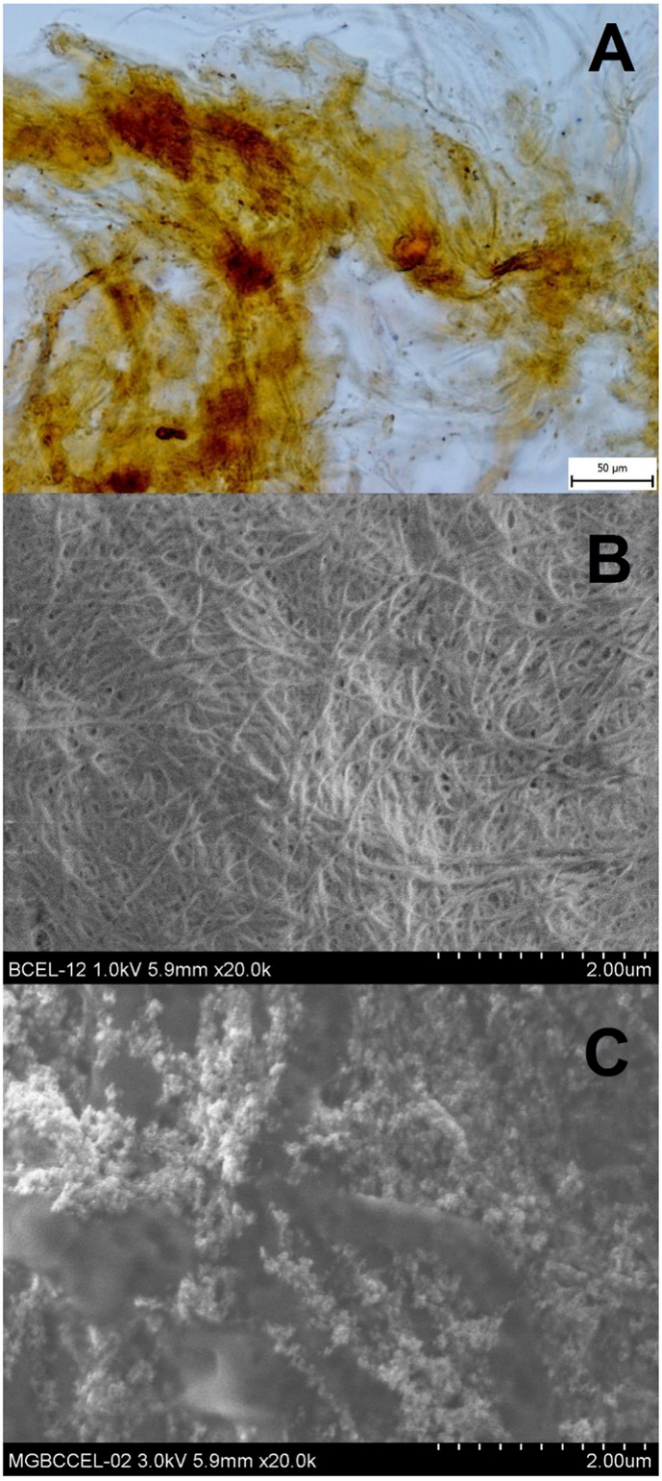

Fig. 2. Optical microscopy of MBC particles (A), SEM image of the surface structure of BC (B) and MBC covered by nanoparticles of iron oxides and their aggregates due to the magnetic fluid treatment (C).

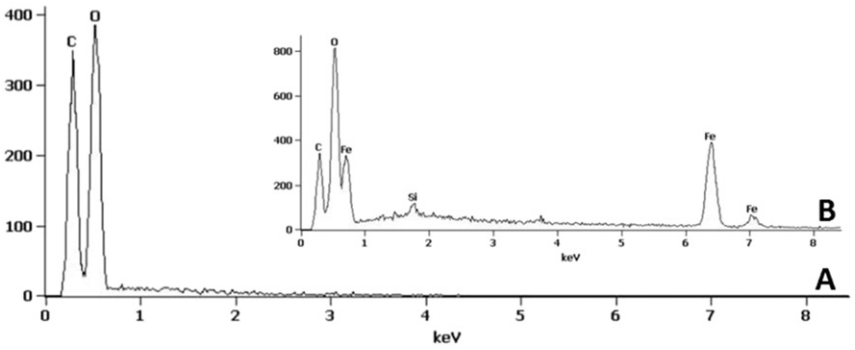

Fig. 3. EDS of native (A) and magnetically modified (B) bacterial cellulose.

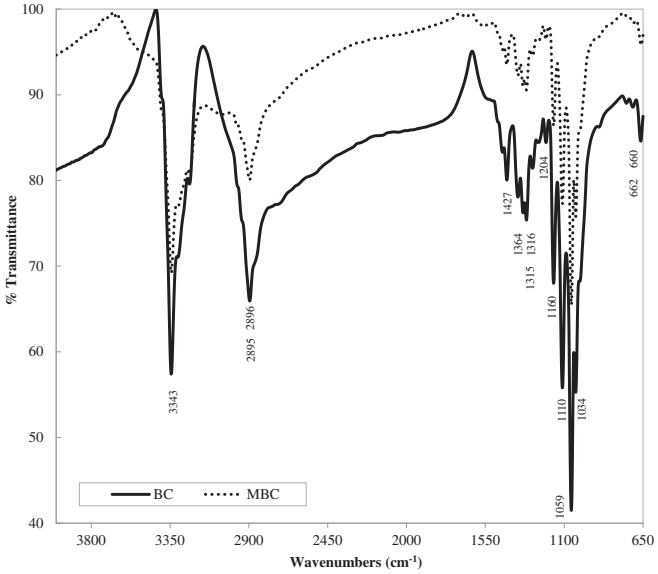

Fig. 4. FTIR spectra of BC (—) and MBC (…).

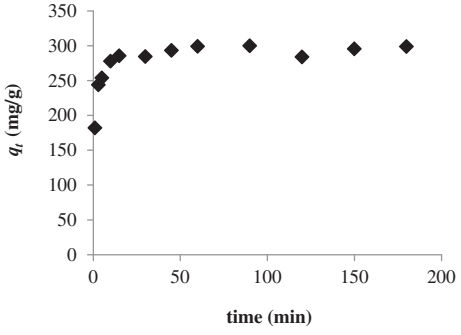

Fig. 5. The time dependence of crystal violet adsorption on PM-MBC (conditions: 0.5 mL of adsorbent, 10 mL of 100 mg/L dye solution, room temperature).

3.2.1. Adsorption kinetics

As can be seen from Fig. 5, adsorption process was very fast; almost 85% was adsorbed within the first 5 min. Although the adsorption equilibrium was reached within 15 min, the incubation time used for isotherm studies was set to 2 h.

Adsorption kinetics was determined using pseudo-first and pseudo-second-order kinetic models and the fitting was assessed on the basis of obtained correlation coefficients. It is apparent from data presented in Table 1 that the correlation coefficient for the pseudo-second-order kinetic model is much higher (0.99) than for pseudo-first-order kinetic model (0.94), thus it can be supposed that investigated adsorption process conformed well the pseudo-second-order kinetic model. This statement is also supported by the calculated q_e value which is in case of pseudo-second-order kinetic model very similar to the experimental q_e value ($q_{e\ exp}$).

3.2.2. Thermodynamics

The obtained thermodynamic data for all tested temperatures are presented in Table 2, the plot of ln K_d versus $1/T$ in Fig. 6. The negative value of Gibbs free energy (ΔG°) indicates the spontaneous process, the negative value of enthalpy (ΔH°) denotes exothermic nature of adsorption and the positive value of entropy ΔS° corresponds to decrease in degree of freedom of the adsorbed species.

3.2.3. Adsorption isotherms

Adsorption data were analyzed by means of two most often used equilibrium adsorption isotherm models, namely the Langmuir and Freundlich ones; related adsorption parameters are summarized in Table 3. The standard error of estimate was also calculated for each case. Fitting of both isotherm models to the experimental data can be determined on the basis of SEE values; it is evident that the Freundlich isotherm model approached the experimental data more closely than the Langmuir one in case of PM-MBC; however, MBC exhibited an

Table 2
Thermodynamic parameters of the adsorption process.

Temperature (K)	ln K_d	ΔG° (kJ/mol)	ΔH° (kJ/mol)	ΔS° (J/mol/K)	R^2
284.15	8.37	−19.769	−27.497	−27.05	0.998
295.15	7.98	−19.586			
313.15	7.30	−18.996			

Table 1
Kinetic parameters.

		Pseudo-first-order model			Pseudo-second-order model		
Initial dye concentration	$q_{e\ exp}$ (mg/g)	q_e (mg/g)	k_1 (1/min)	R^2	q_e (mg/g)	k_2 (g/mg min)	R^2
100 mg/L	300	73.9	0.0695	0.9509	294.1	0.0046	0.9993

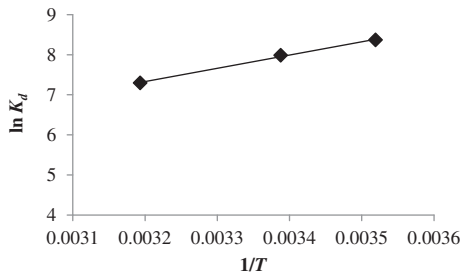

Fig. 6. Plot of Ln K_d versus 1/T.

Table 3
Isotherm parameters for PM-MBC and MBC at tested temperatures.

		PM-MBC			MBC
		Temperature			
Isotherm model	Parameters	11.0 °C	22.0 °C	40.0 °C	22.0 °C
Langmuir	q_m (mg/g)	392.1	388.4	345.1	179.4
	α_L (L/mg)	0.213	0.210	0.351	0.007
	SEE	24.744	31.308	22.355	6.611
Freundlich	K_F [(mg/g) (L/mg)$^{1/n}$]	190.657	182.348	197.520	7.030
	n	7.685	7.298	9.632	1.999
	SEE	8.641	9.731	12.215	11.723

opposite trend. In all cases, the value of the Freundlich constant n is higher than 1, which indicates a physical adsorption.

Phthalocyanine decoration increased the maximum adsorption capacity of MBC more than twice (see Table 3 and/or Fig. 7), from 179 to 388 mg/g at 22.0 °C, respectively. The obtained value is high, and is fully comparable with the results obtained using other adsorbents for crystal violet removal (see Table 4). Therefore, the phthalocyanine-loaded BC could be applied in dye removal process with much higher

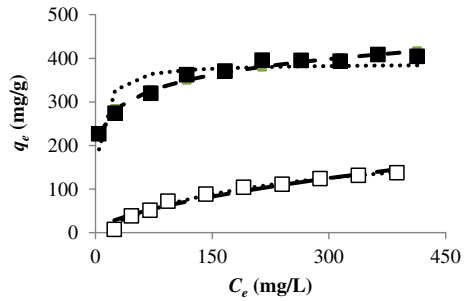

Fig. 7. Adsorption isotherms at 22.0 °C for (■) PM-MBC and (□) MBC.

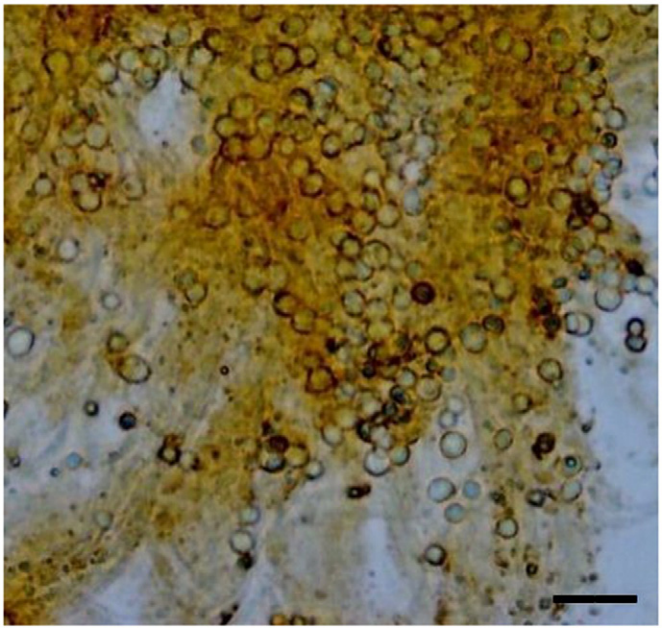

Fig. 8. Appearance of yeast cells entrapped and cross-linked in MBC particles (the bar corresponds to 20 μm).

efficiency. On the contrary, magnetic modification of native bacterial cellulose had only a negligible effect on the nonspecific binding of crystal violet; during three experiments, magnetic modification of BC led to less than 10% decrease of crystal violet adsorption.

3.3. Immobilization of Saccharomyces cerevisiae cells

Yeast cells (*Saccharomyces cerevisiae*) were immobilized on MBC and used as a model whole-cell biocatalyst. Yeast cells were successfully immobilized by both adsorption of cells on MBC with subsequent cross-linking using glutaraldehyde and also by covalent binding on previously activated MBC using sodium periodate and 1,4-butanediol diglycidyl ether. According to the operational stability testing, all three immobilization methods were suitable for yeast cell immobilization (see Fig. 8); after 6 repeated cycles of sucrose solution hydrolysis, immobilized cells retained approximately 90% of their initial activity (similar results for all three samples), see Fig. 9.

3.4. Immobilization of trypsin

Bovine pancreas crystalline trypsin was used as a model enzyme immobilized on MBC using two procedures. Better immobilization method for trypsin was covalent binding after MBC periodate

Table 4
Comparison of maximum adsorption capacities of crystal violet on different adsorbents.

Material	q_m (mg/g)	Other comments	Reference
Carboxylate-functionalized sugarcane bagasse	692.1	At 45 °C, endothermic process, P-2-O model followed	[28]
Bacillus amyloliquefaciens biofilm	582.4	Exothermic process, P-1-O model followed	[29]
Citric acid-NaOH modified magnetic barley straw	410.8	Endothermic process, P-2-O model followed	[18]
Phthalocyanine-modified magnetic bacterial cellulose	392.1	At 11 °C, exothermic process, Freundlich and P-2-O models followed	This paper
Cellulose resin crosslinked with perylene tetracarboxylic diimides	391.7	Exothermic process, Langmuir and P-2-O models followed	[30]
Carboxylate-functionalized cellulose nanocrystals	243.9	Exothermic process, Langmuir and P-2-O models followed	[31]
Magnetic EDTA-modified chitosan/SiO_2/Fe_3O_4 adsorbent	227.3	Exothermic process, Langmuir and P-2-O models followed	[32]
Glycidyl methacrylate/sulfo-salicylic acid modified cellulose	218.8	At 50 °C, endothermic process, Langmuir and P-2-O models followed	[33]
Tea dust	175.4	Langmuir and P-2-O models followed	[34]
Magnetic nanoparticles modified with sodium dodecyl sulphate	166.7	Freundlich and P-2-O models followed	[35]
Magnetically modified activated carbon	67.1	Endothermic process, Langmuir and P-2-O models followed	[36]
Chitosan-graphite oxide modified polyurethane	64.9	Endothermic process, Langmuir and P-2-O models followed	[37]
Carrageenan wet beads	52.0	Endothermic process, Freundlich and P-2-O models followed	[38]
Cellulose modified with maleic anhydride	33.7	Endothermic process, Langmuir and P-2-O models followed	[39]

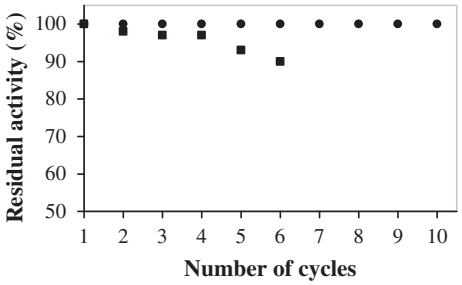

Fig. 9. Operational stability of trypsin and *Saccharomyces cerevisiae* cells immobilized on MBC (• - trypsin immobilized on periodate activated MBC, ■ - yeast cells adsorbed to MBC and cross-linked by glutaraldehyde; initial activity in the first cycle is 100%).

activation; this sample was very stable during operational stability testing, it could be repeatedly used for ten cycles of BAPNA hydrolysis without loss of its initial activity (Fig. 9).

4. Conclusion

Extremely simple procedure for the preparation of magnetically responsive bacterial cellulose was developed. Magnetic modification based on simple mixing of BC with magnetic fluid stabilized by perchloric acid resulted in the formation of magnetically responsive material that could be easily and selectively separated from desired environs (e.g. suspensions, difficult-to-handle media etc.) by means of external magnetic field (using permanent magnet, magnetic separator or electromagnet).

Magnetic cellulose derivative was characterized and subsequently used as a biocompatible carrier for the immobilization of affinity ligands, enzymes and cells. Magnetically responsive bacterial cellulose after copper phthalocyanine decoration exhibited more than twice higher maximum adsorption capacity for crystal violet than the MBC without phthalocyanine treatment. Baker's yeast were successfully immobilized both on native MBC followed by glutaraldehyde cross-linking and on previously activated MBC, and efficiently used for 6 cycles of sucrose hydrolysis. The most suitable method for immobilization of trypsin consisted in covalent binding on MBC activated with sodium periodate; the biocatalyst was very stable and retained its enzyme activity for 10 cycles. Further research on the potential application of the prepared magnetic bacterial cellulose is in progress.

Acknowledgements

The research was supported by the projects LD14075 and LO1305 (Ministry of Education, Youth and Sports of the CR) and by the project 14-11516S (Czech Science Foundation). The authors acknowledge the assistance provided by the Research Infrastructure NanoEnviCz, supported by the Ministry of Education, Youth and Sports of the Czech Republic under Project No. LM2015073. This work was also carried out in the frame of the Cost Action TD1203 entitled “Food waste valorisation for sustainable chemicals, materials & fuels (EUBis)”.

References

[1] M.L. Cacicedo, M.C. Castro, I. Servetas, L. Bosnea, K. Boura, P. Tsafrakidou, A. Dima, A. Terpou, A. Koutinas, G.R. Castro, Progress in bacterial cellulose matrices for biotechnological applications, Bioresour. Technol. 213 (2016) 172–180.
[2] L. Fu, J. Zhang, G. Yang, Present status and applications of bacterial cellulose-based materials for skin tissue repair, Carbohydr. Polym. 92 (2013) 1432–1442.
[3] J. Wippermann, D. Schumann, D. Klemm, H. Kosmehl, S. Satehi-Gelani, T. Wahlers, Preliminary results of small arterial substitute performed with a new cylindrical biomaterial composed of bacterial cellulose, Eur. J. Vasc. Endovasc. 37 (2009) 592–596.
[4] W. Czaja, A. Krystynowicz, S. Bielecki, R.M. Brown, Microbial cellulose - the natural power to heal wounds, Biomaterials 27 (2006) 145–151.
[5] B.V. Mohite, S.V. Patil, A novel biomaterial: bacterial cellulose and its new era applications, Biotechnol. Appl. Biochem. 61 (2014) 101–110.
[6] P. Paximada, E. Tsouko, N. Kopsahelis, A.A. Koutinas, I. Mandala, Bacterial cellulose as stabilizer of o/w emulsions, Food Hydrocoll. 53 (2016) 225–232.
[7] E. Tsouko, C. Kourmentza, D. Ladakis, N. Kopsahelis, I. Mandala, S. Papanikolaou, F. Paloukis, V. Alves, A. Koutinas, Bacterial cellulose production from industrial waste and by-product streams, Int. J. Mol. Sci. 16 (2015) 14832–14849.
[8] I. Safarik, K. Pospiskova, K. Horska, M. Safarikova, Potential of magnetically responsive (nano)biocomposites, Soft Matter 8 (2012) 5407–5413.
[9] I. Safarik, K. Pospiskova, E. Baldikova, M. Safarikova, Magnetically responsive biological materials and their applications, Adv. Mater. Lett. 7 (2016) 254–261.
[10] M. Zeng, A. Laromaine, W. Feng, P.A. Levkin, A. Roig, Origami magnetic cellulose: controlled magnetic fraction and patterning of flexible bacterial cellulose, J. Mater. Chem. C 2 (31) (2014) 6312–6318.
[11] M. Sureshkumar, D.Y. Siswanto, C.K. Lee, Magnetic antimicrobial nanocomposite based on bacterial cellulose and silver nanoparticles, J. Mater. Chem. 20 (33) (2010) 6948–6955.
[12] B. Galateanu, M.C. Bunea, P. Stanescu, E. Vasile, A. Casarica, H. Iovu, A. Hermenean, C. Zaharia, M. Costache, *In vitro* Studies of Bacterial Cellulose and Magnetic Nanoparticles Smart Nanocomposites for Efficient Chronic Wounds Healing, Stem Cells Int. 2015, 2015 (Article ID 195096).
[13] V. Kachrimanidou, N. Kopsahelis, M. Alexandri, A. Strati, C. Gardeli, S. Papanikolaou, M. Komaitis, I.K. Kookos, A.A. Koutinas, Integrated sunflower-based biorefinery for the production of antioxidants, protein isolate and poly(3-hydroxybutyrate), Ind. Crop. Prod. 71 (2015) 106–113.
[14] R. Massart, Preparation of aqueous magnetic liquids in alkaline and acidic media, IEEE Trans. Magn. 17 (2) (1981) 1247–1248.
[15] I. Safarik, Removal of organic polycyclic compounds from water solutions with a magnetic chitosan based sorbent bearing copper phthalocyanine dye, Water Res. 29 (1) (1995) 101–105.
[16] Y.S. Ho, Citation review of Lagergren kinetic rate equation on adsorption reactions, Scientometrics 59 (2004) 171–177.
[17] Y.S. Ho, G. McKay, Sorption of dye from aqueous solution by peat, Chem. Eng. J. 70 (1998) 115–124.
[18] E. Baldikova, D. Politi, Z. Maderova, K. Pospiskova, D. Sidiras, M. Safarikova, I. Safarik, Utilization of magnetically responsive cereal by-product for organic dye removal, J. Sci. Food Agric. 96 (2016) 2204–2214.
[19] I. Safarik, N. Ashoura, Z. Maderova, K. Pospiskova, E. Baldikova, M. Safarikova, Magnetically modified *Posidonia oceanica* biomass as an adsorbent for organic dyes removal, Mediterr. Mar. Sci. 17 (2) (2016) 351–358.
[20] K. Pospiskova, I. Safarik, Magnetically responsive enzyme powders, J. Magn. Magn. Mater. 380 (2015) 197–200.
[21] K. Pospiskova, G. Prochazkova, I. Safarik, One-step magnetic modification of yeast cells by microwave-synthesized iron oxide microparticles, Lett. Appl. Microbiol. 56 (2013) 456–461.
[22] I. Safarik, K. Horska, B. Svobodova, M. Safarikova, Magnetically modified spent coffee grounds for dyes removal, Eur. Food Res. Technol. 234 (2012) 345–350.
[23] V. Palaninathan, N. Chauhan, A.C. Poulose, S. Raveendran, T. Mizuki, T. Hasumura, T. Fukuda, H. Morimoto, Y. Yoshida, T. Maekawa, D.S. Kumar, Acetosulfation of bacterial cellulose: an unexplored promising incipient candidate for highly transparent thin film, Mater. Express 4 (2014) 415–421.
[24] H. Hayatsu, Cellulose bearing covalently linked copper phthalocyanine trisulphonate as an adsorbent selective for polycyclic compounds and its use in studies of environmental mutagens and carcinogens, J. Chromatogr. A 597 (1992) 37–56.
[25] I. Safarik, M. Safarikova, N. Vrchotova, Study of sorption of triphenylmethane dyes on a magnetic carrier bearing an immobilized copper phthalocyanine dye, Collect. Czechoslov. Chem. Commun. 60 (1) (1995) 34–42.
[26] I. Safarik, M. Safarikova, Detection of low concentrations of malachite green and crystal violet in water, Water Res. 36 (2002) 196–200.
[27] Z.Y. Wu, H.W. Liang, C. Li, B.C. Hu, X.X. Xu, Q. Wang, J.F. Chen, S.H. Yu, Dyeing bacterial cellulose pellicles for energetic heteroatom doped carbon nanofiber aerogels, Nano Res. 7 (2014) 1861–1872.
[28] B.C. Silva Ferreira, F.S. Teodoro, A.B. Mageste, L.F. Gil, R.P. de Freitas, L.V. Alves Gurgel, Application of a new carboxylate-functionalized sugarcane bagasse for adsorptive removal of crystal violet from aqueous solution: kinetic, equilibrium and thermodynamic studies, Ind. Crop. Prod. 65 (2015) 521–534.
[29] P. Sun, C. Hui, S. Wang, L. Wan, X. Zhang, Y. Zhao, *Bacillus amyloliquefaciens* biofilm as a novel biosorbent for the removal of crystal violet from solution, Colloids Surf. B: Biointerfaces 139 (2016) 164–170.
[30] H. Guo, Y. Wu, J. Yuan, F. Yang, High-efficiency sorbent for dyes based on cellulose resin crosslinked with perylene tetracarboxylic diimides, Sep. Sci. Technol. 49 (2014) 2548–2556.
[31] H. Qiao, Y. Zhou, F. Yu, E. Wang, Y. Min, Q. Huang, L. Pang, T. Ma, Effective removal of cationic dyes using carboxylate-functionalized cellulose nanocrystals, Chemosphere 141 (2015) 297–303.
[32] Y. Ren, Y. Chen, M. Sun, H. Peng, K. Huang, Rapid and efficient removal of cationic dyes by magnetic chitosan adsorbent modified with EDTA, Sep. Sci. Technol. 49 (2014) 2049–2059.
[33] Y. Zhou, M. Zhang, X. Wang, Q. Huang, Y. Min, T. Ma, J. Niu, Removal of crystal violet by a novel cellulose-based adsorbent: comparison with native cellulose, Ind. Eng. Chem. Res. 53 (2014) 5498–5506.
[34] M.M.R. Khan, M.W. Rahman, H.R. Ong, A.B. Ismail, C.K. Cheng, Tea dust as a potential low-cost adsorbent for the removal of crystal violet from aqueous solution, Desalin. Water Treat. 57 (2016) 14728–14738.

[35] C. Muthukumaran, V.M. Sivakumar, M. Thirumarimurugan, Adsorption isotherms and kinetic studies of crystal violet dye removal from aqueous solution using surfactant modified magnetic nanoadsorbent, J. Taiwan Inst. Chem. Eng. 63 (2016) 354–362.
[36] S. Hamidzadeh, M. Torabbeigi, S.J. Shahtaheri, Removal of crystal violet from water by magnetically modified activated carbon and nanomagnetic iron oxide, J. Environ. Health Sci. Eng. 13 (2015), Article No. 8.
[37] J. Qin, F. Qiu, X. Rong, J. Yan, H. Zhao, D. Yang, Adsorption behavior of crystal violet from aqueous solutions with chitosan-graphite oxide modified polyurethane as an adsorbent, J. Appl. Polym. Sci. 132 (2015), Article No. 41828.
[38] G.R. Mahdavinia, F. Bazmizeynabad, B. Seyyedi, *kappa*-Carrageenan beads as new adsorbent to remove crystal violet dye from water: adsorption kinetics and isotherm, Desalin. Water Treat. 53 (2015) 2529–2539.
[39] Y. Zhou, Q. Jin, X. Hu, Q. Zhang, T. Ma, Heavy metal ions and organic dyes removal from water by cellulose modified with maleic anhydride, J. Mater. Sci. 47 (2012) 5019–5029.

5.3 Adsorpce těžkých kovů

5.3.1 Mikrobiální buňky

Tato přehledná kapitola se zabývá odstraňováním těžkých kovů a radionuklidů pomocí mikrobiálních buněk s adekvátní magnetickou odezvou. Zahrnuty jsou jak kvasinkové (např. *Saccharomyces cerevisiae*, *Kluveromyces marxianus*, *Yarrowia lipolytica* či *Rhodotorula glutinis*), tak bakteriální (např. *Pseudomonas putida*, *Enterobacter* sp. či *Escherichia coli*) buňky, přičemž nezanedbatelná část je věnována magnetotaktickým bakteriím.

První část kapitoly je zaměřena na obecnou charakteristiku biosorpce, fyzikálně-chemického procesu, který v sobě zahrnuje několik různých mechanismů (transport buněčnou membránou, sorpce na buněčné stěny, záchyt do extracelulárních kapsulí apod.). V další části jsou podrobně popisovány dostupné techniky magnetické modifikace, a to od těch běžných až po ty méně časté. Poslední část je věnována samotné problematice odstraňování těžkých kovů s využitím magnetických mikrobiálních buněk. Nechybí zde přehledná tabulka shrnující publikované práce včetně dalších dostupných informací, např. o povaze adsorpčního procesu či možnosti regenerace sorbentu.

V neposlední řadě je zde zmíněno využití magneticky modifikovaných buněk pro předkoncentraci těžkých kovů pomocí extrakce na magnetické pevné fázi.

Publikace je obohacena o snímky z optické, skenovací a transmisní elektronové mikroskopie, které zřetelně demonstrují přítomnost magnetických částic na povrchu mikrobiálních buněk.

Příloha 18:

Magnetically responsive microbial cells for metal ions removal and detection

Safarik I, Pospiskova K, Baldikova E, Safarikova M

In: *Metal-Microbe Interactions and Bioremediation: Principles and Applications for Toxic Metals*, (Das S., Dash H.R., Eds.), CRC Press, **2016**, 769-778

48 Magnetically Responsive Microbial Cells for Metal Ions Removal and Detection

Ivo Safarik, Kristyna Pospiskova, Eva Baldikova, and Mirka Safarikova

CONTENTS

Abstract 769
48.1 Introduction 769
48.2 Biosorption 769
48.3 Preparation of Magnetically Responsive Microbial Cells 770
48.4 Use of Magnetically Responsive Microbial Cells for Metal Ions Removal and Detection 773
48.5 Summary 776
References 776

ABSTRACT

Prokaryotic and eukaryotic cells can interact with various types of magnetic nanoparticles and microparticles. Due to the presence of magnetic particles on the cell surface, in protoplasm or in intracellular organelles, magnetically modified cells can be rapidly, easily, and selectively separated from desired environments by means of magnetic separators. The cell surface contains a wide variety of functional groups that can be efficiently employed in adsorption processes. Magnetically responsive cells are very interesting and easily obtainable biomaterials that are highly usable for the removal and detection of metal ions. Such types of biosorbents can be very promising in environmental technologies in the near future.

48.1 INTRODUCTION

Human activity, as well as natural geochemical processes, is accompanied by the pollution of water, soil, and atmosphere by huge amounts of inorganic and organic pollutants. Toxic metals are extensively employed in electronics, machine construction, high-tech technologies, and many products used in everyday life, such as batteries and accumulators. As a result, toxic metals enter water resources and cause harmful pollution. The main sources of contamination include mining wastes, landfill leaches, municipal wastewater, urban runoff, and industrial wastewaters, particularly from the electroplating, electronic, and metal-finishing industries. Metal concentrations in many aquatic environments are substantially higher than official limits. Heavy metal ions may cause serious health problems in human beings; in water sources, they can pose a threat to a variety of fish and invertebrates. Large acute doses can lead to harmful, even fatal effects. Because of these reasons, heavy metal ions have to be removed to very low levels from water resources (Sharma, 2015).

Various treatment methods for the removal of target metal ions from industrial wastewater have been developed. A number of traditional treatment techniques including ion exchange, chemical precipitation, electrochemical precipitation, adsorption, membrane filtration, reverse osmosis, phytoremediation, photocatalysis, or complexation have been described and used. However, the necessity to reduce the amount of heavy metal ions in wastewater streams has led to an increasing interest in alternative procedures (Sharma, 2015).

48.2 BIOSORPTION

During the last several decades, new processes for the removal of both organic and inorganic pollutants have been developed and tested. A huge amount of procedures is based on the use of materials of biological origin, acting as adsorbents (biosorbents). In general, biosorption has been defined as the property of certain biomaterials to sequester metal ions or other molecules from aqueous solutions. During the removal of metal ions, different processes including transport through the cell membrane, biosorption on cell walls, entrapment in the extracellular capsule, and oxidation/reduction reactions have been observed in nonliving and living microorganisms. Selectivity in removing the desired metal ions is an added advantage of bio-based separation techniques. These techniques have been proved to be some of the most economical and eco-friendly procedures for the removal of metal ions. Biosorption of metal ions has thus become an intensively studied field of research in environmental science and technology.

Diverse types of microalgae, bacteria, fungi, and yeasts have been used as efficient biosorbents of metal ions. In addition to cultivated microbial cells, also low-cost waste biomass can be efficiently used. The metal uptake capacity of various biological materials has usually been evaluated during batch adsorption experiments; equilibrium adsorption isotherms of different types are created and, if possible, maximum adsorption capacities are calculated. The effect of various reaction conditions, including contact time, pH, temperature, biomass loading, ionic strength, etc., has also been studied extensively,

as well as detailed adsorption kinetic studies. Both living and dead microbial biomass can be used as a biosorbent; the optimum form depends on the specific application.

Various mechanisms have been suggested for metal ions removal from model solutions and wastewater using microbial cells. Metal ions can be biosorbed onto the binding sites present in the cellular structure; this process is known as passive uptake. Metal ions can also pass inside the cell across the cell membrane through the cell metabolic cycle; this mode of metal uptake is known as active uptake. The metal uptake by both active and passive modes can be described as bioaccumulation (Sharma, 2015).

In order to simplify manipulation with biosorbents in difficult-to-handle environments, microbial cells are magnetically modified to get magnetically responsive derivatives, which can be easily separated using an appropriate magnetic separator.

48.3 PREPARATION OF MAGNETICALLY RESPONSIVE MICROBIAL CELLS

An absolute majority of prokaryotic and eukaryotic cells exhibit diamagnetic properties. Nevertheless, there is an extraordinary bacterial group called magnetotactic bacteria (MTB) that can synthesize intracellular biogenic magnetic nanoparticles (based either on magnetite (Fe_3O_4) or on greigite (Fe_3S_4)) that enable their magnetic separation and movement; it is generally assumed that magnetosomes (organelles containing individual magnetic nanoparticles covered with a lipid bilayer) are involved in magnetoreception (Schüler, 2007).

Many procedures enabling conversion of diamagnetic cells into their magnetically responsive derivatives have been described recently (Safarik et al., 2014, 2015a). Magnetic modification of cells is based on their interaction with an appropriate magnetic label, usually nanoparticles and microparticles of magnetite (Fe_3O_4) or maghemite (γ-Fe_2O_3); in some cases, ferrite particles (Lee et al., 2004) or chromium dioxide particles (Widjojoatmodjo et al., 1993) have also been used. Alternatively, the modification can be performed by binding paramagnetic cations on acid groups on the cell surface (Zborowski et al., 1992) or by the binding of magnetoferritin (Zborowski et al., 1996) on the cell surface. In general, microbial cells can especially be modified by the nonspecific attachment of magnetic iron oxide nanoparticles (e.g., by the magnetic fluid treatment) (Safarikova et al., 2009), by binding of magnetic microparticles on the cell surface (Pospiskova et al., 2013), by specific interactions with immunomagnetic nanoparticles and microparticles (Safarik and Safarikova, 1999), by covalent immobilization on magnetic carriers (Safarik et al., 2015b), by cross-linking of the cells or isolated cell walls with a bifunctional reagent in the presence of magnetic particles (Patzak et al., 1997), or by entrapment (together with magnetic particles) into biocompatible polymers (Safarik et al., 2008). The individual modification procedures enabling preparation of magnetically responsive microbial biosorbents will be described in more detail in further text.

Magnetic modification of microbial cells can be efficiently performed using appropriate magnetic fluid (ferrofluid). In the simplest way, perchloric acid–stabilized magnetic fluid was mixed with baker's or brewer's yeast cells washed with and suspended in acetate buffer, pH 4.6, or in glycine–HCl buffer, pH 2.2; alternatively, tetramethylammonium hydroxide–stabilized magnetic fluid was used for baker's yeast cells modification in 0.1 M glycine–NaOH buffer, pH 10.6. After a short time period, magnetic particles precipitated on the cell surface (Figure 48.1) (Safarikova et al., 2009). The modified cells can be heated in a boiling water bath to kill the cells; a stable adsorbent for the removal of selected organic and inorganic xenobiotics can be prepared (Safarik et al., 2002). Magnetic modification of dried *Kluyveromyces marxianus* (fodder yeast; Figure 48.2) and *Chlorella vulgaris* cells required thorough washing with 0.1 M acetic acid to remove a substantial portion of soluble macromolecules that otherwise caused spontaneous precipitation of magnetic fluid; after washing and suspending the cells in acetic acid solution, the addition of perchloric acid–stabilized magnetic fluid resulted in the formation of magnetically modified yeast and algae cells (Safarik et al., 2007, 2008).

A simple procedure for the magnetic modification of yeast and algae cells based on the use of microwave-synthesized magnetic iron oxide nanoparticles and microparticles has been developed recently. The particles are usually prepared from ferrous sulfate heptahydrate and sodium or potassium hydroxide; after their mixing and precipitation of mixed iron hydroxides, the suspension underwent the microwave treatment in a regular kitchen microwave oven (700 W, 2450 MHz) and nanoparticles and microparticles of magnetic iron oxides formed (Zheng et al., 2010; Pospiskova et al., 2013). Mixing of magnetic particles with algae cells (*Chlorella vulgaris*) and yeast cells (*Saccharomyces cerevisiae*) suspensions caused cell flocculation and magnetically responsive cell aggregates (usually ca. 100–300 μm in diameter) were formed (Figure 48.3) (Pospiskova et al., 2013; Prochazkova et al., 2013). Alternatively, commercial magnetite microparticles were used to capture bacterial cells (Sze et al., 1996; Wong and Fung, 1997) and fungal biomass (Wainwright et al., 1990). Another adsorbent for capturing bacterial cells was prepared from granular activated carbon after its modification with Mn ferrite (Podder and Majumder, 2016).

In general, microbial cells are covalently bound on magnetic carriers by means of an appropriate coupling agent (e.g., aminosilane, carbodiimide, glutaraldehyde) to introduce a specific group on the carrier surface, which subsequently can interact with reactive groups on the cell surface. In a typical example, magnetic chitosan particles activated by glutaraldehyde have been utilized for *Saccharomyces cerevisiae* immobilization (Figure 48.4) (Safarik et al., 2015b). Alternatively, magnetic cellulose microparticles were activated with periodic acid and subsequently utilized for the immobilization of yeast cells (Ivanova et al., 2011). Silanized magnetite nanoparticles, activated by (3)-aminopropyltriethoxysilane followed by glutaraldehyde treatment, were covalently bound to cells of *Bacillus circulans* (Safarikova et al., 2007). An iron-based ammonia synthesis catalyst covered by a stable film of amino groups containing epoxy resin was used for *Saccharomyces*

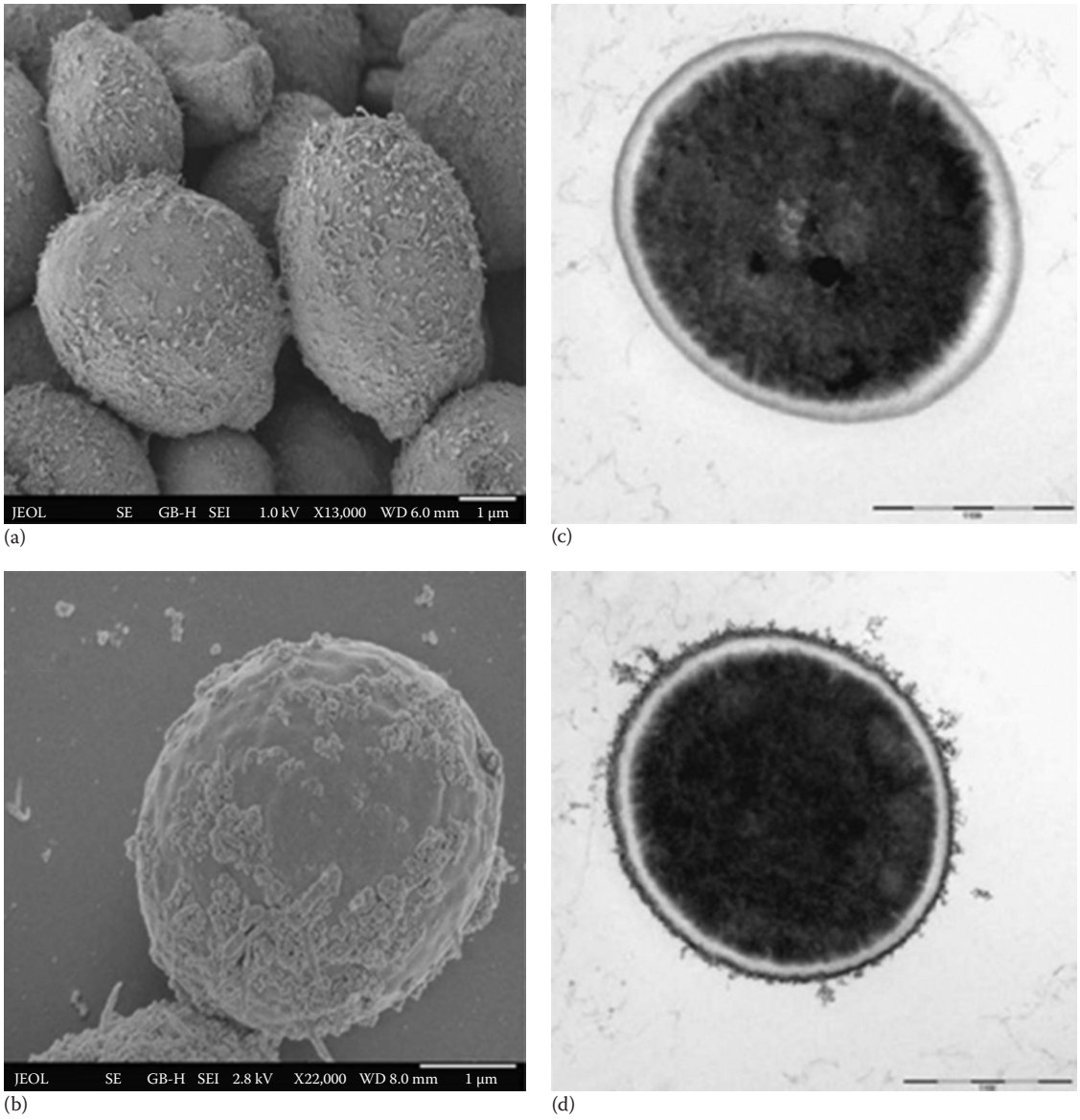

FIGURE 48.1 Scanning electron microscopy micrographs of ferrofluid modified *Saccharomyces cerevisiae* cells showing attached magnetic nanoparticles and their aggregates on the cell surface (a, b; bars: 1 µm). Transmission electron microscopy micrographs of native *S. cerevisiae* cells (c; bar: 1 µm) and ferrofluid modified cells with attached magnetic iron oxide nanoparticles on the cell wall (d; bar: 1 µm). (Reproduced from Safarikova, M. et al., *Food Res. Int*., 42, 521, 2009. With permission.)

cerevisiae cells immobilization after glutaraldehyde activation (Ivanova et al., 1996).

Microbial cell walls contain free amino and/or carboxyl groups, which can easily be cross-linked by bifunctional or multifunctional reagents such as glutaraldehyde or toluene diisocyanate. The cells are usually cross-linked in the presence of an inert protein like gelatine, albumin, raw hen egg white, and collagen. If magnetic particles are used throughout the cross-linking process, magnetic cells or cell walls' derivatives can be prepared (Patzak et al., 1997).

Microbial cells can be entrapped in natural or biocompatible synthetic carriers (gels) that can be formed by various mechanisms, namely, polymerization (e.g., polyacrylamide, polymethacrylate), cross-linking (e.g., proteins), polycondensation (polyurethane, epoxy resins), thermal gelation (e.g., gelatine, agar, agarose), ionotropic gelation (e.g., alginate, chitosan), and precipitation (cellulose, cellulose triacetate). The gel is formed in the presence of the cells and appropriate magnetic materials. There are various methods available to obtain particles (beads) containing entrapped cells and magnetic particles (Safarik et al., 2014).

Magnetically responsive alginate beads containing entrapped *S. cerevisiae* cells and magnetite microparticles were prepared; larger beads (2–3 mm in diameter) were formed by dropping the mixture into a calcium chloride solution, while microbeads (50–100 µm) were prepared using the water-in-oil emulsification process (Figure 48.5). The presence of magnetic material had no negative effect

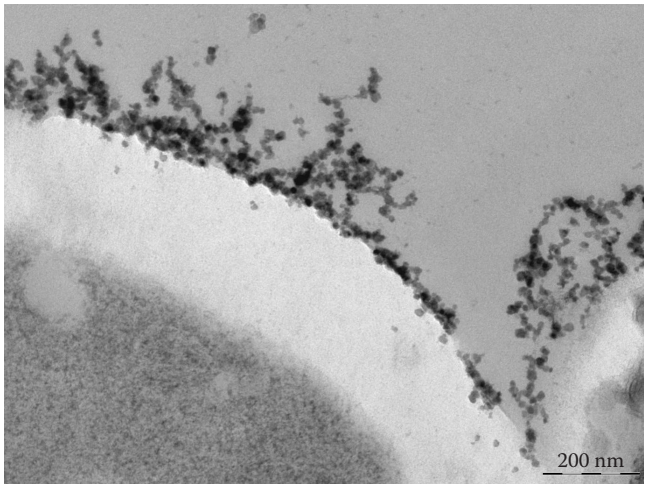

FIGURE 48.2 Transmission electron microscopy picture of magnetically modified dried fodder yeast (*Kluyveromyces marxianus*) cells (bar—200 nm). (Reproduced from Safarik, I. et al., *Enzyme Microb. Technol*., 40, 1551, 2007. With permission.)

on the activity of cells (Safarik et al., 2008). Bacterial alkaliphilic cells *Amphibacillus* sp. KSUCr3 were immobilized in silica-coated magnetic alginate gel beads and applied for detoxification of hexavalent chromate. In comparison with the cells immobilized into a nonmagnetic matrix, the magnetic beads with cells showed approximately 16% higher reduction activity. Coating of magnetic alginate beads with a dense silica layer (using sol-gel procedure; the silica layer was deposited by addition of ammonia and tetraethyl orthosilicate to dispersed beads) improved the physical and mechanical properties and thermal stability of immobilized cells (Ibrahim et al., 2013).

Bacterial cells of *Pseudomonas delafieldii* R-8 were immobilized in magnetic polyvinyl alcohol beads and utilized for biodesulfurization. The suspension of cells in phosphate buffer was mixed with aqueous solution of PVA and oleic acid stabilized magnetic fluid and subsequently dropped into liquid nitrogen for quick freezing. The formed beads with immobilized cells underwent thawing by slow increase of the temperature under vacuum (Guobin et al., 2005).

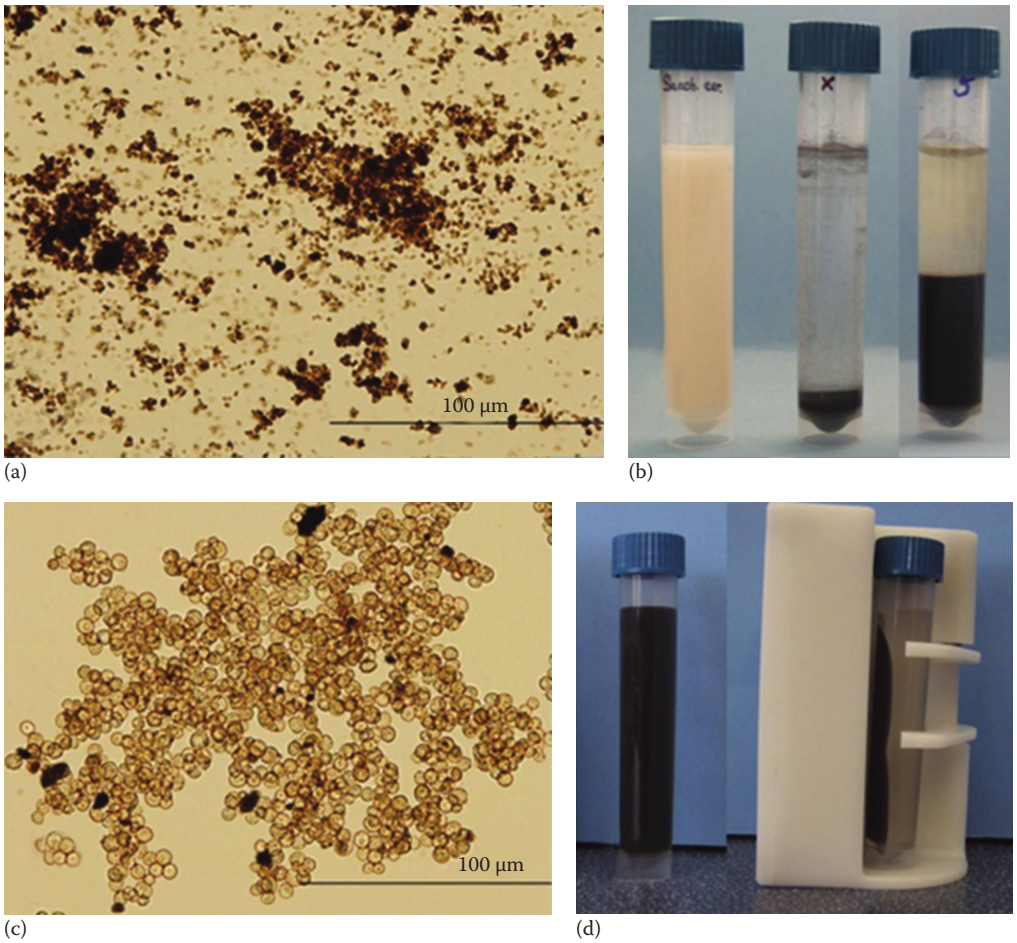

FIGURE 48.3 (a) Optical microscopy of magnetic iron oxide microparticles prepared by microwave-assisted synthesis; (b) process of magnetic modification of yeast cells (left tube, *Saccharomyces cerevisiae* cells suspension; middle tube, sedimented iron oxide microparticles for magnetic modification; right tube, sedimented magnetically modified yeast cells); (c) optical microscopy of *S. cerevisiae* cells modified by iron oxide microparticles; (d) magnetic separation of magnetically modified yeast cells. (Reproduced from Pospiskova, K. et al., *Lett. Appl. Microbiol*., 56, 456, 2013. With permission.)

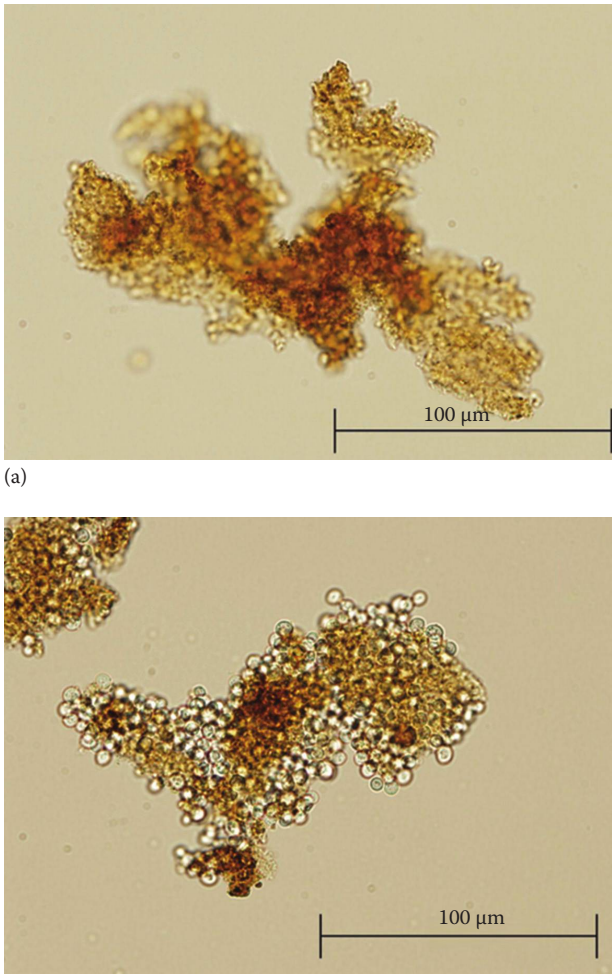

FIGURE 48.4 (a) Optical microscopy images of microwave-synthesized magnetic chitosan microparticles and (b) magnetic chitosan microparticles with immobilized *Saccharomyces cerevisiae* cells. (Reproduced from Safarik, I. et al., *Yeast*, 32, 239, 2015b. With permission.)

48.4 USE OF MAGNETICALLY RESPONSIVE MICROBIAL CELLS FOR METAL IONS REMOVAL AND DETECTION

Various magnetically modified prokaryotic and eukaryotic cells, as well as selected strains of MTB, have been tested as possible biosorbents for a range of metal ions (Tables 48.1 and 48.2). Copper, nickel, cadmium, lead, chromium, mercury, iron, gold, silver, manganese, uranium, arsenic, strontium, plutonium, and cerium ions have served as the tested adsorbates. Most experiments have been performed with model metal ions solutions in a laboratory scale; when the biosorption potential using real industrial wastewater was tested, the efficiency was usually substantially lower.

Yeast biomass represents an important and promising material for metal ions biosorption. Yeast cells of the genus *Saccharomyces* are nonpathogenic, are easily available, and enable simple manipulation. *Saccharomyces cerevisiae* cells (both baker's and brewer's yeasts) can be magnetically modified by contact with perchloric acid–stabilized magnetic fluid (Safarikova et al., 2009; Uzun et al., 2011) or other magnetic nanoparticles (Gorobets et al., 2013; Pospiskova et al., 2013). Alternatively, yeast cells can be magnetically modified with magnetic chitosan particles (Saifuddin and Dinara, 2012; Safarik et al., 2015b), bound to magnetic activated carbon (Abdel-Fattah et al., 2014; Mahmoud et al., 2015) or entrapped in magnetic biopolymer beads (Safarik et al., 2008). Green technologies, especially microwave irradiation, have also been employed during magnetic carriers' synthesis and cells' immobilization (Saifuddin and Dinara, 2012; Pospiskova et al., 2013; Safarik et al., 2015b). In some cases, the yeast cell wall was chemically treated with ethylenediaminetetraacetic dianhydride; this treatment resulted in a high number of carboxyl and amino groups on the cell surface (Xu et al., 2011; Zhang et al., 2011). In order to have stabilized product enabling work for a long period of time, dead yeast cells are

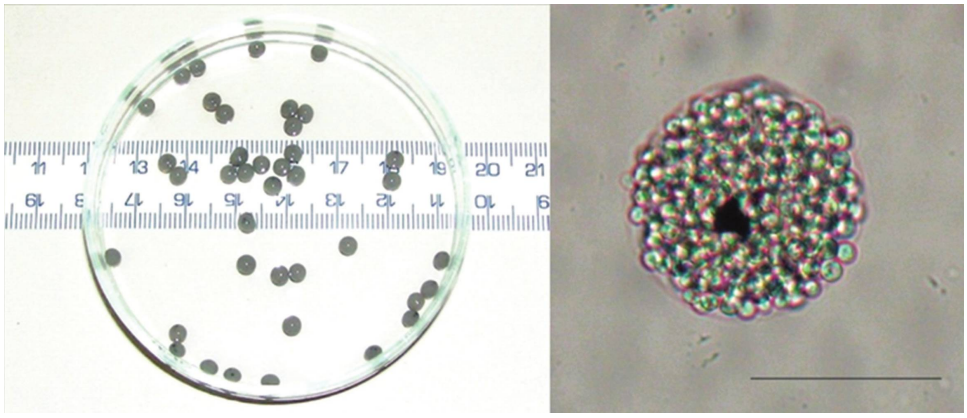

FIGURE 48.5 Magnetically responsive alginate beads containing entrapped *Saccharomyces cerevisiae* cells and magnetite microparticles. (a) Millimeter-sized beads and (b) microbeads. The scale bar corresponds to 50 µm. (Reproduced from Safarik, I. et al., *J. Agric. Food Chem.*, 56, 7925, 2008. With permission.)

TABLE 48.1
Examples of Magnetically Responsive Eukaryotic Microbial Cells and Their Applications as Magnetic Adsorbents for Metal Ions Removal

Microorganism	Magnetic Modification	Adsorbed Ion(s)	Matrix	Other Details	Reference
Baker's yeast	Cells adsorption on activated carbon/nano-Fe_3O_4 composite	Cr(VI) Cr(III)	Aqueous solutions	Removal of chromium species from various real water samples studied	Abdel-Fattah et al. (2014)
Baker's yeast	Cells adsorption on activated carbon/nano-Fe_3O_4 composite	Hg(II)	Model and real aqueous samples	Adsorption follows Langmuir model	Mahmoud et al. (2015)
Baker's yeast biomass	Cross-linked, EDTA-dianhydride modified cells with bound nano-Fe_3O_4	Ca(II) Cd(II) Pb(II)	Model aqueous solutions	Biosorbent with plenty of carboxyl and amino groups introduced by the EDTA molecules	Xu et al. (2011)
Baker's yeast biomass	Cross-linked, EDTA-dianhydride modified cells with bound nano-Fe_3O_4	Pd(II) Cd(II)	Model aqueous solutions	Biosorbent regeneration with 0.1 M HCl	Zhang et al. (2011)
Fungal mycelium (waste)	Composite from waste fungal mycelium, chitosan, and Fe_3O_4 nanoparticles	Cu(II)	Model aqueous solutions	Adsorption equilibrium data fit Langmuir isotherm equation; maximum adsorption capacity 46.25 mg/g	Ren et al. (2008b)
Fungal mycelium (waste)	Composite from waste fungal mycelium, chitosan, and Fe_3O_4 nanoparticles	Cu(II)	Model aqueous solutions	Adsorption equilibrium data fit Langmuir isotherm equation; maximum adsorption capacity 71.36 mg/g	Ren et al. (2008a)
Kluyveromyces marxianus	Treatment with water-based magnetic fluid stabilized with perchloric acid	Sr(II)	Model aqueous solutions	Adsorption equilibrium data fit Langmuir isotherm equation; maximum adsorption capacity 140.8 mg/g	Ji et al. (2010)
Rhizopus cohnii	Immobilization of mycelium and magnetic particles in the matrix of sodium alginate and polyvinyl alcohol	Cr(VI)	Model aqueous solutions	Adsorption equilibrium data fit Langmuir isotherm equation; maximum adsorption capacity 5.79 mg/g	Li et al. (2008)
Rhodotorula glutinis	Treatment with water-based magnetic fluid stabilized with perchloric acid	$UO_2(NO_3)_2$	Model aqueous solutions	Adsorption equilibrium data fit Langmuir isotherm equation; maximum adsorption capacity ca 190 mg/g	Bai et al. (2012)
Saccharomyces cerevisiae	Modification with iron nanoparticles (nZVI)	Ni(II)	Model aqueous solutions	Adsorption equilibrium data fit Langmuir isotherm equation; maximum adsorption capacity 54.23 mg/g	Guler and Ersan (2016)
Saccharomyces cerevisiae	Cells modification with magnetite nanoparticles	Fe(II)	Model aqueous solutions	Adsorption equilibrium data fit Langmuir isotherm equation; maximum adsorption capacity 230 mg/g	Gorobets et al. (2013)
Saccharomyces cerevisiae	Cells bound to cross-linked chitosan-magnetic nanoparticles beads	U(VI)	Model aqueous solutions	Adsorption equilibrium data fit Langmuir isotherm equation; maximum adsorption capacity 72.4 mg/g	Saifuddin and Dinara (2012)
Saccharomyces cerevisiae	Cells immobilized on the surface of chitosan-coated magnetic nanoparticles	Cu(II)	Model aqueous solutions	Adsorption equilibrium data fit Langmuir isotherm equation; maximum adsorption capacity 144.9 mg/g	Peng et al. (2010)
Saccharomyces cerevisiae subsp. *uvarum*	Treatment with water-based magnetic fluid stabilized with perchloric acid	Cu(II)	Model aqueous solutions	Adsorption equilibrium data fit Langmuir isotherm equation; maximum adsorption capacity 1.2 mmol/g	Uzun et al. (2011)
Saccharomyces cerevisiae subsp. *uvarum*	Treatment with water-based magnetic fluid stabilized with perchloric acid	Hg(II)	Model aqueous solutions and artificial wastewater	Adsorption equilibrium data fit Langmuir isotherm equation; maximum adsorption capacity 114.6 mg/g	Yavuz et al. (2006)
Saccharomyces cerevisiae cell walls	Cell walls with covalently and noncovalently bound magnetite	Cu(II) Cd(II) Ag(I)	Model aqueous solutions	Maximum adsorption capacities 50 (Cu), 25 (Cd), and 45 (Ag) μmol/g	Patzak et al. (1997)
Yarrowia lipolytica	Cells modified with phyto-inspired Fe^0/Fe_3O_4 nanoparticles	Cr(VI)	Model aqueous solutions	Adsorption equilibrium data fit Langmuir isotherm equation; maximum adsorption capacity 156.3 mg/g	Rao et al. (2013)
Yeast	Magnetic chitosan/yeast composite	Ce(III)	Aqueous solutions	Adsorption equilibrium data fit Langmuir isotherm equation; maximum adsorption capacity 73.53 mg/g	Ou et al. (2013)
Yeast biomass	Ethylenediamine-modified yeast biomass coated with magnetic chitosan microparticles	Pb(II)	Model aqueous solutions	Adsorption equilibrium data fit Langmuir isotherm equation; maximum adsorption capacity 121.26 mg/g	Li et al. (2013)

TABLE 48.2
Examples of Magnetically Responsive Prokaryotic Microbial Cells and Their Applications as Magnetic Adsorbents for Metal Ions Removal or for Bioreduction

Microorganism	Magnetic Modification	Adsorbed Ion(s)	Matrix	Other Details	Reference
Amphibacillus sp.	Cells immobilized in silica-coated magnetic alginate beads	Cr(VI)	Model aqueous solution	Bioreduction of Cr(VI) studied; magnetically immobilized cells showed 16% higher Cr(VI) reduction activity than nonmagnetic immobilized cells	Ibrahim et al. (2013)
Corynebacterium glutamicum	Cells adsorption on granular activated carbon/ $MnFe_2O_4$ composite	As(III) As(V)	Model aqueous solution	Biosorption of both As(III) and As(V) was spontaneous and exothermic under studied conditions	Podder and Majumder (2016)
Desulfovibrio magneticus	Magnetotactic bacterium	Cd(II)	Model aqueous solution	Electron-dense particles present on cell surface when cultivated in the presence of cadmium ions	Arakaki et al. (2002)
Enterobacter sp.	Cells adsorption on commercial magnetite	Ni(II)	Model aqueous solution	Optimum adsorption at pH 9; elution of adsorbed Ni(II) with diluted citric acid	Wong and Fung (1997)
Escherichia coli	Cells functionalization by magnetic nanobeads	Cd(II) Hg(II)	Model aqueous solutions	Electrochemical biosensor for heavy metal detection constructed	Souiri et al. (2009)
Geobacillus galactosidasius	Cells adsorption on magnetite prepared from Fe^{2+} and Fe^{3+} ions	Pb(II) Cd(II)	Tap and mineral water, food extracts	Preconcentrations of Pb and Cd ions by solid-phase extraction before ICP-OES	Özdemir et al. (2016)
Magnetospirillum gryphiswaldense	Magnetotactic bacterium	Au(III)	Model aqueous solution	Reduction of gold ions to gold nanoparticles	Cai et al. (2011)
Magnetotactic bacterium	—	Pu	Extract from Ravenglass Estuary sediments, UK	Orientation magnetic separation used for cells collection	Bahaj et al. (1998)
Magnetotactic bacterium	—	Au(III) Cu(II)	Model aqueous solutions	Optimum adsorption at pH 1–5.5 for Au(III) and 2.0–4.5 for Cu(II)	Song et al. (2007)
Magnetotactic spirillum	—	Fe(III)	Model aqueous solutions	Orientation magnetic separation used for cells collection	Bahaj et al. (1994)
Pedomicrobium manganicum	Cells adsorption on magnetite particles prepared from crude ore	Mn(II)	Model aqueous solutions	Fluidized bed of magnetized biomass used for manganese removal from water	Sly et al. (1995)
Pseudomonas putida	Cells adsorption on commercial magnetite	Cu(II)	Electroplating effluent	Batch and continuous adsorption in a tank reactor; maximum adsorption capacity 14 and 13.4 mg/g, resp.	Sze et al. (1996)
Pseudomonas putida	Cells adsorption on commercial magnetite	Cu(II)	Industrial waste effluent	Pretreatment of cells by 0.6 M HCl greatly enhances the adsorption capacity	Wang et al. (2000)
Pseudomonas putida	Cells adsorption on commercial magnetite	Cu(II)	Synthetic wastewater	Pretreatment of cells by dilute HCl enhances the adsorption capacity	Chua et al. (1998)
Pseudomonas putida	Cells adsorption on commercial magnetite	Cu(II)	Cu(II)-bearing wastewater	Cu(II) accumulated on the surface of the cell walls; efficient desorption by the acidic treatment	Lei et al. (2000)
Stenotrophomonas sp.	Magnetotactic bacterium	Au(III)	Model aqueous solutions	Reduction of Au(III) to Au(0) by the reductants on the biomass; thiourea used for Au desorption	Song et al. (2008)

preferred. Fodder yeast cells (*Kluyveromyces marxianus*) are usually used in the dried (powdered) form enabling both simple magnetic modification and preparation of a low-cost adsorbent; treatment with magnetic fluid was successfully employed (Safarik et al., 2007).

Magnetically modified baker's, brewer's, and fodder yeast cells were tested as efficient adsorbents of various metal ions, including chromium, mercury, cadmium, lead, nickel, iron, uranium, strontium, and silver ones. The adsorption equilibrium data could usually be well fitted to the Langmuir isotherm. The yeast biomass containing adsorbed metal ions could be easily regenerated by diluted inorganic acids with high efficiency (Yavuz et al., 2006; Ji et al., 2010; Zhang et al., 2011).

Magnetically modified *Rhodotorula glutinis* was used to adsorb uranium from aqueous solutions. The presence of competing cations showed only little effect on uranium sorption. The sorption process was endothermic and spontaneous, implying that it becomes favorable at higher temperature (Bai et al., 2012).

The industrially important yeast *Yarrowia lipolytica* was used for Cr(VI) removal. Due to the cells modification by the phyto-inspired Fe^0/Fe_3O_4 nanocomposite, it was concluded that the yeast cells were efficiently involved in the biosorption of Cr(VI) that was followed by the reduction of Cr(VI) to Cr(III) due to the presence of Fe^{2+} reduction sites in the nanocomposite; the regeneration was caused by electron transfer from Fe^0 particles to Fe^{3+} of magnetite (Rao et al., 2013).

In addition to yeast cells, magnetically modified waste fungal mycelium and *Rhizopus cohnii* mycelium were also tested as adsorbents for copper and chromium ions removal (Li et al., 2008; Ren et al., 2008a,b).

Magnetically modified bacterial cells (especially of the genus *Pseudomonas*) were intensively studied as possible adsorbents for heavy metal ions. *Pseudomonas putida* strain isolated from heavy metal ions contaminated samples exhibited high affinity for Cu(II) ions; pretreatment of the cells with diluted hydrochloric acid (0.6 M) led to the increase in the adsorption capacity. Copper ions were mainly accumulated on the cell surface. EDTA solution (0.1 M) or 0.6 M HCl efficiently removed the adsorbed copper ions from the adsorbent (Sze et al. 1996; Chua et al., 1998; Lei et al., 2000; Wang et al., 2000).

Cr(VI)-reducing *Amphibacillus* cells were immobilized by entrapment in agar, agarose, alginate, or gelatine gels in the presence of Fe_3O_4 nanoparticles; alginate was selected as the best immobilization matrix. In comparison with nonmagnetic immobilized cells, the magnetically immobilized cells exhibited approximately 16% higher Cr(VI) reduction activity. To improve their physical and mechanical properties, the magnetic alginate beads were successfully coated with a dense silica layer using sol-gel chemistry (Ibrahim et al., 2013).

Cells of *Enterobacter* sp. immobilized on magnetite particles could remove large amounts of nickel ions from aqueous solutions. The optimal conditions to remove Ni(II) ions were at an alkaline pH. Complete recovery of adsorbed ions from immobilized cells was achieved by washing with diluted citric acid (Wong and Fung, 1997).

Magnetically modified bacterial cells can also be used for analytical purposes. *Geobacillus galactosidasius* cells modified with maghemite nanoparticles were used for the preconcentrations of Pb and Cd ions by solid-phase extraction before inductively coupled plasma-optical emission spectrometry measurement. Linear calibration curves were constructed in the concentration ranges of 1.0–60 ng/mL for both cations. Maximum adsorption capacities were 47.8 mg/g for Pb and 52.9 mg/g for Cd (Özdemir et al., 2016).

Several strains of MTB have also been tested as potential adsorbents of heavy metal ions and radionuclides. The solution contaminated with plutonium interacted with MTB, and subsequently, orientation magnetic separation was used for cells collection (Bahaj et al., 1998). *Desulfovibrio magneticus* was used in the recovery of cadmium from water solutions (Arakaki et al., 2002). Cells of *Magnetospirillum gryphiswaldense* reduced gold ions to gold nanoparticles that became attached to the bacterial surface (Cai et al., 2011); a similar process was observed in the case of *Stenotrophomonas* sp. (Song et al., 2008).

48.5 SUMMARY

The potential of biosorbents applicable for the removal of heavy metals from aquatic environments has been widely investigated in the last three decades, motivated by the ever-increasing level of water pollution. The sorbents of natural origin are very useful especially for larger-scale applications where good sorption properties combined with lower price (in comparison with other sorbents) are required. Among them, prokaryotic and eukaryotic microbial cells form an intensively studied group of biosorbents enabling the efficient adsorption of heavy metals; sorption processes may also be accompanied with bioremediation. Microbial cells can be modified in order to prepare biosorbents with additional properties; for example, facilitated separation after their magnetic modification is very beneficial and can be one of the future trends in modern technologies improvement. In this chapter, preparation of magnetically responsive microorganisms and their applications for the removal of metal ions have been reviewed. Based on the presented examples of magnetically modified yeast and bacterial cells or fungal mycelia, these types of biosorbents are very promising in environmental technologies. However, their practical applications are not widespread, so further intensive research in this area could be expected in the future.

REFERENCES

Abdel-Fattah, T.M., Mahmoud, M.E., Osmam, M.M., Ahmed, S.B. 2014. Magnetically active biosorbent for chromium species removal from aqueous media. *Journal of Environmental Science and Health, Part A* 49: 1064–1076.

Arakaki, A., Takeyama, H., Tanaka, T., Matsunaga, T. 2002. Cadmium recovery by a sulfate-reducing magnetotactic bacterium, *Desulfovibrio magneticus* RS-1, using magnetic separation. *Applied Biochemistry and Biotechnology* 98: 833–840.

Bahaj, A.S., Croudace, I.W., James, P.A.B., Moeschler, F.D., Warwick, P.E. 1998. Continuous radionuclide recovery from wastewater using magnetotactic bacteria. *Journal of Magnetism and Magnetic Materials* 184: 241–244.

Bahaj, A.S., James, P.A.B., Croudace, I.W. 1994. Metal uptake and separation using magnetotactic bacteria.. *IEEE Transactions on Magnetics* 30: 4707–4709.

Bai, J., Wu, X., Fan, F., Tian, W., Yin, X., Zhao, L., Fan, F., Li, Z., Tian, L., Qin, Z. et al. 2012. Biosorption of uranium by magnetically modified *Rhodotorula glutinis*. *Enzyme and Microbial Technology* 51: 382–387.

Cai, F., Li, J., Sun, J., Ji, Y. 2011. Biosynthesis of gold nanoparticles by biosorption using *Magnetospirillum gryphiswaldense* MSR-1. *Chemical Engineering Journal* 175: 70–75.

Gorobets, S.V., Karpenko, Y.V., Kovalev, O.V., Olishevsky, V.V. 2013. Application of magnetically labeled cells *S. cerevisiae* as biosorbents at treatment plants. *Research Bulletin NTUU 'KPI'* 3: 42–47.

Guler, U.A., Ersan, M. 2016. *S. cerevisiae* cells modified with nZVI: A novel magnetic biosorbent for nickel removal from aqueous solutions. *Desalination and Water Treatment* 57: 7196–7208.

Guobin, S., Jianmin, X., Chen, G., Huizhou, L., Jiayong, C. 2005. Biodesulfurization using *Pseudomonas delafieldii* in magnetic polyvinyl alcohol beads. *Letters in Applied Microbiology* 40: 30–36.

Chua, H., Wong, P.K., Yu, P.H.F., Li, X.Z. 1998. The removal and recovery of copper (II) ions from wastewater by magnetite immobilized cells of *Pseudomonas putida* 5-X. *Water Science and Technology* 38: 315–322.

Ibrahim, A.S.S., Al-Salamah, A.A., El-Toni, A.M., El-Tayeb, M.A., Elbadawi, Y.B., Antranikian, G. 2013. Detoxification of hexavalent chromate by *Amphibacillus* sp KSUCr3 cells immobilised in silica-coated magnetic alginate beads. *Biotechnology and Bioprocess Engineering* 18: 1238–1249.

Ivanova, V., Hristov, J., Dobreva, E., Al-Hassan, Z., Penchev, I. 1996. Performance of a magnetically stabilized bed reactor with immobilized yeast cells. *Applied Biochemistry and Biotechnology* 59: 187–198.

Ivanova, V., Petrova, P., Hristov, J. 2011. Application in the ethanol fermentation of immobilized yeast cells in matrix of alginate/magnetic nanoparticles, on chitosan-magnetite microparticles and cellulose-coated magnetic nanoparticles. *International Review of Chemical Engineering* 3: 289–299.

Ji, Y.-Q., Hu, Y.-T., Tian, Q., Shao, X.-Z., Li, J., Safarikova, M., Safarik, I. 2010. Biosorption of strontium ions by magnetically modified yeast cells. *Separation Science and Technology* 45: 1499–1504.

Lee, D.Y., Oh, Y.I., Kim, D.H., Kim, K.M., Kim, K.N., Lee, Y.K. 2004. Synthesis and performance of magnetic composite comprising barium ferrite and biopolymer. *IEEE Transactions on Magnetics* 40: 2961–2963.

Lei, W., Chua, H., Lo, W.H., Yu, P.H.F., Zhao, Y.G., Wong, P.K. 2000. A novel magnetite-immobilized cell process for heavy metal removal from industrial effluent. *Applied Biochemistry and Biotechnology* 84–86: 1113–1126.

Li, H., Li, Z., Liu, T., Xiao, X., Peng, Z., Deng, L. 2008. A novel technology for biosorption and recovery hexavalent chromium in wastewater by bio-functional magnetic beads. *Bioresource Technology* 99: 6271–6279.

Li, T.-T., Liu, Y.-G., Peng, Q.-Q., Hu, X.-J., Liao, T., Wang, H., Lu, M. 2013. Removal of lead(II) from aqueous solution with ethylenediamine-modified yeast biomass coated with magnetic chitosan microparticles: Kinetic and equilibrium modeling. *Chemical Engineering Journal* 214: 189–197.

Mahmoud, M.E., Ahmed, S.B., Osman, M.M., Abdel-Fattah, T.M. 2015. A novel composite of nanomagnetite-immobilized-baker's yeast on the surface of activated carbon for magnetic solid phase extraction of Hg(II). *Fuel* 139: 614–621.

Ou, H., Bian, W., Weng, X., Huang, W., Zhang, Y. 2013. Adsorption of Ce(III) by magnetic chitosan/yeast composites from aqueous solution: Kinetic and equilibrium studies. In *Energy Engineering and Environmental Engineering*, Pts 1 and 2, ed. T. Sun, pp. 391–394. Zurich, Switzerland: Trans Tech Publications.

Özdemir, S., Kılınç, E., Okumuş, V., Poli, A., Nicolaus, B., Romano, I. 2016. Thermophilic *Geobacillus galactosidasius* sp. nov. loaded γ-Fe_2O_3 magnetic nanoparticle for the preconcentrations of Pb and Cd. *Bioresource Technology* 201: 269–275.

Patzak, M., Dostalek, P., Fogarty, R.V., Safarik, I., and Tobin, J.M. 1997. Development of magnetic biosorbents for metal uptake. *Biotechnology Techniques* 11: 483–487.

Peng, Q., Liu, Y., Zeng, G., Xu, W., Yang, C., Zhang, J. 2010. Biosorption of copper(II) by immobilizing *Saccharomyces cerevisiae* on the surface of chitosan-coated magnetic nanoparticles from aqueous solution. *Journal of Hazardous Materials* 177: 676–682.

Podder, M.S., Majumder, C.B. 2016. Application of granular activated carbon/$MnFe_2O_4$ composite immobilized on *C. glutamicum* MTCC 2745 to remove As(III) and As(V): Kinetic, mechanistic and thermodynamic studies. *Spectrochimica Acta, Part A* 153: 298–314.

Pospiskova, K., Prochazkova, G., Safarik, I. 2013. One-step magnetic modification of yeast cells by microwave-synthesized iron oxide microparticles. *Letters in Applied Microbiology* 56: 456–461.

Prochazkova, G., Safarik, I., Branyik, T. 2013. Harvesting microalgae with microwave synthesized magnetic microparticles. *Bioresource Technology* 130: 472–477.

Rao, A., Bankar, A., Kumar, A.R., Gosavi, S., Zinjarde, S. 2013. Removal of hexavalent chromium ions by *Yarrowia lipolytica* cells modified with phyto-inspired Fe^0/Fe_3O_4 nanoparticles. *Journal of Contaminant Hydrology* 146: 63–73.

Ren, Y., Zhang, M., Zhao, D. 2008a. Synthesis and properties of magnetic Cu(II) ion imprinted composite adsorbent for selective removal of copper. *Desalination* 228: 135–149.

Ren, Y.M., Wei, X.Z., Zhang, M.L. 2008b. Adsorption character for removal Cu(II) by magnetic Cu(II) ion imprinted composite adsorbent. *Journal of Hazardous Materials* 158: 14–22.

Safarik, I., Maderova, Z., Pospiskova, K., Baldikova, E., Horska, K., Safarikova, M. 2015a. Magnetically responsive yeast cells: Methods of preparation and applications. *Yeast* 32: 227–237.

Safarik, I., Maderova, Z., Pospiskova, K., Horska, K., Safarikova, M. 2014. Magnetic decoration and labeling of prokaryotic and eukaryotic cells. In *Cell Surface Engineering*: *Fabrication of Functional Nanoshells*, eds. R.F. Fakhrullin, I. Choi, and Y.M. Lvov, pp. 185–215. Cambridge, U.K.: The Royal Society of Chemistry.

Safarik, I., Pospiskova, K., Maderova, Z., Baldikova, E., Horska, K., and Safarikova, M. 2015b. Microwave-synthesized magnetic chitosan microparticles for the immobilization of yeast cells. *Yeast* 32: 239–243.

Safarik, I., Ptackova, L., Safarikova, M. 2002. Adsorption of dyes on magnetically labeled baker's yeast cells. *European Cells and Materials* 3(Suppl. 2): 52–55.

Safarik, I., Rego, L.F.T., Borovska, M., Mosiniewicz-Szablewska, E., Weyda, F., Safarikova, M. 2007. New magnetically responsive yeast-based biosorbent for the efficient removal of water-soluble dyes. *Enzyme and Microbial Technology* 40: 1551–1556.

Safarik, I., Sabatkova, Z., Safarikova, M. 2008. Hydrogen peroxide removal with magnetically responsive *Saccharomyces cerevisiae* cells. *Journal of Agricultural and Food Chemistry* 56: 7925–7928.

Safarik, I., Safarikova, M. 1999. Use of magnetic techniques for the isolation of cells. *Journal of Chromatography B* 722: 33–53.

Safarikova, M., Atanasova, N., Ivanova, V., Weyda, F., Tonkova, A. 2007. Cyclodextrin glucanotransferase synthesis by Semicontinuous cultivation of magnetic biocatalysts from cells of *Bacillus circulans* ATCC 21783. *Process Biochemistry* 42: 1454–1459.

Safarikova, M., Maderova, Z., Safarik, I. 2009. Ferrofluid modified *Saccharomyces cerevisiae* cells for biocatalysis. *Food Research International* 42: 521–524.

Safarikova, M., Pona, B.M.R., Mosiniewicz-Szablewska, E., Weyda, F., Safarik, I. 2008. Dye adsorption on magnetically modified *Chlorella vulgaris* cells. *Fresenius Environmental Bulletin* 17: 486–492.

Saifuddin, N., Dinara, S. 2012. Immobilization of *Saccharomyces cerevisiae* onto cross-linked chitosan coated with magnetic nanoparticles for adsorption of uranium (VI) ions. *Advances in Natural and Applied Sciences* 6: 249–267.

Schüler, D., ed. 2007. *Magnetoreception and Magnetosomes in Bacteria*. Berlin, Heidelberg: Springer.

Sharma, S.K., ed. 2015. *Heavy Metals in Water*: *Presence, Removal and Safety*. Cambridge, U.K.: The Royal Society of Chemistry.

Sly, L.I., Arunpairojana, V., Dixon, D.R. 1995. Method for removing manganese from water. USA Patent 5,443,729.

Song, H.P., Li, X.G., Sun, J.S., Xu, S.M., Han, X. 2008. Application of a magnetotactic bacterium, *Stenotrophomonas* sp to the removal of Au(III) from contaminated wastewater with a magnetic separator. *Chemosphere* 72: 616–621.

Song, H.P., Li, X.G., Sun, J.S., Yin, X.H., Wang, Y.H., Wu, Z.H. 2007. Biosorption equilibrium and kinetics of Au(III) and Cu(II) on magnetotactic bacteria. *Chinese Journal of Chemical Engineering* 15: 847–854.

Souiri, M., Gammoudi, I., Ouada, H.B., Mora, L., Jouenne, T., Jaffrezic-Renault, N., Dejous, C., Othmane, A., Duncan, A.C. 2009. *Escherichia coli*-functionalized magnetic nanobeads as an ultrasensitive biosensor for heavy metals. *Procedia Chemistry* 1: 1027–1030.

Sze, K.F., Lu, Y.J., Wong, P.K. 1996. Removal and recovery of copper ion (Cu^{2+}) from electroplating effluent by a bioreactor containing magnetite-immobilized cells of *Pseudomonas putida* 5X. *Resources*, *Conservation and Recycling* 18: 175–193.

Uzun, L., Saglam, N., Safarikova, M., Safarik, I., Denizli, A. 2011. Copper biosorption on magnetically modified yeast cells under magnetic field. *Separation Science and Technology* 46: 1045–1051.

Wainwright, M., Singleton, I., Edyvean, R.G.J. 1990. Magnetite adsorption as a means of making fungal biomass susceptible to a magnetic field. *Biorecovery* 2: 37–53.

Wang, L., Chua, H., Wong, P.K., Lo, W.H., Yu, P.H.F., Zhao, Y.G. 2000. An optimal magnetite immobilized *Pseudomonas putida* 5-x cellsystem for Cu^{2+} removal from industrial waste effluent. *Water Science and Technology* 41: 241–246.

Widjojoatmodjo, M.N., Fluit, A.C., Torensma, R., Verhoef, J. 1993. Comparison of immunomagnetic beads coated with protein A, protein G, or goat anti-mouse immunoglobulins. *Journal of Immunological Methods* 165: 11–19.

Wong, P.K., Fung, K.Y. 1997. Removal and recovery of nickel ion (Ni^{2+}) from aqueous solution by magnetite-immobilized cells of *Enterobacter* sp 4–2. *Enzyme and Microbial Technology* 20: 116–121.

Xu, M., Zhang, Y., Zhang, Z., Shen, Y., Zhao, M., Pan, G. 2011. Study on the adsorption of Ca^{2+}, Cd^{2+} and Pb^{2+} by magnetic Fe_3O_4 yeast treated with EDTA dianhydride. *Chemical Engineering Journal* 168: 737–745.

Yavuz, H., Denizli, A., Gungunes, H., Safarikova, M., Safarik, I. 2006. Biosorption of mercury on magnetically modified yeast cells. *Separation and Purification Technology* 52: 253–260.

Zborowski, M., Fuh, C.B., Green, R., Baldwin, N.J., Reddy, S., Douglas, T., Mann, S., Chalmers, J.J. 1996. Immunomagnetic isolation of magnetoferritin-labeled cells in a modified ferrograph. *Cytometry* 24: 251–259.

Zborowski, M., Malchesky, P.S., Jan, T.F., Hall, G.S. 1992. Quantitative separation of bacteria in saline solution using lanthanide Er(III) and a magnetic field. *Journal of General Microbiology* 138: 63–68.

Zhang, Y., Zhu, J., Zhang, L., Zhang, Z., Xu, M., Zhao, M. 2011. Synthesis of EDTAD-modified magnetic baker's yeast biomass for Pb^{2+} and Cd^{2+} adsorption. *Desalination* 278: 42–49.

Zheng, B.Z., Zhang, M.H., Xiao, D., Jin, Y., Choi, M.M.F. 2010. Fast microwave synthesis of Fe_3O_4 and Fe_3O_4/Ag magnetic nanoparticles using Fe^{2+} as precursor. *Inorganic Materials* 46: 1106–1111.

5.4 Adsorpce endokrinních disruptorů

5.4.1 Adsorpce bisfenolu A na biouhel

Bisfenol A je považován za jednu z nejvýznamnějších průmyslových látek napodobujících přírodní hormony v endokrinním systému organismů. Ročně je produkován v ohromném množství (celosvětová produkce se uvádí až pět miliónů tun) a je součástí zejména polykarbonátových plastů a epoxidových pryskyřic. Tato chemická sloučenina je ubikvitní, což dokazuje nejen její přítomnost ve všech typech vod, ale také v moči 90 % testovaných jedinců.

Pro adsorpci bisfenolu A byl testován biouhel získaný jako vedlejší produkt při gasifikaci smrkových štěpek. Magnetická modifikace byla provedena pomocí suspenze MS magnetitu v poměru 1:4 (1 g biouhlu a 4 mL suspenze magnetických částic v obvyklém poměru), která umožnila dostatečně rychlou separaci materiálu. Bisfenol A v modelovém roztoku byl kvantifikován pomocí HPLC vybavenou detektorem s diodovým polem.

V této publikaci byly testovány dva základní faktory ovlivňující účinnost adsorpce, a sice inkubační doba a teplota. Ukázalo se, že adsorpční rovnováha byla dosažena za 120-150 min a že proces adsorpce je spontánní a exotermní. Maximální adsorpční kapacita vypočtená z Langmuirova modelu činila 77,4 mg/g.

Závěrem lze konstatovat, že tento typ biokompozitního materiálu vykazuje nejen relativně vysokou adsorpční účinnost pro testovaný analyt v porovnání s dalšími studovanými biologickými materiály, ale také poskytuje možnost rychlé a selektivní separace z prostředí.

Příloha 19:

Removal of bisphenol A using magnetically responsive spruce chip biochar

Baldikova E, Pospiskova K, Safarik I

Zasláno do redakce

Removal of bisphenol A using magnetically responsive spruce chip biochar

Short title: Bisphenol A removal using magnetic spruce chip biochar

Eva Baldikova[1,2,*], Kristyna Pospiskova[3], Ivo Safarik[1,3]

[1]Department of Nanobiotechnology, Biology Centre, ISB, Czech Academy of Sciences, Na Sadkach 7, 37005 Ceske Budejovice, Czech Republic

[2]Department of Applied Chemistry, Faculty of Agriculture, University of South Bohemia, Branisovska 1457, 37005 Ceske Budejovice, Czech Republic

[3]Regional Centre of Advanced Technologies and Materials, Palacky University, Slechtitelu 27, 78371 Olomouc, Czech Republic

*Corresponding author; email address: baldie@email.cz, phone number: +420387775605

Abstract

Bisphenol A, a representative of significantly extended endocrine disruptor chemicals, was efficiently adsorbed on biochar obtained as a by-product from high temperature gasification of spruce chips. Simple magnetic modification employing microwave-synthesized magnetic iron oxide nano- and microparticles (MS-MIOP) was used for the preparation of the novel magnetically responsive sorbent. Adsorption equilibrium data were analyzed using non-linear regression analysis and the Langmuir and Freundlich isotherm models. The experimental adsorption data for all tested temperatures conformed well to the Langmuir isotherm model, and the maximum adsorption capacity reached the value of 77.4 mg per gram of magnetic material at 282.15 K. Kinetics of sorption process followed the pseudo-second-order kinetic model, and thermodynamic studies described an exothermic and spontaneous adsorption process. The prepared material exhibited high adsorption efficiency of bisphenol A and also a rapid magnetic response to an external magnetic field. These properties predetermine magnetic biochar adsorbent as a prospective material for highly efficient removal of hazardous bisphenol A in environmental applications.

Key words: adsorbent; biochar; bisphenol A; HPLC analysis; magnetic iron oxides; microwave synthesis

Abbreviations and nomenclature

BPA = bisphenol A

EDC = endocrine disruptor compounds

MS-MIOP = microwave-synthesized magnetic iron oxide nano- and microparticles

SEE = the standard error of estimate

C = the constant varied directly with the boundary layer thickness (mg/g)

C_0 = the initial concentration of BPA (mg/L)

C_e = the concentration of free (unbound) BPA in the supernatant (mg/L) in equilibrium

C_t = the concentration of free (unbound) BPA at time t (mg/L)

$\Delta G°$ = the standard free energy change of sorption (J/mol)

$\Delta H°$ = the standard enthalpy change (J/mol)

k_1 = the rate constant of pseudo-first-order kinetic model (1/min)

k_2 = the rate constant of pseudo-second-order kinetic model (g/mg min)

k_{id} = the intra-particle diffusion rate constant (mg/g $min^{1/2}$)

K_D = the thermodynamic equilibrium constant

K_F = the Freundlich isotherm constant related to adsorption capacity [(mg/g) $(L/mg)^{1/n}$]

K_L = the Langmuir constant related to the energy of adsorption (L/mg)

m = weight of adsorbent (g)

n = the Freundlich isotherm constant connected with adsorption intensity

n' = the number of the experimental measurements

p' = the number of parameters

q_e = the amount of BPA bound to the unit mass of the adsorbent (mg/g)

q_m = the maximum adsorption capacity (mg/g)

q_t = the amount of dye bound to the unit mass of the adsorbent at time t (mg/g)

R = the universal gas constant (8.314 J/mol K)

R_L = the separation factor

$\Delta S°$ = the standard entropy change (J/mol K)

t = time (min)

T = temperature (K)

V = volume of solution (L)

y_i = the experimental value of the dependent variable

$y_{i,theor}$ = the estimated value of the dependent variable

Introduction

Bisphenol A (BPA), also known as 2,2-bis(4-hydroxyphenyl)propane or 4,4´-isopropylidenediphenol, belongs to the group of endocrine disruptors (EDCs) - substances that mimic natural hormones in the endocrine system and that cause adverse effects on humans and wildlife.

BPA is utilized as an intermediate (binding, hardening, and plasticizing) in plastics, binding and filling materials, paints/lacquers, and as an additive for brake fluids, flame-retardants, and thermal papers. About 95 % of BPA produced in industry is used to make plastics, in particular polycarbonate (71 %) and epoxy resins (29%) (Careghini et al. 2015). Polycarbonates generally exhibit excellent physical and chemical properties, such as good thermal stability, elasticity, high mechanical strength, and low density, thus have been extensively utilized in pharmaceutical and food packaging, infant bottles, medical equipment, kitchen utensils, computers and electronic devices (compact discs) (Johnson et al. 2015; Sala et al. 2010). Epoxy resins are used as an interior protective lining for food and beverage cans (Johnson et al. 2015).

The world-wide production of BPA was 3.2 million tons in 2005 (Fernandez et al. 2007), 3.8 million tons in 2006 (Rancière et al. 2015), and 5 million tons in 2010 (Huang et al. 2012). Due to the intense and still increasing consumption, BPA is ubiquitous in our environment. Vandenberg et al. (2010) determined that over 90 % of individuals have detectable levels of BPA present in their urine. The presence of BPA has been detected in all types of environmental water, at concentrations ranging from 17.2 mg/L in hazardous waste landfill leachate, to 12 μg/L in stream water and 3.5-59.8 ng/L in drinking water (Bautista-Toledo et al. 2014). BPA can enter water during manufacturing and leach from plastic products (Zhou et al. 2012).

Many techniques can be successfully used for BPA and other EDC removal, including the application of nanofiltration and reverse osmosis membrane (Jin et al. 2010), ozonation (Bila et al. 2007), microbial (Ribeiro et al. 2010) or sonochemical (Ifelebuegu et al. 2014) degradation, coagulation/flocculation or advanced oxidation processes (Lazim et al. 2015),

but these methods are often connected with high cost and very expensive maintenance. Hence, development of effective and low-cost approaches for BPA disposal is necessary. Both aims can be easily achieved by means of biosorption, especially using cheap and easily-available biomaterials. Recently, various biosorbents have been tested for BPA removal, including rice husk ash (Sudhakar et al. 2016), peat, straw and sugarcane bagasse (Zhou et al. 2012), and bamboo fiber powder (Hartono et al. 2015). In order to enhance usually lower maximum adsorption capacity of natural biosorbents, an appropriate chemical treatment can be utilized. For instance, Zhou et al. (2011) modified fibric peat with a surfactant hexadecyltrimethylammonium bromide and increased the maximum adsorption capacity (q_m) from 15.9 to 29.1 mg/g.

In this study, a solid by-product from gasification of spruce chips (biochar) was utilized for BPA adsorption. To simplify manipulation with adsorbent, biochar was magnetically modified. The magnetic biochar demonstrated high maximum adsorption capacity (77.4. mg/g) without modification which allows for economical removal of BPA from environmental water.

Materials and methods

Materials

Ferrous sulfate heptahydrate ($FeSO_4$. 7 H_2O) was supplied by Lachner (Neratovice, Czech Republic), and NaOH by Penta (Prague, Czech Republic). Both chemicals were of GR grade. Bisphenol A (97%) was obtained from Sigma Aldrich (St. Louis, MO, USA) and methanol super gradient (HPLC) from Labscan (Dublin, Ireland).

Adsorbent preparation

Biochar was obtained from the company AIVOTEC s.r.o. (Kromeriz, Czech Republic), in February 2016, as a by-product of gasification of spruce chips using temperature ca.1200^{o}C for 1 h. Obtained biochar was passed through sieves with mesh sizes of 100 and 200 μm (Retsch, Haan, Germany).

Magnetic modification of spruce chip biochar was carried out using microwave-synthesized magnetic iron oxide nano- and microparticles (MS-MIOP) as described previously (Zheng et al. 2010). Briefly, 100 mL of 1% $FeSO_4$ $7H_2O$ solution (w/V) was drop-by-drop alkalized with 1 M NaOH under stirring (Stuart SB 161-3 stirrer; Bibby Scientific Ltd, Stone, UK) until the pH reached the value 12. The total volume was then made up to 200

mL with distilled water and the iron hydroxide suspension underwent microwave irradiation treatment in microwave oven (700W, 2450 MHz) at maximum power for 10 min. The formed MS-MIOP were washed several times with distilled water to obtain a neutral pH of suspension, and allowed to settle under gravity in 50 mL calibrated cylinders for 18 h.

The magnetic derivative of biochar was prepared by thorough mixing of 1 g wood biochar with 4 mL microwave-synthesized iron oxide suspension (1 part settled MS-MIOP and 4 parts water) and subsequent drying at 58 ^{o}C for 24 h.

Material characterization

The morphology of native and magnetically modified biochar was observed by Scanning Electron Microscopy (120 Hitachi SU6600, Hitachi, Tokyo, Japan) with accelerating voltage of 5 kV. Energy Dispersive Spectroscopy (EDS) was carried out using Thermo Noran System 7 acquired in SEM (Thermo Scientific, Waltham, MA, USA) with Si(Li) detector (acquisition time 300 s and accelerating voltage of 15 kV).

Fourier transform infrared (FT-IR) spectroscopy of native and magnetically responsive biochar was performed using FT-IR spectrometer (Thermo Scientific Nicolet iS5, Thermo Nicolet Corp., Madison, WI, USA) with iD Foundation accessory (ZnSe crystal, range 4000–650 cm^{-1}, resolution 4 cm^{-1}, 32 scans). The FT-IR absorption spectra were recorded in advanced attenuated total reflectance (ATR) mode and presented in transmittance.

Batch adsorption experiments

A stock solution of bisphenol A (1mg/mL; pH 7.6) was prepared in methanol (HPLC) due to its low solubility in water; further dilutions were carried out with distilled water. All adsorption experiments were performed in a batch system at natural pH in duplicate; average values are presented. After incubation on rotator mixer (Stuart SB3, Bibby Scientific Ltd, Stone, UK) at 23 rpm for particular time, samples were magnetically separated (magnetic separator Dynamag^{TM}-15, Dynal, Oslo, Norway) and supernatant filtered through 0.22 μm PTFE syringe filters (Membrane Solutions, Dallas,TX, USA). Filtrates were analyzed using HPLC Agilent Series 1100 (Agilent Technologies, Santa Clara, CA, USA) equipped with diode array UV/VIS detector and SGX C18 column (Tessek, Prague, Czech Republic) 150x 4 mm, particles 5 micron. The mobile phase consisted of 70% methanol and 30% distilled water; flow rate 0.5 mL/min and 20 μL of sample were used. Column temperature was set to 30 ^{o}C and absorbance was measured at 278 nm.

The dependence of incubation time, initial concentration and temperature on BPA adsorption was studied in detail. The amount of free (unbound) BPA in equilibrium (C_e; mg/L) or at time t (C_t; mg/L) was calculated from a calibration curve and the amount of BPA adsorbed on unit mass of biochar (q_e and q_t; mg/g) from the following formulae:

$$q_e = \frac{V\,(C_0 - C_e)}{m} \quad (1)$$

$$q_t = \frac{V\,(C_0 - C_t)}{m} \quad (2)$$

Kinetic studies

Adsorption kinetics was studied at room temperature (RT, 295.15 K) using 30 mg of biochar, 10 mL of 250 mg/L BPA solution and time intervals of 5-300 min. Kinetic data were evaluated using the linear forms of pseudo-first-order (Ho 2004), pseudo-second-order (Ho and McKay 1998) and intra-particle diffusion (Weber and Morris 1963) models given as follows (equations 3 – 5):

$$\ln(q_e - q_t) = \ln(q_e) - k_1\, t \quad (3)$$

where k_1 and q_e were calculated from the slope and intercept of the plots of ln(q_e-q_t) versus t.

$$\frac{\mathrm{t}}{\mathrm{q_t}} = \frac{1}{k_2\, {q_e}^2} + \frac{t}{q_e} \quad (4)$$

where the values of k_2 and q_e were calculated from the slope and intercept of the plots of t/q_t versus t.

$$q_t = k_{id} t^{1/2} + C \quad (5)$$

Adsorption isotherms

30 mg of magnetically modified biochar was mixed with 10 mL BPA solution with concentrations ranging from 100-350 mg/L in 15 mL test tubes, and incubated on a rotator mixer at 282.15, 295.15 and 313.15 K overnight.

Adsorption equilibrium data were analyzed by Langmuir and Freundlich adsorption isotherm models using nonlinear regression analysis (Microsoft Excel, function Solver-add).

The Langmuir model, referring to homogeneous monolayer adsorption, is defined as

$$q_e = \frac{K_L\, q_{max}\, C_e}{1 + K_L\, C_e} \quad (6)$$

The Freundlich model, describing the multilayer adsorption on a heterogeneous surface, is expressed as

$$q_e = K_F\, (C_e)^{\frac{1}{n}} \quad (7)$$

Fitting of experimental data to each adsorption isotherm model was assessed using the standard error of estimate (SEE) values calculated as follows:

$$SEE = \sqrt{\sum_{i=1}^{n'} \left(y_i - y_{i,theor}\right)^2 / (n' - p')} \quad (8)$$

Separation factor (R_L) was calculated from the formula:

$$R_L = \frac{1}{1 + K_L\, C_0} \quad (9)$$

Thermodynamics

Adsorption equilibrium isotherms obtained at different temperatures (282.15, 295.15 and 313.15 K) were used for determination of thermodynamic parameters, namely Gibbs free energy (ΔG^o), enthalpy (ΔH^o) and entropy (ΔS^o). The thermodynamic equilibrium constant (K_d) was determined from the intercept of the plots of ln (q_e/C_e) against q_e (Khan and Singh 1987).

ΔG^o was calculated from the following formula:

$$\Delta G^o = -RT \ln(K_d) \quad (10)$$

Enthalpy and entropy values were determined using the Van´t Hoff equation, from the slope and intercept of the linear plot of ln (K_d) versus 1/T, respectively:

$$\ln(K_d) = \frac{\Delta S^o}{R} - \frac{\Delta H^o}{RT} \quad (11)$$

Results and discussion

Magnetic modification and characterization of material

The deposition of magnetic iron oxide nano- and microparticles on wood chip biochar and subsequent thorough drying of composite material resulted in a formation of a magnetic adsorbent typical of a great response to an external magnetic field (permanent magnet, commercially available magnetic separators or electromagnets) as documented by Fig. 1. Furthermore, the binding of MS-MIOP on biochar surface was very stable. After one month of material storage in distilled water at 4 ^{o}C, no release of magnetic particles from biochar was observed.

Recently, it has been proved that the size of magnetic iron oxides synthesized using microwave irradiation ranges from 25 to 100 nm, however, the nanoparticles tend to form stable micro-sized agglomerates (with maximum aggregate size about 20 μm) (Baldikova et al. 2016). The morphology of spruce chip biochar was observed using scanning electron microscopy; appearance of native biochar can be seen in Fig. 2a, and detail of magnetic particles attached on biochar surface in Fig. 2b. The presence of iron was successfully identified by energy dispersive X-ray spectroscopy (Fig. 2c).

FT-IR analysis of native and magnetically modified material revealed absorption spectra without any typical bands (Fig. 3). This result is in accordance with other studies focusing on biochar prepared at temperatures exceeding 700 ^{o}C (Asada et al. 2004).

Adsorption studies

Magnetic wood chip biochar was tested as a potential adsorbent for BPA removal. Agitation time and temperature dependence on adsorption efficiency was studied in detail. Subsequently, the kinetic and thermodynamic parameters were determined.

Incubation time is a significant factor for achieving the adsorption equilibrium. As can be seen from Fig. 4a, the adsorption process for BPA was relatively quick; 95 % of 250 mg/L BPA was adsorbed within 30 min under experimental conditions used (rotation at 23 rpm, total volume 10 mL, RT). Nevertheless, at least 120-150 min is needed to reach the equilibrium.

Equilibrium adsorption data at all tested temperatures were analyzed using the most often used – two parameter - adsorption isotherm models, specifically the Langmuir and Freundlich ones. The Langmuir model assumes monolayer adsorption and no interaction

between adsorbed molecules; whereas the Freundlich model is more suitable for description of multilayer adsorption on a heterogeneous surface. Higher K_L values denote high affinity for sorbate, and higher values of K_F correspond to higher adsorption capacity. The fitting of the experimental data to the both tested adsorption isotherm models were evaluated on the basis of obtained SEE values, summarized in Table 1. In all cases, SEE values for the Langmuir model are lower than for the Freundlich model, thus it can be supposed that adsorption of BPA on magnetic biochar is best described by the Langmuir isotherm.

The type of isotherm can also be determined by the separation factor. If the R_L value is higher than 1, the isotherm is unfavorable. If the R_L value lies between 0 and 1, the process is favorable. $R_L = 1$ indicates linear isotherm and $R_L = 0$ denotes the irreversible process (Kumar et al. 2014). As can be seen from Fig. 5, the adsorption of BPA on magnetically responsive biochar is a favorable process at all tested temperatures and concentrations used.

Kinetic studies

Adsorption kinetics was determined from experimental data describing the effect of contact time on adsorption efficiency (Fig. 4a), at time intervals ranging from 5 to 300 min. Pseudo-first-order, pseudo-second-order kinetic models and the intra-particle diffusion model were used for investigation of kinetic process (see Fig. 4b-d and Table 2).

The intra-particle diffusion plot usually consists of two portions; first portion indicates a boundary layer effect at the initial stage of the adsorption and second portion reflects the gradual adsorption stage with the rate limiting step (Guzel et al. 2015). According to the multi-linear plots demonstrated in Fig. 4d, it can be assumed that intra-particle diffusion plays a significant role but is not the only rate-limiting step.

In general, the applicability of kinetic models used can be evaluated on the basis of the obtained correlation coefficients R^2 and calculated q_e values. As shown in Table 2, the pseudo-second-order kinetic models exhibited both higher R^2 and closer $q_{e\,(calc)}$ value to $q_{e\,(exp)}$ value in comparison to the other two models. This indicates that the sorption mechanism of BPA on magnetically responsive biochar follows the pseudo-second-order kinetic model.

Thermodynamics

Thermodynamic parameters, given in Table 3, were calculated from equilibrium adsorption isotherms performed at 282.15, 295.15 and 313.15 K. The values of Gibbs free energy for all temperatures used are negative which indicates the spontaneous reaction.

Negative enthalpy value denotes the exothermic nature of adsorption process which is also suggested by obtained q_m values that decrease when temperature increases; at 282.15 K the maximum adsorption capacity reached 77.4 mg/g, while at 313.15 K it was only 71.6 mg/g. The negative value of entropy corresponds to a decrease in degree of freedom of the adsorbed species.

Table 4 presents some other adsorbents utilized for BPA adsorption including their maximum adsorption capacities at experimental conditions used and other features characterizing the adsorption process, such as a type of adsorption isotherm, kinetic model and thermodynamic reaction.

Conclusions

Spruce chip biochar was magnetically modified using simple and fast method employing microwave-synthesized magnetic iron oxide nano- and microparticles formed from two cheap and basic chemicals, specifically ferrous sulfate heptahydrate and sodium hydroxide. Thorough mixing of MS-MIOP with biochar and subsequent drying resulted in a formation of material with a great response to external magnetic field. Prepared material can be easily magnetically manipulated and separated from suspensions and difficult-to-handle media.

Magnetically responsive biochar exhibited high adsorption efficiency for BPA removal; the maximum adsorption capacities calculated from the Langmuir isotherm model were found to be 77.4, 72.6 and 71.6 mg/g at 282.15, 295.15 and 313.15 K, respectively. The adsorption equilibrium was achieved within 120-150 min. Adsorption process can be well described with pseudo-second-order kinetic model, is spontaneous and exothermic.

Prepared magnetic adsorbent provides a set of unique characteristics, such as economical convenience, high BPA adsorption efficiency and simultaneously easy manipulation in any environment.

Acknowledgements

This research was supported by the projects LO1305 and LD14066 (Ministry of Education, Youth and Sports of the Czech Republic) and by the COST Action TD1107 "Biochar as option for sustainable resource management". The authors also thank Mr. Jan Kana for providing the biochar sample and Ing. Petra Bazgerova for performing SEM and EDS analysis.

References

Asada T, Oikawa K, Kawata K, Ishihara S, Iyobe T, Yamada A (2004) Study of removal effect of bisphenol A and beta-estradiol by porous carbon. J Health Sci 50: 588-593. doi:10.1248/jhs.50.588

Baldikova E, Politi D, Maderova Z, Pospiskova K, Sidiras D, Safarikova M, Safarik I (2016) Utilization of magnetically responsive cereal by-product for organic dye removal. J Sci Food Agric 96: 2204-2214. doi:10.1002/jsfa.7337

Bautista-Toledo MI, Rivera-Utrilla J, Ocampo-Perez R, Carrasco-Marin F, Sanchez-Polo M (2014) Cooperative adsorption of bisphenol-A and chromium(III) ions from water on activated carbons prepared from olive-mill waste. Carbon 73: 338-350. doi:10.1016/j.carbon.2014.02.073

Bila D, Montalvao AF, Azevedo DdeA, Dezotti M (2007) Estrogenic activity removal of 17 beta-estradiol by ozonation and identification of by-products. Chemosphere 69: 736-746. doi:10.1016/j.chemosphere.2007.05.016

Careghini A, Mastorgio AF, Saponaro S, Sezenna E (2015) Bisphenol A, nonylphenols, benzophenones, and benzotriazoles in soils, groundwater, surface water, sediments, and food: A review. Environ Sci Pollut Res 22: 5711-5741. doi:10.1007/s11356-014-3974-5

Fernandez MF, Arrebola JP, Taoufiki J, Navalon A, Ballesteros O, Pulgar R, Vilchez JL, Olea N (2007) Bisphenol-A and chlorinated derivatives in adipose tissue of women. Reprod Toxicol 24: 259-264. doi:10.1016/j.reprotox.2007.06.007

Guzel F, Saygili H, Saygili GA, Koyuncu F (2015) New low-cost nanoporous carbonaceous adsorbent developed from carob (*Ceratonia siliqua*) processing industry waste for the

adsorption of anionic textile dye: Characterization, equilibrium and kinetic modeling. J Mol Liq 206: 244-255. doi:10.1016/j.molliq.2015.02.037

Hartono MR, Assaf A, Thouand G, Kushmaro A, Chen XD, Marks RS (2015) Use of bamboo powder waste for removal of bisphenol A in aqueous solution. Water Air Soil Pollut 226: 382. doi:10.1007/s11270-015-2644-7

Ho YS (2004) Citation review of Lagergren kinetic rate equation on adsorption reactions. Scientometrics 59: 171-177. doi: 10.1023/B:SCIE.0000013305.99473.cf

Ho YS, McKay G (1998) Sorption of dye from aqueous solution by peat. Chem Eng J 70: 115-124. doi:10.1016/s1385-8947(98)00076-x

Huang YQ, Wong CKC, Zheng JS, Bouwman H, Barra R, Wahlstrom B, Neretin L, Wong MH (2012) Bisphenol A (BPA) in China: A review of sources, environmental levels, and potential human health impacts. Environ Int 42: 91-99. doi:10.1016/j.envint.2011.04.010

Ifelebuegu AO, Onubogu J, Joyce E, Mason T (2014) Sonochemical degradation of endocrine disrupting chemicals 17 beta-estradiol and 17 alpha-ethinylestradiol in water and wastewater. Int J Environ Sci Technol 11: 1-8. doi:10.1007/s13762-013-0365-2

Jin X, Hu J, Ong SL (2010) Removal of natural hormone estrone from secondary effluents using nanofiltration and reverse osmosis. Water Res 44: 638-648. doi:10.1016/j.watres.2009.09.057

Johnson S, Saxena P, Sahu R (2015) Leaching of bisphenol A from baby bottles. Proc Natl Acad Sci, India, Sect B Biol Sci 85: 131-135. doi:10.1007/s40011-013-0246-y

Khan AA, Singh RP (1987) Adsorption thermodynamics of carbofuran on Sn (IV) arsenosilicate in H^+, Na^+ and Ca^{2+} forms. Colloid Surf 24: 33-42.

Kumar PS, Palaniyappan M, Priyadharshini M, Vignesh AM, Thanjiappan A, Fernando PSA, Ahmed RT, Srinath R (2014) Adsorption of basic dy onto raw and surface-modified agricultural waste. Environ Prog Sustain Energy 33: 87-98. doi: 10.1002/ep.11756

Lazim ZM, Hadibarata T, Puteh MH, Yusop Z (2015) Adsorption characteristics of bisphenol A onto low-cost modified phyto-waste material in aqueous solution. Water Air Soil Pollut 226: 34. doi:10.1007/s11270-015-2318-5

Li J, Zhan Y, Lin J, Jiang A, Xi W (2014) Removal of bisphenol A from aqueous solution using cetylpyridinium bromide (CPB)-modified natural zeolites as adsorbents. Environ Earth Sci 72: 3969-3980. doi:10.1007/s12665-014-3286-6

Rancière F, Lyons JG, Loh VHY, Botton J, Galloway T, Wang T, Shaw JE, Magliano DJ (2015) Bisphenol A and the risk of cardiometabolic disorders: A systematic review

with meta-analysis of the epidemiological evidence. Environ Health 14: 1-23. doi:10.1186/s12940-015-0036-5

Ribeiro AR, Carvalho MF, Afonso CMM, Tiritan ME, Castro PML (2010) Microbial degradation of 17-estradiol and 17-ethinylestradiol followed by a validated HPLC-DAD method. J Environ Sci Health Part B-Pestic Contam Agric Wastes 45: 265-273. doi:10.1080/03601231003704523

Sala M, Kitahara Y, Takahashi S, Fujii T (2010) Effect of atmosphere and catalyst on reducing bisphenol A (BPA) emission during thermal degradation of polycarbonate. Chemosphere 78: 42-45. doi:10.1016/j.chemosphere.2009.10.036

Soni H, Padmaja P (2014) Palm shell based activated carbon for removal of bisphenol A: An equilibrium, kinetic and thermodynamic study. J Porous Mat 21: 275-284. doi:10.1007/s10934-013-9772-5

Sudhakar P, Mall ID, Srivastava VC (2016) Adsorptive removal of bisphenol-A by rice husk ash and granular activated carbon-A comparative study. Desalin Water Treat 57: 12375-12384. doi:10.1080/19443994.2015.1050700

Vandenberg LN, Chahoud I, Heindel JJ, Padmanabhan V, Paumgartten FJR, Schoenfelder G (2010) Urinary, circulating, and tissue biomonitoring studies indicate widespread exposure to bisphenol A. Environ Health Perspect 118: 1055-1070. doi:10.1289/ehp.0901716

Weber WJ, Morris JC (1963) Kinetics of adsorption on carbon from solution. J Sanit Eng Division Proc. Am Soc Civil Eng 89: 31-60 .

Wirasnita R, Hadibarata T, Yusoff ARM, Yusop Z (2014) Removal of bisphenol A from aqueous solution by activated carbon derived from oil palm empty fruit bunch. Water Air Soil Pollut 225:2148. doi:10.1007/s11270-014-2148-x

Zheng B, Zhang M, Xiao D, Jin Y, Choi MMF (2010) Fast microwave synthesis of Fe_3O_4 and Fe_3O_4/Ag magnetic nanoparticles using Fe^{2+} as precursor. Inorg Mater 46: 1106-1111. doi:10.1134/s0020168510100146

Zheng S, Sun Z, Park Y, Ayoko GA, Frost RL (2013). Removal of bisphenol A from wastewater by Ca-montmorillonite modified with selected surfactants. Chem Eng J 234: 416-422. doi:10.1016/j.cej.2013.08.115

Zhou Y, Chen L, Lu P, Tang X, Lu J (2011) Removal of bisphenol A from aqueous solution using modified fibric peat as a novel biosorbent. Sep Purif Technol 81: 184-190. doi:10.1016/j.seppur.2011.07.026

Zhou Y, Lu P, Lu J (2012) Application of natural biosorbent and modified peat for bisphenol a removal from aqueous solutions. Carbohydr Polym 88: 502-508. doi:10.1016/j.carbpol.2011.12.034

Legend to Figures and Tables

Figure 1: Magnetic separation of biochar modified with MS-MIOP.

Figure 2: SEM image of a) native biochar and b) detail of magnetic particles attached on modified biochar surface; c) EDS of magnetically modified biochar.

Figure 3: FTIR spectra of native (solid line) and magnetically modified (dashed line) biochar.

Figure 4: Kinetic studies: a) effect of contact time on BPA adsorption; b) pseudo-first-order kinetic plot; c) pseudo-second-order kinetic plot; d) intra-particle diffusion plot.

Figure 5: Separation factor (R_L) for BPA adsorption on magnetically modified biochar at tested temperatures (◊ 282.15 K, □ 295.15 K, ▲313.15 K).

Table 1: Parameters from Langmuir and Freundlich adsorption equilibrium isotherm models at tested temperatures.

Table 2: Parameters from pseudo-first-order, pseudo-second-order and intra-particle diffusion models.

Table 3: Thermodynamic parameters.

Table 4: Examples of adsorbents used for BPA removal (DDTMAB = dodecyl trimethyl ammonium bromide, HDTMAB = hexadecyl trimethyl ammonium bromide, N/A = data not available).

Fig. 1


1 cm

Fig. 2

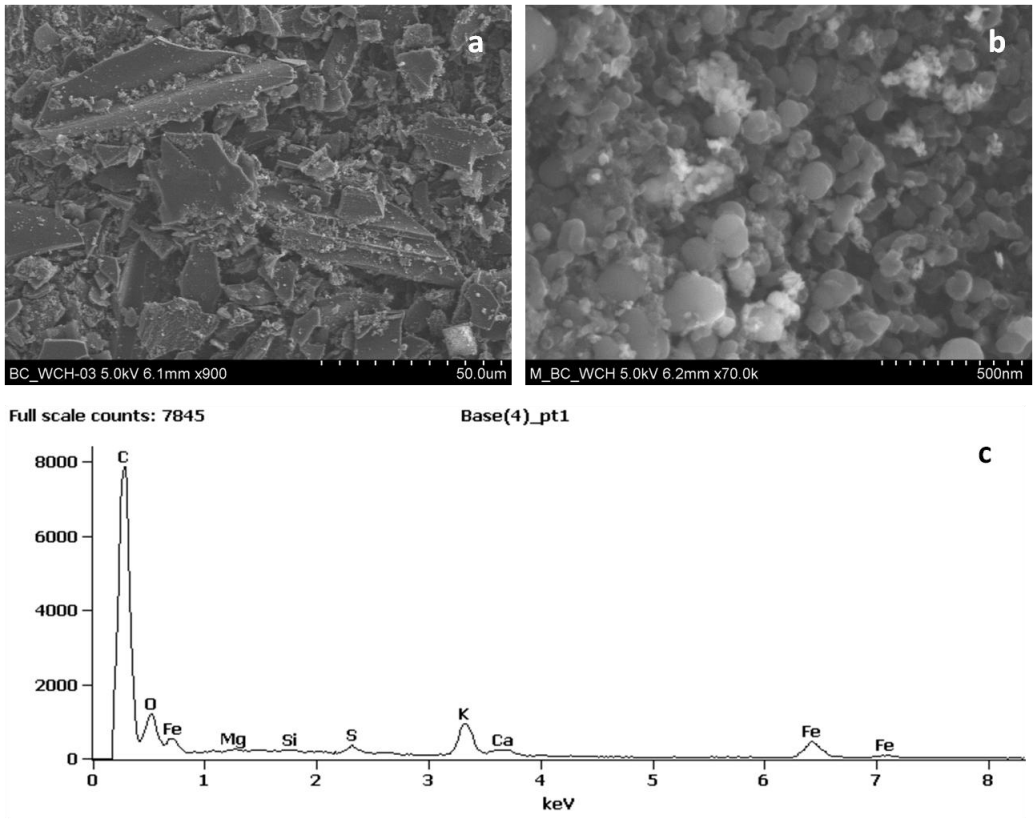
a
BC_WCH-03 5.0kV 6.1mm x900
50.0um
b
M_BC_WCH 5.0kV 6.2mm x70.0k
500nm
Full scale counts: 7845
Base(4)_pt1
c
8000
6000
4000
2000
0
C
O
Fe
Mg
Si
S
K
Ca
Fe
Fe
0
1
2
3
4
5
6
7
8
keV

Fig. 3

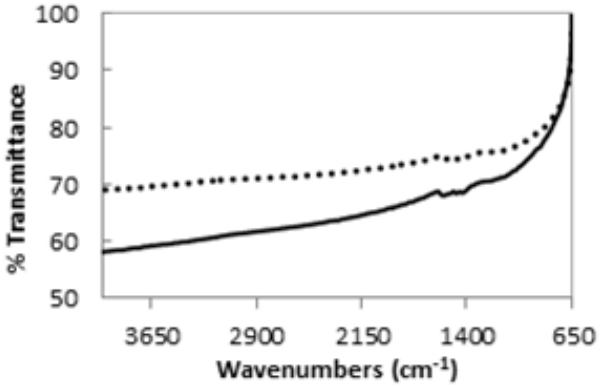
100
90
80
70
60
50
% Transmittance
3650
2900
2150
1400
650
Wavenumbers (cm-1)

Fig. 4

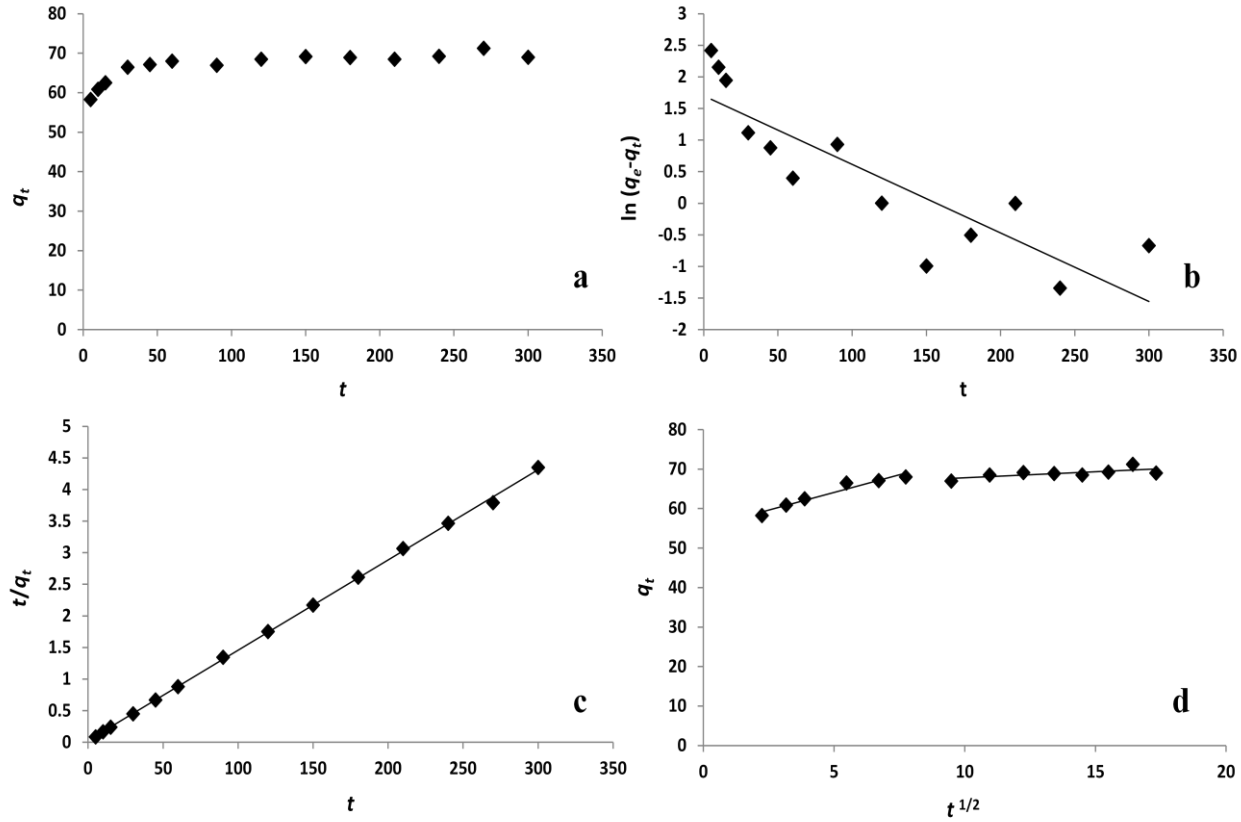
a
b
c
d
qt
t
ln (qe-qt)
t/qt
t 1/2

Fig. 5

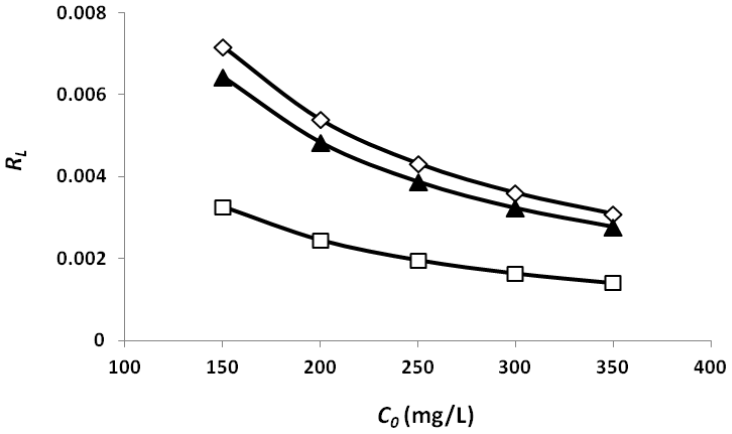

Table 1

Temperature	Langmuir model		Freundlich model	
282.15 K	K_L (L/mg)	0.922	K_F [mg/g) (L/mg]$^{1/n}$]	49.348
	q_m (mg/g)	77.4	*n*	9.377
	SEE	3.366	*SEE*	4.085
295.15 K	K_L (L/mg)	2.032	K_F [mg/g) (L/mg]$^{1/n}$]	45.906
	q_m (mg/g)	72.6	*n*	9.167
	SEE	3.074	*SEE*	5.110
313.15 K	K_L (L/mg)	1.029	K_F [mg/g) (L/mg]$^{1/n}$]	49.998
	q_m (mg/g)	71.6	*n*	12.459
	SEE	1.639	*SEE*	4.178

Table 2

q_e (exp)	Pseudo-first kinetic model		Pseudo-second kinetic model		Intra-particle diffusion model			
69.5	$q_{e\ (calc)}$ (mg/g)	5.5	$q_{e\ (calc)}$ (mg/g)	69.9	*C* (mg/g)	55.2	*C* (mg/g)	64.7
	k_1 (1/min)	0.011	k_2 (g/mg min)	0.007	k_{id1} (mg/g min$^{1/2}$)	1.778	k_{id2} (mg/g min$^{1/2}$)	0.307
	R^2	0.752	R^2	0.999	R^2	0.945	R^2	0.503

Table 3

Temperature (K)	**Ln K_d**	**Δ G^o** (kJ/mol)	**Δ H^o** (kJ/mol)	**Δ S^o** (J/mol K)	**R^2**
282.15	11.646	- 27.319			
295.15	10.844	- 26.610	- 38.959	- 41.46	0.9978
313.15	9.997	- 26.027			

Table 4

Material	**q_m (mg/g)**	**pH**	**Temperature (^{o}C)**	**Adsorption isotherm model**	**Adsorption equilibrium**	**Kinetic model**	**Adsorption process**	**References**
Ca-montmorillonite modified with DDTMAB	106.4	7	24	Langmuir	5 min	pseudo-second	exothermic	(Zheng et al. 2013)
Magnetically modified spruce chip biochar	77.4	N/A	9	Langmuir	2 h	pseudo-second	exothermic	This study
Palm shell activated carbon	62.5	N/A	N/A	Langmuir	8 h	pseudo-second	exothermic	(Soni and Padmaja 2014)
Activated carbon from oil palm empty fruit bunch	42.0	N/A	27	Langmuir	48 h	pseudo-second	N/A	(Wirasnita et al. 2014)
Natural zeolite treated with HDTMAB	33.8	7	30	Langmuir	5 h	pseudo-second	exothermic	(Li et al. 2014)
Peat modified with HDTMAB	29.2	N/A	25	Freundlich	4 h	pseudo-second	N/A	(Zhou et al. 2011)

5.5 Adsorpce ropných derivátů

5.5.1 Odstranění ropných derivátů pomocí ječné slámy

Doposud nepublikované výsledky získané ze zahraniční stáže na Univerzitě v Piraeu v Řecku.

MATERIÁLY A METODY

„Typy“ testovaných slam a příprava:

V rámci těchto experimentů byla testována pšeničná sláma:

1) Nativní (pocházející z ČR a Řecka)
2) Olejová (hydrofobizovaná)
3) Modifikovaná pomocí H_2SO_4 (hydrolyzovaná)

Slámové materiály byly připraveny ve dvou velikostech, tzv. malé (s rozměry částic 0,1-1 mm) a větší (1-2 mm).

Modifikace pšeničné slámy:

Olejová modifikace:

1 g slámy byl smíchán s 1 g slunečnicového oleje a 19 g vody. Směs byla míchána 2 h a poté sušena při teplotě 55 ^{o}C do konstantní hmotnosti.

H_2SO_4 modifikace:

Kyselá hydrolýza probíhala při 100 ^{o}C po dobu 4 hodin. Detailní postup modifikace je uveden v publikaci (Batzias et al., 2009).

Magnetická modifikace:

Magnetická modifikace byla provedena pomocí MS magnetitu, a to v poměrech 1:2, 1:4, 1:6, 1:8 a 1:10.

Adsorpce ropných derivátů:

Adsorpční experimenty vycházely ze standardních metod: ASTM F 726 stanovující množství navázaného oleje (gravimetricky) a ASTM D 95 určující obsah nasorbované vody pomocí destilace.

a) Adsorpce v ideálním prostředí

Sorpce v čistém prostředí byla provedena ve 25 mL ropného derivátu (benzinu, nafty a surové ropy) či destilované vodě za přídavku 0,1- 0,2 g slámového materiálu. Doba adsorpce byla dle metodiky stanovena na 15 min. Poté byl magnetický adsorbent magneticky separován, okapán (30 s) a znovu zvážen. Výpočet navázaného ropného derivátu (q_m v g/g) byl proveden dle následujícího vzorce:

$$q_m = \frac{m_1 - m_0}{m_0} \quad (1)$$

kde: m_1 = váha po sorpci (g), m_0 = váha naváženého materiálu (g).

V rámci experimentů byl zjišťován vliv typu pšeničné slámy (nativní, po H_2SO_4 a olejové modifikaci), velikosti částic (malé 0,1 – 1 mm a větší 1-2 mm), intenzity magnetické modifikace (magnetizace MS magnetitem v poměru 1:6, 1:8 a 1:10), třepání (100 rpm) a použitého adsorbátu (natural 98, diesel, surová ropa) na maximální adsorpční kapacitu (q_m).

b) Adsorpce ve směsném prostředí (ropný derivát/voda)

Adsorpční experimenty byly provedeny v 600 mL kádinkách, s 200 mL vody, 10 mL ropného derivátu a 0,8 g slámového adsorbentu (agitace 150 rpm, 15 min sorpce, 30 s okapání, zvážení a destilace k určení množství navázané vody).

VÝSLEDKY A DISKUSE

a) Adsorpce na pšeničnou slámu modifikovanou MS magnetitem – ideální prostředí

- **Vliv třepání**

Jak je zřejmé z Grafu 1, agitace jak u nativní slámy pocházející z ČR, tak u nativní slámy získané z území Řecka nehraje významnou roli; pouze v případě řecké modifikované slámy dochází k výraznějšímu nárůstu maximání adsorpční kapacity (q_m).

Graf 1: Vliv třepání na maximálních adsorpční kapacitu slámových adsorbentů (malé částice, natural 98).

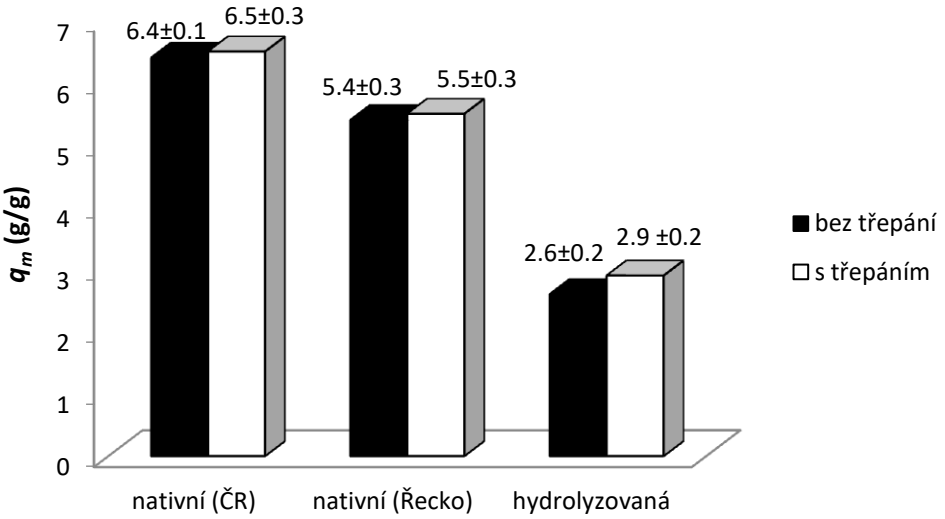

- **Vliv intenzity magnetizace a velikosti částic**

V experimentu, jehož výsledky jsou shrnuty v Tabulce 8, byly testovány magnetizační poměry 1:6, 1:8 a 1:10 a dvě velikosti částic řeckých vzorků slámy, tzv. malé (0.1-1 mm) a větší (1-2 mm). Ukazuje se, že zvyšující se přídavek magnetických částic má spíše negativní účinek na hodnotu maximální adsorpční kapacity (q_m) konkrétně u nativní a olejové (hydrofobizované) slámy. H_2SO_4 hydrolyzovaná sláma vykazuje velmi překvapivě opačný trend, a to i v případě použití velkých částic, u kterých je ve všech ostatních případech zaznamenán prudký pokles q_m oproti hodnotám naměřených u částic malých.

Tabulka 8: Vliv intenzity magnetizace a velikosti částic na maximální adsorpční kapacitu (q_m).

Intenzita magnetizace	q_m (g/g)					
	Nativní		**Hydrolyzovaná**		**Hydrofobizovaná**	
	Malé	Větší	Malé	Větší	Malé	Větší
1:6	5.7 ± 0.11	3.7 ± 0.28	4.4 ± 0.13	5.7 ± 0.21	3.4 ± 0.11	2.3 ± 0.17
1:8	5.3 ± 0.12	3.5 ± 0.38	4.9 ± 0.18	6.2 ± 0.21	3.1 ± 0.1	2.2 ± 0.19
1:10	5.4 ± 0.05	3.4 ± 0.18	5.0 ± 0.23	6.8 ± 0.25	3.1 ± 0.12	2.1 ± 0.07

- **Vliv použitého adsorbátu**

V tomto experimentu byly testovány všechny typy slámy v obou velikostech, magnetizované v poměru 1:8. Výsledky sorpce surové ropy, nafty a vody za využití větších částic slámy jsou ukázány v Grafu 2.

Graf 2: Maximální adsorpční kapacity slámových sorbentů (větší částice) pro různé adsorbáty.

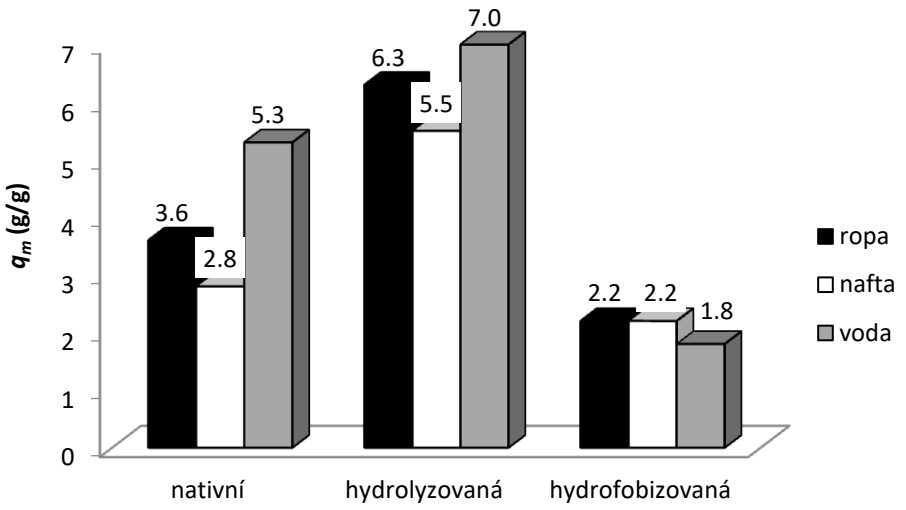

- **Vliv jednotlivých typů pšeničné slámy**

Vliv typu slámy se prolíná ve všech prezentovaných experimentech. Je však nutné vzít v potaz nejen typ slámy, ale také intenzitu magnetizace či velikost částic. Z těchto ohledů lze za nejvhodnější adsorbent pro další adsorpční experimenty či využití v praxi považovat slámu hydrolyzovanou o větší velikosti částic a současně s vyšším zastoupením magnetických částic. Je-li ovšem vyžadováno použití malých

částic ve směsném prostředí (olej/voda), je vhodné zvolit slámu olejovou, která jako jediná drží v olejové vrstvě.

b) Adsorpce na pšeničnou slámu modifikovanou MS magnetitem – směsné prostředí

K tomuto adsorpčnímu experimentu byly použity větší částice nativní a hydrolyzované slámy, neboť se prokázalo, že ty malé nedrží v olejové vrstvě, tudíž nejsou pro pokusy a následnou magnetickou separaci vhodné. Olejová sláma, která byla úspěšně hydrofobizována, byla však použita ve verzi malé. Testovány byly sorpce surové ropy a dieselu. Ve všech případech se za pomoci destilačního přístroje ukázalo, že slámový sorbent ve směsném prostředí neváže žádnou vodu. Hodnoty q_m pro jednotlivé sorbenty jsou uvedeny v Tabulce 9.

Tabulka 9: Maximální adsorpční kapacity slámových sorbentů ve směsném prostředí.

Slámový adsorbent	**q_m (g/g)**	
	Ropa	**Nafta**
Větší částice nativní slámy	3.1 ± 0.3	2.4 ± 0.2
Větší částice hydrolyzované slámy	5.5 ± 0.3	4.7 ± 0.1
Malé částice hydrofobizované slámy	3.0 ± 0.2	2.9 ± 0.2

ZÁVĚR

Z předložených výsledků je patrné, že pšeničná sláma, reprezentující vedlejší produkt zemědělského průmyslu, může být s relativně vysokou účinností využita jako adsorbent pro surovou ropu, diesel i natural 98. Přídavkem magnetických částic získal slámový materiál unikátní vlastnost, a to reakci na vnější magnetické pole, umožňující velmi jednoduchou, selektivní a rychlou separaci připraveného biokompozitu.

6. DISKUSE

Disertační práce byla zaměřena na problematiku přípravy magnetických biokompozitních materiálů a jejich následnou aplikaci v environmentálních technologiích, konkrétně k odstranění organických i anorganických xenobiotik z vod. Významným přínosem magneticky modifikovaných materiálů je jejich odezva vůči vnějšímu magnetickému poli (např. komerčně dostupnému magnetickému separátoru), která umožňuje jejich selektivní separaci z prostředí.

Experimentální část práce se zabývala přípravou nových typů magnetických biokompozitních materiálů rostlinného a mikrobiálního původu s důrazem na zužitkování nejrůznějších odpadních a vedlejších produktů zemědělského a potravinářského průmyslu.

Pro přípravu magnetických materiálů z jejich diamagnetických prekurzorů byly vybrány jednoduché a časově nenáročné techniky magnetické modifikace zahrnující zejména smíchání modifikovaného materiálu s magnetickou kapalinou (Safarik and Safarikova, 2010) či mikrovlnně syntetizovanými magnetickými nano- a mikročásticemi oxidů železa (Safarik and Safarikova, 2014). Pro materiály tvořící po modifikaci vodným MS magnetitem a následným vysušením tvrdé klastry byla vyvinuta jednoduchá modifikace stávající metody založená na převedení MS magnetitu do organického rozpouštědla mísitelného s vodou (Safarik et al., 2016a). Touto vylepšenou technikou byla magnetizována např. makrořasa *Sargassum horneri*, která byla posléze využita pro adsorpci akridinové oranže, krystalové violeti, malachitové zeleně, metylenové modře a safraninu O (Angelova et al., 2016). Morfologie připravených magnetických derivátů byla charakterizována pomocí optické či skenovací elektronové mikroskopie. Přítomnost částic železa na povrchu materiálu byla také detekována prostřednictvím EDS. Vybrané materiály byly podrobeny FTIR analýze ke zjištění změn v přítomnosti funkčních skupin po chemické modifikaci či po sorpci testovaného barviva. U každého materiálu byla také zjišťována stabilita ve vodném prostředí, která byla ve všech případech delší než jeden měsíc.

Magnetická odezva jednotlivých derivátů byla testována reakcí na permanentní magnet. Intenzitu magnetizace (rychlost odezvy) lze jednoduše upravit snížením či zvýšením množství magnetických částic. Navázané magnetické částice lze kvantifikovat prostřednictvím inovativní techniky založené na měření magnetické permeability (Safarik et al., 2016b).

Vyjma adsorpčních experimentů byly připravené magnetické materiály použity jako nosiče pro imobilizované enzymy, buňky či afinitní ligandy. Například na bakteriální celulózu, modifikovanou kyselou MK, byly úspěšně naimobilizovány kvasinkové buňky, trypsin i ostazinová tyrkys. Enzymatickou aktivitu připraveného biokompozitu bylo možné využít opakovaně (Baldikova et al., 2017a). Na částice magnetického mikrovlnně syntetizovaného chitosanu byly kovalentně navázány kvasinkové buňky, jež byly využity jak pro degradaci peroxidu vodíku, tak pro tvorbu inertního cukru (Safarik et al., 2015b). Hydrolýza sacharózy byla také testována na chitosanu magnetizovaném MK stabilizovanou kyselinou polymetakrylovou, na který byly během jeho formace navázány kvasinkové buňky *S. cerevisiae, Candida utilis* a *Kluyveromyces lactis*. U tohoto experimentu bylo prokázáno, že pro průmyslové účely lze účinně použít i jiné zástupce kvasinkových buněk než běžně využívané *S. cerevisiae* (Baldikova et al., 2017b).

Majoritní část experimentální práce byla zaměřena na využití magneticky modifikovaných biokompozitů (často odpadních a vedlejších produktů průmyslu) pro odstraňování organických barviv. Jedny z nejvyšších maximálních adsorpčních kapacit (q_m) byly získány u tepelně ošetřeného aktivovaného kalu modifikovaného pomocí MS magnetitu, kde nejvyšší hodnota q_m dosahovala 768 mg/g (pro anilinovou modř). Následuje magnetická chemicky modifikovaná ječná sláma, u které byla vypočtená hodnota q_m pro Bismarckovu hněď Y rovna 520 mg/g. Vysoké hodnoty q_m byly také zjištěny pro adsorpci krystalové violeti na magnetickou bakteriální celulózu ošetřenou ostazinovou tyrkysí (392 mg/g) či pro adsorpci amidové černě 10B pomocí *Lepthotrix* sp., které byly modifikovány jak kyselou MK (339 mg/g), tak MS magnetitem (286 mg/g). Relativně vysoké hodnoty q_m byly dosaženy také při použití magnetické makrořasy *Sargassum horner*i (110 - 194 mg/g) či mořské trávy *Posidonia oceanica* (88 – 234 mg/g). Nižší hodnoty q_m byly zaznamenány při studiu adsorpce na odpadu čaje Rooibos (62 – 142 mg/g) či na magnetickém biouhlu (19 – 137 mg/g). Ve všech testovaných případech byl adsorpční proces spontánní.

Další experimentálně studovaná xenobiotika zahrnovala bisfenol A, jenž byl sorbován na magneticky modifikovaný biouhel získaný gasifikací smrkových štěpek, či ropné deriváty (surovou ropu, naftu, benzín 98), které byly odstraňovány pomocí magnetické ječné slámy. I u těchto xenobiotik byly dosaženy relativně vysoké q_m hodnoty, které zcela korelují s hodnotami publikovanými ve vědeckých článcích.

Z předložených výsledků je patrné, že magnetické biokompozitní materiály mohou být připraveny pomocí jednoduchých, časově a instrumentálně nenáročných technik a že zejména v případě modifikace odpadních či vedlejších produktů potravinářského a zemědělského průmyslu lze získat extrémně laciný biomateriál s adekvátní odezvou vůči vnějšímu magnetickému poli, který lze aplikovat nejen jako adsorbent xenobiotik, ale také jako nosič pro imobilizované enzymy, buňky či afinitní ligandy.

7. ZÁVĚR

1) Byla vypracována literární rešerše zabývající se problematikou přípravy a následného využití magneticky modifikovaných biokompozitních materiálů jako adsorbentů organických barviv, těžkých kovů, farmaceutických preparátů a přípravků osobní péče společně s endokrinními disruptory, a také ropných derivátů.

2) Byly připraveny nové typy magnetických materiálů zejména rostlinného původu, reprezentující vedlejší a odpadní produkty potravinářského a zemědělského průmyslu. Důraz byl kladen nejen na snadnou dostupnost a nízkou cenu diamagnetických materiálů, ale také na jednoduchost, rychlost a spolehlivost použitých metod magnetické modifikace.

3) U vybraných materiálů byla provedena jednoduchá chemická modifikace využívající účinku kyseliny citronové a hydroxidu sodného, která měla za následek významné (více než čtyřnásobné) navýšení maximálních adsorpčních kapacit pro všechna testovaná organická barviva.

4) Úspěšnost magnetické modifikace byla testována reakcí na permanentní magnet, v některých případech také Perlsovým barvením, které selektivně reaguje se vzniklými Fe(III) ionty. Magnetické částice či jejich agregáty navázané na povrch modifikovaného materiálu byly pozorovány pomocí skenovací elektronové mikroskopie.

5) Proces adsorpce byl studován v modelovém vodném prostředí v nejrůznějších experimentálních podmínkách. Ve všech experimentech byla testována především závislost na čase, neboť správné určení doby inkubace je nezbytné pro modelování adsorpčních izoterem. Dále byl sledován vliv pH a teploty. Ze získaných dat byly vypočteny kinetické a termodynamické parametry popisující povahu adsorpce.

8. LITERÁRNÍ ZDROJE

Abdolali A, Guo WS, Ngo HH, Chen SS, Nguyen NC, Tung KL. Typical lignocellulosic wastes and by-products for biosorption process in water and wastewater treatment: a critical review. *Bioresour. Technol.* 160, **2014**, 57-66.

Akkaya G, Guzel F. Application of some domestic wastes as new low-cost biosorbents for removal of methylene blue: kinetic and equilibrium studies. *Chem. Eng. Commun.* 201, **2014,** 557-578.

Aksu Z. Application of biosorption for the removal of organic pollutants: a review. *Process Biochem.* 40, **2005**, 997-1026.

Angelova R, Baldikova E, Pospiskova K, Maderova Z, Safarikova M, Safarik I. Magnetically modified *Sargassum horneri* biomass as an adsorbent for organic dye removal. *J. Clean Product.* 137, **2016**, 189-194.

Angelova R, Baldikova E, Pospiskova K, Safarikova M, Safarik I. Magnetically modified sheaths of *Leptothrix* sp. as an adsorbent for Amido black 10B removal. *J. Magn. Magn. Mater*. 427, **2017**, 314-319.

Ansone L, Klavins M, Viksna A. Arsenic removal using natural biomaterial-based sorbents. *Environ. Geochem. Health* 35, **2013**, 633-642.

Bai J, Wu X, Fan F, Tian W, Yin X, Zhao L, Fan F, Li Z, Tian L, Qin Z, Guo J. Biosorption of uranium by magnetically modified *Rhodotorula glutinis*. *Enzyme Microb. Technol.* 51, **2012**, 382-387.

Baldikova E, Politi D, Maderova Z, Pospiskova K, Sidiras D, Safarikova M, Safarik I. Utilization of magnetically responsive cereal by-product for organic dye removal. *J. Sci. Food Agric.* 96, **2016**, 2204-2214.

Baldikova E, Pospiskova K, Ladakis D, Kookos IK, Koutinas AA, Safarikova M, Safarik I. Magnetically modified bacterial cellulose: a promising carrier for immobilization of affinity ligands, enzymes, and cells. *Mater. Sci. Eng. C* 71, **2017a**, 214-221.

Baldikova E, Prochazkova J, Stepanek M, Hajduova J, Pospiskova K, Safarikova M, Safarik I. PMAA-stabilized ferrofluid/chitosan/yeast composite for bioapplications. *J. Magn. Magn. Mater.* 427, **2017b**, 29-33.

Banerjee SS, Joshi MV, Jayaram RV. Treatment of oil spill by sorption technique using fatty acid grafted sawdust. *Chemosphere* 64, **2006**, 1026-1031.

Batzias F, Sidiras D, Schroeder E, Weber C. Simulation of dye adsorption on hydrolyzed wheat straw in batch and fixed-bed systems. *Chem. Eng. J.* 148, **2009**, 459-472.

Behnood R, Anvaripour B, Fard NJH, Farasati M. Petroleum hydrocarbons adsorption from aqueous solution by raw sugarcane bagasse. *Int. J. Emerg. Sci. Eng.* 1, **2013**, 96-99.

Brena BM, Batista-Viera F. Immobilization of enzymes: a literature survey. In: *Methods in Biotechnology: Immobilization of Enzymes and Cells* (Guisan JM, Ed.). 2nd edition. Humana Press Inc.: Totowa, **2006**, pp 15-30.

Brodelius P, Vandamme EJ. Immobilized cell systems. In: *Biotechnology: Enzyme Technology* (Kennedy JF, Ed.). VCH Verlagsgesellschaft: Weinheim, **1987**, pp 405-464.

Celekli A, Bozkurt H. Predictive modeling of an azo metal complex dye sorption by pumpkin husk. *Environ. Sci. Pollut. Res.* 20, **2013**, 7355-7366.

Chen XG, Cheng J, Lv SS, Zhang PP, Liu ST, Ye Y. Preparation of porous magnetic nanocomposites using corncob powders as template and their applications for electromagnetic wave absorption. *Compos. Sci. Technol.* 72, **2012**, 908-914.

Cheng Z, Gao Z, Ma W, Sun Q, Wang B, Wang X. Preparation of magnetic Fe_3O_4 particles modified sawdust as the adsorbent to remove strontium ions. *Chem. Eng. J.* 209, **2012**, 451-457.

Chibata I, Toss T, Sato T. Application of immobilized biocatalysts in pharmaceutical and chemical industries. In: *Biotechnology: Enzyme Technology* (Kennedy JF, Ed.). VCH Verlagsgesellschaft: Weinheim, **1987**, pp 653-684.

Choi GG, Oh SJ, Lee SJ, Kim JS. Production of bio-based phenolic resin and activated carbon from bio-oil and biochar derived from fast pyrolysis of palm kernel shells. *Bioresour. Technol.*178, **2015**, 99-107.

Coleman JM, Baker J, Cooper C, Fingas M, Hunt GL, Kvenvolden KA, McDowell JE, Michel J, Michel RK, Phinney J, Pond R, Rabalais NN, Roesner LA, Spies RB. Oil in the sea: inputs, fates, and effects. *Spill Sci. Technol. Bull.* 7, **2012**, 197-199.

Creamer A E, Gao B, Wang S. Carbon dioxide capture using various metal oxyhydroxide-biochar composites. *Chem. Eng. J.* 283, **2016**, 826-832.

Ding C, Cheng W, Sun Y, Wang X. Novel fungus-Fe_3O_4 bio-nanocomposites as high performance adsorbents for the removal of radionuclides. *J. Hazard. Mater.* 295, **2015**, 127-137.

Du ZJ, Zhang Y, Li ZJ, Chen H, Wang Y, Wang GT, Zou P, Chen HP, Zhang YS. Facile one-pot fabrication of nano-Fe_3O_4/carboxyl-functionalized baker's yeast composites and their application in methylene blue dye adsorption. *Appl. Surf. Sci.* 392, **2017**, 312-320.

Dutz S, Clement JH, Eberbeck D, Gelbrich T, Hergt R, Mueller R, Wotschadlo J, Zeisberger M. Ferrofluids of magnetic multicore nanoparticles for biomedical applications. *J. Magn. Magn. Mater.* 321, **2009**, 1501-1504.

Fan Y, Yang RF, Lei ZM, Liu N, Lv JL, Zhai SR, Zhai B, Wang L. Removal of Cr(VI) from aqueous solution by rice husk derived magnetic sorbents. *Korean J. Chem. Eng.* 33, **2016**, 1416-1424.

Fent K, Weston AA, Caminada D. Ecotoxicology of human pharmaceuticals. *Aquat. Toxicol.* 76, **2006**, 122-159.

Gan WT, Gao LK, Zhan XX, Li J. Preparation of thiol-functionalized magnetic sawdust composites as an adsorbent to remove heavy metal ions. *RSC Adv.* 6, **2016a**, 37600-37609.

Gan WT, Gao LK, Zhang WB, Li J, Cai LP, Zhan XX. Removal of oils from water surface via useful recyclable $CoFe_2O_4$/sawdust composites under magnetic field. *Mater. Des.* 98, **2016b**, 194-200.

Gong R, Du Y, Li C, Zhu S, Qiu Y, Jiang J. Thioglycolic acid esterified into rice straw for removing lead from aqueous solution. *Iranian J. Environ. Health Sci. Eng.* 8, **2011**, 219-226.

Gong R, Jin Y, Chen F, Chen J, Liu Z. Enhanced malachite green removal from aqueous solution by citric acid modified rice straw. *J. Hazard. Mater.* 137, **2006**, 865-870.

Gronnow MJ, Budarin VL, Mašek O, Crombie KN, Brownsort PA, Shuttleworth PS, Hurst PR, Clark JH. Torrefaction/biochar production by microwave and conventional slow pyrolysis – comparison of energy properties. *GCB Bioenergy* 5, **2013**, 144-152.

Gui X, Zeng Z, Lin Z, Gan Q, Xiang R, Zhu Y, Cao A, Tang Z., 2013. Magnetic and highly recyclable macroporous carbon nanotubes for spilled oil sorption and separation. *ACS Appl. Mater. Interfaces* 5, **2013**, 5845-5850.

Guler UA, Ersan M. *S. cerevisiae* cells modified with nZVI: a novel magnetic biosorbent for nickel removal from aqueous solutions. *Desalin. Water Treat.* 57, **2016**, 7196-7208.

Gupta VK, Nayak A. Cadmium removal and recovery from aqueous solutions by novel adsorbents prepared from orange peel and Fe_2O_3 nanoparticles. *Chem. Eng. J.* 180, **2012**, 81-90.

Haghighat ZA, Ameri E. Synthesis and characterization of nano magnetic wheat straw for lead adsorption. *Desalin. Water Treat.* 57, **2016**, 9813-9823.

Han R, Zhang L, Song C, Zhang M, Zhu H, Zhang L. Characterization of modified wheat straw, kinetic and equilibrium study about copper ion and methylene blue adsorption in batch mode. *Carbohydr. Polym.* 79, **2010**, 1140-1149.

Hashemian S, Salimi M. Nano composite a potential low cost adsorbent for removal of cyanine acid. *Chem. Eng. J.* 188, **2012**, 57-63.

Hernandez-Mena LE, Pecora AAB, Beraldo AL. Slow pyrolysis of bamboo biomass: analysis of biochar properties. *Chem. Eng. Trans.* 37, **2014**, 115-120.

Hoekman SK, Broch A, Robbins C, Zielinska B, Felix L. Hydrothermal carbonization (HTC) of selected woody and herbaceous biomass feedstocks. *Biomass Conv. Bioref.* 3, **2013**, 113-126.

Hong RY, Li JH, Li HZ, Ding J, Zheng Y, Wei DG. Synthesis of Fe_3O_4 nanoparticles without inert gas protection used as precursors of magnetic fluids. *J. Magn. Magn. Mater.* 320, **2008**, 1605-1614.

Huang YQ, Wong CKC, Zheng JS, Bouwman H, Barra R, Wahlstrom B, Neretin L, Wong MH. Bisphenol A (BPA) in China: a review of sources, environmental levels, and potential human health impacts. *Environ. Int.* 42, **2012**, 91-99.

Husseien M, Amer AA, El-Maghraby A, Taha NA. Availability of barley straw application on oil spill clean up. *Int. J. Environ. Sci. Technol*. 6, **2009**, 123-130.

Ibrahim ASS, Al-Salamah AA, El-Toni AM, El-Tayeb MA, Elbadawi YB, Antranikian G. Detoxification of hexavalent chromate by *Amphibacillus* sp KSUCr3 cells immobilised in silica-coated magnetic alginate beads. *Biotechnol. Bioprocess Eng.* 18, **2013**, 1238-1249.

Ji YQ, Hu YT, Tian Q, Shao XZ, Li J, Safarikova M, Safarik I. Biosorption of strontium ions by magnetically modified yeast cells. *Sep. Sci. Technol.* 45, **2010**, 1499-1504.

Jiang R, Tian J, Zheng H, Qi J, Sun S, Li X. A novel magnetic adsorbent based on waste litchi peels for removing Pb(II) from aqueous solution. *J. Environ. Manage.* 155, **2015**, 24-30.

Jing XR, Wang YY, Liu WJ, Wang YK, Jiang H. Enhanced adsorption performance of tetracycline in aqueous solutions by methanol-modified biochar. *Chem. Eng. J.* 248, **2014**, 168-174.

Jung KW, Hwang MJ, Jeong TU, Ahn KH., 2015. A novel approach for preparation of modified-biochar derived from marine macroalgae: dual purpose electro-modification for improvement of surface area and metal impregnation. *Bioresour. Technol.* 191, **2015**, 342-345.

Khan AA, Singh RP. Adsorption thermodynamics of carbofuran on Sn (IV) arsenosilicate in H^+, Na^+ and Ca^{2+} forms. *Colloid Surf.* 24, **1987**, 33-42.

Khandanlou R, Ahmad MB, Masoumi HRF, Shameli K, Basri M, Kalantari K. Rapid adsorption of copper(II) and lead(II) by rice straw/Fe_3O_4 nanocomposite: optimization, equilibrium isotherms, and adsorption kinetics study. *Plos One* 10(3), **2015**. doi:10.1371/journal.pone.0120264.

Kong X, Liu Y, Pi J, Li W, Liao Q, Shang J., 2017. Low-cost magnetic herbal biochar: characterization and application for antibiotic removal. *Environ. Sci. Pollut. Res.* 24, **2017**, 6679-6687.

Krumphanzl V, Řeháček Z. Mikrobiální technologie: buňka a techniky jejího využití. 1. vyd. Academia Praha: Praha, **1988**, 360 s.

Kudaybergenov KK, Ongarbayev EK, Mansurov ZA. Thermally treated rice husks for petroleum adsorption. *Int. J. Biol. Chem.* 1, **2012**, 3-12.

Kuncová G, Trögl J. Mikroorganismy imobilizované uvnitř anorganických nosičů. *Chem. listy* 105, **2001**, 830-838.

Latha PP, Bhatt M, Jain SL. Sustainable catalysis using magnetic chicken feathers decorated with Pd(0) for Suzuki-cross coupling reaction. *Tetrahedron Lett.* 56, **2015**, 5718-5722.

Laurent S, Forge D, Port M, Roch A, Robic C, Vander Elst L, Muller RN. Magnetic iron oxide nanoparticles: synthesis, stabilization, vectorization, physicochemical characterizations, and biological applications. *Chem. Rev.* 108, **2008**, 2064-2110.

Li H, Li Z, Liu T, Xiao X, Peng Z, Deng L. A novel technology for biosorption and recovery hexavalent chromium in wastewater by bio-functional magnetic beads. B*ioresour. Technol.* 99, **2008**, 6271-6279.

Liu D, Zhang ZP, Ding YG. A simple method to prepare magnetic modified corncobs and its application for congo red adsorption. *J. Dispersion Sci. Technol.* 37, **2016a**, 73-79.

Liu X, Gong W, Luo J, Zou C, Yang Y, Yang S. Selective adsorption of cationic dyes from aqueous solution by polyoxometalate-based metal–organic framework composite. *Appl. Surf. Sci.* 362, **2016b**, 517-524.

Liu YC, Zhu XD, Qian F, Zhang SC, Chen JM. Magnetic activated carbon prepared from rice straw-derived hydrochar for triclosan removal. *RSC Adv.* 4, **2014**, 63620-63626.

Lou JQ, Xu X, Gao YF, Zheng DZ, Wang JY, Li ZG. Preparation of magnetic activated carbon from waste rice husk for the determination of tetracycline antibiotics in water samples. *RSC Adv.* 6, **2016**, 112166-112174.

Lunge S, Singh S, Sinha A. Magnetic iron oxide (Fe_3O_4) nanoparticles from tea waste for arsenic removal. *J. Magn. Magn. Mater.* 356, **2014**, 21-31.

Madrakian T, Afkhami A, Ahmadi M. Adsorption and kinetic studies of seven different organic dyes onto magnetite nanoparticles loaded tea waste and removal of them from wastewater samples. *Spectroc. Acta Pt A-Molec. Biomolec. Spectr.* 99, **2012**, 102-109.

Mahmoud ME, Ahmed SB, Osman MM, Abdel-Fattah TM. A novel composite of nanomagnetite-immobilized-baker's yeast on the surface of activated carbon for magnetic solid phase extraction of Hg(II). *Fuel* 139, **2015**, 614-621.

Massart R. Preparation of aqueous magnetic liquids in alkaline and acidic media. *IEEE Trans. Magn.* 17, **1981**, 1247-1248.

Mohan D, Kumar H, Sarswat A, Alexandre-Franco M, Pittman Jr CU. Cadmium and lead remediation using magnetic oak wood and oak bark fast pyrolysis bio-chars. *Chem. Eng. J.* 236, **2014**, 513-528.

Mosiniewicz-Szablewska E, Safarikova M, Safarik I. Magnetic studies of ferrofluid-modified microbial cells. *J. Nanosci. Nanotechnol.* 10, **2010**, 2531-2536.

Nartey OD, Zhao BW. Biochar preparation, characterization, and adsorptive capacity and its effect on bioavailability of contaminants: an overview. *Adv Mater. Sci. Eng.* 2014, **2014**. doi:10.1155/2014/715398.

Ong ST, Keng PS, Ooi ST, Hung YT, Lee SL. Utilization of fruits peel as a sorbent for removal of methylene blue. *Asian J. Chem.* 24, **2012**, 398-402.

Panneerselvam P, Morad N, Tan KA. Magnetic nanoparticle (Fe_3O_4) impregnated onto tea waste for the removal of nickel(II) from aqueous solution. *J. Hazard. Mater.* 186, **2011**, 160-168.

Parmar A, Nema PK, Agarwal T. Biochar production from agro-food industry residues: a sustainable approach for soil and environmental management. *Curr. Sci.* 107, **2014**, 1673-1682.

Patzak M, Dostalek P, Fogarty RV, Safarik I, Tobin JM. Development of magnetic biosorbents for metal uptake. *Biotechnol. Tech.* 11, **1997**, 483-487.

Peng H, Wang H, Wu J, Meng G, Wang Y, Shi Y, Liu Z, Guo X. Preparation of superhydrophobic magnetic cellulose sponge for removing oil from water. *Ind. Eng. Chem. Res.* 55, **2016**, 832-838.

Peng Q, Liu Y, Zeng G, Xu W, Yang C, Zhang J. Biosorption of copper(II) by immobilizing *Saccharomyces cerevisiae* on the surface of chitosan-coated magnetic nanoparticles from aqueous solution. *J. Hazard. Mater.* 177, **2010**, 676-682.

Pengsaket I, Thamaphat K, Limsuwan P. Removal of Cu^{2+} from aqueous solutions by magnetic nanoparticles-pomelo peel composite. *Key Eng. Mater.* 675-676, **2016**, 154-157.

Pirbazari AE, Saberikhah E, Gorabi NGA. Fe_3O_4 nanoparticles loaded onto wheat straw: an efficient adsorbent for basic blue 9 adsorption from aqueous solution. *Desalin. Water Treat.* 57, **2016**, 4110-4121.

Pospiskova K, Prochazkova G, Safarik I. One-step magnetic modification of yeast cells by microwave-synthesized iron oxide microparticles. *Lett. Appl. Microbiol.* 56, **2013**, 456-461.

Rafatullah M, Sulaiman O, Hashim R, Ahmad A. Adsorption of methylene blue on low-cost adsorbents: a review. *J. Hazard. Mater.* 177, **2010**, 70-80.

Rahnama B, Darban AK, Milani S. Magnetic nano-biosorption of heavy metal from aqueous solutions using sugarcane bagasse. *Iran. J. Sci. Technol.-Trans. Civ. Eng.* 38, **2014**, 137-146.

Rajesh Kumar S, Jayavignesh V, Selvakumar R, Swaminathan K, Ponpandian N. Facile synthesis of yeast cross-linked Fe_3O_4 nanoadsorbents for efficient

removal of aquatic environment contaminated with As(V). *J. Colloid Interface Sci.* 484, **2016**, 183-195.

Rancière F, Lyons JG, Loh VHY, Botton J, Galloway T, Wang T, Shaw JE, Magliano DJ. Bisphenol A and the risk of cardiometabolic disorders: a systematic review with meta-analysis of the epidemiological evidence. *Environ. Health* 14, **2015**, 1-23.

Rao A, Bankar A, Kumar AR, Gosavi, S, Zinjarde, S. Removal of hexavalent chromium ions by *Yarrowia lipolytica* cells modified with phyto-inspired Fe^0/Fe_3O_4 nanoparticles. *J. Contam. Hydrol.* 146, **2013**, 63-73.

Rattanachueskul N, Saning A, Kaowphong S, Chumha N, Chuenchom L. Magnetic carbon composites with a hierarchical structure for adsorption of tetracycline, prepared from sugarcane bagasse via hydrothermal carbonization coupled with simple heat treatment process. *Bioresour. Technol.* 226, **2017**, 164-172.

Reddy DHK, Lee SM. Magnetic biochar composite: facile synthesis, characterization, and application for heavy metal removal. *Colloid Surf. A-Physicochem. Eng. Asp.* 454, **2014**, 96-103.

Reguyal F, Sarmah AK, Gao W. Synthesis of magnetic biochar from pine sawdust via oxidative hydrolysis of $FeCl_2$ for the removal sulfamethoxazole from aqueous solution. *J. Hazard. Mater.* 321, **2017**, 868-878.

Rozumova L, Seidlerova J, Safarik I, Safaríkova M, Cihlarova M, Gabor R. Magnetically modified tea for lead sorption. *Adv. Sci. Eng. Med.* 6, **2014**, 473-476.

Rozumova L, Seidlerova J, Safarik I, Safarikova M, Gabor R, Tanger LTD. Sorption of Pb on magnetically modified biological materials. *Nanocon 2012*, 4th Int. Conference, **2012**, 623-628.

Safarik I, Baldikova E, Pospiskova K, Safarikova M. Magnetic modification of diamagnetic agglomerate forming powder materials. *Particuology* 29, **2016a**, 169-171.

Safarik I, Horska K, Pospiskova K, Filip J, Safarikova M. Mechanochemical synthesis of magnetically responsive materials from non-magnetic precursors. *Mater. Lett.* 126, **2014**, 202-206.

Safarik I, Horska K, Pospiskova K, Maderova Z, Safarikova M. Microwave assisted synthesis of magnetically responsive composite materials. *IEEE Trans. Magn.* 49, **2013**, 213-218.

Safarik I, Horska K, Pospiskova K, Safarikova M. One-step preparation of magnetically responsive materials from non-magnetic powders. *Powder Technol.* 229, **2012a**, 285-289.

Safarik I, Horska K, Safarikova M. Magnetically modified spent grain for dye removal. *J. Cereal Sci.* 53, **2011a**, 78-80.

Safarik I, Horska K, Safarikova M. Magnetically responsive biocomposites for inorganic and organic xenobiotics removal. In: *Microbial Biosorption of Metals* (Kotrba P, Mackova M, Macek T., Eds.). Springer, **2011b**, pp 301-320.

Safarik I, Horska K, Svobodova B, Safarikova M. Magnetically modified spent coffee grounds for dyes removal. *Eur. Food Res. Technol.* 234, **2012b**, 345-350.

Safarik I, Maderova Z, Pospiskova K, Baldikova E, Horska K, Safarikova M. Magnetically responsive yeast cells: methods of preparation and applications. *Yeast* 32, **2015a**, 227-237.

Safarik I, Nydlova L, Pospiskova K, Baldikova E, Maderova Z, Safarikova M. Rapid determination of iron oxide content in magnetically modified particulate materials. *Particuology* 26, **2016b**, 114-117.

Safarik I, Pospiskova K, Baldikova E, Maderova Z, Safarikova M. Magnetic modification of cells. In: *Application of NanoBioMaterials* (Grumezescu A, Ed.). Elsevier: US, **2016c**, pp 145-181.

Safarik I, Pospiskova K, Horska K, Safarikova M. Potential of magnetically responsive (nano)biocomposites. *Soft Matter* 8, **2012c**, 5407-5413.

Safarik I, Pospiskova K, Maderova Z, Baldikova E, Horska K, Safarikova M. Microwave-synthesized magnetic chitosan microparticles for the immobilization of yeast cells. *Yeast* 32, **2015b**, 239-243.

Safarik I, Ptackova L, Safarikova M. Adsorption of dyes on magnetically labeled baker's yeast cells. *Eur. Cells Mater.* 3, **2002**, 52-55.

Safarik I, Rego LFT, Borovska M, Mosiniewicz-Szablewska E, Weyda F, Safarikova M. New magnetically responsive yeast-based biosorbent for the efficient removal of water-soluble dyes. *Enzyme Microb. Technol.* 40, **2007**, 1551-1556.

Safarik I, Safarikova M. Use of magnetic techniques for the isolation of cells. *J. Chromatogr. B* 722, **1999**, 33-53.

Safarik I, Safarikova M. Cells: isolation: magnetic techniques. In: *Encyclopedia of Separation Science* (Wilson ID, Aldar TR, Poole CF, Cool M, Eds.). Academic Press Ltd.: London, **2000**. pp 2260-2267.

Safarik I, Safarikova M. Magnetically modified microbial cells: a new type of magnetic adsorbents. *China Particuology* 5, **2007**, 19-25.

Safarik I, Safarikova M. Magnetically responsive nanocomposite materials for bioapplications. *Solid State Phenomena* 151, **2009**, 88-94.

Safarik I, Safarikova M. Magnetic fluid modified peanut husks as an adsorbent for organic dyes removal. *Phys. Procedia* 9, **2010**, 274-278.

Safarik I, Safarikova M. One-step magnetic modification of non-magnetic solid materials. I*nt. J. Mater. Res.* 105, **2014**, 104-107.

Safarikova M, Pona BMR, Mosiniewicz-Szablewska E, Weyda F, Safarik I. Dye adsorption on magnetically modified *Chlorella vulgaris* cells. *Fresenius Environ. Bull.* 17, **2008**, 486-492.

Safarikova M, Ptackova L, Kibrikova I, Safarik I. Biosorption of water-soluble dyes on magnetically modified *Saccharomyces cerevisiae* subsp *uvarum* cells. *Chemosphere* 59, **2005**, 831-835.

Safarikova M, Safarik I. Magnetické separace v přírodních vědách a biotechnologiích. *Chem. listy* 89, **1995**, 223-252.

Safarikova M, Safarik I. The application of magnetic techniques in bioscience. *Magn. Electr. Sep.* 10, **2001**, 223-252.

Sathasivam K, Haris MRHM. Adsorption kinetics and capacity of fatty acid-modified banana trunk fibers for oil in water. *Water Air Soil Pollut.* 213, **2010**, 413-423.

Sayed SA, Zayed AM. Investigation of the effectiveness of some adsorbent materials in oil spill clean-ups. *Desalination* 194, **2006**, 90-100.

Shah J, Jan MR, Khan M, Amir S. Removal and recovery of cadmium from aqueous solutions using magnetic nanoparticle-modified sawdust: kinetics and adsorption isotherm studies. *Desalin. Water Treat.* 57, **2016**, 9736-9744.

Shen BX, Li GL, Wang FM, Wang YY, He C, Zhang M, Singh S. Elemental mercury removal by the modified bio-char from medicinal residues. *Chem. Eng. J.* 272, **2015**, 28-37.

Sidiras D, Konstantinou I. A new oil spill adsorbent from sulfuric acid modified wheat straw. In: *Latest Trends in Environmental and Manufacturing*

Engineering (Ponis S, Karas IR, Momete DC, Eds.). WSEAS Press: Vienna, **2012**, pp 132-137.

Singha B, Das S. Removal of Pb(II) ions from aqueous solution and industrial effluent using natural biosorbents. *Environ. Sci. Pollut. Res.* 19, **2012**, 2212-2226.

Song W, Gao B, Zhang T, Xu X, Huang X, Yu H, Yue Q. High-capacity adsorption of dissolved hexavalent chromium using amine-functionalized magnetic corn stalk composites. *Bioresour. Technol.* 190, **2015**, 550-557.

Srivastava S, Agrawal SB, Mondal MK. A review on progress of heavy metal removal using adsorbents of microbial and plant origin. *Environ. Sci. Pollut. Res.* 22, **2015**, 15386-15415.

Stenmarck A, Jensen C, Quested T, Moates G. Estimates of European food waste levels. FUSIONS project EU (Grant agreement no. 311972), Reducing food waste through social innovation, **2016**, 79 pages.

Sud D, Mahajan G, Kaur MP. Agricultural waste material as potential adsorbent for sequestering heavy metal ions from aqueous solutions - a review. *Bioresour. Technol.* 99, **2008**, 6017-6027.

Sun PF, Hui C, Khan RA, Du JT, Zhang QC, Zhao,YH. Efficient removal of crystal violet using Fe_3O_4-coated biochar: the role of the Fe_3O_4 nanoparticles and modeling study their adsorption behavior. *Sci. Rep.* 5, **2015**. doi:10.10138/srep12638.

Sun XF, Sun RC, Sun JX. Acetylation of rice straw with or without catalysts and its characterization as a natural sorbent in oil spill cleanup. *J. Agric. Food Chem.* 50, **2002**, 6428-6433.

Taha NA, El-Maghraby A. Magnetic peanut hulls for methylene blue dye removal: isotherm and kinetic study. *Glob. Nest J.* 18, **2016**, 25-37.

Tan KA, Morad N, Teng TT, Norli I, Panneerselvam P. Removal of cationic dye by magnetic nanoparticle (Fe_3O_4) impregnated onto activated maize cob powder and kinetic study of dye waste adsorption. *APCBEE Procedia* 1, **2012**, 83-89.

Tan ZX, Wang YH, Kasiuliene A, Huang CQ, Ai P. Cadmium removal potential by rice straw-derived magnetic biochar. *Clean Technol. Environ. Policy* 19, **2017**, 761-774.

Tian Y, Ji C, Zhao M, Xu M, Zhang Y, Wang R. Preparation and characterization of baker's yeast modified by nano-Fe_3O_4: application of biosorption of methyl violet in aqueous solution. *Chem. Eng. J.* 165, **2010**, 474-481.

Tian Y, Wu M, Lin X, Huang P, Huang Y. Synthesis of magnetic wheat straw for arsenic adsorption. *J. Hazard. Mater.*193, **2011**, 10-16.

Tonk S, Maicaneanu A, Indolean C, Burca S, Majdik C. Application of immobilized waste brewery yeast cells for Cd^{2+} removal. Equilibrium and kinetics. *J. Serb. Chem. Soc.* 76, **2011**, 363-373.

Uzun L, Saglam N, Safarikova M, Safarik I, Denizli A. Copper biosorption on magnetically modified yeast cells under magnetic field. *Sep. Sci. Technol.* 46, **2011**, 1045-1051.

Vandenberg LN, Chahoud I, Heindel JJ, Padmanabhan V, Paumgartten FJR, Schoenfelder G. Urinary, circulating, and tissue biomonitoring studies indicate widespread exposure to bisphenol A. *Environ. Health Perspect.* 118, **2010**, 1055-1070.

Wang H, Ji,Y, Tian Q, Horska K, Shao X, Maderova Z, Miao X, Safarikova M, Safarik I. Biosorption of uranium by magnetically modified wheat bran. *Sep. Sci. Technol.*49, **2014**, 2534-2539.

Wang H, Lin KY, Jing B, Krylova G, Sigmon GE, McGinn P, Zhu Y, Na C. Removal of oil droplets from contaminated water using magnetic carbon nanotubes. *Water Res.* 47, **2013a**, 4198-4205.

Wang H, Xu X, Ren Z, Gao B. Removal of phosphate and chromium(VI) from liquids by an amine-crosslinked nano-Fe_3O_4 biosorbent derived from corn straw. *RSC Adv.* 6, **2016**, 47237-47248.

Wang HY, Gao B, Wang SS, Fang J, Xue YW, Yang K. Removal of Pb(II), Cu(II), and Cd(II) from aqueous solutions by biochar derived from $KMnO_4$ treated hickory wood. *Bioresour. Technol.* 197, **2015**, 356-362.

Wang J, Chen C. Biosorbents for heavy metals removal and their future. *Biotechnol. Adv.* 27, **2009**, 195-226.

Wang SL, Xu XR, Sun YX, Liu JL, Li HB. Heavy metal pollution in coastal areas of South China: a review. *Mar. Pollut. Bull.* 76, **2013b**, 7-15.

Wong KT, Yoon Y, Snyder SA, Jang M. Phenyl-functionalized magnetic palm-based powdered activated carbon for the effective removal of selected

pharmaceutical and endocrine-disruptive compounds. *Chemosphere* 152, **2016**, 71-80.

Wong PK, Fung KY. Removal and recovery of nickel ion (Ni^{2+}) from aqueous solution by magnetite-immobilized cells of *Enterobacter* sp 4-2. *Enzyme Microb. Technol.* 20, **1997**, 116-121.

Wu Y, Zhang L, Gao C, Ma J, Ma X, Han R. Adsorption of copper ions and methylene blue in a single and binary system on wheat straw. *J. Chem. Eng. Data* 54, **2009**, 3229-3234.

Xu M, Zhang Y, Zhang Z, Shen Y, Zhao M, Pan G. Study on the adsorption of Ca^{2+}, Cd^{2+} and Pb^{2+} by magnetic Fe_3O_4 yeast treated with EDTA dianhydride. *Chem. Eng. J.* 168, **2011**, 737-745.

Yakout SM, Daifullah AEHM, El-Reefy SA. Pore structure characterization of chemically modified biochar derived from rice straw. *Environ. Eng. Manage. J.* 14, **2015**, 473-480.

Yamamura APG, Yamaura M, Costa CH. Magnetic biosorbent for removal of uranyl ions. *Int. J. Nucl. Energy Sci.Technol.* 6, **2011**, 8-16.

Yap MW, Mubarak NM, Sahu JN, Abdullah EC. Microwave induced synthesis of magnetic biochar from agricultural biomass for removal of lead and cadmium from wastewater. *J. Ind. Eng. Chem.* 45, **2017**, 287-295.

Yavuz H, Denizli A, Gungunes H, Safarikova M, Safarik I. Biosorption of mercury on magnetically modified yeast cells. *Sep. Purif. Technol.* 52, **2006**, 253-260.

Yu JX, Chi RA, Zhang YF, Xu ZG, Xiao CQ, Guo J. *A situ* co-precipitation method to prepare magnetic PMDA modified sugarcane bagasse and its application for competitive adsorption of methylene blue and basic magenta. *Bioresour. Technol.* 110, **2012**, 160-166.

Yu JX, Wang LY, Chi RA, Zhang YF, Xu ZG, Guo J. Competitive adsorption of Pb^{2+} and Cd^{2+} on magnetic modified sugarcane bagasse prepared by two simple steps. *Appl. Surf. Sci.*268, **2013a**, 163-170.

Yu JX, Wang LY, Chi RA, Zhang YF, Xu ZG, Guo J. A simple method to prepare magnetic modified beer yeast and its application for cationic dye adsorption. *Environ. Sci.Pollut. Res.* 20, **2013b**, 543-551.

Zhang M, Gao B, Varnoosfaderani S, Hebard A, Yao Y, Inyang M. Preparation and characterization of a novel magnetic biochar for arsenic removal. *Bioresour. Technol.* 130, **2013a**, 457-462.

Zhang W, Yan H, Li H, Jiang Z, Dong L, Kan X, Yan H, Li A, Cheng R. Removal of dyes from aqueous solutions by straw based adsorbents: batch and column studies. *Chem. Eng. J.* 168, **2011a**, 1120-1127.

Zhang W, Yang H, Dong L, Yan H, Li H, Jiang Z, Kan X, Li A, Cheng R. Efficient removal of both cationic and anionic dyes from aqueous solutions using a novel amphoteric straw-based adsorbent. *Carbohydr. Polym.* 90, **2012**, 887-893.

Zhang X, Zhang SH, Yang HP, Shi T, Chen YQ, Chen HP. Influence of NH_3/CO_2 modification on the characteristic of biochar and the CO_2 capture. *BioEnergy Res.* 6, **2013b**, 1147-1153.

Zhang Y, Liu W, Zhang L, Wang M, Zhao M. Application of bifunctional *Saccharomyces cerevisiae* to remove lead(II) and cadmium(II) in aqueous solution. *Appl. Surf. Sci.* 257, **2011b**, 9809-9816.

Zhang Y, Zhu J, Zhang,L, Zhang Z, Xu M, Zhao M. Synthesis of EDTAD-modified magnetic baker's yeast biomass for Pb^{2+} and Cd^{2+} adsorption. *Desalination* 278, **2011c**, 42-49.

Zhao Y, Xia YX, Yang HY, Wang YY, Zhao MJ. Synthesis of glutamic acid-modified magnetic corn straw: equilibrium and kinetic studies on methylene blue adsorption. *Desalin. Water Treat.* 52, **2014**, 199-207.

Zheng B, Zhang M, Xiao D, Jin Y, Choi MMF. Fast microwave synthesis of Fe_3O_4 and Fe_3O_4/Ag magnetic nanoparticles using Fe^{2+} as precursor. *Inorg. Mater.* 46, **2010**, 1106-1111.

Zhou Y, Lu P, Lu J. Application of natural biosorbent and modified peat for bisphenol a removal from aqueous solutions. *Carbohydr. Polym.* 88, **2012**, 502-508.

Zou J, Chai W, Liu X, Li B, Zhang X, Yin T. Magnetic pomelo peel as a new absorption material for oil-polluted water. *Desalin. Water Treat.* 57, **2016**, 12536-12545.

Zuorro A, Di Battista A, Lavecchia R. Magnetically modified coffee silverskin for the removal of xenobiotics from wastewater. *Chem. Eng. Trans.* 35, **2013**, 1375-1380.

Zuorro A, Lavecchia R, Natali S. Magnetically modified agro-industrial wastes as efficient and easily recoverable adsorbents for water treatment. *Chem. Eng. Trans.* 38, **2014**, 349-354.

9. PŘÍLOHY

9.1 Seznam obrázků

Obrázek 1: SEM bakterie *Leptothrix* sp. modifikované pomocí kyselé magnetické kapaliny (vlevo) a magnetických oxidů železa syntetizovanými mikrovlnným zářením (vpravo)…….. 17

Obrázek 2: Kvasinkové buňky kovalentně vázané na částice magnetického chitosanu.……... 18

Obrázek 3: Schéma metod magnetické separace mikrobiálních buněk…… 21

Obrázek 4: Ukázka magnetické separace pomocí různých typů komerčně dostupných vsádkových magnetických separátorů……. 22

9.2 Seznam grafů

Graf 1: Vliv třepání na maximálních adsorpční kapacitu slámových adsorbentů (malé částice, natural 98)……... 85

Graf 2: Maximální adsorpční kapacity slámových sorbentů (větší částice) pro různé adsorbáty…….. 86

9.3 Seznam tabulek

Tabulka 1: Nosiče používané pro kovalentní imobilizace…….. 19

Tabulka 2: Rozdělení nosičů dle mechanismu tvorby gelu…… 20

Tabulka 3: Porovnání výtěžnosti biouhlu při použití různých termochemických procesů…….. 25

Tabulka 4: Magnetické biokompozitní materiály pro odstranění organických barviv…… 28

Tabulka 5: Magnetické biokompozitní materiály pro odstranění těžkých kovů…. 32

Tabulka 6: Magnetické biokompozitní materiály pro odstranění PPCP/EDCs….. 38

Tabulka 7: Magnetické biokompozitní materiály pro odstranění ropných látek… 40

Tabulka 8: Vliv intenzity magnetizace a velikosti částic na maximální adsorpční kapacitu (q_m)……..... 86

Tabulka 9: Maximální adsorpční kapacity slámových sorbentů ve směsném prostředí…… 87

9.4 Seznam zkratek

ATB = antibiotika

EDA = etylendiamin

EDCs = endokrinní disruptory

EDS = energiově dispersní spektroskopie

EDTA = etylendiamintetraoctová kyselina

EDTAD = dianhydrid etylendiamintetraoctové kyseliny

FTIR = infračervená spektroskopie s Fourierovou transformací

GA= glutaraldehyd

MES= 2-(N-morfolino)etanosulfonová kyselina

MK = magnetická kapalina

MS = mikrovlnně-syntetizovaný

N/A = neděláno

PMDA = pyromelitický dianhydrid

PPCPs = farmaceutické preparáty a přípravky osobní péče

SEM = skenovací elektronová mikroskopie

SQUID = supravodivé kvantové interferenční zařízení

TEM = transmisní elektronová mikroskopie

TETA = trietylen-tetramin

TRIS = tris(hydroxymetyl)aminometan

XRD = rentgenová difrakční analýza

9.5 Má publikační aktivita

9.5.1 Články v impaktovaných vědeckých časopisech

1) Safarik I., Pospiskova K., Maderova Z., **Baldikova, E**., Horska, K, Safarikova, M. Microwave-synthesized magnetic chitosan microparticles for the immobilization of yeast cells. *Yeast* 32, **2015**, 239-242.
2) Safarik I., Maderova Z., Horska K., **Baldikova E**., Pospiskova K., Safarikova M. Spent rooibos (*Aspalathus linearis*) tea biomass as an adsorbent for organic dyes removal. *Bioremed. J*. 19(3), **2015**, 183-187.
3) **Baldikova E**., Safarikova M., Safarik I. Organic dyes removal using magnetically modified rye straw. *J. Magn. Magn. Mater. 380*, **2015**, 181-185.
4) Safarik I., Maderova Z., Pospiskova K., **Baldikova E**., Horska K., Safarikova M. Magnetically responsive yeast cells: methods of preparation and application. *Yeast* 32, **2015**, 227-237.
5) **Baldikova E**., Politi D., Maderova Z., Pospiskova K., Sidiras D., Safarikova M., Safarik I. Utilization of magnetically responsive cereal by-product for organic dyeremoval. *J. Sci. Food Agric*. 96, **2016**, 2204-2214.
6) **Baldikova E.**, Pospiskova K., Maderova Z., Safarikova M., Safarik I. Příprava magnetických kompozitních materiálů - experimenty pro studenty středních škol. *Chem. listy* 110, **2016**, 64-68.
7) Safarik I., Nydlova L., Pospiskova K., **Baldikova E.**, Maderova Z., Safarikova M. Rapid determination of iron oxides content in magnetically modified particulate materials. *Particuology* 26, **2016**, 114-117.
8) Safarik I., Ashoura N., Maderova Z., Pospiskova K., **Baldikova E.**, Safarikova M. Magnetically modified *Posidonia oceanica* biomass as an adsorbent for organic dyes removal. *Mediterr. Mar. Sci.* 17(2), **2016**, 351-358.
9) Maderova Z., **Baldikova E**., Pospiskova K., Safarik I., Safarikova M. Removal of dyes by adsorption on magnetically modified activated sludge. *Int. J. Environ. Sci. Technol.* 13, **2016,** 1653-1664.
10) Safarik I., Pospiskova K., **Baldikova E.**, Safarikova M. Development of advanced biorefinery concepts using magnetically responsive materials. *Biochem. Eng. J.*, 116, **2016**, 17-26.

11) Safarik I., **Baldikova E.,** Pospiskova K., Safarikova M. Magnetic modification of diamagnetic agglomerate forming powder materials. *Particuology* 29, **2016**, 169-171.
12) Angelova R., **Baldikova E.**, Pospiskova K., Maderova Z., Safarikova M., Safarik I., Magnetically modified *Sargassum horneri* biomass as an adsorbent for organic dye removal. *J. Clean. Product.* 137, **2016**, 189-194.
13) Safarik I., Stepanek M., Uchman M., Slouf M., **Baldikova E.,** Nydlova L., Pospiskova K., Safarikova M. Composite particles formed by complexation of poly(methacrylic acid) - stabilized magnetic fluid with chitosan: Magnetic material for bioapplications. *Mater. Sci. Eng. C* 67, **2016**, 486-492.
14) Safarik I., Maderova Z., Pospiskova K., Schmidt H.P., **Baldikova E.**, Filip J.,Krizek M., Malina O., Safarikova M. Magnetically modified biochar for organic xenobiotics removal. *Water Sci. Technol.* 74(7), **2016**, 1706-1715.
15) **Baldikova E.**, Pospiskova K., Ladakis D., Kookos I.K., Koutinas A.A., Safarikova M., Safarik I. Magnetically modified bacterial cellulose: A promising carrier for immobilization of affinity ligands, enzymes, and cells. *Mater. Sci. Eng. C* 71, **2017**, 214-221.
16) **Baldikova E.**, Prochazkova J., Stepanek M., Hajduova J., Pospiskova K., Safarikova M., Safarik I. PMAA-stabilized ferrofluid/chitosan/yeast composite for bioapplications. *J. Magn. Magn. Mater. 427,* **2017**, 29-33.
17) Angelova R., **Baldikova E.**, Pospiskova K., Safarikova M., Safarik I. Magnetically modified sheaths of *Leptothrix* sp. as an adsorbent for Amido black 10B removal. *J. Magn. Magn. Mater. 427,* **2017**, 314-319.
18) Safarik I., Angelova R., **Baldikova E.**, Pospiskova K., Safarikova M. *Leptothrix* sp. sheats modified with iron oxide particles: Magnetically responsive, high aspect ratio functional material. *Mater. Sci. Eng. C* 71, **2017**, 1342-1346.

9.5.2 Články v neimpaktovaných vědeckých časopisech

1) Safarik I., Pospiskova K., **Baldikova E.**, Safarikova M. Magnetically responsive biological materials and their applications. *Adv. Mater. Lett.* 7(4), **2016**, 254-261.

9.5.3 Knižní kapitoly

1) Safarik I., Pospiskova K., **Baldikova E.**, Maderova Z., Safarikova M.: Magnetic modification of cells. In: *Applications of NanoBioMaterials*, Volume II: Engineering of NanoBioMaterials (Grumezescu, A., ed.), Elsevier: US, **2016**, pp 145 – 181.
2) Safarik I., Pospiskova K., **Baldikova E.,** Safarikova M.: Magnetically responsive microbial cells for metal ions removal and detection. In: *Metal-Microbe Interactions and Bioremediation: Principles and Applications for Toxic Metals*, (Das S., Dash H.R., Eds.), CRC Press, **2017**, 769-777.
3) Safarik I., Pospiskova K., **Baldikova E.**, Safarikova M.: Magnetic particles for microalgae separation and biotechnology. In: *Food Bioactives: Extraction and Biotechnology Applications* (Puri M, Ed.), Springer, **2017**, 153-171.